INTERNATIONAL COUNCIL FOR RESEARCH AND INNOVATION
IN BUILDING AND CONSTRUCTION

WORKING COMMISSION W18 - TIMBER STRUCTURES

CIB - W18

MEETING THIRTY-NINE

FLORENCE

ITALY

AUGUST 2006

Lehrstuhl für Ingenieurholzbau und Baukonstruktionen
Universität Karlsruhe
Germany
Compiled by Rainer Görlacher
2006

ISSN 0945-6996

CONTENTS

0 List of Participants

INTERNATIONAL COUNCIL FOR RESEARCH AND INNOVATION IN BUILDING AND CONSTRUCTION
WORKING COMMISSION W18 - TIMBER STRUCTURES

MEETING THIRTY-NINE
Florence, Italy, 28 - 31 August 2006

LIST OF PARTICIPANTS

AUSTRALIA	
K Crews	University of Technology Sydney UTS
AUSTRIA	
M Augustin	TU Graz
T Bogensperger	TU Graz
A Jöbstel	TU Graz
R Katzengruber	TU Graz
G Schickhofer	TU Graz
CANADA	
A Asiz	University of New Brunswick, Fredericton
E Karacabeyli	Forintek, Vancouver
F Lam	University of BC, Vancouver
P Quenneville	Royal Military College of Canada, Kingston
I Smith	University of New Brunswick, Fredericton
CZECH REPUBLIC	
P Kuklik	TU Prague
DENMARK	
H J Larsen	Copenhagen
H Riberholt	Tech. University of Denmark
FINLAND	
A Hanhijärvi	VTT Technical Research Centre of Finland, Espoo
A Ranta-Maunus	VTT Technical Research Centre of Finland, Espoo
FRANCE	
P Racher	Blaise Pascal University, Aubiere Cedex
GERMANY	
I Bejtka	Universität Karlsruhe
H J Blaß	Universität Karlsruhe
J Denzler	Technical University of Munich
M Deublein	Technical University of Munich
A Döhrer	Bauhaus University, Weimar
J Ehlbeck	Freiburg
B Franke	Bauhaus University, Weimar
S Franke	Bauhaus University, Weimar
M Frese	Universität Karlsruhe
R Görlacher	Universität Karlsruhe
A Heiduschke	TU Dresden

K Rautenstrauch	Bauhaus University, Weimar
J Schänzlin	Universität Stuttgart
T Uibel	Universität Karlsruhe
IRELAND	
A Harte	National University of Ireland, Galway
ITALY	
A Ceccotti	IVALSA-CNR
M Follesa	IVALSA-CNR, Florence
M P Lauriola	IVALSA-CNR, Florence
M Moschi	IVALSA-CNR, Florence
A Palermo	Politecnico di Milano
C Sandhaas	IVALSA-CNR, Florence
M Togni	University of Florence
L Uzielli	University of Florence
JAPAN	
C Minowa	Research Institute for Earth Science and Disaster Prevention
M Yasumura	Shizuoka University
SLOVENIA	
B Dujic	University of Ljubljana
SWEDEN	
B Källsner	SP Trätek, Stockholm
J König	SP Trätek, Stockholm
SWITZERLAND	
A Frangi	ETH Zürich
R Steiger	EMPA Wood Laboratory, Dübendorf
THE NETHERLANDS	
A Jorissen	TU Eindhoven
A Leijten	TU Delft
J W van de Kuilen	TU Delft
NEW ZEALAND	
A Buchanan	University of Canterbury
M Fragiacomo	University of Canterbury
UK	
V Enjily	BRE, Garston
R Marsh	Loubs-Bernac, France
D Trujillo	CCB Evolution, Bristol
USA	
T Williamson	American Plywood Association, Tacoma
B Yeh	American Plywood Association, Tacoma

1. Chairman's Introduction

2. General Topics

3. Stress Grading

4. Stresses for Solid Timber

5. Timber Joints and Fasteners

6. Load Sharing

7. Duration of Load

8. Laminated Members

9. Structural Stability

10. Fire

11. Statistics and Data Analysis

12. Glued Joints

13. Fracture Mechanics

14. Test Methods

15. Loading Codes

16. Any Other Business

17. Venue and Program for Next Meeting

18. Close

INTERNATIONAL COUNCIL FOR RESEARCH AND INNOVATION
IN BUILDING AND CONSTRUCTION

WORKING COMMISSION W18 - TIMBER STRUCTURES

MEETING THIRTY NINE

FLORENCE, ITALY 28 TO 31 AUGUST 2006

M I N U T E S
(F Lam)

1 CHAIRMAN'S INTRODUCTION

Prof. Hans Blass welcomes the delegates to the 39th CIB W18 Meeting in Florence. Sixty delegates registered for this meeting. Ario Ceccotti is hosting the meeting for the third time in 20 years. Two of the meetings are in Florence and one in Venice.

Papers brought directly to the meeting would not be accepted for presentation, discussions, or publication. Papers presented by non-authors or non-coauthors are not recommended except in exceptional situations because the discussion process might be compromised.

The working commission format is not the same as conference meeting. The participants should take advantage of this format of questions and answers and be present in all part of the meeting. Request to move a talk to a particular time slot is not encouraged.

In total there were 31 papers. The presentations should be limited to 20 minutes with 10 minutes discussion period. Presenters were reminded that they should conclude the presentation with a general proposal or statements concerning impact of the research results on existing or future codes and standards. One of the main targets of this group is the translation of research results into design rules in codes or the development and harmonization of existing and new standards.

There were 9 topics covered in this meetings: stress grading (2 papers), stresses for solid timber (2 papers), timber joints and fasteners (6 papers), load sharing (1 paper), duration of load (1 paper), laminated members (5 papers), structural stability (4 papers), fire (3 papers), statistics and data analysis (1 paper), glued joints (2 paper), fracture mechanics (1 paper), test methods (2 papers), and loading codes (1 paper). The program again showed that the area of timber joints and fasteners has the largest research interest.

Questions on meeting proceedings should be directed at R. Görlacher. The participants were asked to check the participant address list under circulation for accuracy.

2 GENERAL TOPICS

J Ehlbeck gave a presentation on the history of CIB W18 meeting started in March 1973 in Princes Risborough in the UK. Scientists from 11 countries (AU, BR, CA, CH, DE, DK, FR, NL, NO, SE, UK, US) established this working group.

The aim of CIB W18 was to promote the exchange of scientific findings in research and development in order to create a uniform basis for guidelines for the development of material design codes and standards. John Sunley (UK) was the first chairman of the group followed by Chris Stieda (Canada) and the current Chair Hans Blass (Germany since

1992). J Ehlbeck also pointed out that the evaluation of the so called "CIB code", first discussed in 1976-1977 with a final version in 1983 (6th edition), is the basis of a draft of the Eurocode 5 and ISO standard. J Ehlbeck also thanked Ario Ceccotti for hosting the current CIB W18 meeting.

M Yasumura invited the delegates to attend the 12th World Conference in Timber Engineering WCTE in June 2008 in Miyazaki Japan.

P Lavisci informed the delegates about a future COST action entitled "Safe Timber – Safety assessment protocol for existing timber structure".

V Enjily asked if COST E34 covered the subject. P Lavisci responded that COST E34 was intended for the dissemination of ideas; therefore, these ideas were mentioned there. The proposal is to create a new group. May be CIB W18 can be the coordinator of these activities.

V Enjily suggested that this is very useful but could create difficulties for timber construction if competing material misused this information. R Marsh suggested incompetent designs would be the issues and this group could help reduce such situation. H Riberholt stated that failure investigation involving a team to study failure 1st hand would not be suitable for CIB W18. H Blass mentioned Austria, Germany and UK already had groups interested in this topic. J Köhler mentioned that there might other COST actions be interested also in this type of activities.

A Ceccotti acknowledged Prof. Uzielli for his contribution in the organization of this event and provided details about the organized activities for this meeting.

A Ceccotti presented gifts to CIB W18 members who attended the Florence meeting 20 years ago.

3 STRESS GRADING

39 - 5 - 1 A Discussion on the Control of Grading Machine Settings – Current Approach, Potential and Outlook - **J Köhler, R Steiger**

Presented by J Köhler

J Denzler asked if the alternative model was used, what could be said about the results. J Köhler responded that the paper discussed general concept of using additional information to enhance the knowledge.

H Riberholt commented that the method depended on the stability of the results, for example the material may be source dependent. J Köhler responded that the same problem existed for current method. The main assumption of the current and proposed approaches would be fairly smooth variability i.e. without large variations.

B Källsner commented that the method is interesting.

A Hanhijärvi asked if it would be possible to consider grading of graded material. J Köhler responded that the intent was not to consider grading.

V. Rajcic commented grading using Neural Network was previously considered and could be considered.

39 - 5 - 2 Tensile Proof Loading to Assure Quality of Finger-Jointed Structural timber -**R Katzengruber, G Jeitler, G Schickhofer**

Presented by R Katzengruber

JW van de Kuilen asked about the issue of influence of moisture content on the curing

time. R Katzengruber responded that the moisture content of the specimens was checked in detail and they were within expectation.

H Riberholt commented that the choice of proof stress level would be important as too high a level would lead to too many failures; therefore, the issue of how much failure would be considered acceptable in practice would be an important issue. Further discussion took place on the suitability of the grading rules in relation with the number of failures observed. As the number of failures was high, the appropriateness of the rules would be in question.

T Williamson commented that in the US finger jointed material for flange stock of I joist have been in use for over 5 years and it is an accepted practice by manufacturers.

4 STRESSES FOR SOLID TIMBER

39 - 6 - 1 Allocation of Central European hardwoods into EN 1912 - **P Glos, J K Denzler**

Presented by J Denzler

F Lam commented that in Canada when new grades containing "something and better" is considered, the relative proportion of the grade needs to be considered carefully so that it can be maintained to prevent possibility of taking some of the high grade material away. J Denzler agreed.

JW van de Kuilen received confirmation that normal distribution was used to represent MOE.

39 - 6 - 2 Revisiting EN 338 and EN 384 Basics and Procedures - **R Steiger, M Arnold, M Fontana**

Presented by R Steiger

A Ranta-Maunus commented that a Finnish paper on similar subject will be presented next year. He also asked why a code change was not proposed although the ratio between tension and bending strength were observed to be higher than assumed in the code. R Steiger answered as structural engineer, one might want to have additional safety for tension compared to bending. A Ranta-Maunus responded that safety and characteristic properties should be dealt with separately.

JW van de Kuilen received confirmation that timber density and bending strength did not show a strong relationship; therefore, the paper focused on the rest of the properties.

F Lam commented in N. American MSR material has stepped tension to bending ratios for different grades.

G Schickhofer stated that this is an important issue for glulam use also.

J Ehlbeck commented that EN338 is only used in Europe and this research focused on wood from Switzerland only. He stated that the discussion was good but cautioned that one must be careful as more information on material from different regions should be considered.

F Lam commented that ISO work on stress class led by D Barrett considered data from Europe, N. America and Australia. A paper was presented in WCTE 2006 in Portland.

P Kuklik received information that static and dynamic MOE information was available in the annex of the paper. R^2 is higher between MOE's but prediction of strength was not as good.

H Riberholt commented that the issue of tension-bending strength relationship of timber and glulam should be considered separately.

5 TIMBER JOINTS AND FASTENERS

39 - 7 - 1 Effective in-row Capacity of Multiple-Fastener Connections - **P Quenneville, M Bickerdike**

Presented by P Quenneville

H Blass asked whether the net tension failure mode in EC5 was considered in the comparison. He commented that 4d or 5d was considered in the study but EC5 only allow as low as 5d and asked whether this would influence the conclusion. P Quenneville responded that net tension was not considered as failure mode but group tear out was. Also 5d was considered within the database.

H Blass stated that load slip curve for single bolt was used in the research and asked how one knew whether this would be appropriate for a group of bolts especially when splitting initiate from a single bolt. P Quenneville replied that the use of single bolt data was an assumption but the results seemed to show that it was appropriate. I Smith suggested that the localized shear failure under the bolt may explain why it worked. He commented that P Quenneville did a lot of work to pull the various databases together.

T Williamson offered explanation why NDS on this topic is not mandatory at this point and USFPL might be doing more work on this issue.

H Riberholt asked about the influence of staggering of bolts. P Quenneville commented that these non-staggered connections are the most common; therefore, staggered system was not considered.

E Karacabeyli and P Quenneville discussed the issue of influence of density and material service condition factor.

A Jorissen questioned about the phi factor. P Quenneville explained the phi factor depended on the variability of failure load and the failure mode.

A Hanhijärvi asked about the details on the gap between the bolts and the wood. P Quenneville explained the computer model did not show dependency on the gap and load slip were treated randomly first. In the final analysis gap was set at 1.6 mm.

39 - 7 - 2 Self-tapping Screws as Reinforcements in Beam Supports - **I Bejtka, H J Blaß**

Presented by I Bejtka

K Crews asked about the thickness of the steel. I Bejtka answered that they were the same as the screw head height.

A Jorissen asked about the linear distribution of axial load. H Blass answered that the real distribution from analysis was used which looked fairly linear as shown in the ppt slide.

Jorissen asked about stiffness as E modulus and why not as a spring. I Bejtka stated that it would also be possible to use a spring.

R Marsh asked about the differences between idealized versus actual system, for example, screw head might not be flush with support in reality. H Blass responded that many test (120) were conducted in this particular issue alone.

P Quenneville asked whether the same equation could be used if a very long screw was used when applied from the top through to the support. H Blass answered that it would work provided the bottom section had the same length of screw.

JW van de Kuilen asked about the use of the screws as shear reinforcement. H Blass answered that it was tried and even at 45 degree but it did not work.

I Smith raised the issue of length of screw versus the depth of the member. I Bejtka replied that 66% was used as the ratio between screw length and timber depth.

H Riberholt asked about the influence of moisture variation. I Bejtka answered that more test would be needed.

39 - 7 - 3 Connectors for Timber-concrete Composite-Bridges - **A Döhrer, K Rautenstrauch**

Presented by A Döhrer

A Asiz asked what kind of long term tests were preformed and were corrosion tests considered. A Döhrer answered that the advantage of this system would be the protection of the connections; therefore, corrosion issue from de-icing would not be of concern.

A Ceccotti stated that in long span timber bridges the issue of differential movement from temperature would be of concern. A Döhrer answered at the span of 10 to 30 m the temperature caused movement should be acceptable.

A Frangi and A Döhrer discussed why the failure mode changed from the ductile (short term) to brittle (2 million cycles). It was the longitudinal compression of the timber that created the ductility.

K Crews commented that at long span the 3 dimensionality of the structure would become important. A Döhrer stated that there was a limitation of lab space to allow this aspect to be tested.

M Fragiacomo stated that in Colorado 20000 cycles rather than 2 million cycles were used and asked whether significant change in stiffness was observed after 2 million cycles. A Döhrer showed the results actually increased in stiffness after 2 million cycles.

39 - 7 - 4 Block Shear Failure at Dowelled Double Shear Steel-to-timber Connections - **A Hanhijärvi, A Kevarinmäki, R Yli-Koski**

Presented by A Hanhijärvi

A Jorissen wondered why values were conservative for glulam but just okay for Kerto LVL.

R Foschi wondered why the research was performed when the code was conservative and received clarification that this mode of failure was not originally considered in EC5 which led to a failure in Finland and A Hanhijärvi further responded that the comparison was focused on the Annex which is a later version of EC5.

J König commented that the designers did not use the right version.

R Foschi commented that many years ago in Canada a similar problem was experienced with glulam rivets. Block shear failure occurred with capacity of ½ of code values. This led to changes in code and increased spacing of rivets. Now both block shear and rivet yielding modes are considered in Canadian code.

J König further commented that the accuracy of manufacturing is important.

P Racher discussed the French experience on this type of connections. Designers would be working outside the code with this type of joints.

P Quenneville added that other types of steel (mild) and larger row spacing can influence the issue. A Hanhijärvi agreed that there were many possibilities. The project objectives were very specific. In Finland the steel typically had higher quality than required. There

would be a risk of bad design if one assumed mild steel.

39 - 7 - 5 *Load Carrying Capacity of Joints with Dowel Type Fasteners in Solid Wood Panels* - **T Uibel, H J Blaß**

Presented by T Uibel

A Buchanan asked about how one could account for the interlaminar slip in nail connected panels. T Uibel answered that it was not considered as glued panels were studied.

P Quenneville discussed the issue of including or exclusion of outlier for plug shear failures. H Blass answered plug shear failure did not always occur, if one took away the outliers, one would have taken away too much.

I Smith asked about shear transfer and load paths. H Blass stated that the behaviour is rather ductile with ~ 15 mm of deformation at the high load level; therefore, load path is of less significant.

J Köhler received confirmation that the load–deformation data was obtained via deformation controlled not force controlled testing and ductility can be achieved.

B Dujic asked about beams columns and moment resisting joints. H Blass stated that both tensile and moment carrying members could be used efficiently. In the tensile members, connections typically governed. Here the connection capacity was improved so this material seemed to be appropriate for a balanced capacity of joint and member.

G Schickhofer asked about other lay-ups such as 5 or 7 layers. T Uibel answered that only 5 layers were studied.

39 - 7 - 6 *Generalised Canadian Approach for Design of Connections with Dowel Fasteners* - **P Quenneville, I Smith, A Asiz, M Snow, Y H Chui**

Presented by P Quenneville

H Larsen asked how would one sell to engineers the concept that capacity would be related the G1.21. P Quenneville stated that refinements would be made.

H Blass stated for yield moment of fasteners steel values are usually minimum values. How would one obtain mean values? I smith commented that this work represented the initial step of a long process.

R Foschi stated that there was too much put on capacity. Information would be needed in the demand area where stiffness would be needed. This is especially true in earthquake engineering area. P Quenneville stated that the lateral section of the code should take care of the seismic part.

A Jorissen asked why group tear out was considered. H Blass stated that this would be an issue for structural composite material and not for timber. I Smith commented on the concept of treating splittable versus non-splittable material differently.

6 LOAD SHARING

39 - 8 -1 *Overview of a new Canadian Approach to Handling System Effects in Timber Structures* - **I Smith, Y H Chui, P Quenneville**

Presented by I Smith

H Larsen commented that it would be useful to define the terms used in the paper such as objective based design and capacity design.

A Buchanan commented that the work would require changes in people's thinking to consider things not within the code structure. He wondered whether it would turn people off timber design and put people towards the use of non timber material. I Smith responded that there would be a need to provide people with tools to make timber design more affordable.

F Lam commented about the philosophical nature of the paper without hard justification of some of the factors. I Smith responded that the paper provided a framework and if acceptable could guide future work.

H Riberholt questioned whether there were discussions of similar concept within competing material and why the member and connection resistance had such a wide separation. I Smith stated that he wanted to test the water within this group on the concept and see what would be the response. If this was not worthwhile, one would be prepared to change track. The separation of member and connection resistance distribution would not be for all situations but could be true for some cases.

J Köhler also questioned why there was such a large difference between member and connection capacity. I Smith mentioned that typically member capacity would be underutilized anyways and for some context the large separation would be valid.

R Foschi provided the following comments: in 1994 Northridge earthquake led to a large study on steel connection. US FEMA created tables for objective based design. There was a lot of talk in the way of definitions with the basic idea to design to some performance level. One would need to tell the engineer that the performance level is tied to some confidence level. Damage forecasting would be important where in Northridge US$10 billion of damage with few collapses were experienced. One would need to focus on what happened in between and not only on ultimate capacity. This would be the difficult part of the work where accurate model and data would be needed to define the entire load deformation history. This calls for a lot of good experimental work. This would be true for concrete and steel also. Then one could focus on reliability of performance. R. Foschi also provided analogy with offshore structures. In summary, he stated that we are always designing buildings. Structural System behaviour needed a lot of work. He did not agree with the statement that engineers would reject work if it was too complicated. He gave example of the Canadian experience of adopting size effect adjustment factors in the 1970's. Consulting engineers in Vancouver are doing time series analysis now but not a few years ago because of availability of fast computers and software.

P Quenneville commented that he had met with some experienced engineers on the issues of who would use system effect approach. There were two reactions 1) rejection outright and 2) if this approach gave them an advantage they would use it.

7 DURATION OF LOAD

39 - 9 - 1 *Simplified Approach for the Long-Term Behaviour of Timber-Concrete Composite Beams According to the Eurocode 5 Provisions* - **M Fragiacomo, A Ceccotti**

Presented by M Fragiacomo

A Hanhijärvi stated that the model contained a creep limit and typical experimental data did not support such a limit. He asked whether the current work had long enough time and moisture fluctuation. One might need to be careful and not to extrapolate although it might not be a problem here. Fragiacomo answered that only data were 2 tests; one in Florence (5yrs) and one in Switzerland (not more than 5 yrs). H Blass said that in Karlsruhe there

were 8 beams loaded for 6 ¼ years with different connections.

R Foschi received clarification that a component on the diffusion problem was considered to account for moisture movement in the wood as relative humidity and temperature changed.

JW van de Kuilen and M Fragiacomo discussed the issue of theoretical limit of changes of moisture content.

A Leijten commented that the EC5 creep coefficient for connection was established on the basis of political agreement not technical agreements.

8 LAMINATED MEMBERS

39 - 12 - 1 Recommended Procedures for Determination of Distribution Widths in the Design of Stress Laminated Timber Plate Decks - **K Crews**

Presented by K Crews

I Smith asked why one did not use special barrel type washers to keep the tension. K Crews stated that it was tried but get some stress losses. Variation due to seasonal changes would be more important than creep losses. One would need to design maintenance procedures to check tension periodically.

G Schickhofer and Crews discussed the issue of shear strength. K Crews stated that shear strength was not an issue unless very short span; therefore in Australia and Canada, it wasn't an issue. T Williamson asked whether FRP rod had been tried to reduce the issue of creep. Crews answered that this would be at an experimental stage. FRP strand rather than FRP rod would be considered as rods might need sophisticated anchorage system.

39 - 12 - 2 In-situ Strengthening of Timber Structures with CFRP - **K U Schober, S Franke, K Rautenstrauch**

Presented by S Franke

K Crews asked how many specimens were tested. S Franke responded that 4 very old beams were tested with debonding failure observed.

P Quenneville received confirmation that the FRP was not prestressed.

H Larsen discussed whether this type of work would be worth continuing on the basis of small gains. R Marsh suggested that the work dealt with existing structures up to 100 years old. Engineers would need guidelines to increase confidence on the performance of such structure to ascertain its engineering or economic life.

R Steiger stated that the R^2 value in figure 5 was meaningless.

L Uzielli wondered what would happen when one made a cut to insert the reinforcement when there was spiral grain. H Blass responded that it would depend on the size of t he cut and the severity of the spiral grain.

B Dujic commented on the issue of higher strength and stiffness but lower ductility would not be desirable.

T Williamson asked about glass versus carbon fibre. S Franke responded that glass fibre would be too soft and other projects have been underway.

39 - 12 - 3 Effect of Checking and Non-Glued Edge Joints on the Shear Strength of Structural Glued Laminated Timber Beams - **B Yeh, T G Williamson, Z A Martin**

Presented by B Yeh

P Quenneville asked whether the effect of checks around the neutral axis would be evaluated. B Yeh stated that it was already done. If the length of crack was too long, one would need to consult engineer to investigate; therefore, only examined the most common cases.

A Ranta-Maunus stated in Finland work was performed in similar issue for the code.

I Smith stated that critical length and real length are very different and natural versus man-made cracks are also very different.

A Leijten commented that there must be natural reasons why these cracks occurred. B Yeh confirmed that the non-glue situation was artificial and not intended for production.

F Lam asked whether the artificially induced crack would close during loading and if so friction might develop. B Yeh stated that the gaps did closed but would not expect large shear transfer.

E Karacabeyli asked if there would be guidance when one had more than one check. B Yeh answered that the neutral axis case should be governing.

J Van de Kuilen suggested the case with cracks near the support, crack near the top of the beam rather than the bottom of the beam would be more serious because of compression perpendicular to grain. B Yeh answered that the bottom of the beam would see more shear stress.

39 - 12 - 4 A Contribution to the Design and System Effect of Cross Laminated Timber (CLT) - **R A Jöbstl, T Moosbrugger, T Bogensperger, G Schickhofer**

Presented by R Jöbstl

A Leijten and R Jöbstl discussed the last formula dependency on COV and why system factors increased when COV increased and the issue of COV for tensile strength became a very important factor.

H Larsen questioned that when one set up the model, why not use the mean values rather than the characteristic values. G Schickhofer stated that this could be done.

B Dujic discussed the possible use of the CLT beam on its side and wondered if one would expect different failure mode. G Schickhofer stated that this was not known as this would be a different system and the current system behaved as a plate.

H Larsen asked how many companies would be making these members. H Blass responded that 7 or 8 German groups were making these systems and the number would increase.

H Larsen wondered would they require EU technical approval if so why these companies were not asked to develop a large database. H Blass stated one system has EU technical approval.

R Foschi asked when you tested these systems what was the failure (1st failure or sequential failures). G Schickhofer stated that it was not a brittle failure mode and sequential failures were observed. R Foschi stated this would explain why system factors would go up with larger COV same as lumber floor system.

A Buchanan asked about nailed system without glue. H Blass stated that nail system and beech dowel as connection system have been approved in Germany. Tests results were

developed but not generally available for the public.

P Quenneville asked about the 4 laminae wide versus larger number of laminae. R Jöbstl answered that it was done.

L Uzielli announced planning a new COST action on wood science concerning conservation of cultural heritage structures. The idea would be to mix structural engineering and wood science as a subject. Interested parties should contact L Uzielli directly.

39 - 12 - 5 Behaviour of Glulam in Compression Perpendicular to Grain in Different Strength Grades and Load Configurations - **M Augustin, A Ruli, R Brandner, G Schickhofer**

Presented by M Augustin

A Leijten commented that the listed references were not cited in text. He stated that when comparing Cases ABC to prismatic case, model was lacking. A model presented in past CIB W18 meeting can be used in here.

H Riberholt discussed the issue of boundary conditions of glulam used in the test. The issue of compression on both top and bottom of beam versus compression on side of beam would influence test results.

H Larsen stated the paper lacked practical implications. The paper missed mean values and COV. One would need this statistical information to assess results. It would not be appropriate if one defined compression perpendicular failure as "collapse" rather than serviceability. M Augustin received confirmation from the Chair that it would be possible to revise the paper.

G Schickhofer stated that one would need to be careful with rounded values in code.

9 STRUCTURAL STABILITY

39 - 15 - 1 Effect of Transverse Walls on Capacity of Wood-Framed Wall Diaphragms - **U A Girhammar, B Källsner**

Presented by B Källsner

H Blass asked how the capacity of the nailed connection was calculated. B Källsner answered that some old test results of similar connections were used for this paper. The work was still a preliminary evaluation and would be doing more.

B Dujic and B Källsner agreed that the influence of length of transfer wall have a limit as maximum value should be the case of fully anchored wall. Also linear beam elements would also influence the load path.

I Smith suggested the completion of the box would be of interest. B Källsner agreed that consideration of the rest of the structure would be important.

E Karacabeyli commented that two story tests without hold-down showed that they behaved well. This analytical approach offered theoretical explanation and support of the experimental results.

B Dujic commented that based on this work every wall with transverse wall can make use of the added capacity.

39 - 15 - 2 Which Seismic Behaviour Factor for Multi-Storey Buildings made of Cross-Laminated Wooden Panels? - **M Follesa, M P Lauriola, C Minowa, N Kawai, C Sandhaas, M Yasumura, A Ceccotti**

Presented by A Ceccotti

H Blass commented that the real time behaviour was better than the static behaviour.

B Dujic commented that the testing of the wall was better than the testing of the anchors. How the anchor behave is important. Two of his walls were recently tested and would present the work next week in a different meeting. He asked about the one story test where q was less than 3.

A Ceccotti stated that the nails were not randomly put. 12 nails were used in an anchor to ensure the nail and not steel failures. Also Additional story improved the behaviour.

A Buchanan stated that the strength of the wall was not chosen for seismic reason. If there were a wood failure would one worry about collapse.

A Ceccotti stated that it would be impossible in this case. The matter is not to make the wall thinner. In Italy and Central Europe people want the feel of solid wall.

I Smith stated that light frame system also behaved better than single wall but this would not be the same in the case of masonry.

F Lam asked about the rigidity of the diaphragm. A Ceccotti stated that the rigid diaphragm was assumed in the model but non rigid diaphragm was observed in test. F Lam also asked whether torsional response was observed in the tests. A Ceccotti stated that it was observed in pseudo dynamic tests but less in the shake table test.

G Schickhofer stated that in Graz a 7x7 system was tested in racking but could not destroy the wall; therefore, the wood failure would be unlikely.

R Steiger stated that in shake table test accurate reproduction of the ground acceleration would obviously be important but what about the displacement. C Minowa stated that the maximum displacement was 10 cm from the supplied record because high pass filter was originally used. In this test low pass filter was used and ~40 cm of peak ground motion was obtained on the table.

R Marsh asked about some shake table test results done in 2001 in Japan. M Yasumura has agreed to check on this.

39 - 15 - 3 Laminated Timber Frames under Dynamic Loadings - **A Heiduschke, B Kasal, P Haller**

Presented by A Heiduschke

R Steiger commented on peak ground displacement of the records (11 and 18 cm). He stated that the equation used in the calculation of period depended on damping; therefore, they were only approximate.

B Dujic commented that free displacement without resistance was shown in the hysteretic loop.

A Ceccotti asked which computer software was used. A Heiduschke answered ANSYS; therefore, simple hysteretic laws were needed.

E Karacabeyli asked would one recommend this type of frame or would one wait for bracing system wall. A Heiduschke answered as pointed out in the conclusion bracing system work would be needed.

A Leijten and A Heiduschke discussed the issue of improving structural performance by

the introduction of stronger and stiffer connections.

39 - 15 - 4 Code Provisions for Seismic Design of Multi-storey Post-tensioned Timber Buildings - **S Pampanin, A Palermo, A Buchanan, M Fragiacomo, B Deam**

Presented by A Palermo

I Smith asked about the need for shear along with moment transfer. A Palermo stated that a shear key could be used.

A Leijten received confirmation that code design recommendations would be intended for next CIB.

A Jorissen and A Palermo discussed the observed failure mode; no fatigue as the number of cycles was low.

V Rajcic and A Palermo discussed shrinkage issue for long span and how to account for loss of tension. There was agreement that more work would be needed.

10 FIRE

39 - 16 - 1 Fire Performance of FRP Reinforced Glulam - **T G Williamson, B Yeh**

Presented by T Williamson

A Buchanan asked whether steel trusses shown in the slide would have a 1 hr fire rating. T Williamson answered in US steel would be considered as non-combustible and fire rating would not be an issue for them.

A Buchanan asked whether a full or reduced design load was used in the fire test. T Williamson answered in US fire tests would be performance at full design load.

A Asiz asked about the fire rating of LVL hybrid glulam. T Williamson stated that LVL member would be typically of smaller dimension and would not seek the same level of rating. But LVL would be expected to perform similar to glulam.

H Larsen asked what would be the economy of this system and could one develop a standard for a patented producer. T Williamson explained the recent history and issues of the patented FRP glulam and that alternative patented products have been introduced into the market. The cost of glass reinforced system would be approximately 20% cheaper than normal glulam and 10% cheaper than steel. Finally ASTM standard would be focused on mechanics based model not patent specific product.

I Smith received clarification that in US only a single passing fire rating test would be required to achieve a certain target fire rating.

J König commented that it is well known that bigger beams would be needed to achieve the target fire rating. He questioned what would the strength of deeper beam be without the FRP in comparison to using the FRP reinforced deeper beam. He commented that since one would need the deeper beam anyway to achieve the fire rating why one would need the FRP.

39 - 16 - 2 An Easy-to-use Model for the Design of Wooden I-joists in Fire - **J König, B Källsner**

Presented by J König

A Frangi asked about the issue of rock fibre versus glass fibre used in the model. J König stated that the model would be okay for cavity and glass fibre would be okay if cladding was intact. After cladding failed the glass fibre performance would be compromised as the

melting point is ~ 500C. H Blass questioned that knowing rock fibre would be better why would one consider glass fibre. J König stated that glass fibre user would need the data.

B Yeh asked about the charring of web material as typical real failure mode. T Williamson stated in US insulation would typically not be provided in the cavity. J König stated that in Sweden no one would use non-insulated system because of sound transmission issue etc.

A Buchanan commented that the model required assumed knowledge of the cladding and glass performance etc which could be product manufacturer dependent. Also the model would be based on standard fire curve and questioned what about parametric fire.

J König stated that full size testing would be needed to calibrate the model. Different gypsum producers would need to provide fire test data to put in the model if they would want their product considered. Finally parametric fire would be tricky. Thermo properties of wood would only be valid for standard fire.

39 - 16 - 3 A Design Model for Timber Slabs Made of Hollow Core Elements in Fire - **A Frangi, M Fontana**

Presented by A Frangi

I Smith and A Frangi discussed the issues of passive versus active resistance in major building.

R Marsh and A Frangi discussed the need of educating insurance company about the latest developments in fire engineering of timber buildings to recognize their performance so that novel timber construction would not be penalized.

A Jorissen questioned whether glass fibre should be banned based on the results. A Frangi replied that banning a particular material would not be the issue but understanding the performance of the material would be of interest.

11 STATISTICS AND DATA ANALYSIS

39 - 17 - 1 Possible Canadian / ISO Approach to Deriving Design Values from Test Data - **I Smith, A Asiz, M Snow, Y H Chui**

Presented by A Asiz

H Larsen stated when you compared test results to theory one should use mean values. However design should not be based on mean values as coefficient of variation would come into play. I Smith answered that as long as results would be similar, it would only depend on how the format was put together. H Larsen disagreed and cited the example of structural timber having high COV compared to glulam. With characteristic values and phi approach the differences would be considered appropriately. Also his supporting document for European design code allowed mean value based test results with large penalty. Alternative approach of polled data to combine various data sets could also be used. Further discussion on the subject took place.

JW van de Kuilen stated that ISO standard on general principle of reliability assessment already existed. What the difference would be between the proposed approach and ISO standard. A Asiz stated 4 ranges of failure modes have been considered in this work.

A Ceccotti suggested that different definition of ductility to be checked. J Köhler and A Asiz discussed the approach of using the approximate formula originated in the 1970 compared to more accurate method. A Asiz stated that this approach would make it easier for engineers to use.

F Lam commented that this simplified approach has limitations because the phi formula

would be based on the assumption of lognormal distributions and we knew loads followed extreme value distribution.

12 GLUED JOINTS

39 - 18 - 1 Comparison of the Pull–out Strength of Steel Bars Glued in Glulam Elements Obtained Experimentally and Numerically - **V Rajcic, A Bjelanovic, M Rak**

Presented by V Rajcic

H Larsen discussed the principle of using glued-in rods where glue in rods should not be used unless ductile failure. In this case test data showed brittle failure. He further commented that the neural network was not verified. V Rajcic stated that the neural network approach would consider both training sample and testing set.

I Smith questioned whether these techniques should be limited to certain moisture class. V Rajcic agreed.

A Jorissen and V Rajcic discussed test setup and boundary conditions in the FEM analysis in relation to the observed failure mode.

39 - 18 - 2 The Influence of the Grading Method on the Finger Joint Bending Strength of Beech - **M Frese, H J Blaß**

Presented by M Frese

I Smith asked about the finger joint profile and whether there had been any optimization work regarding softwood versus hardwood. M Frese answered the profile was based on softwood and more work would be needed to look into the optimization for hardwood.

G Schickhofer asked about bending versus tension testing of finger joint. M Frese answered that tension tests were also performed and the data could be made available.

G Schickhofer asked whether Formula 2 can be used if no finger joint in beam. The answer was yes. One could use higher value of finger joint strength so that tensile strength of the laminae governed. There was confirmation the Formula 2 was derived based on mean test data and beams were modelled to derive characteristic strengths.

H Larsen asked why tensile tests were performed if the model did not need it. H Blass responded that it was not known prior.

13 FRACTURE MECHANICS

39 - 19 - 1 First Evaluation Steps of Design Rules in the European and German codes of Transverse Tension Areas - **S Franke, B Franke, K Rautenstrauch**

Presented by B Franke

H Blass stated that although the results showed values in the German design code to be conservative, volume effect was not considered; therefore, for larger beams this conservatism would disappear. Also S Aicher recently tested 900 mm deep beams with holes and results clearly showed a size effect.

I Smith stated that he planned to perform notch beam tests on large glulam members (7m long). I Smith commented that surface observation versus internal behaviour could be different. Even observation of behaviour on both sides show they are different.

B Franke agreed and thin cross section tended to give better results compared with thick

cross sections.

14 TEST METHODS

39 - 21 - 1 Timber Density Restrictions for Timber Connection Tests According to EN28970/ISO8970 - **A Leijten, J Köhler, A Jorissen**

Presented by A Leijten

H Blass stated that he agreed on the content of the paper; however, the reference section needed improvement. E.g. Eqn 9 was not from Ref 2 and correct paper could be downloaded from Karlsruhe homepage. He also stated that the reference list was incomplete e.g. some of the work done in Delft (Van de Kuilen's dissertation) was not referenced.

I Smith stated that work from TRADA did not show density influence within a species but between species. This was true and A Ceccotti has the report. There was discussion that within piece density variation could influence results and conclusions especially if a group of fasteners was considered rather than a single fastener.

J Köhler said that the aim of the paper was to show that although we might know the information of strength versus density, there might be inconsistency in using the results if a narrow range was considered.

H Larsen commented that code equations was based on assumption of density and strength relationship and suggested wider range should be considered.

39 - 21 - 2 The Mechanical Inconsistence in the Evaluation of the Modulus of Elasticity According to EN384 - **T Bogensperger, H Unterwieser, G Schickhofer**

Presented by T Bogensperger

A Ranta-Maunus wondered why one would need local MOE. If this was not needed, may be one could just work with global MOE with a 5% increase to make adjustment.

G Schickhofer stated that one need to repair the standard.

A Leijten asked about the background of the formula and B Källsner stated the formula originally based on low E material.

I Smith provided caution that some measurements could be subjected to 50% difference.

15 LOADING CODES

39 - 102 -1 Calibration of Partial Factors in the Danish Timber Code - **H Riberholt**

Presented by H Riberholt

I smith asked how would one know that the extreme conditions had been experienced. H Riberholt explained that the wind load several years ago was very high yet no failures were experience; therefore, one would be comfortable with the proposed reduction.

R Marsh stated that one seemed to eliminate the problem during erection. Miss erection would be more of problem. H Riberholt stated that it was assumed for timber structures that the erections were done under normal conditions. A Ranta-Maunus stated that it would be difficult to quantify effect of erection errors. H Larsen stated that control during erection should be considered separately. Larsen did not like the statement that his research demonstrated Euler column formula did not apply to timber column.

16 ANY OTHER BUSINESS

Master copy of the paper with any corrections should be send to R Görlacher at the end of September 2006. Some of the papers will be renumbered. Changes to papers only needed if errors were identified.

Photographs and participant list for 39th CIB W18 and their contact information will be available from the password protected area of the CIB W18 website.

17 VENUE AND PROGRAMME FOR NEXT MEETING

B Dujic invited the participants to attend the 40th CIB W18 meeting in Lake Bled, Slovenia 27-30 August 2007, hosted by University of Ljubljana.

The 2008 meeting will be organized by I Smith around the 3rd week of August in New Brunswick, Canada.

Discussions took place of the 2009 meeting to be organized by R Steiger in Switzerland.

A Buchanan sought feedback from the group of considering the possibility for 2010 CIB W18 meeting in New Zealand in terms of timing and distance of travel.

18 CLOSE

The chair thanked the speakers for their presentations and the delegates for their participation. Also thanks were extended to A Ceccotti and L Uzielli and their team for their efforts to organize the meeting. He also thanked F Lam for recoding the meeting minutes.

19. List of CIB-W18 Papers, Florence, Italy 2006

List of CIB-W18 Papers, Florence, Italy 2006

39 - 5 - 1 A Discussion on the Control of Grading Machine Settings – Current Approach, Potential and Outlook - **J Köhler, R Steiger**

39 - 5 - 2 Tensile Proof Loading to Assure Quality of Finger-Jointed Structural timber - **R Katzengruber, G Jeitler, G Schickhofer**

39 - 6 - 1 Allocation of Central European hardwoods into EN 1912 - **P Glos, J K Denzler**

39 - 6 - 2 Revisiting EN 338 and EN 384 Basics and Procedures - **R Steiger, M Arnold, M Fontana**

39 - 7 - 1 Effective in-row Capacity of Multiple-Fastener Connections - **P Quenneville, M Bickerdike**

39 - 7 - 2 Self-tapping Screws as Reinforcements in Beam Supports - **I Bejtka, H J Blaß**

39 - 7 - 3 Connectors for Timber-concrete Composite-Bridges - **A Döhrer, K Rautenstrauch**

39 - 7 - 4 Block Shear Failure at Dowelled Double Shear Steel-to-timber Connections - **A Hanhijärvi, A Kevarinmäki, R Yli-Koski**

39 - 7 - 5 Load Carrying Capacity of Joints with Dowel Type Fasteners in Solid Wood Panels - **T Uibel, H J Blaß**

39 - 7 - 6 Generalised Canadian Approach for Design of Connections with Dowel Fasteners - **P Quenneville, I Smith, A Asiz, M Snow, Y H Chui**

39 - 8 - 1 Overview of a new Canadian Approach to Handling System Effects in Timber Structures - **I Smith, Y H Chui, P Quenneville**

39 - 9 - 1 Simplified Approach for the Long-Term Behaviour of Timber-Concrete Composite Beams According to the Eurocode 5 Provisions - **M Fragiacomo, A Ceccotti**

39 - 12 - 1 Recommended Procedures for Determination of Distribution Widths in the Design of Stress Laminated Timber Plate Decks - **K Crews**

39 - 12 - 2 In-situ Strengthening of Timber Structures with CFRP - **K U Schober, S Franke, K Rautenstrauch**

39 - 12 - 3 Effect of Checking and Non-Glued Edge Joints on the Shear Strength of Structural Glued Laminated Timber Beams - **B Yeh, T G Williamson, Z A Martin**

39 - 12 - 4 A Contribution to the Design and System Effect of Cross Laminated Timber (CLT) - **R A Jöbstl, T Moosbrugger, T Bogensperger, G Schickhofer**

39 - 12 - 5 Behaviour of Glulam in Compression Perpendicular to Grain in Different Strength Grades and Load Configurations - **M Augustin, A Ruli, R Brandner, G Schickhofer**

20. Current List of CIB-W18(A) Papers

CURRENT LIST OF CIB-W18(A) PAPERS

Technical papers presented to CIB-W18(A) are identified by a code CIB-W18(A)/a-b-c, where:

a denotes the meeting at which the paper was presented. Meetings are classified in chronological order:

1 Princes Risborough, England; March 1973
2 Copenhagen, Denmark; October 1973
3 Delft, Netherlands; June 1974
4 Paris, France; February 1975
5 Karlsruhe, Federal Republic of Germany; October 1975
6 Aalborg, Denmark; June 1976
7 Stockholm, Sweden; February/March 1977
8 Brussels, Belgium; October 1977
9 Perth, Scotland; June 1978
10 Vancouver, Canada; August 1978
11 Vienna, Austria; March 1979
12 Bordeaux, France; October 1979
13 Otaniemi, Finland; June 1980
14 Warsaw, Poland; May 1981
15 Karlsruhe, Federal Republic of Germany; June 1982
16 Lillehammer, Norway; May/June 1983
17 Rapperswil, Switzerland; May 1984
18 Beit Oren, Israel; June 1985
19 Florence, Italy; September 1986
20 Dublin, Ireland; September 1987
21 Parksville, Canada; September 1988
22 Berlin, German Democratic Republic; September 1989
23 Lisbon, Portugal; September 1990
24 Oxford, United Kingdom; September 1991
25 Åhus, Sweden; August 1992
26 Athens, USA; August 1993
27 Sydney, Australia; July 1994
28 Copenhagen, Denmark; April 1995
29 Bordeaux, France; August 1996
30 Vancouver, Canada; August 1997
31 Savonlinna, Finland; August 1998
32 Graz, Austria, August 1999
33 Delft, The Netherlands; August 2000
34 Venice, Italy; August 2001
35 Kyoto, Japan; September 2002
36 Colorado, USA; August 2003
37 Edinburgh, Scotland, August 2004
38 Karlsruhe, Germany, August 2005
39 Florence, Italy, August 2006

b denotes the subject:

1 Limit State Design
2 Timber Columns
3 Symbols
4 Plywood
5 Stress Grading
6 Stresses for Solid Timber
7 Timber Joints and Fasteners
8 Load Sharing
9 Duration of Load
10 Timber Beams
11 Environmental Conditions
12 Laminated Members
13 Particle and Fibre Building Boards
14 Trussed Rafters
15 Structural Stability
16 Fire
17 Statistics and Data Analysis
18 Glued Joints
19 Fracture Mechanics
20 Serviceability
21 Test Methods
100 CIB Timber Code
101 Loading Codes
102 Structural Design Codes
103 International Standards Organisation
104 Joint Committee on Structural Safety
105 CIB Programme, Policy and Meetings
106 International Union of Forestry Research Organisations

c is simply a number given to the papers in the order in which they appear:

Example: CIB-W18/4-102-5 refers to paper 5 on subject 102 presented at the fourth meeting of W18.

Listed below, by subjects, are all papers that have to date been presented to W18. When appropriate some papers are listed under more than one subject heading.

LIMIT STATE DESIGN

1-1-1	Limit State Design - H J Larsen
1-1-2	The Use of Partial Safety Factors in the New Norwegian Design Code for Timber Structures - O Brynildsen
1-1-3	Swedish Code Revision Concerning Timber Structures - B Noren
1-1-4	Working Stresses Report to British Standards Institution Committee BLCP/17/2
6-1-1	On the Application of the Uncertainty Theoretical Methods for the Definition of the Fundamental Concepts of Structural Safety - K Skov and O Ditlevsen
11-1-1	Safety Design of Timber Structures - H J Larsen
18-1-1	Notes on the Development of a UK Limit States Design Code for Timber - A R Fewell and C B Pierce
18-1-2	Eurocode 5, Timber Structures - H J Larsen
19-1-1	Duration of Load Effects and Reliability Based Design (Single Member) - R O Foschi and Z C Yao
21-102-1	Research Activities Towards a New GDR Timber Design Code Based on Limit States Design - W Rug and M Badstube
22-1-1	Reliability-Theoretical Investigation into Timber Components Proposal for a Supplement of the Design Concept - M Badstube, W Rug and R Plessow
23-1-1	Some Remarks about the Safety of Timber Structures - J Kuipers
23-1-2	Reliability of Wood Structural Elements: A Probabilistic Method to Eurocode 5 Calibration - F Rouger, N Lheritier, P Racher and M Fogli
31-1-1	A Limit States Design Approach to Timber Framed Walls - C J Mettem, R Bainbridge and J A Gordon
32 -1-1	Determination of Partial Coefficients and Modification Factors- H J Larsen, S Svensson and S Thelandersson
32 -1-2	Design by Testing of Structural Timber Components - V Enjily and L Whale
33-1-1	Aspects on Reliability Calibration of Safety Factors for Timber Structures – S Svensson and S Thelandersson
33-1-2	Sensitivity studies on the reliability of timber structures – A Ranta-Maunus, M Fonselius, J Kurkela and T Toratti

TIMBER COLUMNS

2-2-1	The Design of Solid Timber Columns - H J Larsen
3-2-1	The Design of Built-Up Timber Columns - H J Larsen
4-2-1	Tests with Centrally Loaded Timber Columns - H J Larsen and S S Pedersen
4-2-2	Lateral-Torsional Buckling of Eccentrically Loaded Timber Columns- B Johansson
5-9-1	Strength of a Wood Column in Combined Compression and Bending with Respect to Creep - B Källsner and B Norén
5-100-1	Design of Solid Timber Columns (First Draft) - H J Larsen
6-100-1	Comments on Document 5-100-1, Design of Solid Timber Columns - H J Larsen and E Theilgaard
6-2-1	Lattice Columns - H J Larsen
6-2-2	A Mathematical Basis for Design Aids for Timber Columns - H J Burgess
6-2-3	Comparison of Larsen and Perry Formulas for Solid Timber Columns- H J Burgess

7-2-1	Lateral Bracing of Timber Struts - J A Simon
8-15-1	Laterally Loaded Timber Columns: Tests and Theory - H J Larsen
17-2-1	Model for Timber Strength under Axial Load and Moment - T Poutanen
18-2-1	Column Design Methods for Timber Engineering - A H Buchanan, K C Johns, B Madsen
19-2-1	Creep Buckling Strength of Timber Beams and Columns - R H Leicester
19-12-2	Strength Model for Glulam Columns - H J Blaß
20-2-1	Lateral Buckling Theory for Rectangular Section Deep Beam-Columns- H J Burgess
20-2-2	Design of Timber Columns - H J Blaß
21-2-1	Format for Buckling Strength - R H Leicester
21-2-2	Beam-Column Formulae for Design Codes - R H Leicester
21-15-1	Rectangular Section Deep Beam - Columns with Continuous Lateral Restraint - H J Burgess
21-15-2	Buckling Modes and Permissible Axial Loads for Continuously Braced Columns - H J Burgess
21-15-3	Simple Approaches for Column Bracing Calculations - H J Burgess
21-15-4	Calculations for Discrete Column Restraints - H J Burgess
22-2-1	Buckling and Reliability Checking of Timber Columns - S Huang, P M Yu and J Y Hong
22-2-2	Proposal for the Design of Compressed Timber Members by Adopting the Second-Order Stress Theory - P Kaiser
30-2-1	Beam-Column Formula for Specific Truss Applications - W Lau, F Lam and J D Barrett
31-2-1	Deformation and Stability of Columns of Viscoelastic Material Wood - P Becker and K Rautenstrauch
34-2-1	Long-Term Experiments with Columns: Results and Possible Consequences on Column Design – W Moorkamp, W Schelling, P Becker, K Rautenstrauch
34-2-2	Proposal for Compressive Member Design Based on Long-Term Simulation Studies – P Becker, K Rautenstrauch
35-2-1	Computer Simulations on the Reliability of Timber Columns Regarding Hygrothermal Effects- R Hartnack, K-U Schober, K Rautenstrauch
36-2-1	The Reliability of Timber Columns Based on Stochastical Principles - K Rautenstrauch, R Hartnack
38-2-1	Long-term Load Bearing of Wooden Columns Influenced by Climate – View on Code - R Hartnack, K Rautenstrauch

SYMBOLS

3-3-1	Symbols for Structural Timber Design - J Kuipers and B Norén
4-3-1	Symbols for Timber Structure Design - J Kuipers and B Norén
28-3-1	Symbols for Timber and Wood-Based Materials - J Kuipers and B Noren
1	Symbols for Use in Structural Timber Design

PLYWOOD

2-4-1	The Presentation of Structural Design Data for Plywood - L G Booth

3-4-1	Standard Methods of Testing for the Determination of Mechanical Properties of Plywood - J Kuipers
3-4-2	Bending Strength and Stiffness of Multiple Species Plywood - C K A Stieda
4-4-4	Standard Methods of Testing for the Determination of Mechanical Properties of Plywood - Council of Forest Industries, B.C.
5-4-1	The Determination of Design Stresses for Plywood in the Revision of CP 112 - L G Booth
5-4-2	Veneer Plywood for Construction - Quality Specifications - ISO/TC 139. Plywood, Working Group 6
6-4-1	The Determination of the Mechanical Properties of Plywood Containing Defects - L G Booth
6-4-2	Comparsion of the Size and Type of Specimen and Type of Test on Plywood Bending Strength and Stiffness - C R Wilson and P Eng
6-4-3	Buckling Strength of Plywood: Results of Tests and Recommendations for Calculations - J Kuipers and H Ploos van Amstel
7-4-1	Methods of Test for the Determination of Mechanical Properties of Plywood - L G Booth, J Kuipers, B Norén, C R Wilson
7-4-2	Comments Received on Paper 7-4-1
7-4-3	The Effect of Rate of Testing Speed on the Ultimate Tensile Stress of Plywood - C R Wilson and A V Parasin
7-4-4	Comparison of the Effect of Specimen Size on the Flexural Properties of Plywood Using the Pure Moment Test - C R Wilson and A V Parasin
8-4-1	Sampling Plywood and the Evaluation of Test Results - B Norén
9-4-1	Shear and Torsional Rigidity of Plywood - H J Larsen
9-4-2	The Evaluation of Test Data on the Strength Properties of Plywood - L G Booth
9-4-3	The Sampling of Plywood and the Derivation of Strength Values (Second Draft) - B Norén
9-4-4	On the Use of the CIB/RILEM Plywood Plate Twisting Test: a progress report - L G Booth
10-4-1	Buckling Strength of Plywood - J Dekker, J Kuipers and H Ploos van Amstel
11-4-1	Analysis of Plywood Stressed Skin Panels with Rigid or Semi-Rigid Connections- I Smith
11-4-2	A Comparison of Plywood Modulus of Rigidity Determined by the ASTM and RILEM CIB/3-TT Test Methods - C R Wilson and A V Parasin
11-4-3	Sampling of Plywood for Testing Strength - B Norén
12-4-1	Procedures for Analysis of Plywood Test Data and Determination of Characteristic Values Suitable for Code Presentation - C R Wilson
14-4-1	An Introduction to Performance Standards for Wood-base Panel Products - D H Brown
14-4-2	Proposal for Presenting Data on the Properties of Structural Panels - T Schmidt
16-4-1	Planar Shear Capacity of Plywood in Bending - C K A Stieda
17-4-1	Determination of Panel Shear Strength and Panel Shear Modulus of Beech-Plywood in Structural Sizes - J Ehlbeck and F Colling
17-4-2	Ultimate Strength of Plywood Webs - R H Leicester and L Pham
20-4-1	Considerations of Reliability - Based Design for Structural Composite Products - M R O'Halloran, J A Johnson, E G Elias and T P Cunningham

21-4-1 Modelling for Prediction of Strength of Veneer Having Knots - Y Hirashima

22-4-1 Scientific Research into Plywood and Plywood Building Constructions the Results and Findings of which are Incorporated into Construction Standard Specifications of the USSR - I M Guskov

22-4-2 Evaluation of Characteristic values for Wood-Based Sheet Materials - E G Elias

24-4-1 APA Structural-Use Design Values: An Update to Panel Design Capacities - A L Kuchar, E G Elias, B Yeh and M R O'Halloran

STRESS GRADING

1-5-1 Quality Specifications for Sawn Timber and Precision Timber - Norwegian Standard NS 3080

1-5-2 Specification for Timber Grades for Structural Use - British Standard BS 4978

4-5-1 Draft Proposal for an International Standard for Stress Grading Coniferous Sawn Softwood - ECE Timber Committee

16-5-1 Grading Errors in Practice - B Thunell

16-5-2 On the Effect of Measurement Errors when Grading Structural Timber- L Nordberg and B Thunell

19-5-1 Stress-Grading by ECE Standards of Italian-Grown Douglas-Fir Dimension Lumber from Young Thinnings - L Uzielli

19-5-2 Structural Softwood from Afforestation Regions in Western Norway - R Lackner

21-5-1 Non-Destructive Test by Frequency of Full Size Timber for Grading - T Nakai

22-5-1 Fundamental Vibration Frequency as a Parameter for Grading Sawn Timber - T Nakai, T Tanaka and H Nagao

24-5-1 Influence of Stress Grading System on Length Effect Factors for Lumber Loaded in Compression - A Campos and I Smith

26-5-1 Structural Properties of French Grown Timber According to Various Grading Methods - F Rouger, C De Lafond and A El Quadrani

28-5-1 Grading Methods for Structural Timber - Principles for Approval - S Ohlsson

28-5-2 Relationship of Moduli of Elasticity in Tension and in Bending of Solid Timber - N Burger and P Glos

29-5-1 The Effect of Edge Knots on the Strength of SPF MSR Lumber - T Courchene, F Lam and J D Barrett

29-5-2 Determination of Moment Configuration Factors using Grading Machine Readings - T D G Canisius and T Isaksson

31-5-1 Influence of Varying Growth Characteristics on Stiffness Grading of Structural Timber - S Ormarsson, H Petersson, O Dahlblom and K Persson

31-5-2 A Comparison of In-Grade Test Procedures - R H Leicester, H Breitinger and H Fordham

32-5-1 Actual Possibilities of the Machine Grading of Timber - K Frühwald and A Bernasconi

32-5-2 Detection of Severe Timber Defects by Machine Grading - A Bernasconi, L Boström and B Schacht

34-5-1 Influence of Proof Loading on the Reliability of Members – F Lam, S Abayakoon, S Svensson, C Gyamfi

36-5-1 Settings for Strength Grading Machines – Evaluation of the Procedure according to prEN 14081, part 2 - C Bengtsson, M Fonselius

36-5-2 A Probabilistic Approach to Cost Optimal Timber Grading - J Köhler, M H Faber

36-7-11 Reliability of Timber Structures, Theory and Dowel-Type Connection Failures - A Ranta-Maunus, A Kevarinmäki

38-5-1 Are Wind-Induced Compression Failures Grading Relevant - M Arnold, R Steiger

39-5-1 A Discussion on the Control of Grading Machine Settings – Current Approach, Potential and Outlook - J Köhler, R Steiger

39-5-2 Tensile Proof Loading to Assure Quality of Finger-Jointed Structural timber - R Katzengruber, G Jeitler, G Schickhofer

STRESSES FOR SOLID TIMBER

4-6-1 Derivation of Grade Stresses for Timber in the UK - W T Curry

5-6-1 Standard Methods of Test for Determining some Physical and Mechanical Properties of Timber in Structural Sizes - W T Curry

5-6-2 The Description of Timber Strength Data - J R Tory

5-6-3 Stresses for EC1 and EC2 Stress Grades - J R Tory

6-6-1 Standard Methods of Test for the Determination of some Physical and Mechanical Properties of Timber in Structural Sizes (third draft) - W T Curry

7-6-1 Strength and Long-term Behaviour of Lumber and Glued Laminated Timber under Torsion Loads - K Möhler

9-6-1 Classification of Structural Timber - H J Larsen

9-6-2 Code Rules for Tension Perpendicular to Grain - H J Larsen

9-6-3 Tension at an Angle to the Grain - K Möhler

9-6-4 Consideration of Combined Stresses for Lumber and Glued Laminated Timber - K Möhler

11-6-1 Evaluation of Lumber Properties in the United States - W L Galligan and J H Haskell

11-6-2 Stresses Perpendicular to Grain - K Möhler

11-6-3 Consideration of Combined Stresses for Lumber and Glued Laminated Timber (addition to Paper CIB-W18/9-6-4) - K Möhler

12-6-1 Strength Classifications for Timber Engineering Codes - R H Leicester and W G Keating

12-6-2 Strength Classes for British Standard BS 5268 - J R Tory

13-6-1 Strength Classes for the CIB Code - J R Tory

13-6-2 Consideration of Size Effects and Longitudinal Shear Strength for Uncracked Beams - R O Foschi and J D Barrett

13-6-3 Consideration of Shear Strength on End-Cracked Beams - J D Barrett and R O Foschi

15-6-1 Characteristic Strength Values for the ECE Standard for Timber - J G Sunley

16-6-1 Size Factors for Timber Bending and Tension Stresses - A R Fewell

16-6-2 Strength Classes for International Codes - A R Fewell and J G Sunley

17-6-1 The Determination of Grade Stresses from Characteristic Stresses for BS 5268: Part 2 - A R Fewell

17-6-2 The Determination of Softwood Strength Properties for Grades, Strength Classes and Laminated Timber for BS 5268: Part 2 - A R Fewell

18-6-1 Comment on Papers: 18-6-2 and 18-6-3 - R H Leicester

18-6-2 Configuration Factors for the Bending Strength of Timber - R H Leicester

18-6-3	Notes on Sampling Factors for Characteristic Values - R H Leicester
18-6-4	Size Effects in Timber Explained by a Modified Weakest Link Theory- B Madsen and A H Buchanan
18-6-5	Placement and Selection of Growth Defects in Test Specimens - H Riberholt
18-6-6	Partial Safety-Coefficients for the Load-Carrying Capacity of Timber Structures - B Norén and J-0 Nylander
19-6-1	Effect of Age and/or Load on Timber Strength - J Kuipers
19-6-2	Confidence in Estimates of Characteristic Values - R H Leicester
19-6-3	Fracture Toughness of Wood - Mode I - K Wright and M Fonselius
19-6-4	Fracture Toughness of Pine - Mode II - K Wright
19-6-5	Drying Stresses in Round Timber - A Ranta-Maunus
19-6-6	A Dynamic Method for Determining Elastic Properties of Wood - R Görlacher
20-6-1	A Comparative Investigation of the Engineering Properties of "Whitewoods" Imported to Israel from Various Origins - U Korin
20-6-2	Effects of Yield Class, Tree Section, Forest and Size on Strength of Home Grown Sitka Spruce - V Picardo
20-6-3	Determination of Shear Strength and Strength Perpendicular to Grain - H J Larsen
21-6-1	Draft Australian Standard: Methods for Evaluation of Strength and Stiffness of Graded Timber - R H Leicester
21-6-2	The Determination of Characteristic Strength Values for Stress Grades of Structural Timber. Part 1 - A R Fewell and P Glos
21-6-3	Shear Strength in Bending of Timber - U Korin
22-6-1	Size Effects and Property Relationships for Canadian 2-inch Dimension Lumber - J D Barrett and H Griffin
22-6-2	Moisture Content Adjustements for In-Grade Data - J D Barrett and W Lau
22-6-3	A Discussion of Lumber Property Relationships in Eurocode 5 - D W Green and D E Kretschmann
22-6-4	Effect of Wood Preservatives on the Strength Properties of Wood - F Ronai
23-6-1	Timber in Compression Perpendicular to Grain - U Korin
24-6-1	Discussion of the Failure Criterion for Combined Bending and Compression - T A C M van der Put
24-6-3	Effect of Within Member Variability on Bending Strength of Structural Timber - I Czmoch, S Thelandersson and H J Larsen
24-6-4	Protection of Structural Timber Against Fungal Attack Requirements and Testing- K Jaworska, M Rylko and W Nozynski
24-6-5	Derivation of the Characteristic Bending Strength of Solid Timber According to CEN-Document prEN 384 - A J M Leijten
25-6-1	Moment Configuration Factors for Simple Beams- T D G Canisius
25-6-3	Bearing Capacity of Timber - U Korin
25-6-4	On Design Criteria for Tension Perpendicular to Grain - H Petersson
25-6-5	Size Effects in Visually Graded Softwood Structural Lumber - J D Barrett, F Lam and W Lau
26-6-1	Discussion and Proposal of a General Failure Criterion for Wood - T A C M van der Put

27-6-1	Development of the "Critical Bearing": Design Clause in CSA-086.1 - C Lum and E Karacabeyli
27-6-2	Size Effects in Timber: Novelty Never Ends - F Rouger and T Fewell
27-6-3	Comparison of Full-Size Sugi (Cryptomeria japonica D.Don) Structural Performance in Bending of Round Timber, Two Surfaces Sawn Timber and Square Sawn Timber - T Nakai, H Nagao and T Tanaka
28-6-1	Shear Strength of Canadian Softwood Structural Lumber - F Lam, H Yee and J D Barrett
28-6-2	Shear Strength of Douglas Fir Timbers - B Madsen
28-6-3	On the Influence of the Loading Head Profiles on Determined Bending Strength - L Muszyñsky and R Szukala
28-6-4	Effect of Test Standard, Length and Load Configuration on Bending Strength of Structural Timber- T Isaksson and S Thelandersson
28-6-5	Grading Machine Readings and their Use in the Calculation of Moment Configuration Factors - T Canisius, T Isaksson and S Thelandersson
28-6-6	End Conditions for Tension Testing of Solid Timber Perpendicular to Grain - T Canisius
29-6-1	Effect of Size on Tensile Strength of Timber - N Burger and P Glos
29-6-2	Equivalence of In-Grade Testing Standards - R H Leicester, H O Breitinger and H F Fordham
30-6-1	Strength Relationships in Structural Timber Subjected to Bending and Tension - N Burger and P Glos
30-6-2	Characteristic Design Stresses in Tension for Radiata Pine Grown in Canterbury - A Tsehaye, J C F Walker and A H Buchanan
30-6-3	Timber as a Natural Composite: Explanation of Some Peculiarities in the Mechanical Behaviour - E Gehri
31-6-1	Length and Moment Configuration Factors - T Isaksson
31-6-2	Tensile Strength Perpendicular to Grain According to EN 1193 - H J Blaß and M Schmid
31-6-3	Strength of Small Diameter Round Timber - A Ranta-Maunus, U Saarelainen and H Boren
31-6-4	Compression Strength Perpendicular to Grain of Structural Timber and Glulam - L Damkilde, P Hoffmeyer and T N Pedersen
31-6-5	Bearing Strength of Timber Beams - R H Leicester, H Fordham and H Breitinger
32-6-1	Development of High-Resistance Glued Robinia Products and an Attempt to Assign Such Products to the European System of Strength Classes - G Schickhofer and B Obermayr
32-6-2	Length and Load Configuration Effects in the Code Format - T Isaksson
32-6-3	Length Effect on the Tensile Strength of Truss Chord Members - F Lam
32-6-4	Tensile Strength Perpendicular to Grain of Glued Laminated Timber - H J Blaß and M Schmid
32-6-5	On the Reliability-based Strength Adjustment Factors for Timber Design - T D G Canisius
34-6-1	Material Strength Properties for Canadian Species Used in Japanese Post and Beam Construction - J D Barrett, F Lam, S Nakajima
35-6-1	Evaluation of Different Size Effect Models for Tension Perpendicular to Grain Design - S Aicher, G Dill-Langer

35-6-2 Tensile Strength of Glulam Perpendicular to Grain - Effects of Moisture Gradients - J Jönsson, S Thelandersson

36-6-1 Characteristic Shear Strength Values Based on Tests According to EN 1193 - P Glos, J Denzler

37-6-1 Tensile Strength of Nordic Birch - K H Solli

37-6-2 Effect of Test Piece Orientation on Characteristic Bending Strength of Structural Timber - P Glos, J K Denzler

37-6-3 Strength and Stiffness Behaviour of Beech Laminations for High Strength Glulam - P Glos, J K Denzler, P W Linsenmann

37-6-4 A Review of Existing Standards Related to Calculation of Characteristic Values of Timber - F Rouger

37-6-5 Influence of the Rolling-Shear Modulus on the Strength and Stiffness of Structural Bonded Timber Elements - P Fellmoser, H J Blass

38-6-1 Design Specifications for Notched Beams in AS:1720 - R H Leicester

38-6-2 Characteristic Bending Strength of Beech Glulam - H J Blaß, M Frese

38-6-3 Shear Strength of Glued Laminated Timber - H Klapp, H Brüninghoff

39-6-1 Allocation of Central European hardwoods into EN 1912 - P Glos, J K Denzler

39-6-2 Revisiting EN 338 and EN 384 Basics and Procedures - R Steiger, M Arnold, M Fontana

TIMBER JOINTS AND FASTENERS

1-7-1 Mechanical Fasteners and Fastenings in Timber Structures - E G Stern

4-7-1 Proposal for a Basic Test Method for the Evaluation of Structural Timber Joints with Mechanical Fasteners and Connectors - RILEM 3TT Committee

4-7-2 Test Methods for Wood Fasteners - K Möhler

5-7-1 Influence of Loading Procedure on Strength and Slip-Behaviour in Testing Timber Joints - K Möhler

5-7-2 Recommendations for Testing Methods for Joints with Mechanical Fasteners and Connectors in Load-Bearing Timber Structures - RILEM 3 TT Committee

5-7-3 CIB-Recommendations for the Evaluation of Results of Tests on Joints with Mechanical Fasteners and Connectors used in Load-Bearing Timber Structures - J Kuipers

6-7-1 Recommendations for Testing Methods for Joints with Mechanical Fasteners and Connectors in Load-Bearing Timber Structures (seventh draft) - RILEM 3 TT Committee

6-7-2 Proposal for Testing Integral Nail Plates as Timber Joints - K Möhler

6-7-3 Rules for Evaluation of Values of Strength and Deformation from Test Results - Mechanical Timber Joints - M Johansen, J Kuipers, B Norén

6-7-4 Comments to Rules for Testing Timber Joints and Derivation of Characteristic Values for Rigidity and Strength - B Norén

7-7-1 Testing of Integral Nail Plates as Timber Joints - K Möhler

7-7-2 Long Duration Tests on Timber Joints - J Kuipers

7-7-3 Tests with Mechanically Jointed Beams with a Varying Spacing of Fasteners - K Möhler

7-100-1 CIB-Timber Code Chapter 5.3 Mechanical Fasteners;CIB-Timber Standard 06 and 07 - H J Larsen

9-7-1 Design of Truss Plate Joints - F J Keenan

9-7-2 Staples - K Möhler

11-7-1	A Draft Proposal for International Standard: ISO Document ISO/TC 165N 38E
12-7-1	Load-Carrying Capacity and Deformation Characteristics of Nailed Joints - J Ehlbeck
12-7-2	Design of Bolted Joints - H J Larsen
12-7-3	Design of Joints with Nail Plates - B Norén
13-7-1	Polish Standard BN-80/7159-04: Parts 00-01-02-03-04-05. "Structures from Wood and Wood-based Materials. Methods of Test and Strength Criteria for Joints with Mechanical Fasteners"
13-7-2	Investigation of the Effect of Number of Nails in a Joint on its Load Carrying Ability - W Nozynski
13-7-3	International Acceptance of Manufacture, Marking and Control of Finger-jointed Structural Timber - B Norén
13-7-4	Design of Joints with Nail Plates - Calculation of Slip - B Norén
13-7-5	Design of Joints with Nail Plates - The Heel Joint - B Källsner
13-7-6	Nail Deflection Data for Design - H J Burgess
13-7-7	Test on Bolted Joints - P Vermeyden
13-7-8	Comments to paper CIB-W18/12-7-3 "Design of Joints with Nail Plates"- B Norén
13-7-9	Strength of Finger Joints - H J Larsen
13-100-4	CIB Structural Timber Design Code. Proposal for Section 6.1.5 Nail Plates - N I Bovim
14-7-1	Design of Joints with Nail Plates (second edition) - B Norén
14-7-2	Method of Testing Nails in Wood (second draft, August 1980) - B Norén
14-7-3	Load-Slip Relationship of Nailed Joints - J Ehlbeck and H J Larsen
14-7-4	Wood Failure in Joints with Nail Plates - B Norén
14-7-5	The Effect of Support Eccentricity on the Design of W- and WW-Trussed with Nail Plate Connectors - B Källsner
14-7-6	Derivation of the Allowable Load in Case of Nail Plate Joints Perpendicular to Grain - K Möhler
14-7-7	Comments on CIB-W18/14-7-1 - T A C M van der Put
15-7-1	Final Recommendation TT-1A: Testing Methods for Joints with Mechanical Fasteners in Load-Bearing Timber Structures. Annex A Punched Metal Plate Fasteners - Joint Committee RILEM/CIB-3TT
16-7-1	Load Carrying Capacity of Dowels - E Gehri
16-7-2	Bolted Timber Joints: A Literature Survey - N Harding
16-7-3	Bolted Timber Joints: Practical Aspects of Construction and Design; a Survey - N Harding
16-7-4	Bolted Timber Joints: Draft Experimental Work Plan - Building Research Association of New Zealand
17-7-1	Mechanical Properties of Nails and their Influence on Mechanical Properties of Nailed Timber Joints Subjected to Lateral Loads - I Smith, L R J Whale, C Anderson and L Held
17-7-2	Notes on the Effective Number of Dowels and Nails in Timber Joints - G Steck
18-7-1	Model Specification for Driven Fasteners for Assembly of Pallets and Related Structures - E G Stern and W B Wallin

18-7-2	The Influence of the Orientation of Mechanical Joints on their Mechanical Properties - I Smith and L R J Whale
18-7-3	Influence of Number of Rows of Fasteners or Connectors upon the Ultimate Capacity of Axially Loaded Timber Joints - I Smith and G Steck
18-7-4	A Detailed Testing Method for Nailplate Joints - J Kangas
18-7-5	Principles for Design Values of Nailplates in Finland - J Kangas
18-7-6	The Strength of Nailplates - N I Bovim and E Aasheim
19-7-1	Behaviour of Nailed and Bolted Joints under Short-Term Lateral Load - Conclusions from Some Recent Research - L R J Whale, I Smith and B O Hilson
19-7-2	Glued Bolts in Glulam - H Riberholt
19-7-3	Effectiveness of Multiple Fastener Joints According to National Codes and Eurocode 5 (Draft) - G Steck
19-7-4	The Prediction of the Long-Term Load Carrying Capacity of Joints in Wood Structures - Y M Ivanov and Y Y Slavic
19-7-5	Slip in Joints under Long-Term Loading - T Feldborg and M Johansen
19-7-6	The Derivation of Design Clauses for Nailed and Bolted Joints in Eurocode 5 - L R J Whale and I Smith
19-7-7	Design of Joints with Nail Plates - Principles - B Norén
19-7-8	Shear Tests for Nail Plates - B Norén
19-7-9	Advances in Technology of Joints for Laminated Timber - Analyses of the Structural Behaviour - M Piazza and G Turrini
19-15-1	Connections Deformability in Timber Structures: A Theoretical Evaluation of its Influence on Seismic Effects - A Ceccotti and A Vignoli
20-7-1	Design of Nailed and Bolted Joints-Proposals for the Revision of Existing Formulae in Draft Eurocode 5 and the CIB Code - L R J Whale, I Smith and H J Larsen
20-7-2	Slip in Joints under Long Term Loading - T Feldborg and M Johansen
20-7-3	Ultimate Properties of Bolted Joints in Glued-Laminated Timber - M Yasumura, T Murota and H Sakai
20-7-4	Modelling the Load-Deformation Behaviour of Connections with Pin-Type Fasteners under Combined Moment, Thrust and Shear Forces - I Smith
21-7-1	Nails under Long-Term Withdrawal Loading - T Feldborg and M Johansen
21-7-2	Glued Bolts in Glulam-Proposals for CIB Code - H Riberholt
21-7-3	Nail Plate Joint Behaviour under Shear Loading - T Poutanen
21-7-4	Design of Joints with Laterally Loaded Dowels. Proposals for Improving the Design Rules in the CIB Code and the Draft Eurocode 5 - J Ehlbeck and H Werner
21-7-5	Axially Loaded Nails: Proposals for a Supplement to the CIB Code - J Ehlbeck and W Siebert
22-7-1	End Grain Connections with Laterally Loaded Steel Bolts A draft proposal for design rules in the CIB Code - J Ehlbeck and M Gerold
22-7-2	Determination of Perpendicular-to-Grain Tensile Stresses in Joints with Dowel-Type Fasteners - A draft proposal for design rules - J Ehlbeck, R Görlacher and H Werner
22-7-3	Design of Double-Shear Joints with Non-Metallic Dowels A proposal for a supplement of the design concept - J Ehlbeck and O Eberhart
22-7-4	The Effect of Load on Strength of Timber Joints at high Working Load Level - A J M Leijten

22-7-5	Plasticity Requirements for Portal Frame Corners - R Gunnewijk and A J M Leijten
22-7-6	Background Information on Design of Glulam Rivet Connections in CSA/CAN3-086.1-M89 - A proposal for a supplement of the design concept - E Karacabeyli and D P Janssens
22-7-7	Mechanical Properties of Joints in Glued-Laminated Beams under Reversed Cyclic Loading - M Yasumura
22-7-8	Strength of Glued Lap Timber Joints - P Glos and H Horstmann
22-7-9	Toothed Rings Type Bistyp 075 at the Joints of Fir Wood - J Kerste
22-7-10	Calculation of Joints and Fastenings as Compared with the International State - K Zimmer and K Lissner
22-7-11	Joints on Glued-in Steel Bars Present Relatively New and Progressive Solution in Terms of Timber Structure Design - G N Zubarev, F A Boitemirov and V M Golovina
22-7-12	The Development of Design Codes for Timber Structures made of Compositive Bars with Plate Joints based on Cyclindrical Nails - Y V Piskunov
22-7-13	Designing of Glued Wood Structures Joints on Glued-in Bars - S B Turkovsky
23-7-1	Proposal for a Design Code for Nail Plates - E Aasheim and K H Solli
23-7-2	Load Distribution in Nailed Joints - H J Blass
24-7-1	Theoretical and Experimental Tension and Shear Capacity of Nail Plate Connections - B Källsner and J Kangas
24-7-2	Testing Method and Determination of Basic Working Loads for Timber Joints with Mechanical Fasteners - Y Hirashima and F Kamiya
24-7-3	Anchorage Capacity of Nail Plate - J Kangas
25-7-2	Softwood and Hardwood Embedding Strength for Dowel type Fasteners - J Ehlbeck and H Werner
25-7-4	A Guide for Application of Quality Indexes for Driven Fasteners Used in Connections in Wood Structures - E G Stern
25-7-5	35 Years of Experience with Certain Types of Connectors and Connector Plates Used for the Assembly of Wood Structures and their Components- E G Stern
25-7-6	Characteristic Strength of Split-ring and Shear-plate Connections - H J Blass, J Ehlbeck and M Schlager
25-7-7	Characteristic Strength of Tooth-plate Connector Joints - H J Blass, J Ehlbeck and M Schlager
25-7-8	Extending Yield Theory to Screw Connections - T E McLain
25-7-9	Determination of k_{def} for Nailed Joints - J W G van de Kuilen
25-7-10	Characteristic Strength of UK Timber Connectors - A V Page and C J Mettem
25-7-11	Multiple-fastener Dowel-type Joints, a Selected Review of Research and Codes - C J Mettem and A V Page
25-7-12	Load Distributions in Multiple-fastener Bolted Joints in European Whitewood Glulam, with Steel Side Plates - C J Mettem and A V Page
26-7-1	Proposed Test Method for Dynamic Properties of Connections Assembled with Mechanical Fasteners - J D Dolan
26-7-2	Validatory Tests and Proposed Design Formulae for the Load-Carrying Capacity of Toothed-Plate Connectored Joints - C J Mettem, A V Page and G Davis
26-7-3	Definitions of Terms and Multi-Language Terminology Pertaining to Metal Connector Plates - E G Stern

26-7-4 Design of Joints Based on in V-Shape Glued-in Rods - J Kangas

26-7-5 Tests on Timber Concrete Composite Structural Elements (TCCs) - A U Meierhofer

27-7-1 Glulam Arch Bridge and Design of it's Moment-Resisting Joints - K Komatsu and S Usuku

27-7-2 Characteristic Load - Carrying Capacity of Joints with Dowel - type Fasteners in Regard to the System Properties - H Werner

27-7-3 Steel Failure Design in Truss Plate Joints - T Poutanen

28-7-1 Expanded Tube Joint in Locally DP Reinforced Timber - A J M Leijten, P Ragupathy and K S Virdi

28-7-2 A Strength and Stiffness Model for the Expanded Tube Joint - A J M Leijten

28-7-3 Load-carrying Capacity of Steel-to Timber Joints with Annular Ring Shanked Nails. A Comparison with the EC5 Design Method - R Görlacher

28-7-4 Dynamic Effects on Metal-Plate Connected Wood Truss Joints - S Kent, R Gupta and T Miller

28-7-5 Failure of the Timber Bolted Joints Subjected to Lateral Load Perpendicular to Grain - M Yasumura and L Daudeville

28-7-6 Design Procedure for Locally Reinforced Joints with Dowel-type Fasteners - H Werner

28-7-7 Variability and Effects of Moisture Content on the Withdrawal Characteristics for Lumber as Opposed to Clear Wood - J D Dolan and J W Stelmokas

28-7-8 Nail Plate Capacity in Joint Line - A Kevarinmäki and J Kangas

28-7-9 Axial Strength of Glued-In Bolts - Calculation Model Based on Non-Linear Fracture Mechanics - A Preliminary Study - C J Johansson, E Serrano, P J Gustafsson and B Enquist

28-7-10 Cyclic Lateral Dowel Connection Tests for seismic and Wind Evaluation - J D Dolan

29-7-1 A Simple Method for Lateral Load-Carrying Capacity of Dowel-Type Fasteners - J Kangas and J Kurkela

29-7-2 Nail Plate Joint Behaviour at Low Versus High Load Level - T Poutanen

29-7-3 The Moment Resistance of Tee and Butt - Joint Nail Plate Test Specimens - A Comparison with Current Design Methods - A Reffold, L R J Whale and B S Choo

29-7-4 A Critical Review of the Moment Rotation Test Method Proposed in prEN 1075 - M Bettison, B S Choo and L R J Whale

29-7-5 Explanation of the Translation and Rotation Behaviour of Prestressed Moment Timber Joints - A J M Leijten

29-7-6 Design of Joints and Frame Corners using Dowel-Type Fasteners - E Gehri

29-7-7 Quasi-Static Reversed-Cyclic Testing of Nailed Joints - E Karacabeyli and A Ceccotti

29-7-8 Failure of Bolted Joints Loaded Parallel to the Grain: Experiment and Simulation - L Davenne, L Daudeville and M Yasumura

30-7-1 Flexural Behaviour of GLT Beams End-Jointed by Glued-in Hardwood Dowels - K Komatsu, A Koizumi, J Jensen, T Sasaki and Y Iijima

30-7-2 Modelling of the Block Tearing Failure in Nailed Steel-to-Timber Joints - J Kangas, K Aalto and A Kevarinmäki

30-7-3 Cyclic Testing of Joints with Dowels and Slotted-in Steel Plates - E Aasheim

30-7-4 A Steel-to-Timber Dowelled Joint of High Performance in Combination with a High Strength Wood Composite (Parallam) - E Gehri

30-7-5 Multiple Fastener Timber Connections with Dowel Type Fasteners - A Jorissen

30-7-6 Influence of Ductility on Load-Carrying Capacity of Joints with Dowel-Type Fasteners - A Mischler

31-7-1 Mechanical Properties of Dowel Type Joints under Reversed Cyclic Lateral Loading - M Yasumura

31-7-2 Design of Joints with Laterally Loaded Dowels - A Mischler

31-7-3 Flexural Behaviour of Glulam Beams Edge-Jointed by Lagscrews with Steel Splice Plates - K Komatsu

31-7-4 Design on Timber Capacity in Nailed Steel-to-Timber Joints - J Kangas and J Vesa

31-7-5 Timber Contact in Chord Splices of Nail Plate Structures - A Kevarinmäki

31-7-6 The Fastener Yield Strength in Bending - A Jorissen and H J Blaß

31-7-7 A Proposal for Simplification of Johansen`s Formulae, Dealing With the Design of Dowelled-Type Fasteners - F Rouger

31-7-8 Simplified Design of Connections with Dowel-type fasteners - H J Blaß and J Ehlbeck

32-7-1 Behaviour of Wood-Steel-Wood Bolted Glulam Connections - M Mohammad and J H P Quenneville

32-7-2 A new set of experimental tests on beams loaded perpendicular-to-grain by dowel-type joints- M Ballerini

32-7-3 Design and Analysis of Bolted Timber Joints under Lateral Force Perpendicular to Grain - M Yasumura and L Daudeville

32-7-4 Predicting Capacities of Joints with Laterally Loaded Nails - I Smith and P Quenneville

32-7-5 Strength Reduction Rules for Multiple Fastener Joints - A Mischler and E Gehri

32-7-6 The Stiffness of Multiple Bolted Connections - A Jorissen

32-7-7 Concentric Loading Tests on Girder Truss Components - T N Reynolds, A Reffold, V Enjily and L Whale

32-7-8 Dowel Type Connections with Slotted-In Steel Plates - M U Pedersen, C O Clorius, L Damkilde, P Hoffmeyer and L Esklidsen

32-7-9 Creep of Nail Plate Reinforced Bolt Joints - J Vesa and A Kevarinmäki

32-7-10 The Behaviour of Timber Joints with Ring Connectors - E Gehri and A Mischler

32-7-11 Non-Metallic, Adhesiveless Joints for Timber Structures - R D Drake, M P Ansell, C J Mettem and R Bainbridge

32-7-12 Effect of Spacing and Edge Distance on the Axial Strength of Glued-in Rods - H J Blaß and B Laskewitz

32-7-13 Evaluation of Material Combinations for Bonded in Rods to Achieve Improved Timber Connections - C J Mettem, R J Bainbridge, K Harvey, M P Ansell, J G Broughton and A R Hutchinson

33-7-1 Determination of Yield Strength and Ultimate Strength of Dowel-Type Timber Joints – M Yasumura and K Sawata

33-7-2 Lateral Shear Capacity of Nailed Joints – U Korin

33-7-3 Height-Adjustable Connector for Composite Beams – Y V Piskunov and E G Stern

33-7-4 Engineering Ductility Assessment for a Nailed Slotted-In Steel Connection in Glulam– L Stehn and H Johansson

33-7-5	Effective Bending Capacity of Dowel-Type Fasteners - H J Blaß, A Bienhaus and V Krämer
33-7-6	Load-Carrying Capacity of Joints with Dowel-Type Fasteners and Interlayers - H J Blaß and B Laskewitz
33-7-7	Evaluation of Perpendicular to Grain Failure of Beams caused by Concentrated Loads of Joints – A J M Leijten and T A C M van der Put
33-7-8	Test Methods for Glued-In Rods for Timber Structures – C Bengtsson and C J Johansson
33-7-9	Stiffness Analysis of Nail Plates – P Ellegaard
33-7-10	Capacity, Fire Resistance and Gluing Pattern of the Rods in V-Connections – J Kangas
33-7-11	Bonded-In Pultrusions for Moment-Resisting Timber Connections – K Harvey, M P Ansell, C J Mettem, R J Bainbridge and N Alexandre
33-7-12	Fatigue Performance of Bonded-In Rods in Glulam, Using Three Adhesive Types - R J Bainbridge, K Harvey, C J Mettem and M P Ansell
34-7-1	Splitting Strength of Beams Loaded by Connections Perpendicular to Grain, Model Validation – A J M Leijten, A Jorissen
34-7-2	Numerical LEFM analyses for the evaluation of failure loads of beams loaded perpendicular-to-grain by single-dowel connections – M Ballerini, R Bezzi
34-7-3	Dowel joints loaded perpendicular to grain - H J Larsen, P J Gustafsson
34-7-4	Quality Control of Connections based on in V-shape glued-in Steel Rods – J Kangas, A Kevarinmäki
34-7-5	Testing Connector Types for Laminated-Timber-Concrete Composite Elements – M Grosse, S Lehmann, K Rautenstrauch
34-7-6	Behaviour of Axially Loaded Glued-in Rods - Requirements and Resistance, Especially for Spruce Timber Perpendicular to the Grain Direction – A Bernasconi
34-7-7	Embedding characteristics on fibre reinforcement and densified timber joints - P Haller, J Wehsener, T Birk
34-7-8	GIROD – Glued-in Rods for Timber Structures – C Bengtsson, C-J Johansson
34-7-9	Criteria for Damage and Failure of Dowel-Type Joints Subjected to Force Perpendicular to the Grain – M Yasumura
34-7-10	Interaction Between Splitting and Block Shear Failure of Joints – A J M Leijten, A Jorissen, J Kuipers
34-7-11	Limit states design of dowel-fastener joints – Placement of modification factors and partial factors, and calculation of variability in resistance – I Smith, G Foliente
34-7-12	Design and Modelling of Knee Joints - J Nielsen, P Ellegaard
34-7-13	Timber-Steel Shot Fired Nail Connections at Ultimate Limit States - R J Bainbridge, P Larsen, C J Mettem, P Alam, M P Ansell
35-7-1	New Estimating Method of Bolted Cross-lapped Joints with Timber Side Members - M Noguchi, K Komatsu
35-7-2	Analysis on Multiple Lag Screwed Timber Joints with Timber Side Members - K Komatsu, S Takino, M Nakatani, H Tateishi
35-7-3	Joints with Inclined Screws - A Kevarinmäki
35-7-4	Joints with Inclined Screws - I Bejtka, H J Blaß
35-7-5	Effect of distances, Spacing and Number of Dowels in a Row an the Load Carrying Capacity of Connections with Dowels failing by Splitting - M Schmid, R Frasson, H J Blaß
35-7 6	Effect of Row Spacing on the Capacity of Bolted Timber Connections Loaded Perpendicular-to-grain - P Quenneville, M Kasim

35-7-7 Splitting Strength of Beams Loaded by Connections, Model Comparison - A J M Leijten

35-7-8 Load-Carrying Capacity of Perpendicular to the Grain Loaded Timber Joints with Multiple Fasteners - O Borth, K U Schober, K Rautenstrauch

35-7-9 Determination of fracture parameter for dowel-type joints loaded perpendicular to wooden grain and its application - M Yasumura

35-7-10 Analysis and Design of Modified Attic Trusses with Punched Metal Plate Fasteners - P Ellegaard

35-7-11 Joint Properties of Plybamboo Sheets in Prefabricated Housing - G E Gonzalez

35-7-12 Fiber-Reinforced Beam-to-Column Connections for Seismic Applications - B Kasal, A Heiduschke, P Haller

36-7-1 Shear Tests in Timber-LWAC with Screw-Type Connections - L Jorge, H Cruz, S Lopes

36-7-2 Plug Shear Failure in Nailed Timber Connections: Experimental Studies - H Johnsson

36-7-3 Nail-Laminated Timber Elements in Natural Surface-Composite with Mineral Bound Layer - S Lehmann, K Rautenstrauch

36-7-4 Mechanical Properties of Timber-Concrete Joints Made With Steel Dowels - A Dias, J W G van de Kuilen, H Cruz

36-7-5 Comparison of Hysteresis Responses of Different Sheating to Framing Joints - B Dujič, R Zarnić

36-7- 6 Evaluation and Estimation of the Performance of the Nail Joints and Shear Walls under Dry/Humid Cyclic Climate - S Nakajima

36-7-7 Beams Transversally Loaded by Dowel-Type Joints: Influence on Splitting Strength of Beam Thickness and Dowel Size - M Ballerini, A Giovanella

36-7-8 Splitting Strength of Beams Loaded by Connections - J L Jensen

36-7-9 A Tensile Fracture Model for Joints with Rods or Dowels loaded Perpendicular-to-Grain - J L Jensen, P J Gustafsson, H J Larsen

36-7-10 A Numerical Model to Simulate the Load-Displacement Time-History of Mutiple-Bolt Connections Subjected to Various Loadings - C P Heine, J D Dolan

36-7-11 Reliability of Timber Structures, Theory and Dowel-Type Connection Failures - A Ranta-Maunus, A Kevarinmäki

37-7-1 Development of the "Displaced Volume Model" to Predict Failure for Multiple-Bolt Timber Joints - D M Carradine, J D Dolan, C P Heine

37-7-2 Mechanical Models of the Knee Joints with Cross-Lapped Glued Joints and Glued in Steel Rods - M Noguchi, K Komatsu

37-7-3 Simplification of the Neural Network Model for Predicting the Load-Carrying Capacity of Dowel-Type Connections - A Cointe, F Rouger

37-7-4 Bolted Wood Connections Loaded Perpendicular-to-Grain- A Proposed Design Approach - M C G Lehoux, J H P Quenneville

37-7-5 A New Prediction Formula for the Splitting Strength of Beams Loaded by Dowel Type Connections - M Ballerini

37-7-6 Plug Shear Failure: The Tensile Failure Mode and the Effect of Spacing - H Johnsson

37-7-7 Block Shear Failure Test with Dowel-Type Connection in Diagonal LVL Structure - M Kairi

37-7-8 Glued-in Steel Rods: A Design Approach for Axially Loaded Single Rods Set Parallel to the Grain - R Steiger, E Gehri, R Widmann

37-7-9 Glued in Rods in Load Bearing Timber Structures - Status regarding European Standards for Test Procedures - B Källander

37-7-10 French Data Concerning Glued-in Rods - C Faye, L Le Magorou, P Morlier, J Surleau

37-7-11 Enhancement of Dowel-Type Fasteners by Glued Connectors - C O Clorius, A Højman

37-7-12 Review of Probability Data for Timber Connections with Dowel-Type Fasteners - A J M Leijten, J Köhler, A Jorissen

37-7-13 Behaviour of Fasteners and Glued-in Rods Produced From Stainless Steel - A Kevarinmäki

37-7-14 Dowel joints in Engineered Wood Products: Assessment of Simple Fracture Mechanics Models - M Snow, I Smith, A Asiz

37-7-15 Numerical Modelling of Timber and Connection Elements Used in Timber-Concrete-Composite Constructions - M Grosse, K Rautenstrauch

38-7-1 A Numerical Investigation on the Splitting Strength of Beams Loaded Perpendicular-to-grain by Multiple-dowel Connections – M Ballerini, M Rizzi

38-7-2 A Probabilistic Framework for the Reliability Assessment of Connections with Dowel Type Fasteners - J Köhler

38-7-3 Load Carrying Capacity of Curved Glulam Beams Reinforced with self-tapping Screws - J Jönsson, S Thelandersson

38-7-4 Self-tapping Screws as Reinforcements in Connections with Dowel-Type Fasteners- I Bejtka, H J Blaß

38-7-5 The Yield Capacity of Dowel Type Fasteners - A Jorissen, A Leijten

38-7-6 Nails in Spruce - Splitting Sensitivity, End Grain Joints and Withdrawal Strength - A Kevarinmäki

38-7-7 Design of Timber Connections with Slotted-in Steel Plates and Small Diameter Steel Tube Fasteners - B Murty, I Smith, A Asiz

39-7-1 Effective in-row Capacity of Multiple-Fastener Connections - P Quenneville, M Bickerdike

39-7-2 Self-tapping Screws as Reinforcements in Beam Supports - I Bejtka, H J Blaß

39-7-3 Connectors for Timber-concrete Composite-Bridges - A Döhrer, K Rautenstrauch

39-7-4 Block Shear Failure at Dowelled Double Shear Steel-to-timber Connections - A Hanhijärvi, A Kevarinmäki, R Yli-Koski

39-7-5 Load Carrying Capacity of Joints with Dowel Type Fasteners in Solid Wood Panels - T Uibel, H J Blaß

39-7-6 Generalised Canadian Approach for Design of Connections with Dowel Fasteners - P Quenneville, I Smith, A Asiz, M Snow, Y H Chui

LOAD SHARING

3-8-1 Load Sharing - An Investigation on the State of Research and Development of Design Criteria - E Levin

4-8-1 A Review of Load-Sharing in Theory and Practice - E Levin

4-8-2 Load Sharing - B Norén

19-8-1 Predicting the Natural Frequencies of Light-Weight Wooden Floors - I Smith and Y H Chui

20-8-1 Proposed Code Requirements for Vibrational Serviceability of Timber Floors - Y H Chui and I Smith

21-8-1 An Addendum to Paper 20-8-1 - Proposed Code Requirements for Vibrational Serviceability of Timber Floors - Y H Chui and I Smith

21-8-2 Floor Vibrational Serviceability and the CIB Model Code - S Ohlsson

22-8-1 Reliability Analysis of Viscoelastic Floors - F Rouger, J D Barrett and R O Foschi

24-8-1 On the Possibility of Applying Neutral Vibrational Serviceability Criteria to Joisted Wood Floors - I Smith and Y H Chui

25-8-1 Analysis of Glulam Semi-rigid Portal Frames under Long-term Load - K Komatsu and N Kawamoto

34-8-1 System Effect in Sheathed Parallel Timber Beam Structures – M Hansson, T Isaksson

35-8-1 System Effects in Sheathed Parallel Timber Beam Structures part II. - M Hansson, T Isaksson

39-8-1 Overview of a new Canadian Approach to Handling System Effects in Timber Structures - I Smith, Y H Chui, P Quenneville

DURATION OF LOAD

3-9-1 Definitions of Long Term Loading for the Code of Practice - B Norén

4-9-1 Long Term Loading of Trussed Rafters with Different Connection Systems - T Feldborg and M Johansen

5-9-1 Strength of a Wood Column in Combined Compression and Bending with Respect to Creep - B Källsner and B Norén

6-9-1 Long Term Loading for the Code of Practice (Part 2) - B Norén

6-9-2 Long Term Loading - K Möhler

6-9-3 Deflection of Trussed Rafters under Alternating Loading during a Year - T Feldborg and M Johansen

7-6-1 Strength and Long Term Behaviour of Lumber and Glued-Laminated Timber under Torsion Loads - K Möhler

7-9-1 Code Rules Concerning Strength and Loading Time - H J Larsen and E Theilgaard

17-9-1 On the Long-Term Carrying Capacity of Wood Structures - Y M Ivanov and Y Y Slavic

18-9-1 Prediction of Creep Deformations of Joints - J Kuipers

19-9-1 Another Look at Three Duration of Load Models - R O Foschi and Z C Yao

19-9-2 Duration of Load Effects for Spruce Timber with Special Reference to Moisture Influence - A Status Report - P Hoffmeyer

19-9-3 A Model of Deformation and Damage Processes Based on the Reaction Kinetics of Bond Exchange - T A C M van der Put

19-9-4 Non-Linear Creep Superposition - U Korin

19-9-5 Determination of Creep Data for the Component Parts of Stressed-Skin Panels - R Kliger

19-9-6 Creep an Lifetime of Timber Loaded in Tension and Compression - P Glos

19-1-1 Duration of Load Effects and Reliability Based Design (Single Member) - R O Foschi and Z C Yao

19-6-1 Effect of Age and/or Load on Timber Strength - J Kuipers

19-7-4 The Prediction of the Long-Term Load Carrying Capacity of Joints in Wood Structures - Y M Ivanov and Y Y Slavic

19-7-5 Slip in Joints under Long-Term Loading - T Feldborg and M Johansen

20-7-2 Slip in Joints under Long-Term Loading - T Feldborg and M Johansen

22-9-1 Long-Term Tests with Glued Laminated Timber Girders - M Badstube, W Rug and W Schöne

22-9-2 Strength of One-Layer solid and Lengthways Glued Elements of Wood Structures and its Alteration from Sustained Load - L M Kovaltchuk, I N Boitemirova and G B Uspenskaya

24-9-1 Long Term Bending Creep of Wood - T Toratti

24-9-2 Collection of Creep Data of Timber - A Ranta-Maunus

24-9-3 Deformation Modification Factors for Calculating Built-up Wood-Based Structures - I R Kliger

25-9-2 DVM Analysis of Wood. Lifetime, Residual Strength and Quality - L F Nielsen

26-9-1 Long Term Deformations in Wood Based Panels under Natural Climate Conditions. A Comparative Study - S Thelandersson, J Nordh, T Nordh and S Sandahl

28-9-1 Evaluation of Creep Behavior of Structural Lumber in Natural Environment - R Gupta and R Shen

30-9-1 DOL Effect in Tension Perpendicular to the Grain of Glulam Depending on Service Classes and Volume - S Aicher and G Dill-Langer

30-9-2 Damage Modelling of Glulam in Tension Perpendicular to Grain in Variable Climate - G Dill-Langer and S Aicher

31-9-1 Duration of Load Effect in Tension Perpendicular to Grain in Curved Glulam - A Ranta-Maunus

32-9-1 Bending-Stress-Redistribution Caused by Different Creep in Tension and Compression and Resulting DOL-Effect - P Becker and K Rautenstrauch

32-9-2 The Long Term Performance of Ply-Web Beams - R Grantham and V Enjily

36-9-1 Load Duration Factors for Instantaneous Loads - A J M Leijten, B Jansson

39-9-1 Simplified Approach for the Long-Term Behaviour of Timber-Concrete Composite Beams According to the Eurocode 5 Provisions - M Fragiacomo, A Ceccotti

TIMBER BEAMS

4-10-1 The Design of Simple Beams - H J Burgess

4-10-2 Calculation of Timber Beams Subjected to Bending and Normal Force - H J Larsen

5-10-1 The Design of Timber Beams - H J Larsen

9-10-1 The Distribution of Shear Stresses in Timber Beams - F J Keenan

9-10-2 Beams Notched at the Ends - K Möhler

11-10-1 Tapered Timber Beams - H Riberholt

13-6-2 Consideration of Size Effects in Longitudinal Shear Strength for Uncracked Beams - R O Foschi and J D Barrett

13-6-3 Consideration of Shear Strength on End-Cracked Beams - J D Barrett and R O Foschi

18-10-1 Submission to the CIB-W18 Committee on the Design of Ply Web Beams by Consideration of the Type of Stress in the Flanges - J A Baird

18-10-2 Longitudinal Shear Design of Glued Laminated Beams - R O Foschi

19-10-1 Possible Code Approaches to Lateral Buckling in Beams - H J Burgess

19-2-1 Creep Buckling Strength of Timber Beams and Columns - R H Leicester

20-2-1 Lateral Buckling Theory for Rectangular Section Deep Beam-Columns - H J Burgess

20-10-1 Draft Clause for CIB Code for Beams with Initial Imperfections - H J Burgess

20-10-2 Space Joists in Irish Timber - W J Robinson

20-10-3 Composite Structure of Timber Joists and Concrete Slab - T Poutanen

21-10-1 A Study of Strength of Notched Beams - P J Gustafsson

22-10-1 Design of Endnotched Beams - H J Larsen and P J Gustafsson

22-10-2 Dimensions of Wooden Flexural Members under Constant Loads - A Pozgai

22-10-3 Thin-Walled Wood-Based Flanges in Composite Beams - J König

22-10-4 The Calculation of Wooden Bars with flexible Joints in Accordance with the Polish Standart Code and Strict Theoretical Methods - Z Mielczarek

23-10-1 Tension Perpendicular to the Grain at Notches and Joints - T A C M van der Put

23-10-2 Dimensioning of Beams with Cracks, Notches and Holes. An Application of Fracture Mechanics - K Riipola

23-10-3 Size Factors for the Bending and Tension Strength of Structural Timber - J D Barret and A R Fewell

23-12-1 Bending Strength of Glulam Beams, a Design Proposal - J Ehlbeck and F Colling

23-12-3 Glulam Beams, Bending Strength in Relation to the Bending Strength of the Finger Joints - H Riberholt

24-10-1 Shear Strength of Continuous Beams - R H Leicester and F G Young

25-10-1 The Strength of Norwegian Glued Laminated Beams - K Solli, E Aasheim and R H Falk

25-10-2 The Influence of the Elastic Modulus on the Simulated Bending Strength of Hyperstatic Timber Beams - T D G Canisius

27-10-1 Determination of Shear Modulus - R Görlacher and J Kürth

29-10-1 Time Dependent Lateral Buckling of Timber Beams - F Rouger

29-10-2 Determination of Modulus of Elasticity in Bending According to EN 408 - K H Solli

29-10-3 On Determination of Modulus of Elasticity in Bending - L Boström, S Ormarsson and O Dahlblom

29-10-4 Relation of Moduli of Elasticity in Flatwise and Edgewise Bending of Solid Timber - C J Johansson, A Steffen and E W Wormuth

30-10-1 Nondestructive Evaluation of Wood-based Members and Structures with the Help of Modal Analysis - P Kuklik

30-10-2 Measurement of Modulus of Elasticity in Bending - L Boström

30-10-3 A Weak Zone Model for Timber in Bending - B Källsner, K Salmela and O Ditlevsen

30-10-4 Load Carrying Capacity of Timber Beams with Narrow Moment Peaks - T Isaksson and J Freysoldt

37-10-1 Design of Rim Boards for Use with I-Joists Framing Systems - B Yeh, T G Williamson

ENVIRONMENTAL CONDITIONS

5-11-1 Climate Grading for the Code of Practice - B Norén

6-11-1 Climate Grading (2) - B Norén

9-11-1 Climate Classes for Timber Design - F J Keenan

19-11-1 Experimental Analysis on Ancient Downgraded Timber Structures - B Leggeri and L Paolini

19-6-5 Drying Stresses in Round Timber - A Ranta-Maunus

22-11-1 Corrosion and Adaptation Factors for Chemically Aggressive Media with Timber Structures - K Erler

29-11-1 Load Duration Effect on Structural Beams under Varying Climate Influence of Size and Shape - P Galimard and P Morlier

30-11-1 Probabilistic Design Models for the Durability of Timber Constructions - R H Leicester

36-11-1 Structural Durability of Timber in Ground Contact – R H Leicester, C H Wang, M N Nguyen, G C Foliente, C McKenzie

38-11-1 Design Specifications for the Durability of Timber – R H Leicester, C-H Wang, M Nguyen, G C Foliente

38-11-2 Consideration of Moisture Exposure of Timber Structures as an Action - M Häglund, S Thelandersson

LAMINATED MEMBERS

6-12-1 Directives for the Fabrication of Load-Bearing Structures of Glued Timber - A van der Velden and J Kuipers

8-12-1 Testing of Big Glulam Timber Beams - H Kolb and P Frech

8-12-2 Instruction for the Reinforcement of Apertures in Glulam Beams - H Kolb and P Frech

8-12-3 Glulam Standard Part 1: Glued Timber Structures; Requirements for Timber (Second Draft)

9-12-1 Experiments to Provide for Elevated Forces at the Supports of Wooden Beams with Particular Regard to Shearing Stresses and Long-Term Loadings - F Wassipaul and R Lackner

9-12-2 Two Laminated Timber Arch Railway Bridges Built in Perth in 1849 - L G Booth

9-6-4 Consideration of Combined Stresses for Lumber and Glued Laminated Timber - K Möhler

11-6-3 Consideration of Combined Stresses for Lumber and Glued Laminated Timber (addition to Paper CIB-W18/9-6-4) - K Möhler

12-12-1 Glulam Standard Part 2: Glued Timber Structures; Rating (3rd draft)

12-12-2 Glulam Standard Part 3: Glued Timber Structures; Performance (3 rd draft)

13-12-1 Glulam Standard Part 3: Glued Timber Structures; Performance (4th draft)

14-12-1 Proposals for CEI-Bois/CIB-W18 Glulam Standards - H J Larsen

14-12-2 Guidelines for the Manufacturing of Glued Load-Bearing Timber Structures - Stevin Laboratory

14-12-3 Double Tapered Curved Glulam Beams - H Riberholt

14-12-4 Comment on CIB-W18/14-12-3 - E Gehri

18-12-1 Report on European Glulam Control and Production Standard - H Riberholt

18-10-2 Longitudinal Shear Design of Glued Laminated Beams - R O Foschi

19-12-1 Strength of Glued Laminated Timber - J Ehlbeck and F Colling

19-12-2 Strength Model for Glulam Columns - H J Blaß

19-12-3 Influence of Volume and Stress Distribution on the Shear Strength and Tensile Strength Perpendicular to Grain - F Colling

19-12-4 Time-Dependent Behaviour of Glued-Laminated Beams - F Zaupa

21-12-1 Modulus of Rupture of Glulam Beam Composed of Arbitrary Laminae - K Komatsu and N Kawamoto

21-12-2	An Appraisal of the Young's Modulus Values Specified for Glulam in Eurocode 5- L R J Whale, B O Hilson and P D Rodd
21-12-3	The Strength of Glued Laminated Timber (Glulam): Influence of Lamination Qualities and Strength of Finger Joints - J Ehlbeck and F Colling
21-12-4	Comparison of a Shear Strength Design Method in Eurocode 5 and a More Traditional One - H Riberholt
22-12-1	The Dependence of the Bending Strength on the Glued Laminated Timber Girder Depth - M Badstube, W Rug and W Schöne
22-12-2	Acid Deterioration of Glulam Beams in Buildings from the Early Half of the 1960s - Prelimination summary of the research project; Overhead pictures - B A Hedlund
22-12-3	Experimental Investigation of normal Stress Distribution in Glue Laminated Wooden Arches - Z Mielczarek and W Chanaj
22-12-4	Ultimate Strength of Wooden Beams with Tension Reinforcement as a Function of Random Material Properties - R Candowicz and T Dziuba
23-12-1	Bending Strength of Glulam Beams, a Design Proposal - J Ehlbeck and F Colling
23-12-2	Probability Based Design Method for Glued Laminated Timber - M F Stone
23-12-3	Glulam Beams, Bending Strength in Relation to the Bending Strength of the Finger Joints - H Riberholt
23-12-4	Glued Laminated Timber - Strength Classes and Determination of Characteristic Properties - H Riberholt, J Ehlbeck and A Fewell
24-12-1	Contribution to the Determination of the Bending Strength of Glulam Beams - F Colling, J Ehlbeck and R Görlacher
24-12-2	Influence of Perpendicular-to-Grain Stressed Volume on the Load-Carrying Capacity of Curved and Tapered Glulam Beams - J Ehlbeck and J Kürth
25-12-1	Determination of Characteristic Bending Values of Glued Laminated Timber. EN-Approach and Reality - E Gehri
26-12-1	Norwegian Bending Tests with Glued Laminated Beams-Comparative Calculations with the "Karlsruhe Calculation Model" - E Aasheim, K Solli, F Colling, R H Falk, J Ehlbeck and R Görlacher
26-12-2	Simulation Analysis of Norwegian Spruce Glued-Laminated Timber - R Hernandez and R H Falk
26-12-3	Investigation of Laminating Effects in Glued-Laminated Timber - F Colling and R H Falk
26-12-4	Comparing Design Results for Glulam Beams According to Eurocode 5 and to the French Working Stress Design Code (CB71) - F Rouger
27-12-1	State of the Art Report: Glulam Timber Bridge Design in the U.S. - M A Ritter and T G Williamson
27-12-2	Common Design Practice for Timber Bridges in the United Kingdom - C J Mettem, J P Marcroft and G Davis
27-12-3	Influence of Weak Zones on Stress Distribution in Glulam Beams - E Serrano and H J Larsen
28-12-1	Determination of Characteristic Bending Strength of Glued Laminated Timber - E Gehri
28-12-2	Size Factor of Norwegian Glued Laminated Beams - E Aasheim and K H Solli
28-12-3	Design of Glulam Beams with Holes - K Riipola
28-12-4	Compression Resistance of Glued Laminated Timber Short Columns- U Korin
29-12-1	Development of Efficient Glued Laminated Timber - G Schickhofer

30-12-1 Experimental Investigation and Analysis of Reinforced Glulam Beams - K Oiger

31-12-1 Depth Factor for Glued Laminated Timber-Discussion of the Eurocode 5 Approach - B Källsner, O Carling and C J Johansson

32-12-1 The bending stiffness of nail-laminated timber elements in transverse direction- T Wolf and O Schäfer

Internal Stresses in the Cross-Grain Direction of Wood Induced by Climate Variation – J Jönsson and S Svensson

34-12-1 High-Strength I-Joist Compatible Glulam Manufactured with LVL Tension Laminations – B Yeh, T G Williamson

34-12-2 Evaluation of Glulam Shear Strength Using A Full-Size Four-Point Test Method – B Yeh, T G Williamson

34-12-3 Design Model for FRP Reinforced Glulam Beams – M Romani, H J Blaß

34-12-4 Moisture induced stresses in glulam cross sections – J Jönsson

34-12-5 Load Carrying Capacity of Nail-Laminated Timber under Concentrated Loads – V Krämer, H J Blaß

34-12-6 Determination of Shear Strength Values for GLT Using Visual and Machine Graded Spruce Laminations – G Schickhofer

34-12-7 Mechanically Jointed Beams: Possibilities of Analysis and some special Problems – H Kreuzinger

35-12-1 Glulam Beams with Round Holes – a Comparison of Different Design Approaches vs. Test Data - S Aicher L Höfflin

36-12-1 Problems with Shear and Bearing Strength of LVL in Highly Loaded Structures - H Bier

36-12-2 Weibull Based Design of Round Holes in Glulam - L Höfflin, S Aicher

37-12-1 Development of Structural LVL from Tropical Wood and Evaluation of Their Performance for the Structural Components of Wooden Houses. Part-1. Application of Tropical LVL to a Roof Truss - K Komatsu, Y Idris, S Yuwasdiki, B Subiyakto, A Firmanti

37-12-2 Reinforcement of LVL Beams With Bonded-in Plates and Rods - Effect of Placement of Steel and FRP Reinforcements on Beam Strength and Stiffness - P Alam, M P Ansell, D Smedley

39-12-1 Recommended Procedures for Determination of Distribution Widths in the Design of Stress Laminated Timber Plate Decks - K Crews

39-12-2 In-situ Strengthening of Timber Structures with CFRP - K U Schober, S Franke, K Rautenstrauch

39-12-3 Effect of Checking and Non-Glued Edge Joints on the Shear Strength of Structural Glued Laminated Timber Beams - B Yeh, T G Williamson, Z A Martin

39-12-4 A Contribution to the Design and System Effect of Cross Laminated Timber (CLT) - R Jöbstl, T Moosbrugger, T Bogensperger, G Schickhofer

39-12-5 Behaviour of Glulam in Compression Perpendicular to Grain in Different Strength Grades and Load Configurations - M Augustin, A Ruli, R Brandner, G Schickhofer

PARTICLE AND FIBRE BUILDING BOARDS

7-13-1 Fibre Building Boards for CIB Timber Code (First Draft)- O Brynildsen

9-13-1 Determination of the Bearing Strength and the Load-Deformation Characteristics of Particleboard - K Möhler, T Budianto and J Ehlbeck

9-13-2 The Structural Use of Tempered Hardboard - W W L Chan

11-13-1	Tests on Laminated Beams from Hardboard under Short- and Longterm Load - W Nozynski
11-13-2	Determination of Deformation of Special Densified Hardboard under Long-term Load and Varying Temperature and Humidity Conditions - W Halfar
11-13-3	Determination of Deformation of Hardboard under Long-term Load in Changing Climate - W Halfar
14-4-1	An Introduction to Performance Standards for Wood-Base Panel Products - D H Brown
14-4-2	Proposal for Presenting Data on the Properties of Structural Panels - T Schmidt
16-13-1	Effect of Test Piece Size on Panel Bending Properties - P W Post
20-4-1	Considerations of Reliability - Based Design for Structural Composite Products - M R O'Halloran, J A Johnson, E G Elias and T P Cunningham
20-13-1	Classification Systems for Structural Wood-Based Sheet Materials - V C Kearley and A R Abbott
21-13-1	Design Values for Nailed Chipboard - Timber Joints - A R Abbott
25-13-1	Bending Strength and Stiffness of Izopanel Plates - Z Mielczarek
28-13-1	Background Information for "Design Rated Oriented Strand Board (OSB)" in CSA Standards - Summary of Short-term Test Results - E Karacabeyli, P Lau, C R Henderson, F V Meakes and W Deacon
28-13-2	Torsional Stiffness of Wood-Hardboard Composed I-Beam - P Olejniczak

TRUSSED RAFTERS

4-9-1	Long-term Loading of Trussed Rafters with Different Connection Systems - T Feldborg and M Johansen
6-9-3	Deflection of Trussed Rafters under Alternating Loading During a Year - T Feldborg and M Johansen
7-2-1	Lateral Bracing of Timber Struts - J A Simon
9-14-1	Timber Trusses - Code Related Problems - T F Williams
9-7-1	Design of Truss Plate Joints - F J Keenan
10-14-1	Design of Roof Bracing - The State of the Art in South Africa - P A V Bryant and J A Simon
11-14-1	Design of Metal Plate Connected Wood Trusses - A R Egerup
12-14-1	A Simple Design Method for Standard Trusses - A R Egerup
13-14-1	Truss Design Method for CIB Timber Code - A R Egerup
13-14-2	Trussed Rafters, Static Models - H Riberholt
13-14-3	Comparison of 3 Truss Models Designed by Different Assumptions for Slip and E-Modulus - K Möhler
14-14-1	Wood Trussed Rafter Design - T Feldborg and M Johansen
14-14-2	Truss-Plate Modelling in the Analysis of Trusses - R O Foschi
14-14-3	Cantilevered Timber Trusses - A R Egerup
14-7-5	The Effect of Support Eccentricity on the Design of W- and WW-Trusses with Nail Plate Connectors - B Källsner
15-14-1	Guidelines for Static Models of Trussed Rafters - H Riberholt
15-14-2	The Influence of Various Factors on the Accuracy of the Structural Analysis of Timber Roof Trusses - F R P Pienaar

15-14-3	Bracing Calculations for Trussed Rafter Roofs - H J Burgess
15-14-4	The Design of Continuous Members in Timber Trussed Rafters with Punched Metal Connector Plates - P O Reece
15-14-5	A Rafter Design Method Matching U.K. Test Results for Trussed Rafters - H J Burgess
16-14-1	Full-Scale Tests on Timber Fink Trusses Made from Irish Grown Sitka Spruce - V Picardo
17-14-1	Data from Full Scale Tests on Prefabricated Trussed Rafters - V Picardo
17-14-2	Simplified Static Analysis and Dimensioning of Trussed Rafters - H Riberholt
17-14-3	Simplified Calculation Method for W-Trusses - B Källsner
18-14-1	Simplified Calculation Method for W-Trusses (Part 2) - B Källsner
18-14-2	Model for Trussed Rafter Design - T Poutanen
19-14-1	Annex on Simplified Design of W-Trusses - H J Larsen
19-14-2	Simplified Static Analysis and Dimensioning of Trussed Rafters - Part 2 - H Riberholt
19-14-3	Joint Eccentricity in Trussed Rafters - T Poutanen
20-14-1	Some Notes about Testing Nail Plates Subjected to Moment Load - T Poutanen
20-14-2	Moment Distribution in Trussed Rafters - T Poutanen
20-14-3	Practical Design Methods for Trussed Rafters - A R Egerup
22-14-1	Guidelines for Design of Timber Trussed Rafters - H Riberholt
23-14-1	Analyses of Timber Trussed Rafters of the W-Type - H Riberholt
23-14-2	Proposal for Eurocode 5 Text on Timber Trussed Rafters - H Riberholt
24-14-1	Capacity of Support Areas Reinforced with Nail Plates in Trussed Rafters - A Kevarinmäki
25-14-1	Moment Anchorage Capacity of Nail Plates in Shear Tests - A Kevarinmaki and J. Kangas
25-14-2	Design Values of Anchorage Strength of Nail Plate Joints by 2-curve Method and Interpolation - J Kangas and A Kevarinmaki
26-14-1	Test of Nail Plates Subjected to Moment - E Aasheim
26-14-2	Moment Anchorage Capacity of Nail Plates - A Kevarinmäki and J Kangas
26-14-3	Rotational Stiffness of Nail Plates in Moment Anchorage - A Kevarinmäki and J Kangas
26-14-4	Solution of Plastic Moment Anchorage Stress in Nail Plates - A Kevarinmäki
26-14-5	Testing of Metal-Plate-Connected Wood-Truss Joints - R Gupta
26-14-6	Simulated Accidental Events on a Trussed Rafter Roofed Building - C J Mettem and J P Marcroft
30-14-1	The Stability Behaviour of Timber Trussed Rafter Roofs - Studies Based on Eurocode 5 and Full Scale Testing - R J Bainbridge, C J Mettern, A Reffold and T Studer
32-14-1	Analysis of Timber Reinforced with Punched Metal Plate Fasteners- J Nielsen
33-14-1	Moment Capacity of Timber Beams Loaded in Four-Point Bending and Reinforced with Punched Metal Plate Fasteners – J Nielsen
36-14-1	Effect of Chord Splice Joints on Force Distribution in Trusses with Punched Metal Plate Fasteners - P Ellegaard

36-14-2 Monte Carlo Simulation and Reliability Analysis of Roof Trusses with Punched Metal Plate Fasteners - M Hansson, P Ellegaard

36-14-3 Truss Trouble – R H Leicester, J Goldfinch, P Paevere, G C Foliente

STRUCTURAL STABILITY

8-15-1 Laterally Loaded Timber Columns: Tests and Theory - H J Larsen

13-15-1 Timber and Wood-Based Products Structures. Panels for Roof Coverings. Methods of Testing and Strength Assessment Criteria. Polish Standard BN-78/7159-03

16-15-1 Determination of Bracing Structures for Compression Members and Beams - H Brüninghoff

17-15-1 Proposal for Chapter 7.4 Bracing - H Brüninghoff

17-15-2 Seismic Design of Small Wood Framed Houses - K F Hansen

18-15-1 Full-Scale Structures in Glued Laminated Timber, Dynamic Tests: Theoretical and Experimental Studies - A Ceccotti and A Vignoli

18-15-2 Stabilizing Bracings - H Brüninghoff

19-15-1 Connections Deformability in Timber Structures: a Theoretical Evaluation of its Influence on Seismic Effects - A Ceccotti and A Vignoli

19-15-2 The Bracing of Trussed Beams - M H Kessel and J Natterer

19-15-3 Racking Resistance of Wooden Frame Walls with Various Openings - M Yasumura

19-15-4 Some Experiences of Restoration of Timber Structures for Country Buildings - G Cardinale and P Spinelli

19-15-5 Non-Destructive Vibration Tests on Existing Wooden Dwellings - Y Hirashima

20-15-1 Behaviour Factor of Timber Structures in Seismic Zones. - A Ceccotti and A Vignoli

21-15-1 Rectangular Section Deep Beam - Columns with Continuous Lateral Restraint - H J Burgess

21-15-2 Buckling Modes and Permissible Axial Loads for Continuously Braced Columns- H J Burgess

21-15-3 Simple Approaches for Column Bracing Calculations - H J Burgess

21-15-4 Calculations for Discrete Column Restraints - H J Burgess

21-15-5 Behaviour Factor of Timber Structures in Seismic Zones (Part Two) - A Ceccotti and A Vignoli

22-15-1 Suggested Changes in Code Bracing Recommendations for Beams and Columns - H J Burgess

22-15-2 Research and Development of Timber Frame Structures for Agriculture in Poland- S Kus and J Kerste

22-15-3 Ensuring of Three-Dimensional Stiffness of Buildings with Wood Structures - A K Shenghelia

22-15-5 Seismic Behavior of Arched Frames in Timber Construction - M Yasumura

22-15-6 The Robustness of Timber Structures - C J Mettem and J P Marcroft

22-15-7 Influence of Geometrical and Structural Imperfections on the Limit Load of Wood Columns - P Dutko

23-15-1 Calculation of a Wind Girder Loaded also by Discretely Spaced Braces for Roof Members - H J Burgess

23-15-2	Stability Design and Code Rules for Straight Timber Beams - T A C M van der Put
23-15-3	A Brief Description of Formula of Beam-Columns in China Code - S Y Huang
23-15-4	Seismic Behavior of Braced Frames in Timber Construction - M Yasumara
23-15-5	On a Better Evaluation of the Seismic Behavior Factor of Low-Dissipative Timber Structures - A Ceccotti and A Vignoli
23-15-6	Disproportionate Collapse of Timber Structures - C J Mettem and J P Marcroft
23-15-7	Performance of Timber Frame Structures During the Loma Prieta California Earthquake - M R O'Halloran and E G Elias
24-15-2	Discussion About the Description of Timber Beam-Column Formula - S Y Huang
24-15-3	Seismic Behavior of Wood-Framed Shear Walls - M Yasumura
25-15-1	Structural Assessment of Timber Framed Building Systems - U Korin
25-15-3	Mechanical Properties of Wood-framed Shear Walls Subjected to Reversed Cyclic Lateral Loading - M Yasumura
26-15-1	Bracing Requirements to Prevent Lateral Buckling in Trussed Rafters - C J Mettem and P J Moss
26-15-2	Eurocode 8 - Part 1.3 - Chapter 5 - Specific Rules for Timber Buildings in Seismic Regions - K Becker, A Ceccotti, H Charlier, E Katsaragakis, H J Larsen and H Zeitter
26-15-3	Hurricane Andrew - Structural Performance of Buildings in South Florida - M R O'Halloran, E L Keith, J D Rose and T P Cunningham
29-15-1	Lateral Resistance of Wood Based Shear Walls with Oversized Sheathing Panels - F Lam, H G L Prion and M He
29-15-2	Damage of Wooden Buildings Caused by the 1995 Hyogo-Ken Nanbu Earthquake - M Yasumura, N Kawai, N Yamaguchi and S Nakajima
29-15-3	The Racking Resistance of Timber Frame Walls: Design by Test and Calculation - D R Griffiths, C J Mettem, V Enjily, P J Steer
29-15-4	Current Developments in Medium-Rise Timber Frame Buildings in the UK - C J Mettem, G C Pitts, P J Steer, V Enjily
29-15-5	Natural Frequency Prediction for Timber Floors - R J Bainbridge, and C J Mettem
30-15-1	Cyclic Performance of Perforated Wood Shear Walls with Oversize Oriented Strand Board Panels - Ming He, H Magnusson, F Lam, and H G L Prion
30-15-2	A Numerical Analysis of Shear Walls Structural Performances - L Davenne, L Daudeville, N Kawai and M Yasumura
30-15-3	Seismic Force Modification Factors for the Design of Multi-Storey Wood-Frame Platform Construction - E Karacabeyli and A Ceccotti
30-15-4	Evaluation of Wood Framed Shear Walls Subjected to Lateral Load - M Yasumura and N Kawai
31-15-1	Seismic Performance Testing On Wood-Framed Shear Wall - N Kawai
31-15-2	Robustness Principles in the Design of Medium-Rise Timber-Framed Buildings - C J Mettem, M W Milner, R J Bainbridge and V. Enjily
31-15-3	Numerical Simulation of Pseudo-Dynamic Tests Performed to Shear Walls - L Daudeville, L Davenne, N Richard, N Kawai and M Yasumura
31-15-4	Force Modification Factors for Braced Timber Frames - H G L Prion, M Popovski and E Karacabeyli
32-15-1	Three-Dimensional Interaction in Stabilisation of Multi-Storey Timber Frame Buildings - S Andreasson

32-15-2 Application of Capacity Spectrum Method to Timber Houses - N Kawai

32-15-3 Design Methods for Shear Walls with Openings - C Ni, E Karacabeyli and A Ceccotti

32-15-4 Static Cyclic Lateral Loading Tests on Nailed Plywood Shear Walls - K Komatsu, K H Hwang and Y Itou

33-15-1 Lateral Load Capacities of Horizontally Sheathed Unblocked Shear Walls – C Ni, E Karacabeyli and A Ceccotti

33-15-2 Prediction of Earthquake Response of Timber Houses Considering Shear Deformation of Horizontal Frames – N Kawai

33-15-3 Eurocode 5 Rules for Bracing – H J Larsen

34-15-1 A simplified plastic model for design of partially anchored wood-framed shear walls – B Källsner, U A Girhammar, Liping Wu

34-15-2 The Effect of the Moisture Content on the Performance of the Shear Walls – S Nakajima

34-15-3 Evaluation of Damping Capacity of Timber Structures for Seismic Design – M Yasumura

35-15-1 On test methods for determining racking strength and stiffness of wood-framed shear walls - B Källsner, U A Girhammar, L Wu

35-15-2 A Plastic Design Model for Partially Anchored Wood-framed Shear Walls with Openings - U A Girhammar, L Wu, B Källsner

35-15-3 Evaluation and Estimation of the Performance of the Shear Walls in Humid Climate - S Nakajima

35-15-4 Influence of Vertical Load on Lateral Resistance of Timber Frame Walls - B Dujič, R Žarnić

35-15-5 Cyclic and Seismic Performances of a Timber-Concrete System - Local and Full Scale Experimental Results - E Fournely, P Racher

35-15-6 Design of timber-concrete composite structures according to EC5 - 2002 version - A Ceccotti, M Fragiacomo, R M Gutkowski

35-15-7 Design of timber structures in seismic zones according to EC8- 2002 version - A Ceccotti, T Toratti, B Dujič

35-15-8 Design Methods to Prevent Premature Failure of Joints at Shear Wall Corners - N Kawai, H Okiura

36-15-1 Monitoring Light-Frame Timber Buildings: Environmental Loads and Load Paths – I Smith et al.

36-15-2 Applicability of Design Methods to Prevent Premature Failure of Joints at Shear Wall Corners in Case of Post and Beam Construction - N Kawai, H Isoda

36-15-3 Effects of Screw Spacing and Edge Boards on the Cyclic Performance of Timber Frame and Structural Insulated Panel Roof Systems - D M Carradine, J D Dolan, F E Woeste

36-15-4 Pseudo-Dynamic Tests on Conventional Timber Structures with Shear Walls - M Yasumura

36-15-5 Experimental Investigation of Laminated Timber Frames with Fiber-reinforced Connections under Earthquake Loads - B Kasal, P Haller, S Pospisil, I Jirovsky, A Heiduschke, M Drdacky

36-15-6 Effect of Test Configurations and Protocols on the Performance of Shear Walls - F Lam, D Jossen, J Gu, N Yamaguchi, H G L Prion

36-15-7 Comparison of Monotonic and Cyclic Performance of Light-Frame Shear Walls - J D Dolan, A J Toothman

37-15-1 Estimating 3D Behavior of Conventional Timber Structures with Shear Walls by Pseudodynamic Tests - M Yasumura, M Uesugi, L Davenne

37-15-2	Testing of Racking Behavior of Massive Wooden Wall Panels - B Dujič, J Pucelj, R Žarnić
37-15-3	Influence of Framing Joints on Plastic Capacity of Partially Anchored Wood-Framed Shear Walls - B Källsner, U A Girhammar
37-15-4	Bracing of Timber Members in Compression - J Munch-Andersen
37-15-5	Acceptance Criteria for the Use of Structural Insulated Panels in High Risk Seismic Areas - B Yeh, T D Skaggs, T G Williamson Z A Martin
37-15-6	Predicting Load Paths in Shearwalls - Hongyong Mi, Ying-Hei Chui, I Smith, M Mohammad
38-15-1	Background Information on ISO STANDARD 16670 for Cyclic Testing of Connections - E Karacabeyli, M Yasumura, G C Foliente, A Ceccotti
38-15-2	Testing & Product Standards – a Comparison of EN to ASTM, AS/NZ and ISO Standards – A Ranta-Maunus, V Enjily
38-15-3	Framework for Lateral Load Design Provisions for Engineered Wood Structures in Canada - M Popovski, E Karacabeyli
38-15-4	Design of Shear Walls without Hold-Downs - Chun Ni, E Karacabeyli
38-15-5	Plastic design of partially anchored wood-framed wall diaphragms with and without openings - B Källsner, U A Girhammar
38-15-6	Racking of Wooden Walls Exposed to Different Boundary Conditions - B Dujič, S Aicher, R Žarnić
38-15-7	A Portal Frame Design for Raised Wood Floor Applications - T G Williamson, Z A Martin, B Yeh
38-15-8	Linear Elastic Design Method for Timber Framed Ceiling, Floor and Wall Diaphragms - Jarmo Leskelä
38-15-9	A Unified Design Method for the Racking Resistance of Timber Framed Walls for Inclusion in EUROCODE 5 - R Griffiths, B Källsner, H J Blass, V Enjily
39-15-1	Effect of Transverse Walls on Capacity of Wood-Framed Wall Diaphragms - U A Girhammar, B Källsner
39-15-2	Which Seismic Behaviour Factor for Multi-Storey Buildings made of Cross-Laminated Wooden Panels? - M Follesa, M P Lauriola, C Minowa, N Kawai, C Sandhaas, M Yasumura, A Ceccotti
39-15-3	Laminated Timber Frames under dynamic Loadings - A Heiduschke, B Kasal, P Haller
39-15-4	Code Provisions for Seismic Design of Multi-storey Post-tensioned Timber Buildings - S Pampanin, A Palermo, A Buchanan, M Fragiacomo, B Deam

FIRE

12-16-1	British Standard BS 5268 the Structural Use of Timber: Part 4 Fire Resistance of Timber Structures
13-100-2	CIB Structural Timber Design Code. Chapter 9. Performance in Fire
19-16-1	Simulation of Fire in Tests of Axially Loaded Wood Wall Studs - J König
24-16-1	Modelling the Effective Cross Section of Timber Frame Members Exposed to Fire - J König
25-16-1	The Effect of Density on Charring and Loss of Bending Strength in Fire - J König
25-16-2	Tests on Glued-Laminated Beams in Bending Exposed to Natural Fires - F Bolonius Olesen and J König
26-16-1	Structural Fire Design According to Eurocode 5, Part 1.2 - J König

31-16-1 Revision of ENV 1995-1-2: Charring and Degradation of Strength and Stiffness - J König

33-16-1 A Design Model for Load-carrying Timber Frame Members in Walls and Floors Exposed to Fire - J König

33-16-2 A Review of Component Additive Methods Used for the Determination of Fire Resistance of Separating Light Timber Frame Construction - J König, T Oksanen and K Towler

33-16-3 Thermal and Mechanical Properties of Timber and Some Other Materials Used in Light Timber Frame Construction - B Källsner and J König

34-16-1 Influence of the Strength Determining Factors on the Fire Resistance Capability of Timber Structural Members – I Totev, D Dakov

34-16-2 Cross section properties of fire exposed rectangular timber members - J König, B Källsner

34-16-3 Pull-Out Tests on Glued-in Rods at High Temperatures – A Mischler, A Frangi

35-16-1 Basic and Notional Charring Rates - J König

37 - 16 - 1 Effective Values of Thermal Properties of Timber and Thermal Actions During the Decay Phase of Natural Fires - J König

37 - 16 - 2 Fire Tests on Timber Connections with Dowel-type Fasteners - A Frangi, A Mischler

38-16-1 Fire Behaviour of Multiple Shear Steel-to-Timber Connections with Dowels - C Erchinger, A Frangi, A Mischler

38-16-2 Fire Tests on Light Timber Frame Wall Assemblies - V Schleifer, A Frangi

39-16-1 Fire Performance of FRP Reinforced Glulam - T G Williamson, B Yeh

39-16-2 An Easy-to-use Model for the Design of Wooden I-joists in Fire - J König, B Källsner

39-16-3 A Design Model for Timber Slabs Made of Hollow Core Elements in Fire - A Frangi, M Fontana

STATISTICS AND DATA ANALYSIS

13-17-1 On Testing Whether a Prescribed Exclusion Limit is Attained - W G Warren

16-17-1 Notes on Sampling and Strength Prediction of Stress Graded Structural Timber - P Glos

16-17-2 Sampling to Predict by Testing the Capacity of Joints, Components and Structures - B Norén

16-17-3 Discussion of Sampling and Analysis Procedures - P W Post

17-17-1 Sampling of Wood for Joint Tests on the Basis of Density - I Smith, L R J Whale

17-17-2 Sampling Strategy for Physical and Mechanical Properties of Irish Grown Sitka Spruce - V Picardo

18-17-1 Sampling of Timber in Structural Sizes - P Glos

18-6-3 Notes on Sampling Factors for Characteristic Values - R H Leicester

19-17-1 Load Factors for Proof and Prototype Testing - R H Leicester

19-6-2 Confidence in Estimates of Characteristic Values - R H Leicester

21-6-1 Draft Australian Standard: Methods for Evaluation of Strength and Stiffness of Graded Timber - R H Leicester

21-6-2 The Determination of Characteristic Strength Values for Stress Grades of Structural Timber. Part 1 - A R Fewell and P Glos

22-17-1 Comment on the Strength Classes in Eurocode 5 by an Analysis of a Stochastic Model of Grading - A proposal for a supplement of the design concept - M Kiesel

24-17-1 Use of Small Samples for In-Service Strength Measurement - R H Leicester and F G Young

24-17-2 Equivalence of Characteristic Values - R H Leicester and F G Young

24-17-3 Effect of Sampling Size on Accuracy of Characteristic Values of Machine Grades - Y H Chui, R Turner and I Smith

24-17-4 Harmonisation of LSD Codes - R H Leicester

25-17-2 A Body for Confirming the Declaration of Characteristic Values - J Sunley

25-17-3 Moisture Content Adjustment Procedures for Engineering Standards - D W Green and J W Evans

27-17-1 Statistical Control of Timber Strength - R H Leicester and H O Breitinger

30-17-1 A New Statistical Method for the Establishment of Machine Settings - F Rouger

35-17-1 Probabilistic Modelling of Duration of Load Effects in Timber Structures - J Köhler, S Svenson

38-17-1 Analysis of Censored Data - Examples in Timber Engineering Research - R Steiger, J Köhler

39-17-1 Possible Canadian / ISO Approach to Deriving Design Values from Test Data - I Smith, A Asiz, M Snow, Y H Chui

GLUED JOINTS

20-18-1 Wood Materials under Combined Mechanical and Hygral Loading - A Martensson and S Thelandersson

20-18-2 Analysis of Generalized Volkersen - Joints in Terms of Linear Fracture Mechanics - P J Gustafsson

20-18-3 The Complete Stress-Slip Curve of Wood-Adhesives in Pure Shear - H Wernersson and P J Gustafsson

22-18-1 Perspective Adhesives and Protective Coatings for Wood Structures - A S Freidin

34-18-1 Performance Based Classification of Adhesives for Structural Timber Applications - R J Bainbridge, C J Mettem, J G Broughton, A R Hutchinson

35-18-1 Creep Testing Wood Adhesives for Structural Use - C Bengtsson, B Källander

38-18-1 Adhesive Performance at Elevated Temperatures for Engineered Wood Products - B Yeh, B Herzog, T G Williamson

39-18-1 Comparison of the Pull–out Strength of Steel Bars Glued in Glulam Elements Obtained Experimentally and Numerically - V Rajčić, A Bjelanović, M Rak

39-18-2 The Influence of the Grading Method on the Finger Joint Bending Strength of Beech - M Frese, H J Blaß

FRACTURE MECHANICS

21-10-1 A Study of Strength of Notched Beams - P J Gustafsson

22-10-1 Design of Endnotched Beams - H J Larsen and P J Gustafsson

23-10-1 Tension Perpendicular to the Grain at Notches and Joints - T A C M van der Put

23-10-2 Dimensioning of Beams with Cracks, Notches and Holes. An Application of Fracture Mechanics - K Riipola

23-19-1 Determination of the Fracture Energie of Wood for Tension Perpendicular to the Grain - W Rug, M Badstube and W Schöne

23-19-2 The Fracture Energy of Wood in Tension Perpendicular to the Grain. Results from a Joint Testing Project - H J Larsen and P J Gustafsson

23-19-3 Application of Fracture Mechanics to Timber Structures - A Ranta-Maunus

24-19-1 The Fracture Energy of Wood in Tension Perpendicular to the Grain - H J Larsen and P J Gustafsson

28-19-1 Fracture of Wood in Tension Perpendicular to the Grain: Experiment and Numerical Simulation by Damage Mechanics - L Daudeville, M Yasumura and J D Lanvin

28-19-2 A New Method of Determining Fracture Energy in Forward Shear along the Grain - H D Mansfield-Williams

28-19-3 Fracture Design Analysis of Wooden Beams with Holes and Notches. Finite Element Analysis based on Energy Release Rate Approach - H Petersson

28-19-4 Design of Timber Beams with Holes by Means of Fracture Mechanics - S Aicher, J Schmidt and S Brunold

30-19-1 Failure Analysis of Single-Bolt Joints - L Daudeville, L Davenne and M Yasumura

37 - 19 - 1 Determination of Fracture Mechanics Parameters for Wood with the Help of Close Range Photogrammetry - S Franke, B Franke, K Rautenstrauch

39-19-1 First Evaluation Steps of Design Rules in the European and German codes of Transverse Tension Areas - S Franke, B Franke, K Rautenstrauch

SERVICEABILITY

27-20-1 Codification of Serviceability Criteria - R H Leicester

27-20-2 On the Experimental Determination of Factor k_{def} and Slip Modulus k_{ser} from Short- and Long-Term Tests on a Timber-Concrete Composite (TCC) Beam - S Capretti and A Ceccotti

27-20-3 Serviceability Limit States: A Proposal for Updating Eurocode 5 with Respect to Eurocode 1 - P Racher and F Rouger

27-20-4 Creep Behavior of Timber under External Conditions - C Le Govic, F Rouger, T Toratti and P Morlier

30-20-1 Design Principles for Timber in Compression Perpendicular to Grain - S Thelandersson and A Mårtensson

30-20-2 Serviceability Performance of Timber Floors - Eurocode 5 and Full Scale Testing - R J Bainbridge and C J Mettem

32-20-1 Floor Vibrations - B Mohr

37 - 20 - 1 A New Design Method to Control Vibrations Induced by Foot Steps in Timber Floors - Lin J Hu, Y H Chui

37 - 20 - 2 Serviceability Limit States of Wooden Footbridges. Vibrations Caused by Pedestrians - P Hamm

TEST METHODS

31-21-1 Development of an Optimised Test Configuration to Determine Shear Strength of Glued Laminated Timber - G Schickhofer and B Obermayr

31-21-2 An Impact Strength Test Method for Structural Timber. The Theory and a Preliminary Study - T D G Canisius

35-21-1 Full-Scale Edgewise Shear Tests for Laminated Veneer Lumber- B Yeh, T G Williamson

39-21-1 Timber Density Restrictions for Timber Connection Tests According to EN28970/ISO8970 - A Leijten, J Köhler, A Jorissen

39-21-2 The Mechanical Inconsistence in the Evaluation of the Modulus of Elasticity According to EN384 - T Bogensperger, H Unterwieser, G Schickhofer

CIB TIMBER CODE

2-100-1 A Framework for the Production of an International Code of Practice for the Structural Use of Timber - W T Curry

5-100-1 Design of Solid Timber Columns (First Draft) - H J Larsen

5-100-2 A Draft Outline of a Code for Timber Structures - L G Booth

6-100-1 Comments on Document 5-100-1; Design of Solid Timber Columns - H J Larsen and E Theilgaard

6-100-2 CIB Timber Code: CIB Timber Standards - H J Larsen and E Theilgaard

7-100-1 CIB Timber Code Chapter 5.3 Mechanical Fasteners; CIB Timber Standard 06 and 07 - H J Larsen

8-100-1 CIB Timber Code - List of Contents (Second Draft) - H J Larsen

9-100-1 The CIB Timber Code (Second Draft)

11-100-1 CIB Structural Timber Design Code (Third Draft)

11-100-2 Comments Received on the CIB Code
U Saarelainen; Y M Ivanov, R H Leicester, W Nozynski, W R A Meyer, P Beckmann; R Marsh

11-100-3 CIB Structural Timber Design Code; Chapter 3 - H J Larsen

12-100-1 Comment on the CIB Code - Sous-Commission Glulam

12-100-2 Comment on the CIB Code - R H Leicester

12-100-3 CIB Structural Timber Design Code (Fourth Draft)

13-100-1 Agreed Changes to CIB Structural Timber Design Code

13-100-2 CIB Structural Timber Design Code. Chapter 9: Performance in Fire

13-100-3a Comments on CIB Structural Timber Design Code

13-100-3b Comments on CIB Structural Timber Design Code - W R A Meyer

13-100-3c Comments on CIB Structural Timber Design Code - British Standards Institution

13-100-4 CIB Structural Timber Design Code. Proposal for Section 6.1.5 Nail Plates - N I Bovim

14-103-2 Comments on the CIB Structural Timber Design Code - R H Leicester

15-103-1 Resolutions of TC 165-meeting in Athens 1981-10-12/13

21-100-1 CIB Structural Timber Design Code. Proposed Changes of Sections on Lateral Instability, Columns and Nails - H J Larsen

22-100-1 Proposal for Including an Updated Design Method for Bearing Stresses in CIB W18 - Structural Timber Design Code - B Madsen

22-100-2 Proposal for Including Size Effects in CIB W18A Timber Design Code
- B Madsen

22-100-3 CIB Structural Timber Design Code - Proposed Changes of Section on Thin-Flanged Beams - J König

22-100-4 Modification Factor for "Aggressive Media" - a Proposal for a Supplement to the CIB Model Code - K Erler and W Rug

22-100-5 Timber Design Code in Czechoslovakia and Comparison with CIB Model Code - P Dutko and B Kozelouh

LOADING CODES

4-101-1	Loading Regulations - Nordic Committee for Building Regulations
4-101-2	Comments on the Loading Regulations - Nordic Committee for Building Regulations
37-101-1	Action Combination Processing for the Eurocodes Basis of Software to Assist the Engineer - Y Robert, A V Page, R Thépaut, C J Mettem

STRUCTURAL DESIGN CODES

1-102-1	Survey of Status of Building Codes, Specifications etc., in USA - E G Stern
1-102-2	Australian Codes for Use of Timber in Structures - R H Leicester
1-102-3	Contemporary Concepts for Structural Timber Codes - R H Leicester
1-102-4	Revision of CP 112 - First Draft, July 1972 - British Standards Institution
4-102-1	Comparsion of Codes and Safety Requirements for Timber Structures in EEC Countries - Timber Research and Development Association
4-102-2	Nordic Proposals for Safety Code for Structures and Loading Code for Design of Structures - O A Brynildsen
4-102-3	Proposal for Safety Codes for Load-Carrying Structures - Nordic Committee for Building Regulations
4-102-4	Comments to Proposal for Safety Codes for Load-Carrying Structures - Nordic Committee for Building Regulations
4-102-5	Extract from Norwegian Standard NS 3470 "Timber Structures"
4-102-6	Draft for Revision of CP 112 "The Structural Use of Timber" - W T Curry
8-102-1	Polish Standard PN-73/B-03150: Timber Structures; Statistical Calculations and Designing
8-102-2	The Russian Timber Code: Summary of Contents
9-102-1	Svensk Byggnorm 1975 (2nd Edition); Chapter 27: Timber Construction
11-102-1	Eurocodes - H J Larsen
13-102-1	Program of Standardisation Work Involving Timber Structures and Wood-Based Products in Poland
17-102-1	Safety Principles - H J Larsen and H Riberholt
17-102-2	Partial Coefficients Limit States Design Codes for Structural Timberwork - I Smith
18-102-1	Antiseismic Rules for Timber Structures: an Italian Proposal - G Augusti and A Ceccotti
18-1-2	Eurocode 5, Timber Structures - H J Larsen
19-102-1	Eurocode 5 - Requirements to Timber - Drafting Panel Eurocode 5
19-102-2	Eurocode 5 and CIB Structural Timber Design Code - H J Larsen
19-102-3	Comments on the Format of Eurocode 5 - A R Fewell
19-102-4	New Developments of Limit States Design for the New GDR Timber Design Code - W Rug and M Badstube
19-7-3	Effectiveness of Multiple Fastener Joints According to National Codes and Eurocode 5 (Draft) - G Steck
19-7-6	The Derivation of Design Clauses for Nailed and Bolted Joints in Eurocode5 - L R J Whale and I Smith
19-14-1	Annex on Simplified Design of W-Trusses - H J Larsen

20-102-1 Development of a GDR Limit States Design Code for Timber Structures - W Rug and M Badstube

21-102-1 Research Activities Towards a New GDR Timber Design Code Based on Limit States Design - W Rug and M Badstube

22-102-1 New GDR Timber Design Code, State and Development - W Rug, M Badstube and W Kofent

22-102-2 Timber Strength Parameters for the New USSR Design Code and its Comparison with International Code - Y Y Slavik, N D Denesh and E B Ryumina

22-102-3 Norwegian Timber Design Code - Extract from a New Version - E Aasheim and K H Solli

23-7-1 Proposal for a Design Code for Nail Plates - E Aasheim and K H Solli

24-102-2 Timber Footbridges: A Comparison Between Static and Dynamic Design Criteria - A Ceccotti and N de Robertis

25-102-1 Latest Development of Eurocode 5 - H J Larsen

25-102-1A Annex to Paper CIB-W18/25-102-1. Eurocode 5 - Design of Notched Beams - H J Larsen, H Riberholt and P J Gustafsson

25-102-2 Control of Deflections in Timber Structures with Reference to Eurocode 5 - A Martensson and S Thelandersson

28-102-1 Eurocode 5 - Design of Timber Structures - Part 2: Bridges - D Bajolet, E Gehri, J König, H Kreuzinger, H J Larsen, R Mäkipuro and C Mettem

28-102-2 Racking Strength of Wall Diaphragms - Discussion of the Eurocode 5 Approach - B Källsner

29-102-1 Model Code for the Probabilistic Design of Timber Structures - H J Larsen, T Isaksson and S Thelandersson

30-102-1 Concepts for Drafting International Codes and Standards for Timber Constructions - R H Leicester

33-102-1 International Standards for Bamboo – J J A Janssen

35-102-1 Design Characteristics and Results According to EUROCODE 5 and SNiP Procedures - L Ozola, T Keskküla

35-102-2 Model Code for the Reliability-Based Design of Timber Structures - H J Larsen

36-102-1 Predicted Reliability of Elements and Classification of Timber Structures - L Ozola, T Keskküla

36-102-2 Calibration of Reliability-Based Timber Design Codes: Choosing a Fatigue Model - I Smith

38-102-1 A New Generation of Timber Design Practices and Code Provisions Linking System and Connection Design - A Asiz, I Smith

38-102-2 Uncertainties Involved in Structural Timber Design by Different Code Formats - L Ozola, T Keskküla

38-102-3 Comparison of the Eurocode 5 and Actual Croatian Codes for Wood Classification and Design With the Proposal for More Objective Way of Classification - V Rajcic A Bjelanovic

39-102-1 Calibration of Partial Factors in the Danish Timber Code - H Riberholt

INTERNATIONAL STANDARDS ORGANISATION

3-103-1 Method for the Preparation of Standards Concerning the Safety of Structures (ISO/DIS 3250) - International Standards Organisation ISO/TC98

4-103-1 A Proposal for Undertaking the Preparation of an International Standard on Timber Structures - International Standards Organisation

5-103-1 Comments on the Report of the Consultion with Member Bodies Concerning ISO/TC/P129 - Timber Structures - Dansk Ingeniorforening

7-103-1 ISO Technical Committees and Membership of ISO/TC 165

8-103-1 Draft Resolutions of ISO/TC 165

12-103-1 ISO/TC 165 Ottawa, September 1979

13-103-1 Report from ISO/TC 165 - A Sorensen

14-103-1 Comments on ISO/TC 165 N52 "Timber Structures; Solid Timber in Structural Sizes; Determination of Some Physical and Mechanical Properties"

14-103-2 Comments on the CIB Structural Timber Design Code - R H Leicester

21-103-1 Concept of a Complete Set of Standards - R H Leicester

JOINT COMMITTEE ON STRUCTURAL SAFETY

3-104-1 International System on Unified Standard Codes of Practice for Structures - Comité Européen du Béton (CEB)

7-104-1 Volume 1: Common Unified Rules for Different Types of Construction and Material – CEB

37-104-1 Proposal for a Probabilistic Model Code for Design of Timber Structures - J Köhler, H Faber

CIB PROGRAMME, POLICY AND MEETINGS

1-105-1 A Note on International Organisations Active in the Field of Utilisation of Timber - P Sonnemans

5-105-1 The Work and Objectives of CIB-W18-Timber Structures - J G Sunley

10-105-1 The Work of CIB-W18 Timber Structures - J G Sunley

15-105-1 Terms of Reference for Timber - Framed Housing Sub-Group of CIB-W18

19-105-1 Tropical and Hardwood Timbers Structures - R H Leicester

21-105-1 First Conference of CIB-W18B, Tropical and Hardwood Timber Structures Singapore, 26 - 28 October 1987 - R H Leicester

INTERNATIONAL UNION OF FORESTRY RESEARCH ORGANISATIONS

7-106-1 Time and Moisture Effects - CIB W18/IUFRO 55.02-03 Working Party

INTERNATIONAL COUNCIL FOR RESEARCH AND INNOVATION
IN BUILDING AND CONSTRUCTION

WORKING COMMISSION W18 - TIMBER STRUCTURES

A DISCUSSION ON THE CONTROL OF GRADING MACHINE SETTINGS

J Köhler

Swiss Federal Institute of Technology ETH, Zürich

R Steiger

EMPA, Swiss Federal Laboratories for Materials Testing and Research, Duebendorf

SWITZERLAND

MEETING THIRTY-NINE

FLORENCE

ITALY

AUGUST 2006

Presented by J Köhler

J Denzler asked if the alternative model was used, what could be said about the results. J Köhler responded that the paper discussed general concept of using additional information to enhance the knowledge.

H Riberholt commented that the method depended on the stability of the results, for example the material may be source dependent. J Köhler responded that the same problem existed for current method. The main assumption of the current and proposed approaches would be fairly smooth variability i.e. without large variations.

B Källsner commented that the method is interesting.

A Hanhijärvi asked if it would be possible to consider grading of graded material. J Köhler responded that the intent was not to consider grading.

V. Rajcic commented grading using Neural Network was previously considered and could be considered.

A discussion on the control of grading machine settings

Jochen Köhler

Swiss Federal Institute of Technology ETH, Zurich, Switzerland

René Steiger

EMPA, Swiss Federal Laboratories for Materials Testing and Research, Dübendorf, Switzerland

1. Background

Typical problems in structural engineering such as design, assessment, inspection and maintenance planning are decision problems subject to a combination of inherent, modelling and statistical uncertainties. Recent developments in the field of structural reliability together with the formulation of probabilistic models for the structural response and for loads enable the structural engineer to quantify these uncertainties and establish his decisions on a consistent basis. The results of these advances are summarized in the Probabilistic Model Code (PMC) published by the Joint Committee on Structural Safety (JCSS) [1].

The PMC contains general guidelines for uncertainty modelling, reliability assessment and probabilistic models for loads and material resistance for building materials as concrete and steel. Lately, also a probabilistic model code for structural timber has been developed by an international group of researchers organized under the umbrella of the COST action E24 'Reliability of Timber Structures'[2], [3]. During the COST action E24 it has become apparent that several fundamental issues require more research and development. In particular it has been found that the present practice in regard to strategies to quality control or grading of timber raw material introduces significant uncertainties on the performance of timber structural components. In the present paper control schemes for timber grading machines are discussed from the perspective of the probabilistic modelling of material properties of graded timber.

2. Introduction

Reliability analysis of structures for the purpose of code calibration in general or for the reliability verification of specific structures requires that the relevant failure modes be represented in terms of limit state functions. The limit state functions define the realizations of resistance parameters, i.e. the material properties and the load variables resulting in structural failure. In reliability analysis of timber structures the probabilistic modelling of the material properties is an issue of special interest due to the particular way this material is "produced".

Timber is by nature a very inhomogeneous building material. On a large scale the material properties are a product of e.g. the specific wood species and the geographical location where the wood has been grown. Given species and geographical location the material properties depend on factors such as the age, the diameter of the timber logs and the number of knots together with the moisture contents and the duration of loading. In comparison to other building materials such as steel and concrete, the properties of timber materials are not designed or produced by means of some recipe but may be ensured to fulfil given requirements only by quality control procedures – hereafter referred to as grading. Quality control and selection schemes are implemented in the production line, typically already at the sawmills where the construction timber is produced from the timber logs. Various schemes for grading have been developed using different principles, however, the basic idea behind them all is that the material properties of interest such as, e.g. the ultimate compression stress, are assessed indirectly by means of other properties such as e.g. the density or the modulus of elasticity (see for example Madsen [4], Walker et al. [5] and Green and Kretschmann [6]).

2.1 The Strength Class System

As a result of grading, timber is provided to the market as a graded material. The grades imply that the material properties lie within desirable and predictable limits. However, the material properties of timber grades have to be considered as random variables and the properties of timber grades are characterised (and communicated) through specific fractile values of the assumed probability distribution functions of the material properties of interest.

In general, structural timber is assigned to a specific strength class. Several strength class systems exist on an international scale, e.g. in Europe it is the EN 338 which constitutes the classification of timber based on the prescription of characteristic values or the mean values for the material properties; i.e. for every timber strength class a characteristic value or a mean value for every relevant material property is given. In EN 338 the characteristic values for the strength properties and the density are defined as the 5% fractile values of the underlying distribution functions. The modulus of elasticity (MOE) and the shear modulus are specified by mean values. For the assignment of a timber population to a certain grade, values for three material properties are mandatory; the 5% fractile value of the bending strength, the 5% fractile value of the density and the mean value of the bending MOE.

2.2 Grading Strategies

In general two different strategies of timber grading exist: visual grading and machine grading.

Visual Grading

Visual grading is based on visual inspection of timber structural elements. Visible defects, such as knots, fissures and cross grain are assessed and according to the appearance of timber structural elements in regard to these defects they are sorted to a certain grade. Some more or less rudimentary forms of visual strength grading have been used since timber was utilised as a construction material. The first formal visual grading rules, the USA ASTM Standard D245 were published in 1927 (Madsen [4]). Since the 1930s formalized rules for visual grading were introduced in the European countries (Glos in [7]). These rules are further developed until today, however they differ widely with respect to grading criteria, number of grades and grade limits. Recent efforts to harmonize these visual grading rules at least throughout Europe have not been successful because no single set of grading rules would cover the different species, timber dimensions and uses in a satisfactory manner (Glos in [7]). However, for Europe some general requirements for regional visual grading codes are prescribed (EN 14081-1); the following has to be taken into account:

- limitations for visible strength and stiffness reducing characteristics: knots, slope to the grain, rate of growth (annual ring width), fissures,
- limitations for geometrical characteristics: wane, distortion,
- limitations concerning damages caused by biological attack: insect and fungal damage.

It has to be considered that the visual grading of a timber structural element in the usual production line takes place within 2-4 seconds (Glos in [7]); the before mentioned characteristics are not measured by some device, they are subjectively estimated and it is decided within seconds whether the structural element belongs to a certain grade or not. Visual grading has proven as an efficient tool to reduce the variability of timber material properties, however, the grading effect strongly depends on the person who is performing the visual grading. The statistical characteristics of the material properties of visual graded timber are therefore difficult to assess explicitly based on information about the applied visual grading rules.

Machine Grading

The above mentioned disadvantages of visual strength grading may be overcome by machine grading, where a more formal assessment of the grading process can be performed. In contrast to visual grading, machine grading is in general based on indicative characteristics of a timber structural element which can be measured non-destructively by some device. The indicative characteristics have to be related to the basic material properties of interest. Typical indicative properties are:

- Directly related to the MOE: flat wise bending stiffness, ultrasonic pulse measurement, frequency response measurement.
- Directly related to the density: measurements of weight and dimensions, γ-ray detection.
- Directly related to visible defects: microwave response, optical detection and subsequent image processing.

A good overview about the different measuring schemes can be found in Thelandersson and Larsen [8]. It is the result from several research projects (e.g. Johansson et al. [9], Boström [10]) that measurements related to the MOE are also highly related to the bending strength. That is why several grading machines operate with a single MOE related

indicator as the flat wise bending stiffness and deliver comparable results compared to more complex machines measuring several indicators (Thelandersson and Larsen [8]).

Several grading machine systems can be found at the market, however they operate according to similar principles; one or more indicative properties of the timber to be graded are measured by the machine and based on these measurements a population of un-graded timber is subdivided into sub-populations of graded timber material. The grading acceptance criteria are formulated in form of boundary values for indicative properties which have to be matched to qualify a piece of timber to a certain grade. These boundaries are also termed grading machine settings. The performance, i.e. the statistical characteristics of the output of grading machines strongly depends on these settings, and in general very much attention is kept on how to control these machine settings.

3. Control of Grading Machine Settings

Commonly, grading machines are operating either machine controlled or output controlled. The output controlled grading system was developed in North America. Control is based on frequent destructive strength testing or proof loading of control samples of the machine graded timber. This system is relatively costly but it permits a modification of the machine settings in order to optimise the yield, i.e. the predictability of the properties of the graded timber material. This method requires large quantities of timber of similar dimension and origin, so that it can be assumed that the characteristics of the timber are stationary. These conditions rarely exist in Europe, where a variety of sizes, species and grades in small quantities are typical. For these conditions the machine controlled systems are developed. Machine control means that the settings are derived within a substantial assessment procedure prior to the operation phase of the machine. The settings are optimised to a representative un-graded timber population which might be typical for the daily use of the grading machine. In general these assessments are done for entire geographical regions, e.g. assessments for the gross supply in France or Scandinavia suggest common settings for certain grading machines used in these countries or regions.

Rules for machine grading are described in products standards such as EN 14081 in Europe, AS 4490 and AS 3519 in Australia, ASTM D6570 in the US and NLGA SPS2 in Canada. Except of the US where in general exclusively the output controlled system is used, both, the output controlled and machine controlled system is used. For the output control in general the so called *CUSUM* methods are used for the continuous control of the grading machine output. In the EN 14081 an explicit description of a machine controlled system is given. Both methods are briefly described in the following.

3.1 CUSUM – An Output Control Scheme

3.1.1 Description of the CUSUM method

The most common used schemes for continuous output control of machine grading systems are the cumulative sum (*CUSUM*) methods. *CUSUM* methods for quality control problems are described e.g. in Ewan and Kemp [11] and linked to the timber grading problem in Warren [12]. To date *CUSUM* methods are proposed by building or products standards as the NLGA SPS2 (Canada) and EN 14081 (Europe).

The principle feature of *CUSUM* techniques is that successive values of a variable, e.g. mean values of control samples, are compared with a predetermined target or reference value, and the cumulative sum of deviations from this value is plotted on a chart or recorded in tabulation. If the accumulation reaches or exceeds a pre-determined decision interval, this is taken to indicate that a change has occurred in the mean level of the variable. The decision interval may represent either an ordinal distance on a chart having time or sample number as its abscissa, or a constant for tabulation. To illustrate the main aspects of *CUSUM* methods a possible layout for output controlled machine timber grading is described, mainly following an example given in Leicester and Breitinger [13].

3.1.2 Attribute chart and variable chart procedure

It is differentiated between the attribute chart and the variable chart procedure. The attribute chart procedure is based on measuring the number of times that a required attribute, $c_{att,i}$ is missing. Specifically the attribute is taken as the event e.g. a strength value is in excess of the value of the proof load. The variable chart procedure is based on measuring a mean value, $m_{sc,i}$ of a control sample taken frequently from the output. A common sample size for these samples is $n = 5$. The charting procedure is based on three control parameters k_c, y_c and z_c, where $y_c < z_c$. The values for the control parameters depend on the size n of the control sample, the coefficient of variation of the variable of interest and are different for the attribute and variable chart procedure. For example, if the size of the control sample is $n = 5$ and the coefficient of variation (cov) of the property to be controlled is 25% the control parameters k_c, y_c and z_c can be specified as:

- Attribute Chart (Indep. from cov): $(k_c, y_c, z_c) = (1,1,6)$
- Variable Chart : $(k_c, y_c, z_c) = (0.9625\mu, 0.475\mu, 0.672\mu)$

where μ is the mean value of the property to be controlled.

For the $i-th$ sample, a sum can be computed as:

$$SUM_i = CUSUM_{i-1} + (c_{att,i} - k_c) \tag{1}$$

for an attributes chart and

$$SUM_i = CUSUM_{i-1} + (k_c - m_{sc,i}) \tag{2}$$

for a variable chart. $CUSUM_{i-1}$ denotes the value of *CUSUM* after the previous sample is tested. E.g. the actual $CUSUM_i$ for the variable chart is derived according to Table 1.

When the process switches to 'out-of-control', in general, some check of the stress grading process must be performed. If no processing errors are detected, an intensive sampling is performed, e.g. more samples are collected. If the process does not return to 'in-control' the production is stopped. This procedure is illustrated in Figure 1.

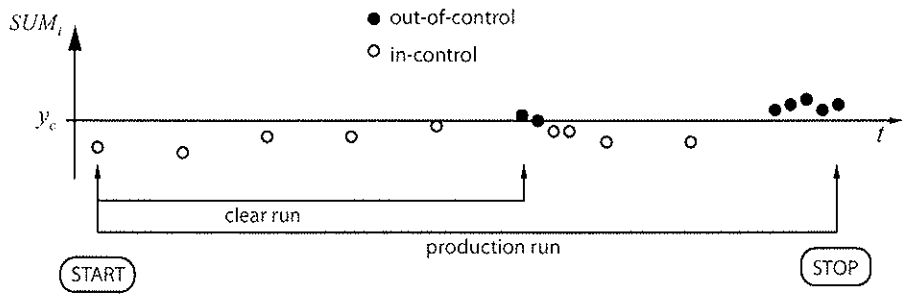

Figure 1 *Principle of CUSUM control procedure.*

Table 1 *Rules for computing CUSUM (Leicester and Breitinger [13]).*

Previous $CUSUM_{i-1}$	Actual $CUSUM_i$				
	$SUM_i \le 0$	$0 < SUM_i < y_c$	$SUM_i \le y_c$	$y_c < SUM_i < z_c$	$SUM_i \ge z_c$
$CUSUM_{i-1} = 0$	0	SUM_i	z_c	z_c	z_c
$0 \le CUSUM_{i-1} < y_c$	0	SUM_i	z_c	z_c	z_c
$y_c \le CUSUM_{i-1} < z_c$	0	0	0	SUM_i	z_c
$CUSUM_{i-1} = z_c$	0	0	0	SUM_i	z_c
$CUSUM_{i-1} \le y_c$: Process is in-control $CUSUM_{i-1} > y_c$: Process is out-of-control					

3.1.3 Discussion of the CUSUM method

Being a common control procedure in the general field of quality control the *CUSUM* method has proven to be an operational scheme for the output control of timber machine grading systems. However, the control mechanism concentrates on mean values of variables of interest and is not sensitive to possible changes of the variance of the variables which are assumed to be known and constant. This could be seen as a reasonable assumption, but on the other hand it could be interpreted as a shortcoming of the method, since changes in variance may be present and lower fractile values are sensitive to these changes.

As an alternative to the *CUSUM* method, a Bayesian updating scheme could be employed to integrate the gathered information more efficiently, i.e. continuously gain more information about the variable and its statistical properties.

3.2 The EN 14081 approach for machine controlled systems

3.2.1 Description of the EN 14081 approach

The new European grading code EN 14081 prescribes an approach for the derivation of grading machine settings according to the machine controlled system. The basis of this approach is first introduced in Rouger [14]. The machines' grading performance is compared with that of a perfect machine capable of grading each piece of timber to its

optimum grade. The comparison is made by assigning utilities for wrongly graded timber. In the following the main aspects of this approach are summarised and discussed.

1) Optimum Grade:

Timber grades are defined by requirements which have to be fulfilled in terms of the statistical properties of some material properties of the graded sub-population. In Europe these requirements are defined through a strength class system given in EN 338 and are referred to the:

- 5%-fractile value of the bending strength,
- 50%-fractile value of the bending stiffness (MOE),
- 5%-fractile value of the wood density,

All properties measured in tests according to EN 408. The characteristic values are derived following the guidelines of EN 384.

The optimal set of different timber grades for a given population is defined as a set where every single component is assigned to its highest possible grade. To obtain this set the following steps are examined (Rouger [14]):

a) For a specific geographic region a large ($n \geq 900$) and representative sample is assessed in regard to measurements on the bending moment capacity $r_{m,i}$, the bending stiffness $moe_{m,i}$, the density $\rho_{den,i}$ and the indicative properties.

b) The values of the measurements are ranked in ascending order that:

$\mathbf{r}_m = \left(r_{m,1}, r_{m,2}, ..., r_{m,n}\right)$ with $r_{m,1} \leq r_{m,2} \leq ... \leq r_{m,n}$;

$\mathbf{moe}_m = \left(moe_{m,1}, moe_{m,2}, ..., moe_{m,n}\right)$ with $moe_{m,1} \leq moe_{m,2} \leq ... \leq moe_{m,n}$;

$\boldsymbol{\rho}_{den} = \left(\rho_{den,1}, \rho_{den,2}, ..., \rho_{den,n}\right)$ with $\rho_{den,1} \leq \rho_{den,2} \leq ... \leq \rho_{den,n}$.

Note that following this approach $r_{m,i}, moe_{m,i}, \rho_{den,i}$ do not essentially correspond to the same specimen. The ranked data is plotted in a quantile plot.

c) For the highest grade the sample is cut at a quantile level such, that the sub-sample above the cut level fulfils the requirements of this grade. If the cutting levels are at different quantiles for the different properties the cutting level with the greatest rank has to be taken as being the relevant.

d) The sub-sample below the cutting level is taken to be cut again to obtain a sub-sample corresponding to the next timber grade below and so on (see Figure 2).

e) The optimal grading is defined as the proportions of different grades assigned according to the segmentation procedure as described above. Typically the proportion of the highest grade is large. A possible optimal grading could be as given in Table 2.

2) A model which relates bending strength with the indicating properties of the machine has to be established. Beside linear regression models also more complex models can be used.

3) A set of machine settings which results in timber grades by using the model derived in '2)' must be determined.

4) The entire population is (virtually) graded according to these settings, into the so-called

assigned grades.

The assigned grades are compared with the optimal grades in a so-called size matrix. A possible size matrix could be as given in

5) Table 3.

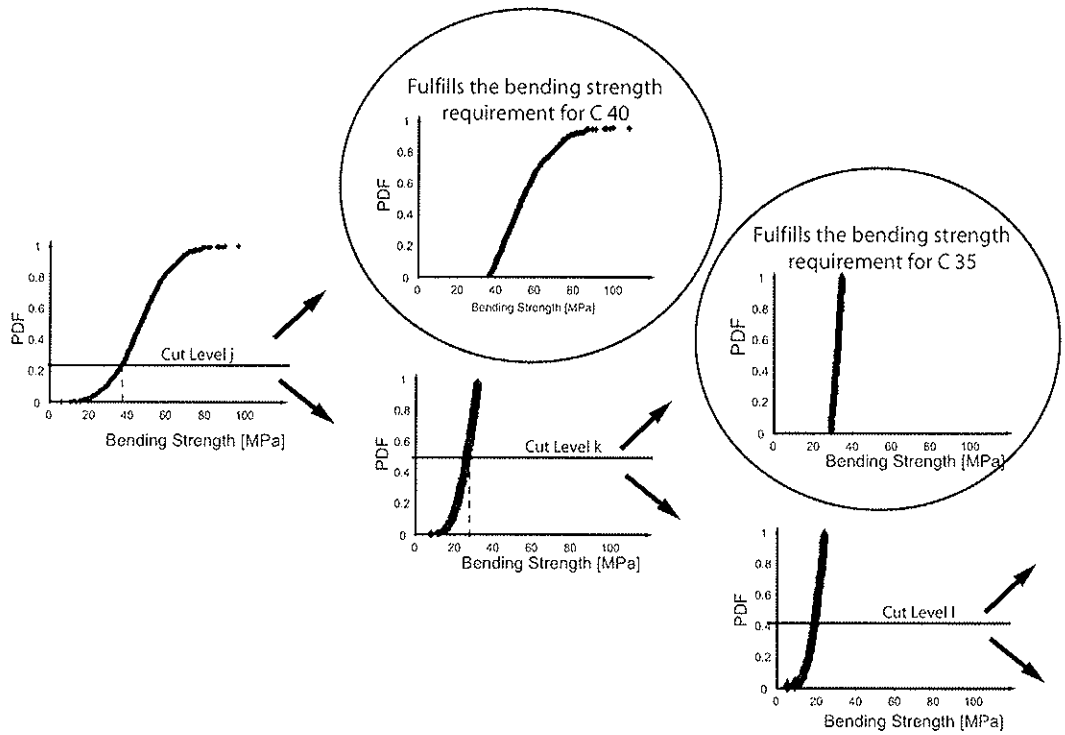

Figure 2 *The principle of the segmentation method exemplified on the bending strength (arbitrary but typical example).*

Table 2 *Optimal Grading (arbitrary but typical example).*

Grade	Proportion
C40	720 (72%)
C30	130 (13%)
C24	89 (8.9%)
reject	61 (6.1%)

Table 3 *A possible size matrix for the grade combination C40-C30-C24-reject (arbitrary but typical example).*

Optimum Grade	Assigned Grades			
	C40	C30	C24	eject
C40	254	412	51	3
C30	11	28	87	4
C24	1	20	45	23
eject	0	3	48	10

6) The determination of an elementary Cost Matrix.

According to Rouger [15] it is considered as unprofitable if timber is assigned to a grade greater than its optimal grade (upgrading) or if timber is assigned to a grade less than its optimal grade (downgrading). Both up- and downgrading is assumed to be associated with costs derived according to the scheme described next.

a) Upgrading:

The mean value of the optimum grade $\mu_{X,opt}$ is calculated based on its characteristic value, i.e. the 5%-fractile value $x_{0.05,opt}$ and assuming that the property is lognormal distributed with a coefficient of variation (cov) of 30%:

$$\mu_{X,opt} = \exp\left(\ln\left(x_{0.05,opt}\right) + \left(0.5\,\mathrm{cov}^2 + 1.645\,\mathrm{cov}\right)\right) \tag{3}$$

Similar, the mean value of the assigned grade $\mu_{X,ass}$ is estimated.

By assuming a target reliability index of $\beta_{target} = 3.0$, an stress applicable to the timber of the assigned grade s_{ass} is calculated as:

$$s_{ass} = \mu_{X,ass} - \beta_{target}\mu_{X,ass}\,\mathrm{cov} \tag{4}$$

s_{ass} is then applied to the timber sub-population corresponding to the optimum grade and a reliability index β is calculated as:

$$\beta = \frac{\mu_{X,opt} - s_{ass}}{\mu_{X,opt}\,\mathrm{cov}} \tag{5}$$

A cost of upgrading is then defined as the difference between this reliability index and the target reliability index:

$$Cost\left(upgrading\right) = \beta_{target} - \beta \tag{6}$$

b) Downgrading:

The cost of downgrading is assigned to be related to the over-dimensioning of beam-type elements in deflection (it is considered that deflection in most cases is the decisive design criteria):

$$Cost(downgrading) = \sqrt[3]{\frac{moe_{m,opt}}{moe_{m,ass}}} - 1 \qquad (7)$$

where $moe_{m,opt}$ and $moe_{m,ass}$ are the MOE's of the optimum and the assigned grade.

Based on the above calculations a so-called Cost Matrix can be derived. A possible Cost Matrix is shown in Table 4.

Table 4 *A possible elementary Cost Matrix (upgrading, dark grey; downgrading, light grey), (arbitrary but typical example).*

Optimum Grade	Assigned Grades			
	C40	C30	C24	eject
C40	0	0.053	0.084	0.326
C30	0.111	0	0.029	0.26
C24	0.222	0.083	0	0.224
eject	0.778	0.5	0.333	0

7) The determination of the global Cost Matrix.

Each value $global_{ij}$ in the global Cost Matrix is obtained by multiplying the corresponding number in each cell of the size matrix $size_{ij}$ by the corresponding value of the elementary Cost Matrix $elementary_{ij}$ and then by dividing by the total number of pieces in the assigned grade, as:

$$global_{ij} = \frac{elementary_{ij} size_{ij}}{\sum_i size_{ij}} \qquad (8)$$

A possible global Cost Matrix is given in Table 5.

Table 5 *A possible global Cost Matrix (arbitrary but typical example).*

Optimum Grade	Assigned Grades			
	C40	C30	C24	eject
C40	0	0.047162	0.018545	0.02445
C30	0.00459	0	0.010922	0.026
C24	0.000835	0.003585	0	0.1288
eject	0	0.00324	0.069195	0

8) Assessment of the global Cost Matrix.

The grading machine settings are considered as appropriate when all global upgrading costs are lower than 0.02. In Table 5 this requirement is not fulfilled.

3.2.2 Discussion of the EN 14081 approach

The principles of the procedure for the derivation of grading machine settings according to EN 14081-2 are briefly summarized above. In the opinion of the authors the procedure exhibits several shortcomings in both, the practical and the theoretical point of view:

Practically, it is considered as a disadvantage that the procedure does not allow for a probabilistic assessment of the material properties based on the derived grading settings. I.e. the gathered information cannot be directly used for the estimation of distribution parameters of the graded timber.

From the theoretical viewpoint several inadequacies can be identified, which, in the opinion of the authors, are too severe to be considered as simplifications or assumptions. The general set up of the method, the assignment of so-called optimum grades by the segmentation technique (compare Figure 2) and taking these segments as a reference is debatable. Furthermore, it seems incorrect to assign Lognormal distributions with a coefficient of variation (cov) of 30% to these segments and perform a reliability calculation (see Equations (3) and (5)). By inspecting the right part of Figure 2 it is clear that the segments are not lognormal distributed and the coefficient of variation is not 30%. In addition, the assumption is not consistent, i.e. for some of the optimum grades the assumption is less inadequate than for others. Another feature which appears inappropriate is the assumption that the cost for upgrading is proportional to the reliability index. Possible cost, however, would better be related to the probability of failure.

Even more features of the method could be questioned; however, the discussion is not continued here.

Quite recently the EN 14081 reached its approval phase. A future task for the research community is to reflect upon the proposed method for the derivation of grading machine settings. Real costs are involved in the structural timber production line and one major issue of competitiveness of structural timber is the consistent representation of the uncertainties according to the timber material properties. It is expected that new more efficient methods will come up soon.

An example for an alternative procedure is presented in the following. Referring to Faber et al. [16] and Köhler and Faber [17] a procedure for the derivation and the control of grading machine settings is presented.

4. Proposed scheme for the derivation and control of grading machine settings

In reliability analysis of timber structures, for the purpose of code calibration in general or for the reliability verification of specific structures, the probabilistic modeling of the material properties is an issue of special interest. As mentioned earlier, at the market timber is always represented as a graded material. It is thus of utmost importance that probabilistic models for timber material properties take the timber grading process into account. Traditionally, this is done implicitly, i.e. by the statistical analysis of populations which are graded to a certain strength class, see, e.g. in Ranta-Maunus et al. [18] or Sørensen et al. [19]. The results of such investigations are highly contradicting; in terms of the proposed distribution functions and in terms of the corresponding distribution parameters. Sometimes it is found that the investigated graded populations are by far 'better' than expected / required (e.g. the fractile values of the basic material properties are

larger than the values required), on the other hand it is sometimes found that graded populations are 'worse' than expected / required. The reason for this situation is that the statistical properties of graded timber material properties are highly dependent on the statistical properties of the underlying population of ungraded timber and on the grading scheme which is applied (comprised of the grading technology and the applied acceptance criteria).

4.1. Accounting for grading scheme and statistical properties of the ungraded population

As demonstrated in Faber et al. [16] the probability distribution function for graded timber material properties can be assessed by taking the statistical properties of the material properties of the ungraded population and the applied grading scheme explicitly into account. The approach is explained along a simple example with one material property of interest σ_C and one indicative property I which is measured non-destructively by a grading machine. The statistical properties of the ungraded population in regard to σ_C are modelled by the prior density function $f'_{\sigma_C}(s)$. When a grading procedure has been applied the prior density function is no longer representative for the graded timber specimens. In order to assess the representative probability density function use may be made of Bayes's rule yielding the posterior probability density function $f''_{\sigma_C}(s)$, i.e. the probability density function, which can be assumed for the material property σ_C, categorized into a particular grade by application of the grading acceptance criteria A_C.

$$f''_{\sigma_C}(s) = P\left(\sigma_C = s \middle| A_C\right) = \frac{1}{c} f'_{\sigma_C}(s) \cdot P(A_C | \sigma_C = s) \tag{9}$$

where $c = P(A_C)$.

It is seen from Equation (9) that it is necessary to estimate the likelihood of the implementation of the selection acceptance criteria, i.e. $P(A_C|\sigma_C = s)$ as a function of the specific value of the material property σ_C. This likelihood may, however, be assessed if test results are available from timber specimens tested both, in regard to the indirect characteristic I, e.g. the flatwise bending stiffness, and the material property of interest σ_C, e.g. the edgewise bending strength. Assuming that such test results are available a regression analysis can be performed based on which the statistical characteristics of the indicator, e.g. the flatwise bending stiffness can be assessed for a given value of the relevant material property.

The regression analysis takes basis in n simultaneous observations of the material property of interest $\sigma_C = (\sigma_{C,1}, \sigma_{C,2}, ..., \sigma_{C,n})^T$ and of the indicator $I = (I_1, I_2, ..., I_n)^T$. Assuming that at least locally a linear relationship between σ_C and I exists, the regression may be performed on the basis of

$$I = a_0 + a_1 \cdot \sigma_C + \varepsilon \tag{10}$$

where a_0 and a_1 are the regression coefficients and ε is an error term. Assuming that the error term ε is normally distributed with zero mean and unknown standard deviation σ_ε the maximum likelihood method, see e.g. Lindley [20] may be used to estimate the mean values and covariance matrix for the parameters a_0, a_1, σ_ε.

The acceptance criteria applied for the categorization of timber into different grades may be formulated in terms of the values of the indicators. Typically the criteria have the following appearance

$$A_C = \{b_L \leq I \leq b_U\} \tag{11}$$

where b_L and b_U are lower and upper bounds of the indicators for a particular grade.

Having performed the regression analysis, it is possible to assess the acceptance probability i.e. $P(A_C|\sigma_C = s)$ by

$$P(A_C|\sigma_C = s) = P(b_L \leq a_0 + a_1 \cdot \sigma_C + \varepsilon \leq b_U|\sigma_C = s) = P(b_L \leq a_0 + a_1 s + \varepsilon \leq b_U) \tag{12}$$

which is straight forward to assess recognizing that the indicator I is normal distributed.

4.2. Identification of a (cost) optimal grading procedure

Based on the explicit formulation of quality control in Equation (9), it is possible to select an optimal grading procedure by utilizing a cost benefit criterion. This is proposed in Köhler and Faber [17] where the idea is illustrated along an indicative example. In the following the basic idea is summarized.

The benefit of a set of timber grades identified by the grading procedure GP may be written as

$$B_T(f'_{\sigma_C}(s), A_C, GP) = \mathbf{V}^T \cdot \mathbf{C}_{grade} \tag{13}$$

where $\mathbf{V}$ is a vector of volumes of particular grades, which can be identified depending on the prior probability distribution of the relevant material property, the set of acceptance criteria and the grading procedure. $\mathbf{C}_{grade}$ is a vector of the (monetary) benefit of the timber grades per unit volume. If the prior probability distribution of the relevant material property, the grading procedure, the set of timber grades and their monetary benefits are known, the optimal set of acceptance criteria A_C may be found by solving the following optimization problem.

$$\max_{A_c} B_T(f'_{\sigma_C}(s), A_C, GP) \quad \text{subject to: } \mathbf{N}_{req}, \mathbf{C}_{grade} \tag{14}$$

subject to normative requirements which have to be fulfilled by the grades, $\mathbf{N}_{req}$, and the cost vector $\mathbf{C}_{grade}$. Involving the investment, maintenance over lifetime costs, costs for personnel, etc. of a particular grading procedure by the function $C_G(GP)$ the optimal grading procedure may be identified by solving

$$\max_{GP}\left[\left(\max_{\substack{A_c \\ \text{subject to: } \mathbf{N}_{req}, \mathbf{C}_{grade}}} B_T(f'_{\sigma_C}(s), A_C, GP)\right) - C_G(GP)\right] \tag{15}$$

4.3. Updating the probabilistic framework for timber grading by using new information – link to the output control scheme

The framework proposed in section 4.1. and 4.2. corresponds to a machine controlled scheme; the so-called grading machine settings are established based on a substantiated analysis prior to the operation phase of the grading machine. In general, such an analysis is performed once and it is assumed that the calibrated grading machine settings provide a stable and efficient output in terms of reaching the prescribed timber grade requirements for the envisaged grades. This assumption includes that the statistical properties of the ungraded material are stable, i.e. that the gross supply of ungraded timber is randomly sampled from identical populations. It is self evident that mostly this is not the case. The statistical properties of the ungraded material vary as the origin of the timber and the processing practice varies. It is important that the grading scheme can take this variation into account, i.e. that the parameters of the prior probability distribution and the parameters of the regression equation can be updated according to new information which might be available during the operation of the grading machine.

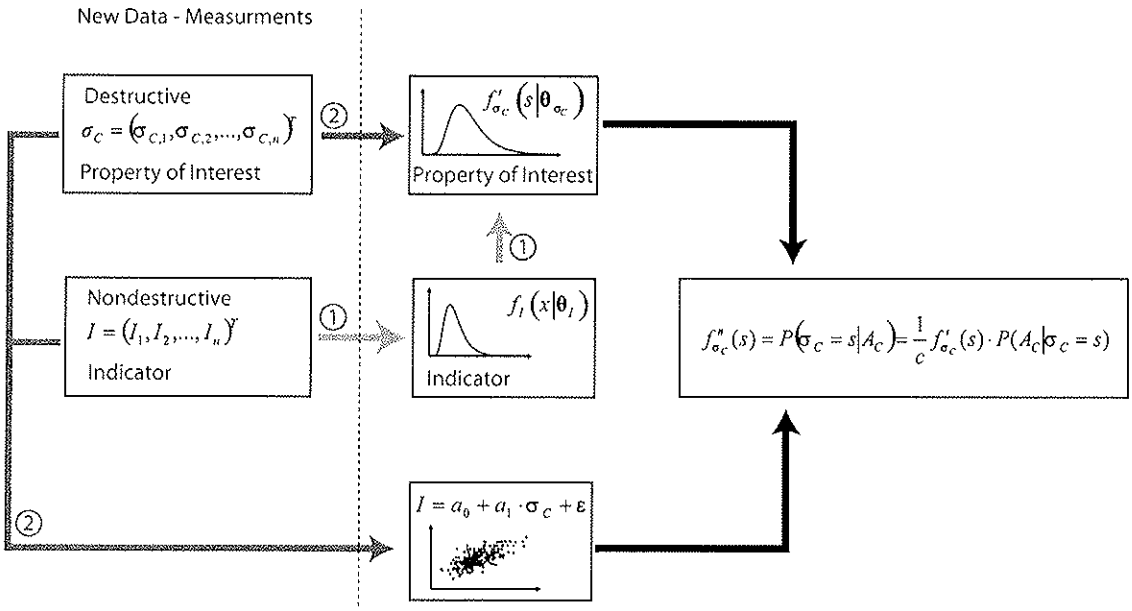

Figure 3 *Possibilities for updating the grading scheme; 1. updating the prior probability distribution by using indirect information, 2. updating the prior probability distribution and the regression by using direct information.*

In Figure 3 the different possibilities for upgrading the grading scheme are illustrated. Possibility '1' is denoted as the utilisation of information about the indicator, i.e. the grading machine measurements, for updating the prior density function of the material property of interst. It is evident that this information is always available during the operation phase of the grading machine, thus, using this information for updating the grading scheme represents a very efficient way for the (output) control of the grading machine. It can also be imagined to perform destructive test of the grading machine output in regard to the material property of interest. The gathered (direct) information might then be used for updating the prior density function of the material property of interst, but also for updating the regression parameters (as indicated as possibility '2' in Figure 3). A further possibility to enter new information which can be utilized for updating is the use of

proof loading data. Proof loading data represents qualitative information, which can be integrated properly. The methodological framework for updating is 'Baysian statistics' and for the corresponding inference it is referred to literature, as for example Lindley [20].

5. Conclusion and Summary

Machine grading is introduced as a prerequisite for the safe and efficient utilization of timber in load bearing construction. It is focused on machine grading schemes and the currently applied strategies for the control of grading machine settings are discussed. The *CUSUM* method is described as a typical methodology for output controlled systems, the methodology first proposed in Rouger [15] and now implemented in the European Standard EN 14081 is taken as an example for a machine controlled system. It is noted that both control methods do not allow for a probabilistic assessment of the graded timber material properties based on the corresponding formalism of the control methods. Furthermore, several shortcomings within the machine controlled method according to the European standard EN 14081 are outlined and discussed.

Based on Faber et al. [16] an alternative method is described; the statistical assessment of timber material properties has been considered with special emphasis on the modelling of the effect of different schemes for quality control and grading of timber. The suggested approach not only forms a very strong tool for the statistical quantification of the material characteristics of timber but furthermore provides a consistent basis for quantifying the efficiency of different quality control and grading procedures. The probabilistic models for the graded timber material properties have been formulated such that they readily may be applied in structural reliability analysis.

It is of utmost importance that the statistical characteristics of timber material properties are assessed and treated in consistency with the implemented quality control and grading procedures. Only then a consistent basis may be established for the quantification of the reliability of timber structures - the basis for codification of design and assessment. The suggested probabilistic modelling seems to provide the required framework for establishing such a basis by means of quantifying the efficiency of the different quality control and grading procedures. It is envisaged that different quality control grading procedures may be described by means of their regression characteristics and acceptance probability curves corresponding to different grading criteria. A format for the standardisation of the probabilistic modelling of timber materials subject to different quality control and grading procedures is suggested in Faber et al. [16]. It is important that the appropriateness of such a format is discussed and that a consensus is achieved in this respect in the near future.

Based on Köhler and Faber [17] in section 4.2 it has been demonstrated how an optimal (in terms of monetary benefit) set of timber grades can be identified through the solution of an optimisation problem. The objective function of the optimisation problem is defined based on the methodology presented in section 4.1. The implementation of the proposed approach in practice would have to incorporate factors such as the marked price of timber, potential demand of the building sector, etc into the formulation of the benefit function. Further studies in close collaboration with the timber industry should be undertaken and discussed to clarify these aspects and to set up a rational basis for their assessment. However, according to the preferences of a sawmill owner the proposed approach facilitates the identification and the calibration of a grading procedure and thus an increase in the overall production benefit.

It is also discussed how new information obtained during the operation phase of the grading machine can be used for updating the model parameters involved. Bayesian statistics constitutes the basis for these updating schemes and a publication is plan which aims the illustration of typical updating situations in timber engineering along some illustrative examples.

References

[1] Joint Committee of Structural Safety (JCSS, 2001). Probabilistic Model Code, Internet Publication: www.jcss.ethz.ch.

[2] COST Action E 24, Reliability of timber structures. Several meetings and Publications, Internet Publication: http://www.km.fgg.uni-lj.si/coste24/coste24.htm, 2005.

[3] Köhler J., Sorensen J.D., Faber M.H. (2005) Probabilistic Modeling of Timber Structures. Proceedings of the international Conference on Probabilistic Models in Timber Engineering, Arcachon, France 2005.

[4] Madsen B. (1992). Structural Behaviour of Timber. Timber Engineering Ltd., Vancouver, Canada.

[5] Walker J. C. F. (1993). Primary Wood Processing. Chapman & Hall.

[6] Green, D.W. and Kretschmann, D.E. (1997). "Properties and Grading of Southern Pine Timbers", Forest Products Journal, Vol.47, No.9.

[7] Blass H.J. (editor) (1995) STEP 1: Timber Engineering, Basis of Design, Material Properties, Structural Components and Joints. Centrum Hout, The Netherlands.

[8] Thelandersson S. and Larsen H. J. (2003). Timber Engineering. John Wiley & Sons Ltd. Chichester, UK.

[9] Johansson C.-J., Brundin, J. and Gruber R. (1992). Stress grading of Swedish and German timber. A comparison of machine stress grading. SP REPORT 1992:23.

[10] Boström L. (1994). Machine strength grading. Comparison of four different grading systems. Swedisch National Testing and Research Institute, SP REPORT 1994:49.

[11] Ewan W. D., Kemp K. W. (1960). Sampling inspection of continuous processes with no autocorrelation between successive results. Biometrika 47, pp. 363-380.

[12] Warren W. G. (1978). Recent developments in statistical quality control procedures for MSR. Proceedings of Fourth Nondestructive Testing of Wood Symposium. Vancouver, Canada.

[13] Leicester R. H. and Breitinger H. O. (1994). Statistical control of timber strength. Proceedings of the 27th Meeting, International Council for Research and Innovation in Building and Construction, Working Commission W18 – Timber Structures, CIB-W18, Paper No. 27-17-1, Sydney, Australia, 1994.

[14] Rouger F. (1996). Application of a modified statistical segmentation method to timber machine strength grading. Wood and Fibre Science. 28(4).

[15] Rouger F. (1997). A new statistical method for the establishment of machine settings. Proceedings of the 30th Meeting, International Council for Research and Innovation in Building and Construction, Working Commission W18 – Timber Structures, CIB-W18, Paper No. 30-17-1, Vancouver, Canada, 1997.

[16] Faber M. H., Köhler J. and Sørensen, J. D. (2004). Probabilistic modelling of graded timber material properties. Journal of Structural Safety, 26(3), pp. 295-309.

[17] Köhler J., Faber M. H. (2003). A probabilistic approach to cost optimal timber grading. Proceedings of the 36th Meeting, International Council for Research and Innovation in Building and Construction, Working Commission W18 – Timber Structures, CIB-W18, Paper No. 36-5-2, Colorado, USA, 2003.

[18] Ranta-Maunus A., Fonselius M., Kurkela J. and Toratti T. (2001). Reliability Analysis of Timber Structures. VTT Research Notes, Espoo, Finland.

[19] Sorensen J. D. and Hoffmeyer P. (2001). Statistical Analysis of Data for Timber Strength. Paper No 206, Structural Reliability Theory, Dep. Of Building Technology and Structural Engineering, Aalbourg University.

[20] Lindley D. V. (1965). Introduction to Probability & Statistics. Cambridge University Press.

AS 3519: Standards Australia: Timber – Stress graded – Procedures for monitoring structural properties. Sydney, Australia, 1997.

AS 4490: Standards Australia: Timber – Machine proof grading. Sydney, Australia, 1997.

ASTM D 245: Standard practice for establishing structural grades and related allowable properties for visually graded lumber. ASTM Book of Standards.

ASTM D 6570: Standard Practice for Assigning Allowable Properties for Mechanically-Graded Lumber. ASTM Book of Standards.

EN 14081 part 1-4: Timber Structures – Strength Graded Timber with rectangular Cross Section. Comité Européen de Normalisation, Brussels, Belgium, 2005.

EN 338: Structural Timber – Strength Classes. Comité Européen de Normalisation, Brussels, Belgium, 2003.

EN 408: European Standard: Timber structures - Structural Timber - Determination of some physical and mechanical properties. Comité Européen de Normalisation, Brussels, Belgium, 2004.

ISO 8375: Solid timber in structural sizes – determination of some physical and mechanical properties. International Organisation for Standardisation, 1985.

NBCC (1980): (National Building Code of Canada), National Research Council of Canada.

INTERNATIONAL COUNCIL FOR RESEARCH AND INNOVATION
IN BUILDING AND CONSTRUCTION

WORKING COMMISSION W18 - TIMBER STRUCTURES

TENSILE PROOF LOADING TO ASSURE QUALITY OF FINGER-JOINTED STRUCTURAL TIMBER

R Katzengruber
G Schickhofer
Institute for Timber Engineering and Wood Technology
Graz University of Technology

G Jeitler
holz.bau forschungs gmbh
Graz

AUSTRIA

MEETING THIRTY-NINE
FLORENCE
ITALY
AUGUST 2006

Presented by R Katzengruber
JW van de Kuilen asked about the issue of influence of moisture content on the curing time. R Katzengruber responded that the moisture content of the specimens was checked in detail and they were within expectation.
H Riberholt commented that the choice of proof stress level would be important as too high a level would lead to too many failures; therefore, the issue of how much failure would be considered acceptable in practice would be an important issue. Further discussion took place on the suitability of the grading rules in relation with the number of failures observed. As the number of failures was high, the appropriateness of the rules would be in question.
T Williamson commented that in the US finger jointed material for flange stock of I joist have been in use for over 5 years and it is an accepted practice by manufacturers.

Tensile Proof Loading to assure Quality of Finger-Jointed Structural Timber

Katzengruber, R.[1], Jeitler, G.[2], Schickhofer, G.[3]

Institute for Timber Engineering and Wood Technology, Graz University of Technology[1,3]

holz.bau forschungs gmbh[2]

Graz, Austria, Europe

1 Introduction / Problem / Motivation

Timber as a natural growing raw material displays large variations in its mechanical characteristics like strength and stiffness in comparison to other materials such as e.g. steel. These variations can be considerable precise with the beam-shaped product structural timber, characterised by lack of homogenisation over the cross-section through gluing of individual components. A statistical 'system effect' which can be considered for glulam or bi- or trilam is not present for single sections. Although grading criterions are defined in DIN 4074-1 with the currently common grading processes strength reducing defects such as the global and local grain deviation, compression failures, reaction wood, pre-broken timber or damage of tree-top are only with difficulty and often not economically ascertainable. Rogues in the lowest quantile area of strength cannot be excluded for sure. The grading process within the production of structural timber is therefore still a challenge.

Even so, performance and minimum production requirements for finger joints of structural timber are regulated in EN 385, a similar difficulty comes up with the joining. This is because for internal and external quality control only the bending strength and mode of failure of few randomly taken finger joint samples are determined in destructive tests. This also results in the fact that structural timber with features responsible for poor finger joint strength can reach the customers.

2 State of the Art

2.1 Grading of Structural Timber

In the German speaking area the most common grading method for structural timber is done by visual inspection according to DIN 4074. The structural timber is mostly graded to class S10 which is assigned strength grade C24 pursuant to EN 338. The grading criterions most commonly used are knottiness, cracks, deformations, annual ring width, wane and discolouration. For the product KVH® *(Konstruktionsvollholz)* additional stricter requirements like the moisture content ($u_m = 15 \pm 3\%$), sawing pattern (pith separated), the dimensional stability (± 1 mm for cross-sections ≤ 100 mm, ± 1.5 mm for cross-sections > 100 mm) and visual appearance (seasoning cracks, knottiness, discolorations, warping, surface quality, wane) are to be obtained. The requirements for KVH® differentiate between applications in visible and non-visible areas.

Stress grading of structural timber by means of bending machines, which determine average Modulus of Elasticity *(MOE)* over short lengths, is because of the limited operating range restricted to the grading of glulam laminations and scaffold boards with a maximum thickness of 75 mm. By use of X-ray radiation and vibration measurements (eigenfrequency) joists and beams up to 100 mm can be graded [4]. The preferred cross sections (width $\leq$ 140 mm, thickness $\leq$ 240 mm) used for KVH® production go beyond the capabilities of approved grading machines.

2.2 Proof Loading

Commonly spoken, *'proof loading'* as a testing method is defined by specimens which are subjected to a defined and generally brief mechanical loading. All samples not reaching a set proof level due to premature material failure can be separated from those with greater strength. Proof loading is a recognized quality control technique to improve the characteristics of the lower tail of strength distribution. Numerous scientific research works on the topic and especially in respect of possibly damaging the material have been published since the late sixties of the last century. Proof of any possible damage is generally considered to be very difficult to impossible. Strickler et al. (1969) for example investigated in [7] proof loaded finger joints and concluded that a bending proof load up to 90 % of the expected ultimate strength did not significantly reduce the strength and by comparison, a tensile proof load was considered feasible, without qualification.

Woeste et al. (1987) conducted in [8] experiments on 1,200 pieces of lumber with single and reverse bending loads and detected no damage due to proof loading. Heatwole et al (1991) stated the following in their literary research on damage [9]: *'Based on published research it is valid to assume there is no appreciable damage to surviving lumber due to proof loading in tension or bending at these low load levels'*. Lam et al. (2003) pointed out in [10] that one of the difficulties is the need of rather large sample sizes for an experimental-based study to develop statistical solutions to quantify the effectiveness on the use of proof loading in relation to the proof level, the potential damage on the members and the improvement of performance in the context of reliability based design methods.

Proof loading is therefore not a new development in the timber construction sector; it is rather already familiar for many years, primarily from North America and Australia and also embedded in manuals [5] and standards [6]. Whereas in Europe apart from those stress grading machines mentioned in 2.1, which in principal do a proof loading of the material in bending, the authors know of no approved industrial proof loading application for structural timber. Test methods working with tensile loads are still uncommon obviously due to the difficulties of applying the loads.

3 Tensile Proof Loading / Functioning of the Testing Device

The target definition of the research project 'qm_online' was the development of a quality control method to assure high product performance of finger jointed structural timber especially in respect to strength characteristics. In particular the following aspects should be fulfilled:

- Every produced piece and therefore the whole volume of the material should be tested.
- No dents should remain on the surface and damage is allowed.
- Testing has to be integrated in production and must not reduce production output.

- Information valuable for design purposes - like strength and stiffness - should be available.

The approach to comply with all defined aspects was tensile proof loading at a high production level. Because loading in bending is difficult to achieve with cross sections typical for structural timber and has disadvantages when stress reducing failures have to be detected in the compression zone, loading in tension was selected. Further this implies, in contrast to bending, a constant stress distribution over the entire timber volume within the free test length.

For development of an appropriate device for industrial applications research was carried out in respect of determination of the most significant mechanical parameters of the testing device (maximum tensile force, clamping plate geometry and surface structure, capacity of the machine and measuring technique) and to determine the time dependant strength of the adhesive used for the finger joints [11]. The 8 to 18 m long rods are individually loaded into the transverse conveyor of the proof loading device at least two hours after the finger jointing process. A curing time of 120 minutes for the PU adhesive Purbond® HB 530 is considered as sufficient for the application of a proof level up to 10 N/mm² without damage of the finger joint. Tensile tests on not fully cured finger joints were worked out to for confirmation. The PU adhesive Purbond® HB 530 showed that already after 90 minutes a strength level is achieved which is within the scattering of the end strength determined on fully cured joints.

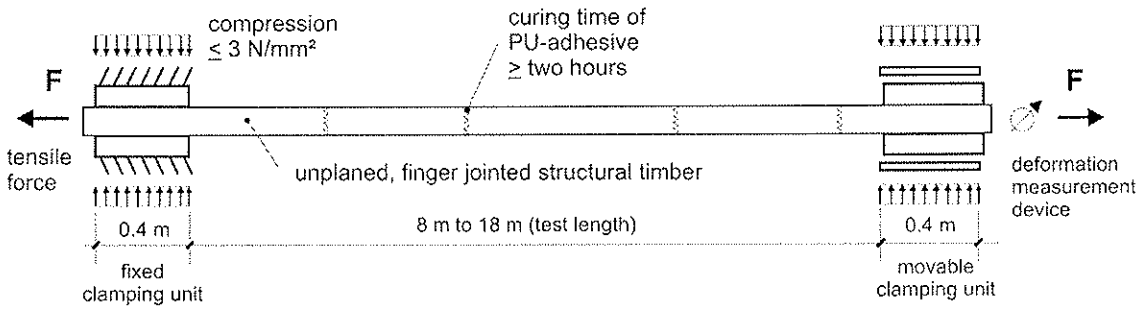

Fig. 1: System sketch of the tensile proof loading device for industrial application

Within the proof loading process a centering device puts each beam into a defined test position. As shown in figure 1 the beam ends are then clamped with profiled steel plates over a length of 400 mm and the corresponding section width. In this way the structural timber is subjected to a defined stress in terms of duration and load factor. During the stress test the proof load and associated deformations are continuously recorded, whereby the mean MOE over the full length up to 18 m can be determined. Rejection parameters of the control program can be sudden drops of the tensile force, too great deflections or when the set proof level is not reached in a certain time or held constant over the defined period. Only those rods running through the test without fraction or error in the control program are fed to the following profiling process. Adjustment to the length of the structural timbers to be tested is provided by the lengthways continuously movable clamping unit.

4 Cyclic Tensile Proof Loading / Experience

Especially to clarify the risk of eventually damaging the material within a tensile proof loading process a cyclic stressing of finger jointed structural timber was analysed with a high number of specimens. Therefore, within special observation periods timber with various cross sections and lengths were produced. All rods were mechanically tested

(proof loaded) using the device as described in figure 1 in industrial environment. In principle two different series (A and B) were investigated in respect of type of loading. Within series A the specimens were tensile stressed to approximately 7 N/mm² and after a short release to a level of approximately 8 N/mm². In contrast the specimens of series B were stressed three times to 12.8 N/mm² but had the same level of release as in series A. Within all cycles the time of effectively loading the material at constant stress was in the range of 1.3 to 2.0 seconds. The speed of loading was, depending on the actual cross section, in the range of 20 to 30 kN/s. Within the total time of loading data (time, tensile force, and extension of end grain) was recorded automatically at a rate of 4 Hz. In table 1 the proof loading programmes are illustrated exemplarily.

Double stress test (Series A)	**Triple stress test** (Series B)
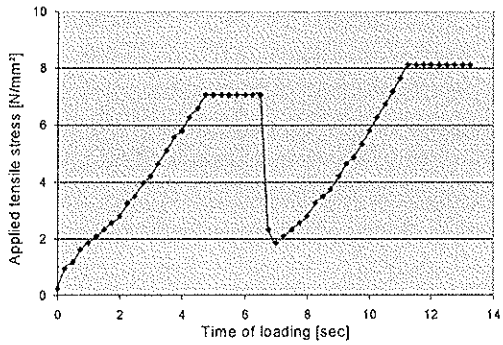	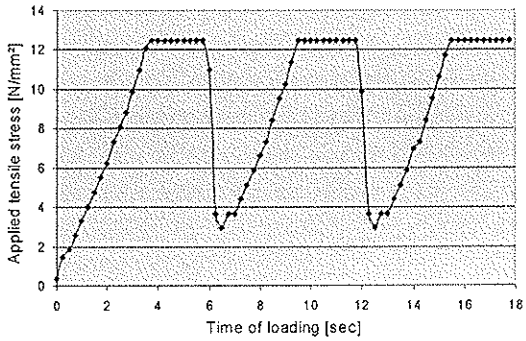
proof level_1 = 7 N/mm², level_2 = 8 N/mm²	proof level_1 = level_2 = level_3 = 12.8 N/mm²
Various cross sections: 65 mm < width < 125 mm, 105 mm < height < 285 mm	Cross section: 63 x 145 mm²
Tested volume: ~ 1.100 m³ number of tested rods: 4,886 # (39,000#) number of tested finger joints: ~ 30,000 #	Tested volume: 63 m³ number of tested rods: 575 # (5,480#) number of tested finger joints: ~ 3,000 #

Tab. 1: Test series to clarify risk of damage when tensile proof loading

The tested volume equals approximately one thousand one hundred (!) cubic meters and 63 m³ of structural timber in series A and series B, respectively. The mean free testing length for both series was approximately 12.0 m. Transposed onto the referred test piece length, acc. to EN 408 of nine times the larger cross-sectional dimension, this would roughly equal 39,000 (!) and 5,480 (!) tests with a free span of approximately 1.6 m und 1.3 m for series A and series B, respectively.

The timber (spruce and pine) for both series was graded acc. DIN 4074 to class S10 by means of visual inspection and an X-ray scanner. There was no separation of higher class material. The finger joints, fulfilling the requirements acc. to EN 385, were characterized by a finger length of 20 mm and a distance between fingers of 5 mm.

The results of the cyclic stress tests are summarized in table 2.

Double stress test (Series A)	**Triple stress test** (Series B)
Number of fractures: within 1st loading: 37 # within 2nd loading: 28 # within 2nd loading and below level_1: 2 #	Number of fractures: within 1st loading: 79 # within 2nd loading: 3 # within 3rd loading: 1 #
Magnitude of damage expressed as loss of strength = 9 % resp. 12 %	Magnitude of damage expressed as loss of strength = 0 %

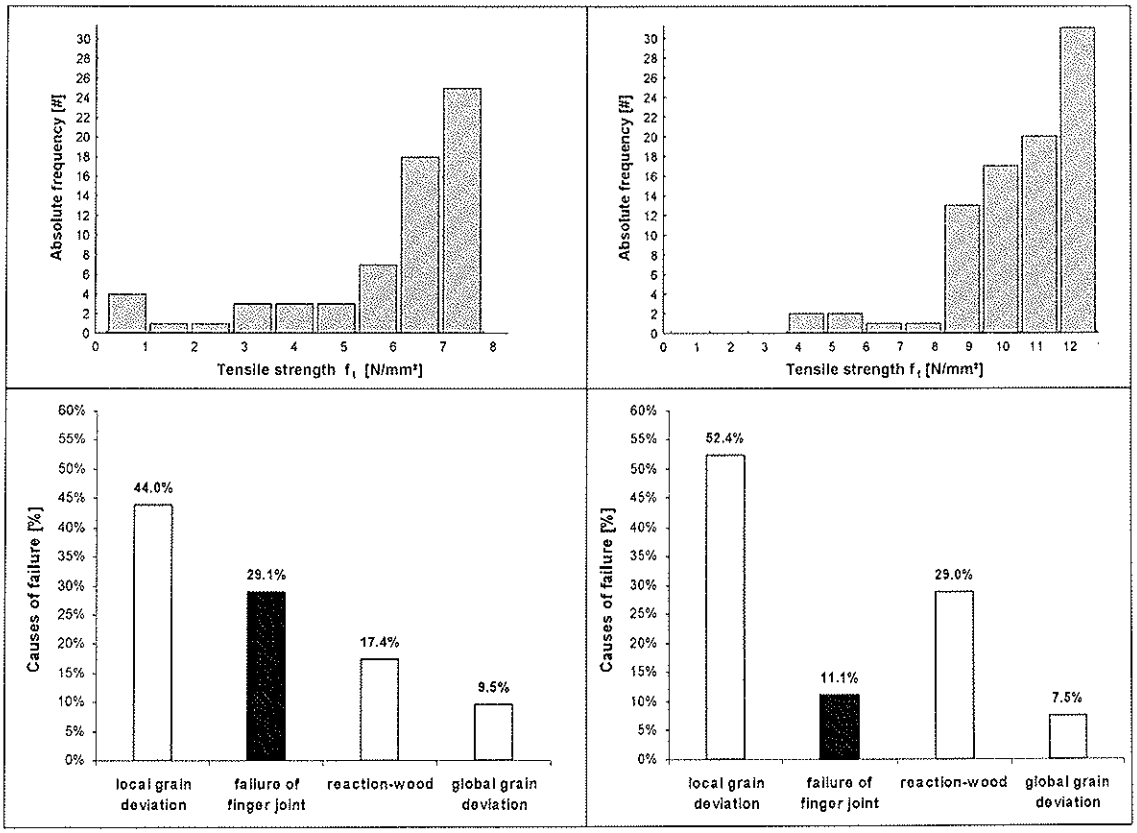

Tab. 2: Results of cyclic stress tests of finger jointed structural timber

In total 65 rods (out of 4,886 #) failed within the double stress test of series A due to fracture of the material or the joints. 37 rods failed before stress was relieved the first time ($\leq$ 7 N/mm²) and 28 rods within the second proof loading step ($\leq$ 8 N/mm²). Only 2 of those rods which failed within the second step failed on a level below proof level_1 thus indicating having been damaged. The extent of damage, expressed as loss of strength, was in the range of 9 to 12 %.

Within series B 79 rods out of 575 # failed before the timber was released the first time. Only 3 rods and 1 rod failed within the 2nd and 3rd cycle, respectively. All these fractures occurred within time of holding the proof level constant. The observed extent of damage, expressed as loss of strength, was therefore in this case 0 % (no damage).

The frequency distribution of tensile strength of all broken specimens and causes of failure are shown in table 2. It is conspicuous that near zero an accumulation is observed for series A. This is because the specimens with nearly 'no strength' are related to faults of finger joints due to deficiencies in joint production. The rest of the lower tail of strength distribution shows the expected characteristic of rampant increase of failures with increased tensile strength.

The dominant cause of failure within the lower tail of strength distribution was, as shown in table 2, **failure of the wood** at 70.9 % and 88,9 % for A and B, respectively. The failure analysis further shows that the local grain deviation often associated with the surrounding area of knots, knot clusters or a broken tree-top is thereby the main cause of failure of this material. It has to be noted that many of the failure causing features could only be detectable with difficulty and apparently not with the applied grading procedure. This was confirmed by close examination of the broken pieces in respect to the grading criterions.

Hence the associated grading represents the limiting factor for structural timber from this production.

The following figures show some typical examples of severe timber defects which could be detected by means of tensile proof loading. Figure 2 shows an extreme local grain deviation caused by a **broken tree top** responsible for low tensile strength. It was also observed that not only one defect causes the failure, rather as illustrated in figure 3, it is a combination - often with **reaction wood**.

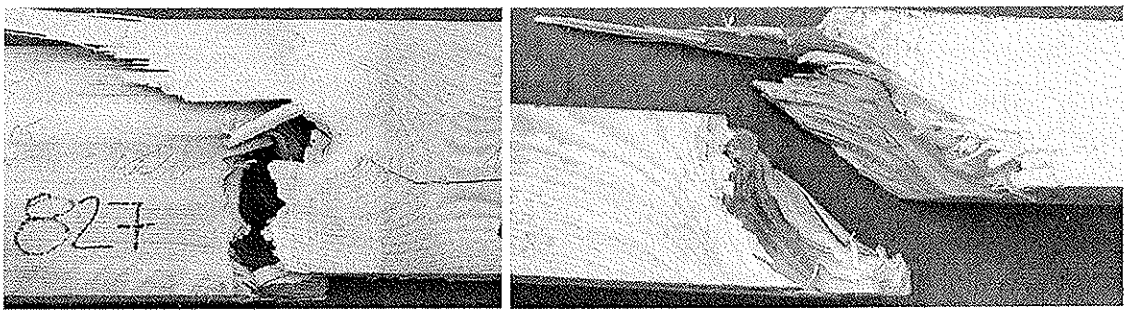

Fig. 2: Low tensile strength due to local grain deviation caused by a broken tree-top (Spec.Nr.827)

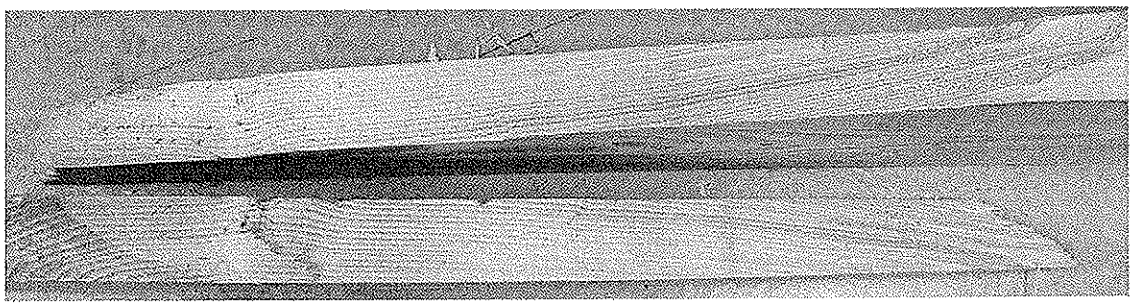

Fig. 3: Tensile strength = 5.8 N/mm² due to reaction-wood and global grain deviation (Spec.Nr.1333)

Compression damages are due to deformations of the wood fibres resulting from excessive compression shakes (impacts) along the grain. They may develop in standing trees due to high loads from storm or snow. They also may result from stresses imposed by lumbering or inadequate handling. As shown in figure 4 (left) they are very difficult to detect on planed surfaces. Because the distorted fibres lead to brittle fracture in processed timber already at relatively low stresses, compression damages can be detected with a tensile proof loading procedure.

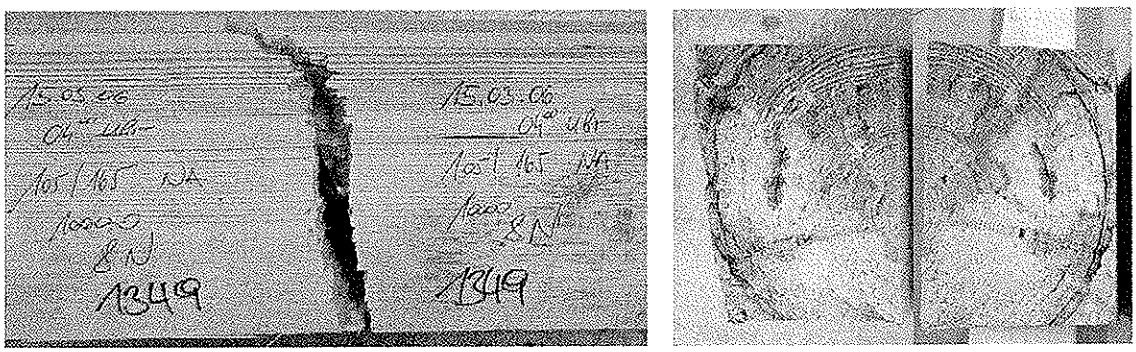

Fig. 4: Tensile strength = 6.4 N/mm² due to compression damage of the timber (Spec.Nr.1349)

5 Discussion and Conclusions

The completed cyclic stress tests, as described in point 4, confirm that a low tensile stress not leading to failure, only minimally affects the strength of structural timber. The evidence that the material is not significantly damaged is herewith clearly adduced. The number of tested specimens (4,886 #) or rather 39.000 # with the referred test length of 1.6 m of series A in relation to the number of faults with slightly reduced strength characteristics (2 #) after the first stressing seems to be sufficient to confirm that statement. The triple stress test of series B confirm further, that a tensile load that could be sustained once (not leading to failure) can be sustained in 99,47 % of the cases again and in 99,29 % of the cases a third time, indicating not being damaged. The results of experimental research work as presented on that high number of specimens show clearly that there is NO appreciable damage to surviving timber due to tensile proof loading at low load levels. Or in other words: The timber is not significantly damaged within tensile proof loading as described in this paper.

The conclusion therefore clearly is that it is better to have tensile proof loaded timber in structural applications than the risk of 'rogues' with poor strength characteristics. Further there should not be any doubt of stressing timber up to the level of design strength which is specified for grade C24 with $f_{t,0,d} = f_{t,0,k} / \gamma_m * k_{mod} = 14 / 1.3 * 1.1 = 11.8$ N/mm², assuming an instantaneous load duration.

Because the length effect (k_{length}) in wood is characterised by reduced scatter and decreased strength characteristics with increasing length its consideration is important for design purposes when it comes to long structural elements. However the testing length has no influence on the result of tensile proof loading in respect to failure recognition. When at a certain point of the specimen the fracture occurs due to the loading the residual volume is released. Further defects of the specimen with also poor strength characteristics, but higher than the one before can only be detected within a repeated proof loading process. In connection with the failure modes and the associated 'learning effect', the proof loading method represents a significant possibility of systematically improving grading within the production process, whether visual or mechanical.

A further area of application of the test method presented here and implanted on an industrial level exists for other sawn timber products in the branch. Glulam production is particularly considered here. It is conceivable to also implement the presented proof loading method in an adapted form for the online quality assurance of finger jointed single lamellas. Furthermore application of the method for testing finger jointed flange sections of I-profiles and nail plate binders is considered sound.

Generally, a timber product with a more reliable minimum strength should be made available to the construction industry by the presented tensile proof loading method as every piece in the lower area of the strength distribution is rejected. The increased reliability for proof loaded finger jointed structural timber could also be reflected in a more favourable partial-coefficient. The corresponding quantification in dependency of the proof level and coefficient of variation of the base material is part of further investigations in cooperation with G.I. Schuëller (Institute of Engineering Mechanics, Leopold-Franzens University, Innsbruck, Austria).

6 Relevance to the European Standards

In consideration of the fact that grading processes of timber still can have inaccuracies and not every strength reducing timber feature can be detected for sure, tensile proof loading should be a recognized quality control system within the European Standards. In particular the 'factory production control' of EN 14081-1 and -3 is addressed here.

The use of a tensile proof loading device is also a very good way to safely ensure that finger joints responsible for poor tensile strength do not reach the customers. Tensile proof loading represents a valuable extension of internal quality control of the finger joint production process - due to the fact that unknown deficiencies in the joining processes can occur. In contrast of bending a few randomly taken specimen as claimed in prEN 15497 (following EN 385) stressing every finger joint in tension is rather more sensitive in respect of failure recognition due to the uniform stress level over the whole volume. Especially in prEN 15497 the following sentence should be included in clause 6.3.4.1 (Sampling within the factory production control):

'If all finger joints are proof loaded according to a harmonized technical specification then the sampling and testing may be omitted.'

In this respect a national standard (ON) is worked out at the moment in Austria within the National Standard Committee (ON-K 012), which will define the technical specification in detail.

7 Acknowledgements

The presented research work was carried out within a project of the competence centre holz.bau forschungs gmbh in collaboration with the Institute for Timber Engineering and Wood Technology of Graz University of Technology for 'Holzindustrie Leitinger GmbH'. The project was supported with funds from the Federal Ministry of Economics and Labour (BMWA), of the province of Styria and the city of Graz as part of the programme Centres and Networks of Excellence for Technology Development of the BMWA.

We would like to thank the chairman of the supervisory board H.P. Leitinger for his always positive attitude to research and development and his team, particularly A. Huber and A. Steinberger. Special thanks go to the scientific advisory board of the holz.bau forschungs gmbh (H.J. Blaß, J. Eberhardsteiner, E. Gehri, W. Guggenberger, H. Kreuzinger, A. Reiterer) for the valuable discussions in the course of the board-meetings. G. Ledinek also deserves mentioning for his readiness to build a pilot tensile proof loading device.

8 References

[1] DIN 4074-1:2003. *Strength grading of wood - Part 1: Coniferous sawn timber.*

[2] EN 385:2001. *Finger jointed structural timber - Performance requirements and minimum production requirements.*

[3] EN 338:2003. *Structural timber - strength classes.*

[4] EN 14081-4:2005. *Timber structures - Strength graded structural timber with rectangular cross section - Part 1: General requirements, Part 3: Machine grading; additional requirements for factory production control, Part 4: Machine Grading - Grading machine settings for machine controlled systems.*

[5] AITC 200-2004. *Manufacturing quality control systems manual for structural glued laminated timber.* American Institute of Timber construction, pp. 55-57.

[6] AS 3519-1993. *Timber - Machine proof-grading.* Australian Standard.

[7] Strickler, M.D., Pellerin, R.F., Talbott, J.W., 1970. *Experiments in Proof Loading Structural End-Jointed Lumber.* Forest Products Journal Vol. 20, No.2., pp. 29-35.

[8] Woeste, F.E., Green, D.W., Tarbell, K.A., Marin, L.A., 1987. *Proof loading to assure lumber strength.* Wood and Fibre Science, pp. 283-297.

[9] Heatwole, E., Woeste, F.E., Green, D.W., 1991. *Allowable bending strength enhancement of 2 by 4 lumber by tension & compression proof loading.* Wood and Fibre Science 23(1), pp.1-14.

[10] Lam, F., Abayakoon, S., Svensson, S., Gyamfi, C. 2001. *Influence of Proof Loading on the Reliability of Members.* Holz als Roh- und Werkstoff 61, 432-438.

[11] Katzengruber, R., Jeitler, G., Schickhofer, G., 2005. *Nondestructive quality assurance of finger jointed structural timber based on a tensile proof loading procedure.* 14th International symposium on non-destructive testing of wood, pp. 225-234.

[12] EN 408:1995. *Timber structures - Structural timber and glued laminated timber – Determination of some physical and mechanical properties.*

[13] Weibull,W., 1939. *A statistical strength theory of the strength of materials.* Ingeniörsveteskapsakademiens Handlingar Nr. 151, Generalstabens Litografiska Anstalts Förlag, Stockholm.

[14] prEN 15497:2006. *Finger jointed structural timber - Performance requirements and minimum production requirements.*

INTERNATIONAL COUNCIL FOR RESEARCH AND INNOVATION
IN BUILDING AND CONSTRUCTION

WORKING COMMISSION W18 - TIMBER STRUCTURES

ALLOCATION OF CENTRAL EUROPEAN HARDWOODS INTO EN 1912

P Glos
J K Denzler

Holzforschung München

GERMANY

MEETING THIRTY-NINE
FLORENCE
ITALY
AUGUST 2006

Presented by J Denzler
F Lam commented that in Canada when new grades containing "something and better" is considered, the relative proportion of the grade needs to be considered carefully so that it can be maintained to prevent possibility of taking some of the high grade material away. J Denzler agreed.
JW van de Kuilen received confirmation that normal distribution was used to represent MOE.

Allocation of Central European hardwoods into EN 1912

P. Glos, J.K. Denzler
Holzforschung München, Germany

1 Introduction

Up to now Central European hardwoods are scarcely used as structural timber. However, due to ecological reasons an increasing amount of hardwoods is being produced in Central European forests. As hardwoods exhibit higher strength and stiffness values they could be used to produce high strength timber products, e.g. glulam.

For long span structures modulus of elasticity is often the limiting factor in design. Therefore, modulus of elasticity is an important material property and it is important that EN 338 reflects the strength-stiffness relationship correctly.

Test results of bending and tension tests of German beech and oak specimens showed that the modulus of elasticity values for given strength levels are higher than those tabled in EN 338. In order to be able to make the best possible use of home grown hardwoods, the strength profiles in EN 338 should be modified.

The aim of this paper is to suggest a more appropriate relationship between strength and stiffness for hardwoods in EN 338 in order to use the full capacity of hardwoods as structural timber of high strength and stiffness.

Moreover, the paper discusses how the characteristic strength and stiffness values of a grade depend on the combination of grades graded in one pass and that this effect has to be taken into account when assigning grades to strength classes.

2 Allocation of Beech (Fagus sylvatica) graded according to DIN 4074-5

223 beech scantlings with three different cross sections (35x70, 60x120, 60x180 mm²) and 571 beech boards with six different cross sections (25x100, 25x150, 32x120, 32x165, 35x100, 35x150 mm²) were collected from three different sawmills in Germany (GLOS & NAEHER 2005). The length of the boards and scantlings varied from 4,000 to 5,000 mm. All specimens were kiln-dried to a target moisture content of 12 %.

The specimens were visually graded according to DIN 4074-5 with respect to all relevant parameters. After grading the scantlings were tested in bending and the boards (32x120, 32x165 mm²) were tested in tension according to EN 384 and EN 408. The other boards were tested with a test length less than 9 times the width. Therefore, these results are

indicative only. Moisture content, growth ring orientation and density were measured according to ISO 3131, respectively, using a 2 cm thick defect-free test slice of full cross section cut from the test specimen near the failure zone.

Table 1 (Annex) summarises the test results of 177 beech scantlings of the visual grades LS 10, LS 10 & better and LS 13 (46 specimens did not meet the grade LS 10 and were rejected). According to EN 384 all test values were adjusted to 12% moisture content. Modulus of elasticity was adjusted to a pure bending modulus of elasticity and bending strength to 150 mm height. No length adjustment was applied because the specimens were tested with a span of 18 times the height and a distance between the inner loading points of 6 times the height. All specimens were tested with the critical defect on the tension edge. Therefore, the 7.5^{th} percentile was used to calculate the characteristic bending strength (GLOS & DENZLER 2004).

The visual grade LS 10 includes only 56 specimens. This is not sufficient to establish mechanical properties. The visual grade LS 10 & better includes all specimens which belong to the grades LS 10 and LS 13. Based on their characteristic strength, the visual grades LS 10 & better and LS 13 fit into the strength classes D 35 and D 40 of EN 338 (see Table 2). The modulus of elasticity of these two grades is $E_{m,0,mean}$ = 15,900 N/mm² and $E_{m,0,mean}$ = 16,100 N/mm², respectively. These values are much higher than the values according to strength class D 35 and D 40 (Figure 1). As modulus of elasticity is strongly correlated with density, density shows the same tendency: The density values of the grades LS 10 & better (ρ_{mean} = 741 kg/m³, ρ_k= 683 kg/m³) and LS 13 (ρ_{mean} = 738 kg/m³, ρ_k= 682 kg/m³) exceed the values of the strength classes D 35 and D 40, respectively.

Table 2: Stiffness and density values in EN 338.

strength class	[-]	D 30	D 35	D 40	D 50	D 60	D 70
$f_{m,k}$	[N/mm²]	30	35	40	50	60	70
$f_{t,0,k}$	[N/mm²]	18	21	24	30	36	42
$E_{0,mean}$	[N/mm²]	10,000	10,000	11,000	14,000	17,000	20,000
ρ_{mean}	[kg/m³]	640	670	700	780	840	1080
ρ_k	[kg/m³]	530	560	590	650	700	900

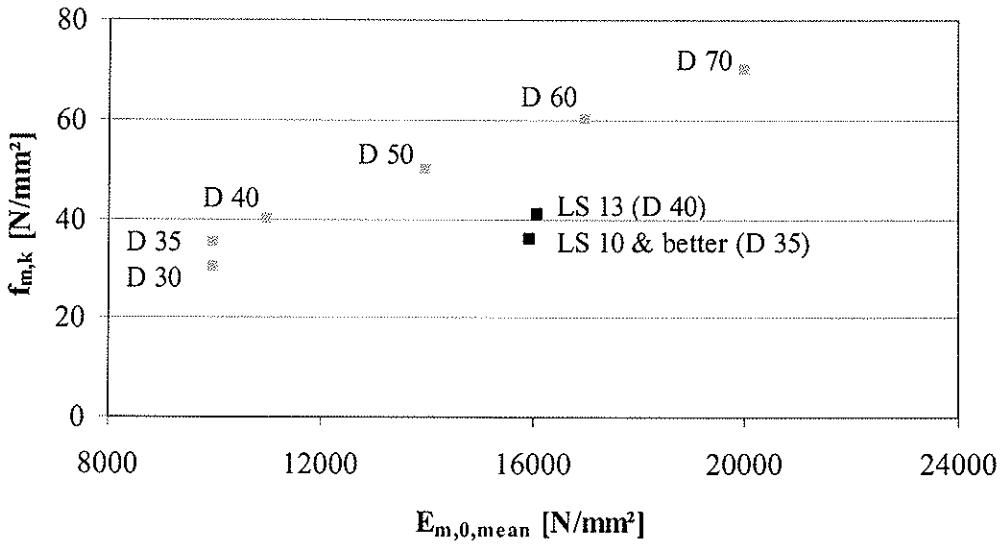

Figure 1: Relationship between $f_{m,k}$ and $E_{m,0,mean}$ given in EN 338 compared with test results for bending tests of beech scantlings.

Table 3 (Annex) summarises the test results of 355 beech boards of the visual grades LS 10, LS 10 & better and LS 13 (216 specimens did not meet the grade LS 10 and were rejected). According to EN 384 all test values were adjusted to 12% moisture content and tension strength was adjusted to 150 mm width. For tension strength no length adjustment factor is given in EN 384. All cross sections not tested with 9 times the height are therefore painted in grey and the results are indicative only.

The visual grade LS 10 includes 75 specimens. This is not regarded to be sufficient to establish mechanical properties. The visual grade LS 10 & better includes all specimens which belong to the grades LS 10 and LS 13 and therefore, contains enough specimens per sample to establish the required characteristic values. These results confirm the allocation of visual grade LS 10 & better to strength class D 35 for Central European beech. Based on its characteristic strength the visual grade LS 13 fits even into strength class D 50.

Modulus of elasticity of the two grades exceeds the required characteristic values of D 35 and D 50, not taking into account the factor of 1.09 between tensile and bending modulus of elasticity (BURGER & GLOS 1995). Moreover, the grade determining defect was always located within the gauge length for the MOE measurement, which probably leads to lower mean values than a random measurement within the specimen length.

The density of the grade LS 10 & better (ρ_{mean} = 720 kg/m³, ρ_k = 656 kg/m³) exceeds the required density of strength class D 35, the mean density of the grade LS 13 (ρ_{mean} = 721 kg/m³) is lower than the mean density of strength class D 50. However, the characteristic density of the grade LS 13 (ρ_k = 655 kg/m³) meets the required value of strength class D 50 given in EN 338.

3 Allocation of Oak (Quercus petraea, Quercus robur) graded according to DIN 4074-5

337 oak scantlings with three different cross sections (40x80, 60x120, 60x180 mm²) were collected from one German sawmill. Their length varied from 3,000 to 4,000 mm. Oak is highly durable and, therefore, often used in outdoor and hence in wet conditions. For this reason the oak specimens were not kiln-dried before testing and had an average moisture content of 32.6%.

The specimens were visually graded according to DIN 4074-5 with respect to all relevant parameters and tested in bending according to EN 384 and EN 408. Moisture content, growth ring orientation and density were measured according to ISO 3131, respectively, using a 2 cm thick defect-free test slice of full cross section cut from the test specimen near the failure zone.

Table 4 (Annex) summarises the test results of 239 oak scantlings of the visual strength class LS 10 & better (98 specimens did not meet the grade LS 10 and were rejected). According to EN 384 all test values were adjusted to u = 12% moisture content. For specimens with u > 18% the adjustment was based on a moisture content of u = 18% to prevent unreliable values for modulus of elasticity. For strength an adjustment factor of 1.16 was used. This factor was based on the following information:

1. From tests with matched specimens with u=12% and u>20% an adjustment factor of 1.21 was detected (GLOS & LEDERER 2000).
2. According to the German standard DIN 1052-1, 5.1.7, strength values must be reduced by 1/6 = 16% for u>18%.
3. According to the Eurocode 5 EN 1995-1-1, 3.1.3, the k_{mod}-value of service class 1 (u=12%) and service class 3 (u>20%) differs between 16% and 22% depending on the load duration class.

Modulus of elasticity was adjusted to a pure bending modulus of elasticity and the bending strength to 150 mm height. No length adjustment was necessary because the specimens were tested with a span of 18 times the height and a distance between the inner loading points of 6 times the height. All specimens were tested with the critical defect on the tension edge. Therefore, the 7.5^{th} percentile was used to calculate the characteristic bending strength (GLOS & DENZLER 2004).

Based on its characteristic strength Central European oak of the visual grade LS 10 & better fits into strength class D 30. The modulus of elasticity of this grade is $E_{m,0,mean}$ = 11,500 N/mm². This value is higher than the required modulus of elasticity of strength class D 30. The density values of this grade (ρ_{mean} = 715 kg/m³, ρ_k= 634 kg/m³) exceed the required density values of strength class D 30.

4 Relationship between strength and stiffness

The strength-stiffness-relationship of a grade depends on the combination of grades graded in one pass. This influence gets stronger with increasing number of grades to be graded in one pass. This is the case in machine grading as well as in visual grading. To show this influence the database of Holzforschung München was used to simulate mechanical grading of 2343 spruce specimens (Picea abies) tested in tension according to EN 384 and EN 408.

Grading was based on size and location of knots, density and cross-sectional dimensions as is the case in existing X-ray grading machines, e.g. the GoldenEye 702. An indicating property was calculated for each test piece and settings were derived so that each grade fulfilled the required characteristic strength values of so called L-classes L 17 to L 40, not taking into account the characteristic value of modulus of elasticity and density of each grade.

Figure 2 shows the relationship between strength and stiffness of each strength class, dependent on the respective grade combination, e.g. L 17, L 17 and L 30, L 17 and L 36 or L 17 and L 40, whereas the yield is optimised in the highest strength classes. For strength class L 17 the modulus of elasticity (tension) varies between 9,200 N/mm² and 11,700 N/mm² depending on the applied grade combination. If more than two grades are graded in one pass the relationship may get even worse. Figure 3 shows the corresponding coefficients of variation (COV) of tensile strength of each strength class, dependent on the respective grade combination. Most of the COV are greater than 30 %. Figure 4 shows the relationship between strength and density, respectively. The effect on characteristic density is not consistent if the assumption of normal distribution is used because the standard deviation may be reduced when more than one grade is graded in one pass leading to higher characteristic values.

In order to specify a relationship between strength and stiffness for one grade it is necessary to either take this effect into account or to restrict the grade to only those specimens within one grade and to exclude all specimens that exceed the upper grade limit.

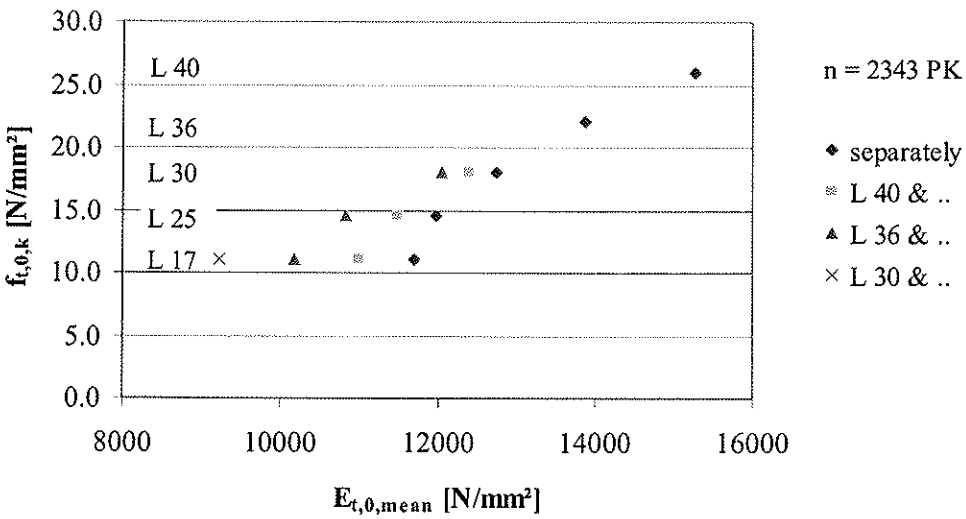

Figure 2: Relationship between $f_{t,0,k}$ and $E_{t,0,mean}$ for different strength classes and strength class combinations.

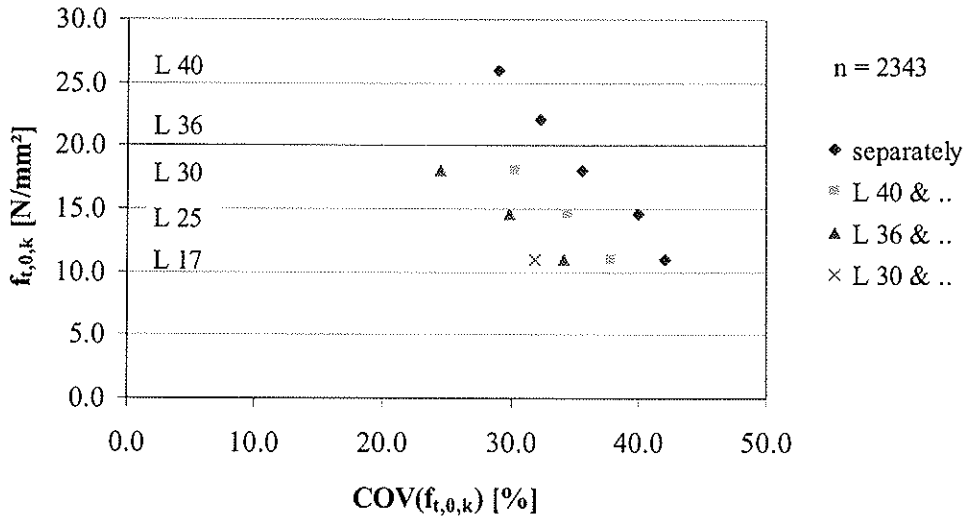

Figure 3: Relationship between $f_{t,0,k}$ and COV($f_{t,0,k}$) for different strength classes and strength class combinations.

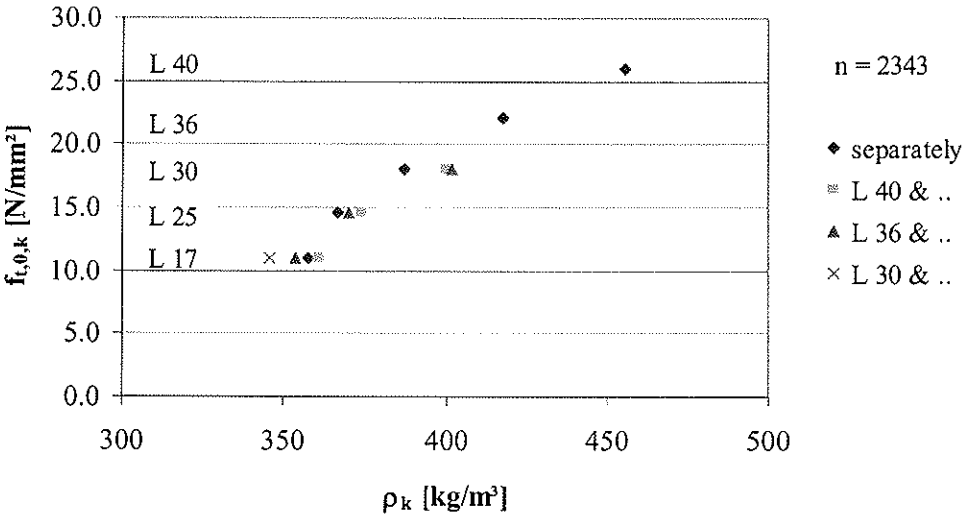

Figure 4: Relationship between $f_{t,0,k}$ and ρ_k for different strength classes and strength class combinations.

5 Conclusion

The aim of this paper is to propose a relationship between strength and stiffness for tempered hardwoods in EN 338. In order to be able to use tempered hardwoods efficiently and keeping in mind that in the near future there will be no need for a great variety of different grades for hardwoods it is recommended to accept grades like "LS 10 & better" and define strength profiles in EN 338 based on such grades. Therefore, the following stiffness and density values are proposed for the strength classes in EN 338 (see Table 5).

Table 5: Proposal for modified stiffness and density values in EN 338.

strength class	**[-]**	**D30**	**D35**	**D40**	**D50**
$f_{m,k}$	[N/mm²]	30	35	40	50
$f_{t,0,k}$	[N/mm²]	18	21	24	30
existing $E_{0,mean}$	[N/mm²]	10,000	10,000	11,000	14,000
proposed $E_{0,mean}$	**[N/mm²]**	**11,500**	**14,500**	**15,500**	**16,500**
existing ρ_{mean}	[kg/m³]	640	670	700	780
proposed ρ_{mean}	**[kg/m³]**	**710**	**720**	**720**	**720**
existing ρ_k	[kg/m³]	530	560	590	650
proposed ρ_k	**[kg/m³]**	**630**	**650**	**650**	**650**

Based on the test results it is proposed to add German beech of the grades LS 10 & better and LS 13 to strength class D 35 and D 40, respectively, in EN 1912. Additionally, German oak of the grade LS 10 & better can be allocated to strength class D 30.

6 Literature

BURGER, N.; GLOS, P. (1995)
Verhältnis zwischen Zug- und Biege-Elastizitätsmoduln von Vollholz. Holz Roh- Werkst. 53 (1995): 73-74. (only available in German)

DIN 1052-1:1988-04
Design of timber structures - General rules and rules for buildings. Normenausschuss Bauwesen (NABau) im DIN (Deutsches Institut für Normung e.V.), Berlin. 34.
(only available in German)

DIN 4074-5:2003-06
Strength grading of wood - Part 5: Sawn hard wood. Normenausschuss Bauwesen (NABau) im DIN (Deutsches Institut für Normung e.V.), Berlin. 20. (only available in German)

EN 338:2003-04
Structural timber - Strength classes. CEN European Committee for Standardization, Bruessel. 9.

EN 384:2004-01
Structural timber - Determination of characteristic values of mechanical properties and density. CEN European Committee for Standardization, Bruessel. 15.

EN 408:2003-08
Timber structures - Structural timber and glued laminated timber - Determination of some physical and mechanical properties. CEN European Committee for Standardization, Bruessel. 32.

EN 1912:2004-12
Structural timber - Strength classes - Assignment of visual grades and species. CEN European Committee for Standardization, Bruessel. 15.

EN 1995-1-1:2004-11
Eurocode 5 - Design of timber structures - Part 1-1: General - Common rules and rules for buildings. CEN European Committee for Standardization, Bruessel. 132.

GLOS, P.; DENZLER, J.K. (2004)
Effect of Test Piece Orientation on Characteristic Bending Strength of Structural Timber. Proc. of CIB-W18 Meeting, Paper 37-6-2. Edinburgh, Scotland. 8.

GLOS, P.; LEDERER, B. (2000)
Sortierung von Buchen- und Eichenschnittholz nach der Tragfähigkeit und Bestimmung der zugehörigen Festigkeits- und Steifigkeitskennwerte. Bericht Nr. 98508, Holzforschung München, Technische Universität München. 41. (only available in German)

GLOS, P.; NAEHER, T. (2005)
Aufnahme der einheimischen Holzarten Buche (Fagus sylvatica), Eiche (Quercus petraea, Quercus robur) und Douglasie (Pseudotsuga menziesii) in die europäische Norm EN 1912. Bericht Nr. 05510, Holzforschung München, Technische Universität München. München, Germany. 30. (only available in German)

ISO 3131:1975-11
Wood; Determination of density for physical and mechanical tests. ISO International Organization for Standardization. 2.

7 Annex

Table 1: Bending test results of beech scantlings.

species	[-]	**Beech** (Fagus sylvatica)											
source	[-]	**Germany**											
grade	[-]	**LS 10**				**LS10 & better**				**LS 13**			
n	[-]	9	36	11	56	48	93	36	177	39	57	25	121
thickness	[mm]	35	60	60	all	35	60	60	all	35	60	60	all
height	[mm]	70	120	180	all	70	120	180	all	70	120	180	all
u_{mean}	[%]	11.8	12.0	11.1	11.8	11.5	11.9	11.0	11.6	11.4	11.8	11.0	11.5
$SD(u_{mean})$	[%]	0.4	0.7	0.3	0.7	0.3	0.7	0.3	0.6	0.3	0.6	0.3	0.6
$f_{m,mean}$	[N/mm²]	53.7	70.7	59.4	65.7	74.4	78.6	69.1	75.5	79.2	83.5	73.3	80.0
$SD(f_{m,mean})$	[N/mm²]	9.7	22.9	17.2	21.2	17.6	20.9	17.4	19.6	15.5	17.9	16.0	17.1
$k_h=(150/h)^{0.2}$	[-]	1.16	1.05	0.96	-	1.16	1.05	0.96	-	1.16	1.05	0.96	-
$f_{m,k(5)}$	[N/mm²]	31.9	22.4	37.5	30.4	34.7	37.2	38.9	38.0	43.1	50.3	40.4	44.2
$f_{m,k(7.5)}$	[N/mm²]	31.9	33.2	37.5	36.3	41.5	40.8	39.9	41.2	43.5	51.1	43.1	48.5
k_s	[-]		-		-		0.88		-		0.87		-
$f_{m,k}$	**[N/mm²]**		**-**		**-**		**35.9**		**-**		**40.9**		**-**
$E_{m,0,mean}$	[kN/mm²]	13.1	16.3	15.4	15.6	14.4	16.7	16.1	15.9	14.7	16.9	16.4	16.1
$E_{m,0,mean}$	**[kN/mm²]**		**15.6**		**-**		**15.9**		**-**		**16.1**		**-**
ρ_{mean}	[kg/m³]	738	758	718	747	720	754	733	741	715	752	740	738
ρ_{mean}	**[kg/m³]**		**747**		**-**		**741**		**-**		**738**		**-**
ρ_k	[kg/m³]	696	692	659	681	679	686	679	677	677	682	691	675
ρ_k	**[kg/m³]**		**686**		**-**		**683**		**-**		**682**		**-**

Table 3: Tension test results of beech boards.

species	[-]	**Beech** (Fagus sylvatica)																		
source	[-]	**Germany**																		
grade	[-]	**LS 10**							**LS10 & better**							**LS 13**						
n	[-]	19	10	13	19	7	7	75	78	63	60	67	43	44	355	59	53	47	48	36	37	280
thickness	[mm]	25	25	32	32	35	35	all	25	25	32	32	35	35	all	25	25	32	32	35	35	all
width	[mm]	100	150	120	165	100	150	all	100	150	120	165	100	150	all	100	150	120	165	100	150	all
u_{mean}	[%]	11.4	11.6	10.6	9.9	11.2	11.4	10.9	11.3	11.4	10.6	9.9	11.4	11.5	10.9	11.2	11.3	10.5	9.9	11.4	11.5	11.0
$SD(u_{mean})$	[%]	0.7	0.6	0.3	0.3	0.3	0.9	0.9	0.7	0.6	0.2	0.3	0.4	0.7	0.8	0.7	0.5	0.2	0.3	0.4	0.7	0.8
$f_{t,0,mean}$	[N/mm²]	48.3	42.6	37.8	37.0	51.6	46.3	43.0	84.3	71.5	57.3	55.8	92.6	74.9	71.9	95.9	76.9	62.7	63.2	100.6	80.4	79.7
$SD(f_{t,0,mean})$	[N/mm²]	18.2	12.1	15.6	12.9	15.3	11.8	15.4	36.4	32.9	24.4	22.6	31.6	26.7	32.4	33.0	32.8	23.8	21.3	27.5	25.3	31.4
$k_h=(150/h)^{0.2}$	[-]	1.08	1.00	1.05	0.98	1.08	1.00	-	1.08	1.00	1.05	0.98	1.08	1.00	-	1.08	1.00	1.05	0.98	1.08	1.00	-
$f_{t,0,k(5)}$	[N/mm²]	22.6	30.3	19.1	14.8	30.1	33.1	22.4	29.3	30.3	23.2	25.8	35.5	34.1	29.3	40.6	33.2	28.2	32.8	47.6	36.7	34.6
k_s	[-]	-						-	1.00						-	1.00						-
$f_{t,0,k}$	**[N/mm²]**	-						-	**27.9**						-	**33.9**						-
$E_{t,0,mean}$	[kN/mm²]	11.7	10.3	12.2	12.7	10.8	10.7	11.7	14.1	13.5	13.7	14.5	14.6	13.8	14.0	14.8	14.1	14.1	15.3	15.4	14.4	14.7
$E_{t,0,mean}$	**[kN/mm²]**	**11.7**						-	**14.0**						-	**14.7**						-
ρ_{mean}	[kg/m³]	703	710	734	717	712	712	714	714	712	726	721	732	721	720	717	712	724	723	736	723	721
ρ_{mean}	**[kg/m³]**	**714**						-	**720**						-	**721**						-
ρ_k	[kg/m³]	652	685	677	642	654	667	657	646	652	655	658	658	672	655	645	648	649	665	660	673	654
ρ_k	**[kg/m³]**	**660**						-	**656**						-	**655**						-

Table 4: Bending test results of oak scantlings.

species	[-]	**Oak** (Quercus petraea, Quercus robur)			
source	[-]	**Germany**			
grade	[-]	**LS10 & better**			
n	[-]	111	62	66	239
thickness	[mm]	40	60	60	all
height	[mm]	80	120	180	all
u_{mean}	[%]	26.1	34.5	41.8	32.6
$SD(u_{mean})$	[%]	6.7	6.0	8.5	9.7
$f_{m,mean}$	[N/mm²]	48.9	46.0	41.2	46.0
$SD(f_{m,mean})$	[N/mm²]	12.3	11.0	8.8	11.5
adj.factor u[1)]	[-]	1/1.16	1/1.16	1/1.16	1/1.16
$k_h=(150/h)^{0.2}$	[-]	1.13	1.05	0.96	-
$f_{m,k(5)}$	[N/mm²]	28.6	30.4	29.3	30.1
$\mathbf{f_{m,k(7.5)}}$	[N/mm²]	31.6	32.9	33.0	32.2
k_s	[-]		0.93		-
$\mathbf{f_{m,k}}$	**[N/mm²]**		**30.0**		-
$E_{m,0,mean}$	[kN/mm²]	11.1	12.6	11.2	11.5
$E_{m,0,mean}$	**[kN/mm²]**		**11.5**		-
ρ_{mean}	[kg/m³]	692	741	728	715
$\boldsymbol{\rho_{mean}}$	**[kg/m³]**		**715**		-
ρ_k	[kg/m³]	599	677	651	626
ρ_k	**[kg/m³]**		**634**		-

[1)] The adjustment factor 1.16 for m/c is based on the following information:

1. From tests with matched specimens with u=12% and u>20% an adjustment factor of 1.21 was detected (GLOS & LEDERER 2000).
2. According to the German standard DIN 1052-1, 5.1.7, strength values must be reduced by 1/6 = 16% for u>18%.
3. According to the Eurocode 5 EN 1995-1-1, 3.1.3, the k_{mod}-value of service class 1 (u=12%) and service class 3 (u>20%) differs between 16% and 22% depending on the load duration class.

INTERNATIONAL COUNCIL FOR RESEARCH AND INNOVATION
IN BUILDING AND CONSTRUCTION

WORKING COMMISSION W18 - TIMBER STRUCTURES

REVISITING EN 338 AND EN 384 BASICS AND PROCEDURES

R Steiger

M Arnold

Swiss Federal Laboratories for Materials Testing and Research EMPA

M Fontana

ETH Zürich

SWITZERLAND

MEETING THIRTY-NINE

FLORENCE

ITALY

AUGUST 2006

Presented by R Steiger

A Ranta-Maunus commented that a Finnish paper on similar subject will be presented next year. He also asked why a code change was not proposed although the ratio between tension and bending strength were observed to be higher than assumed in the code. R Steiger answered as structural engineer, one might want to have additional safety for tension compared to bending. A Ranta-Maunus responded that safety and characteristic properties should be dealt with separately.

JW van de Kuilen received confirmation that timber density and bending strength did not show a strong relationship; therefore, the paper focused on the rest of the properties.

F Lam commented in N. American MSR material has stepped tension to bending ratios for different grades.

G Schickhofer stated that this is an important issue for glulam use also.

J Ehlbeck commented that EN338 is only used in Europe and this research focused on wood from Switzerland only. He stated that the discussion was good but cautioned that one must be careful as more information on material from different regions should be considered.

F Lam commented that ISO work on stress class led by D Barrett considered data from Europe, N. America and Australia. A paper was presented in WCTE 2006 in Portland.

P Kuklik received information that static and dynamic MOE information was available in the annex of the paper. R^2 is higher between MOE's but prediction of strength was not as good.

H Riberholt commented that the issue of tension-bending strength relationship of timber and glulam should be considered separately.

Revisiting EN 338 and EN 384 basics and procedures

R. Steiger [1], M. Arnold [1], M. Fontana [2]

[1] Swiss Federal Laboratories for Materials Testing and Research EMPA, Switzerland

[2] ETH Zurich, Switzerland

1 Introduction

The European standard EN 338 "Timber structures - Strength classes" [1] provides a strength class system for structural timber. The actual grade of a timber sample depends on the characteristic values of the bending strength $f_{m,k}$ and the density r_k, as well as on the mean value of the modulus of elasticity (MOE) parallel to the grain $E_{0,mean}$. Additional mechanical properties listed in EN 338 are derived from these basic values by relationships given in EN 384 "Structural timber – Determination of characteristic values of mechanical properties and density" [2] and in the informative annex A of EN 338 respectively.

In the course of an upcoming revision of EN 338, any confirmatory or contradictory information on the profiles of the EN 338 strength classes is of interest. Based on a series of tests with Swiss grown spruce structural timber, the following property relationships are analysed in this paper:

- bending strength f_m and flexural MOE E_m,
- simultaneous matching of basic values: characteristic bending strength $f_{m,k}$, mean MOE parallel to the grain $E_{0,mean}$ (usually understood as flexural MOE E_m) and density r_k,
- characteristic tensile and compression strength parallel to the grain $f_{t,0,k}$ and $f_{c,0,k}$ with respect to the corresponding characteristic bending strength $f_{m,k}$,
- MOE for bending E_m, compression $E_{c,0}$ and tensile $E_{t,0}$,
- 5^{th}-percentiles and mean values of density r and MOE E_0.

Furthermore, the size adjustment factors proposed by EN 384 to account for the influences of depth and width of structural elements on the bending and tensile strength are assessed. Since the database results from tests not specially designed for the evaluation of size effects, data analysis shows only tendencies and derived conclusions are just indicative.

2 Strength class system for softwoods provided by EN 338

2.1 Assignment of strength classes according to EN 338

2.1.1 Strength class system

The current 2003 version of EN 338 defines twelve strength classes for softwoods, prefixed C: C14, C16, C18, C20, C22, C24, C27, C30, C35, C40, C45 and C50. The numbers represent the characteristic bending stress $f_{m,k}$ for each strength class.

A specific population can be assigned to a certain strength class, if the characteristic values of density r_k and bending strength $f_{m,k}$ (both of them are 5th-percentiles) as well as MOE (mean value, usually derived from bending tests) match or exceed the values of the desired class.

2.1.2 Test procedure and determination of characteristic values

The characteristic values have to be determined according to EN 384 and testing shall be carried out in accordance with EN 408 [3]. The critical section shall be in a position that can be tested. For a bending test to determine strength or MOE, the tension edge shall be selected *at random*. The test piece, having a minimum length of 19 times the depth of the section, shall be simply supported and symmetrically loaded in bending at two points over a span of 18 times the depth. For a compression test parallel to the grain, the specimen (being of full cross section) shall have a length of six times the smaller cross-sectional dimension. For a tension test parallel to the grain, the timber has to be of full cross section and test length clear of the machine grips has to be nine times the width of the specimen.

2.1.3 Reference conditions

The reference wood moisture content (MC) shall be consistent with 20°C and 65% relative humidity, which for most softwoods corresponds to a MC of about 12%. For samples not tested at reference conditions but having a mean MC in the range of 10 to 18%, adjustment of lower 5th-percentile or mean values to 12% MC shall be as follows:

- for bending and tensile strength: no adjustment
- for compression parallel to the grain strength: 3% change for every percentage point difference in MC (1)
- for MOE: 2% change for every percentage point difference in MC

The adjustments are to be carried out in a way that the above-quoted properties increase if the data are adjusted from a higher MC, and vice versa.

For bending strength, the reference condition corresponds to a depth of 150 mm and to the standard test set-up proportions of four point bending with loads applied in the third points and an overall span of 18 times the specimen depth. Tensile strength is given for a reference width of 150 mm. For samples not tested at reference conditions, EN 384 gives adjustment factors. Size adjustment to 150 mm depth or width can be made by dividing the 5th-percentile by:

$$k_h = \left(\frac{150}{h}\right)^{0.2} \tag{2}$$

2.2 Relationships of mechanical properties

2.2.1 Relationship of bending strength and flexural MOE

Flexural MOE correlates with bending strength and therefore is a very important parameter for machine grading. Coefficients of correlation R up to 0.7 – 0.8 are reported in the literature [4].

2.2.2 Ratio of tensile strength parallel to the grain vs. bending strength

According to EN 384 the characteristic values of tensile strength parallel to the grain $f_{t,0,k}$ for softwood species can be calculated with the following Equation (3):

$$f_{t,0,k} = 0.6 \cdot f_{m,k} \tag{3}$$

This constant ratio is used in most strength class systems for structural timber [5], although it was shown in several studies not to be constant but rather to depend on timber quality. Burger and Glos [6] found a noticeable effect of both grading method and dimensions on the f_t/f_m ratio. The ratio f_t/f_m rises with increasing cumulative frequency and thus with increasing strength or wood quality. Burger and Glos reported a f_t/f_m ratio of 0.69 for the 5th percentile level while the ratio on the 50th percentiles level was found to be 0.76.

In the course of their discussion of timber property relationships in Eurocode 5, Green and Kretschmann [7] compared ultimate bending strength and tensile strength parallel to the grain for In-Grade data resulting from tests of different softwood species (Douglas Fir, Larch, Hemlock and Southern Pine). For values of ultimate tensile strength up to 55 N/mm^2 the average ratio was $f_{t,0,k}/f_{m,k} = 0.59$. Above that limit, the ratio increased slightly. The authors however suggested retaining Equation (3).

2.2.3 Relationship between compression strength parallel to the grain and bending strength

EN 384 gives Equation (4) to derive the characteristic values of compression strength parallel to the grain $f_{c,0,k}$ for softwood species from the corresponding bending strength $f_{m,k}$:

$$f_{c,0,k} = 5 \cdot \left(f_{m,k}\right)^{0.45} \tag{4}$$

For In-Grade tested Douglas Fir-Larch, Hem-Fir and Southern Pine, Green and Kretschmann [7] found the trend of the relationship to be virtually identical to the data presented by Curry and Fewell [8], which forms the basis of the above Equation (4). In earlier [9] and recent [10] publications a strong correlation between compression strength parallel to the grain and wood density is reported.

2.2.4 Ratio of MOE in bending, tension and compression parallel to the grain

Most investigations on the ratio between the moduli of elasticity were carried out with small clear specimens [11]. Burger and Glos [12] showed that the MOE in tension and in bending of full-size structural timber, in contrast to small clear specimens, depends on the type of load as well as on timber quality. The authors evaluated test results of 147 European spruce specimens dimensioned 50/120 (54 specimens) and 60/105 (93 specimens). On average, bending flexural MOE E_m was 9% higher than the tensile MOE E_t and the following regression Equation was found:

$$E_m = 90 + 1.077 \cdot E_t \quad [\text{N/mm}^2] \qquad \text{with } R = 0.94 \quad (R^2 = 0.88) \tag{5}$$

Timber being a composite material, Gehri [13] suspects differences in flexural and tensile MOE to depend on sawing pattern. Clear specimens exhibit identical tensile and compression MOE [14].

2.2.5 Ratio of 5th-percentile and mean value of MOE

EN 384 assumes a constant ratio of 5th-percentile and mean value of MOE:

$E_{05}/E_{mean} = 0.67$ for softwood species. (6)

For infinite sized normally distributed samples, this fractile ratio corresponds to a coefficient of variation (COV) of 20%. Green and Kretschmann [7] suggested to lower the ratio and to make it a function of strength class.

2.2.6 Ratio of 5th-percentile to mean value of density

The ratio of the characteristic to the mean value of density given in EN 338 varies between 0.82 and 0.85 with an average of 0.84. This variation results from rounding. Former editions of EN 384 explicitly assumed a constant ratio of 0.84 for softwood species, which in case of a normally distributed sample is identical to a COV of 10%.

Green and Kretschmann [7] reported an average ratio of 0.80 with a range of 0.78 to 0.83 for three major species groups (Douglas Fir-Larch, Hem-Fir and Southern Pine). The average ratio for all species was 0.83.

2.3 Size effects on bending and tensile strength

2.3.1 Bending

The basis for the theoretical models is the weakest link theory put forward by Pierce [15] and Tucker [16] and mathematically formulated by Weibull [17, 18]:

$$\frac{\sigma_2}{\sigma_1} = \left(\frac{V_1}{V_2}\right)^{\frac{1}{k}} = \left(\frac{V_1}{V_2}\right)^{m} \tag{7}$$

Madsen and Buchanan [19] suggested a modification of Equation (7) to account for size effects in longitudinal and in both cross-sectional dimensions b and h.

$$\frac{\sigma_2}{\sigma_1} = \left(\frac{V_1}{V_2}\right)^{m} \approx \left(\frac{\ell_1}{\ell_2}\right)^{m_\ell} \cdot \left(\frac{b_1}{b_2}\right)^{m_b} \cdot \left(\frac{h_1}{h_2}\right)^{m_h} \tag{8}$$

For beams with a constant ratio of depth to length $\ell_1/h_1 = \ell_2/h_2$ a size factor m_R can be derived [20]:

$$\frac{\sigma_2}{\sigma_1} = \left(\frac{\ell_1}{\ell_2}\right)^{m_\ell} \cdot \left(\frac{h_1}{h_2}\right)^{m_h} = \left(\frac{h_1}{h_2}\right)^{m_\ell} \cdot \left(\frac{h_1}{h_2}\right)^{m_h} = \left(\frac{h_1}{h_2}\right)^{m_\ell + m_h} = \left(\frac{h_1}{h_2}\right)^{m_R} \tag{9}$$

with $m_\ell = 0.15 - 0.20$ $m_h = 0 - 0.23$ $m_R = 0.20 - 0.40$

EN 384 accounts for the size effect only in one direction by adjusting characteristic values resulting from test samples with depths different from h = 150 mm to reference condition with an exponent of $m_R = 0.20$. Tests have to be carried out according to EN 408 and thus with a constant span to depth ratio of $\ell = 18\ h$. If the bending test arrangement is not as in EN 408 (i.e. span $\ell = 18\ h$ and distance between inner load points $a_f = 6\ h$), then the 5th-percentile bending strength according to EN 384 can be adjusted to reference conditions by dividing by:

$$k_\ell = \left(\frac{\ell_{es}}{\ell_{et}}\right)^{m_\ell} \qquad m_\ell = 0.2 \tag{10}$$

ℓ_{es} or $\ell_{et} = \ell + 5\ a_f$ standard geometry: index es (11)

chosen test geometry: index et

2.3.2 Tension

Burger and Glos showed in [21] that the weakest link theory is applicable for tension members as well. Madsen [22] proposed the following factors:

effect of length:	mean level	$m_\ell = 0.20$	10^{th} percentile	$m_\ell = 0.15$
effect of width:	mean level	$m_h = 0.15$	10^{th} percentile	$m_h = 0.10$

Barrett and Griffin [23] determined an effect of width of $m_h = 0.22$ irrespective of wood species and quality. Various test lengths were converted into uniform length using a factor of $m_\ell = 0.15$. Barrett and Fewell [24] proposed values of $m_\ell = 0.17$ and $m_h = 0.23$ based on combined Canadian, American and English test results. Glos [25] suggested a factor of $m_\ell = 0.15$. Barrett et al. [26] studied the effect of size on the strength of visually graded softwood structural timber. They found factors of $m_\ell = 0.17$, $m_h = 0.23$ and $m_R = 0.40$. Rouger and Fewell [27] postulated the size effect being influenced by timber quality. Burger and Glos [21] found that tensile strength is mainly affected by the length of a structural member rather than by its width and that there would be no need to consider a size factor m_h.

EN 384 accounts for the size effect only in one direction by adjusting characteristic values resulting from test samples with widths different from $h = 150$ mm to reference condition with an exponent of $m_R = 0.20$. The underlying test standard EN 408 demands tests with a constant length to width ratio of $\ell = 9h$. If however tests are not carried out with this ratio, results have to be adjusted to reference length with regard to length effect, using Equation (10).

3 Experiments and analysis of data

3.1 Material

The test results, which form the basis of the present study, are taken from three different research projects carried out in Switzerland and referenced (i) to (iii):

(i) In the early 1990s an extensive test program was launched at the ETH Zurich, which aimed to evaluate the mechanical properties of Swiss grown Spruce structural timber [28-30]. An additional objective was to relate the traditional Swiss strength classes FK I to III (being quite similar to the German strength classes GK I to III) to a new "C-equivalent" provided by EN 338.

(ii) The second source of data is an extensive project started after the extraordinarily violent winter storm 'Lothar' in Central Europe in December 1999, aiming at collecting more information regarding the extent and location, the causes, the detection, and the consequences of wind-induced compression failures [31]. For the study about property relationships presented in this paper, only data resulting from reference tests on samples *without* any visible storm damages were used.

(iii) A third source of data is a PhD thesis [32] dealing with the influence of long-term log storage in the forest on the mechanical properties of timber.

3.2 Test procedures

3.2.1 Determination of wood moisture content and density

MC was measured by the electric resistance method. Density was determined from the mass and the volume of the whole specimen. When assigning samples to EN 338 strength classes the "global" density values were adjusted to the density of small defect-free prisms (ISO 3131:1975) by dividing by 1.05.

3.2.2 Measurement of ultrasonic wave velocity

The longitudinal ultrasonic wave velocity was calculated from specimen length and travel time of the signal. The ultrasonic testers Steinkamp BP V (frequency = 50 kHz) and Sylvatest (frequency = 16 kHz) were used. To account for the influence of moisture on the ultrasonic wave velocity, Equations (12) [33] and (13) were used. Equation (13) is a linearization of (12), which for MCs of 10 to 20% is equal to Equation (12).

$$v_1 = \frac{v_2}{[1 - 0.0053 \cdot (MC2 - MC1)]} \qquad \text{for MC} < 28\% \qquad (12)$$

$$v_1 = v_2 + 29 \cdot (MC2 - MC1) \qquad \text{for MC} < 28\% \qquad (13)$$

3.2.3 Determination of bending strength and flexural MOE

Tests to derive flexural MOE and bending strength were performed in edgewise position. MOE was measured within the loading points. In the course of the ETHZ project (i), the concept of proof loading with a threshold of 40 N/mm^2 was used, resulting in 214 values of flexural MOE but in only 88 bending strength values. With respect to notations in Fig. 1, Table 1 lists geometrical properties of bending tests carried out.

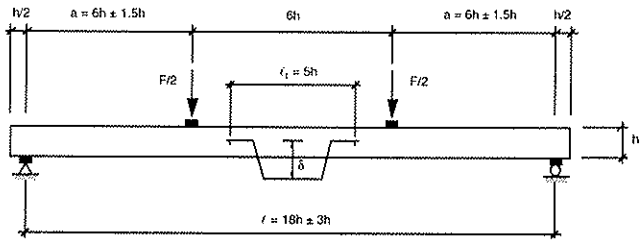

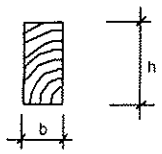

Fig. 1: Test arrangement to derive bending strength and flexural MOE.

Table 1: Geometrical properties of specimens tested in edgewise bending.

Source	Cross section b/h [mm]	Sample size n	Span ℓ [mm]	Distance between loading points $\cdot \ell - 2a$ [mm]	Gauge length ℓ_1 [mm]
(i)	60/120	53	2160 = 18·h	720 = 6·h	500 = 4.17·h
	80/160 and 100/160 [1)]	244 [1)]	2700 = 16.88·h	900 = 5.62·h	600 = 3.75·h
	80/160	36	2760 = 17.25·h	920 = 5.75·h	600 = 3.75·h
(ii)	95/110	363	1980 = 18·h	660 = 6·h	550 = 5·h
EN 408 specifications:			18·h	6·h	5·h

[1)] Proof loaded sample with 214 MOE and density values and 88 bending strength values

3.2.4 Determination of tensile strength and MOE parallel to the grain

Geometrical properties of specimens subjected to tension tests are presented in Table 2 with notations according to Fig. 2. Tests were carried out with a special test equipment set up and optimised based on preliminary studies presented in [34].

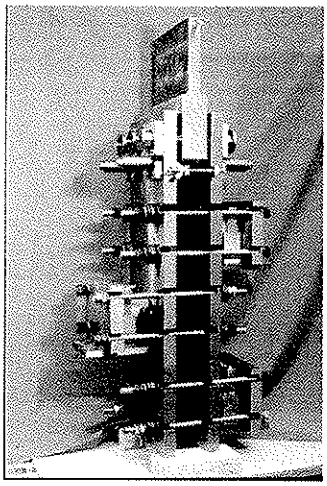

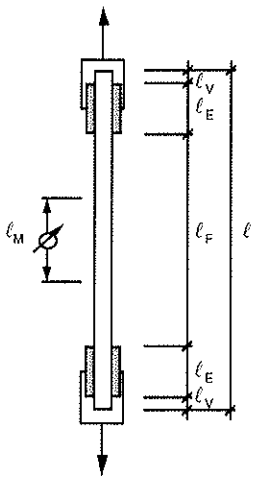

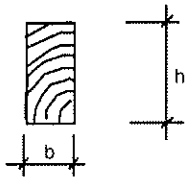

Fig. 2: Test arrangement and equipment to derive tensile strength and MOE.

Table 2: Geometrical properties of specimens tested in tension parallel to the grain.

Source	Cross section b/h [mm]	Sample size n	Free length ℓ_F [mm]	Gauge length ℓ_M [mm]
(i)	10/180	7	910 to 1220 = 5.06·h to 6.78·h	900 = 5·h
	20/180	21	1640 = 9.11·h	900 = 5·h
	30/180	50	1640 = 9.11·h	900 = 5·h
	40/180	21	1640 = 9.11·h	900 = 5·h
	30/150	34	1620 = 10.80·h	900 = 6·h
	80/80	40	1200 = 15·h	900 = 11.25·h
	80/120	46	1200 = 10·h	900 = 7.50·h
	80/160	19	1100 = 6.88·h	900 = 5.63·h
	80/180	21	1200 = 6.67·h	900 = 5·h
	60/180	42	1200 = 6.67·h	900 = 5·h
(ii)	45/150	104	4300 = 28.67·h	750 = 5·h
(iii)	29/150	126	3300 = 22·h	750 = 5·h
	45/150	156		
	49/150	109		
EN 408 specifications:			9·h	5·h

3.2.5 Determination of parallel to the grain compression strength and MOE

Compression tests were carried out with lateral restraints at half-length to prevent the specimens from buckling (Fig. 3). Geometrical properties are listed in Table 3. Compression test sample sizes are smaller because they were not treated with the same priority within the project and furthermore it could be assumed that variation of test values would be smaller compared to tension and bending tests.

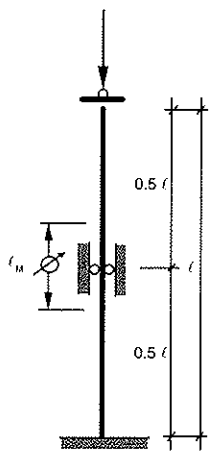

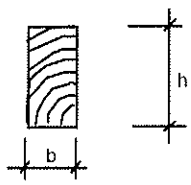

Fig. 3: Compression tests parallel to the grain.

Table 3: Geometrical properties of specimens tested in compression parallel to the grain.					
Source	Cross section b/h [mm]	Sample size n	Length ℓ [mm]	Free length $0.5 \cdot \ell$ [mm] [1)]	Gauge length ℓ_M [mm] [2)]
(i)	60/120	46	$1000 = 8.33 \cdot h$	$500 = 8.33 \cdot b$	$600 = 10 \cdot b$
	80/160	19	$1500 = 9.38 \cdot h$	$750 = 9.38 \cdot b$	$900 = 11.25 \cdot b$
	100/160	40	$1500 = 9.38 \cdot h$	$750 = 7.50 \cdot b$	$900 = 9 \cdot b$
	140/240	47	$1500 = 6.25 \cdot h$	$750 = 5.36 \cdot b$	$700 = 5 \cdot b$
EN 408 specifications:			–	$6 \cdot b$	$4 \cdot b$

3.3 Assessment of timber quality

The MOE, although not being a direct parameter to define strength, but depending on the same factors (which define strength), is the best single indicator of timber quality. The dynamic MOE E_{dyn} was used in this analysis as a reference indicator of quality. E_{dyn} was calculated from the velocity of an ultrasonic wave passing the specimen longitudinally and from the specimen's density:

$$E_{dyn} = r \cdot v^2 \tag{14}$$

E_{dyn} can be measured non-destructively and is a reliable indicator of actual stiffness (MOE) and strength of timber in bending, tension and compression as shown in Figs. 16 to 20 in annex A.1.

3.4 Analysis of data

According to EN 384 characteristic values (sample 5th-percentiles) are to be estimated by determining the 5th-percentiles of ranked samples. With regard to the samples of sometimes smaller size, our analysis to calculate 5th-percentiles used parametric methods in order to take into account all the information provided by the test results. In case of strength variables, a lognormal distribution was used. MOE and density data were analysed on base of normal distributions.

Tensile strength data resulting from tests with different lengths were adjusted to reference length by using Equation (9) with an exponent of $m_\ell = 0.15$.

Dynamic MOE E_{dyn} was used to group test values according to timber quality. Grouping always aimed to get at least 40 specimens in each group. Usually groups contained more than 60 – 80 values.

4 Results

4.1 Relationship of bending strength and flexural MOE

The correlation of bending strength f_m and flexural MOE E_m derived from static bending tests is shown in Fig. 4. The coefficient of correlation amounts to $R = 0.66$ ($R^2 = 0.43$), which compared to other studies reported in [4] is lower.

The EN 338 strength class values (characteristic bending strength $f_{m,k}$ and MOE parallel to the grain $E_{0,mean}$) follow the trend of the experimental data up to strength class C24. In strength classes C27 to C50, flexural MOE found in tests is higher than the assigned strength class value.

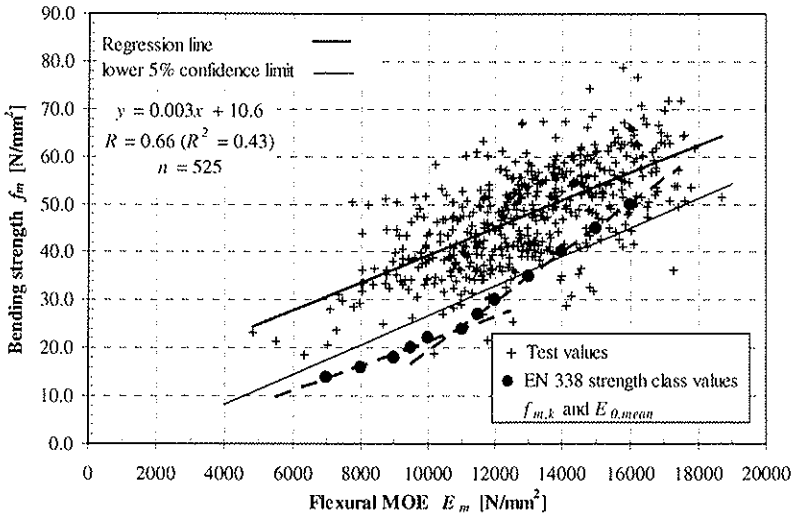

Fig. 4: Bending strength f_m versus flexural MOE E_m derived by static tests (edgewise). The dots indicate pairs of ($f_{m,k}$; $E_{0,mean}$) given in EN 338.

4.2 Profile of basic values $f_{m,k}$, $E_{0,mean}$ and r_k

In order to be able to assign a sample to a certain strength class provided by EN 338, three criterions have to be fulfilled: the characteristic values (5th-percentiles) of bending strength $f_{m,k}$ and density r_k as well as the mean MOE parallel to the grain $E_{0,mean}$. All of them have to match or exceed the class values. The data derived from bending tests (sample size n= 522) was divided into 6 equally sized groups according to measured dynamic MOE E_{dyn}. The above-mentioned characteristic values were calculated for each group and compared to the code values given in EN 338. Fig. 5 shows that the test data match the strength class profile given by EN 338 very well. For strength classes with MOE > 13000 N/mm^2 the tests exhibit somewhat higher MOE values than assigned by EN 338.

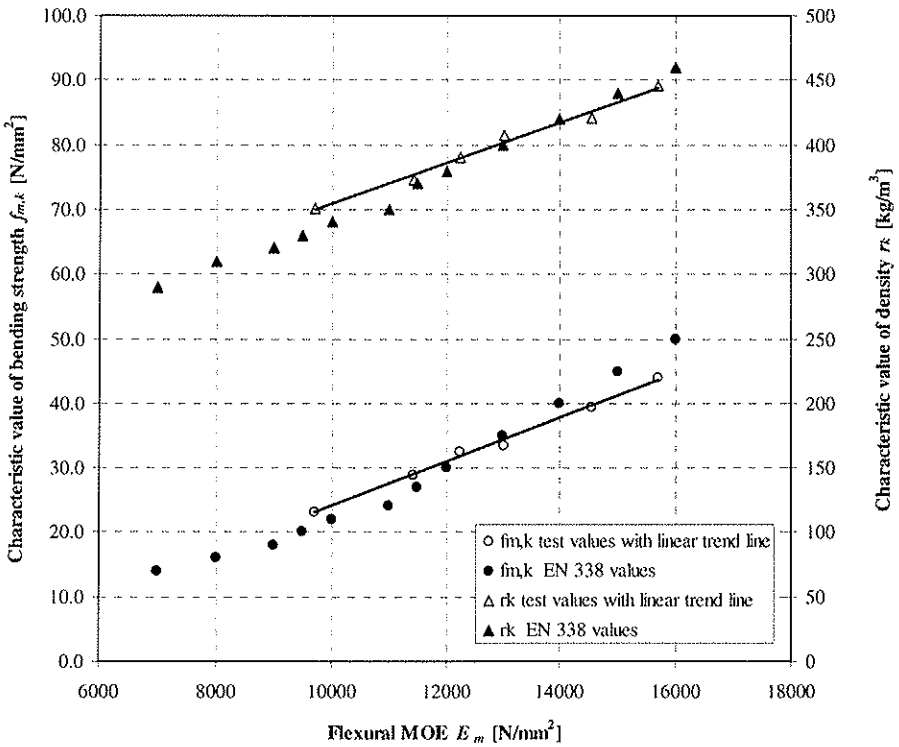

Fig. 5: Comparison of EN 338 strength class values $f_{m,k}$, $E_{0,mean}$ and r_k and test values (with linear trend lines).

4.3 Ratio of tensile strength parallel to the grain to bending strength

A direct comparison of bending and tensile strength is not possible since one cannot test the same specimen to failure in bending and in tension. The ratio of characteristic values of tensile strength $f_{t,0,k}$ to bending strength $f_{m,k}$ shown in Fig. 6 was therefore derived from data grouped (5 groups) according to the dynamic MOE E_{dyn} with equal class boundaries for both bending and tensile strength data sets.

The ratio of tensile to bending strength obviously is not constant but rather depends on timber quality. Ratios of mean values and characteristic values exhibit the same trend. Assuming a constant ratio of f_t/f_m = 0.6 gives safe results for strength classes C22 and higher. Below strength class C22 however, the ratio derived from the test results is smaller than 0.6!

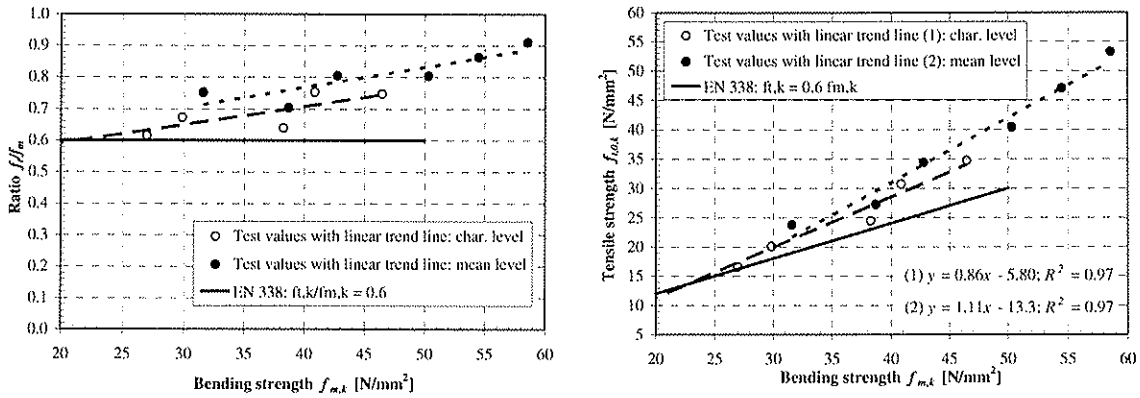

Fig. 6: Ratio (left) and relationship (right) of bending strength f_m and tensile strength f_t.

4.4 Relationship between compression and bending strength

Again, a direct comparison of bending and compression strength is not possible since one cannot test the same specimen to failure in bending and in compression. The ratio of characteristic values of compression strength $f_{c,0,k}$ to bending strength $f_{m,k}$ shown in Fig. 7 was derived from data grouped (4 groups) according to the dynamic MOE E_{dyn} with equal class boundaries for both bending and compression strength data sets. Compared to our test results the EN approach is more conservative for strength classes ≥ C24. The trend line fitting the test results progresses equally on the mean and on the characteristic level. An extrapolation of the trend to strength classes lower than C24 however, results in lower $f_{c,0,k}$ values compared to the characteristic values assigned by EN 338.

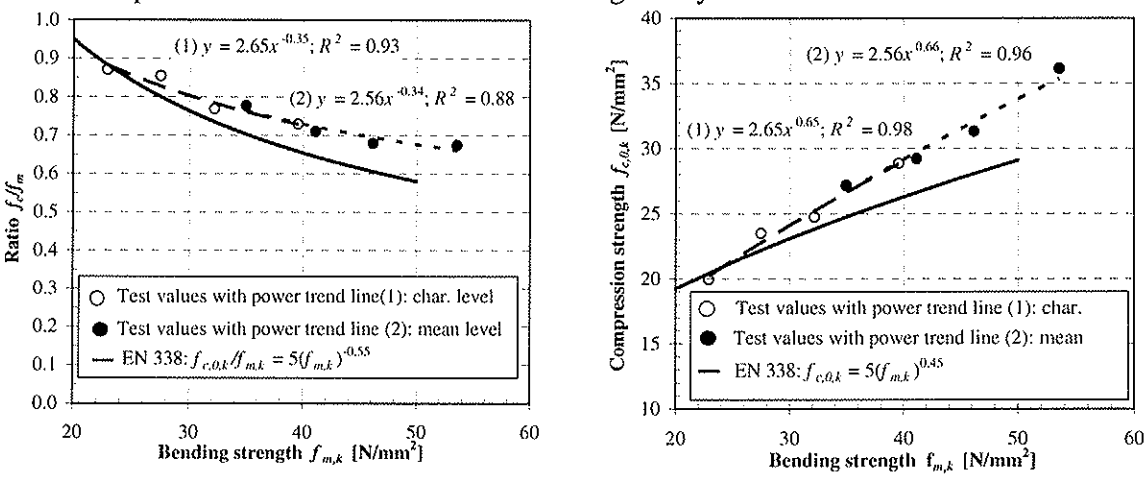

Fig. 7: Ratio (left) and relationship (right) of bending strength f_m compression strength f_c.

EN 338 values as well as test values (4 groups graded according to E_{dyn}) exhibit a linear relationship between the compression strength parallel to the grain $f_{c,0}$ and the wood density r (Fig. 8). The slope of the regression line found in our tests however is almost twice the slope of the trend line fitted to the code values. As an alternative to the code approach (Equation (4)), the compression strength parallel to the grain could be derived from the wood density using a linear model.

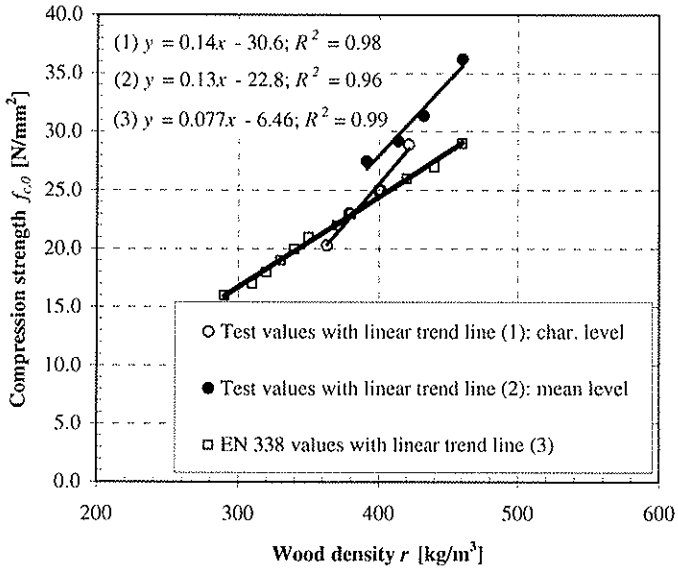

Fig. 8: Relationship between compression strength parallel to the grain $f_{c,0}$ and wood density r: test results and EN 338 values.

4.5 Ratio of MOE in bending, tension and compression

The data analysed here was collected in the course of interaction tests on 80/160 mm beams simultaneously loaded by a bending moment and a normal (tension or compression) force [35] being part of project (i) (see 3.1). All specimens were cut according to the pattern shown in Fig. 9. The relationships of flexural MOE E_m and tensile MOE E_t or compression MOE E_c are shown in Fig. 10.

Fig. 9: Sawing pattern of interaction test specimens (80/160 mm).

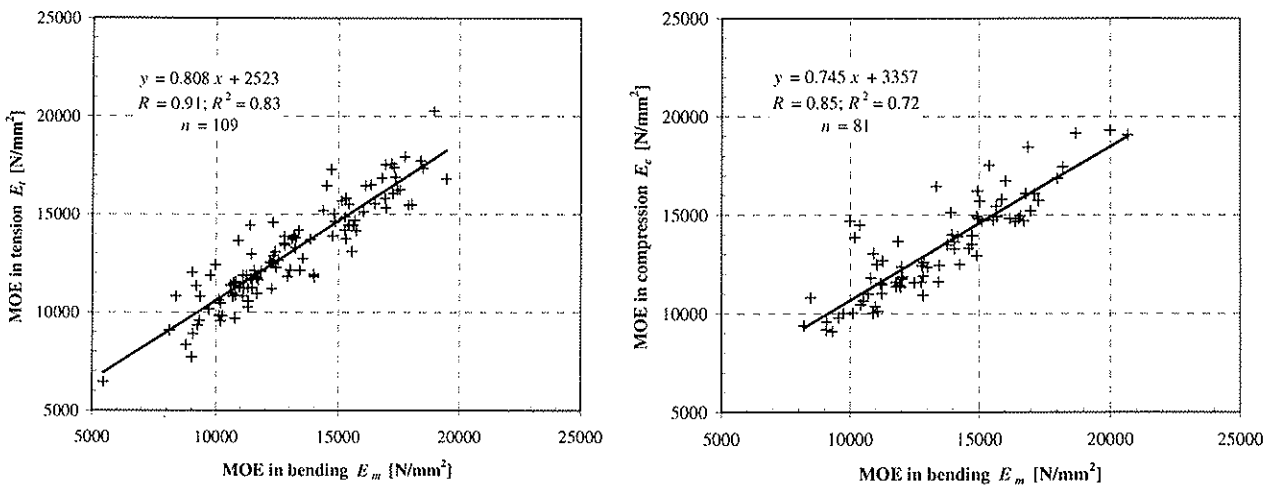

Fig. 10: Flexural MOE E_m versus tensile MOE E_t (left) and versus MOE in compression E_c (right) for Swiss grown Spruce structural timber with cross section 80/160 mm.

The following linear regression Equation could be derived from the tests:

$$E_t = 0.808 \cdot E_m - 2523 \qquad \text{with } R = 0.91 \quad (R^2 = 0.83) \qquad (15)$$

$$E_c = 0.745 \cdot E_m + 3357 \qquad \text{with } R = 0.85 \quad (R^2 = 0.72) \qquad (16)$$

An evaluation of the regression Equation for the EN 338 strength classes spectrum results in MOE ratios given in Table 4 and plotted in Fig. 11. On average, flexural MOE according to EN 408 differed only by 1% from MOE in tension or in compression. However, the ratios are not constant; they depend on timber quality and on sawing pattern:

- low-quality timber (for example class C18): $E_t/E_m = 1.09$ $E_c/E_m = 1.12$
- normal-quality timber of classes C24 to C30: $E_t/E_m = 1.03$ $E_c/E_m = 1.04$
- high-quality timber of classes C35 and C40: $E_t/E_m = 1.00$ $E_c/E_m = 1.00$.

Timber members assigned to classes C35 and C40 are free of defects. That is why such members behave similar to small clear specimens resulting in identical MOE E_t, E_c, E_m.

Table 4: Ratios of flexural MOE and MOE in tension or in compression for Swiss grown Spruce solid timber with cross section 80/160 mm.

Strength class	E_m [N/mm^2] acc. EN 338	E_t [N/mm^2] calc. with (15)	E_c [N/mm^2] calc. with (16)	Ratio E_t/E_m	Ratio E_c/E_m
C14	*7000*	*8193*	*8607*	*1.17*	*1.23*
C16	*8000*	*9003*	*9357*	*1.13*	*1.17*
C18	9000	9813	10107	1.09	1.12
C20	9500	10218	10482	1.08	1.10
C22	10000	10623	10857	1.06	1.09
C24	**11000**	**11433**	**11607**	**1.04**	**1.06**
C27	**11500**	**11838**	**11982**	**1.03**	**1.04**
C30	**12000**	**12243**	**12357**	**1.02**	**1.03**
C35	13000	13053	13107	1.00	1.01
C40	14000	13863	13857	0.99	0.99
C45	15000	14673	14607	0.98	0.97
C50	16000	15483	15357	0.97	0.96

italic: extrapolation **bold: normal-quality timber**

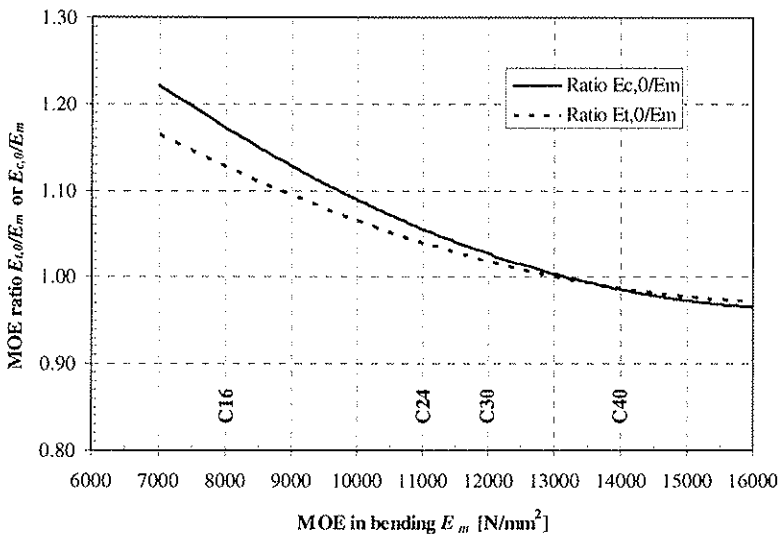

Fig. 11: MOE ratios: tension / bending and compression / bending.

4.6 Ratio of 5th-percentile and mean value of MOE and density

4.6.1 MOE in bending

The ratio of characteristic to mean MOE calculated based on all results of bending tests (n = 668) yields in E_{05}/E_{mean} = 0.70. The coefficient of variation is 18.4% and a normal distribution fits the data reasonably well (Fig. 12).

4.6.2 Density

The ratio between characteristic and mean value of density (MC = 12%) of all 1640 specimens tested results in r_k/r_{mean} = 0.84. The mean value is 450 kg/m^3 and the coefficient of variation amounts to approximately 9.7%. The normal probability plot (Fig. 13) confirms the assumption of a normal distribution for density.

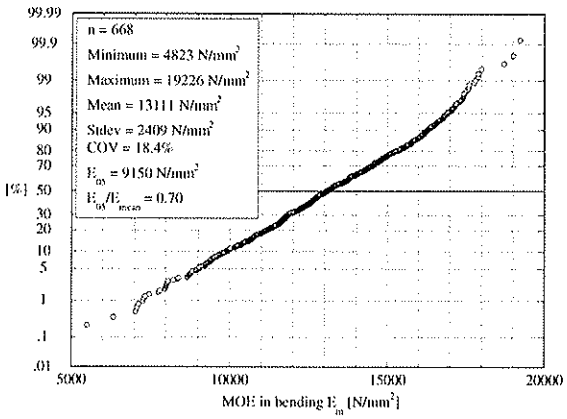

Fig. 12: Normal probability plot of flexural MOE for a MC of 12%.

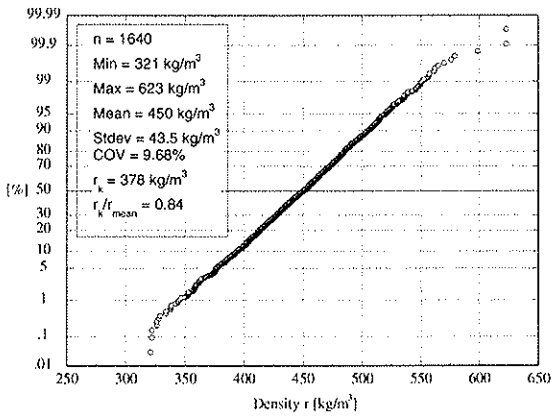

Fig. 13: Normal probability plot of density for a MC of 12%.

4.7 Influence of cross section on bending and on tensile strength

The database analysed in this paper results from tests not especially designed for the evaluation of size effects. Concerning the influence of size and shape of the cross section on bending and tensile strength only tendencies can be shown. Derived relationships are just indicative. Regarding the influence of size on the bending strength, a trend line fit based on a power model according to Equation (9) tends towards an exponent of m_R = -0.19 (Fig. 14) and confirms the EN 384 approach (m_R = -0.20). The coefficient of determination R^2 is low.

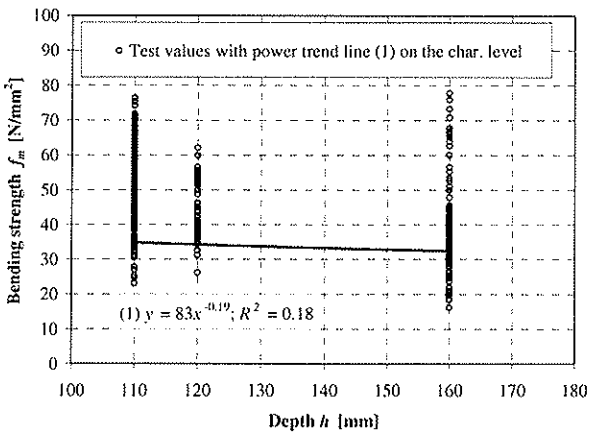

Fig. 14: Influence of depth on bending strength.

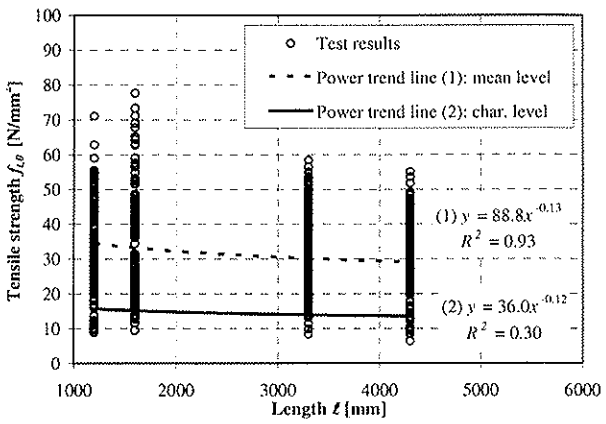

Fig. 15: Influence of length on tensile strength.

The characteristic value of tensile strength parallel to the grain $f_{t,0,k}$ was found to be affected by member length (Fig. 15) but no influence of width on tensile strength could be shown. These results are in line with the findings of Burger and Glos [21], where tensile strength is reported to decrease with increasing member length (m_ℓ = -0.13 on the mean level) and an effect of width as suggested in European standards could not be confirmed.

5 Conclusions

Our investigations lead to the following conclusions:

- The correlation of bending strength and flexural MOE derived from static bending tests is consistent with other studies. The regression line however does not follow exactly the trend of pairs ($f_{m,k}$; $E_{0,mean}$) given for the strength classes in EN 338. In classes C27 to C50 flexural MOE found in tests was higher than indicated in EN 338.
- Tensile to bending strength ratio was found not to be constant, but to depend on timber quality. Ratios for strength classes above C22 amounted to 0.8 – 1.1. Nevertheless, for design practice the use of a conservative value of 0.6 is reasonable.
- The relationship between the characteristic values of compression and bending strength parallel to the grain given in EN 384 is more conservative than our test results. As an alternative to the existing approach, the compression strength parallel to the grain could be derived from wood density using a linear model.
- The ratios of MOE of full-size structural timber in tension, compression and bending differ depending on timber quality. Differences up to 9% between tensile and flexural MOE were found. Regarding compression MOE, the maximum difference to the bending MOE was 12%. For normal quality timber of classes C24 to C30 (mostly used in practice), the differences between E_t, E_c and E_m account to not more than approximately 5%. With regard to a simple design process, the current practice of using one single MOE value should therefore not be changed. But when assigning timber populations to strength classes based on tension MOE instead of flexural MOE, the differences have to be taken into account. In this case, timber must be regarded as a composite material having zones of different MOE within cross sections depending on sawing pattern.
- The calculated fractile ratios for density r_k/r_{mean} and for MOE parallel to the grain $E_{0,05}/E_{0,mean}$ were 0.84 and 0.70. These values correspond well to the ratios assumed in EN 384 and EN 338 (0.84 and 0.67) assuming a COV of 10% and 20% respectively.
- The influence of depth h on the bending strength was confirmed to follow a power trend with an exponent of m_R = 0.2. The tensile strength was not found to be influenced by member width but rather by its length. Consequently the EN 384 approach should be reconsidered where tensile strength is regarded to follow a power function of width with an exponent of m_R = 0.2.

To sum up:
Based on our test results the strength class profiles given in EN 338 are confirmed and regarding the parameters r_k, $f_{m,k}$, $f_{c,0,k}$, $f_{t,0,k}$ and E_0 no reason for substantial changes were found. Instead of deriving the compression strength parallel to the grain from the bending strength, the wood density might be taken as basis. Doing so the importance of density as a classification criterion would be increased. The size adjustment factor for tensile strength however should be reconsidered.

6 References

[1] Comité Européen de Normalisation CEN, 2003 : EN 338: Structural timber - Strength classes.

[2] Comité Européen de Normalisation CEN, 2004 : EN 384: Structural timber - Determination of characteristic values of mechanical properties and density.

[3] Comité Européen de Normalisation CEN, 2003: EN 408: Timber structures - Structural Timber and glued laminated timber - Determination of some physical and mechanical properties.

[4] Glos P., 1995: Step A6: Festigkeitssortierung. In: Holzbauwerke nach Eurocode 5, Step 1: Bemessung und Baustoffe. Informationsdienst Holz der Arbeitsgemeinschaft Holz e. V. Düsseldorf. p. A6/1 – A6/9.

[5] Green D. W., Kretschmann D. E., 1990: Stress class systems - An idea whose time has come? Forest Products Laboratory. Madison, Wisconsin, USA.

[6] Burger N., Glos. P., 1997: Strength relationships in structural timber subjected to bending and tension. Paper 30-6-1 in: Proceedings of CIB-W18 Meeting 30. Vancouver, Canada.

[7] Green D. W., Kretschmann D. E., 1989: A discussion of lumber property relationships in Eurocode 5. Paper 22-6-3 in: Proceedings of CIB-W18 Meeting 22. Berlin, German Democratic Republic.

[8] Curry W. T., Fewell A. R., 1997: The relations between the ultimate tension and ultimate compression strength of timber and its modulus of elasticity. Princes Risborough Laboratory, Building Research Establishment BRE. Buckinghamshire, Great Britain.

[9] Ylinen A., 1942.: Über den Einfluss des Spätholzanteiles und der Rohwichte auf die Festigkeits- und elastischen Eigenschaften des Nadelholzes. Acta forest. Fenn. 5:1. In Kollmann F. F. P., Côté Jr. W. A., 1968: Principles of Wood Science and Technology - Part 1: Solid Wood. p. 346.

[10] Ruli A., 2004: Determination of the compression strength of glulam - longitudinal and perpendicular to the grain. Institute of timber engineering and wood technology, Graz University of Technology, Austria.

[11] Conners T. E., Medvecz P. J., 1992: Wood as a bimodular material. Wood and Fiber Science **24** (4). p. 413-423.

[12] Burger N., Glos P., 1995: Relationship of moduli of elasticity in tension and in bending of solid timber. Paper 28-5-2 in: Proceedings of CIB-W18 Meeting 28. Copenhagen, Denmark.

[13] Gehri E., 1997: Timber as natural composite: explanation of some peculiarities in the mechanical behaviour - Case: Assessment of the modulus of elasticity of timber parallel to grain. Paper 30-6-3 in: Proceedings of CIB-W18 Meeting 30. Vancouver, Canada.

[14] Thunell B., 1941: Über die Elastizität schwedischen Kiefernholzes. Holz als Roh- und Werkstoff **4** (1). p. 15-18.

[15] Pierce F. T., 1926: Tensile tests for cotton yarns. Textile Institute Journal **17**. p. T355-T368.

[16] Tucker J., 1927: A study of the compression strength dispersion of materials with applications. Journal of the Franklin Institute **204**. p. 751-781.

[17] Weibull W., 1939: A statistical theory of the strength of materials. In: Proceedings of the Royal Swedish Institute of Engineering Research. Bulletin No. 151:1. Royal Technical University of Stockholm, Sweden.

[18] Weibull W., 1939: The phenomenon of rupture in solids. In: Proceedings of the Royal Swedish Institute of Engineering Research. Bulletin No. 153. Royal Technical University of Stockholm, Sweden.

[19] Madsen B., Buchanan A. H., 1986: Size Effects in Timber Explained by a Modified Weakest Link Theory. Canadian Journal of Civil Engineering **13** (2). p. 218-232.

[20] Rouger F., 1995: Step B1: Einfluss des Volumens und der Spannungsverteilung auf die Festigkeit. In: Holzbauwerke nach Eurocode 5, Step 1: Bemessung und Baustoffe. Informationsdienst Holz der Arbeitsgemeinschaft Holz e. V. Düsseldorf. p. B1/1 – B1/8.

[21] Burger N., Glos P., 1996: Effect of size on tensile strength of timber. Paper 29-6-1 in: Proceedings of CIB-W18 Meeting 29. Bordeaux, France.

[22] Madsen B., 1992: Structural behaviour of timber. Timber Engineering Ltd. North Vancouver, B. C, Canada.

[23] Barrett J. D., Griffin. H., 1989: Size effects and property relationships for Canadian 2-inch dimension lumber. Paper 22-6-1 in: Proceedings of CIB-W18 Meeting 22. Berlin, German Democratic Republic.

[24] Barrett J. D., Fewell A. R., 1990: Size factors for the bending and tension strength of structural timber. Paper 23-10-3 in: Proceedings of CIB-W18 Meeting 23. Lisbon, Portugal.

[25] Glos P., 1990: Vergleichende Berechnungen für Bauteile und Verbindungsmittel auf der Grundlage des neuen Sicherheitssystems - EUROCODE 5 - Holzbauwerke - Teilprojekt I: Baustoffe. Bericht 89501. Institut für Holzforschung, Universität München, Deutschland.

[26] Barrett J. D., Lam F., Lau W., 1992: Size effects in visually graded softwood structural lumber. Paper 25-6-5 in: Proceedings of CIB-W18 Meeting 25. Ahus, Sweden.

[27] Rouger F., Fewell A. R., 1994: Size effects in timber: Novelty never ends. Paper 27-6-2 in: Proceedings of CIB-W18 Meeting 27. Sydney, Australia.

[28] Steiger R., 1995: Biege-, Zug- und Druckversuche an Schweizer Fichtenholz. Institut für Baustatik und Konstruktion IBK, ETH Zürich. Bericht Nr. 207. Birkhäuser Verlag, Basel.

[29] Steiger R., 1995: Versuche an Fichten-Kanthölzern: Biegemoment - Normalkraft – Interaktion. Institut für Baustatik und Konstruktion IBK, ETH Zürich. Bericht Nr. 209. Birkhäuser Verlag, Basel, Schweiz.

[30] Steiger R., 1996: Mechanische Eigenschaften von Schweizer Fichten-Bauholz bei Biege-, Zug-, Druck- und kombinierter M/N-Beanspruchung. Institut für Baustatik und Konstruktion IBK, ETH Zürich. Bericht Nr. 221. Birkhäuser Verlag, Basel, Schweiz.

[31] Arnold M., Steiger R., 2006: The influence of wind-induced compression failures on the mechanical properties of spruce structural timber. Materials and Structures, published online June 2006.

[32] Mischler-Schrepfer V., 2000: Der Einfluss der Waldlagerung von Fichten-Rundholz auf die Längs-Zugeigenschaften des Schnittholzes. Dissertation Nr. 13857, ETH Zürich, Schweiz.

[33] Sandoz J.-L., 1990 : Triage et fiabilité des bois de construction validité de la méthode ultrason. Dissertation Nr. 851, EPF Lausanne, Schweiz.

[34] Steiger R., Arm H., Gehri E., 1994: Einspannvorrichtung für Zugversuche an Holzproben grösseren Querschnitts. Institut für Baustatik und Konstruktion IBK, ETH Zürich. Bericht Nr. 204. Birkhäuser Verlag, Basel, Schweiz.

[35] Steiger R., Fontana M., 2005: Bending moment and axial force interacting on solid timber beams. Materials and Structures **38** (279). p. 507-513.

Annex

A.1 Correlation of dynamic MOE E_{dyn} and mechanical properties

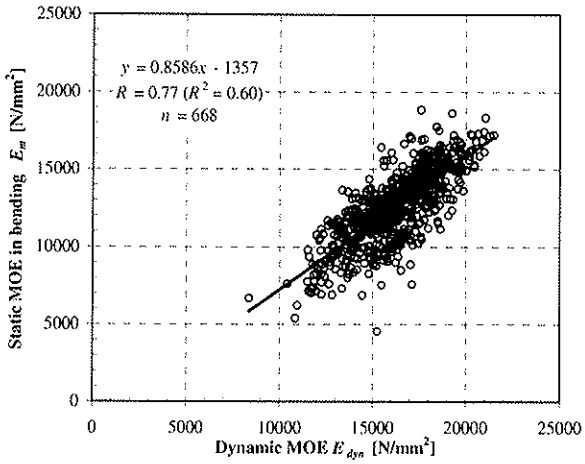

Fig. 16: MOE in bending E_m vs. E_{dyn}.

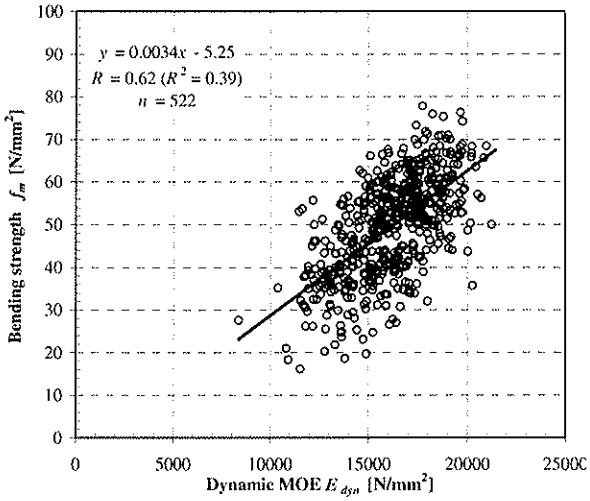

Fig. 17: Bending strength f_m vs. E_{dyn}.

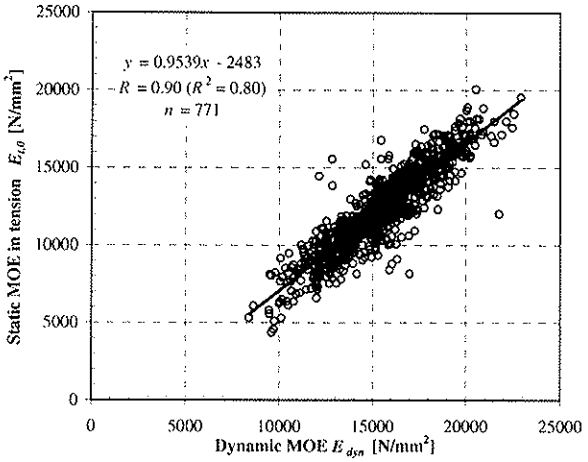

Fig. 18: MOE in tension $E_{t,0}$ vs. E_{dyn}.

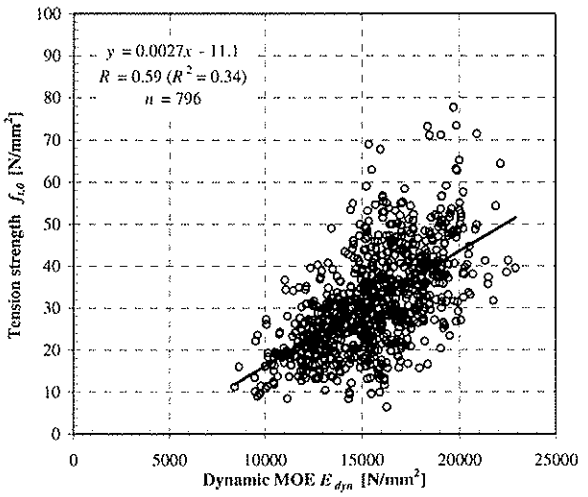

Fig. 19: Tensile strength $f_{t,0}$ vs. E_{dyn}.

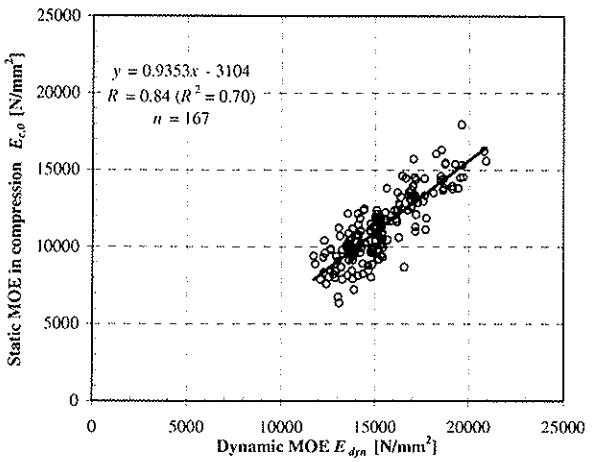

Fig. 20: MOE in compression $E_{c,0}$ vs. E_{dyn}.

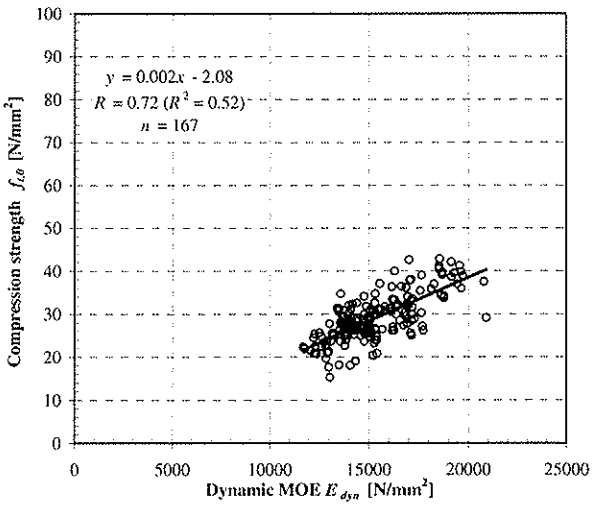

Fig. 21: Compression strength $f_{c,0}$ vs. E_{dyn}.

INTERNATIONAL COUNCIL FOR RESEARCH AND INNOVATION
IN BUILDING AND CONSTRUCTION

WORKING COMMISSION W18 - TIMBER STRUCTURES

EFFECTIVE IN-ROW CAPACITY OF MULTIPLE-FASTENER CONNECTIONS

P Quenneville
M Bickerdike

Royal Military College of Canada
Kingston

CANADA

MEETING THIRTY-NINE
FLORENCE
ITALY
AUGUST 2006

Presented by P Quenneville
H Blass asked whether the net tension failure mode in EC5 was considered in the comparison. He commented that 4d or 5d was considered in the study but EC5 only allow as low as 5d and asked whether this would influence the conclusion. P Quenneville responded that net tension was not considered as failure mode but group tear out was. Also 5d was considered within the database.
H Blass stated that load slip curve for single bolt was used in the research and asked how one knew whether this would be appropriate for a group of bolts especially when splitting initiate from a single bolt. P Quenneville replied that the use of single bolt data was an assumption but the results seemed to show that it was appropriate. I Smith suggested that the localized shear failure under the bolt may explain why it worked. He commented that P Quenneville did a lot of work to pull the various databases together.
T Williamson offered explanation why NDS on this topic is not mandatory at this point and USFPL might be doing more work on this issue.
H Riberholt asked about the influence of staggering of bolts. P Quenneville commented that these non-staggered connections are the most common; therefore, staggered system was not considered.
E Karacabeyli and P Quenneville discussed the issue of influence of density and material service condition factor.
A Jorissen questioned about the phi factor. P Quenneville explained the phi factor depended on the variability of failure load and the failure mode.
A Hanhijärvi asked about the details on the gap between the bolts and the wood. P Quenneville explained the computer model did not show dependency on the gap and load slip were treated randomly first. In the final analysis gap was set at 1.6 mm.

Effective in-row capacity of multiple-fastener connections

Pierre Quenneville, Morgan Bickerdike
Royal Military College of Canada
Kingston, Canada

1 Introduction

It is well accepted that the effective in-row capacity of multiple-fasteners is potentially less than the sum of the capacity of each individual fastener in the row. Since most design procedures are based on principles developed for single fasteners failing in a ductile mode, multiple-fastener connection resistances could not be reasonably predicted for all cases. To overcome this shortcoming, design procedures would include modification factors that took various geometric variables into account, trying to cover all possible situations. In recent past, research observations have shown that this decrease from the optimal resistance is due to the brittle failures of the wood fibers surrounding the fasteners. Multiple-fastener connections would fail in row-shear, group tear-out, or splitting.

A numerical model based on the load-slip behaviour of single fastener connections was developed to study the behaviour of multiple fastener connections failing in row-shear. Variables taken into account include single fastener load-slip curves with varying resistances, stiffness and ultimate slip, fastener gaps, and number of in-row fasteners. The numerical model was developed using the finite element software ANSYS. Numerical predictions of the connection ultimate load were compared to available experimental results of the modelled connection configurations, showing good agreement. The model was then used to predict the ultimate resistances of connection configurations for various end distances and fastener spacings. From these predictions, a design equation for row-shear was developed.

This design equation is presented and compared to the Canadian, European and American design provisions for the in-row connection resistance.

2 Numerical model

The numerical model from Bickerdike (2006) was developed to simulate the ultimate strength of multiple-bolt connections failing in row-shear. This model uses 2-dimensional finite elements from the ANSYS software. The connection geometry and material properties are built, and the non-linear static analysis is executed by utilizing a pre-written batch file code. A significant component of the analysis was to randomize (1) the initial

bolt hole gap of each fastener in the connection, and (2) the load-slip relationship of each fastener from known variances and average values determined from experimental tests.

A schematic of the loading mechanism on a single fastener within the model is presented in Figure 1. The wood, steel plates and bolts are represented as linear-elastic elements. Non-linear spring elements are implemented in the model to represent the experimentally tested load-slip curves of single bolt connections at 4d, 7d and 10d end distances, at slenderness ratios of 4.2 and 6.8. An example of a single fastener load-slip curve is illustrated in Figure 2, where the ultimate strength is 49.5 kN and the slip limit is 20.2 mm.

The failure modes of these experimental tests range from various forms of EYM ductile failure to the brittle case of row-shear. A displacement is applied to the elements representing the steel plates. Once the bolt comes in contact with the wood surface, the non-linear spring is engaged in compression. As the load-slip curve reaches its slip limit, the load is removed while the slip continues to increase. In order to adequately simulate the load-slip response of the non-linear springs, no failure in the wood elements is possible.

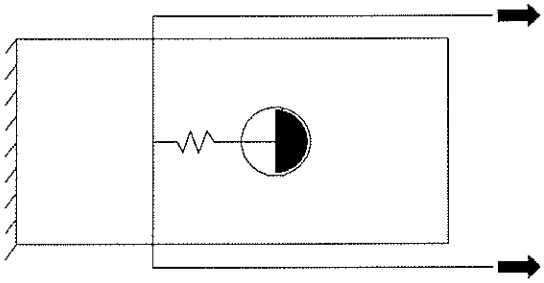

Figure 1 – Single Bolt Spring Representation

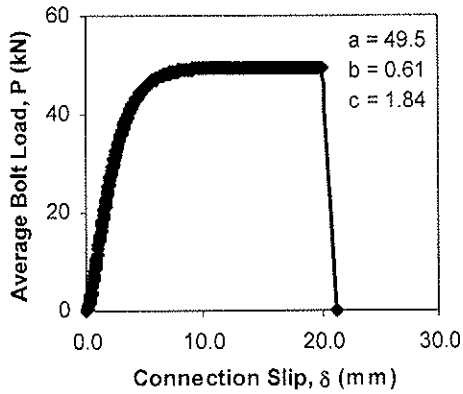

Figure 2 – Single 19.1 mm Bolt Load-Slip Curve in 80 mm S-P Glulam

A series of single-bolt connections of varying end distances were tested to obtain the shape of their load-slip curves. For each test, the load-slip curve (refer to Figure 2) was idealized by the relationship in equation (1) where the coefficients a, b, and c describe its shape. From the assemblage of single-fastener tests, average and COV values for these coefficients were determined to permit for possible variations to each individual bolt.

$$P = a\left(1 - \exp^{(-b\delta)}\right)^c \qquad (1)$$

Once the shape of each load-slip curve is obtained, the average slip limit (δ_x) along with variances was established for each of the 4d, 7d, and 10d end distances. This would instruct the model to cut-off the load-slip curve for a single fastener at a certain point, otherwise simulating failure in that spring. A summary of the randomized variables for a 19.1 mm diameter bolt in 80 mm thick Spruce-Pine (S-P) glulam is presented in Table 1.

Table 1 – Random Input Variables for 80 mm S-P Glulam Numerical Model

	Initial Gap	a	b	c	δ_{4d}	δ_{7d}	δ_{10d}
	mm	kN	mm^{-1}		mm	mm	mm
Average	0.8	49.55	0.61	1.84	4.51	7.50	17.70
St. Dev.		5.45	0.20	0.73	1.51	1.81	5.30

A relationship between the end distance and the corresponding single fastener slip limit was established for both average and COV slip values. The relationships in equations (2) and (3) allow for the computer model to generate the load-slip response for each fastener in the model at any end distance (e) or bolt spacing (s_B). In these equations, (x) refers to the e/d or s_B/d ratio for the individual fastener, and utilize the information for δ_x presented in Table 1.

$$\delta_x = 3.26 + 0.24\exp^{(0.41x)} \quad (2)$$

$$\delta_x \text{st.dev} = 1.51 + 0.001\exp^{(0.85x)} \quad (3)$$

With all of the variations applied, the non-linear springs describing the load-slip relationships will have a unique shape for each bolt in the modelled configuration. The number of rows (n_R), number of bolts in-the-row (n_{fi}), member thickness (t), and bolt diameter (d) were all set in the model, while the variables in Table 1 were randomly assigned for each bolt in a non-linear analysis. In total, 40 simulation loops were required for a specific configuration. The set of randomized variables are assigned unique values for each simulation loop, thus producing a scatter of ultimate loads that would typically be found through experimental testing.

Numerical predictions were first made on experimentally tested connection configurations failing in row-shear to assess the ability of the computer model to predict the ultimate strength of connections failing in this brittle manner. In total, 40 non-linear analyses of the 6 steel-wood-steel (SWS) configurations comprised of S-P glulam material were modelled, and the results in comparison to tested data are presented in Table 2. For cases of two rows of bolts, a row spacing (s_R) of 5d was sufficient to permit a row-shear failure. From the information presented in this table, confidence in the computer model was achieved.

Table 2 – Comparison of Numerical vs. Experimental Average Ultimate Loads

Dimension	d	n_R	n_{fi}	e	s_B	s_R	P_{avg} (kN)		% Diff
mm x mm	mm						Predicted	Actual	
80 x 190	19.1	1	2	7d	4d	--	82	78	5.1
80 x 190	19.1	1	2	10d	4d	--	85	92	-7.6
80 x 152	19.1	1	3	7d	4d	--	121	118	2.5
80 x 190	19.1	1	4	7d	4d	--	152	141	7.8
80 x 190	19.1	2	3	7d	4d	5d	228	242	-2.8
130 x 190	19.1	2	4	7d	4d	5d	394	408	-3.4

The numerical model was further utilized to predict the ultimate loads of various connection configurations. Table 3 presents the average predicted connection strength (P_{avg}) of 18 SWS configurations with 19.1 mm diameter bolts in 80 mm x 190 mm S-P glulam. From the predicted results of the configurations presented in Table 3, the ultimate load of connections failing in row-shear showed a significant dependency on the minimum of either the end distance or bolt spacing in-the-row, min(e,s_B). The bolt in the model with the minimum of these two geometric parameters along with the minimum initial gap was the fastener responsible for triggering failure. The trend observed from these predictions was that connections with min(e,s_B) = 4d parameter had ultimate loads significantly lower than for connections with min(e,s_B) = 10d. A similar tendency was observed for a minimum parameter of 7d but to a lesser extent.

Table 3 – Prediction Results from 2-D Finite Element Analysis

e	s_B	s_R	Group 1 n_R=2, n_{fi}=2 P_{avg} (kN)	Group 2 n_R=2, n_{fi}=3 P_{avg} (kN)
4d			151	223
7d	4d	5d	156	228
10d			158	228
4d			158	240
7d	7d	5d	187	279
10d			189	281
4d			158	240
7d	10d	5d	189	284
10d			198	297

3 Proposed design procedures and equations

The format of the proposed design approach for parallel-to-grain loading involves the determination of the ultimate strength (p_u) for each mode of ductile and brittle failure. The design criteria would therefore be the minimum lateral strength value determined from this set of equations. This design provision eliminates the reliance on modification factors that account for brittle situations.

$$\text{Strength} = \min \begin{cases} \phi_y p_{uB} \\ \phi_w p_{uRS} \\ \phi_w p_{uGT} \\ \phi_w p_{uT} \end{cases} \tag{4}$$

The lateral strength of connections failing in a ductile manner, p_{uB}, uses the minimum load-carrying capacity value of a single fastener found by the set of equations outlined by the EYM, and is further multiplied by the number of fasteners in the connection.

The numerical model presented above was created to simulate the strength characteristics of multiple-bolt connections failing in row-shear (RS). The results of this model showed that the lateral strength of the row-shear failure mode is strongly dependent on the minimum parameter of either the end distance or bolt spacing, otherwise referred to as the triggering length. From this observation, the proposed design procedure for predicting the lateral strength of row-shear failure follows the guideline in equation (5).

The best fit for the row-shear design equation is found when the longitudinal shear strength (f_v) is divided by 3. Further, a factor of 0.65, based on the work of Mohammad and Quenneville (2001), is required for connections with single shear members. The comparison between the theoretical values of the proposed approach and the experimental values for connections failing in row-shear are presented in Figure 3. The connections in this figure are in the form of steel-wood (SW), wood-steel-wood (WSW) or steel-wood-steel (SWS). The experimentally determined results used to validate the proposed row-shear design equation are obtained from the configurations outlined in Quenneville and Mohammad (2000) and Mohammad and Quenneville (2001).

$$p_{uRS} = \sum_{i=1}^{n_R} 2\,RS_i \qquad (5)$$

Where:

RS_i = $f_v\,K_{ls}\,t\,n_{fi}\,a_{cr}$
f_v = $16.6 \cdot G^{0.85}/3 = 5.53 \cdot G^{0.85}$, in MPa. From [5].
K_{ls} = 0.65, for wood side member(s)
= 1.0, for wood internal member
G = mean oven dry relative density
t = member thickness, in mm
n_{fi} = number of fasteners in row "i"
a_{cr} = min(e,s_B), in mm
n_R = number of rows

The equation describing group tear-out (GT) failure is also created with reference to the triggering length parameter, min(e,s_B). The lateral strength of this mode of failure is determined for connections with more than one row of fasteners, and is outlined in equation (6). Note that this equation will produce the same lateral resistance as the row-shear design equation if only one row of fasteners is used.

$$p_{uGT} = \left(RS_i + RS_{nr}\right) + \frac{f_t\,A_{cr}}{3} \qquad (6)$$

Where:

f_t = $170.7 \cdot G^{1.01}$, in MPa. From [5].
A_{cr} = $(n_R\text{-}1)\cdot[s_R\text{-}(d+2)]\cdot t$, in mm
s_R = row spacing, in mm

Figure 4 represents the comparison between theoretical predictions and experimental values of connections failing by group tear-out, obtained from Mohammad and Quenneville (2001).

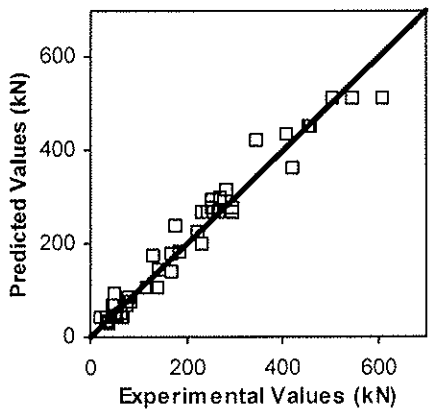

Figure 3 – Prediction vs. Experimental Ultimate Loads for Connections Failing in Row-Shear (RS)

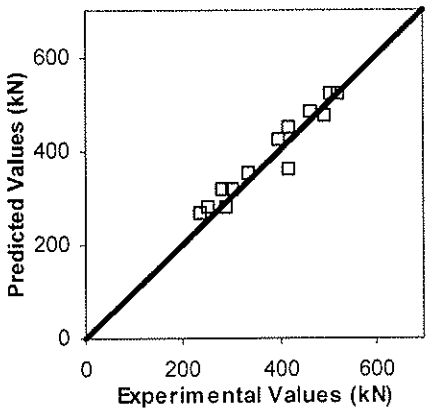

Figure 4 – Prediction vs. Experimental Ultimate Loads for Connections Failing in Group Tear-out (GT)

According to Figure 3 and Figure 4, both the row-shear and group tear-out design equations are able to adequately predict lateral resistances for their respective failure modes. The proposed design approach is a valid representation for the behaviour of laterally loaded bolted connections as these comparisons were made on configurations with varying end distances (e), bolt spacing in-the-row (s_B), row spacing (s_R), number of rows (n_R), number of bolts in the row (n_{fi}), species, bolt diameters and cross-sectional dimensions.

The last mode of brittle failure involves tension (T) fracture along the cross-section of the timber member. This is simply calculated by the following equation:

$$p_{uT} = \min\begin{cases} f_{tg} A_g \\ f_{tn} A_n \end{cases} \qquad (7)$$

Where:

f_{tg} = tension gross-section strength, in MPa
f_{tn} = net gross-section strength, in MPa
A_g = gross cross-sectional area, in mm^2
A_n = net cross-sectional area, in mm^2

A graphical representation of the proposed design approach is presented in Figure 5 for a steel-wood-steel connection with its corresponding dimensional properties as listed in Table 4. In this figure, the effective number of fasteners (n_{ef}) is plotted versus incrementing number of bolts in-the-row (n_{fi}) for the calculated strengths of each failure mode of this specific connection configuration. The design criterion is therefore the minimum lateral strength determined from the proposed set of equations.

Table 4 – Properties of Bolted Connection

Layout	SWS	
Species	S-P	Glulam
t_w	80	mm
b_w	190	mm
t_s	6.35	mm
b_s	152	mm
d	19.1	mm
n_R	2	
e	7d	
s_B	4d	
s_R	5d	

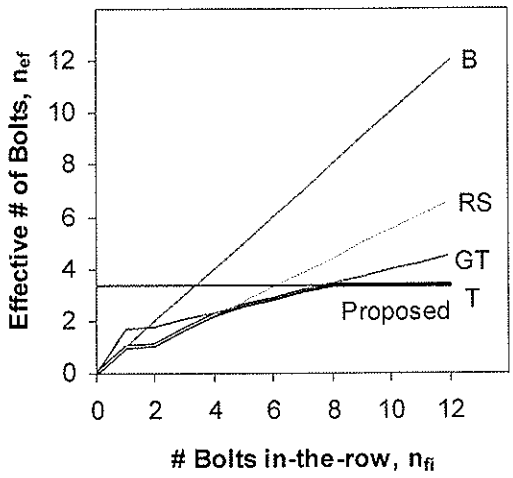

Figure 5 – Effective Number of Fasteners for Proposed Design Approach

Curve B represents ductile failure where n_{ef} is proportional to n_{fi}. The brittle failure modes show a reduced efficiency on a per bolt basis as the ductile strength is not achieved for an incrementing number of bolts in-the-row for this specific connection layout. According to this figure, there is no mechanical advantage for this configuration if more than 8 bolts in-the-row are used, as the effective number of bolts will never exceed 3.35 due to the occurrence of tensile fracture.

4 Effective number of fasteners, n_{ef}

In current design standards, brittle modes of failure are accounted for with the application of modification factors to the ductile lateral resistance design format. This methodology converts the number of bolts in-the-row (n_{fi}) to the effective number of fasteners (n_{ef}), and is then subsequently multiplied by n_{fi} to obtain the connection strength. The adjustments utilized by each international design standard are derived from numerical theories and/or limited independent experimental data, which has resulted in a noticeable strength prediction disagreement from one standard to another with respect to laterally loaded, bolted timber connections.

The National Design Specifications (NDS) utilized in the United States is based on Allowable Stress Design (ASD) format. This design standard implements a group action factor (C_g) where the number of effective fasteners can be obtained by multiplying C_g by n_{fi}. The group factor is based on the elastic numerical model derived by Lantos (1969), and is determined by the relationship in equation (8).

$$C_g = \left[\frac{m\left(1-m^{2n}\right)}{n\left[\left(1+R_{EA}m^{n}\right)\left(1+m\right)-1+m^{2n}\right]}\right]\left[\frac{1+R_{EA}}{1-m}\right] \qquad (8)$$

The European Design Standard, Eurocode 5, for bolted timber connections determines the effective number of fasteners by the relationship in equation (9), where (n) refers to the number of bolts in-the-row, and (a_1) refers to the spacing between bolts in the grain direction.

$$n_{ef} = \min\begin{cases} n \\ n^{0.9}\sqrt[4]{\frac{a_1}{13d}} \end{cases} \tag{9}$$

The Canadian design standard accounts for brittle behaviour by applying a set of modification factors in the form of equation (10). The group factor (J_G) is a numerical interpretation of available experimental data that takes into account the number of bolts in-the-row. For this modification factor, (t) refers to the thickness of the thinnest timber member, (s) refers to the bolt spacing in-the-row, and (N) refers to the number of bolts in-the-row.

$$J_F = J_G\, J_L\, J_R \tag{10}$$

Where:

$$J_G = 0.33\left(\frac{t}{d}\right)^{0.5}\left(\frac{s}{d}\right)^{0.2} N^{-0.3} \le 1.0$$

$$J_L = \begin{cases} 1.0 & \text{for } e = 10d \\ & \text{linear interpolation for intermediate values} \\ 0.75 & \text{for } e = 7d \end{cases}$$

$$J_R = \begin{cases} 1.0 & \text{for 1 row} \\ 0.8 & \text{for 2 rows} \\ 0.6 & \text{for 3 rows} \end{cases}$$

Graphical comparisons of the effective number of bolts (n_{ef}) are made between the existing modification factors of international design codes versus the proposed design approach. Six groups representing different connection configurations are presented where the geometric attributes are varied. These configurations are outlined in Table 5, along with their corresponding graphs in Figure 6 of the effective number of fasteners for each group.

Table 5 – Connection Configurations Used to Compare n_{ef} of Proposed Design Approach to n_{ef} of Existing Standards

Group	Glulam Species	t_w mm	b_w mm	d mm	n_R	e	s_B	s_R
a	S-P	80	190	19.1	1	7d	4d	--
b	S-P	80	190	19.1	1	7d	7d	--
c	S-P	130	266	19.1	2	7d	4d	3d
d	D-Fir	130	304	12.7	2	10d	7d	5d
e	S-P	80	114	10.0	1	7d	4d	--
f	S-P	80	228	8.0	3	7d	4d	5d

For the one-row configuration of group (a), the proposed design format produces a similar n_{ef} relationship to Eurocode 5 (EN5-2004). The proposed line describes the n_{ef} values determined by the row-shear design equation, which otherwise suggests that this mode of failure will occur for any number of bolts in-the-row. Further, group tear-out will not govern since group (a) has one row of fasteners.

The only difference between the configurations of group (a) and group (b) is the in-the-row bolt spacing. If this parameter is increased, then the shape of the proposed line will adjust as the line in row-shear will tend more so towards the EYM, and tension fracture will become a possibility. The configuration of group (b) ably demonstrates the flexibility of the new design approach by accounting for variations towards bolt spacings.

The specifications of group (c) are a replicate of the configurations tested by Massé et al. for which the modification factors of the current Canadian design provisions (CSA-2001) are based upon. As seen in the graphical representation of this group, the proposed design approach produces a nearly identical response to the n_{ef} obtained from CSA-2001. The shape of the line describing the proposed design approach follows the equation for group tear-out failure.

Group (d) further attests to the flexibility of the new design approach as variations are permitted to all of the parameters in Table 5. This example falls within close proximity of the existing design standards, more specifically the NDS group factor. The final two examples emphasize the use of slender dowels where in group (e), the proposed design approach produces an effective number of fasteners much like the values obtained from the Eurocode 5 design provisions. Furthermore, the final group implements three rows of slender dowels where group tear-out failure governs the design for this particular dimensional configuration beyond four bolts in-the-row.

Comparisons are not limited to the six configurations presented; rather this can be accomplished for any possible connection permutation. The ones presented reveal and attest to the capabilities of this simple yet robust proposed design approach.

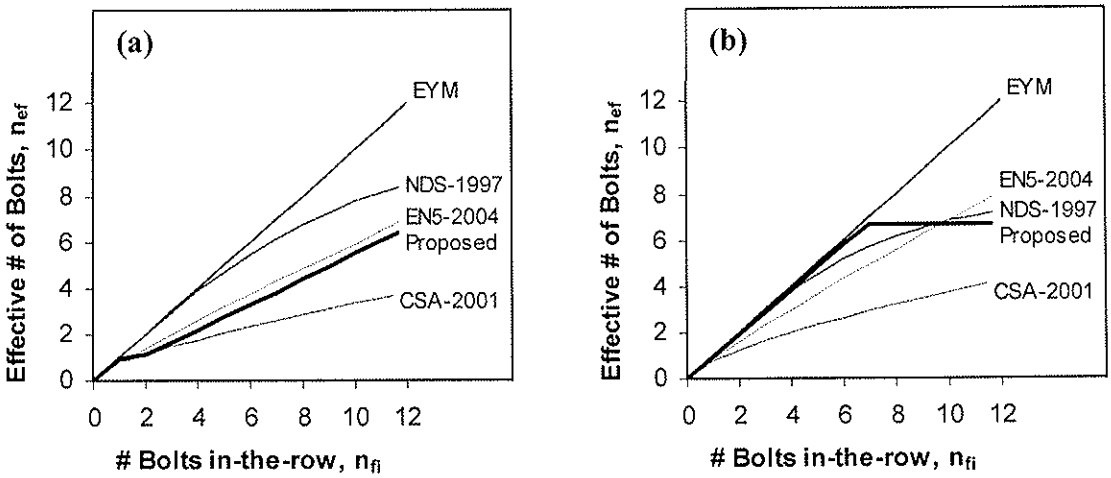

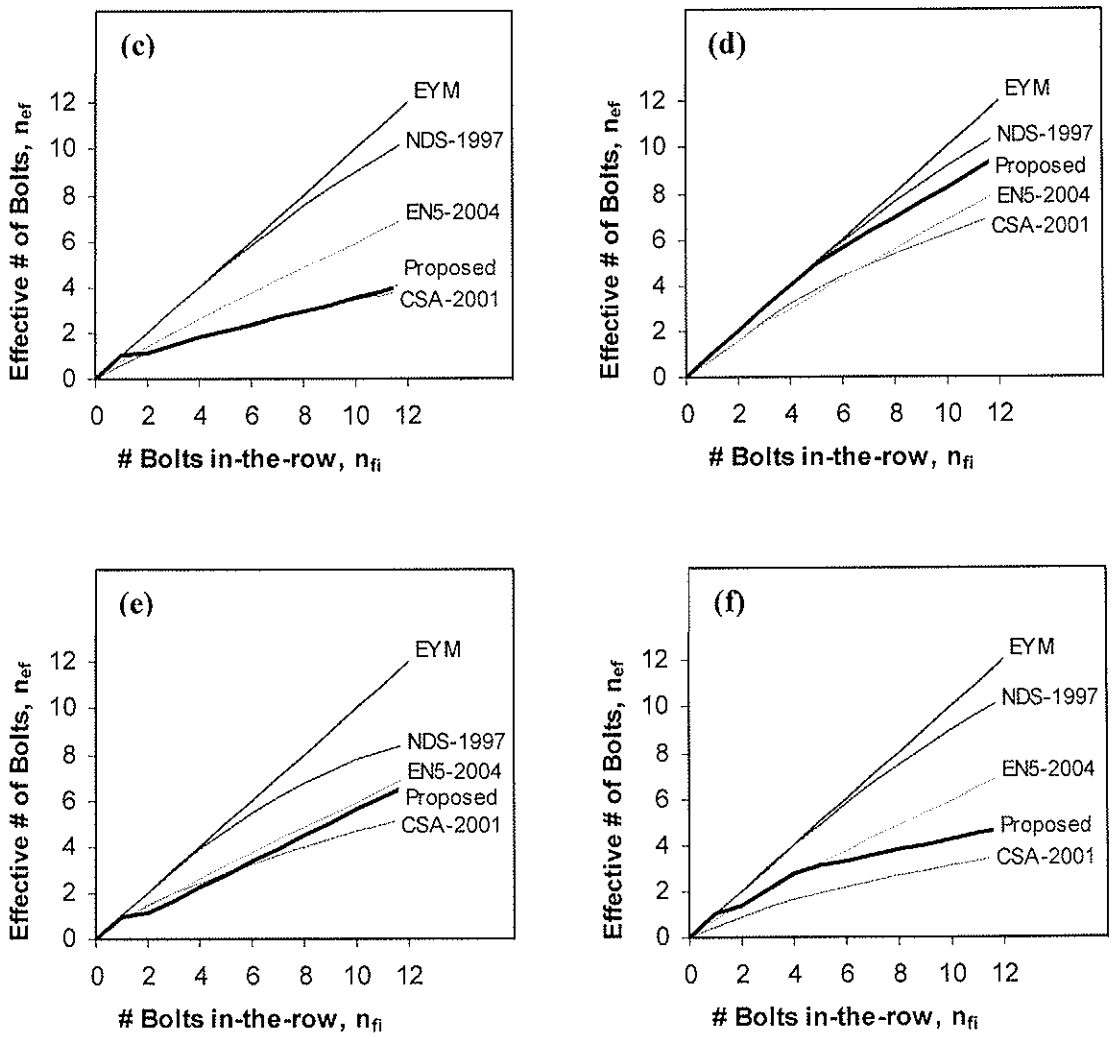

Figure 6 – Comparison of Existing Standards to Proposed Design Approach, Groups a-f

5. Conclusions

A set of design equations to predict the resistance of dowelled connections failing in a brittle manner (row-shear, group tear-out, and net tension) for parallel-to-grain loading is proposed. These equations are based on experimental information along with the results from the numerical model of Bickerdike (2006), and prove to be an effective method of predicting the strength of bolted timber connections loaded in the parallel-to-grain direction.

The relationship of effective number of fasteners to the number of bolts in-the-row was used to compare the proposed set of equations to existing design standards. The proposed design approach replicates the effective number of fasteners for the configurations that were used to develop the Eurocode and Canadian code.

Utilizing the minimum resistance determined from all possible failure modes provides the flexibility to consider all possible connection scenarios in the parallel-to-grain loading direction.

References

[1] Bickerdike, M. 2006. Predicting the row shear failure mode and strength of bolted timber connections loaded parallel-to-grain. M.A.Sc. Thesis, Department of Civil Engineering, Royal Military College of Canada, Kingston, Canada. 231 p.

[2] Bickerdike, M., and Quenneville, J.H.P. 2006. Predicting row shear failure mode in parallel-to-grain bolted connections. Proceedings of the 9th World Conference on Timber Engineering, Portland, Oregon, 8 p..

[3] CSA O86-01. 2001. Engineering design in wood. Canadian Standards Association, Toronto, Canada.

[4] EN 1995-1-1. 2004. Eurocode 5 – Design of timber structures. CEN, Brussels.

[5] Forest Products Society. 1999. Wood handbook: Wood as an engineering material. Forest Products Laboratory General Technical Report FPL-GTR-113. United States of America.

[6] Massé, D., Salinas, J., and Turnbull, J. 1988. Lateral strength and stiffness of single and multiple bolts in glue-laminated timber loaded parallel to grain. Engineering and Statistical Research Centre, Research Branch, Agriculture, Ottawa. 29 p.

[7] Mohammad, M., and Quenneville, J.H.P. 2001. Bolted wood-steel and wood-steel-wood connections: verification of a new design approach. Canadian Journal of Civil Engineering. Vol. 28, pp. 254-263.

[8] NDS-1997. 1997. National Design Specification (NDS) for wood construction. American Forest & Paper Association, Inc., United States of America.

[9] Quenneville, J.H.P., and Mohammad, M. 2000. On the failure modes and strength of steel-wood-steel bolted timber connections loaded parallel-to-grain. Canadian Journal of Civil Engineering. Vol. 27, pp. 761-773.

INTERNATIONAL COUNCIL FOR RESEARCH AND INNOVATION
IN BUILDING AND CONSTRUCTION

WORKING COMMISSION W18 - TIMBER STRUCTURES

SELF-TAPPING SCREWS AS REINFORCEMENTS IN BEAM SUPPORTS

I Bejtka
H J Blaß

Lehrstuhl für Ingenieurholzbau und Baukonstruktionen
Universität Karlsruhe

GERMANY

MEETING THIRTY-NINE
FLORENCE
ITALY
AUGUST 2006

Presented by I Bejtka
K Crews asked about the thickness of the steel. I Bejtka answered that they were the same as the screw head height.
A Jorissen asked about the linear distribution of axial load. H Blass answered that the real distribution from analysis was used which looked fairly linear as shown in the ppt slide.
Jorissen asked about stiffness as E modulus and why not as a spring. I Bejtka stated that it would also be possible to use a spring.
R Marsh asked about the differences between idealized versus actual system, for example, screw head might not be flush with support in reality. H Blass responded that many test (120) were conducted in this particular issue alone.
P Quenneville asked whether the same equation could be used if a very long screw was used when applied from the top through to the support. H Blass answered that it would work provided the bottom section had the same length of screw.
JW van de Kuilen asked about the use of the screws as shear reinforcement. H Blass answered that it was tried and even at 45 degree but it did not work.
I Smith raised the issue of length of screw versus the depth of the member. I Bejtka replied that 66% was used as the ratio between screw length and timber depth.
H Riberholt asked about the influence of moisture variation. I Bejtka answered that more test would be needed.

Self-tapping screws as reinforcements in beam supports

I. Bejtka, H.J. Blaß
Lehrstuhl für Ingenieurholzbau und Baukonstruktionen
Universität Karlsruhe, Germany

1 Introduction

The compressive strength of timber perpendicular to the grain is much lower than the respective strength value parallel to the grain. The ratio of the characteristic compressive strength perpendicular to the grain to the compressive strength parallel to the grain for solid timber is about 1/8. Particularly beam supports should hence be detailed in order to minimise compressive stresses perpendicular to the grain.

Increasing the load-carrying capacity of beam supports may be obtained by enlarging the area loaded perpendicular to the grain or by reinforcing the beam support area. Self-tapping screws with continuous threads represent a simple and economic reinforcement method. The screws are placed at the beam support perpendicular to the grain direction. To evenly apply the support load on the screws and on the timber, a steel plate is placed between the beam surface and the support.

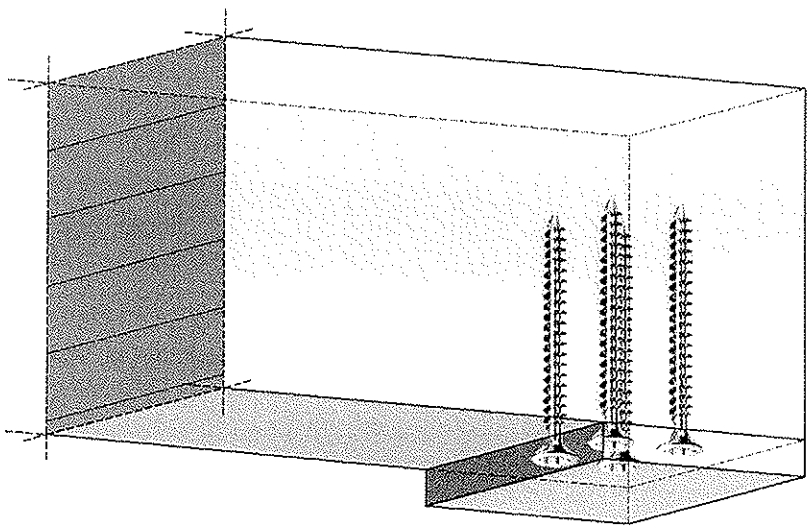

Fig. 1: Bottom view of a reinforced beam support

Comparing the test results, the load-carrying capacity of reinforced beam supports was at maximum 300% higher than the load-carrying capacity of non-reinforced beam supports.

The maximum ratio between the stiffness perpendicular to the grain of reinforced beam supports and the corresponding stiffness of non-reinforced beam supports was about 5.

To calculate the load-carrying capacity and to estimate the stiffness of reinforced beam supports two calculation models were derived. In this paper both calculation models will be presented.

2 Calculation model for the load-carrying capacity

2.1 Assumptions

The load-carrying capacity of reinforced beam supports is calculated taking into account three different failure modes. The governing failure mode depends primarily on the geometry of the beam support and on the geometry of the reinforcing screws i.e. their slenderness ratio. Further parameters influencing the load-carrying capacity are the number and the yield strength of the screws and the strength class of the timber.

The first failure mode occurs in reinforced beam supports with a low number of short screws. In this case, the load-carrying capacity of the reinforced beam support is characterised by pushing the screws into the timber. Simultaneously, the compressive strength perpendicular to the grain at the contact surface is reached. For screws the pushing-in capacity is considered equal to the withdrawal capacity.

The second failure mode occurs in beam supports with slender screws. Here, the reinforcing screws are prone to buckle. Simultaneously, as in the first failure mode, the compressive strength perpendicular to the grain at the contact surface is reached. A typical buckling shape of slender reinforcing screws is shown left in *Fig. 2*.

The third and last failure mode is observed in beam supports with multiple short screws. Here, the load-carrying capacity of the reinforced beam support is characterised by reaching the compressive strength of timber perpendicular to the grain in a plane formed by the screw tips (right in *Fig. 2*).

Taking into account the three possible failure modes, the pushing-in capacity and the buckling load of the reinforcing screws and the compressive strength perpendicular to the grain at the contact surface as well as in a plane formed by the screw tips affect the load-carrying capacity of reinforced beam supports. The compressive strength perpendicular to the grain at the contact surface may be calculated according to [4] (see also in [1]). The pushing-in capacity and the buckling load of the reinforcing screw as well as the compressive strength perpendicular to the grain in a plane formed by the screw tips are presented subsequently.

For the first two failure modes it is assumed, that the compressive strength perpendicular to the grain at the contact surface of the beam and the load-carrying capacity of the axially loaded screws are reached at the same time. For the compressive strength perpendicular to the grain a linear-elastic - ideal-plastic and for the axially loaded screw a linear-elastic load-displacement behaviour is adopted. In spite of different load-displacement behaviour, numerical and analytical calculations confirm that the load-carrying capacity of the axially loaded screws is reached when the compressive strength of the timber is already reached. For this reason, both load-carrying capacities can be added to calculate the load-carrying capacity of reinforced beam supports.

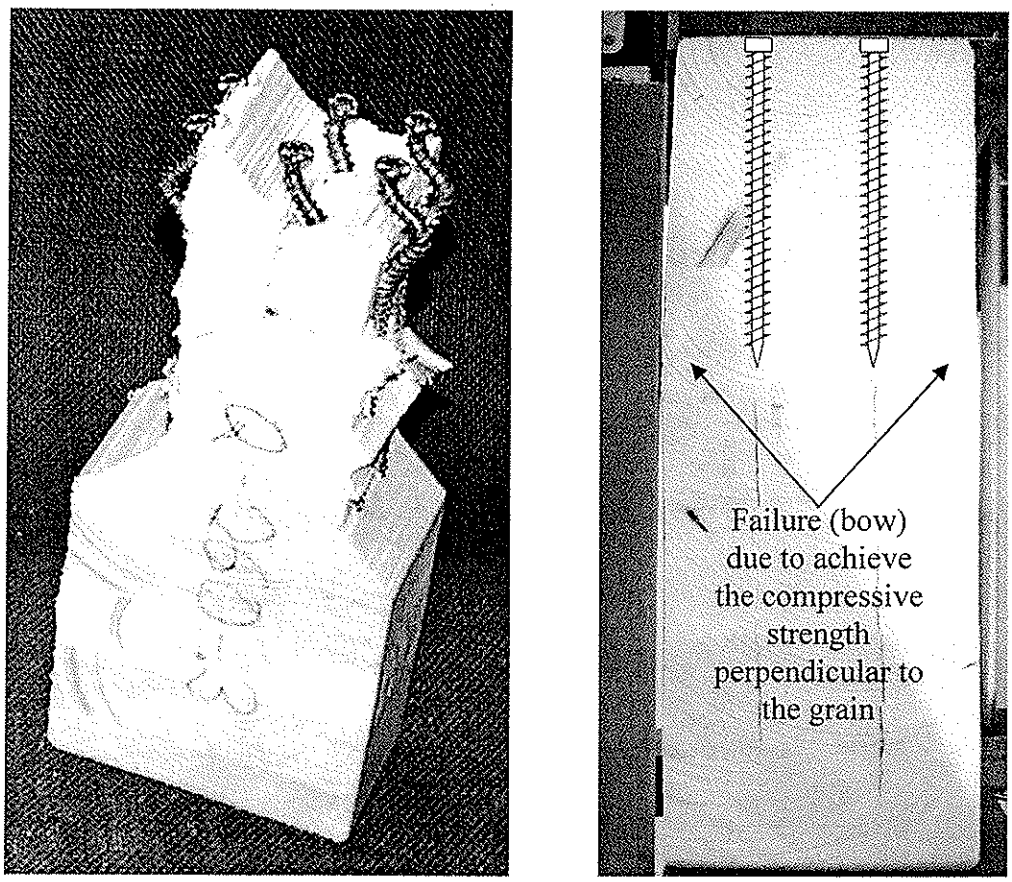

Fig. 2: Buckling of the screws and timber failure in a plane formed by the screw tips

2.2 Pushing-in capacity of self-tapping screws

Preliminary tests have confirmed, that the pushing-in capacity of self-tapping screws is equal to the withdrawal capacity R_{ax}. To determine the pushing-in capacity, 413 withdrawal tests with self-tapping screws were performed. Here, the screw diameter d between 6 and 12 mm and the penetration length of the screw ℓ_S in the timber between 3,33·d and 16·d were varied. The angle between the screw axis and the grain direction was 90°. The best correlation between the test results and the calculated values can be achieved, when the withdrawal capacity is calculated by the following equation.

$$R_{ax} = 0,6 \cdot \sqrt{d} \cdot \ell_S^{0,9} \cdot \rho^{0,8} \qquad (1)$$

The best correlation between characteristic values and test results can be achieved by replacing the factor 0,6 by 0,56 in eq. (1) (see *Fig. 3*).

In *Fig. 3* the calculated characteristic withdrawal capacities in comparison to the test results are displayed.

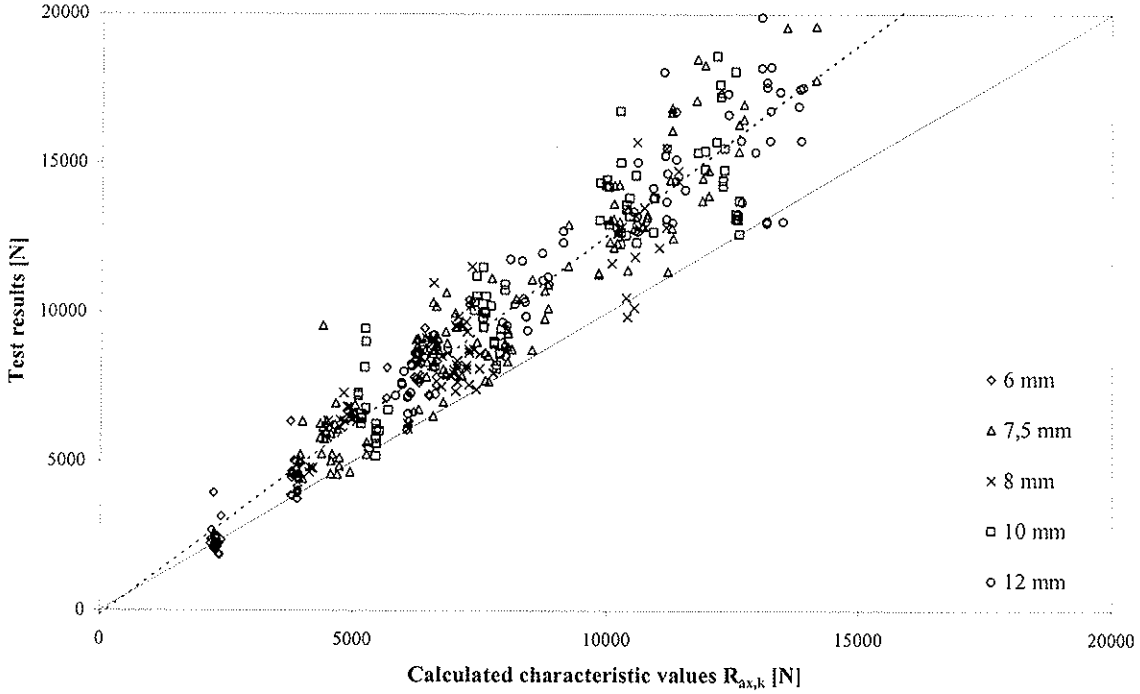

Fig. 3: Calculated characteristic withdrawal capacities in comparison to the test results

2.3 Buckling load of self-tapping screws as reinforcements

The second failure mode is characterised by screw buckling. Here, the reinforcing screws are axially loaded in compression. The ultimate load-carrying capacity for buckling of screws with a circular cross section can be calculated taking into account amongst others the buckling load. The buckling load for axially loaded screws, which are embedded in the timber, was determined by a numerical model (*Fig. 4*).

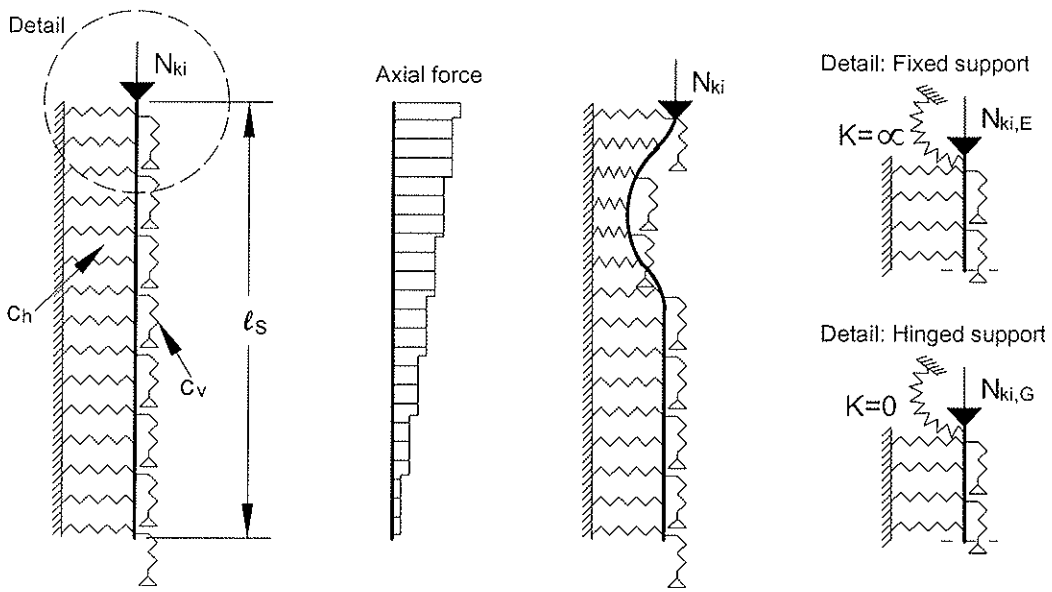

Fig. 4: Numerical model to determine the buckling load N_{ki}

The axially loaded screw with the elastic foundation c_h and with the elastic support c_v is displayed left in *Fig. 4*. The elastic foundation c_h was determined from tests to determine the embedding strength of the timber loaded by screws (400 tests). The elastic support c_v was determined from tests to determine the withdrawal or pushing-in capacity of the screws (300 tests).

The best correlation between the test results and the calculated values can be achieved, when the elastic foundation c_h is calculated by the following equation.

$$c_h = \frac{(0,22 + 0,014 \cdot d) \cdot \rho}{1,17 \cdot \sin^2 \alpha + \cos^2 \alpha} \tag{2}$$

The angle α is the angle between the grain and the force direction. For $\alpha = 90°$ the elastic foundation is smaller than the representative value for an angle of 0°. Hence, reinforcing screws bedded into the timber are prone to buckle perpendicular to the grain.

For the elastic support c_v, the best correlation between the test results and the calculated values can be achieved, when the elastic support c_v is calculated by the following equation.

$$c_v = 234 \cdot \frac{(\rho \cdot d)^{0,2}}{\ell_S^{\,0,6}} \tag{3}$$

The distribution of the axial force (*Fig. 4*) depends on the ratio between the elastic support c_v and the longitudinal stiffness of the screw. An approximately triangle-shaped distribution of the normal force leads to buckling of the screw close to the screw head.

Taking into account the elastic foundation c_h and the elastic support c_v, the buckling loads for screws as reinforcements were calculated by a finite element calculation. Thereby, a clamped screw head support and a hinged screw head support were modelled.

A hinged screw head support must be assumed, when the surface of the screw heads is flush with the beam surface. In this case, using a steel plate, loads from the beam support can be transferred simultaneously into the timber and into the screws. A clamped screw head support may only be assumed by clamping the screw heads i.e. in the steel plate. For this, it is necessary to countersink the steel plate in the form of the screw heads in such a way as the surface of the screw heads is flush with the lower steel plate surface.

The buckling loads were derived depending on the screw length and on the density of the timber, for hinged and clamped screw head supports, with $E_S = 210000$ N/mm^2 and with a ratio between the core and the thread diameter of $d_k/d = 0,7$ (see *Tab. 1 and 2*).

Tab. 1: Characteristic buckling loads for hinged screw head supports

$N_{ki,G,k}$ [kN]		ρ_k = 310 kg/m³					ρ_k = 380 kg/m³					ρ_k = 410 kg/m³					ρ_k = 450 kg/m³				
		Screw diameter [mm]					Screw diameter [mm]					Screw diameter [mm]					Screw diameter [mm]				
		4	6	8	10	12	4	6	8	10	12	4	6	8	10	12	4	6	8	10	12
Screw length l_S [mm]	20	3,99	4,51	4,95	5,37	5,79	4,85	5,52	6,06	6,58	7,10	5,22	5,95	6,54	7,10	7,66	5,70	6,53	7,18	7,79	8,40
	40	7,50	12,5	14,5	15,9	17,3	8,38	14,9	17,6	19,5	21,1	8,73	16,0	19,0	21,0	22,8	9,16	17,3	20,7	23,0	25,0
	60	7,44	16,4	24,2	28,3	31,2	8,30	18,4	28,7	34,3	38,1	8,64	19,2	30,5	36,8	41,0	9,08	20,2	32,7	40,1	44,8
	80	7,41	16,5	28,5	39,0	45,4	8,24	18,5	32,2	45,9	54,7	8,58	19,2	33,6	48,7	58,6	9,00	20,2	35,4	52,1	63,7
	100		16,6	29,0	43,9	56,9		18,6	32,5	49,7	66,7		19,3	34,0	52,1	70,6		20,3	35,8	55,0	75,4
	120			29,4	44,9	62,4			33,0	50,6	71,1			34,4	52,9	74,5			36,2	55,8	78,8
	140			29,7	45,7	64,2			33,2	51,4	72,5			34,6	53,7	75,9			36,4	56,7	80,2
	160	7,25			46,4	65,4	8,06			52,1	73,9	8,38			54,3	77,3	8,80			57,2	81,6
	180		16,7		46,8	66,5		18,6		52,4	75,0		19,3		54,7	78,4		20,3		57,6	82,7
	200			29,8		67,4			33,3		75,8			34,7		79,2			36,5		83,5
	220				47,1	68,1				52,7	76,4				55,0	79,7				57,8	84,0
	>240					68,6					76,9					80,2					84,4
$N_{ki,k}$ [1)]		6,81	16,1	29,9	48,6	72,6	7,54	17,8	33,1	53,8	80,4	7,83	18,5	34,3	55,9	83,5	8,20	19,4	36,0	58,5	87,5

Tab. 2: Characteristic buckling loads for clamped screw head supports

$N_{ki,E,k}$ [kN]		ρ_k = 310 kg/m³					ρ_k = 380 kg/m³					ρ_k = 410 kg/m³					ρ_k = 450 kg/m³				
		Screw diameter [mm]					Screw diameter [mm]					Screw diameter [mm]					Screw diameter [mm]				
		4	6	8	10	12	4	6	8	10	12	4	6	8	10	12	4	6	8	10	12
Screw length l_S [mm]	20	13,3	16,9	18,5	20,0	21,6	14,5	20,7	22,6	24,6	26,5	15,0	22,4	24,4	26,5	28,6	15,7	24,6	26,8	29,1	31,3
	40	16,2	24,5	36,1	39,1	42,2	19,1	28,2	44,2	47,9	51,7	20,3	29,8	47,7	51,7	55,8	21,7	32,0	50,8	56,8	61,2
	60	17,2	31,9	41,1	56,4	62,7	19,3	38,0	48,4	64,4	76,9	20,1	40,5	51,5	67,8	82,9	21,2	43,7	55,6	72,3	91,0
	80	17,2	36,6	51,2	61,7	76,5	19,1	41,2	61,4	73,3	89,1	19,8	43,0	65,6	78,2	94,5	20,8	45,3	71,2	84,8	102
	100	15,6	36,9	60,7	73,9	85,7	17,3	41,7	69,5	88,9	102	17,9	43,6	72,8	95,2	110	18,8	46,0	77,0	103	119
	120		36,1	62,1	86,8	99,8		40,0	70,5	102	120		41,6	74,0	108	129		43,7	78,4	115	140
	140			63,7	92,2	115			72,3	105	137			75,7	111	146			80,0	117	157
	160				94,5	126				108	145				114	153				121	163
	180			64,8	97,2	130			73,0	111	149			76,2	116	157			80,3	123	167
	200					134					154				117	162					172
	220				99,1	137				112	157					165				124	175
	>240					140					159					167					177
$N_{ki,k}$ [2]		13,6	32,1	59,7	97,2	145	15,1	35,6	66,1	108	161	15,7	37,0	68,7	112	167	16,4	38,7	72,0	117	175

Useful for comparison, the buckling loads $N_{ki,k}$[1] and $N_{ki,k}$[2] are displayed in the bottom line in *Tab. 1* and *Tab. 2*. Here, $N_{ki,k}^{1)} = \sqrt{c_h \cdot E_S \cdot I_S}$ corresponds to the buckling load for elasticly bedded beams without supports (Zimmermann, 1905). The buckling load for elasticly bedded beams on two supports can be calculated by $N_{ki,k}^{2)} = 2 \cdot \sqrt{c_h \cdot E_S \cdot I_S}$ (Engesser, 1884). For slender and long beams, $N_{ki,k}$[1] and $N_{ki,k}$[2] is independent of the beam length. Subject to these limitations, the buckling load for long screws can be easily calculated using $N_{ki,k}$[1] or $N_{ki,k}$[2], E_S = 210000 N/mm² and $I_S = \frac{\pi}{64} \cdot (0,7 \cdot d)^4$.

2.4 Load distribution in beam supports

The load-carrying capacity for the third failure mode is characterised by reaching the compressive strength perpendicular to the grain in a plane formed by the screw tips. In this case, the load-carrying capacity for this failure mode depends on the compressive strength perpendicular to the grain and on the compressed area in a plane formed by the screw tips. The load distribution and consequently the length of the plane formed by the screw tip where compressive stresses occur were determined from a numerical calculation (see [2]). Two different beam supports were studied: Directly loaded sleepers and indirectly loaded beam supports.

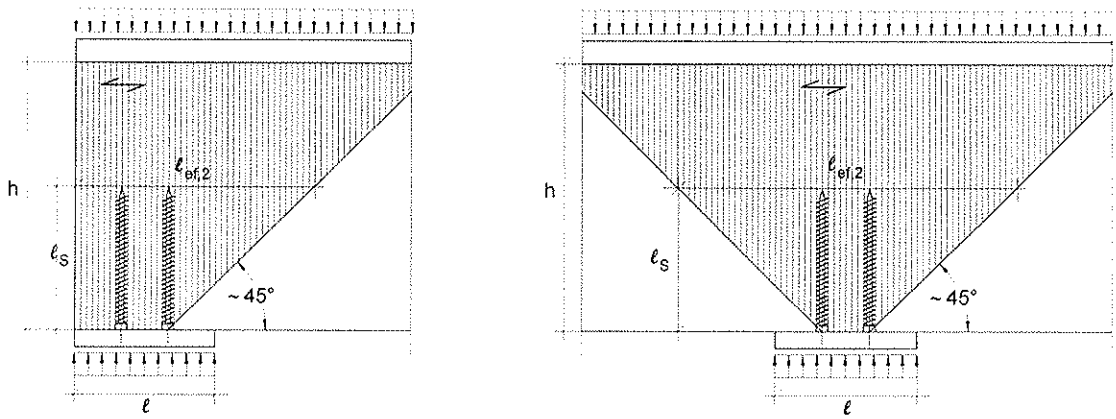

Fig. 5: Load distribution in directly loaded beam supports

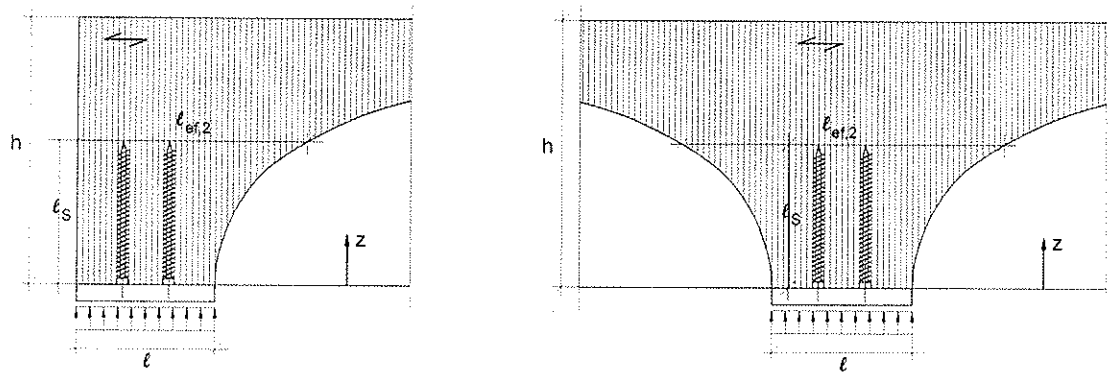

Fig. 6: Load distribution in indirectly loaded beam supports

In directly loaded sleepers a linear load distribution may approximately be assumed (see in *Fig. 5*). The length of the plane formed by the screw tips where compressive stresses occur can be calculated taking into account the length of the screws and the length of the beam support. In contrast, the load distribution in indirectly loaded beam supports is nonlinear and the increase becomes less with increasing beam height (see in *Fig. 6*).

As a result of the nonlinear load distribution in indirectly loaded beam supports (see in *Fig. 6*), the length of the plane formed by the screw tips where compressive stresses occur can be calculated as follows. For single-sided load distribution see eq. (4), for double-sided load distribution see eq. (5).

$$\ell_{ef,2} = \ell + 0,25 \cdot \ell_S \cdot e^{3,3 \cdot \frac{\ell_S}{h}} \tag{4}$$

$$\ell_{ef,2} = \ell + 0,58 \cdot \ell_S \cdot e^{3,6 \cdot \frac{\ell_S}{h}} \tag{5}$$

2.5 Design equations for the load-carrying capacity of reinforced beam supports

Taking into account the three different failure modes, the load-carrying capacity $R_{90,d}$ of a reinforced beam support may be calculated as follows:

$$R_{90,d} = \min \begin{Bmatrix} n \cdot R_d + k_{c,90} \cdot \ell_{ef} \cdot b \cdot f_{c,90,d} \\ b \cdot \ell_{ef,2} \cdot f_{c,90,d} \end{Bmatrix} \tag{6}$$

where

$$R_d = \min \left\{ R_{ax,d} \; ; \; R_{c,d} \right\} \tag{7}$$

$$R_{c,d} = \kappa_c \cdot N_{pl,d} \tag{8}$$

$$\kappa_c = 1 \qquad \text{for} \quad \overline{\lambda} \le 0,2$$

$$\kappa_c = \frac{1}{k + \sqrt{k^2 - \overline{\lambda}^2}} \qquad \text{for} \quad \overline{\lambda} > 0,2 \tag{9}$$

with

$$k = 0,5 \cdot \left[1 + 0,49 \cdot \left(\overline{\lambda} - 0,2\right) + \overline{\lambda^2}\right] \tag{10}$$

$$\overline{\lambda} = \sqrt{\frac{N_{pl,d}}{N_{ki,d}}} \tag{11}$$

and

$R_{ax,d}$ Design value of the withdrawal capacity (see eq. (1)) calculated with k_{mod} and $\gamma_M = 1,3$.

n Number of screws

b Width of the beam

l_{ef} $l_{ef} = l + max\ \{l\ ;\ 30\ mm\}$ for single-sided load distribution, see in [1]

$l_{ef} = l + 2 \cdot max\ \{l\ ;\ 30\ mm\}$ for double-sided load distribution, see in [1]

$l_{ef,2}$ see in *Fig. 5 and 6*

$k_{c,90}$ Coefficient $k_{c,90} \in [1\ ;\ 1,75]$ for the load distribution, see in [1]

$f_{c,90,d}$ Design value of the compressive strength perpendicular to the grain

$N_{pl,d}$ Design value of the plastic load-carrying capacity calculated with the cross section of the core diameter of the screw.

$N_{ki,d}$ Design value of the buckling load for a screw taking into account the elastic foundation perpendicular to the screw axis, a triangular normal load distribution along the screw axis as well as the support condition of the screw head. For hinged head supports the design values of the buckling load are summarised in *Tab. 1*. For clamped head supports see *Tab. 2*. The design value is calculated from the characteristic value with k_{mod} and $\gamma_M = 1,3$.

3 Calculation model for the stiffness

The effective stiffness perpendicular to the grain in the range of the reinforced beam support is derived using the Volkersen Theory (1953). The complete derivation for the effective stiffness of a reinforced beam support is specified in [2]. The effective stiffness of a reinforced beam support can be estimated by the following equation:

$$E_{tot} = \frac{E_{90} \cdot f_{LD} \cdot n \cdot \ell_S \cdot \left(\frac{\psi}{n} + 1\right) \cdot \omega \cdot \sinh\left(\omega \cdot \ell_S\right)}{\phi - \psi + n \cdot \left(\frac{\psi}{n} + 1\right) \cdot \cosh\left(\omega \cdot \ell_S\right) + 0,7 \cdot f_{LD} \cdot \ell_S \cdot \phi \cdot \omega \cdot \sinh\left(\omega \cdot \ell_S\right)} \tag{12}$$

with the load distribution factor f_{LD} for a linear load distribution

$$f_{LD} = \sqrt{1 + L \cdot \frac{\ell_S}{\ell} \cdot \tan\alpha} \tag{13}$$

and with the ratio between the extensional stiffness of the timber and the screw ϕ as well as the coefficient ψ and ω:

$$\phi = \frac{E_{90} \cdot A}{E_S \cdot A_S} \qquad \psi = \frac{n + \phi \cdot \cosh(\omega \cdot \ell_S)}{\cosh(\omega \cdot \ell_S) - 1} \cdot f_{LD} \qquad \omega = \sqrt{\left(\frac{1}{E_S \cdot A_S} + \frac{n}{E_{90} \cdot A}\right) \cdot c_v} \tag{14}$$

Further notation:

n	Number of screws
$E_{90} \cdot A$	extensional stiffness of the beam at the beam support perpendicular to the grain direction
$E_S \cdot A_S$	extensional stiffness of the reinforcing screw
c_v	see eq. (3)
l_S, l, $\alpha = 45$	see in *Fig. 5*
L	$L = 1$ for single-sided, $L = 2$ for double-sided load distribution

It must be pointed out, that the effective stiffness estimated by eq. 12 to 14 is only valid for reinforced beam supports using self-tapping screws. Furthemore, the equations only apply for a linear load distribution, such as in directly loaded beam supports. The effective stiffness for reinforced beam supports in the range of the reinforcing screws is only valid, when the surface of the screw heads is exactly flush with the surface of the beam support. To receive an impression about the size of E_{tot} depending on the reinforcement, two diagrams were generated. Left in *Fig. 7* the effective stiffness depending on the screw number n and the screw length l_S is displayed for a screw with 6 and 12 mm diameter. Remarkable is the increasing of E_{tot} with increasing screw length. Right in *Fig. 7* the effective stiffness depending on the beam support area and the screw diameter for one screw (n = 1) is displayed. Remarkable is the increase of E_{tot} with decreasing spacing between the screws. For large screw spacing, E_{tot} is hardly higher than the MOE for solid timber perpendicular to the grain.

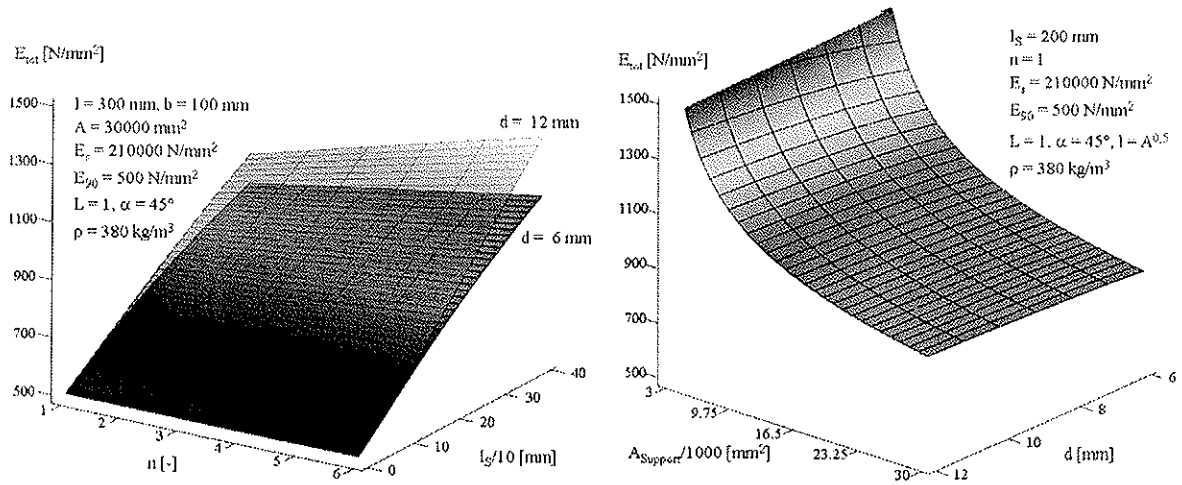

Fig. 7: E_{tot} depending on l_S and n (left) and E_{tot} depending on A and d (right)

4 Tests

To verify the calculation models, different reinforced beam supports were tested (15 test series). To demonstrate the effectiveness of reinforced beam supports, further non-reinforced beam supports were tested (4 test series). All tested specimens are specified in *Tab. 3*. The averaged load-carrying capacity for each test series is displayed in column four.

In the following column the averaged effective stiffness of the reinforced beam supports is displayed. Information about the geometry of the beam support and the screws as well as the plastic load-carrying capacity N_{pl} for the screws are displayed in column 6 to 12.

A remarkable effect of this reinforcing method is the high increase in load-carrying capacity compared to the non-reinforced geometrically identical beam supports. For example, the averaged load-carrying capacity for the test series A_6_6 is 132 kN and consequently 130% higher than the corresponding value for the test series A_2. The greatest increase in load-carrying capacity was reached with the test series D_8b_6. Here, compared to the test series D_2, the increase in load-carrying capacity was 330%.

Furthermore, for reinforced beam supports a high increase in stiffness perpendicular to the grain direction is observed. Compared to solid timber with a MOE perpendicular to the grain of about 300 – 500 N/mm^2, the effective stiffness E_{tot} perpendicular to the grain in the range of the reinforcing screws reached a maximum value of about 1870 N/mm^2.

Tab. 3: Properties of tested beam supports and test results

specimen	number of spec.	mean density	mean load-carrying capacity	mean MOE	beam support			reinforcing screws			
					direct/ indirect	width	length	number of screws	screw diameter	length of the threaded part	ductile axial force
	n	ρ	R_{90}	E_{tot}		t	l_{ef}	n	d	l_S	N_{pl}
[-]	[-]	[kg/m^3]	[kN]	[N/mm^2]	[-]	[mm]	[mm]	[-]	[mm]	[mm]	[kN]
A_1	5	463	**43,2**	-	indirekt	100	80	-	-	-	-
A_7_2	5	444	**77,5**	**790**	indirect	100	80	2	7,5	180	32,7
A_8_2	5	459	**92,0**	**1293**	indirect	100	80	2	8	340	32,7
A_10_2	5	448	**104**	**845**	indirect	100	80	2	10	200	51,8
A_7_4	4	446	**126**	**635**	indirect	100	120	4	7,5	180	32,7
A_10_4	5	449	**133**	**764**	indirect	100	120	4	10	200	51,8
A_2	10	464	**57,1**	-	indirekt	120	90	-	-	-	-
A_6_6	10	466	**132**	**861**	indirect	120	90	6	6,5	115/160	22,5
D_1	5	451	**46,0**	-	direkt	100	80	-	-	-	-
D_7_2	5	460	**96,1**	**1050**	direct	100	80	2	7,5	180	34,2
D_8_2	5	425	**98,0**	**1350**	direct	100	80	2	8	340	32,7
D_10_2	5	439	**104**	**1119**	direct	100	80	2	10	200	51,8
D_7_4	14	443	**127**	**985**	direct	100	120	4	7,5	180	34,2
D_8_4	6	445	**169**	**1247**	direct	100	120	4	8	340	32,7
D_10_4	5	456	**173**	**836**	direct	100	120	4	10	200	51,8
D_2	3	450	**56,4**	-	direkt	120	90	-	-	-	-
D_7_6	3	459	**195**	**1196**	direct	120	90	6	7,5	180	34,2
D_8a_6	3	453	**228**	**1435**	direct	120	90	6	8	260	39,1
D_8b_6	3	455	**242**	**1870**	direct	120	90	6	8	400	37,5

In the following *Fig. 8* and *Fig. 9* the test results (R_{90} and E_{tot}) for each test series are compared with the calculated values. All values were calculated with the averaged density and the averaged plastic load-carrying capacity for the screws. Furthermore, the

compressive strength perpendicular to the grain was assumed as 5 N/mm^2. The effective stiffness perpendicular to the grain E_{tot} was calculated using a MOE of 300 N/mm^2.

The calculated values show a good agreement with the test results. Furthermore, the calculated failure modes mainly correspond to the failure modes observed in the tests (see in *Fig. 8*).

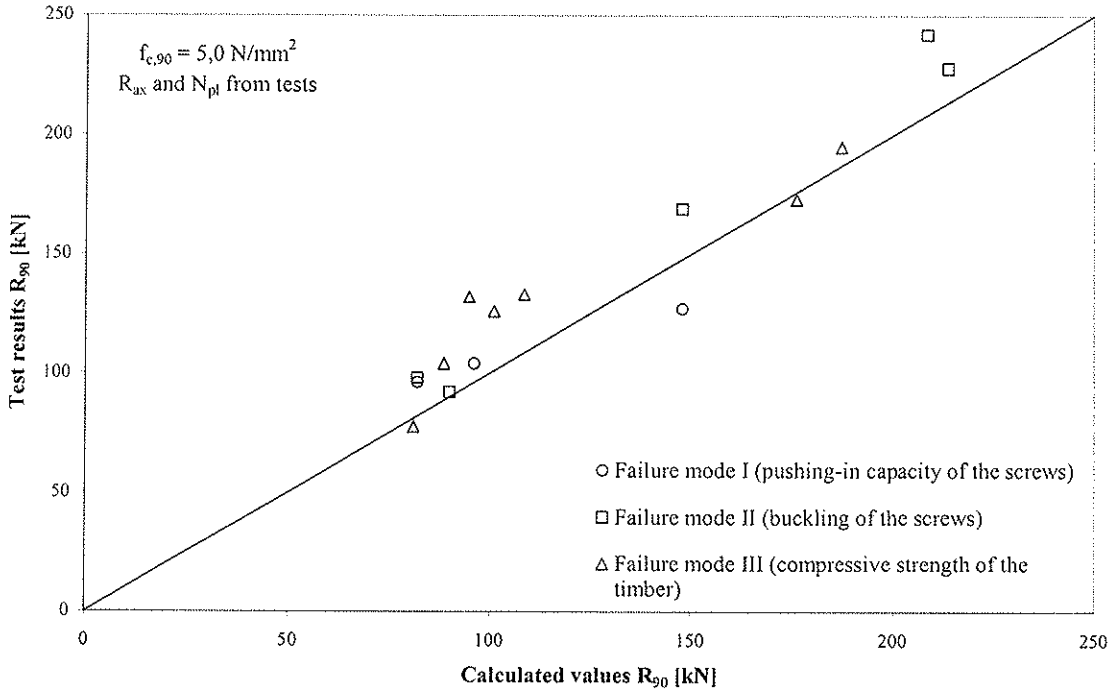

Fig. 8: Calculated load-carrying capacities in comparison with the test results

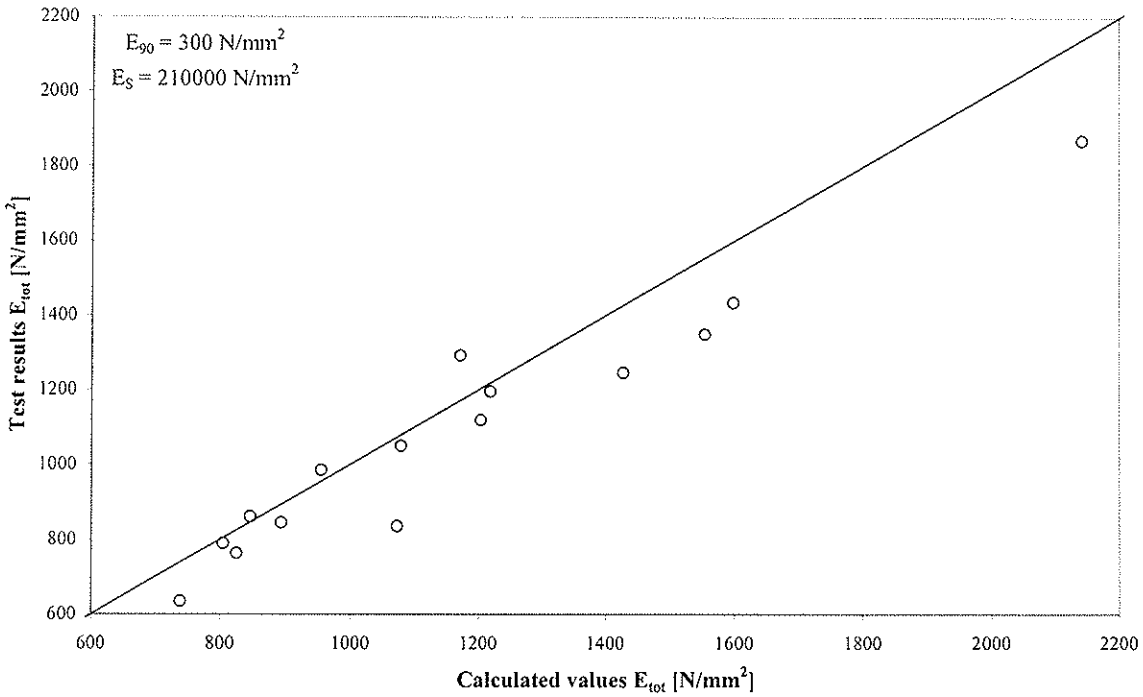

Fig. 9: Calculated effective stiffness in comparison with the test results

5 Summary

Self-tapping screws with continuous threads provide a good opportunity to reinforce beam supports and consequently to increase the load-carrying capacity and the stiffness perpendicular to the grain or to minimize the elastic displacement perpendicular to the grain. In this paper a calculation model for the load-carrying capacity and for the effective stiffness reinforced beam supports using self-tapping screws is presented. With the first calculation model it is possible to calculate the load-carrying capacity and to predict the failure mode of a reinforced beam support. The second calculation model may be used to estimate the stiffness or the elastic displacement perpendicular to the grain in the support area. Both calculation models were verified by test.

6 References

[1] DIN 1052:2004-08, Entwurf, Berechnung und Bemessung von Holzbauwerken – Allgemeine Bemessungsregeln und Bemessungsregeln für den Hochbau

[2] Bejtka, I. (2005). Verstärkung von Bauteilen aus Holz mit Vollgewindeschrauben. Band 2 der Reihe Karlsruher Berichte zum Ingenieurholzbau. Herausgeber: Universität Karlsruhe (TH), Lehrstuhl für Ingenieurholzbau und Baukonstruktionen, Univ.-Prof. Dr.-Ing. H.J. Blaß. ISSN 1860-093X,ISBN 3-937300-54-6

[3] Volkersen, O. (1953). Die Schubkraftverteilung in Kleb-, Niet- und Bolzenverbindungen. Aus Energie und Technik, March.1953

[4] Blaß, H.J.; Görlacher, R. (2004). Compression perpendicular to the grain. In proceedings of the 8th World Conference on Timber Engineering – Volume II, page 435 – 440; WCTE 2004, June 14-17, 2004 in Lahti, Finland

INTERNATIONAL COUNCIL FOR RESEARCH AND INNOVATION
IN BUILDING AND CONSTRUCTION

WORKING COMMISSION W18 - TIMBER STRUCTURES

CONNECTORS FOR TIMBER-CONCRETE COMPOSITE-BRIDGES

A Döhrer

K Rautenstrauch

Bauhaus-University Weimar

GERMANY

MEETING THIRTY-NINE

FLORENCE

ITALY

AUGUST 2006

Presented by A Döhrer

A Asiz asked what kind of long term tests were preformed and were corrosion tests considered. A Döhrer answered that the advantage of this system would be the protection of the connections; therefore, corrosion issue from de-icing would not be of concern.

A Ceccotti stated that in long span timber bridges the issue of differential movement from temperature would be of concern. A Döhrer answered at the span of 10 to 30 m the temperature caused movement should be acceptable.

A Frangi and A Döhrer discussed why the failure mode changed from the ductile (short term) to brittle (2 million cycles). It was the longitudinal compression of the timber that created the ductility.

K Crews commented that at long span the 3 dimensionality of the structure would become important. A Döhrer stated that there was a limitation of lab space to allow this aspect to be tested.

M Fragiacomo stated that in Colorado 20000 cycles rather than 2 million cycles were used and asked whether significant change in stiffness was observed after 2 million cycles. A Döhrer showed the results actually increased in stiffness after 2 million cycles.

Connectors for timber-concrete composite-bridges

Antje Döhrer, Karl Rautenstrauch
Bauhaus-University Weimar, Germany

1 Introduction

The construction method using timber-concrete composites has been developed in the field of building engineering. This technology will also be interesting for bridge constructions in the future. Combining concrete in the compression zone with timber in the tension zone to a composite structure, the favourable properties of both materials could be used efficiently. Especially the combination of log-glued laminated beams with concrete slabs will establish new opportunities for the building of road bridges [8].

Many problems occurring at timber road bridges could be solved by this new type of hybrid timber-concrete composite-bridges. The concrete deck provides an ideal constructive wood preservation. The distribution of high loads per axle and the transmission of horizontal loads can be realised much easier by the concrete deck. Construction details proved in building of concrete bridges and accepted by the national highway administrations could be transferred. In comparison to simple concrete bridges the superstructure is much lighter, so costs in the fields of foundations could be reduced. Using precast concrete units a high prefabrication level could be realised.

The development and use of sufficient stiff connectors between timber and concrete is very important for those composite bridge constructions. EC5 [1] previously only included regulations concerning bolted steel fasteners and grooves. Tests are demanded for other connections. For these tests it is necessary to take the different time-, temperature- and moisture-dependent behaviour of both composite materials into consideration, especially under conditions of service class 2.

At the Bauhaus-University Weimar, short-time shear tests, long-time shear tests and push-out-tests under cyclic loading with three different types of connectors were arranged. The paper will present the results of these tests. The decrease of the stiffness influenced by long-term loading under conditions of service class 2 and under cyclic loading will also be discussed. These results could contribute to verify the shear stiffness approach of the connection between timber and concrete being the fundamental construction parameter for this new type of hybrid road bridges.

2 Development status of connectors

The construction of the shear-joint is very important for the load-bearing capacity of timber-concrete composite structures. The stiffness of the bridge structure is considerably

determined by the stiffness of the connectors, its quantity and assembly in the cross section. Most of the researched connectors have been developed for the use in slabs of structural engineering. For building road bridges their ultimate loads and stiffness are too small. An overview of joints being appropriate to road bridges because of its load-deformation-behaviour is given in Tab. 1. All stated average values result from the tested geometry and are not generally valid.

Tab. 1: Appropriate connectors for hybrid timber road bridges

connector typ	**test numbers** short-time/ long-time/ dynamic shear tests	**ultimate load F_{max} [kN] (average value)**	**view**
		Slip modulus K_{ser} [kN/mm] (average value)	
		creep coefficient (loading period)	
stud connector (cam depth 50 mm, timber length in front of the joint 500 – 700 mm, incline of cam edge 75°) [9]	2/0/0	458	
		466	
		-	
X-connector [6] (2 tension bars ∅10, 1 compression bar ∅10, glueing length 250 mm, incline 45°, partly with grooves)	6/0/2	126 ... 212	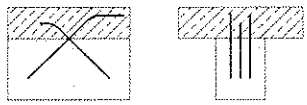
		175 ... 390	
		-	
groove with steel connectors (depth 20 mm, timber length in front of the joint 150-250 mm, incline of cam edge 90°) [5]	30/3/0	263 ... 543	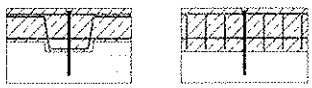
		382 ... 1158	
		0,55 ... 0,62 (1a)	
console cam (cam depth 50-70 mm, incline of cam edge 90°) [3]	24/3/0	71 ... 178	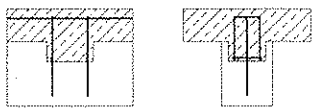
		155 ... 291	
		1,5 (335d)	
BVD-anchor [2]	-	(perm T = 57...200)	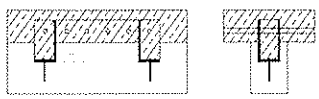
		-	
		-	

The stud connector has been developed in 2 short-time shear tests by *Steurer* [9]. It has already been practically used in the building of the Crestawald Bridge near Sufers (CH). The connector consists of a steel plate with 4 studs on concrete side and a welded trapezoid border on timber side. So the bond to timber functions analogue to the traditional step joint, while the bond to concrete is realised by a standardised connector of steel-concrete composite construction.

In Finland a great research program – the Nordic timber bridge project - has been initiated to promote timber bridges. Within the scope of this project lots of joints for timber-concrete composite bridges have been tested in shearing [6][10]. The so called X-connector consisting of inclined-glued reinforcing steel bars has been used in all pilot bridges.

The groove connector that has been developed by *Natterer* [7] is the only one joint being mentioned with regard to its design in a code [1]. A steel connector is demanded in the

code to protect the lift-off between concrete and timber, though it has been found in [5], that the concrete is solely able to transfer the eccentric moment resulting of the shear force.

A similar joint using the step joint principle is the console cam developed by *Glaser* [3]. The tension force in the console is transferred by a grid-shaped reinforcement bar being glued into the timber.

Another connector which has already been used in practice is the BVD-anchor [2]. The anchor is a frame-shaped steel unit transferring the shear force by two contact edges. It has only been tested in bending, therefore there are no data for modulus of displacement and the permitted shear forces are calculated values.

The comparison of the connectors (Tab. 1) shows, that any sufficient stiff and sustainable joints have been developed. But the quantity of realised tests under short-time, long-time and dynamic loading is too small for a standardised regulation.

3 Experimental investigations

3.1 Test configuration and specimens

In the following systematic tests with three special connectors will be presented. The experimental program consisted of shear tests under short-time, long-time and dynamic loading. All shear tests were arranged as "push-out-tests" with specimens consisting of a centrically located timber part and two bordering concrete layers. Short-time shear tests have been performed to determine the stiffness and the ultimate load of each joint at the initial state. The influence of moisture and temperature variation under long-term loading in service class 2 on the stiffness of the connectors has been recorded by long-time shear tests. Shear tests under cyclic loading have been arranged for the evaluation of fatigue behaviour. These tests should show, whether the stiffness decreases and the slip between the composite materials increases.

In figure 1 the tested connector types are shown. Respectively 9 test specimens per connector type have been fabricated, so each 4 pieces have been short-time tested (series K-K, S-K, X-K), each 3 pieces have been tested under long-time loading (series K-L, S-L, X-L) and each 2 pieces have been made for dynamic tests (series K-D, S-D, X-D). All specimens consisted of glued laminated timber GL28h and reinforced concrete C25/30. The average of the timber moisture amounted to 11% at the time of the tests.

The transmission of the shear forces in series K only occurred at grooves being milled 2 cm deep into timber and filled with concrete. The connector of series S consisted of a 2 cm thick steel plate anchored in concrete with 2 welded studs of 19 mm diameter. The dimension of S-connectors aimed at timber failure, because failure in the concrete part is known from steel-concrete composite structures and could be regulated by variation of the geometry of the studs. In series X respectively 2 tension and compression reinforcing bars (diameter 14 mm) were inclined glued 50 cm into the timber part. A two-component epoxy resin adhesive has been used for gluing.

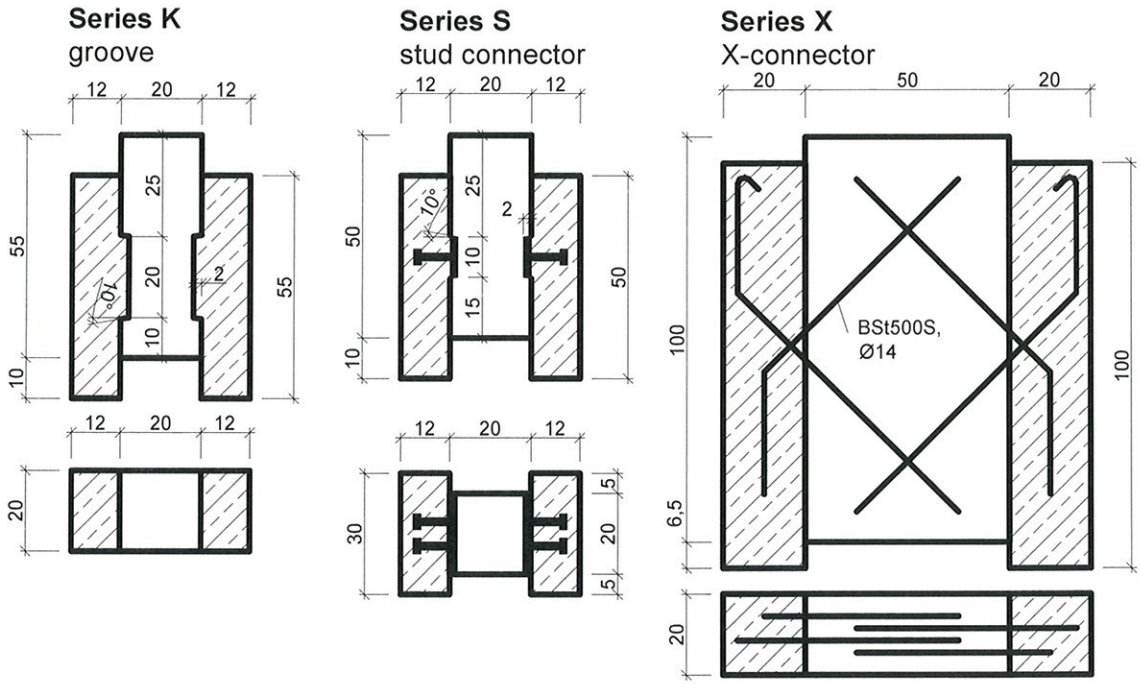

figure 1: Test specimens

3.2 Short-time shear tests

In September 2005 short-time shear tests were accomplished with the described composite elements at the Bauhaus-University Weimar. Experimental procedure and load history were chosen according to DIN EN 26891 (figure 2). Two direct current differential transformers having been placed centrically to the connectors on each side of the specimens recorded the relative displacement between timber and concrete. The joint opening was also measured by analogue equipment.

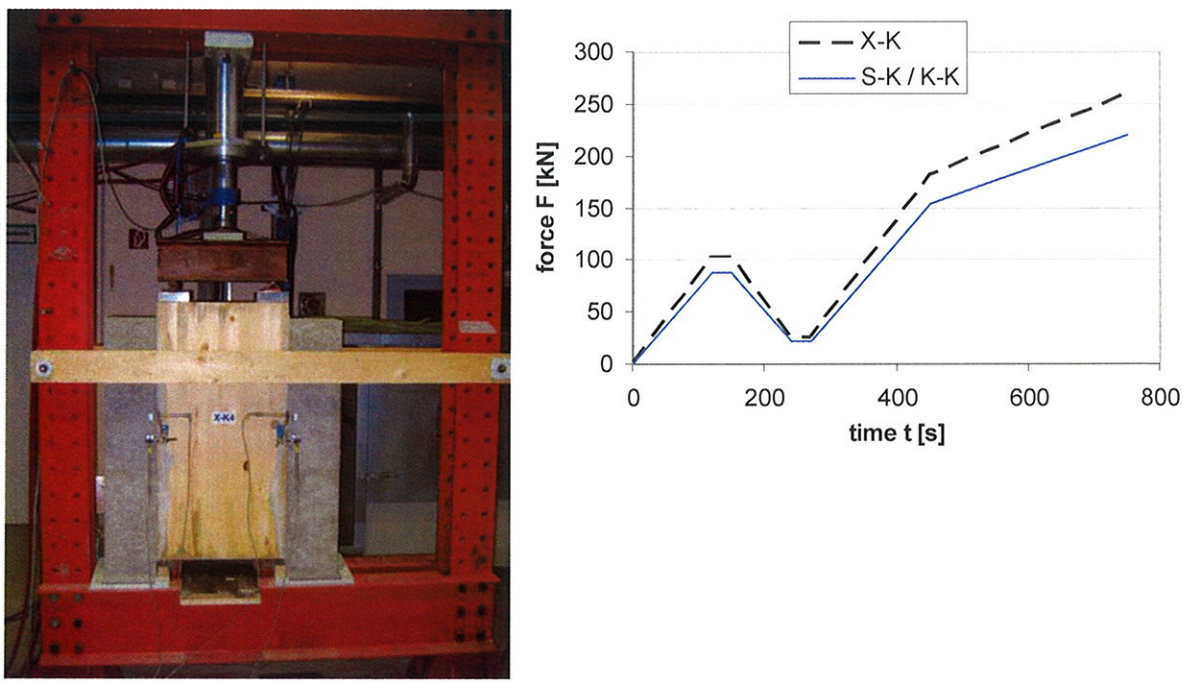

figure 2: Experimental procedure and load history of short-time shear tests

In figure 3 the averaged load-slip-curves are shown for each series. All test specimens showed a very ductile behaviour until fracture. Specimens of series X reached the highest stiffness and ultimate load, but the slip modulus highly dispersed. Stiffness and load-bearing capacity depend on specimens geometries and could be adjusted to required values by variation of the geometrical parameters.

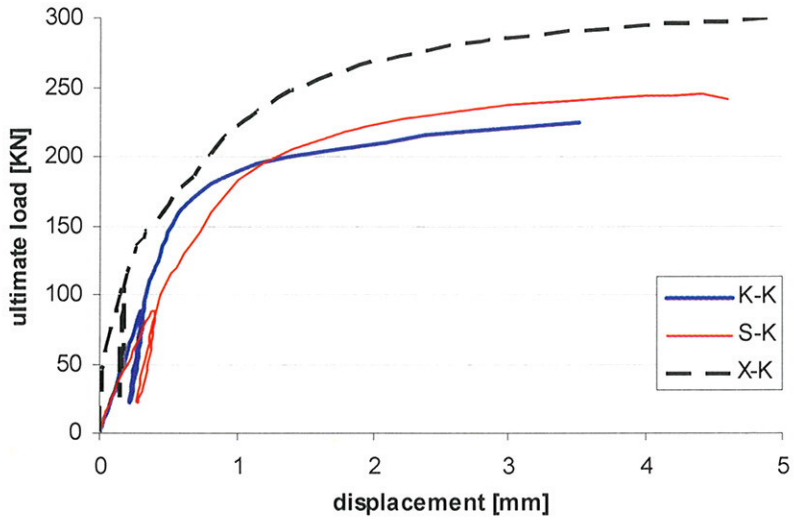

figure 3: Load-slip-curves of short-time shear tests

Longitudinal compressive deformation (figure 4) and shear failure in timber as well as cracking in the concrete groove characterised the fracture mode in series K. S-specimens also failed after plastic compressive deformation parallel to the grain by shearing of the timber part in front of the joint (figure 5). Fracture of series X was caused by rupture of a tension bar after reaching high joint displacements.

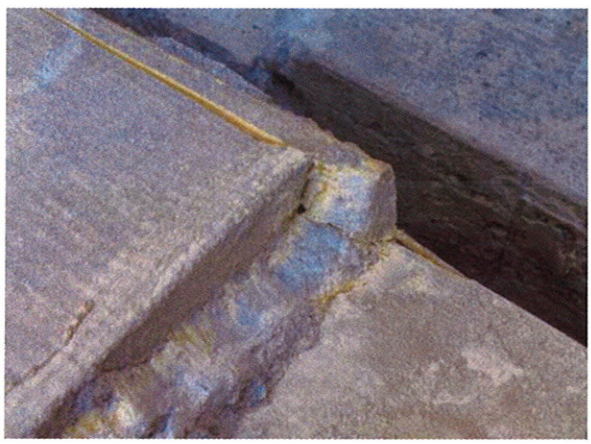

figure 4: Plastic deformation of timber fibre at the groove edge (Series K)

figure 5: Failure cause of series K and S - shearing of timber in front of the joint

In analysis of the tests the ultimate loads and slip modulus shown in figure 6 have been investigated.

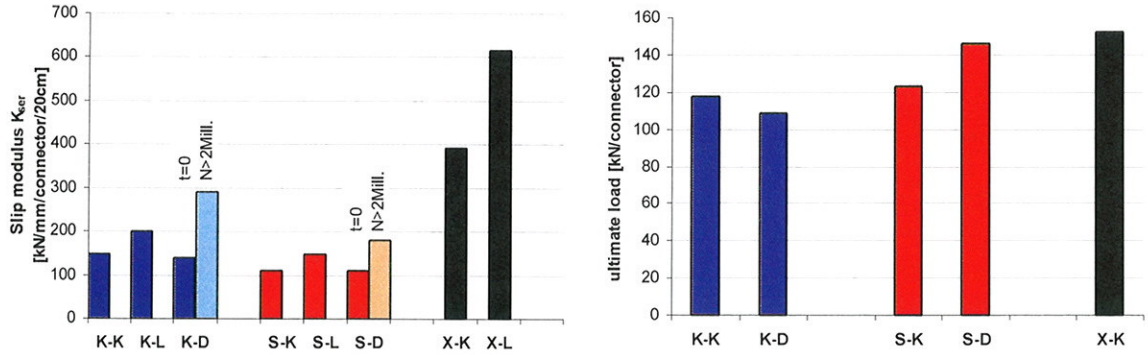

figure 6: Slip modulus and ultimate loads of all test series (averaged values)

3.3 Long-time shear tests

Since December 2005 long-time shear tests have been accomplished with 3 specimens per series. At the beginning all specimens were loaded with the ramp of the short-time shear tests to evaluate the initial slip modulus (figure 6). In the following a permanent load of approximately 30 % of the ultimate load of the short-time tests was adopted by a spring construction. This load level represents the serviceability state. The system was over-stressed about 10 % to compensate its alteration during the load transformation.

The load varies about less than 1% in spite of the spring construction because of the temperature extension of the tension bars. The length variations of the springs have also been measured to include this influence. At every measurement cycle it is possible to determine the actual load by the gauged characteristic curve of each spring.

All specimens are stored outside and roofed. This storage represents the climate of service class 2, which will occur in real bridge constructions [12]. Climate chronicle has still being permanently digitally recorded (1 measurement per hour - figure 7) while displacement has only been captured digitally in the first 2 days. Since the specimens have been displaced from the loading frame the slip has been recorded manually by a dial indicator with a precision of 0,01mm. The measurement cycles decrease by increasing of the load duration. The moisture of the timber has been recorded at each measurement cycle by electrodes staying permanently in the specimens. Test configuration and measurement system are adjusted to the climate conditions of a 5 year roofed outside-storage (figure 9).

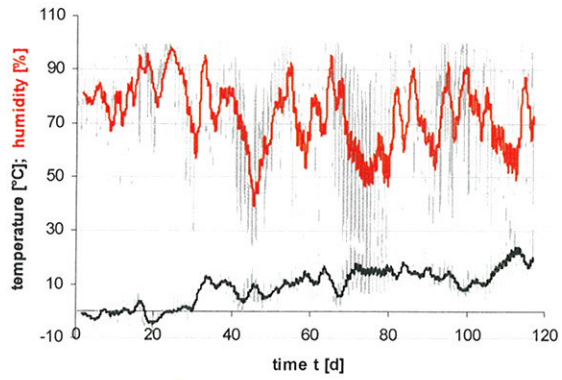

figure 7: Outside climate for long-time shear tests

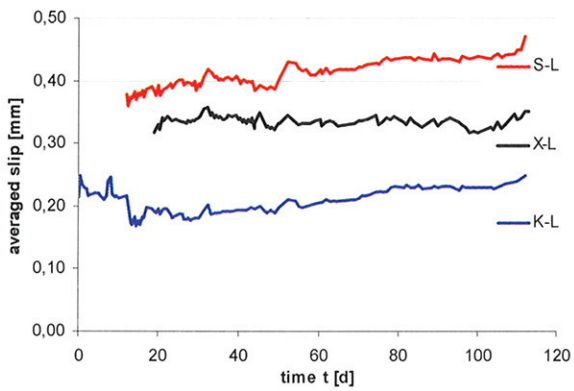

figure 8: Increasing slip of all series under 120 d long-time loading

figure 9: Long-time shear tests (specimens stored outside and roofed)

In figure 8 the development of the slip between timber and concrete for all series is shown over a test period of 120 days. The slips of all specimens have been increasing. The highest rising occurred at S-series by 24% of the starting value, the lowest one at X-series by 10% of the starting value. Tests have been running and will be analysed periodically to gain more information about the creep effect at the connectors.

3.4 Dynamic shear tests

Dynamic shear tests have been arranged since Mai 2006. Up to now there are test results of series S and K. Tests with specimens of series X are still running.

Load history for dynamic tests has been chosen so, that stress amplitudes and load cycles of road bridges have been reached. Up to now there are no standardisations for dynamic tests of timber-concrete composites and only a few tests have been published internationally (Tab. 2). Preliminary calculations have been done at a framework model to establish a relationship between the load amplitude in test series and the loads acting in a real bridge. In this context the variation range of the connector's shear forces at the instant and final state has been determined. Therefore two example bridges with spans of 10 and 25 m with respectively two borderline specification of joint stiffness have been generated. On the basis of the slip modulus gotten from the short-time shear tests and the calculation results, the minimal and maximal load values for all series have been defined (Tab. 2).

Tab. 2: Dynamic shear tests on timber-concrete composite elements (P_{ult} = ultimate load of short-time shear tests)

Reference	**number of specimens**	**P_{min} / P_{max} [KN]**	**frequency [Hz]**	**number of cycles [mill.]**
[6]	3	0,04/ 0,57...0,65 P_{ult}	6	0,1 ... 1,69
[10]	4	0,01...0,02 / 0,17 ... 0,26 P_{ult}	no data	1 ... 2,1
[11]	3	0,19 ... 0,43 P_{ult}	3	2
own tests	6	0,06 ... 0,35 P_{ult}	3	≥ 2

During the cyclic loading static load ramps have been placed analogue to the short-time loading. So the development of the connector's stiffness should also be observed beside the deformation increase. After the fatigue tests the specimens were path-controlled loaded up to failure. The load history consisted of the following phases (figure 10):

Phase I: load ramp analogue to short-time loading (to get the initial stiffness)

Phase II: sinusoidal fatigue cycles in threshold range with static load ramps inside (load-controlled)

Phase III: path-controlled fracture test (degree of speed analogue phase I and static load ramps)

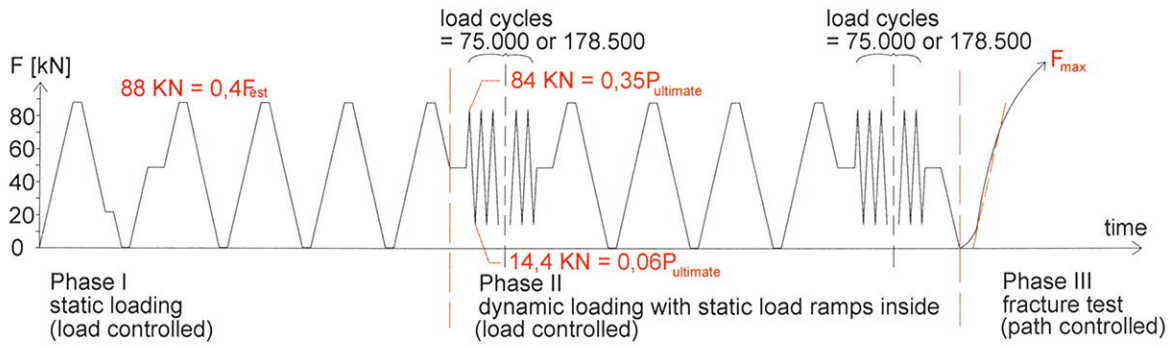

figure 10: Load history of dynamic tests of S-specimens

In figure 11 the development of slips under fatigue loads is shown at the P_{min}-load level. Overall the total slips remained after unloading were smaller than 0,5 mm. Averaged slip of series S increased by 87% under fatigue loading while the average of series K rised by 66%. The most increase of the slips happened at the first 500000 cycles and especially at the initial ramp about 30% of the total slip developed (figure 12). In contrast to [11] a stabilization of the slips after a certain number of cycles has not been observed.

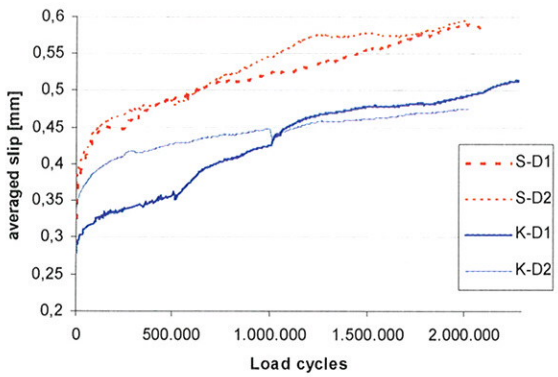

figure 11: Development of slip under fatigue loading at P_{min}

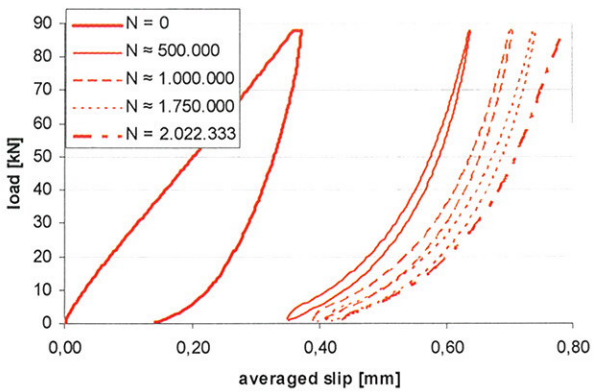

figure 12: Development of slip and stiffness at N load cycles (specimen S-D2)

The averaged values of slip modulus and failure loads are shown in figure 6. The K-D2 specimen has not been included into the averaging of failure tests because it failed unscheduled by a machine error. As also stated in [11] the fatigued specimens exhibited no loss of ultimate capacity and showed an increase of stiffness. The slip modulus increased by 107 % for series K and by 63 % for series S. The stiffer response of the fatigued specimens could be caused by a local wood densification of the loaded area.

At the fracture tests K-D1- and all S-D-specimens failed analogue to the short-time shear tests by shearing of timber in front of the joint. But no more ductility could be observed

because the timber's longitudinal compression in loading area had already been happened during fatigue loading.

4 Discussion and conclusion

The construction method using timber and concrete in a composite action is an expedient alternative to the conventional bridge building. To make this method negotiable further investigations are required in the fields of connectors being suitable for bridge building. The paper focused on systematic tests on three types of suitable shear connectors. Shear tests have been arranged under short-time, long-time and dynamic loading. First the initial values of stiffness and ultimate loads were determined. Then the influences of creeping under conditions of service class 2 and of more than 2 million load cycles were investigated. Based on the experimental research the following conclusions can be drawn:

All tested connectors are suitable for bridge building. They performed superior stiffness and higher ultimate loads in short-time shear tests in comparison to joints being well-known from building construction. Grooves and stud connectors behaved well under fatigue loading exhibiting no loss of ultimate loads and stiffness. Fatigue tests at X-connectors and long-time tests have still been running and will be analysed periodically. However, the presented tests have only been done for orientation. More extensive tests are necessary to get statistically confirmed values of stiffness and ultimate loads. Such tests will be performed with the stud connector at the Bauhaus-University next month.

Finally, the tests results will be verified by a computation model using a complex 3-dimensional nonlinear material model for timber that had been developed at the Bauhaus-University Weimar [4].

5 References

[1] DIN EN 1995-2: Eurocode 5: Design of timber structures – Part 2: Bridges; German Version EN 1995-2:2004, Februar 2006

[2] Ebert, K.: *Tragfähigkeitsversuche an Holz-Beton-Verbundträgern.* Untersuchungsbericht Nr. 1316/Eb im Auftrag des Ingenieurbüros für Tragwerksplanung P. Bertsche, MPA Bau der Technischen Universität München, 1997

[3] Glaser, R.: *Zum Kurz- und Langzeitverhalten von Holz-Beton-Verbundkonstruktionen*, Dissertation, Brandenburgische Technische Universität Cottbus, 2005

[4] Grosse, M.: *Zur numerischen Simulation des physikalisch nichtlinearen Kurzzeittragverhaltens von Nadelholz am Beispiel von Holz-Beton-Verbundkonstruktionen,* Dissertation, Bauhaus-Universität Weimar, 2005

[5] Kuhlmann, U.; Aicher, S.; Michelfelder, B.: *Trag- und Verformungsverhalten von Kerven mit Schlüsselschrauben als Schubverbindung bei Holz-Beton-Verbunddecken.* Schlussbericht zum AiF-Forschungsvorhaben

[6] Mäkipuro, R. u. a.: Wood-concrete Composite Bridges, Nordic Timber Council 1996, Stockholm

[7] Natterer, J. K.: Tendencies in bridge construction. *Proceedings of the 5th World Conference on Timber Engineering*, S. 100-107, Montreux, Schweiz 1998

[8] Rautenstrauch, K.; Döhrer, A.; Schaffitzel, J.: Moderne Brücken in Holz-Beton-Verbundbauweise – Eine Projektskizze, in: König, G.; Holschemacher, K.; Dehn, F. (Hrsg.): *Holz-Beton-Verbund.* Bauwerk Verlag, Berlin, 2004, S. 313-334

[9] Steurer, A.: Holz/Beton-Verbund im Brückenbau – Die Crestawald-Brücke bei Sufers (GR), in: 31. SAH-Fortbildungskurs: *Tragende Verbundkonstruktionen mit Holz*; Weinfelden, November 1999, S. 245-258

[10] Tommola, J.; Salokangas, L.; Jutila, A.: Wood-concrete composite bridges - Tests on Shear Connectors. Nordic Timber Council, 1999, Stockholm

[11] Weaver, C. A.; Davids, W. G.; Dagher, H. J.: Testing and analysis of partially composite fiber-reinforced polymer-glulam-concrete bridge girders. *Journal of bridge engineering*, Juli/August 2006, S. 316-325

[12] Yttrup, P.: *Concrete and timber composite construction for enhanced strength, stiffness and service life for timber bridges.* http.//aok.arch.utas.edu.au/research/bridge/sem3.html

INTERNATIONAL COUNCIL FOR RESEARCH AND INNOVATION
IN BUILDING AND CONSTRUCTION

WORKING COMMISSION W18 - TIMBER STRUCTURES

BLOCK SHEAR FAILURE AT DOWELLED STEEL-TO-TIMBER CONNECTIONS

A Hanhijärvi
A Kevarinmäki
R Yli-Koski

VTT

FINLAND

MEETING THIRTY-NINE
FLORENCE
ITALY
AUGUST 2006

Presented by A Hanhijärvi
A Jorissen wondered why values were conservative for glulam but just okay for Kerto LVL.
R Foschi wondered why the research was performed when the code was conservative and received clarification that this mode of failure was not originally considered in EC5 which led to a failure in Finland and A Hanhijärvi further responded that the comparison was focused on the Annex which is a later version of EC5.
J König commented that the designers did not use the right version.
R Foschi commented that many years ago in Canada a similar problem was experienced with glulam rivets. Block shear failure occurred with capacity of ½ of code values. This led to changes in code and increased spacing of rivets. Now both block shear and rivet yielding modes are considered in Canadian code.
J König further commented that the accuracy of manufacturing is important.
P Racher discussed the French experience on this type of connections. Designers would be working outside the code with this type of joints.
P Quenneville added that other types of steel (mild) and larger row spacing can influence the issue. A Hanhijärvi agreed that there were many possibilities. The project objectives were very specific. In Finland the steel typically had higher quality than required. There would be a risk of bad design if one assumed mild steel.

Block shear failure at dowelled steel-to-timber connections

Antti Hanhijärvi, Ari Kevarinmäki, Rainer Yli-Koski
VTT, Finland

1 Introduction

The design of dowel type joints of timber is well established in the Eurocode 5 by the use of the Johansen theory (Johansen 1949). It has shown to perform well when the fastener diameter is small and consequently the fasteners are slender (see Hilson 1995). With the increase of span length in large timber structures, the use of high capacity dowel type joints is necessary. The high capacity dowelled connections are often implemented by slotted in steel plates and large diameter dowels or bolts. With the increase of the diameter the rigidity of the dowel increases more than the embedment capacity. Therefore with large diameter rigid dowels, also the failure of timber at the joint area becomes more easily critical for the capacity of the connection – not only as embedment failure but through failure of the whole joint area by tension or shear. The failure mechanisms in this manner at the connection area are known as block shear or plug shear.

The lack of design against timber failure as consequence of shear and tension at the connection area (block shear) was found to be the partial reason for a recent failure of a large roof structure in Finland (Anon. 2004, Ranta-Maunus and Kevarinmäki 2003). Although the primary reason for the failure was a manufacturing fault in one connection (missing dowels) of a large glulam truss, the failure would not have proceeded to a catastrophic one, unless the true capacity of the properly manufactured joint had not been much lower than the capacity assumed in the design, which did not include any consideration of timber failure at the joint area. The true capacity of the connection was tested later after the collapse in a full-scale test, in which it was found that the true capacity was only appr. 50% of the design value (Ranta-Maunus and Kevarinmäki 2003). The tests showed also clearly the importance of the block shear failure mechanism as the critical one. At the time of the design of the roof, the ENV-version of the Eurocode 5 did not contain any mention of this type of failure mechanisms.

The aim of the present work is to improve the grounds for design of heavy-duty dowelled connections by experimental investigation of the timber failure at the joint area in joints implemented by steel plates loaded in tension. Alltogether more than 150 tension tests were made with glulam and Kerto-LVL specimens. The experimental program contained tests of both double-shear and multiple shear (4- and 6- shear) plane connections. In double shear, both timber-steel-timber and steel-timber-steel specimens were tested. In multiple shear the outermost parts were allways timber.

2 Symbols

a_1 dowel spacing parallel to grain
a_2 dowel spacing perpendicular to grain
a_3 dowel end distance
a_4 dowel edge distance
B specimen height
b block shear failure mechanism
b-r block shear failure mechanism with calculational shear failure capacity > tension failure capacity
b-t block shear failure mechanism with calculational tension failure capacity > shear failure capacity
CoV coefficient of variation
d dowel diameter
DF design failure mode (critical failure mechanism according to design)
F_{max} failure load in tests
F_{Bk} calculated characteristic load-carrying capacity of connection according to EC5 Annex A (block/plug shear)
F_{Bm} calculated load-carrying capacity of connection according to EC5 Annex A (block/plug shear) and using mean properties
F_{Rk} calculated characteristic load-carrying capacity of connection according to EC5 assuming $n_{ef} = n$
F_{Rm} calculated load-carrying capacity according to EC5 assuming $n_{ef} = n$ and using mean properties of the test material
F_{Sk} calculated characteristic load-carrying capacity according to EC5 assuming splitting etc. ($n_{ef} \neq n$) but not block/plug shear
F_{Sm} calculated load-carrying capacity according to EC5 assuming splitting etc. ($n_{ef} \neq n$) but not block/plug shear and using mean properties of the test material
F_{Tm} calculated capacity according to the EC5 assuming only tension failure and using mean properties of the test material and cross-section reduction due to dowel holes
N number of specimens
n number of dowels in a row
n_{ef} effective number of dowels in a row
m number of dowel rows
p plug shear failure
row row shear failure
s/r splitting or row shear failure
T tension failure mechanism (of cross-section)
TF test failure mode (prevailing failure mechanism in test)
t_1 thickness of outer timber member
t_2 thickness of inner timber member
t_S thickness of steel plate
v_{max} connection slip at maximum load
ρ_m mean density of the test material

3 Material

All glulam for the tests was manufactured in an industrial process from spruce (*Picea abies*) wood. To get more homogenious properties, the lamellas were specially selected.

The selection was made using a commercial strength grading machine, which measures the natural frequency (Dynagrader). First, a sufficiently large batch of lamellas was graded with settings of grade MT30 (=C30). Second, the pieces which had passed the requirements of this grade were re-graded using the settings of MT40 and only those pieces with failed this higher criterion were taken for the production of the test glulam. Thus the lamellas had properties exceeding the requirements for MT30 but not MT40. The LVL for the tests was produced at the Kerto-LVL factory of Finnforest Oyj in Lohja, Finland.

Dowels were produced by cutting and machining from cold drawn steel bars. The binder bolts were produced from the same material as the dowels and the smooth length was always at least a few mm's longer than the width of the joint, i.e. in no case did the threaded part touch the wood or the steel plates. The dimensional accuracy of the diameter of the dowels and bolts was very good.

The steel plates were manufactured by laser cutting from steel quality S355 using an NC-machine tool. The dowel holes were cut to diameter Ø13 mm and Ø8.7 mm for the dowel diameters 12 and 8 mm, respectively.

All test specimens were manufactured so that a similar dowelled connection was manufactured at both ends of the specimen. Thus, actually, twice as many joints were tested than the number of specimens shows. However, the actual strength of only the weaker one of the pair of joints in one specimen was obtained – and it can be only said that the other one was at least as strong.

3.1 Double shear connection specimens

The double-shear test series are listed in Tables 1 and 2 for glulam and Kerto-LVL, respectively. Double shear test series of the timber-steel-timber type were made with unattached timber parts: For glulam the two halves were obtained by splitting a glulam beam into two and manufacturing the specimen using the two halves but leaving them unattached in the middle part. For LVL specimens the two halves were obtained from two pieces of LVL coming from the same manufacture batch. Both standard type Kerto-S and cross-veneered Kerto-Q were tested.

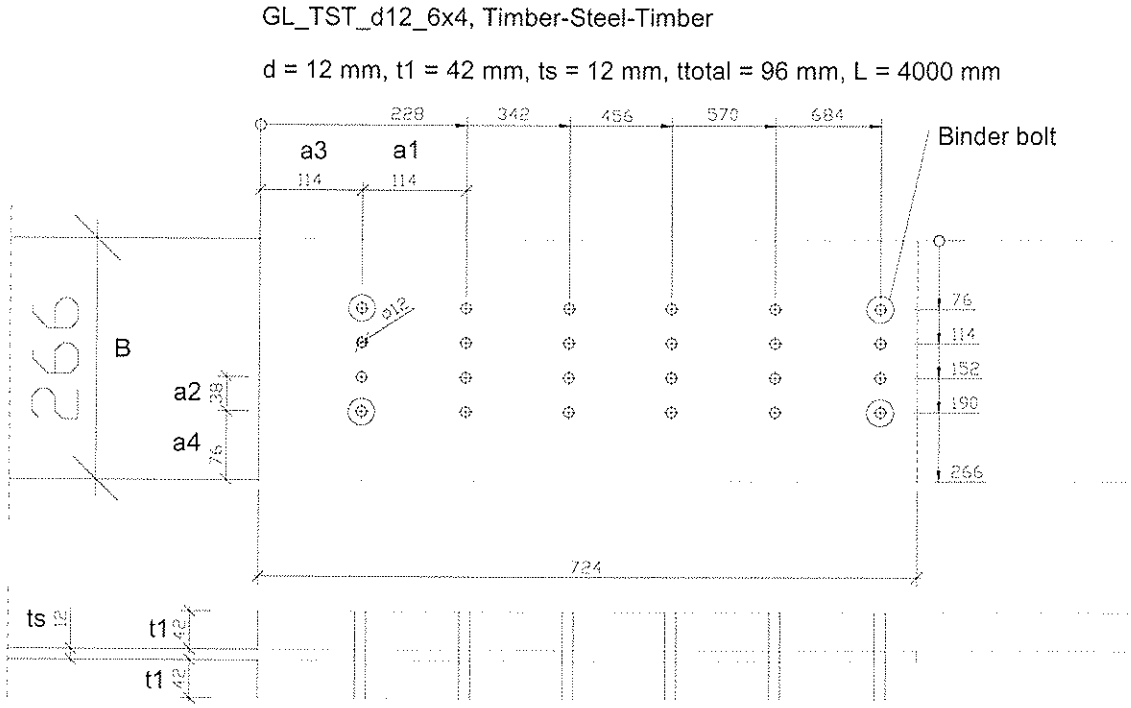

Figure 1. Example of a double shear dowelled timber-steel-timber connection used in the tests (GL_TST_d12_6x4).

Table 1. Glulam series with double-shear dowelled connections.

Series name	Dowel pattern n x m	dowel diam. d mm	thick-ness t_1 or t_2 mm	width B mm	steel plate t_s mm	spacing parall. a_1 mm	spacing, perp. a_2 mm	end dist. a_3 mm	edge dist. a_4 mm	N
Timber-Steel-Timber, Dowel diameter 12mm										
GL28h, t_1 = 42 mm, d = 12 mm, dowel strength.cl. 8.8, a_2 = 38 mm, a_3 = a_1										
GL_TST_d12_12x2	12 x 2	12	42	220	12	93	38	93	91	3
GL_TST_d12_8x3	8 x 3	12	42	244	12	105	38	105	84	3
GL_TST_d12_6x4	6 x 4	12	42	266	12	114	38	114	76	5
GL_TST_d12_4x6	4 x 6	12	42	296	12	114	38	114	53	3
Steel-Timber-Steel, Dowel diameter 12mm										
GL28h, t_2 = 90 mm, d = 12 mm, dowel strength cl. 8.8, a_3 = max(a_1; 84 mm), t_s = 6 mm										
GL_STS_d12_12x2	12 x 2	12	90	250	6	84	48	84	101	3
GL_STS_d12_8x3	8 x 3	12	90	262	6	120	48	120	83	3
GL_STS_d12_6x4	6 x 4	12	90	276	6	60	58	84	51	5
GL_STS_d12_4x6	4 x 6	12	90	304	6	60	40	84	52	3
GL_STS_d12_3x8	3 x 8	12	90	372	6	84	36	84	60	3
Timber-Steel-Timber, Dowel diameter 8mm										
GL28h, t_1 = 28 mm, d = 8 mm, dowel strength cl. 10.9, a_2 = 26 mm, a_3 = 80 mm										
GL_TST_d8_12x2	12 x 2	8	28	158	8	64	26	80	66	3
GL_TST_d8_6x4	6 x 4	8	28	192	8	80	26	80	57	3
Steel-Timber-Steel, Dowel diameter 8mm										
GL28h, t_2 = 60 mm, d = 8 mm, dowel strength cl. 10.9, a_3 = 80 mm, t_s = 4 mm										
GL_STS_d8_12x2	12 x 2	8	60	174	4	56	32	80	71	3
GL_STS_d8_6x4	6 x 4	8	60	190	4	40	40	80	35	3

Table 2. Kerto-LVL series with double-shear dowelled connections. Kerto-S is standard LVL and Kerto-Q is cross veneered.

Series name	Dowel pattern n x m	dowel diam. d mm	thick-ness t_1 or t_2 mm	width B mm	steel plate t_s mm	spacing parall. a_1 mm	spacing, perp. a_2 mm	end dist. a_3 mm	edge dist. a_4 mm	N
Timber-Steel-Timber, Dowel diameter 12mm										
Kerto-S, t_1 = 39 mm, d = 12 mm, dowel strength cl 8.8, a_2 = 38 mm, a_3 = max(a_1; 105mm)										
KS_TST_d12_12x2	12x2	12	39	162	12	84	38	105	62	3
KS_TST_d12_8x3	8x3	12	39	180	12	93	38	105	52	3
KS_TST_d12_6x4	6x4	12	39	204	12	105	38	105	45	5
KS_TST_d12_4x6	4x6	12	39	266	12	105	38	105	38	3
Kerto-Q, t_1 = 39 mm, d = 12 mm, dowel strength cl. 8.8, a_2 = 38 mm, a_3 = 105mm										
KQ_TST_d12_6x4	6x4	12	39	258	12	105	38	105	72	3
Steel-Timber-Steel, Dowel diameter 12mm										
Kerto-S, t_2 = 75 mm, d = 12 mm, dowel strength cl. 8.8, a_3 = 105 mm, t_s = 6 mm, F_{Rk} = 624 kN										
KS_STS_d12_12x2	12x2	12	75	228	6	84	48	105	90	3
KS_STS_d12_8x3	8x3	12	75	224	6	105	48	105	64	3
KS_STS_d12_6x4	6x4	12	75	252	6	84	60	105	36	5
KS_STS_d12_4x6	4x6	12	75	272	6	84	40	105	36	3
KS_STS_d12_3x8	3x8	12	75	324	6	84	36	105	36	3
Timber-Steel-Timber, Dowel diameter 8mm										
Kerto-S, t_1 = 27 mm, d = 8 mm, dowel strength cl. 10.9, a_2 = 26 mm, a_3 = 105 mm										
KS_TST_d8_12x2	12x2	8	27	116	8	56	26	105	45	3
KS_TST_d8_6x4	6x4	8	27	138	8	64	26	105	30	3
Steel-Timber-Steel, Dowel diameter 8mm										
Kerto-S, t = 51 mm, d = 8 mm, dowel strength cl. 10.9, a_3 = 105 mm, t_s = 4 mm										
KS_STS_d8_12x2	12x2	8	51	160	4	56	32	105	64	3
KS_STS_d8_6x4	6x4	8	51	174	4	56	42	105	24	3
Kerto-Q, t = 51 mm, d = 8 mm, dowel strength cl. 10.9, a_3 = 60 mm, t_s = 4 mm										
KQ_STS_d8_12x2	12x2	8	51	210	4	56	32	60	89	3
KQ_STS_d8_6x4	6x4	8	51	224	4	56	42	60	49	3

3.2 Multiple shear connection specimens

The multiple shear tests series are shown in Tables 3 and 4 for glulam and LVL, respectively.

Multiple shear test series were made with connected members except one series (GL-4Sh_d8_AZ). The glulam specimens were manufactured from split glulam, but the split parts were glued together using two battens of either 14 mm thickness or 10 mm thickness depending on the steel plate thickness 12 mm or 8 mm, respectively. Similarly, LVL-specimens were manufactured by gluing the parts together. The gluing was made as screw-gluing with polyurethane glue. Series GL-4Sh_d8_6x4_AZ was made with unattached members and was used as a parallel series to GL-4Sh_d8_6x4_A to see, if the capacity depends on whether the timber members are glued together or not.

Table 3. Glulam series with multiple shear dowelled connections.

Series name	Dowel pattern n x m	dowel diam. d mm	thick-ness t_1 / t_2 mm	width B mm	steel plate t_s mm	spacing parall. a_1 mm	spacing perp. a_2 mm	end dist. a_3 mm	edge dist. a_4 mm	N
4-Shear, Timber-Steel-Timber-Steel-Timber, Dowel diameter 12mm										
GL28h, d = 12 mm, dowel strength cl. 8.8, a_2 = 38 mm, a_3 = a_1, t_s = 12 mm										
GL_4Sh_d12_12x2A	12x2	12	42 / 90	250	12	93	38	93	106	3
GL_4Sh_d12_12x2B	12x2	12	35 / 104	250	12	93	38	93	106	3
GL_4Sh_d12_6x4A	6x4	12	42 / 90	276	12	114	38	114	81	3
GL_4Sh_d12_6x4B	6x4	12	35 /104	276	12	114	38	114	81	3
4-Shear, Timber-Steel-Timber-Steel-Timber, Dowel diameter 8mm										
GL28h, d = 8 mm, dowel strength class10.9, a_2 = 26 mm, a_3 = 80 mm, t_s = 8 mm										
GL_4Sh_d8_12x2A	12x2	8	28 / 60	174	8	64	26	80	74	3
GL_4Sh_d8_12x2B	12x2	8	22 / 72	174	8	64	26	80	74	3
GL_4Sh_d8_6x4AZ(*	6x4	8	28 / 60	192	8	80	26	80	57	3
GL_4Sh_d8_6x4B	6x4	8	22 / 72	192	8	80	26	80	57	3
GL_4Sh_d8_6x4A(*	6x4	8	28 / 60	192	8	80	26	80	57	3
6-Shear, Timber-Steel-Timber-Steel-Timber-Steel-Timber, Dowel diameter 8mm										
GL28h, d = 8 mm, dowel strength class10.9, a_2 = 26 mm, a_3 = 80 mm, t_s = 8 mm										
GL_6Sh_d8_12x2	12x2	8	28 / 60	174	8	64	26	80	74	3

Table 4. Kerto-LVL series with multiple shear dowelled connections.

Series name	Dowel pattern n x m	dowel diam. d mm	thick-ness t_1 / t_2 mm	width B mm	steel plate t_s mm	spacing parall. a_1 mm	spacing perp. a_2 mm	end dist. a_3 mm	edge dist. a_4 mm	N
4-Shear, Timber-Steel-Timber-Steel-Timber, Dowel diameter 12mm										
Kerto-S, d = 12 mm, Dowel strength class 8.8, a_2 = 48 mm, a_3 = 105 mm, t_s = 8 mm										
KS_4Sh_d12_12x2	12 x 2	12	38 / 72	228	8	84	48	105	90	3
KS_4Sh_d12_6x4	6 x 4	12	38 / 72	252	8	105	48	105	54	3
Kerto-Q, d = 12 mm, Dowel strength class 8.8, a_2 = 48 mm, a_3 = 105 mm, t_s = 8 mm										
KQ_4Sh_d12_5x4	5 x 4	12	38 / 72	322	8	105	48	105	89	3
4-Shear, Timber-Steel-Timber-Steel-Timber, Dowel diameter 8mm										
Kerto-S, d = 8 mm, Dowel strength class 10.9, a_2 = 32 mm, a_3 = 105 mm, t_s = 8 mm										
KS_4Sh_d8_12x2A	12 x 2	8	26 / 49	160	8	56	32	105	64	3
KS_4Sh_d8_12x2B	12 x 2	8	20 / 61	160	8	56	32	105	64	3
KS_4Sh_d8_6x4A	6 x 4	8	26 / 49	176	8	56	32	105	40	3
KS_4Sh_d8_6x4B	6 x 4	8	20 / 61	176	8	56	32	105	40	3
Kerto-Q, d = 8 mm, Dowel strength class 10.9, a_2 = 32 mm, a_3 = 60 mm, t_s = 8 mm										
KQ_4Sh_d12_6x4	6 x 4	8	26 / 49	226	8	56	32	60	65	3
6-Shear, Timber-Steel-Timber-Steel-Timber-Steel-Timber, Dowel diameter 8mm										
Kerto-S, d = 8 mm, Dowel strength class 10.9, a_2 = 32 mm, a_3 = 105 mm, t_s = 8 mm										
KS_6Sh_d8_12x2	6 x 4	8	26 / 49	176	8	56	32	105	40	3

4 Methods

The dowel holes for glulam were drilled using a numerical control (NC) machine tool. The glulam specimens were first allowed to reach equilibrium moisture content in a climate chamber with relative humidity of 65% and temperature 20°C (corresponding to equilibrium moisture content 12%) and drilled within 12h from taking outside the chamber. Then the specimens were taken back to the climate chamber. After that, the steel plates were put in place, dowels inserted as well as the binderbolts and nuts assembled. The LVL

specimens were also drilled using a numerical control machine tool, at the Kerto-LVL factory.

All series were kept in a climate chamber (20°C, 65%RH) long enough that they reached the equilibrium moisture content before manufacturing of joints and testing.

The loading was made according to EN26891:1991

5 Results and analysis

The results of the double shear tests are presented in Tables 5 and 6 and the multiple shear tests in Tables 7 and 8 for glulam and LVL, respectively. The presented test results contain the measured mean density, mean maximum slip (v_{max}) and mean maximum load (F_{max}) and its coefficient of variation. The observed failure mechanism is also reported. The prevailing failure mechanism was block shear (Fig. 2), but also tensile failures occurred as well as a few rowshear failures. However, no plug shear failures were detected.

For better comparison of the test results to the design formulas of Eurocode 5 (EC5, EN 1995-1-1:2004) some calculated values based on EC5 equations are also added to Table 5-8. The calculated values represent either characteristic values (subscript k) or mean values (subscript m) and are explained in the list of symbols (Chapter 2). The characteristic values have been calculated based on characteristic material properties as obtained from standards. The mean values are based on the measured values of density of timber and tensile strength of dowels. The mean values of non-measured properties have been assumed the following values:

– Glulam: $f_{tm} = 1.3 * f_{tk} = 29$ N/mm^2, $f_{vm} = 1.3 * f_{vk} = 4.9$ N/mm^2
– Kerto-S: $f_{tm} = 43$ N/mm^2, $f_{vm,edge} = 4.9$ N/mm^2, $f_{vm,flat} = 3.0$ N/mm^2
– Kerto-Q: $f_{tm} = 33$ N/mm^2, $f_{vm,edge} = 5.4$ N/mm^2, $f_{vm,flat} = 1.7$ N/mm^2

The above values for Kerto-LVL are estimated based on initial tests made at VTT according to the product standard EN14374. The values for glulam are an estimation based on experience.

The load-carrying capacity in case of splitting or rowshear is calculated by a reduction of the number of dowels n and capacity given by Johansen theory (EC5, Eqs. 8.1, 8.34):

$$F_{Sk} = \frac{n_{ef}}{n} F_{Rk}, \quad where \ n_{ef} = \min\left(n, n^{0.9} \left(\frac{a_1}{13d} \right)^{0.25} \right) \tag{1}$$

where F_{Rk} is the capacity by the Johansen theory.

The load-carrying capacity in case of block or plug shear failure has been calculated by the formula (A.1) in the Annex A of EC5:

$$F_{bs,Rk} = F_{Bk} = \max \begin{cases} 1.5 A_{net,t} f_{t,0,k} \\ 0.7 A_{net,v} f_{v,k} \end{cases} \tag{2}$$

where $f_{t,0,k}$ and $f_{v,k}$ are the tensile and shear strengths of the material, respectively, and $A_{net,t}$ and $A_{net,v}$ are the areas along the assumed failure surface that are under tension and shear stress, respectively. The areas are calculated as (Annex A Eq. A.2, A.3):

$$A_{net,t} = L_{net,t} t_1 \tag{3}$$

$$A_{\text{net,v}} = \begin{cases} L_{\text{net,v}}\, t_1 & \text{embedment fail. or steel – timber – steel connection} \\ \dfrac{L_{\text{net,v}}}{2}\left(L_{\text{net,t}} + 2t_{ef}\right) & \text{other cases} \end{cases} \quad (3)$$

where t_{ef} is the calculational distance from the surface to the dowel plastic hinge according to the Johansen theory. The magnitudes of $L_{\text{net,t}} = (m\text{-}1)*(a_2\text{-}d)$ and $L_{\text{net,v}} = (n\text{-}1)*(a_1\text{-}d)+(a3\text{–}d)$ (see Fig. 2).

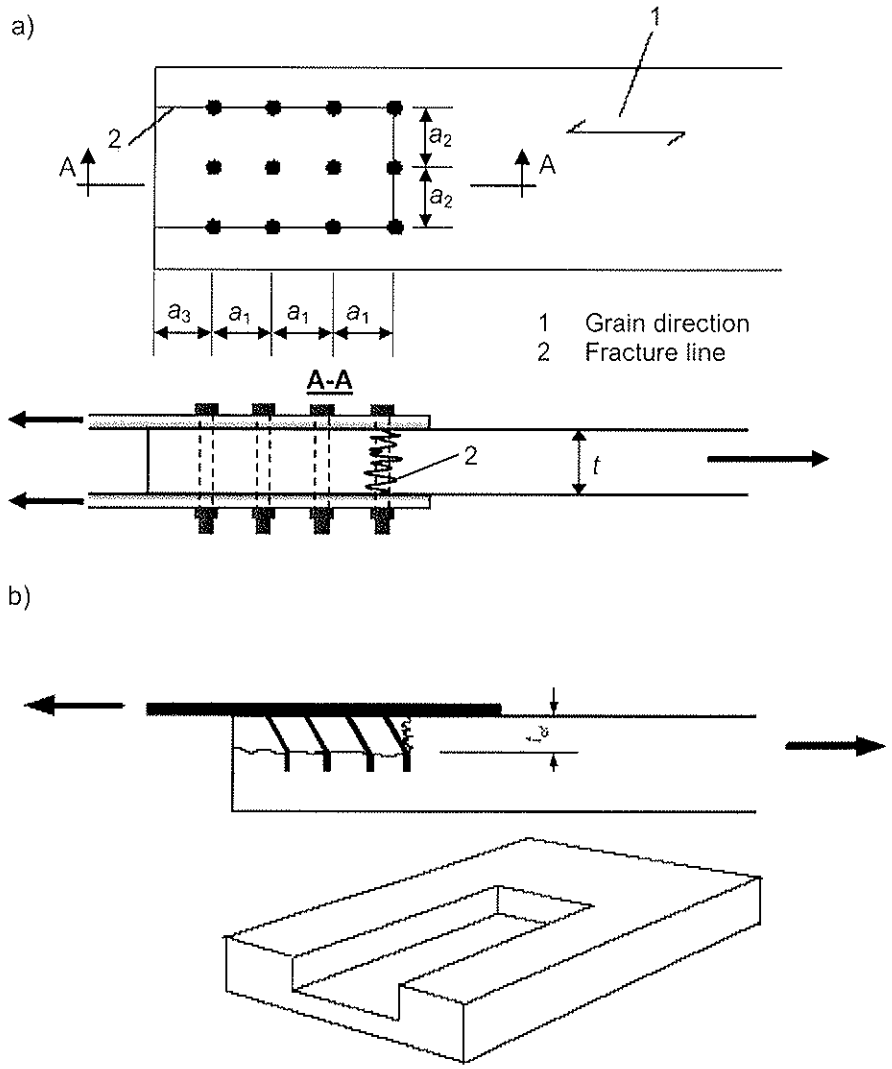

Figure 2. a) Block shear failure and b) plug shear failure of a dowelled connection.

Table 5. The calculated capacities and test results of the glulam series with double-shear dowelled connections. Symbols: see Chapter 2.

Series name	F_{Sk} kN	F_{Bk} kN	DF	F_{Rm} kN	F_{Sm} kN	F_{Bm} kN	F_{Tm} kN	ρ_m kg/m^3	v_{max} mean mm	F_{max} mean kN	F_{max} CoV %	TF	F_{max} / F_{Sm}	F_{max} / F_{Bm}
Timber-Steel-Timber, Dowel diameter 12mm														
GL28h, t_1 = 42 mm, d = 12 mm, Dowel strength cl. 8.8, F_{Rk} = 520 kN														
GL_TST_d12_12x2	356	297	p	579	397	385	459	466	1.9	424	8.3	b	1.07	1.10
GL_TST_d12_8x3	382	315	p	574	422	409	487	460	2.0	504	11.6	b	1.19	1.23
GL_TST_d12_6x4	402	332	p	585	452	430	511	474	2.3	529	4.4	b	1.17	1.23
GL_TST_d12_4x6	418	319	p	577	464	415	525	464	2.8	571	6.2	b	1.23	1.38
Steel-Timber-Steel, Dowel diameter 12mm														
GL28h, t_2 = 90 mm, d = 12 mm, dowel strength cl. 8.8, F_{Rk} = 576 kN														
GL_STS_d12_12x2	385	353	b-r	635	424	459	567	462	2.4	537	2.8	b	1.27	1.17
GL_STS_d12_8x3	438	353	b-r	644	490	459	567	475	3.7	646	7.4	b	1.32	1.41
GL_STS_d12_6x4	379	363	b-t	625	411	472	572	447	3.0	606	10.1	b	1.47	1.28
GL_STS_d12_4x6	395	369	b-t	638	438	479	582	467	2.6	552	6.0	b	1.26	1.15
GL_STS_d12_3x8	442	442	b-t	638	490	575	693	466	4.0	671	1.5	row	1.37	1.17
Timber-Steel-Timber, Dowel diameter 8mm														
GL28h, t_1 = 28 mm, d = 8 mm, dowel strength cl. 10.9, F_{Rk} = 279 kN														
GL_TST_d8_12x2	193	148	p	314	217	191	222	472	1.9	266	5.6	b	1.23	1.39
GL_TST_d8_6x4	218	164	p	296	232	214	250	425	1.6	238	17.7	b	1.03	1.11
Steel-Timber-Steel, Dowel diameter 8mm														
GL28h, t_2 = 60 mm, d = 8 mm, dowel strength cl. 10.9, F_{Rk} = 318 kN														
GL_STS_d8_12x2	212	163	b-r	355	237	212	264	468	2.6	295	21.6	b	1.24	1.39
GL_STS_d8_6x4	209	168	b-t	353	232	219	264	462	2.0	299	4.8	(*	1.29	1.37

*) the dominating failure mode is unclear

Table 6. The calculated capacities and results of the LVL series with double-shear dowelled connections. Symbols: see Chapter 2.

Series name	F_{Sk} kN	F_{Bk} kN	DF	F_{Rm} kN	F_{Sm} kN	F_{Bm} kN	F_{Tm} kN	ρ_m kg/m^3	v_{max} mean mm	F_{max} mean kN	F_{max} CoV %	TF	F_{max} / F_{Sm}	F_{max} / F_{Bm}
Timber-Steel-Timber, Dowel diameter 12mm														
Kerto-S, t_1 = 39 mm, d = 12 mm, Dowel strength cl. 8.8, F_{Rk} = 563 kN														
KS_TST_d12_12x2	376	331	p	594	397	395	506	499	2.6	400	7.9	b	1.01	1.01
KS_TST_d12_8x3	402	347	p	588	420	414	528	492	2.3	460	6.8	b	1.10	1.11
KS_TST_d12_6x4	426	378	p	603	456	449	572	512	2.6	507	6.1	b	1.11	1.13
KS_TST_d12_4x6	444	532	s/r	586	462	649	711	488	3.1	598	0.8	b	1.29	0.92
Kerto-Q, t_1 = 39 mm, d = 12 mm, Dowel strength cl. 8.8, F_{Rk} = 542 kN														
KQ_TST_d12_6x4	411	237	p	561	425	297	586	482	2.6	447	2.1	T	1.05	1.51
Steel-Timber-Steel, Dowel diameter 12mm														
Kerto-S, t_2 = 75 mm, d = 12 mm, Dowel strength cl. 8.8, F_{Rk} = 665 kN														
KS_STS_d12_12x2	444	386	b-r	722	483	459	719	523	2.7	500	5.2	b	1.04	1.09
KS_STS_d12_8x3	489	325	b-r	726	534	387	662	527	3.2	568	0.8	b	1.06	1.47
KS_STS_d12_6x4	476	567	s/r	736	527	692	719	537	3.7	591	7.1	b	1.12	0.85
KS_STS_d12_4x6	496	551	s/r	753	562	673	705	556	2.8	570	4.9	b	1.01	0.85
KS_STS_d12_3x8	510	662	s/r	717	551	807	803	518	2.8	561	7.3	b	1.02	0.70
Timber-Steel-Timber, Dowel diameter 8mm														
Kerto-S, t_1 = 27 mm, d = 8 mm, Dowel strength cl. 10.9, F_{Rk} = 303 kN														
KS_TST_d8_12x2	203	167	p	324	216	199	254	502	1.8	200	7.6	b	0.93	1.01
KS_TST_d8_6x4	224	180	p	328	243	214	269	514	1.7	241	13.0	b	0.99	1.13
Steel-Timber-Steel, Dowel diameter 8mm														
Kerto-S, t_2 = 51 mm, d = 8 mm, Dowel strength cl. 10.9, F_{Rk} = 344 kN														
KS_STS_d8_12x2	230	185	b-r	374	250	220	345	524	2.8	296	2.0	b	1.18	1.35
KS_STS_d8_6x4	246	273	s/r	380	272	333	340	518	3.8	336	2.3	b	1.25	1.01
Kerto-Q, t_2 = 51 mm, d = 8 mm, Dowel strength cl. 10.9, F_{Rk} = 333 kN														
KQ_STS_d8_12x2	223	188	b-r	341	228	226	354	492	3.7	308	7.0	T	1.35	1.36
KQ_STS_d8_6x4	239	203	b-t	348	249	254	350	501	3.9	335	7.3	b,T	1.35	1.32

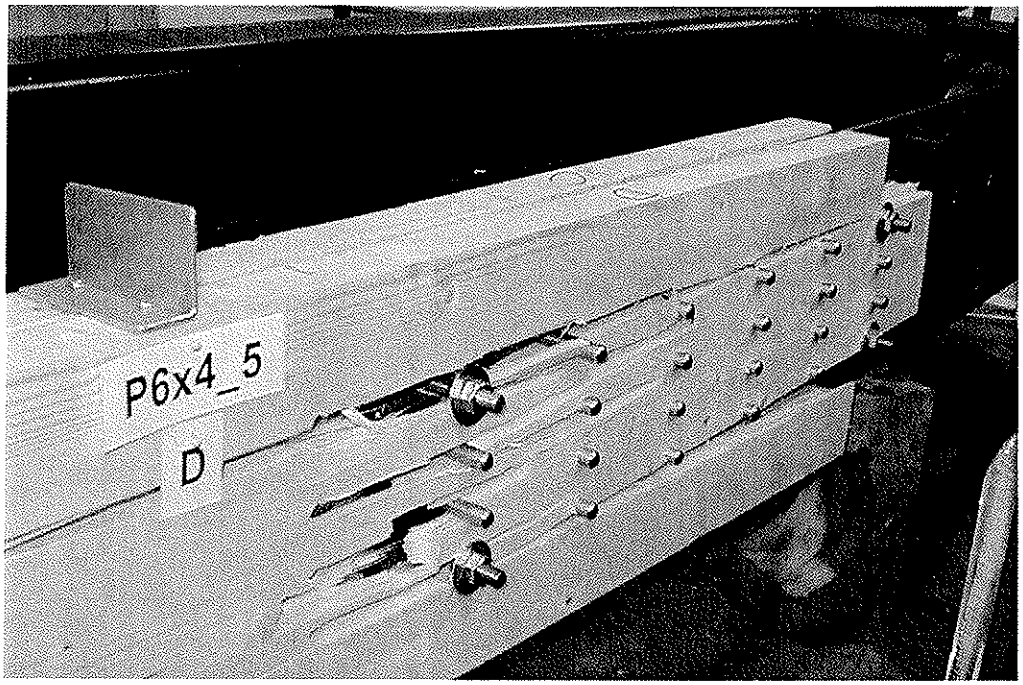

Figure 3. Typical failure by the block shear failure mechanism.

Table 7. The calculated capacities and test results of the Glulam series with multiple-shear dowelled connections. Symbols: see Chapter 2.

Series name	F_{Sk} kN	F_{Bk} kN	DF	F_{Rm} kN	F_{Sm} kN	F_{Bm} kN	F_{Tm} kN	ρ_m kg/m^3	v_{max} mm	F_{max} mean kN	F_{max} CoV %	TF	F_{max} / F_{Sm}	F_{max} / F_{Bm}
4-Shear, Dowel diameter 12mm														
GL28h, d = 12 mm, dowel str. cl. 10.9, t_s = 12 mm, F_{Rk} = 1040 kN (A), 1122 kN (12x2B), 1447 (6x4B)														
GL_4Sh_d12_12x2A	781	702	p,b-r	1216	833	910	1096	447	2.0	968	6.9	b,b	1.16	1.06
GL_4Sh_d12_12x2B	769	744	p,b-r	1196	820	965	1096	449	2.1	1084	5.7	b,b	1.32	1.12
GL_4Sh_d12_6x4A	881	589	p,b-r	1240	958	762	1106	463	1.4	856	5.9	b,b	0.89	1.12
GL_4Sh_d12_6x4B	1118	616	p,b-r	1592	1230	798	1106	462	1.8	1069	6.3	b,b	0.87	1.34
4-Shear, Dowel diameter 8mm														
GL28h, d = 8 mm, dowel strength class10.9, t_s = 8 mm, F_{Rk} = 558 kN (A), 689 kN (B)														
GL_4Sh_d8_12x2A	385	335	p,b-r	598	413	435	511	447	2.0	501	20.3	b,b	1.21	1.15
GL_4Sh_d8_12x2B	476	363	b-r,b-r	791	546	468	511	471	1.9	530	4.3	b,b	0.97	1.13
GL_4Sh_d8_6x4AZ	437	282	p,b-r	606	474	366	518	458	2.0	586	6.1	b,b	1.24	1.60
GL_4Sh_d8_6x4B	539	299	b-r,b-r	765	599	388	517	455	1.8	478	15.9	b,b	0.80	1.23
GL_4Sh_d8_6x4A	437	282	p,b-r	596	467	366	518	444	1.8	546	4.5	b,b	1.17	1.49
6-Shear, Dowel diameter 8mm														
GL28h, d = 8 mm, dowel strength class10.9, t_s = 8 mm, F_{Rk} = 837 kN														
GL_6Sh_d8_12x2	655	400	p,b-r	879	688	521	786	431	1.7	765	11.7	b,b	1.11	1.47

Table 8. The calculated capacities and test results of the LVL series with multiple-shear dowelled connections. Symbols: see Chapter 2.

Series name	F_{Sk} kN	F_{Bk} kN	DF	F_{Rm} kN	F_{Sm} kN	F_{Bm} kN	F_{Tm} kN	ρ_m kg/m^3	v_{max} mm	F_{max} mean kN	F_{max} CoV %	TF	F_{max} / F_{Sm}	F_{max} / F_{Bm}
4-Shear, Dowel diameter 12mm														
Kerto-S, d = 12 mm, Dowel strength class 10.9, F_{Rk} = 1226kN														
KS_4Sh_d12_12x2	819	758	p,b-r	1314	878	898	1418	525	2.3	898	7.6	b,b	1.02	1.00
KS_4Sh_d12_6x4	928	886	b-t,b-t	1312	993	1065	1418	523	2.2	1157	1.2	b,b	1.17	1.09
Kerto-Q, d = 12 mm, Dowel strength class 10.9, F_{Rk} = 1188kN														
KQ_4Sh_d12_5x4	900	623	b-t,b-r	1272	963	779	1449	527	4.3	1196	3.1	b,b	1.24	1.53
4-Shear, Dowel diameter 8mm														
Kerto-S, d = 8 mm, Dowel strength class 10.9, F_{Rk} =604kN (A), F_{Rk} = 702 kN (B)														
KS_4Sh_d8_12x2A	404	364	p,b-r	658	440	431	683	538	1.8	460	8.8	b,b	1.05	1.07
KS_4Sh_d8_12x2B	469	396	b-r,b-r	790	528	468	684	540	2.0	511	2.5	b,b	0.97	1.09
KS_4Sh_d8_6x4A	433	382	b-t,b-t	660	473	466	683	541	1.5	492	1.1	b,b	1.04	1.06
KS_4Sh_d8_6x4B	503	419	b-t,b-t	772	553	504	684	528	1.7	528	2.8	b,b	0.95	1.05
Kerto-Q, d = 8 mm, Dowel strength class 10.9, F_{Rk} = 584 kN														
KQ_4Sh_d12_6x4	418	324	b-t,b-t	618	443	396	701	518	2.3	584	4.9	b,b	1.31	1.47
6-Shear, Dowel diameter 8mm														
Kerto-S, d = 8 mm, Dowel strength class 10.9, F_{Rk} = 906 kN														
KS_6Sh_d8_12x2	649	567	b-t,b-t	876	627	462	670	550	1.7	729	8.8	b,b	1.16	1.58

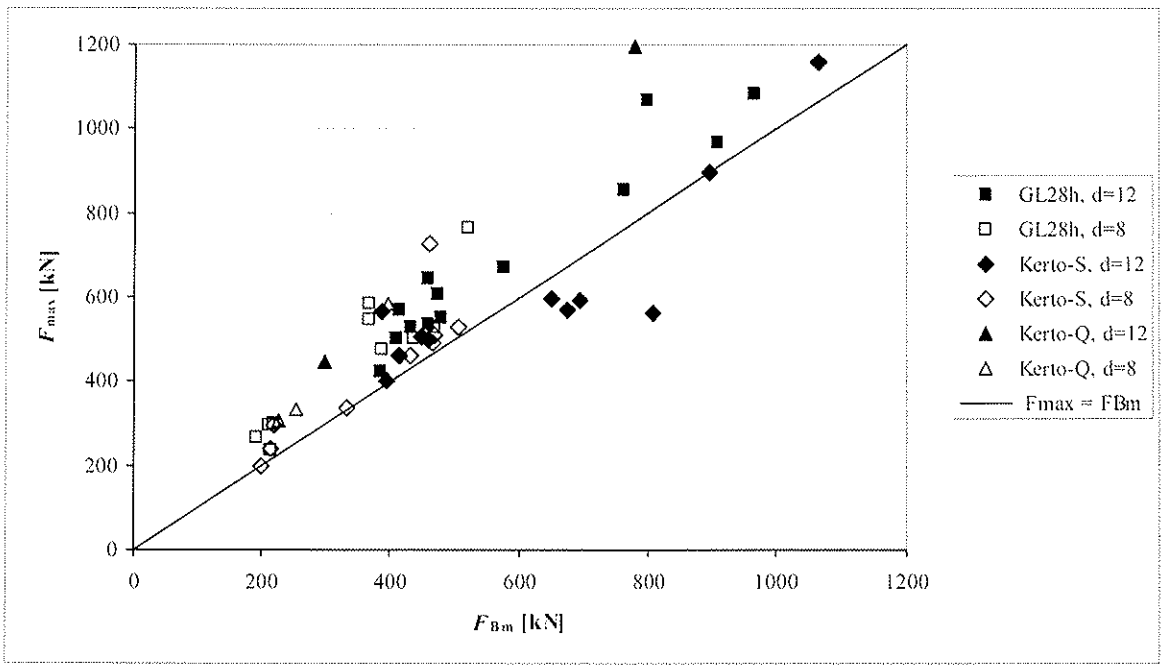

Figure 4. F_{max} plotted agains F_{Bm}. Each point is the mean result of one series. Note that in all four series which are under the F_{max} = F_{Bm} line, the critical design is not due to block shear but splitting or rowshear, represented by F_S, and in all four cases $F_{max} > F_{Sm}$.

6 Discussion

One surprising feature in the results is that the observed failure mode is in a large proportion different than what the calculation of the capacity value is based on (EN1995-1-1:2004). Especially this concerns the double-shear timber-steel-timber series and the outer

timber members of the multiple-shear series. In a large part of the series of these kinds, the calculation of the capacity is based on the plug-shear failure mechanisms, whereas the observed failure was block shear. In fact, in no cases was plug shear observed. For the Kerto-Q LVL the plug shear failure design value is in some cases very low, due to the low shear strength of the cross-veneers (rolling shear). However, in no cases was the plug shear observed for the Kerto-Q specimens, either. The plug shear failure does not occur, because the dowels remain straight or bend very little before failure and failure occurs as block shear.

Another general observation is that, even if according to the design equations the failure load due to block or plug shear and splitting (F_{Bm} and F_{Sm}) are very close to each other, and F_{Sm} is even lower than F_{Bm}, there were almost no cases of splitting or rowshear failure detected, which should be represented by F_{Sm} (only few series showed rowshear). This indicates that the equation by which F_{Sm} is calculated is too conservative for these types of connections, although the dowels were rather rigid.

Kerto-Q behaves differently from what could be anticipated from design equations. The low value of flatwise shear strength leads calculationally to very low capacity, if the critical failure mechanism is plug shear. However, in practice the plug shear does not occur due to rigid dowels and the capacity is much higher than expected by design calculations.

7 Conclusions

Based on the large experimental data that has been gathered by the loading of more than 150 specimens and 300 connections, the following recommendations can be given for the development of the design of dowelled timber-to-steel connections:

- The plug shear failure mechanism does not occur in the connection area contrarily to what the design equations in EC5 (EN 1995-1-1:2004; Annex A) suggest. This is due to the fact that the relatively rigid dowels remain straight or bend very little before failure, which is then mostly due to the block shear mechanism. Failure by plug shear would probably require the development of fully developed plastic hinges, which does not occur at the failure level of block shear. The design equations assume the fully developed plastic hinges in order to determine the failure mechanism based on the Johansen theory.
- If the mean material property values are substituted in the design equations of EC5, the value of F_{Sm} and F_{Bm}, representing splitting or rowshear failure and block shear or plug shear failure, respectively, are often very close to each other. In many cases the value of F_{Sm} is lower that F_{Bm}. However, in these experimental tests no pure splitting failure was observed and rowshear in only few series. This indicates that the equation for the reduction effect of the number of dowels in a row is too conservative for these connections, because it does not take into account the slenderness of the dowels.
- Connections with cross-veneered Kerto-Q-LVL showed much higher experimental capacities than could be anticipated from the design calculations using the characteristic values in EC5. This is due to the fact that the plug shear failure does not occur because of rigid dowels and because the low flatwise shear strength reduces the calculational capacity dramatically in case of plug shear.
- When the calculational failure mode of EC5 is block shear (b-r, b-t) it can be concluded that the formulas result usually in clearly conservative design for glulam,

but they are approximately on the right level for Kerto-S-LVL. Higher coefficients (instead of 1.5 and 0.7) could therefore be used for glulam in Eq. (2). However, the following additional condition should be given for the failure mode b-r (block-shear with shear capacity higher than tension): it works only if the edge distance a_3 is sufficiently large so that the tensile capacity of the outermost timber strips is enough to carry the whole failure load. It is apparent that, in most block shear failure cases, a simultaneous combination of tensile and shear stress is acting.

Acknowledgements

This work was financed by The Technology Agency of Finland, Finnforest Oyj, Versowood Oyj, SPU-Systems Oy, LATE-Rakenteet Oy, Exel Oyj and VTT which is gratefully acknowledged.

References

Anon. 2004. Tutkintaselostus. Messuhallin katon romahtaminen Jyväskylässä 1.2.2003. (Fair centre roof collapsing in Jyväskylä, Finland, on 1 Feb 2003.) Accident Investigation Report. Accident Investigation Board of Finland Report B 2/2003 Y

Hilson B.O. 1995. Joints with dowel type fasteners – Theory. STEP Lecture C3. In: Blass H.J., Aune P., Choo B.S., Görlacher R., Griffiths D.R., Hilson B.O., Racher P., Steck G. (Eds.): Timber Engineering STEP 1. Basis of design, material properties, structural components and joints. Centrum Hout, The Netherlands.

Johansen K.W. 1949. Theory of timber connections. International Association of Bridge and Structural Engineering. Publication No. 9:249-262. Bern.

Ranta-Maunus A., Keverinmäki A. 2003. Reliability of timber structures, theory and dowel-type connection failures. CIB-W18/36-7-11, Colorado, USA, August 2003.

INTERNATIONAL COUNCIL FOR RESEARCH AND INNOVATION
IN BUILDING AND CONSTRUCTION

WORKING COMMISSION W18 - TIMBER STRUCTURES

LOAD CARRYING CAPACITY OF JOINTS WITH DOWEL TYPE FASTENERS IN SOLID WOOD PANELS

T Uibel
H J Blaß

Lehrstuhl für Ingenieurholzbau und Baukonstruktionen
Universität Karlsruhe

GERMANY

MEETING THIRTY-NINE
FLORENCE
ITALY
AUGUST 2006

Presented by T Uibel
A Buchanan asked about how one could account for the interlaminar slip in nail connected panels. T Uibel answered that it was not considered as glued panels were studied.
P Quenneville discussed the issue of including or exclusion of outlier for plug shear failures. H Blass answered plug shear failure did not always occur, if one took away the outliers, one would have taken away too much.
I Smith asked about shear transfer and load paths. H Blass stated that the behaviour is rather ductile with ~ 15 mm of deformation at the high load level; therefore, load path is of less significant.
J Köhler received confirmation that the load–deformation data was obtained via deformation controlled not force controlled testing and ductility can be achieved.
B Dujic asked about beams columns and moment resisting joints. H Blass stated that both tensile and moment carrying members could be used efficiently. In the tensile members, connections typically governed. Here the connection capacity was improved so this material seemed to be appropriate for a balanced capacity of joint and member.
G Schickhofer asked about other lay-ups such as 5 or 7 layers. T Uibel answered that only 5 layers were studied.

Load Carrying Capacity of Joints with Dowel Type Fasteners in Solid Wood Panels

T. Uibel, H.J. Blaß

Lehrstuhl für Ingenieurholzbau und Baukonstruktionen

Universität Karlsruhe, Germany

1 Introduction

Solid wood panels with cross layers (Fig. 1) have been used more and more frequently in timber engineering in recent years. Their use in constructions requires their connection with each other and with other components of the construction. To that purpose dowel-type fasteners can be used. It is possible to position the fasteners perpendicular to the plane of the panels or in their narrow sides. In this paper only the first possibility will be discussed.

The load carrying capacity for dowel-type fasteners is usually calculated according to Johansen's yield theory [3], [4]. Embedding strength as well as the yield moment of the fasteners are important parameters in this calculation. Withdrawal strength is needed to calculate the load carrying capacity of axially loaded screws or nails. The aim of a current research project at the University of Karlsruhe is to develop a proposal for calculating the load carrying capacity of joints with dowel type fasteners in solid wood panels.

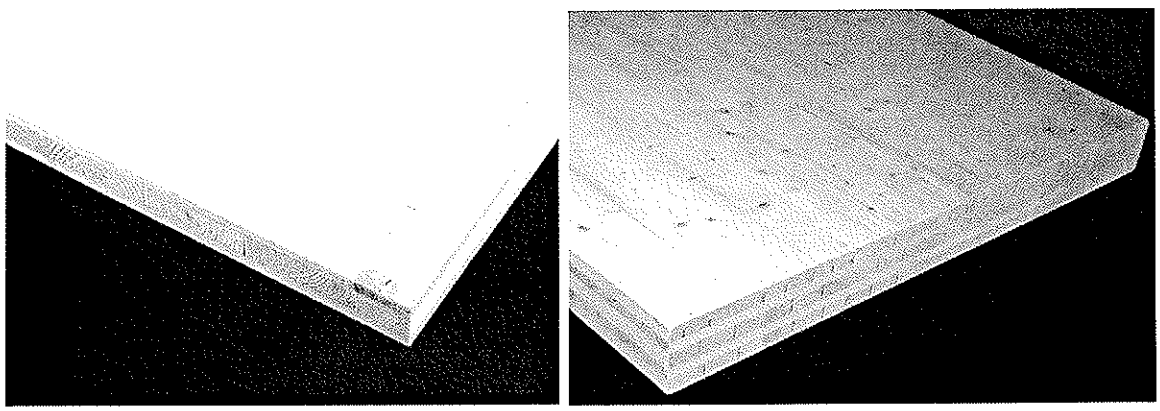

Fig. 1: Solid wood panels with cross layers - two examples of products (pictures: Informationsdienst Holz)

2 Characteristics of the test material

Solid wood panels consist of boards crosswise laminated with a minimum of three layers. Some panels are produced with gaps between the narrow sides of the boards. The maximum width of gaps is limited to 6 mm. In addition, grooves with a width of about 2,5 mm are sawn into the boards of some products. Fig. 2 shows cross-sections of different solid wood panel products. Table 1 gives some statistic information about the gaps.

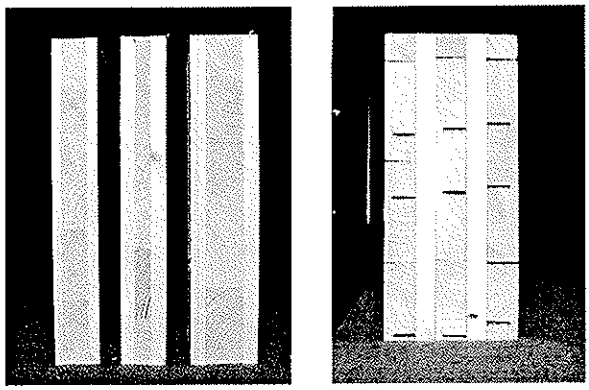

Fig. 2: Cross-sections of panels without and with gaps between boards and grooves

Table 1: Width of gaps between boards of one layer for some different products

Manufacturer/ product	Build-up	Width [mm] of gaps in								
		Outer layers			Interlayers			Centre layer		
		mean	max.	95% fractile	mean	max.	95% fractile	mean	max.	95% fractile
1	17-17-17-17-17	0,6	2,1	1,6	1,6	7,3	3,4	1,0	3,0	2,3
2	19-22-19	0,4	2,0	1,3	-	-	-	0,5	2,2	1,8
2	34-13-34-13-34	0,2	1,0	1,0	1,4	6,8	3,3	2,0	6,7	4,5
4	9,5-6,8-9,5-6,8-9,5	0	0	0	0,6	5,4	3,5	0	0	0

The characteristic density (at normal climate, 20°C/65% RH) of solid wood panels was determined by analysing altogether 2299 test specimens out of a range of products from different manufacturers (Table 2). This revealed a minimum 5th percentile density of 400 kg/m³ for product 2. Taking this result into account a characteristic density of 400 kg/m³ is proposed for solid wood panels made of European spruce (*Picea abies*).

Table 2: Density of solid wood panels

Manufacturer/ product	n	ρ_{mean} kg/m³	ρ_{min} kg/m³	ρ_{max} kg/m³	Coefficient of variation %	$\rho_{0,05}$ kg/m³
1	515	470	415	630	5,11	430
2	906	437	372	578	6,02	400
3	208	458	406	507	5,18	423
4	670	459	397	558	5,75	419

3 Embedding strength

3.1 Test set-up

To determine the embedding strength of solid wood panels with cross layers 620 embedment tests according to EN 383 [5] were carried out, involving tests with a load under 0°, 45° and 90° to the grain of the outer layers. Furthermore the position of fasteners was varied, as shown in Fig. 3. They were placed in areas without gaps (pos. 1), placed in gaps (pos. 2 to 4) or over gaps (pos. 5).

For tests with fasteners loaded parallel and perpendicular to the grain direction of the outer layers it was possible to apply the geometry of test specimens as specified in EN 383. To carry out embedment tests with fasteners loaded under 45° to the grain the size of test specimens had to be increased due to plug shear failure in outer layers.

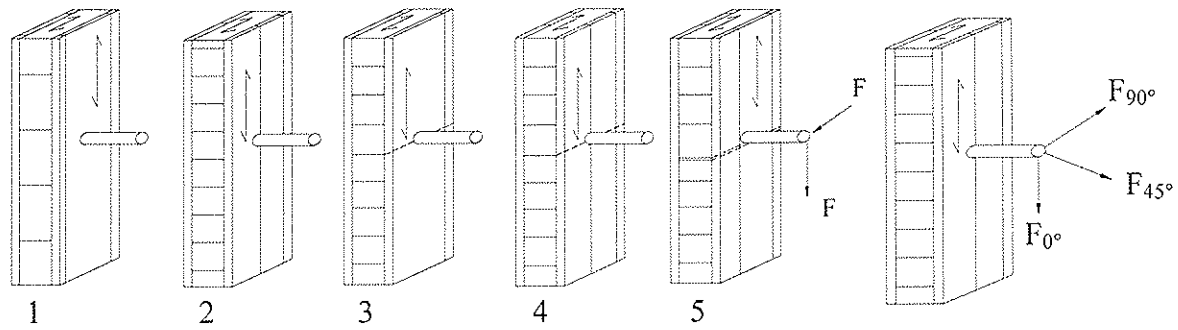

Fig. 3: Positions of fasteners and load direction in embedment tests, schematic sketch

3.2 Results for dowels

For dowels it was possible to develop the following two models for embedment strength on the basis of a multiple regression analysis of 438 test results. In the first model the embedment strength as given in equation (1) is independent of the build-up of the panels. The correlation coefficient r is equal to 0,75. The embedment strength depends on the diameter d of the dowel, the density ρ of the solid wood panel and the angle α between load and grain direction of the outer layer.

$$f_{h,pred} = \frac{0,035 \cdot (1 - 0,015 \cdot d) \cdot \rho^{1,16}}{1,1 \cdot \sin^2\alpha + \cos^2\alpha} \quad \text{in N/mm}^2 \qquad (1)$$

$r = 0,75$

Additionally the second model (eq. (2)) takes into account the build-up of the panels as defined in Fig. 4.

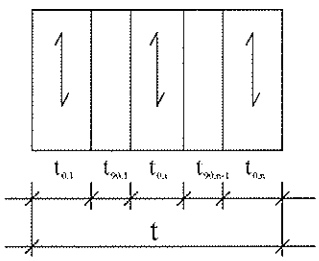

Fig. 4: Definition of thickness of layers for eq. (2) and (3), in case of a panel with 5 layers

$$f_{h,pred} = 0,037 \cdot (1 - 0,016 \cdot d) \cdot \rho^{1,16} \cdot \left[\frac{\sum_{i=1}^{n} t_{0,i}}{t \cdot \left(1,2 \cdot \sin^2\alpha + \cos^2\alpha\right)} + \frac{\sum_{j=1}^{n-1} t_{90,j}}{t \cdot \left(1,2 \cdot \cos^2\alpha + \sin^2\alpha\right)} \right] \quad \text{in N/mm}^2 \qquad (2)$$

$r = 0,74$

The validity of equation (1) and (2) is limited to panels which fulfill the following conditions:

- Maximum thickness of one layer: 40 mm
- Ratio of layers with different grain directions as defined in Fig. 4:

$$0,95 < \frac{\sum t_{0,i}}{\sum t_{90,j}} < 2,1 \qquad (3)$$

Fig. 5 shows the results of embedment tests over the predicted values for model 1.

The characteristic embedment strength on basis of equation (1) for a characteristic density of 400 kg/m³ can be calculated according to the following expression:

$$f_{h,k} = \frac{0,031 \cdot (1 - 0,015 \cdot d) \cdot \rho_k^{1,16}}{1,1 \cdot \sin^2\alpha + \cos^2\alpha} = 32 \cdot \frac{1 - 0,015 \cdot d}{1,1 \cdot \sin^2\alpha + \cos^2\alpha} \quad \text{in N/mm}^2 \qquad (4)$$

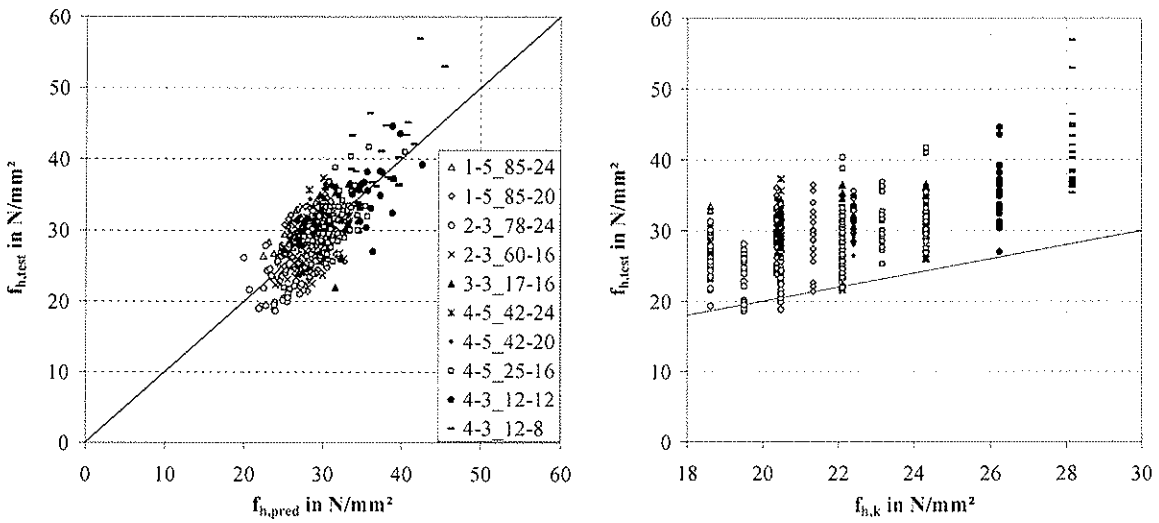

Fig. 5: Comparison of test results and predicted resp. characteristic values for dowels

3.3 Results for screws and nails

On the basis of a regression analysis of 179 tests with screws and nails the embedment strength can be derived as:

$$f_{h,pred} = 0,13 \cdot d^{-0,53} \cdot \rho^{1,05} \quad \text{in N/mm}^2 \qquad (5)$$

$r = 0,83$

A comparison of predicted values and test results is shown in Fig. 6. The correlation coefficient was determined as r = 0,83. At present the validity of equation (5) has to be limited to panels with layers thinner than 7 mm. In equation (5) the embedding strength is independent of the angle α. This result corresponds to the research results of Blaß and Bejtka [1], [2] for self-tapping screws.

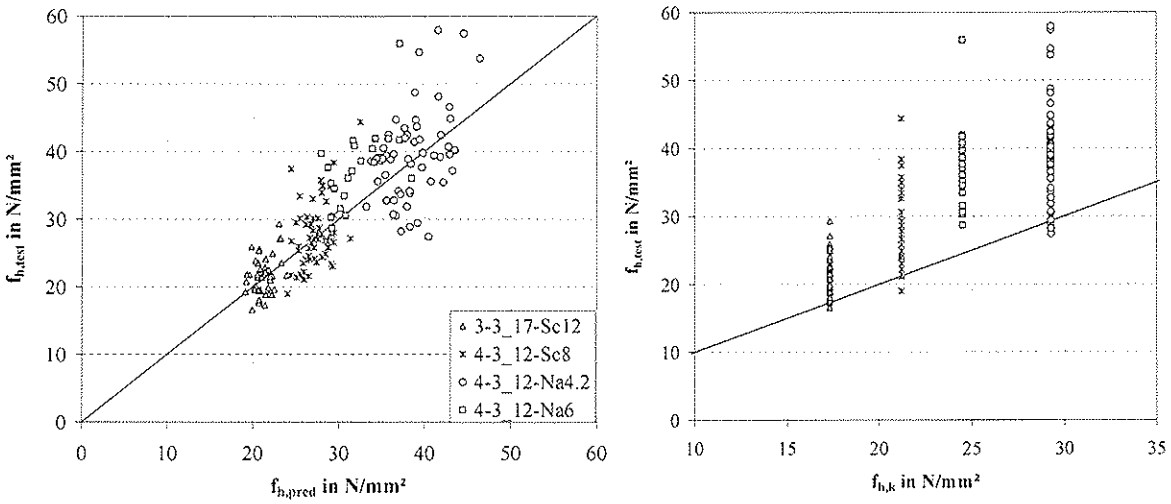

Fig. 6: Comparison of test results and predicted resp. characteristic values (screws/nails)

By inserting a characteristic density of 400 kg/m³ in equation (5) the characteristic embedment strength can be proposed as:

$$f_{h,k} = 0{,}112 \cdot d^{-0{,}5} \cdot \rho_k^{1{,}05} = 60 \cdot d^{-0{,}5} \quad \text{in N/mm}^2 \qquad (6)$$

4 Load carrying capacity

4.1 Calculation Model

The load carrying capacity of joints in solid wood panels under lateral load can be determined according to Johansen's yield theory. For connections with screws and nails in solid wood panels with thin layers ($t_j \leq 7$ mm) it is possible to use the embedment strength from equation (5) resp. (6) for the calculation.

In other cases the embedment strength depends on the angle between load and grain direction so that additional investigations are necessary. Here obviously the embedment strength of a layer loaded in grain direction is larger than of one loaded perpendicular to the grain (see Fig. 7). In the following the load carrying capacity of dowels in a steel-to-solid-wood-panel connection with an inner steel plate is derived exemplarily. According to Johansen's yield theory three failure modes are possible. The load carrying capacity is the minimum value of these three modes. Failure mode 1 is characterized by an embedment failure of all layers as shown in Fig. 7.

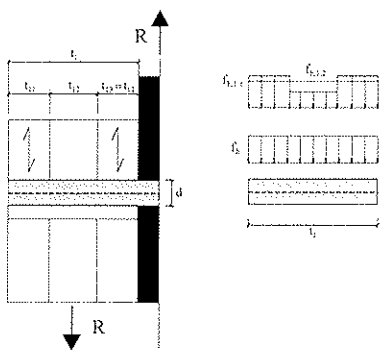

Fig. 7: Failure mode 1

In this failure mode the load carrying capacity can be directly calculated by using the embedment strength from equation (6).

$$R = f_h \cdot d \cdot t_1 \tag{7}$$

In the second failure mode with one plastic hinge the load carrying capacity depends on the distance x (Fig. 8). For a solid wood panel with three layers two cases (2.1 and 2.2) have to be taken into consideration as shown in Fig. 8.

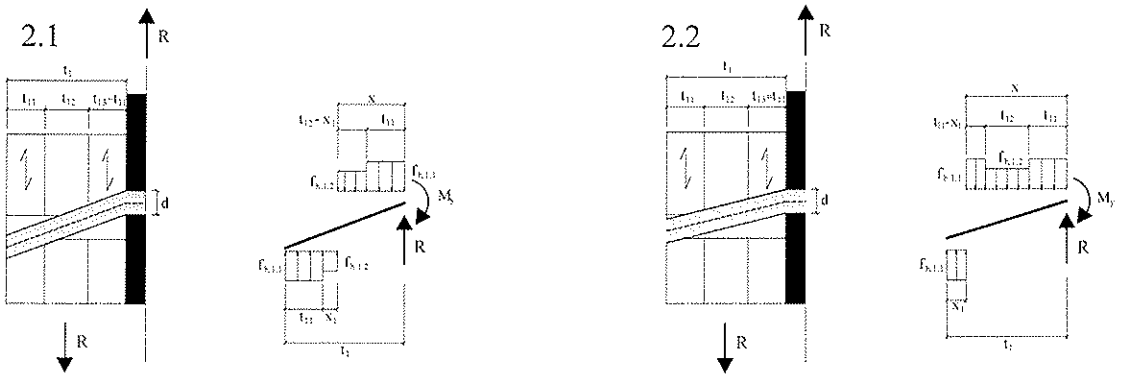

Fig. 8: Failure mode 2.1 and 2.2

By using the substitutions

$$\beta_{1,2}=f_{h,1,2}/f_{h,1,1} \tag{8}$$

and

$$\psi=t_{11}/t_1 \tag{9}$$

the load carrying capacity for failure mode 2.1 and 2.2 can be calculated as follows.

Failure mode 2.1:

$$R = f_{h,1,1} \cdot d \cdot t_1 \cdot \left[\sqrt{2} \cdot \sqrt{\beta_{1,2} \cdot \left(\beta_{1,2} \cdot \left(2 \cdot \psi^2 - 2\psi + 1\right) + 2 \cdot \psi \left(1 - \psi\right) + \frac{2 \cdot M_y}{f_{h,1,1} \cdot d \cdot t_1^2} \right)} - \beta_{1,2} \right] \tag{10}$$

for

$$\psi \le \frac{1}{2} \left(\beta_{1,2} + 1 - \sqrt{\beta_{1,2}^2 + 1 + \frac{4 \cdot M_y}{d \cdot f_{h,1,1} \cdot t_1^2}} \right) \tag{11}$$

Failure mode 2.2:

$$R = f_{h,1,1} \cdot d \cdot t_1 \left(\sqrt{2} \cdot \sqrt{\psi \cdot \left(2 \cdot \beta_{1,2} - 2\right) + 2 - \beta_{1,2} + \frac{2 \cdot M_y}{f_{h,1,1} \cdot d \cdot t_1^2}} + 2 \cdot \psi + \beta_{1,2} \cdot \left(1 - 2 \cdot \psi\right) - 2 \right) \tag{12}$$

for

$$\psi \ge \frac{1}{2} \left(\beta_{1,2} + 1 - \sqrt{\beta_{1,2}^2 + 1 + \frac{4 \cdot M_y}{d \cdot f_{h,1,1} \cdot t_1^2}} \right) \tag{13}$$

In failure mode three the load carrying capacity depends on the position of the second plastic hinge. For a panel with three layers there are three cases to be considered as follows.

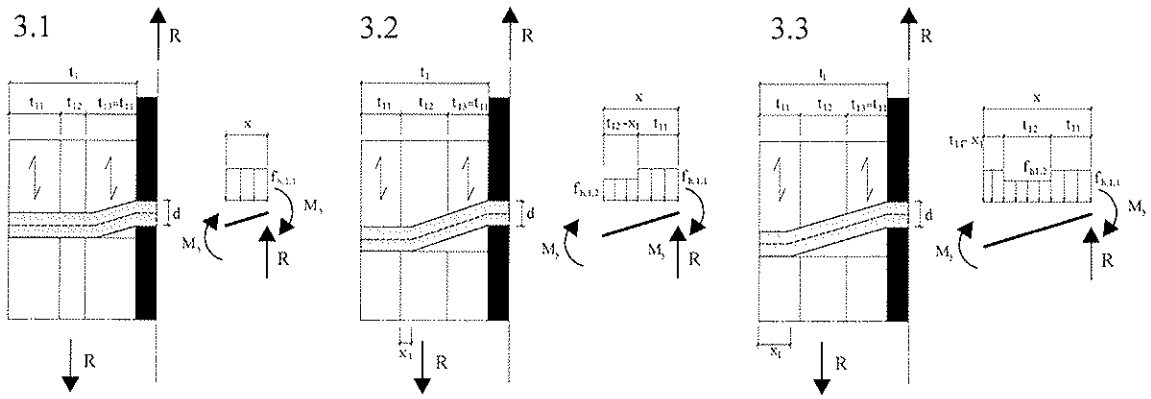

Fig. 9: Failure mode 3.1 to 3.3

Failure mode 3.1:

$$R = \sqrt{2}\sqrt{2 \cdot f_{h,1,1} \cdot M_y \cdot d} \qquad \text{for} \quad \psi \geq 2 \cdot \sqrt{\frac{M_y}{f_{h,1,1} \cdot d \cdot t_1^2}} \tag{14}$$

Failure mode 3.2:

$$R = f_{h,1,1} \cdot d \cdot t_1 \cdot \psi \left(1 - \beta_{1,2} + \sqrt{\beta_{1,2} \cdot \left(\beta_{1,2} - 1 + \frac{4 \cdot M_y}{f_{h,1,1} \cdot d \cdot t_1^2 \cdot \psi^2} \right)} \right) \tag{15}$$

for

$$\psi \leq 2 \cdot \sqrt{\frac{M_y}{f_{h,1,1} \cdot d \cdot t_1^2}} \quad \text{and} \quad \frac{\psi}{\beta_{1,2}} \cdot \sqrt{\beta_{1,2} \cdot \left(\beta_{1,2} - 1 + \frac{4 \cdot M_y}{f_{h,1,1} \cdot d \cdot t_1^2 \cdot \psi^2} \right)} + \psi \leq 1 \tag{16}$$

Failure mode 3.3:

$$R = f_{h,1,1} \cdot d \cdot t_1 \left(\beta_{1,2} (1 - 2 \cdot \psi) + 2 \cdot \psi - 1 + \sqrt{2 \cdot \psi (\beta_{1,2} - 1) - \beta_{1,2} + 1 + \frac{4 \cdot M_y}{f_{h,1,1} \cdot d \cdot t_1^2}} \right) \tag{17}$$

for

$$\psi \leq 2 \cdot \sqrt{\frac{M_y}{f_{h,1,1} \cdot d \cdot t_1^2}} \quad \text{and} \quad \sqrt{2 \cdot \psi \cdot (\beta_{1,2} - 1) - \beta_{1,2} + 1 + \frac{4 \cdot M_y}{f_{h,1,1} \cdot d \cdot t_1^2}} + \psi \geq 1 \tag{18}$$

The shown way of calculation is already complex for a panel with three layers. Besides the variability of the density of different layers and gaps are not taken into account.

In many cases, which are dependent on the type of connection, the build-up of the solid wood panels and the diameter and yield moment of the fastener, a simplified calculation of the load carrying capacity using the embedment strength given in paragraph 3 is possible. For some configurations the yield moment develops in the outermost layers. This allows to directly use their embedment strength for the calculation. In conclusion, the limits for the application of simplified calculations have to be defined for different build-ups of solid wood panels.

4.2 Tests

In order to confirm the calculated load carrying capacities 88 tests with connections with dowel type fasteners positioned perpendicular to the plane of solid wood panels were planned. The tests also provide a basis for the required spacing, edge and end distances for the fasteners. Table 3 shows the specimen parameters and table 4 shows the results of the first 28 tests. The test set-up is documented in Fig. 10. A comparison between test results and calculated load carrying capacities is given in Fig. 11. A significant difference between the calculated load carrying capacity and the test results is determined only for specimen 1-24-2S_1.1 (R_{test}/R_{cal}=0,85). It is assumed that a plug shear failure which occurred in the outer layers is the reason for this discrepancy.

In most of the tests a displacement of more than 15 mm was reached. Even if a plug shear failure or splitting occurred in the outer layers, the load kept a constant level or dropped only marginally. Typical load-displacement-curves are displayed in Fig. 12. Fig. 10 (right) shows an opened connection after the test.

Table 3: Specimen parameters

Specimen	n	Type	Fasteners									Build-up of solid wood panel	
			Type	d mm	M_y Nm	t_1 mm	t_2 mm	$a_{1,t}$	a_1	$a_{2,c}$	Number of fasteners per row	Side members	Middle member
1-24-2S_1.1	4	T-S-T	dowels	24	1191	60	-	7·d	5·d	3·d	3 (one row)	19-22-19	steel plate
1-20-22_1.1	6	T-T-T	dowels	20	779	60	128	5·d	5·d	3·d	3 (one row)	19-22-19	34-13-34-13-34
1-20-22_1.2	6	T-T-T	dowels	20	779	60	128	5·d	4·d	3·d	3 (one row)	19-22-19	34-13-34-13-34
1-20-22_1.3	3	T-T-T	dowels	20	779	60	128	4·d	4·d	3·d	3 (one row)	19-22-19	34-13-34-13-34
1-12-42_1.1	3	T-T-T	screws	12	58,5	27	146	10·d	4·d	2,5·d	2 (one row)	8,5-10-8,5	34-22-34-22-34
1-12-42_1.2	3	T-T-T	screws	12	58,5	27	146	12·d	5·d	3·d	2 (one row)	8,5-10-8,5	34-22-34-22-34
1-12-42_1.3	3	T-T-T	screws	12	58,5	27	146	6·d	3·d	3·d	2 (one row)	8,5-10-8,5	34-22-34-22-34

Table 4: Results of the tests

Specimen	Number of Specimens n	Mean density ρ_m in kg/m³		Load carrying capacity per fastener and shear plane $F_{u,mean}$ in kN
		Side members	Middle members	
1-24-2S_1.1	4/3)[1]	435	-	31,7
1-20-22_1.1	6	430	417	24,7
1-20-22_1.2	6/5)[1]	425	433	22,1
1-20-22_1.3	3	463	433	23,5
1-12-42_1.1	3/2)[1]	440	411	7,28
1-12-42_1.2	3	438	430	7,49
1-12-42_1.3	3	424	438	6,88
)[1] 1 specimen with tensile failure				

Fig. 10: Test-set-up for connections 1-24-2S_1.1 and 1-12-42_1.2,
opened connection 1-20-22_1.2.2 (right)

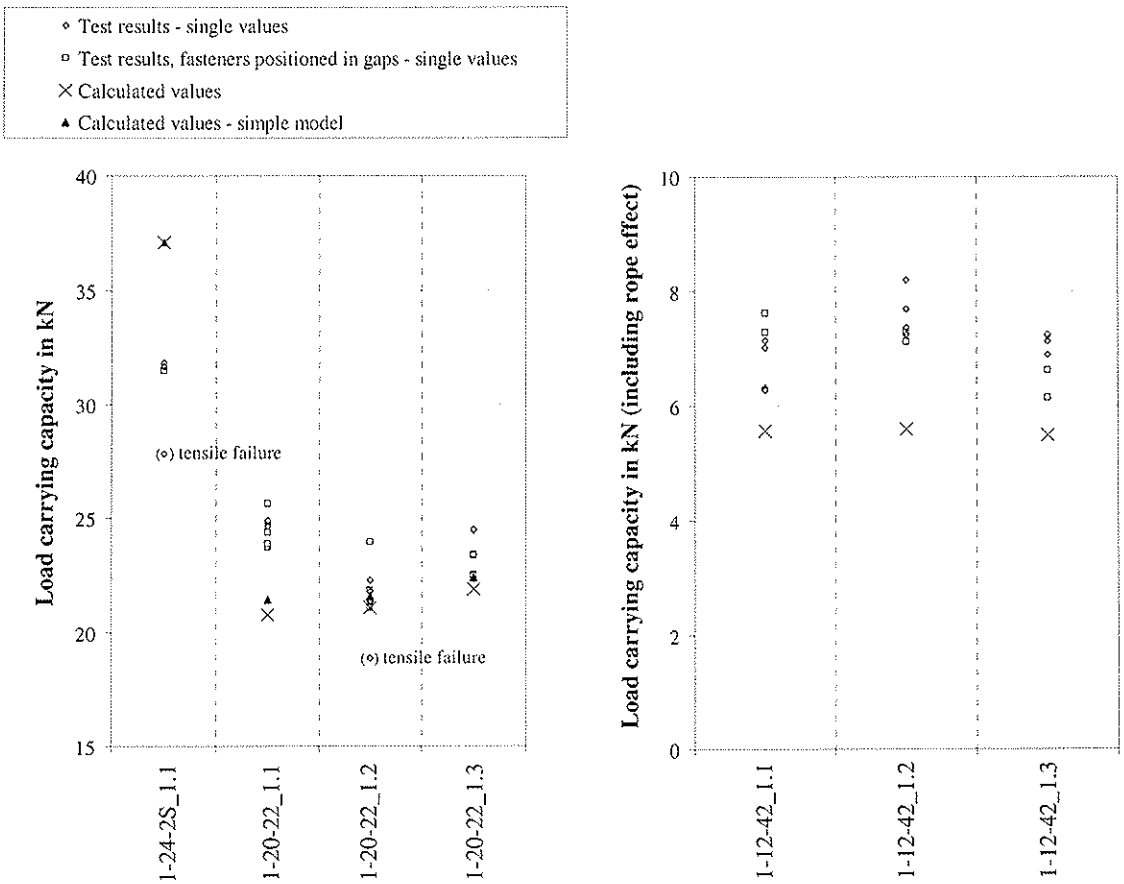

Fig. 11: Comparison between test results and calculated load carrying capacities

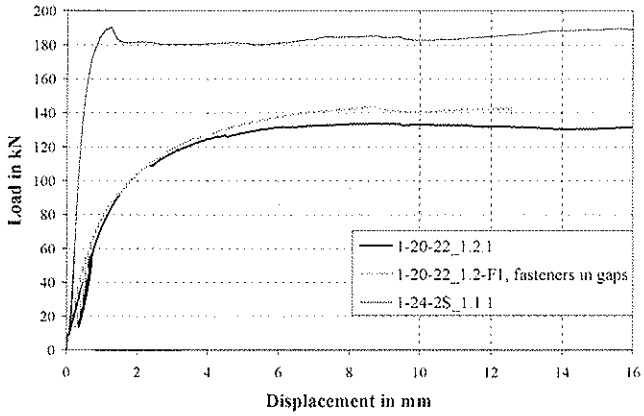

Fig. 12: Typical load-displacement-curves

5 Conclusions

The parameters of solid wood panels with cross layers for calculating the load carrying capacity of dowel type fasteners were examined. For the characteristic density of solid wood panels made of spruce a value of 400 kg/m³ is proposed. On the basis of a statistical analysis of 617 embedment tests it was possible to determine the embedment strength of solid wood panels for dowel type fasteners. The presented functions depend on type and diameter of fasteners, density and particularly on the angle between load and grain direction of the outer layers. Proposals for characteristic values are also given. For the example of a steel-to-solid-wood-panel connection the load carrying capacity is derived. First results of tests with connections in solid wood panels are presented. These tests are important to verify a simplified calculation model. Furthermore they are required to determine the minimum edge and end distances and spacings of fasteners. When the load in the tests reaches the load-carrying capacity, the connections show almost ideal plastic load-displacement behaviour. Even plug shear or splitting of the outer layers do not initiate a brittle failure. These facts show the reinforcement effect in crosswise laminated structures. Further investigations are necessary to determine the influence of plug shearing on the load carrying capacity.

6 References

[1] Bejtka, I.: Verstärkungen von Bauteilen aus Holz mit Vollgewindeschrauben. *Karlsruher Berichte zum Ingenieurholzbau*, Band 2, Lehrstuhl für Ingenieurholzbau und Baukonstruktionen (Ed.), Universität Karlsruhe (TH), Karlsruhe, 2005

[2] Blaß, H. J., Bejtka, I., Uibel, T.: Tragfähigkeit von Verbindungen mit selbstbohrenden Holzschrauben mit Vollgewinde. *Karlsruher Berichte zum Ingenieurholzbau*, Band 4, Lehrstuhl für Ingenieurholzbau und Baukonstruktionen (Ed.), Universität Karlsruhe (TH), Karlsruhe, 2006

[3] Hilson, B. O. : Verbindungen mit stiftförmigen Verbindungsmitteln – Theorie. In: Blaß, H. J.; Görlacher, R.; Steck, G. (Ed.): *Holzbauwerke STEP1 – Bemessung und Baustoffe*, Fachverlag Holz, Düsseldorf, 1995

[4] Johansen, K. W.: Theory of timber connections. International Association of bridge and structural Engineering, Bern, 1949, p. 249-262

[5] EN 383: 1993 – Timber structures; Test methods; Determination of embedding strength and foundation values for dowel type fasteners

INTERNATIONAL COUNCIL FOR RESEARCH AND INNOVATION
IN BUILDING AND CONSTRUCTION

WORKING COMMISSION W18 - TIMBER STRUCTURES

GENERALISED CANADIAN APPROACH FOR DESIGN OF CONNECTIONS WITH DOWEL FASTENERS

P Quenneville
Department of Civil Engineering, Royal Military College
Kingston, ON

Ian Smith
Andi Aziz
Monica Snow
Ing Hei Chui
Faculty of Forestry and Environmental Management
University of New Brunswick, Fredericton, NB

CANADA

MEETING THIRTY-NINE
FLORENCE
ITALY
AUGUST 2006

Presented by P Quenneville
H Larsen asked how would one sell to engineers the concept that capacity would be related the G1.21. P Quenneville stated that refinements would be made.
H Blass stated for yield moment of fasteners steel values are usually minimum values. How would one obtain mean values? I smith commented that this work represented the initial step of a long process.
R Foschi stated that there was too much put on capacity. Information would be needed in the demand area where stiffness would be needed. This is especially true in earthquake engineering area. P Quenneville stated that the lateral section of the code should take care of the seismic part.
A Jorissen asked why group tear out was considered. H Blass stated that this would be an issue for structural composite material and not for timber. I Smith commented on the concept of treating splittable versus non-splittable material differently.

Generalised Canadian approach for design of connections with dowel fasteners

Pierre Quenneville
Department of Civil Engineering, Royal Military College
Kingston, ON, Canada

and

Ian Smith, Andi Aziz, Monica Snow and Ing Hei Chui
Faculty of Forestry and Environmental Management
University of New Brunswick, Fredericton, NB, Canada

1 Background

There is already agreement in principle that there will be radical overhaul during the 2005-2010 code cycle of the philosophy underpinning, and detailed provisions of, dowel fastener connection design provisions in the Canadian code CAN/CSA Standard 086-01 "Engineering design in wood". Agreed principles include: that 'calculation based' methods for assigning Load and Resistance Factor Design (LRFD) capacities for connections must be based on recognised mechanics models, and that models must identify each potential mode of failure. Failure modes to be considered are ductile 'yield failure' and brittle 'fracturing failure' in wood or other components of a connection. The mode with the lowest estimated capacity will be the governing situation. Each mode may encompass a range of mechanisms. For example, ductile modes will encompass the mechanisms associated with 'Johansen type' dowel connection yield models, the so-called European Yield Model (EYM). Brittle modes will consider mechanisms like 'tear out' of a fastener groups and 'row shear failure' in lines of fasteners. It is also already decided that resistance factors will be estimated based on reliability concepts appropriate to connection design. The scope involves members manufactured from sawn lumber, glulam, Structural Composite Lumber (SCL), wood-based structural panels (plywood and OSB), and light gauge or plate steel. Fastener types to be included will be nails, rivets, screws (wood, self-tapping and lag), plain dowels and drift pins, bolts and tubes.

As it is the case in every other design standard, the current Canadian approach (CSA, 2005) for the design of multiple-bolted connections is solely based on the EYM, further modified in certain cases to attempt to account for potential brittle failure modes. As a result of the many recent studies on the brittle behaviour of connections in timber structures (Quenneville and Mohammad, 2000; Smith and Chui, 2006; Leijten and Jorissen, 2001; Ballerini, 1999), the fracture failure modes have been identified and are as shown in Figure 1. Below reference is made to fasteners loading members at various angles relative to the main member axis. However because for members made from SCL, structural panels and potentially other types of wood-based composites, grain direction has

no unique meaning, the intent is that readers should take grain direction to mean the strong in-plane direction.

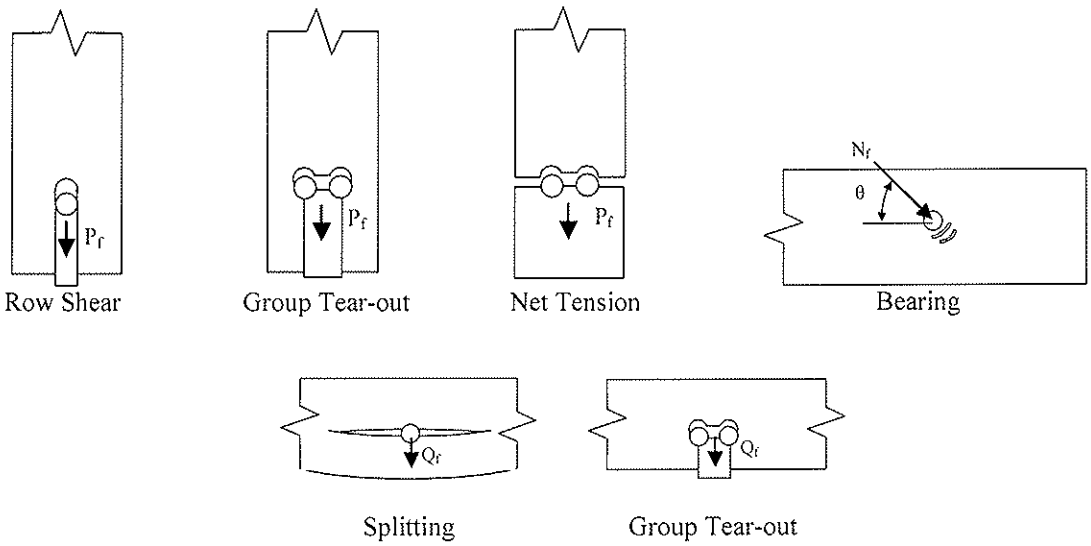

Figure 1. Potential failure modes, ductile and brittle for dowelled connections.

2 Proposed Design Approach

2.1 Resistance Verification

The design capacity of dowel fasteners will be the minimum value determined from a series of possible failure scenarios. Not all failure modes are possible in either parallel or perpendicular-to-grain and appropriate capacities will be compared to either the load applied or a function of its component parallel or perpendicular-to-grain. Basically, the designer will need to verify the following three cases:

$$N_f \leq N_r \quad [1]$$

$$N_f \cos(\theta) = P_f \leq \text{Minimum } (RS_r, GT_r, T_{nr}) \cdot (K_D K_{SF} K_T) \quad [2]$$

$$N_f \sin(\theta) = Q_f \leq \text{Minimum } (S_{pr}, GTp_r) \cdot (K_D K_{SF} K_T) \quad [3]$$

Where: N_f = factored design loads, N_r = yield factored resistance, RS_r = row shear resistance, GT_r = group tear-out resistance, Sp_r = splitting resistance, GTp_r = group tear-out resistance and K_D, K_{SF} and K_T are modification factors for load duration, service conditions and treatment respectively. This format is based on the assumption that the brittle failure modes are uncoupled. This needs to be verified.

2.2 Reliability Factors

The expression for calculating resistance factors (phi values) for joints is given in Ravinda and Galambos, 1978 and is expressed as:

For average characteristic resistance: $\phi = \exp(-C\beta V)$ [4]

For 5th % characteristic resistance: $$\phi = \exp(-C\beta V)\frac{R_{av}}{R_{0.05}} \quad [5]$$

where: C = a calibrated constant, set at 0.75, β = reliability index, V = coefficient of variation in resistance, R_{av} = average resistance, and $R_{0.05}$ = 5th % resistance. Previous reliability studies for wood (mainly for isolated lumber members) by Foschi et al (1989), and isolated structural steel members and joints by Ravinda and Galambos (1978) suggest that acceptable nominal values for the reliability index β lie in the range 2.4 to 3.4, as shown in Figure 2. Here is presumed that 5-percentile characteristic resistance will be the basis of connection design equations in the next revision of the Canadian timber design code, to match what is currently done for lumber, glulam and structural panels. This means that equation [5] will likely be adopted rather than equation [4]. However for the longer term doing the reverse might be most appropriate (Smith and Chui, 2006; Smith et al, 2006). The phi values in Figure 2 are calculated based on equation [5]. In structural steel design it is traditional to design joints stronger than the members, which predisposes structural steel systems to fail in the members, reflecting that members tend to fail by ductile mechanisms. Consequently β values for structural steel joints are in the region of 3.5, while β values for structural steel members are 3.0 or less. By contrast in structural wood design, because either members or connections can fail by ductile or brittle mechanisms, either type of component can be the element(s) controlling system capacity.

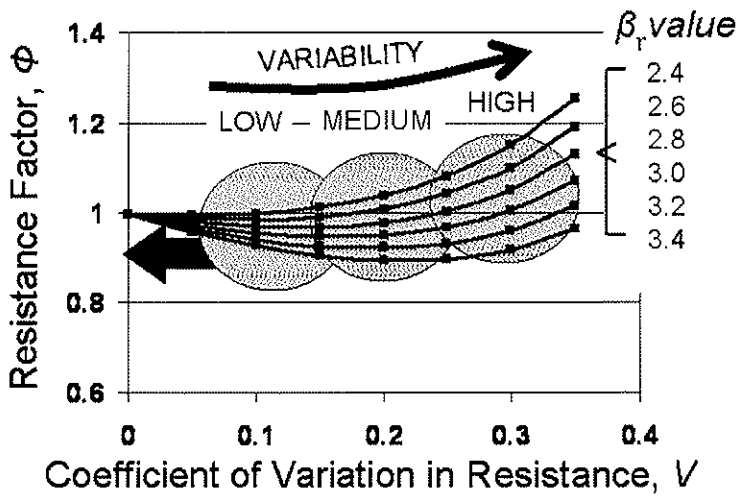

Figure 2. Relationship between the resistance factor ϕ and the coefficient of variability in resistance V (C = 0.75, β_r = 2.4 to 3.5).

Translated into practical format, this results in ϕ values that generally will be 0.9, which matches the values currently assigned in the Canadian timber code to most other types of component. It is anticipated that for situations like fasteners resisting withdrawal loads, lesser values will actually be adopted. Traditionally conservatism prevails in situations where there is most uncertainty about performance of fasteners in service.

2.3 Yield equation

For dowel type fasteners failing in a ductile mode, the design equations would be:

$$N_r = \phi\, n_{yu}\, n_s\, n_f \quad [6]$$

where

ϕ = 0.9 = resistance factor

n_{yu} = minimum lateral strength resistance for yielding (from the European Yield Model equations)

n_s = number of shear planes

n_f = total number of fasteners in the joint

where the yielding lateral strength per fastener, per shear plane is obtained from either equation 7 for one shear plane or 8, for two shear planes, whichever is applicable.

$$n_{yu} = \text{minimum} \begin{cases} f_{1\theta}\, d\, t_1 \\ f_{2\theta}\, d\, t_2 \\ \dfrac{f_{1\theta}\, d\, t_2}{1+\beta}\left[\sqrt{\beta + 2\beta^2\left(1+\dfrac{t_2}{t_1}+\left(\dfrac{t_2}{t_1}\right)^2\right)+\beta^3\left(\dfrac{t_2}{t_1}\right)^2}-\beta\left(1+\dfrac{t_2}{t_1}\right)\right] \\ \dfrac{f_{1\theta}\, d\, t_1}{2+\beta}\left[\sqrt{2\beta(1+\beta)+\dfrac{4\beta(2+\beta)M_y}{f_{1\theta}\, d\, t_1^2}}-\beta\right] \\ \dfrac{f_{1\theta}\, d\, t_2}{1+2\beta}\left[\sqrt{2\beta^2(1+\beta)+\dfrac{4\beta(1+2\beta)M_y}{f_{1\theta}\, d\, t_2^2}}-\beta\right] \\ \sqrt{\dfrac{2\beta}{1+\beta}}\sqrt{2M_y f_{1\theta} d} \end{cases} \quad [7]$$

or

$$n_{yu} = \text{minimum} \begin{cases} f_{1\theta}\, d\, t_1 \\ 0.5\, f_{2\theta}\, d\, t_2 \\ \dfrac{f_{1\theta}\, d\, t_1}{2+\beta}\left[\sqrt{2\beta(1+\beta)+\dfrac{4\beta(2+\beta)M_y}{f_{1\theta}\, d\, t_1^2}}-\beta\right] \\ \sqrt{\dfrac{2\beta}{1+\beta}}\sqrt{2M_y f_{1\theta} d} \end{cases} \quad [8]$$

where $f_{i\theta}$ = embedment strength calculated in accordance with equation [9], β = ratio of embedment strength of main (or inner) member, $f_{2\theta}$ to embedment strength of side

member(s), $f_{i\theta}$, and M_y = fastener yield moment, N-mm. For steel or concrete, the embedment values would be 3.75 F_u (F_u being the ultimate resistance) and 125 MPa, respectively.

For each wood member loaded at an angle θ, the embedment strength is obtained from:

$$f_{i\theta} = \frac{f_{i\,para}\, f_{i\,perp}}{f_{i\,para} \sin^2(\theta) + f_{i\,perp} \cos^2(\theta)} K_D K_{SF} K_T \qquad [9]$$

where:

$f_{i\theta}$ = embedment strength of member "i" for a fastener bearing at angle θ relative to the strong material axis (MPa).

$f_{i\,para}$ = tabulated average test embedment strength for fastener bearing parallel to the strong material axis (θ = 0°), from Table 2 (MPa).

$f_{i\,perp}$ = tabulated average test embedment strength for fastener bearing perpendicular to the strong material axis (θ = 90°), from Table 1 (MPa).

θ = angle of bearing relative to the strong material axis (parallel to grain of member).

Table 1. Normalized embedment strengths for fasteners in wood-based materials.

Fastener type	Wood-based material	Normalized embedment strength (MPa)
nails (all types), screws (all types), hollow tubes	sawn lumber, glulam, SCL (other than LSL)	$f_{i\,par} / \rho_{OD} = 72(1\text{-}0.01d)$ $f_{i\,perp} / \rho_{OD} = 70d^{-0.5}$
nails (all types), screws (all types), bolts, plain dowels, hollow tubes	LSL, plywood	$f_{i\,par} / \rho_{OD} = 104(1\text{-}0.01d)$ $f_{i\,perp} / \rho_{OD} = 60$
nails (all types), screws (all types), bolts	OSB, tempered hardboard	$f_{i\,par} / \rho_{Dry} = 104(1\text{-}0.01d)$ $f_{i\,perp} / \rho_{Dry} = 40$
timber rivets, bolts, plain dowels	sawn lumber, glulam, SCL	$f_{i\,par} / \rho_{OD} = 53\ (1\text{-}0.01d)$ $f_{i\,perp} / \rho_{OD} = 55\ (1\text{-}0.01d)$

Notes:
Values are for standard term duration load.
ρ_{OD} = mean relative density of the wood-based material, also known as specific gravity, for the oven dry condition. It is calculated as the density of the material for the oven dry condition normalized relative to the density of water, based on mass and volume after oven drying.
ρ_{Dry} = mean relative density of the wood-based material for the dry service condition. It is calculated as the density of the material for dry service conditions normalized relative to the density of water, based on mass and volume of the material in service. Values applicable to proprietary structural wood based materials should be obtained from product suppliers.

A composite adjustment for duration of load, fabrication and service condition adjustments like the one in Eurocode 5 is the target for future code discussions.

2.4 Row shear equation

The total factored row shear strength of fasteners in a given member is given by:

$$RS_r = \phi \sum_{i=1}^{n_r} 2\, RS_i\ (K_D K_{SF} K_T) \qquad [10]$$

where

ϕ = 0.9 = resistance factor (it is possible that this value will be lowered to 0.8 based on committee judgement)

RS_i = shear resistance along one shear plane of row "i", in N

$= \frac{(f_{v\,avg} \cdot 0.60)}{3 \cdot 1.25} K_{ls}\, t\, n_{fi}\, a_{cr} = \frac{(16.6 \cdot G^{0.85} \cdot 0.60)}{3.75} K_{ls}\, t\, n_{fi}\, a_{cr} = 2.66\, G^{0.85} K_{ls}\, t\, n_{fi}\, a_{cr}$

$f_{v\,avg}$ = member average shear strength, MPa, equal to $16.6\, G^{0.85}$.

0.60 = factor to convert average to 5th percentile resistances, assuming a normal distribution and a COV of 25%.

K_{ls} = factor for member loaded surfaces
= 0.65 for side member
= 1 for internal member

t = member thickness, mm

n_{fi} = number of fasteners in row "i"

a_{cr} = minimum of a_{3t} and a_l, mm

a_l = fastener spacing, in the row, mm

a_{3t} = fastener end distance when member is in tension, mm

1.25 = factor to convert test to short load duration

G = mean relative density of the wood-based material

Note that row shear is not possible if the member is in compression. The designer must ensure that each member of a joint can resist its share of the force transferred.

2.5 Group tear-out equation

The total factored group tear-out strength of fasteners in a given member is given by:

$$GT_r = \phi\, GT\, (K_D K_{SF} K_T) \qquad [11]$$

where

ϕ = 0.9 = resistance factor (it is possible that this value will be lowered to 0.8 based on committee judgement)

$GT = (RS_1 + RS_{nr}) + \frac{(f_{t\,avg} \cdot 0.60 \cdot A_{GT\text{-}net})}{3 \cdot 1.25} = (RS_1 + RS_{nr}) + \frac{(170.7\, G^{1.01} \cdot 0.60 \cdot A_{GT\text{-}net})}{3.75}$

$= (RS_1 + RS_{nr}) + (27.3\, G^{1.01} \cdot A_{GT\text{-}net})$

RS_1 = shear resistance along row 1 bounding the fastener group, equal to $2.66\, G^{0.85} K_{ls}\, t\, n_{fi}\, a_{cr}$

RS_{nr} = shear resistance along row "n_r" bounding the fastener group, equal to $2.66\, G^{0.85} K_{ls}\, t\, n_{fi}\, a_{cr}$

0.60 = factor to convert average to 5th percentile resistances, assuming a normal distribution and a COV of 25%.

$f_{t\,avg}$ = member average tension strength, MPa, equal to $170.7\, G^{1.01}$

$A_{GT\text{-}net}$ = critical area between the two outer rows, mm^2

1.25 = factor to convert test to short load duration

Note that group tear-out (parallel) is not possible if the member is in compression. The designer must ensure that each member of a connection can resist its share of the force transferred.

Note that equation [11] is for full fastener penetration. Group tear-out for partial penetration is under investigation.

2.6 Net tension equation

The factored lateral net tension strength of a member at a group of dowel fasteners is given by:

$$T_{nr} = \phi\, T_n\, (K_D K_{SF} K_T)$$

where

ϕ = 0.9 = resistance factor
T_n = $f_t A_n$
A_n = net area, mm^2
f_t = member specified tension strength parallel-to-grain, MPa

2.7 Splitting equation

The factored lateral splitting strength of a dowel connector loaded perpendicular-to-grain in a given member is given by:

$$S_{pr} = \phi\, S_p\, (K_D K_{SF} K_T)$$

where

ϕ = 0.9 = resistance factor (it is possible that this value will be lowered to 0.8 based on committee judgement)

$$S_p = \frac{0.3\,(n_r\, d\, t_2)^{0.8}\; 0.6\, K_{LOC}}{1.25\, A_b\, B_b\, C_b\, (N\, d)^{0.2}} = \frac{0.144\,(n_r\, d\, t_2)^{0.8}\, K_{LOC}}{A_b\, B_b\, C_b\, (N\, d)^{0.2}}$$

K_{LOC} = factor to take into account position of connection
= 1 for interior connection, i.e. $a_3 \geq$ depth – a_{4t}
= 0.5 for exterior connection, i.e. $a_3 \leq$ depth – a_{4t}

0.60 = factor to convert average to 5th percentile resistances, assuming a normal distribution and a COV of 25%.

1.25 = factor to convert test to short load duration

A_b = 0.85 - 0.3(N-1) - 0.45(n_r - 1)

B_b = 1.22 - 0.0041a_2 for 1 row of bolts
= 0.976 + 0.0053a_2 – 0.0023a_1 for 2 rows of bolts

$$C_b = 5 \exp\left(-1.867\left(\frac{\text{depth} - a_{4t}}{\text{depth}}\right)\right)$$

For the group tear-out perpendicular-to-grain, which is possible for Structural Composite Lumber materials, the equation is still under development.

The authors wish to remind the readers that the format presented is a generalization and by no means, constitute a final document version. Other documentation, such as recommendations for fastener spacings, hole sizes, etc… needs to be included.

3 Discussion

The effectiveness of the various equations in predicting the mode of failure and resistance of connections tested in various laboratory studies is best shown graphically. Figures 3 to 5 show graphs with the experimental average values and associated predictions of the resistance of bolted connections. The experimental data is for test duration and has not

been modified. The predictions are for averages and thus, the factor to convert average to 5^{th} % values has been omitted.

It can be seen that the agreement is adequate for code purposes. The fact that the design equations for the various modes of failure (ductile and brittle) can adequately predict the experimental resistances for experimental values available in the literature (Quenneville et Mohammad, 2000; Mohammad and Quenneville, 2001; Massé et al., 1988; Jorissen, 1998) provides a strong argument for robustness. This robustness is also shown in Quenneville and Bickerdike (2006).

For the graphs in Figures 3 to 5, the symbols are as follow:

◇ RMC steel-wood-steel
△ RMC wood-steel-wood
□ RMC Wood-steel
○ Massé, Salinas & Turnbull (1988) and Jorissen (1998)

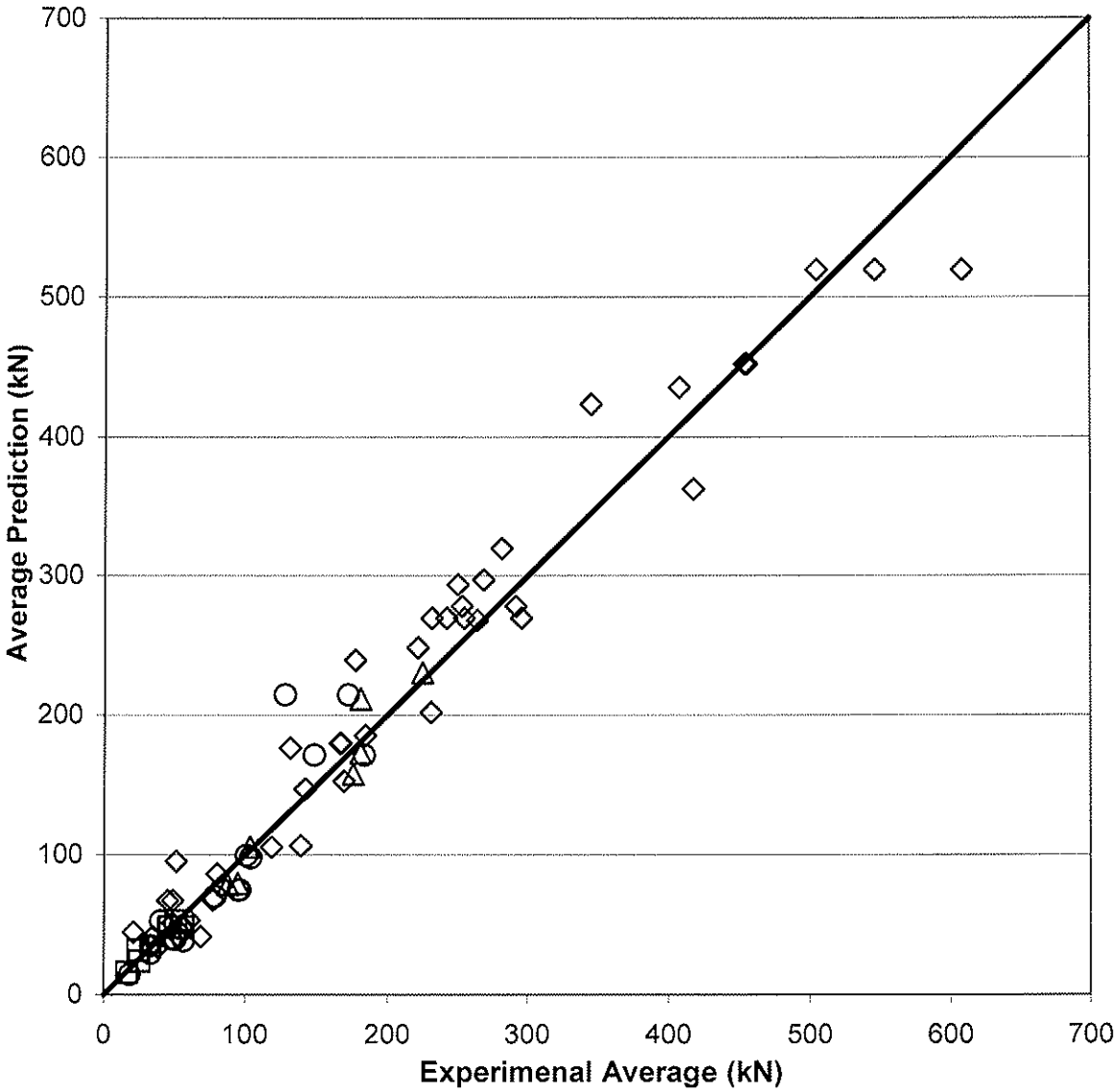

Figure 3. Comparison of experimental and design prediction averages for Row Shear.

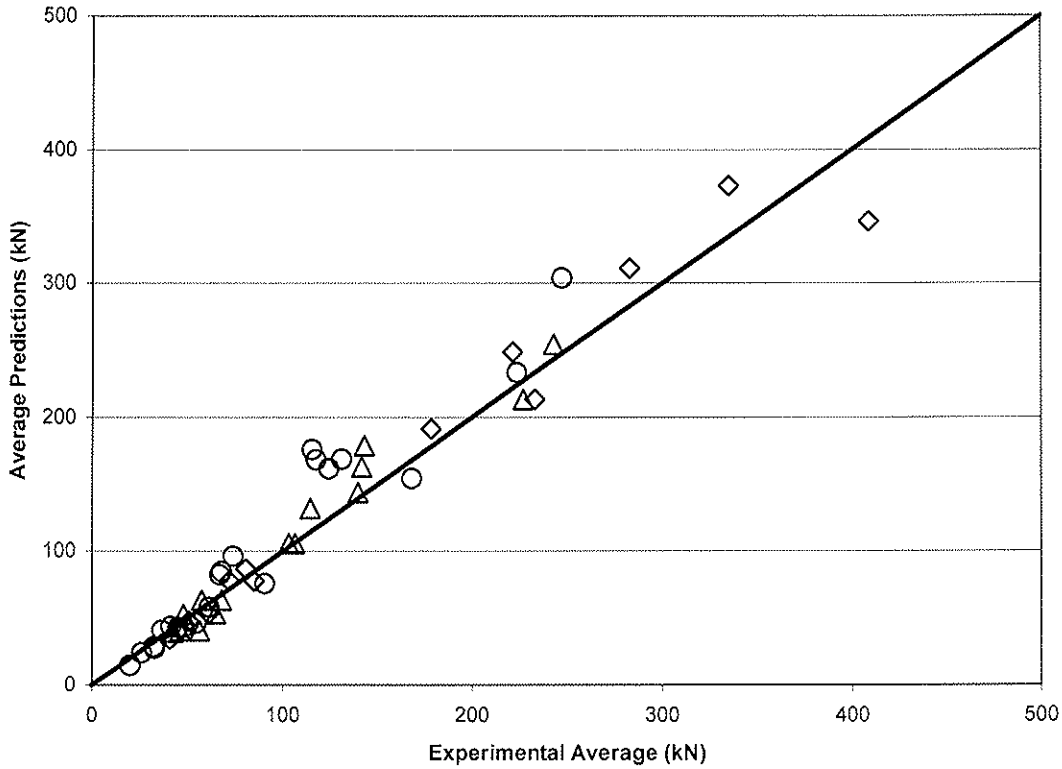

Figure 4. Comparison of experimental and design prediction averages for Yielding.

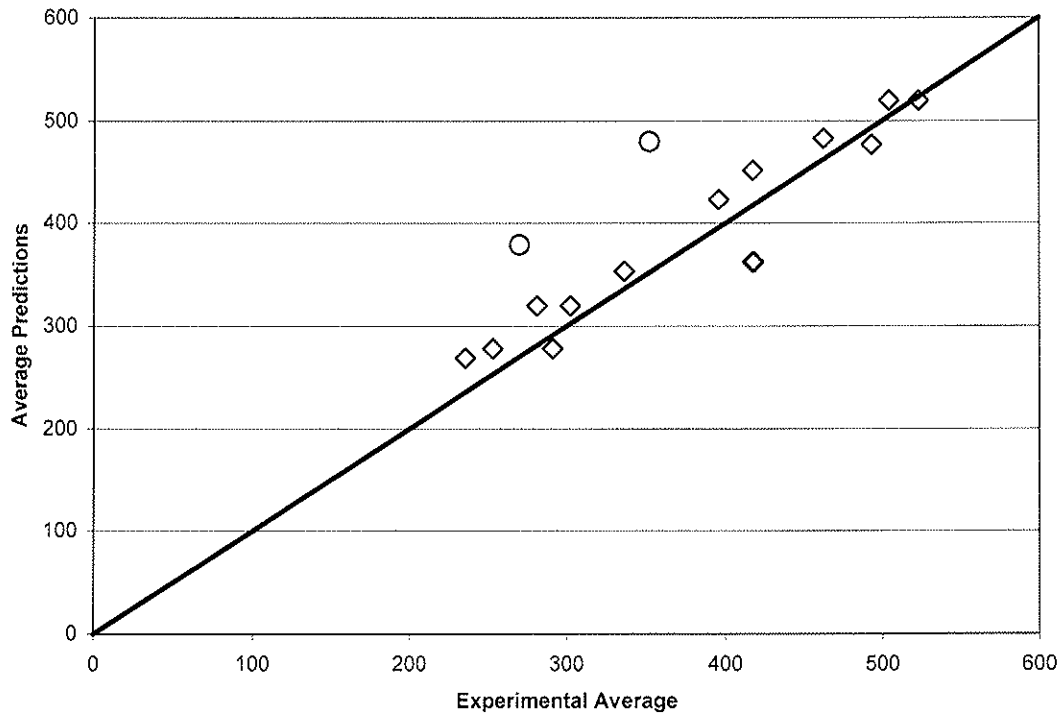

Figure 5. Comparison of experimental and design prediction averages for Group Tear-out.

Conclusions

A generalized design procedure that addresses all potential ductile and brittle modes of failure of dowelled connections is presented. It offers the required framework to design most possible connection configurations with an adequate degree of precision. It is hoped that it will provide both the flexibility and rigour to address all possible design challenges associated with the various connection configurations.

References

Ballerini, M. 1999. "A new set of experimental tests on beams loaded perpendicular-to-grain by dowel-type-joints", CIB-W18 meeting Proceedings, paper 32-7-2, Graz, Austria.

Canadian Standard Association, 2005. "CAN/CSA-O86-01 Engineering Design in Wood", Mississauga, Canada.

Foschi, R.O., Folz, B.R. and Yao, F.Z., 1989, "Reliability-Based Design of Wood Structures", Structural Research Series, Report 34, Dept of Civil Engineering, University of British Columbia, Vancouver, Canada, 282 p.

Johansen, K.W. 1949. "Theory of Timber Connectors". Publications of the International Association of Bridge and Structural Engineering. No. 9: 249-262. Bern, General Secretariat.

Jorissen, A. 1998. "Double Shear Timber Connections With Dowel Type Fasteners", PhD thesis, Delft University Press, The Netherlands, 264 p.

Leijten, A.J.M., and Jorissen, A. 2001. "Splitting strength of beams loaded by connections perpendicular-to-grain, model comparison", CIB-W18 meeting Proceedings, paper 34-7-1, Venice, Italy.

Mohammad, M. and Quenneville, J.H.P. 2001. "Behaviour of wood-steel-wood bolted glulam connections." CJCE, **28**, pp. 254-263.

Quenneville, J.H.P., and Mohammad, M. 2000. "On the failure modes and strength of steel-wood-steel bolted timber connections loaded parallel-to-grain." CJCE, **27**, pp. 761-773.

Quenneville, P., and Bickerdike, M. 2006. "Effective in-row capacity of Multiple - fastener connections, CIB-W18 meeting Proceedings, Florence, Italy, in press.

Ravinda M.K. and Galambos T.V. 1978. "Load and resistance factor design for steel", ASCE Journal. of the Structural. Division., 104(ST9): 1337-1353.

Smith, I., and Chui, Y. H., 2006. "Principles of connection design.", ISO TC165 WG7 meeting discussion document. Portland, Oregon, 17p.

Smith, I., Asiz, A., Snow, M. and Chui, Y.H. 2006. "Possible Canadian / ISO approach to deriving design values from test data", CIB-W18 Meeting in Florence (*in press*).

INTERNATIONAL COUNCIL FOR RESEARCH AND INNOVATION
IN BUILDING AND CONSTRUCTION

WORKING COMMISSION W18 - TIMBER STRUCTURES

OVERVIEW OF A NEW APPROACH TO HANDLING SYSTEM EFFECTS IN TIMBER STRUCTURES

I Smith
Ying Hei Chui
University of New Brunswick, Fredericton, NB

Pierre Quenneville
Royal Military College, Kingston, ON

CANADA

MEETING THIRTY-NINE
FLORENCE
ITALY
AUGUST 2006

Presented by I Smith
H Larsen commented that it would be useful to define the terms used in the paper such as objective based design and capacity design.
A Buchanan commented that the work would require changes in people's thinking to consider things not within the code structure. He wondered whether it would turn people off timber design and put people towards the use of non timber material. I Smith responded that there would be a need to provide people with tools to make timber design more affordable.
F Lam commented about the philosophical nature of the paper without hard justification of some of the factors. I Smith responded that the paper provided a framework and if acceptable could guide future work.
H Riberholt questioned whether there were discussions of similar concept within competing material and why the member and connection resistance had such a wide separation. I Smith stated that he wanted to test the water within this group on the concept and see what would be the response. If this was not worthwhile, one would be prepared to change track. The separation of member and connection resistance distribution would not be for all situations but could be true for some cases.
J Köhler also questioned why there was such a large difference between member and connection capacity. I Smith mentioned that typically member capacity would be underutilized anyways and for some context the large separation would be valid.
R Foschi provided the following comments: in 1994 Northridge earthquake led to a large study on steel connection. US FEMA created tables for objective based design. There was a lot of talk in the way of definitions with the basic idea to design to some performance level. One would need to tell the engineer that the performance level is tied to some confidence level. Damage forecasting would be important where in Northridge US$10 billion of damage with few collapses were experienced. One would need to focus on what happened in between and not only on ultimate capacity. This would be the difficult part of the work where accurate model and data would be needed to define the entire load deformation history. This calls for a lot of good experimental work. This would be true for concrete and steel also. Then one could focus on reliability of performance. R. Foschi also provided analogy with offshore structures. In summary, he stated that we are always designing buildings. Structural System behaviour needed a lot of work. He did not agree with the statement that engineers would reject work if it was too complicated. He gave example of the Canadian experience of adopting size effect adjustment factors in the 1970's. Consulting engineers in Vancouver are doing time series analysis now but not a few years ago because of availability of fast computers and software.
P Quenneville commented that he had met with some experienced engineers on the issues of who would use system effect approach. There were two reactions 1) rejection outright and 2) if this approach gave them an advantage they would use it.

Overview of a New Approach to Handling System Effects in Timber Structures

Ian Smith and Ying Hei Chui
University of New Brunswick, Fredericton, NB, Canada

Pierre Quenneville
Royal Military College, Kingston, ON, Canada

Abstract

In Canada ideas are being formulated about how system design can be implemented within the national timber design code. Momentum for this comes from need to address the changing nature of the construction industry and allied professional engineering practice. The end product needs to be something that can be seamlessly transitioned into design practice. System design is not envisaged as an approach that will yield unfamiliar solutions for familiar problems. Rather it is seen as supporting creation of timber solution in new situations. This paper attempts to identify the major framework issues, starting with the question of what the term system should mean. There is no attempt to follow faddish trends that fly under the same label. It is thought that landscape level changes will shape system design in Canada, and presumably elsewhere, and will concern evolution of architectural solutions, rapid broadening in the available range of structural products (wood, non-wood and composite varieties), changing construction methods and practices, and evolution in regulatory regimes. Detailed technical issues such as what constitute acceptable 'search tree' and 'structural reliability' algorithms will need to be addressed at some point, but that should be after framework issues have been resolved.

1. Introduction

Currently the timber design code in Canada gives cursory guidance on system level issues and detailed guidance on 'free body sizing' of components. The focus of this discussion is a transition from that to a document that gives integrated guidance on design of structural systems constructed mainly from wood products. The transition should mostly be about philosophical shifting of emphasis, with the intent that a restructured code will support systemic thinking. This will not, of course, diminish the need for technical updating of detailed component sizing rules, but it will modify the range of factors that enter them.

Although emphasis here is on the broad issues, it is recognized that fine details and the mathematical intricacies must be addressed at some stage. However, doing that now would as the old British saying goes "to put the cart before the horse".

Formulation of design codes is (like design itself) an essentially subjective process founded as much on professional judgment as exact data and precise formulae. Legendary statistician George Box is credited with saying "All models are wrong, some models are useful". By analogy, all codes are based on inexact concepts, but despite this, they usually are useful aids to engineering practice. One can add that codes remain useful as long as they support contemporary needs. There can never be any best way of formulating a design code, just as no single design solution is correct. Criteria for measuring perfection are subjective and discourse, and suggestions here are simply one of many parallel tracks that could lead to creation of effective code provisions.

Under existing timber design codes the procedures result in what have been proven, by practical experience, to be acceptable design solutions for recurring types of design problem. Therefore, if the nature of timber construction were never to evolve further practices formulated in those documents would continue to result in adequate solutions. With adequate solutions being those acceptable to society in terms of balancing structural safety, material conservation and cost. However, as is abundantly clear in Canada and other parts of the westernized world, the nature of construction of all types is changing rapidly. The driving forces are well beyond the control of the timber community and include aging and more urbanization populations, resource scarcity, climate change and international trade practices [1, 2]. Evolving tastes, needs of society and business, and technological development drive architectural design. Future practices will not replicate past utilization of construction materials. Architecture of buildings is changing, e.g. more wall openings, more irregularity in plans and roofs. There is rapid broadening in available types of structural products and connection hardware (not just wood products). Construction methods and practices are changing, as are regulatory regimes that control design and construction practices. What in Canada is called Objective Based Design [3] is helping change the landscape. Although not yet impacting design in Canada, it is clear from international trends that future design practices will need to address more than traditional loading scenarios. For example, avoidance of disproportional collapse under accidental or deliberate blast loads has becoming an important issue [4]. Avoidance of disproportionate collapse whatever the causal agent of damage is an excellent example of an issue that can only be handled properly via systemic design approaches.

Systems design methods are believed necessary mainly because they embody the approach most likely to result in robust ways of doing new things under new regulatory regimes. In practical terms, systems level design becomes necessary when:

- non-traditional loads must be resisted (e.g. bomb blasts),
- non-traditional structural forms are employed (e.g. very large wall openings, complex roofs),
- non-traditional combinations of materials are employed (e.g. wood-plastic composites), or
- non-traditional intra or inter component, or system support, connections are employed (e.g. proprietary hardware).

As already indicated, when only common traditional timber products are employed within traditional structural forms existing approaches are adequate. This is because the free body sizing rules for components implicitly acknowledge, i.e. were calibrated to incorporate, the system context. For example, it is implicit that small dimension sawn lumber joists will be used in load-sharing arrangements. For traditional combinations of materials and traditional connections it is known by experience that component deformation characteristics will be compatible. Also, that problems due to factors like excessive mechanosorptive creep and local instabilities are unlikely. However, to again illustrate in terms of floors, when wood I-joist and open-web joist products with tall cross-sections were first employed, codified design practices based on experience with systems having sawn lumber joists broke down. This was because the rules no longer implicitly reflected the appropriate system issues. Usually the problem was that the new products altered the two-way structural action within floor systems, or that warping and instability of joists became issues. The strategy to achieve satisfactory design solutions using new joist products was to substitute proprietary design methods in lieu of code rules.

Rapid evolution is occurring in many countries with respect to the range of available: construction products and materials, construction methods and structural design tools. Concurrently, the range of options for how new products and technologies can enter the marketplace is being opened up. Often this is for trade reasons, and because of a broad public and political perception that a more open regime will provide society with better purchasing choices. Regulatory frameworks are moving towards greater choice concerning how acceptability of engineering designs can be demonstrated.

In Canada under Objective Base Design using rules in material codes, such as the CAN/CSA timber design code [5], has become just one of several optional parallel approaches to proving acceptability of any design. So far the 'other approaches' are only selectively employed to justifying acceptability of proprietary components or systems. If in even the medium term (circa > 5 years from now) the timber design code in Canada, and presumably those elsewhere, is to remain relevant to needs of structural designers that document will have to be subjected to more than cosmetic or incremental surgery.

This discussion is predicated on the assumption that timber design codes need to be reshaped so that they focus more directly on how wood products are utilized.

Option 1: Make systems level design mandatory.

Option 2: Maintain existing style provisions for traditional wood products (sawn lumber, glulam and panel products) in traditional applications employing traditional connections; in parallel with new systems level provisions that can be applied to all wood products.

2. What is a Structural System?

It is proposed that the term structural system means any arrangement of components capable of developing collapse mechanisms (internal to its domain) that involve deformation or failure of more than one component. In essence, any stable arrangement with inter-component connections would be a system.

A secondary consideration is what constitutes a component. To be consistent with the proposed definition of a system, a component must be any manufactured or prefabricated part that can develop failure mechanisms that are completely internal to its domain. Types of parts easily classed as components include sawn timber framing and glued-laminated timber members in 'post and beam' construction; wall, floor and roof panels; and connections. Other parts may not be easily classified because their end use will determine whether they behave as systems or components (e.g. trusses, spaced columns).

Depending on the complexity and size of a building structure, a design engineer might need to define and analyse a nested series of systems, with higher level systems incorporating the lower level systems (subsystems). The mechanisms considered would differ between the nested systems.

At the purely practical level a system would be any arrangement for which an engineer decides that a separate structural analysis is required. Engineers will resolve dilemmas through professional judgement, as at present.

Reference above to free body sizing of components means the consideration of only the effects that internal forces have on any component that has been abstracted from its parent system. Under the free body approach (which is the basis of existing timber design codes [e.g. 5]) sizing of components is independent of the nature of the parent system once the internal forces have been estimated. Thus the essential difference between what the authors call systemic design and current practice is that under system level design both the nature of system mechanisms and the consequences of any particular component failing would enter component sizing rules. Thus necessary sizes of components would not just reflect the magnitude of factored free body forces.

Recommendation 1: Classify systems according to the structural form, and components according to the type of materials.

Recommendation 2: Provide explicit guidance on the necessity to consider both system and component level failure mechanisms.

Recommendation 3: Make sizing rules a function of system and component classifications and the expected consequences of component failures.

3. Seamless and Shock Free Transition

Complaints from practicing engineers have arisen following previous revisions of timber design and other codes. Concerns focussed on:

- Whether revisions result in meaningful differences in design solutions.
- The extent of retraining necessary to learn about content and how to apply new codes.

These two aspects can be traded off because practitioners realise that retraining is worthwhile provided there are substantive gains in terms of material economies and flexibility in specifying design solutions.

The last major restructuring of the Canadian timber design codes took place in 1984 when the Allowable Stress Design (ASD) code was supplemented by a Load and Resistance Factor Design (LRFD) code. The ASD code was not revised between 1984 and when it was theoretically withdrawn in 1994. In practice the ASD code remained in wide use until at least about 2001. During the same period the parallel LRFD code was revised three times. Initially only a relatively short transition period was intended before the ASD code was eliminated. Use of ASD persisted in Canada because many engineers preferred the older option, and in response building authorities in provinces, territories and cities permitted the practice. Anecdotally it is understood that many older engineers still use the ASD code! Clearly there exists the perception that inadequate benefits accrued from code changes. The experience is understood to have been replicated elsewhere (e.g. UK, USA).

Recommendation 4: Major modifications should only be made to design codes if that results in substantive alterations to design solutions, and/or they expand the range of what can be done with wood products.

Recommendation 5: To be consistent with the philosophy behind Objective Based or Performance Based Code and minimize the 'shock factor', new provisions should be transparent with respect to intent, intuitively consistent with engineering principles (avoid empiricism), and minimize format and content changes to design equations.

4. Scope of System Design Provisions

Figure 1 summarizes, in the Canadian context, the proposed scope of system level design provisions within the timber design code, and how those should compliment those in the national building code.

NATIONAL BUILDING CODE (NBC)	TIMBER DESIGN CODE
- Scope of checks (safety, serviceability)	- Definition and classification of systems
- Global stability checks	- Classification of materials
- Load cases to be considered	- Classification of systems
- Format of design equations	- Sizing rules for components

Figure 1 – Proposed scope of system design provisions

Figure 2 shows the proposed sequence of design decisions around which code rules should be

shaped. The intent is that the timber design code would explicitly define how choice of any particular combinations of structural form, wood product construction material(s) and connection methods affects the expected system failure mechanisms. The nature of the system and its expected failure mechanism would govern the assignment of system related factors entering component design equations. This should encourage designers to make direct links between design decisions and efficiency with which materials can be utilized. For example, if designers select statically determinate structural forms and splitting prone members, and therefore failure of any one component would result in system collapse, component sizing rules should be relatively conservative (i.e. aimed at attaining a relatively high reliability level). By contrast, if statically indeterminate structural forms are selected and failure of one or more components would not result in system collapse, or if ductile failure mode was ensured through the capacity design approach, then sizing rules could be relatively liberal. For all systems the level of ductility achievable in connections should also enter the sizing rules for other components [6].

Recommendation 6: Embed 'rewards' into design code rules so that there is incentive to refine design practices, i.e. make it possible to achieve higher component resistances and to do new things by adopting systemic design practices.

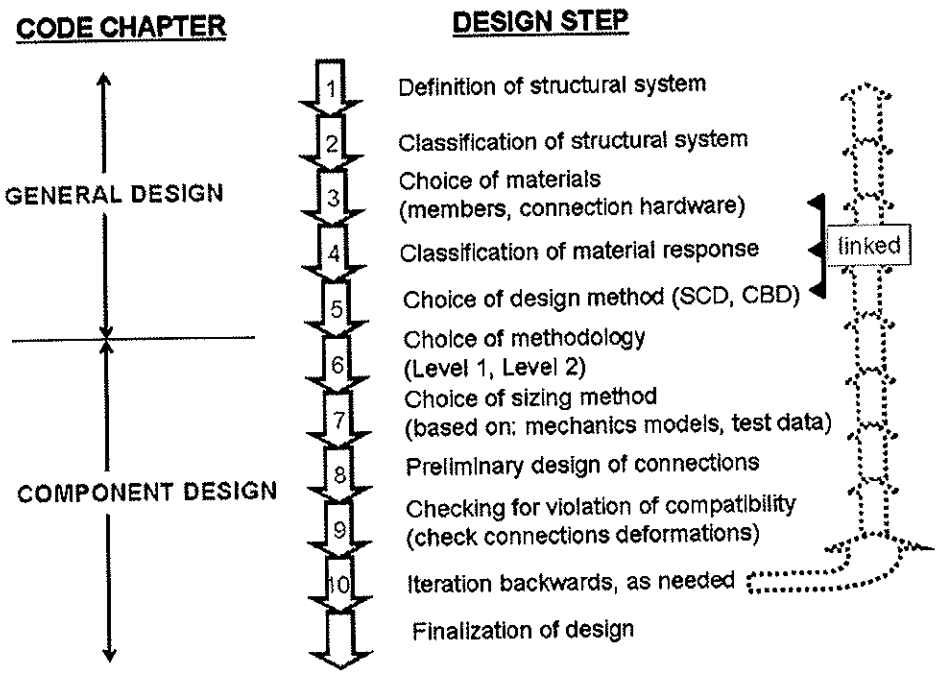

Figure 2 – Proposed sequence of design decisions

Within step 5 in Figure 2 choice of design method refers to the possibility of what here is called Strong Component Design (SCD) or Capacity Based Design (CBD), with the former being equivalent to current practice [5]. CBD concepts were originally developed for design of reinforced concrete structural systems [7] but could be applied to timber structures [8]. The choice of Level 1 versus Level 2 methodologies in step 6 relates essentially to the notion of permitting designers to select between alternatives of simple or complex sizing methods for components.

5. Format of Design Equations

For consistency with *Recommendations 4 to 6* it is proposed that under the systemic approach the design equations for sizing component be simple modifications of existing LRFD equations. Below only the strength LRFD equations applicable under SCD are given. For other situations like CBD or serviceability calculations the approach would be consistent with what is shown here. Whether

serviceability should be addressed as part of component design is a contentious issue. The authors favour the approach that codes simply give guidance on assigning load-deformation characteristics to components for various service situations. Design engineers could then exercise professional judgement about serviceability issues. Preferably serviceability would be assessed at the system rather that component level.

The SCD design strength checking equation should take the generic form:

$$\phi R \geq \text{effects of factored loads} \quad \ldots\ldots\ldots\ldots (1)$$

where: ϕ= resistance factor, R= resistance adjusted for all design specific considerations. The adjusted resistance is calculated according to the generic form:

$$R = R_s k_S k_T k_N k_H \quad \ldots\ldots\ldots\ldots (2)$$

where: R_s= standardized specified resistance, k_S= service factor, k_T= treatment factor, k_N= number of components in series factor, k_H= system failure factor (Sections 7 and 8). The factor k_S accounts for the coupled cumulative effects of loading and service conditions. Specifics of equations (1) and (2) will vary depending on sensitivities of resistances to design variables, and exactly what parameters need appear will vary from situation to situation. It is of course necessary to have prior applicable evidence, or to collect such evidence by testing. A companion paper by Smith et al [9] discusses some related issues.

Recommendation 7: Introduce into design equations for component sizing modification factors accounting for the number of components and the system characteristics.

As suggested under *Option 2* one possibility is to create dual level design methods. If this was done Level 1 provisions could be similar in nature to those in the present Canadian code [5] and permit only SCD. There could still be explicit recognition of the difference in failure characteristics and inherent levels of variability exhibited by various wood products and connection methods (Section 6 and 7). Also there could be recognition in assignment of Level 1 ϕ values of the natures of the governing failure mechanisms for components. However there would be no account taken of the nature of the parent structural system. Sizing of components would therefore be uncoupled from system design. Familiar solutions would result for familiar problems.

The Level 2 approach would fully implement all possible enhancements of design discussed in this paper and companion papers [6, 9].

Recommendation 7: The structured decision sequence illustrated in Figure 2 be embedded directly in design codes irrespective of whether Level 1 or Level 2 methodologies are followed.

Option 3: Permit dual level practices that give designers the option of ignoring or explicitly embracing new systemic concepts. The applicable generic SCD factored resistances for strength limit states would be:

Level 1: $\phi R = \phi R_S k_S k_T \leq$ effects of factored loads ..... (3)

Level 2: $\phi R = \phi R_S k_S k_T k_N k_H \leq$ effects of factored loads ..... (4)

6. Classification of Systems, Materials and Connections

Tables 1 to 4 illustrate preliminary thinking about classification decisions embedded in the decision sequence of Figure 2. Only two classes of wood products are suggested, Table 3, because ability of systems to achieve the more refined four-level classifications scheme of Table 1 is mostly a function of the connection characteristics. The notion that member materials can be divided into splitting and no-splitting categories reflects direct experience in tests conducted by the authors for a

broad range of wood products (e.g. sawn lumber, glulam, Engineered Wood Products, Structural Panels).

Table 1 – Tentative classification of failure mechanisms based on *Ductility Ratio (D)*, and the associated *Reliability Index* (β value)

Classification of failure mechanism of a component	***Brittle***	***Low-ductility***	***Moderate-ductility***	***High-ductility***
	$D \leq 2$	$2 < D \leq 4$	$4 < D \leq 6$	$D > 6$
Type of parent system (Table 2)	**β value**			
No alternative load paths possible	4.5	4.0	3.5	3.0
Alternative load paths possible	4.0	3.5	3.0	2.5

Table 2 – Proposed classification of structural systems

Classification	***Description***
Light frame *without* capability to develop alternative load paths	Systems where less than four linked and parallel framing members or subsystems act together.
Light frame *with* capability to develop alternative load paths	Systems where four or more linked and parallel framing members or subsystems act together.
Heavy frame *without* capability to develop alternative load paths	Statically determinate, or other, systems where failure of one component would cause disproportional system damage.
Heavy frame *with* capability to develop alternative load paths	Statically indeterminate systems where failure of one component would not cause disproportional system damage.
Shell and plate structures	Those structures depending on two-way curvature and folded plate action for stability.
Other	Any system not within another classification.

Table 3 – Proposed classification and expected behaviours of structural wood products

Classification	***Expected behaviour***	***Examples***
Splitting	Brittle response	sawn timber, un-reinforced glulam, LVL, PSL
Non-splitting	Ductile response	reinforced-glulam, plywood, OSB, LSL

Table 4 – Example: Proposed classification of failure mechanisms of connections (*when capacities and failure mode are estimated using mechanics based models)*

Connection Classification (Table 1)	***Member Classification*** (Table 3) (for least ductile joined material)		***Governing mechanism*** (Examples only)
	Splitting	Non-splitting	
Brittle	X		row tear out, block shear, net section, member interference
Low-ductility	X		bearing failure beneath fasteners with only rigid body movements of fasteners
	X	X	all connection level mechanisms
Moderate-ductility	X		plastic hinges formed in fasteners
High-ductility		X	all joint mechanisms

The intent is that classifications in Table 1 will be used within reliability calculation processes that scale resistance factors (ϕ values) for components, and classifications in Table 2 would be used during assignment of system failure factors (k_H values) for components. Classifications in Tables 3 and 4 would be subsidiary information entering detailed sizing rules for components. The logic that

underpins Table 4 is that in recent studies the authors have found that a correlation often exists between the type of failure mechanism for components and their ductility ratios. Thus when capacities for various mechanisms are estimated using mechanics based models, the nature of the mechanism can be employed as a surrogate in lieu of direct evidence concerning the magnitude of the ductility ratio (D). Obviously, when mechanisms and capacities are determined directly from test data [9], classification of the response on the basis of Table 1 would be straightforward.

So far the authors have not formulated firm ideas about how system ductility can be estimated without recourse to complex analyses. One possibility is to create an indexing method that assigns system ductility as a function of component ductility, and employing classifications in Tables 3 and 4. Possibly contributions of individual components could be weighted as is commonly done in post-disaster 'use assessments' of buildings. Numerical case studies are expected to be an appropriate means for focussing insight and clarifying suitable approaches.

Recommendation 8: Reliability index values, and consequently resistance factors, for component design should be a function of the classification of the expected failure mechanism and whether a system is capable of developing alternative load paths following component failure.

7. System Failure Mode

Design of systems involves aggregation of effects of mechanisms for components and identification of possible global failure mechanisms associated with the overall system assembly. Failure mechanisms individually or in combination define the failure mode of a system. It is proposed that the term failure mode be reserved for describing the gross nature of the failure in any complete system.

Currently in Canada the timber design code [5] together with the national building code [3] specifies global design requirements and the loads to be considered. Provisions recognize that structural engineers must pay attention to whole system behaviour. System level design checks required by the building code relate to maintenance of equilibrium under pseudo-static design rules, avoidance of instability, and avoidance of excessive deformations. Member design rules distinguish between heavy-framed and light-framed construction systems. Light-frame systems are assumed capable of load sharing behaviour if certain prescriptively defined caveats are met (e.g. spacing of structural members). No load-sharing capability in heavy-framed systems is acknowledged by the code. The stipulations do not reflect how light or heavy frame systems actually behave. Relatively recently, circa the last 10 years, the Canadian design code has had major modification to its provisions related to the design of shear walls. New design rules treat shear walls as systems that correspond to complete length walls. However as yet there is no linking of shear wall design to the nature of the parent system. Design of connections totally ignores systemic issues.

Recommendation 9: System design level design guidance and required design checks should remain the prerogative of the parent building code.

Recommendation 10: Timber design codes should draw attention to and amplify, if appropriate to use of wood products, system design level requirements in the parent building code.

The first of these recommendations reflects the opinion that the broad guidance on systemic aspects of design that is contained in the Canadian building code is adequate. Also that it does not (and should not) impinge on ability of designers to exercise their professional skills. The second recommendation recognises that currently the timber design code does not go far enough in contextualizing guidance on the systemic aspects of design using wood products.

8. System Related Modification Factors (k_N and k_H)

The notion behind the modification factor k_N which accounts for the number of components in a system is that the apparent resistances of components decrease in proportion to the 'stressed volume' of material in structures.

There has been discussion for many years in timber engineering circles about the inverse relationship between the amount of material that members contain and their apparent material strength. Various empirical explanations and even some theories have been advanced in respect of size of member effects on apparent strength, especially for sawn timber, structural composite lumber and glulam. Many influences are at play, but the most important factor is that as sizes of components and systems increase the ratio of strain energy released during component failures is increased relative to the energy required to create new fracture surface [4, 10]. The apparent brittleness of components and systems tends to increase with size, and hence apparent strength reduces, because the ratio of energy released as the result of a part failing increases compared with the energy consumed in breaking that part [4, 10]. Brittleness and reductions in apparent strength do not (cannot) occur indefinitely as systems get bigger [10] and that needs to be recognized.

Tentatively it is suggested that the number of components in a system be considered a surrogate for introducing a relationships between system size and apparent decreases in material resistances of components. How significant the issue is will depend on the nature of the component failure and the characteristics of systems [4].

Recommendation 11: Detailed case studies be performed across a range of structural systems to determine the significance of system size effects on brittleness and apparent strength.

The notion behind the modification factor k_H which accounts for the nature of the parent system and the expected classification of the system failure mode is that not all systems are equally capable of permitting components to attain their free body capacity. For members this could possibly be an extension of the current approach in the Canadian design code [5], wherein factors are applied to enhance isolated component capacities provided that the system meets certain criteria (Section 7). For connections considerations and approaches can be expected to be quite different from current approaches for members. Incorporating connections into systems can either enhance or diminish their isolated component capacities, depending on the basis of those capacities. To illustrate, assume that capacities of connections are based on post-yield resistance (ultimate capacity) when loaded in isolation. However, intra system compatibility constraints resulting from the structural forms of systems would not always allow connections to attain displacement levels necessary to mobilize their ultimate resistances, prior to the complete system collapsing. Such a possible situation occurs for nailed joints in shell structures. Similar situations can be envisaged for members. The system classification scheme in Table 2 could be a surrogate for linking attainable component resistances to system type.

Recommendation 12: Detailed case studies should be performed across a range of structural systems to determine how best to handle effects of system type on the ability of components to achieve free body capacities. Consideration should also be given to what constitutes the most appropriate interpretation of the resistance responses of components.

9. Adoption of Reliability Concepts

So far reliability concepts have supported code committee decision making in North America in respect of load and resistance factors under LRFD formats. This applies only to component design

(members and structural panels). Approaches adopted are based on so-called nominal rather than true reliability. Analyses imply nominal failure rates of about 1 per 1000 over the design lifetime ($2.4 \leq \beta \leq 3.0$). Of course this is far from realistic and reflects that neither structural representations of components nor the reliability techniques are fully realistic. Nevertheless they are useful, as George Box eloquently implied. For systems, or indeed some types of components (certainly connections) currently applied reliability methods will undoubtedly need to be supplemented or even totally changed [9]. Undoubtedly it will be necessary to get closer than now to dealing in terms of true reliability, and with realistically acceptable failure rates.

Recommendation 13: Options for system level reliability concepts need to be fully investigated.

It is important that this last recommendation not be thought of as only addressing the need for debate on mathematical intricacies. As was stated at the outset of this discourse, it is necessary to adopt a much broader perception of what is needed, and to create something that engineers will want to use.

10. Concluding Comments

The authors do not imagine that they have identified all the relevant issues, nor do they imagine that the approaches suggested will meet with universal support even in Canada. They hope that this "Aunt Sally" will promote debate on issues surrounding the introduction of systems level design into timber design codes. Not debating this creates the risk that such documents become obsolete and that a changing world passes them by.

References

1. Brown, L.B. 2006. "Plan B 2.0: Rescuing a planet under stress and a civilization in trouble", W. W. Norton & Company, New York, p. 365.
2. Smith, I. 2006. "Reaching for the limits with timber construction", Symposium - Responding to Tomorrow's Challenges in Structural Engineering, Budapest, September 13-15, International Association for Bridge and Structural Engineering (*in press*).
3. NRC. 2005. "National building code", National Research Council, Ottawa, ON.
4. Smith, J.W. 2006. "Structural robustness analysis and the fast fracture analogy", *Structural Engineering International,* 16(2): 118-123.
5. Canadian Standards Association (CSA). 2005. "Engineering design in wood", CAN/CSA Standard 086-01, CSA, Toronto, ON, Canada.
6. Quenneville, P., Smith, I., Asiz, A., Snow, M. and Chui, Y.H. 2006. "Generalised Canadian approach for design of connections". CIB-W18 Meeting in Florence (*in press*).
7. Paulay T. 1981. "Developments in the seismic design of reinforced concrete frames in New Zealand", Canadian Journal of Civil Engineering, 8: 91-113.
8. Chui Y.H. and Smith, I. 1993. "Capacity design of wood structures", Proceedings of Annual Conference of Canadian Society for Civil Engineering, II: 365-374.
9. Smith, I., Asiz, A., Snow, M. and Chui, Y.H. 2006. "Possible Canadian / ISO approach to deriving design values from test data", CIB-W18 Meeting in Florence (*in press*).
10. Smith, I., Landis, E. and Gong, M. 2003. "Fracture and fatigue in wood", John Wiley and Sons, Chichester, UK.

INTERNATIONAL COUNCIL FOR RESEARCH AND INNOVATION
IN BUILDING AND CONSTRUCTION

WORKING COMMISSION W18 - TIMBER STRUCTURES

SIMPLIFIED APPROACH FOR THE LONG-TERM BEHAVIOUR OF TIMBER-CONCRETE COMPOSITE BEAMS ACCORDING TO THE EUROCODE 5 PROVISIONS

M Fragiacomo
Department of Civil Engineering
University of Canterbury, Christchurch

NEW ZEALAND

A Ceccotti
IVALSA Trees and Timber Institute
CNR, Sesto Fiorentino (Florence)

ITALY

MEETING THIRTY-NINE
FLORENCE
ITALY
AUGUST 2006

Presented by M Fragiacomo
A Hanhijärvi stated that the model contained a creep limit and typical experimental data did not support such a limit. He asked whether the current work had long enough time and moisture fluctuation. One might need to be careful and not to extrapolate although it might not be a problem here. Fragiacomo answered that only data were 2 tests; one in Florence (5yrs) and one in Switzerland (not more than 5 yrs). H Blass said that in Karlsruhe there were 8 beams loaded for 6 ¼ years with different connections.
R Foschi received clarification that a component on the diffusion problem was considered to account for moisture movement in the wood as relative humidity and temperature changed.
JW van de Kuilen and M Fragiacomo discussed the issue of theoretical limit of changes of moisture content.
A Leijten commented that the EC5 creep coefficient for connection was established on the basis of political agreement not technical agreements.

Simplified approach for the long-term behaviour of timber-concrete composite beams according to the Eurocode 5 provisions

Massimo Fragiacomo[1] and Ario Ceccotti[2]

[1] Department of Civil Engineering, University of Canterbury, Christchurch, New Zealand

[2] IVALSA Trees and Timber Institute, CNR, Sesto Fiorentino (Florence), Italy

1 Introduction

The timber-concrete composite beam (TCC) is a construction technique extensively used for both upgrading of existing floors and new buildings. Many advantages can be achieved by connecting a lower timber beam with an upper concrete slab, including increase in strength and stiffness, better seismic performance, larger thermal mass and fire resistance, better acustic separation, and the possibility to maintain the timber floor when restoring existing buildings (Ceccotti 1995).

The design of the TCC must satisfy both ultimate (ULS) and serviceability (SLS) limit states (CEN 2003). The former are controlled by evaluating the maximum stresses in the component materials (concrete, timber and connection system) using an elastic analysis (Ceccotti 1995). Such approaches generally lead to solutions sufficiently accurate provided that realistic properties of the connection system are employed (Ceccotti et al. 2006).

The SLS are checked by evaluating the maximum deflection both in the short- and long-term. Timber, concrete and connection systems, in fact, all show time-dependent behaviour. Concrete is characterised by creep, shrinkage and thermal strains; timber exhibits creep, mechano-sorptive creep, which is the increase in delayed strains due to cycles of moisture content, shrinkage/swelling, and thermal strains; the connection system itself is also characterised by creep and mechano-soprtive creep. This results in the long-term behaviour being affected also by the environmental conditions. Some numerical models have been proposed in order to evaluate rigorous solutions (Fragiacomo 2005, Schänzlin 2003). The former FE model was compared against a number of long-term experimental tests (Fragiacomo and Ceccotti 2006) showing the possibility to predict accurate results. The software accounts for all of the aforementioned time-dependent phenomena using the Toratti's rheological model (Toratti 1992) for the creep and mechano-sorptive creep of timber and connections system, and the CEB-FIP Model Code 1990 formulas (CEB 1993) for the creep and shrinkage of concrete. The actual distribution of moisture content, which was proved to be highly variable over the timber cross-section (Fragiacomo and Ceccotti 2006), is computed by solving the diffusion problem for a given

history of environmental relative humidity. The temperature distribution, much less variable, is instead considered as constant over the cross-section but variable in time.

A simplified analytical approach was also proposed (Ceccotti 1995), however further research highlighted that some phenomena ignored in such an approach such as concrete shrinkage and inelastic strains due to environmental conditions may lead to significant errors and make the simplified solution not conservative (Ceccotti et al. 2006, Fragiacomo 2006, Fragiacomo et al. 2006a). Some more accurate methods for the long-term behaviour have then been proposed. Kuhlmann and Schänzlin (2003) proposed the use of effective values of creep and shrinkage to take into account the different trends in time of those coefficients in the component materials (timber, concrete and connection system). Fragiacomo (2006) proposed an improvement of the Ceccotti's approach in order to account for the mechano-soprtive creep, concrete shrinkage, and inelastic strains/stresses due to environmental temperature and relative humidity variations.

The aim of this paper is to propose a simplified yet accurate solution for the long-term behaviour of TCC's. The approach will allow the designer to account for the whole loading history of the structure including concrete shrinkage, effect of props during construction, and inelastic strains due to environmental variations. The accuracy will be assessed by comparison with numerical solutions on a number of TCC's of technical interest. Finally the influence of different environmental conditions such as outdoor and heated indoor conditions on the long-term performance will be discussed.

2 Prediction of the long-term behaviour of TCC's

2.1 Current approach

The current approach proposed by Ceccotti (1995) superimposes the effects in time of the dead and live loads applied on the TCC. Let g_1, g_2 and $\psi_2 q$ be the self weight of the TCC, the other part of the dead load, and the quasi-permanent part of the live load q (ψ_2 is equal to 0.3 for domestic and office floors) respectively. t_1, t_2 and t_3 are the times when the loads are applied (t_1 is the time when the props are removed from the TCC) measured from the concrete pouring. A generic effect S (S may signify the deflection, the shear force in the connection system, the stress in the concrete or timber beam) at the time t can be evaluated by superimposing the effects of the different loads:

$$S = S(g_1) + S(g_2) + S(\psi_2 q) \tag{1}$$

where the effect of each load $S(g_i)$ is calculated using the formulas for composite beams with flexible connection suggested by the Annex B of the Eurocode 5-Part 1-1 (EC5) (CEN 2003). The global creep behaviour is taken into account by replacing the elastic E_j (j=c,t) and slip moduli K_{ser} with the effective moduli $E_{j,eff}(t)$ and $K_{eff}(t)$ in the EC5 formulas:

$$E_{c,eff}(t) = \frac{E_c(t_i)}{1+\phi_c(t,t_i)} \qquad E_{t,eff}(t) = \frac{E_t}{1+\phi_t(t-t_i)} \qquad K_{eff}(t) = \frac{K_{ser}}{1+\phi_f(t-t_i)} \tag{2) (3) (4}$$

where ϕ_j are the creep coefficients of concrete (subscript c), timber (t) and connection system (f). The trend in time of the concrete creep coefficient ϕ_c and Young's modulus E_c can be calculated using the CEB formulas (CEB 1993). For timber, the current version of the EC5 suggests the final value (for t–t_i=50 years) of the creep coefficient ϕ_t, which is denoted with k_{def}, for different service classes. The trend in time (Fig. 1) can be obtained by

interpolation of the values for different load duration classes (that is the quantity $t-t_i$) reported in an earlier (1995) version of the EC5. For the connection, the EC5 suggests that a creep coefficients twice as large as the timber one is adopted.

2.2 Proposed approach

The main advantage of the current approach is the simplicity, being based on closed form solutions. However a number of approximations are made, which were found to lead in some cases to significant errors (Fragiacomo 2006). The mechano-soprtive effect is not explicitely considered since there is no direct dependence of the creep coefficient upon the history of moisture content. An indirect allowance for the global time-dependent behaviour (creep and mechano-sorptive creep) is done by making the final creep coefficient dependent upon the service class. Some other phenomena are ignored, such as the concrete shrinkage, and the variation of temperature and relative humidity of the environment. Moisture content variations in timber and environmental temperature variations cause eigenstresses into the TCC. The proposed approach aims at improving the current approach by accounting for the aforementioned phenomena.

2.2.1 Dependence of the creep coefficient on the moisture content

The explicit dependence of the creep coefficient on the timber moisture content is assumed according to the Toratti's model (1992). For a piecewise linear history of moisture content with amplitude Δu [%] and period Δt, the creep coefficient of timber is given by:

$$\phi_i(t-t_i)=\phi_{tc}(t-t_i)+\phi_{tms}(t-t_i)=\left(\frac{t-t_i}{t_d}\right)^m+\phi^\infty\left[1-e^{-c\frac{2\Delta u}{100\Delta t}(t-t_i)}\right] \tag{5}$$

where ϕ_{tc}, ϕ_{tms} are the creep part and the mechano-sorptive part of the total creep coefficient of timber, t_d, m, ϕ^∞ and c are material parameters assumed equal to 29500 days, 0.21, 0.7 and 2.5, respectively. The moisture content distribution $u=u(P,t)$ is not constant over the timber cross-section but highly dependent upon the location of the point P. Furthermore, also the variation over time of the moisture content, which is influenced by the history of environmental relative humidity $RH=RH(t)$, is different over the timber cross-section. In order to simplify the problem, reference is made on the history of average moisture content $u_{aver}=u_{aver}(t)$, which is assumed to be uniform in each point P of the timber cross-section. Such a history is then approximated by a piecewise linear curve on a yearly scale, where $\Delta u=u_{aver,max}-u_{aver,min}$ represents the yearly fluctuation, and Δt=365 days. Eq. (5) is hence substituted into eq. (3) and (4) to account for the mechano-sorptive effect.

The comparison among the creep coefficients suggested by the EC5 for the different service classes and the creep coefficients evaluated according to the Toratti's model is reported in Fig. 1. It can be observed that the yearly variation of moisture content affects the rate of increase in time of the creep coefficient in the Toratti's model. However, the final value is independent of Δu for amplitudes larger than 1.65% (which is the case of technical interest), and is slightly lower than the value suggested by the EC5 for the 3rd service class. For no moisture content variations (Δu=0), the Toratti's model leads to a final value slightly higher than the EC5 final value for the 2nd service class, which may be considered as representative of an environmental condition with no significant moisture content variations and, therefore, no mechano-sorptive effect. Fig. 2 reports the comparison among the creep coefficients of timber, the creep coefficients of connection evaluated by doubling the creep coefficients of timber, and the values obtained by extrapolating the

outcomes of an experimental test recently performed on the Tecnaria shear stud connection (Fragiacomo et al. 2006b). The figure points out that the creep coefficients suggested by the EC5 are far too large compared with the experimental values. When the outcomes of long-term experimental tests are not available, a more reasonable assumption for the connection creep coefficient seems to be the value of the creep coefficient of timber: $\phi_f=\phi_t$. This outcome is confirmed also by other experimental tests performed on glued rebar (Bonamini et al. 1990) and notched (Kuhlmann and Michelfelder 2004) connections. However, to be consistent with the provisions of the EC5, the assumption $\phi_f=2\phi_t$ will be made in all analyses carried out in the following.

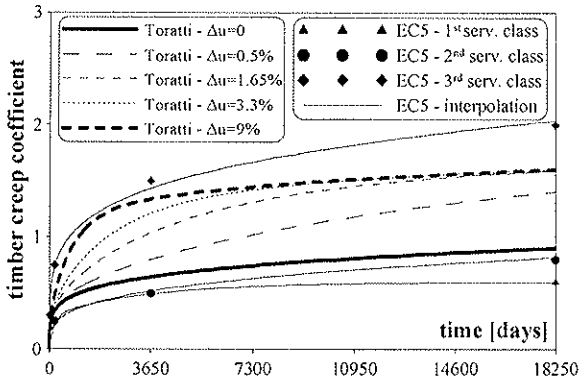

Fig. 1: creep coefficients of timber

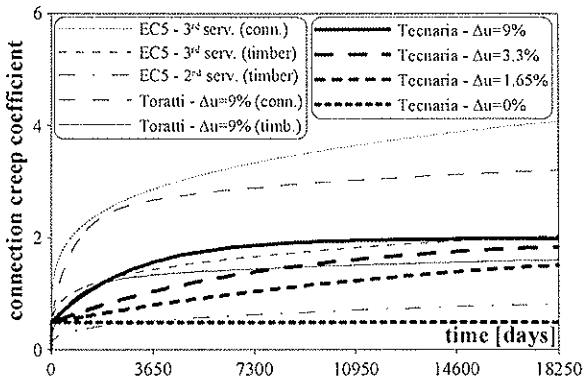

Fig. 2: creep coefficients of connection

2.2.2 Effect of concrete shrinkage

The effect of concrete shrinkage, ε_{cs}, is accounted for by using the closed form solutions for simply supported TCC's with flexible connections subjected to inelastic strains reported in Appendix (Fragiacomo 2006). In such formulas, the following substitutions are made:

$$\Delta\varepsilon_n = -\Delta\varepsilon_{n,c} = -\varepsilon_{cs}(t) + \varepsilon_{cs}(t_s) \qquad E_{c,eff}(t) = \frac{E_c(t)}{1+\phi_c(t,t_s)} \qquad (6)\ (7)$$

where ε_{cs} (<0) signifies the concrete shrinkage, which can be evaluated according to the CEB formulas (CEB 1993), and t_s signifies the time of concrete curing (usually 1 to 7 days after the pouring), when concrete begins shrinking. The influence of concrete, timber and connection creep is taken into account using the effective modulus method (eq. (7) for concrete, and eqs. (3)-(4) for timber and connections, with $t_i=t_s$ and ϕ_t, ϕ_f given by eq. (5)). It is interesting to point out that the construction type (propped or unpropped) does not markedly influence the effect of the concrete shrinkage on the TCC. Figures 3 and 4 report

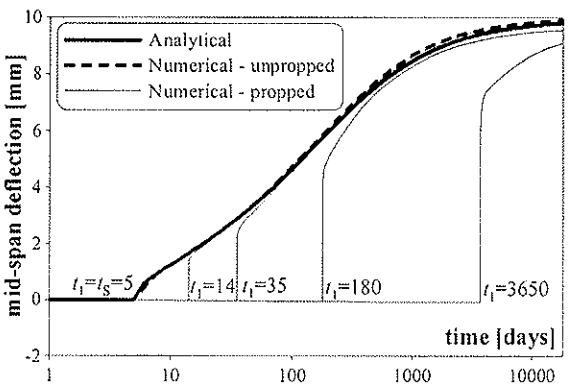

Fig. 3: mid-span deflection due to concrete shrinkage only

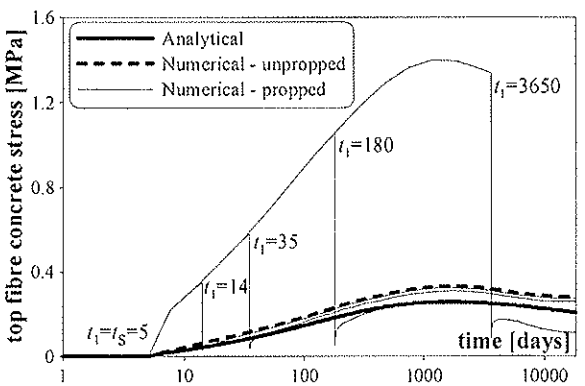

Fig. 4: stress at the top fibre of the concrete slab due to concrete shrinkage only

the trends in time of the mid-span deflection and concrete stress in the top fibre for the Florence TCC (see Table 1) subjected to concrete shrinkage only. The approximate curve carried out using the proposed method is compared against the curves obtained using a rigorous finite element program (Fragiacomo 2005). The mechano-sorptive effect has been neglected in this example. It can be observed that for any time of prop removal t_1, the numerical curve of the propped construction approaches the curve of the unpropped beam, which is well approximated by the analytical curve. The proposed approximate solution for concrete shrinkage can hence be used to evaluate any effect $S(t)$ for $t \geq t_1$.

2.2.3 Effect of shrinkage/swelling due to environmental variations

Environmental variations of relative humidity and temperature with respect to the values at the time of concrete curing t_s cause eigenstresses and deflection in the TCC. The variations of relative humidity $RH=RH(t)$ lead to changes in moisture content $\Delta u=\Delta u(P,t)$ with different amplitudes over the timber cross-section. The corresponding inelastic strains are evaluated with reference to the piecewise-linear curves approximating the yearly fluctuations of the moisture content averaged over the timber cross-section, $u_{aver}(t)$-$u_{aver}(t_s)$. The variation of environmental temperature leads to eigenstresses and inelastic strains in the TCC because of the different thermal expansion coefficients of timber and concrete. It was demonstrated (Fragiacomo and Ceccotti 2006) that the yearly variations of temperature in concrete and timber are almost the same as the environmental ones: $\Delta T_{c,y}=\Delta T_{t,y}=T_{y,max}-T_{y,min}$. Day-to-night variations are the same amplitude as the environmental ones for concrete: $\Delta T_{c,d}=\Delta T_d$, while for timber a reduction factor k should be applied, the amount of which depends on the size of the cross-section (k=0.8 for beams with breadth b_t=125 mm, k=1 for narrow joists with breadth b_t=38 mm): $\Delta T_{t,d}=k\Delta T_d$. The inelastic strains are evaluated with reference to a piecewise-linear curve approximating the yearly trend of the environmental temperature, $T(t)$-$T(t_s)$, and to the day-to-night variations, ΔT_d. The effect of yearly, $\Delta\varepsilon_y$, and daily environmental variations, $\Delta\varepsilon_d$, is accounted for using the elastic solution reported in Appendix with the following substitutions:

$$\Delta\varepsilon_n = \Delta\varepsilon_y = \alpha_{t,u}\left[u_{aver}(t)-u_{aver}(t_s)\right]+\alpha_{t,T}\left[T(t)-T(t_s)\right]-\alpha_{c,T}\left[T(t)-T(t_s)\right] \quad (8)$$

$$\Delta\varepsilon_n = \Delta\varepsilon_d = \alpha_{t,T}k\Delta T_d - \alpha_{c,T}\Delta T_d \quad (9)$$

Since the inelastic strains change in time with cyclic trend, the effect of creep and mechano-sorptive creep is negligible, therefore the Young's moduli of concrete, $E_c(t)$, timber, E_t, and connection, K_{ser} are employed in the formulas.

2.3.4 Superposition

The solution S of the TCC at a generic time t according to the proposed approach is carried out by superimposing the effects of the different loading conditions:

$$S = S(g_1)+S(g_2)+S(\psi_2 q)+S(\varepsilon_{cs})+S(\Delta\varepsilon_y)+S(\Delta\varepsilon_d) \quad (10)$$

where the effects of creep and mechano-sorptive creep are taken into account on the solutions $S(g_1)$, $S(g_2)$, $S(\psi_2 q)$ and $S(\varepsilon_{cs})$ using the effective modulus method (eqs. (2)-(4) and (7)) and the Toratti's model (eq. (5)).

2.4 Numerical-analytical comparison

The accuracy of the proposed (eq. (10)) and current (eq. (1)) approach is assessed against the rigorous numerical solutions carried out using a FE model purposely developed

(Fragiacomo 2005). Four TCC's are analysed: the 'Florence' beam, a long-span composite beam with glued rebar connection and deep glulam beam (Capretti and Ceccotti 1996); the 'Padua' beam, a medium-span composite beam with glued rebar connection typical of upgrading of ancient wooden floors (Turrini and Piazza 1983); the 'Cardington' beam, a short-span beam with narrow timber joists and inclined SFS screws representative of a possible upgrading of a domestic wooden floor (Grantham et al. 2004); the 'Fort Collins' beam, a short-span wood-concrete composite floor/deck system with shear/key anchor connection detail (Fragiacomo et al. 2006a). Geometrical and mechanical properties of the beams are summarized in Table 1 (see the Appendix for the meaning of the symbols).

Table 1: Geometrical and mechanical properties of the beams analysed

	Florence	Padua	Carding.	Fort Coll.		Florence	Padua	Carding.	Fort Coll.
g_1 [kN/m]	2.34	1.65	0.86	0.404	A_s [mm^2]	94	57	85	158
g_2 [kN/m]	0.6	0.6	0.36	0.114	t [mm]	50	25	15	0
$\psi_2 q$ [kN/m]	1.2	1.2	0.45	1.14	K_{ser} [N/mm]	25000	15750	9357	156213
l [mm]	10000	5800	3600	3600	s_{min} [mm]	300	110	100	454.5
b_c [mm]	1000	550	600	190.5	s_{max} [mm]	450	250	200	454.5
h_c [mm]	50	60	50	63.5	b_t [mm]	125	160	38	190.5
f_{cm} [MPa]	30.43	31.24	31.24	17.89	h_t [mm]	500	230	225	88.9
h [mm]	100	120	100	47.6	E_t [GPa]	10	9	8	8.605

The loads g_1, g_2 and $\psi_2 q$ have been applied at the times t_1=14, t_2=35 and t_3=180 days from the concrete pouring for all the composite beams. The time of concrete curing t_s has been assumed as equal to 5 days. The Young's modulus, creep function and shrinkage of concrete have been computed according to the CEB formulas (CEB 1993) by assuming an average environmental relative humidity RH=75%, the mean compressive strength f_{cm} and the notational thickness h specified in Table 1. The area of reinforcement A_s in the concrete slab, considered in the numerical solution, has been neglected in the analytical approach.

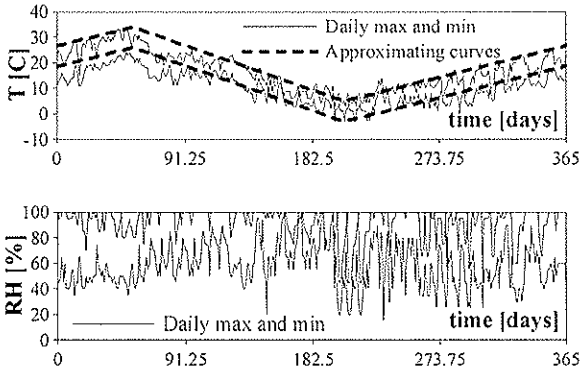

Fig. 5: maximum and minimum daily temperature (top) and relative humidity (bottom) monitored in Florence

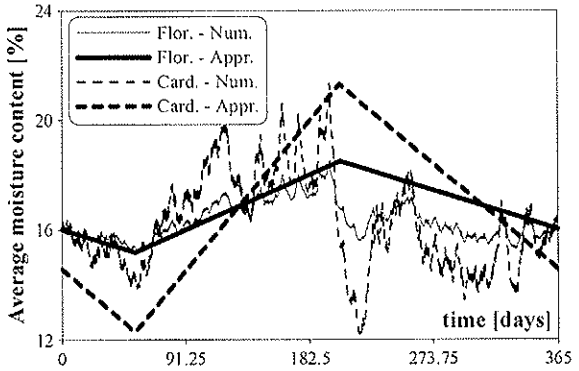

Fig. 6: trend in time of the moisture content averaged over the timber cross-section

All beams have been regarded as exposed to sheltered outdoor conditions (3rd service class according to the EC5, see Ceccotti et al. 2006). The histories of environmental temperature and relative humidity monitored in Florence in the period 9 June 1994 - 8 June 1995 have been assumed in all the analyses. The trends in time of the maximum and minimum daily temperatures are displayed in Fig. 5 (top) including the approximating piecewise-linear curves. The average day-to-night variation is 8 Celsius degrees, while the amplitude of the yearly fluctutation is 29 Celsius degrees. The trends in time of the maximum and minimum daily relative humidities are displayed in Fig. 5 (bottom), with an average daily fluctuation of 34%. The trends in time of the average moisture content over the timber cross-section

are displayed in Fig. 6 for the Florence and Cardington beams, together with the approximating piecewise-linear curves. The curves have been obtained using a numerical program which solves the diffusion problem of moisture content over the timber cross-section for the history of environmental relative humidity monitored in Florence and displayed in Fig. 5, on the bottom, as maximum and minimum daily values. The breadth of the timber beam plays a significant role on the amplitude of the yearly moisture content variation: $\Delta u = u_{aver,max} - u_{aver,min} = 3.3\%$ for the Florence beam (b_t=125 mm), and 9% for the Cardington beam (b_t=38 mm), with values closed to those of the Florence beam for the Padua (3%) and Fort Collins (3.8%) beams, respectively.

Fig. 7 displays the numerical and analytical solutions for the Florence beam in terms of mid-span deflection, concrete and timber stresses in the outer fibres, and connector shear force over the support. Fig. 8 displays the mid-span deflections for the other beams. The analytical solutions are obtained using the proposed approach (dashed line) and the current approach (thick solid line). In all the solutions, the Toratti's rheological model has been used. For the sake of clarity, the yearly and daily fluctuations due to environmental variations have been plotted only for the last year. The use of the proposed approach leads to very accurate results in terms of deflections and stresses (see Table 2). Conversely, the current approach markedly underestimates deflection and stresses. The concrete shrinkage, in fact, represents a significant component of the long-term deflection and, as such, should not be neglected. The yearly and daily fluctuations are also important, however not as much as the concrete shrinkage. The proposed method should hence be used for the design of the composite beam in the long-term, especially for an accurate evaluation of the deflection.

When the time of construction is unknown, the entire yearly and daily moisture content

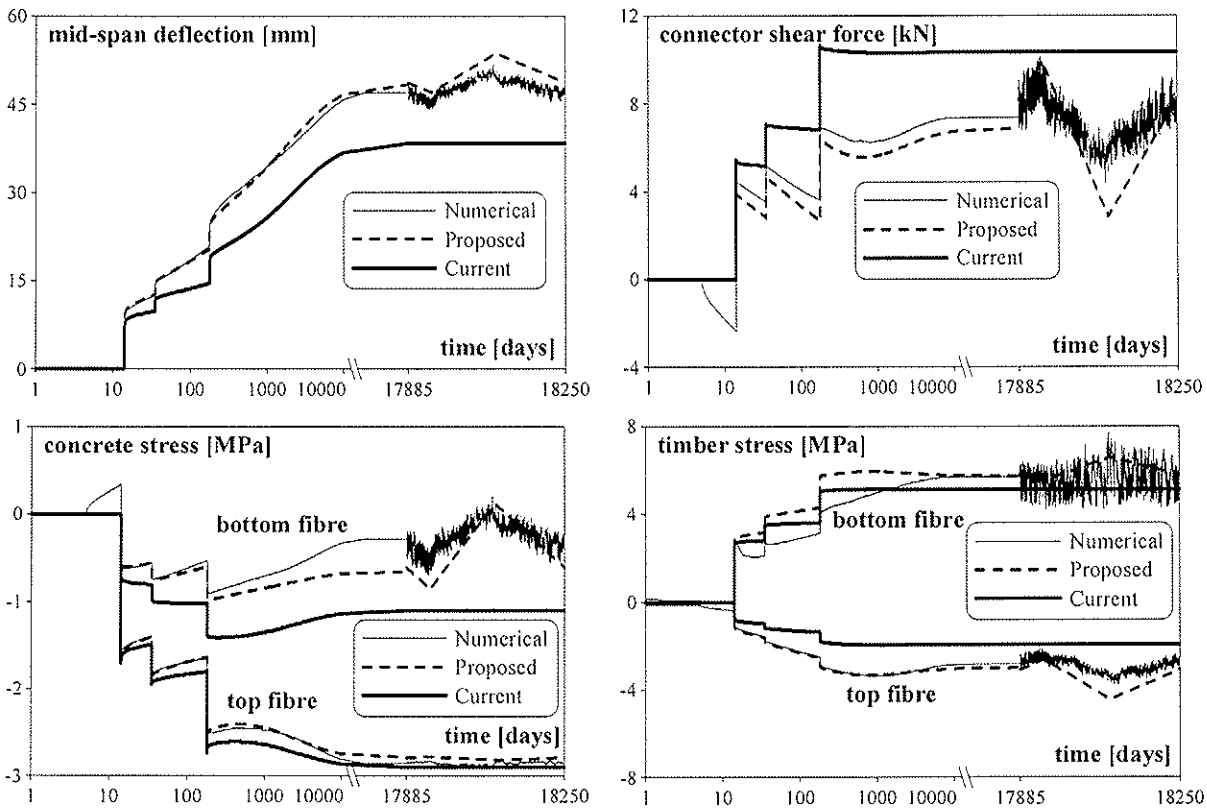

Fig. 7: trends in time of the mid-span deflection (top, left), connector shear force over the support (top, right), outer fibre concrete stresses at mid-span (bottom, left), and outer fibre timber stress at mid-span (bottom, right) for the Florence beam

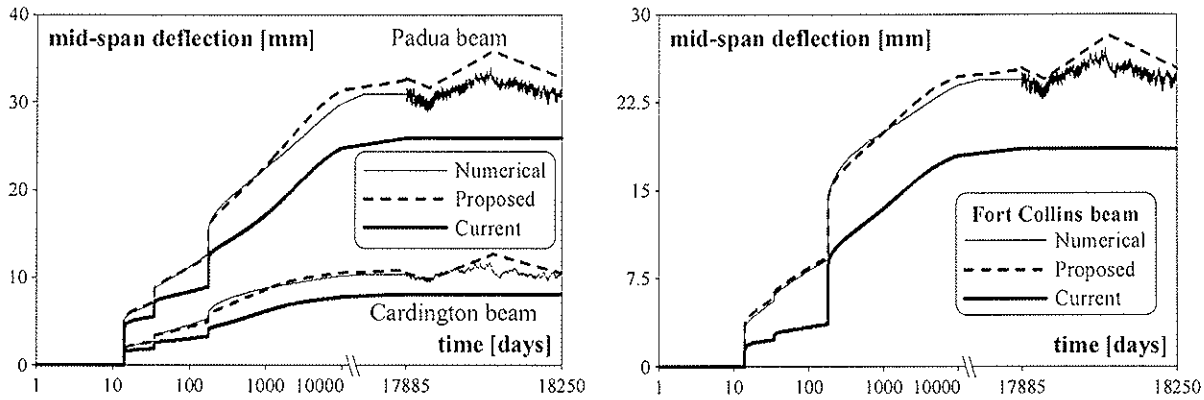

Fig. 8: trend in time of the mid-span deflection for the Padua and Cardington beams (left) and for the Fort Collins beam (right)

Table 2: Percentages of error between numerical and analytical results, as an average on all the beams

	Proposed	Current
Mid-span defl.	5.1	-28.0
Shear force	2.4	7.6
Top fibre concrete stress	3.2	-18.2
Bottom fibre concrete stree	26.3	-39.9
Top fibre timber stress	17.1	-56.9
Bottom fibre timber stress	-14.2	-34.1

Table 3: Differences in percentage between outdoor and diverse indoor conditions, as an average on the Florence and Cardingt. beams

	Δu, ΔT/3	Δu/2, ΔT/3	No Δu, ΔT/3
Mid-span defl.	-4.0	-6.6	-25.3
Shear force	-15.5	-17.3	-33.9
Top fibre concrete stress	-0.2	-0.7	-16.9
Bottom fibre concrete stress	-100.4	-101.6	-106.5
Top fibre timber stress	-11.1	-14.6	-6.8
Bottom fibre timber stress	-1.5	-13.3	-20.9

and temperature variations should be considered in the design of the beam in order to evaluate the most conservative solution:

$$\Delta\varepsilon_y = \alpha_{t,u}(u_{aver,\max} - u_{aver,\min}) + \alpha_{t,T}(T_{y,\max} - T_{y,\min}) - \alpha_{c,T}(T_{y,\max} - T_{y,\min}) \quad (11)$$

$$\Delta\varepsilon_d = \alpha_{t,T} k \Delta T_d - \alpha_{c,T} \Delta T_d \quad (12)$$

Then the yearly $\Delta\varepsilon_y$ and daily $\Delta\varepsilon_d$ environmental variations should be combined with the other loads (dead and live loads $g_1+g_2+\psi_2 q$, shrinkage ε_{cs}) in order to produce the worst effect. For the environmental conditions monitored in Florence, the largest deflection and bending moments in concrete and timber are given by the load combination $S'=g_1+g_2+\psi_2 q+\varepsilon_{cs}-\Delta\varepsilon_y-\Delta\varepsilon_d$, while the largest connector shear force and axial force in timber and concrete are given by the load combination $S''=g_1+g_2+\psi_2 q+\varepsilon_{cs}+\Delta\varepsilon_y+\Delta\varepsilon_d$.

3 Influence of different environmental conditions

The analyses carried out above refer to the case of a TCC exposed to outdoor conditions. Even though the timber beam is protected from direct contact with the rain by the concrete slab, the beam should be assigned to the 3rd service class according to the EC5 (Ceccotti et al. 2006). For TCC's in heated indoor conditions, the environmental variations will be characterised by reduced fluctuations. Some research suggested that in indoor conditions the moisture content variations should be halved with respect to outdoor conditions (Limträhandbok 2001). However, other recent studies (Häglund and Thelandersson 2005)

pointed out that the same amplitude of the moisture content variations can be expected in timber beams exposed to outdoor and heated indoor conditions, with a value of about 7 to 10%. In terms of temperature variations, the whole yearly indoor fluctuation including daily variations can be assumed as little as one-third of the environmental fluctuations.

It is then interesting to investigate which differences can be expected in the response of TCC's in indoor conditions (service class 1 and 2 according to EC5) compared to outdoor conditions. The Florence and Cardington beams have been analysed under indoor conditions by assuming one-third of the environmental temperature variations, and the three cases of equal, half and no moisture content variation in each fiber of the timber beam. The outcomes are reported in Table 3 in terms of numerical solutions, and in Figure 9 as analytical solutions using the proposed approach. For the sake of clarity, the yearly fluctuations due to environmental variations have been plotted only for the last year, and the numerical solutions have not been reported being very close one to another.

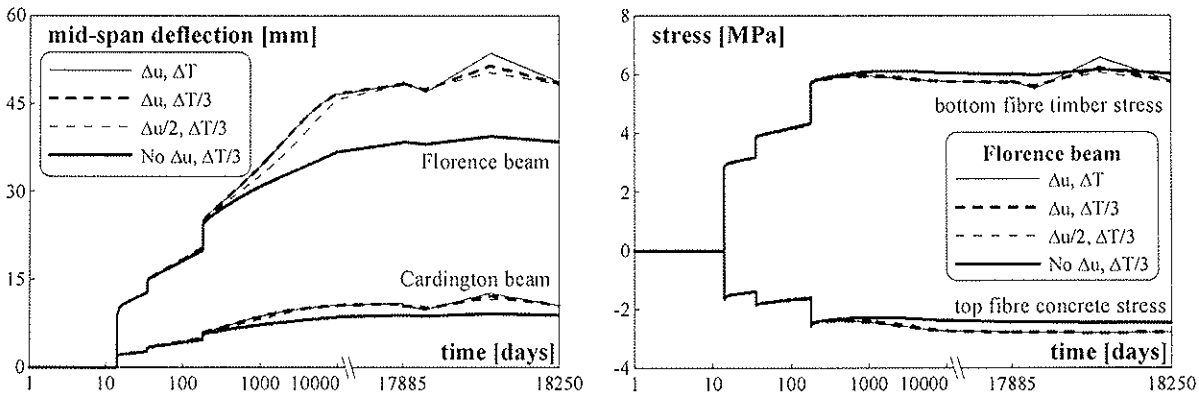

Fig. 9: comparison among the deflections (left) and stresses (right) at mid-span for the Florence and Cardington beams exposed to different environmental conditions

It can be observed that the differences among the solutions in outdoor (Δu, ΔT) and indoor (Δu, $\Delta T/3$, and $\Delta u/2$, $\Delta T/3$) conditions are generally low (max 17%). Those differences are mainly due to the reduced amplitude of the environmental yearly and daily fluctuations, while the long-term effects of the load and concrete shrinkage are hardly affected by the reduction of the yearly moisture content variation from Δu to $\Delta u/2$. This can be justified by the mechano-sorptive effect being almost independent, in the long-term, of the yearly moisture content variations for values of technical interest (Δu>1.65%), as discussed in par. 2.2.1 and depicted in Figs. 1 and 2. A significant difference is observed only when no moisture content variation is considered (Δu=0) where, according to the Toratti's model, the mechano-sorptive effect becomes zero for timber and connection. In this case the creep coefficient of timber and connection approaches the value suggested by the Eurocode 5 for the 2nd service class. The stresses are less affected by the environmental conditions than the deflection. The 100% differences reported in Table 3 refer to very low value of stresses in the concrete, and as such is not representative of a significant variation. This outcome agrees with the evidence that the rheological phenomena mainly affect the deflection of a TCC, while the effect on the stresses is generally limited (Fragiacomo et al. 2006a).

4 Conclusions

The paper investigates the long-term behaviour of timber-concrete composite beams (TCC's). A simplified yet accurate approach based on simple closed form solutions has

been proposed for the prediction of all relevant quantities. The approach is an extension of the method suggested by Ceccotti to account for the mechano-soprtive effect, concrete shrinkage, shrinkage/swelling of timber and concrete due to environmental variations, and modality of construction (propped construction). The proposed approach has been compared with the current approximate method and with the numerical solution carried out using a rigorous Finite Element program. The influence of different environmental conditions (outdoor, heated indoor conditions) on the behaviour of the TCC has also been investigated. The primary observations of this research are reported herein after.

1) the Toratti's rheological model, which accounts for the mechano-sorptive effect, is hardly dependent, in the long-term, upon the yearly moisture content variation Δu for values larger than 1.65%.

2) the creep coefficient of connection, assumed by the EC5 twice as large as the creep coefficient of timber, seems to be overestimated according to the outcomes of some tests.

3) the use of the effective modulus method for evaluating the effect on the TCC beam of creep and mechano-sorptive creep leads to accurate results.

4) the effect of concrete shrinkage can be precisely calculated using the rigorous elastic formulas for TCC's with flexible connection, with the inelastic strain due to shrinkage being measured from the time of concrete curing. The creep is taken into account using the effective modulus method, and the influence of the props is negligible.

5) the shrinkage/swelling due to environmental variations can be taken into account using the rigorous elastic formulas for TCC's with flexible connection. The temperature variations in the concrete and timber beams are assumed equal to the environmental one. The moisture content variation in the timber beam is assumed constant in each point and equal to the average value over the cross-section.

6) the numerical-analytical comparison points out that the proposed approach leads to accurate results in terms of deflections and stresses. Conversely, the use of the current approach which neglects concrete shrinkage and shrinkage/swelling due to environmental variations leads to non-conservative and, therefore, unacceptable approximations.

7) the change of environment from outdoor to indoor heated conditions, characterised by one-third of temperature variations and the same or half moisture content variations, leads to minor reductions in deflections and stresses. Some major reductions take place only if no moisture content variations occur at all. However, this case seems more a pure theoretical limit than a real possibility. According to these outcomes, which are based on the use of the Toratti's rheological model, the type of environment (outdoor, or heated indoor) does not seem to play an important role on the performance of the TCC beam. However, since this outcome is strongly dependent on the type of the rheological model used for timber, a confirmation should be searched using other types of rheological models.

5 References

Bonamini, G., Ceccotti, A., and Uzielli, L. (1990). "Short- and long-term experimental tests on concrete-antique oak and larch timber composite systems." *Proc., The 8th C.T.E. Conference*, Bologna, Italy (in Italian).

Capretti, S., and Ceccotti, A. (1996). "Service behaviour of timber-concrete composite beams: a 5-year monitoring and testing experience." *Proc., International Wood Engineering Conference*, New Orleans, USA, 3, 443-449.

Ceccotti, A. (1995). "Timber-concrete composite structures." *Timber Engineering, Step 2*, First Edition, Centrum Hout, The Netherlands, E13/1-E13/12.

Ceccotti, A., Fragiacomo, M., and Giordano, S. (2006). "Long-term and collapse tests on a timber-concrete composite beam with glued-in connection." *Materials and Structures*, Special Volume on Timber, in press.

Comité Euro-International du Béton (1993). "CEB-FIP Model Code 90." *CEB Bull. No. 213/214*, Lausanne, Switzerland.

Comité Européen de Normalisation (2003). "Eurocode 5 – Design of Timber Structures – Part 1-1: General Rules and Rules for Buildings." *prEN 1995-1-1*, Bruxelles, Belgium.

Fragiacomo, M. (2005). "A finite element model for long-term analysis of timber-concrete composite beams." *Structural Engineering & Mechanics*, 20(2), 173-189.

Fragiacomo, M., and Ceccotti, A. (2006). "Long-term behavior of timber-concrete composite beams. I: Finite element modeling and validation." *Journal of Structural Engineering*, 132(1), 13-22.

Fragiacomo, M. (2006). "Long-term behavior of timber-concrete composite beams. II: Numerical analysis and simplified evaluation." *Journal of Struct. Engineer.*, 132(1), 23-33.

Fragiacomo, M., Gutkowski, R.M., Balogh, J., and Fast, R.S. (2006a). "Long-term behaviour of wood-concrete composite floor/deck systems with shear key connection detail." Submitted for possible publication on *Journal of Structural Engineering*.

Fragiacomo, M., Amadio, C., and Macorini, L. (2006b). "Short- and long-term performance of the "Tecnaria" stud connector for timber-concrete composite beams." Submitted for possible publication on *Materials and Structures*.

Grantham, R., Enjily, V., Fragiacomo, M., Nogarol, C., Zidaric, I., and Amadio, C. (2004). "Potential upgrade of timber frame buildings in the UK using timber-concrete composites." *Proc., The 8th World Conference on Timber Engineering*, Lahti, Finland, Vol. 2, 59-64.

Häglund, M., and Thelandersson, S. (2005). "Consideration of moisture exposure of timber structures as an action." *Proc., Meeting thirty-eight of the Working Commission W18-Timber Structures, CIB,* Karlsruhe, Germany, 11 pp.

Limträhandbook (2001). "Nordic design manual for glulam." Svenskt Limträ AB, Stockholm, Sweden (in Swedish).

Kuhlmann, U., and Michelfelder, B. (2004). "Grooves as shear-connectors in timber-concrete composite structures." *Proc., The 8th World Conference on Timber Engineering*, Lahti, Finland, Vol. 1, 301-306.

Kuhlmann, U., and Schänzlin, J. (2004). "Time dependent behaviour of timber-concrete composite structures." *Proc., The 8th World Conference on Timber Engineering, WCTE 2004*, Lahti, Finland, Vol. 1, 313-318.

Schänzlin, J. (2003). "About the time dependent behavior of composite of board stacks and concrete." *Ph.D. Thesis*, University of Stuttgart, Germany (in German).

Toratti, T. (1992). "Creep of timber beams in a variable environment." *Report No. 31*, Helsinki University of Technology, Helsinki, Finland.

Turrini, G., and Piazza, M. (1983). "The static behaviour of the timber-concrete composite structure." Recuperare, Vol. 2 No. 6, 215-225 (in Italian).

6 Appendix

This Appendix reports the rigorous formulae for elastic analyses of simply supported TCC's with flexible connection subjected to inelastic strains in the concrete slab and timber beam (Fragiacomo 2006):

$$u_{\max} = u_{\max,full} \cdot \gamma_u \qquad u_{\max,full} = \frac{\Delta\varepsilon_n}{H} \cdot \frac{(EI)_{full} - (EI)_{abs}}{(EI)_{full}} \cdot \frac{l^2}{8} \qquad (13)\ (14)$$

$$\gamma_u = 1 - \frac{8}{(\alpha l)^2} \cdot \left[1 - \frac{1}{\cosh(0.5\alpha l)}\right] \qquad s_f(x) = s_{f,\max,abs} \cdot \gamma_s(x) \qquad (15)\ (16)$$

$$s_{f,\max,abs} = -\Delta\varepsilon_n \cdot \frac{l}{2} \qquad \gamma_s(x) = \frac{1}{0.5\alpha l} \cdot [\tanh(0.5\alpha l) \cdot \cosh(\alpha x) - \sinh(\alpha x)] \qquad (17)\ (18)$$

$$F(x) = K_{ser} \cdot s_f(x) \qquad N_t(x) = -N_c(x) = N_{t,\max,full} \cdot \gamma_g(x) \qquad (19)\ (20)$$

$$N_{t,\max,full} = -\frac{\Delta\varepsilon_n}{H} \cdot \frac{(EI)_{full} - (EI)_{abs}}{(EI)_{full}} \cdot \frac{(EI)_{abs}}{H} \qquad M_i(x) = M_{i,\max,full} \cdot \gamma_g(x) \qquad (21)\ (22)$$

$$M_{i,\max,full} = \frac{\Delta\varepsilon_n}{H} \cdot \frac{(EI)_{full} - (EI)_{abs}}{(EI)_{full}} \cdot E_i I_i \quad \text{with } i = c,t \qquad (23)$$

$$\gamma_g(x) = 1 + \tanh(0.5\alpha l) \cdot \sinh(\alpha x) - \cosh(\alpha x) \qquad \Delta\varepsilon_n = \Delta\varepsilon_{n,t} - \Delta\varepsilon_{n,c} \qquad (24)\ (25)$$

$$(EI)_{abs} = E_c I_c + E_t I_t \qquad (EI)_{full} = (EI)_{abs} + (EA)^* \cdot H^2 \qquad (26)\ (27)$$

$$(EA)^* = \frac{E_c A_c E_t A_t}{(EI)_{abs}} \qquad \alpha = \sqrt{\frac{K_{ser}}{s_{ef}(EA)^*} \cdot \frac{(EI)_{full}}{(EI)_{abs}}} \qquad (28)\ (29)$$

$$s_{ef} = 0.75 s_{\min} + 0.25 s_{\max} \qquad H = 0.5h_c + t + 0.5h_t \qquad A_i = b_i h_i \qquad (30)\ (31)\ (32)$$

$$I_i = \frac{b_i h_i^3}{12} \qquad \sigma_t = -\sigma_c = \frac{N_t}{A_t} \qquad \sigma_{m,i} = \frac{M_i}{I_i} \cdot \frac{h_i}{2} \quad \text{with } i = c,t \qquad (33)\ (34)\ (35)$$

where:

u, s_f, F, N_i, M_i are the deflection, relative slip between concrete slab and timber beam, connector shear force, axial force and bending moment in the i member;

the subscript ' max ' refers to the maximum value of an effect along the beam axis;

the subscripts ' *abs* ' and ' *full* ' refer to the cases of TCC's with no connection and with rigid connection, respectively;

the subscripts 'c' and 't' refer to the concrete slab and timber beam, respectively;

x is the distance of the cross-section from the support, and l is the beam length;

$\Delta\varepsilon_{n,i}$ is the inelastic strain, uniformly distributed over the cross-section of the i member;

K_{ser} is the slip modulus of the connector for serviceability limit state verifications;

E_i, A_i, I_i, b_i, h_i, σ_i, $\sigma_{m,i}$ are the Young's modulus, cross-sectional area, second moment of area, breadth, depth, stress due to the axial force and stress due to the bending moment in the i member, respectively;

t, $s_{\min}$, $s_{\max}$ are the flooring thickness, minimum and maximum connector spacing, respectively.

INTERNATIONAL COUNCIL FOR RESEARCH AND INNOVATION
IN BUILDING AND CONSTRUCTION

WORKING COMMISSION W18 - TIMBER STRUCTURES

RECOMMENDED PROCEDURES FOR DETERMINATION OF DISTRIBUTION WIDTHS IN THE DESIGN OF STRESS LAMINATED TIMBER PLATE DECKS

K Crews

Centre for Built Infrastructure Research
University of Technology, Sydney

AUSTRALIA

MEETING THIRTY-NINE
FLORENCE
ITALY
AUGUST 2006

Presented by K Crews
I Smith asked why one did not use special barrel type washers to keep the tension. K Crews stated that it was tried but get some stress losses. Variation due to seasonal changes would be more important than creep losses. One would need to design maintenance procedures to check tension periodically.
G Schickhofer and Crews discussed the issue of shear strength. K Crews stated that shear strength was not an issue unless very short span; therefore in Australia and Canada, it wasn't an issue. T Williamson asked whether FRP rod had been tried to reduce the issue of creep. Crews answered that this would be at an experimental stage. FRP strand rather than FRP rod would be considered as rods might need sophisticated anchorage system.

RECOMMENDED PROCEDURES FOR DETERMINATION OF DISTRIBUTION WIDTHS IN THE DESIGN OF STRESS LAMINATED TIMBER PLATE DECKS

Professor Keith Crews
Deputy Director, Centre for Built Infrastructure Research
University of Technology, Sydney, Australia

SYNOPSIS

Stress laminated timber (SLT) decks are constructed by laminating individual pieces of timber placed side by side (on edge), until a solid deck of the desired width is achieved. The laminating is achieved by compressing individual timber members together by applying a prestress in the transverse direction, which "squeezes" the individual pieces of timber together, creating an orthotropic plate.

A number of approaches have been adopted for modelling the orthotropic behaviour of SLT plate decks. BS EN 1995-2: 2004 presents three of these as basic methods for design of SLT plate decks – orthotropic plate methods, grid (or grillage) modelling and the so called simplified method, which uses the concept of distribution width, to design the deck as a "wide beam."

This paper discusses the basis for modelling deck behaviour adopted in North America, Australia and Europe and compares the various predictions of distribution width, for a given material. Modification to some aspects of BS EN 1995-2: 2004 (Eurocode 5: Design of timber structures – Part 2: Bridges) are recommended that would lead to increased efficiencies in design using the "simplified method", based on the results of research in North America and Australia.

1 INTRODUCTION

Stress laminated timber decks are constructed by laminating individual pieces of timber placed side by side, until a solid deck of the desired width is achieved. The laminating is achieved by compressing individual timber members together by applying a prestress in the transverse direction as indicated in Figure 1, which "squeezes" the individual pieces of timber together, creating a solid timber deck.

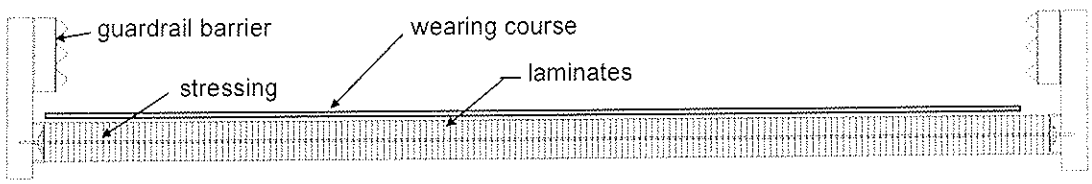

Figure 1 - Section through a Stress Laminated Timber Plate Bridge Deck

The system serves a dual purpose in providing a deck which is both the support for the wearing surface and also the structural system which resists the imposed loads and transfers resultant forces through to the substructure.

Once the prestress force is applied and maintained at or above the minimum design level, the stressed deck will behave as an orthotropic plate, effectively resisting loads, since these can be distributed laterally across some finite width of the deck (the distribution width) and then transferred longitudinally to the sub-structure. The most critical factor for design and maintenance of stress laminated timber deck systems, is to achieve and maintain adequate prestress force between the laminates so that the orthotropic plate action is maintained.

The compression force due to prestress allows transfer of vertical shear between the laminates through friction and also resists transverse bending which is induced by the loads, as shown in Figure 2. The initial compressive stresses commonly used in practice (in Australia) are of the order of 1200 kPa (1.2 N/mm^2) between the timber laminates.

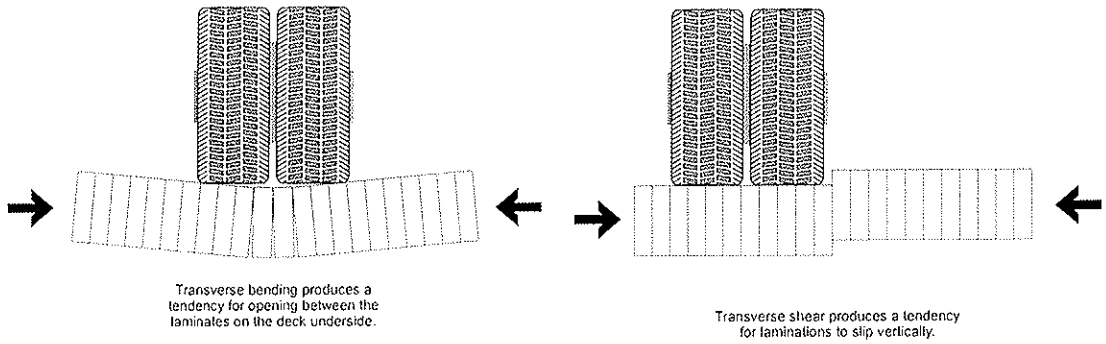

Figure 2 - Structural Actions of a Stress Laminated Timber Plate Bridge deck

2 DESIGN PROCESS FOR SLT PLATE DECKS

The critical phases in designing an SLT deck are:

- Designing the timber elements to have adequate stiffness and strength under flexural loading. This requires the use of a suitable model to represent the orthotropic plate behaviour and must also account for the effect of non continuous laminations (butt joints). Shear effects for longitudinal decks are not significant and are not considered.
- Selecting a suitable stressing system – bar sizes and spacings, such that the desired pressure between laminates is obtained, whilst minimising the effects of prestress losses
- Designing an anchorage and bearing system that transfers the post tensioning load into the deck
- Ensuring that the timber has adequate perpendicular to grain compression capacity to resist the prestress forces

3 MODELLING DECK BEHAVIOUR

A number of approaches have been adopted for modelling the behaviour of SLT plate decks. The basic analysis methods which can be used are as follows:

- Grillage Models
- Finite Element Models
- Orthotropic plate Models
- Modified Beam Models

BS EN1995-2: 2004 presents three of these as basic methods for design of SLT plate decks – orthotropic plate methods, grid (or grillage) modelling and the so called simplified method.

3.1 GRILLAGE MODELS

Grillage models are widely accepted for use in modelling and designing concrete decks. As such, some bridge designers adapt a grillage to model SLT decks and the use of grid or grillage is an acceptable means of analysis under Section 5.1 of BS EN1995-2: 2004.

In a study investigating the applicability of grid modelling, West [*1993*] demonstrated that calibrated grillage models can be used to accurately predict deflections and approximate moment distributions, particularly longitudinal moments, in stress laminated timber decks. However, calibration of material properties for lateral stiffness was necessary and the study concluded that the use of grillage models for design of SLT decks was considerably more complicated and time consuming than alternative methods, without providing any significant advantages for design.

3.2 FINITE ELEMENT MODELS

Finite element models can also be used in a similar way to orthotropic plate and grillage models for predicting plate performance with a reasonable degree of accuracy. However, once again the mesh

density determines the sensitivity of the model and accurate material properties in all principal axes are necessary in order to develop a reasonable model which gives good predictive results for in-service performance of a stress laminated timber deck. In addition, modelling the effects of prestress levels on transverse stiffness can also be problematic.

Both grillage and FEM methods are numerically intensive to varying extents and are generally more sophisticated than is necessary in order for designers to get a reasonably accurate prediction of SLT deck performance.

3.3 ORTHOTROPIC PLATE MODELS

In order to undertake an orthotropic plate analysis, three essential material properties are required. These are the longitudinal elastic bending modulus of the material E_L (based on four point modulus of elasticity (MoE) testing), the transverse stiffness based upon the transverse modulus properties of a plate E_T (determined from transverse loading) and the shear modulus for the timber plate G_{LT} which is generally determined by twisting plate tests and other methods.

The first comprehensive research program involving determination of elastic properties for orthotropic SLT plates was undertaken at Queens University, Ontario. These tests were based on twisting "square" plates approximately 1200mm x 1200mm x 120mm thick, using a method proposed by Tsai [*1965*]. During the mid 1980's, extensive testing was also undertaken at the University of Wisconsin and the Forest Products Laboratory - Madison, to verify the Canadian test results, characterise the behaviour of plate decks and develop analytical modelling techniques for predicting behaviour of SLT decks.

This testing program involved simulated truck loadings on full scale single lane decks spanning up to 24ft (7.3m) and investigated the effect of different anchorage systems, stress bar spacings and levels of prestress on deck behaviour [*Oliva et al - 1990*]. The results quantified the effect of prestress on apparent longitudinal stiffness and load distribution (which the smaller Canadian test specimens had failed to identify) and characterised plate parameters by undertaking twisting plate tests similar to those completed at Queens University. However, the relationships determined from both programs for characterising the transverse stiffness and shear modulus plate parameters differed significantly, with the Queens University tests yielding values between 35% and 50% higher than the FPL results, for the serviceability range of prestress (350 to 700 kPa or 0.35 to 0.7 N/mm^2).

In the period 1990 to 1992, R&D undertaken at the University of Technology, Sydney investigated orthotropic plate properties for various locally used timber species, and these values are listed below in Table 1. Unlike the North American tests which were based on plates 1.2m square, the transverse stiffness and the shear modulus for Australian timbers were derived from testing plate decks 3.6 metres by 3.6 metres, with depths of up to 290mm.

Table 1 - Orthotropic Plate parameters (prestress of 700 kPa)

timber species:	*Average* E_L *(MPa or N/mm^2)*	E_T / E_L	G_{LT} / E_L
Seasoned Hardwood (planed)	18500	1.8 %	2.2 %
Australian Pine (planed)	12000	2.0 %	2.9 %
Douglas fir (sawn)	9500	1.5 %	2.5 %

A comparison of orthotropic plate parameters (based on a reference prestress level of 700 kPa) is presented in Table 2, which highlights the variability of results derived using different testing methods and different species. Whilst surface finish clearly has a significant influence on the values of E_T (as does the level of prestress) there is basic agreement on these values internally. However, there is much more variability inherent in the derived values for G_{LT}, which does not appear to be as sensitive to variation in the surface finish. Basically, the higher MoE timbers used in Canada, and timber species tested in the USA and Australia, all have ratio values about 3%, whilst the Canadian timbers with lower MoE's and the specified European values are twice these value at 6%.

Table 2 – International Comparison of Orthotropic Plate parameters

Region / timber	E_T / E_L	G_{LT} / E_L
Australian – sawn	1.5 %	2.5 %
Australian – planed	2.0 %	3.0 %
Canadian – high MoE	2.0 %	3.5 %
Canadian – low MoE	2.5 %	5.5 %
USA – sawn	1.3 %	3.0 %
BS EN1995-2: 2004 – sawn	1.5 %	6.0 %
BS EN1995-2: 2004 – planed	2.0 %	6.0 %

Whilst surface finish clearly has a significant influence on the values of E_T (as does the level of prestress) there is basic agreement on these values internationally, at about 2% of E_L, as noted in Table 2. However, there is much more variability inherent in the derived values for G_{LT}, which does not appear to be as sensitive to variation in the surface finish.

Orthotropic plate models have been widely used to validate plate behaviour observed in laboratory tests and on prototype bridges constructed in Australia and the United States. These models are very similar and have been calibrated using both laboratory data and load test data obtained from field load testing of prototype bridges (see Figure 3).

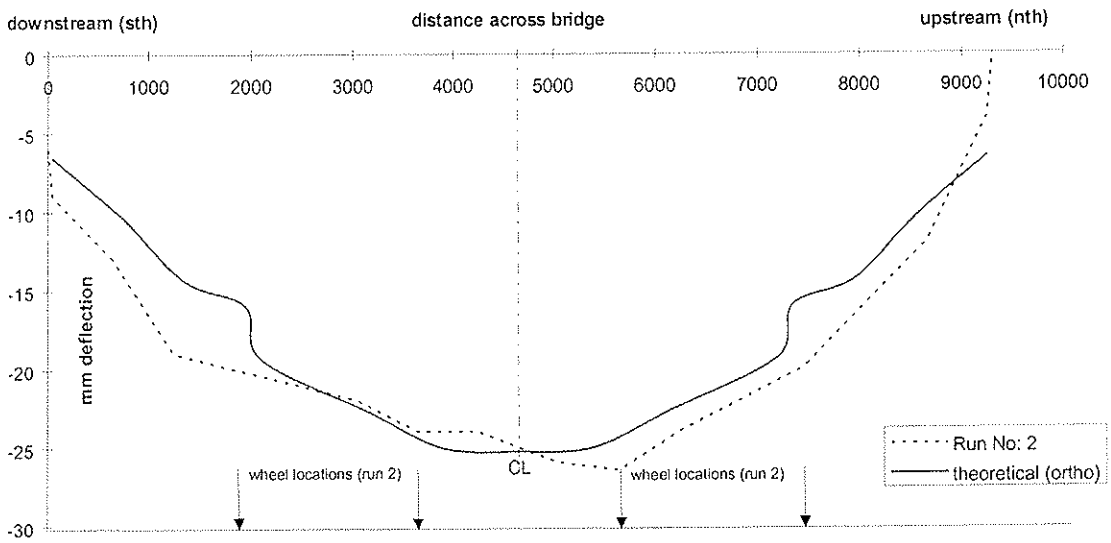

Figure 3 - Comparison of actual and predicted deflection plots

Whilst the orthotropic plate model provides a fairly accurate method of predicting deflections and moment distributions within a stress laminated timber deck (once the relevant plate properties are known), undertaking design using this analysis method is reasonably complex and can be computationally intensive. The method is also inherently sensitive to boundary conditions and as such it is best used as a research tool rather than as a routine design aid.

3.4 EQUIVALENT BEAM OR SIMPLIFIED ANALYSIS

The fourth method which is the most commonly used, is design the deck simply as a beam. The depth of this beam is equal to the deck thickness, whilst the width represents an idealised portion of the orthotropic plate deck over which the imposed loads (travelling along a wheel path) are distributed and resisted, as indicated in Figure 4.

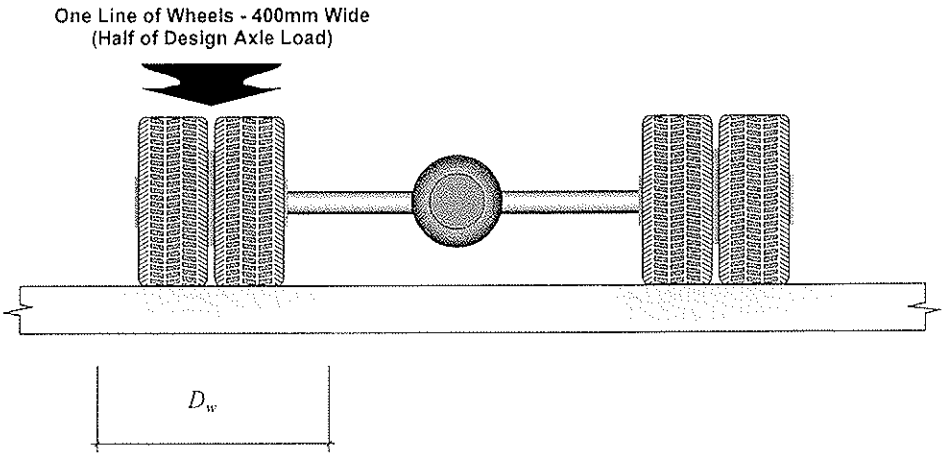

Figure 4 - Distribution widths for "normal" design vehicle

The width of this "equivalent beam" is known as the "distribution width" and it is used for predicting both the deflections (serviceability limit states) and longitudinal flexural capacity (ultimate strength limit state) of a stress laminated deck. As can be seen in Figure 3, the usual deflection profile for an SLT plate deck can be approximated by a parabolic distribution. However, this can be simplified by assuming that the peak deflection of the deck under load for the "equivalent beam" is constant across the distribution width, which is assumed to take all the load, whilst the remainder of the plate is assumed to carry no load and hence has deflections equal to zero. This is illustrated in Figure 5.

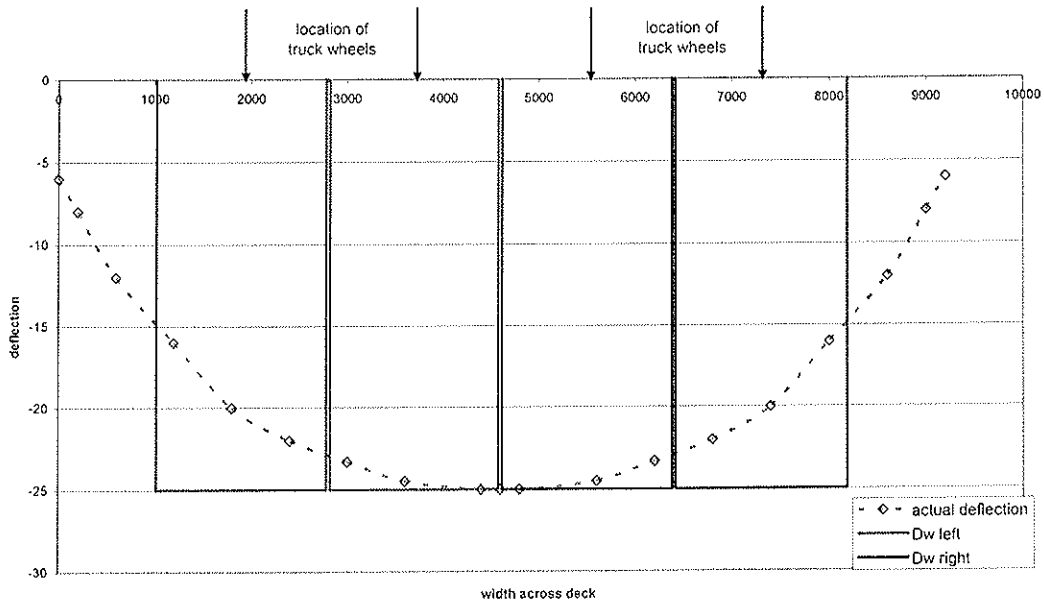

Figure 5 – Equivalent beams modelling the deflection of an SLT deck

Initial design procedures developed in the United States relied upon a series of nomographs for determining distribution widths, which were empirically derived as a function of the orthotropic plate properties and deck geometry. Most other design approaches involve use of a simple formula for estimating distribution widths. Either way, once the distribution width is determined, a stress laminated timber bridge deck can be analysed as either a simply supported or continuous beam.

The key element of these procedures and the extent of their accuracy is dependent upon the method used to determine the effective width of the beam. Provided the estimations for distribution width are representative of the true structural response of the bridge deck, modelling the decks as linear elastic beams is simple and the results obtained are accurate.

4 METHODS FOR DERIVING DISTRIBUTION WIDTH

Whilst the concept of a distribution width is familiar to most bridge engineers, the basis for derivation of such widths for SLT decks is not widely understood. Essentially, distribution widths specified in design codes for SLT decks have been derived in two ways; either by theoretical assumptions about load distribution in the deck, or on the basis of empirical data derived from testing.

4.1 SIMPLIFIED METHOD

The simplified method specified in Clause 5.1.3 of BS EN1995-2: 2004 is based upon a theoretical approach to the assumed dispersion of load through the timber laminations. For longitudinal laminations as used in most applications of SLT decks, the distribution beyond the edge of the actual wheel path is assumed to be 75 degrees to the horizontal. In other words, for a wheel path 400mm wide, and a deck depth of 300mm, the load dispersion is assumed to be approximately 561mm, and when combined with a distribution factor, the distribution width is 861mm, as indicated in Figure 6.

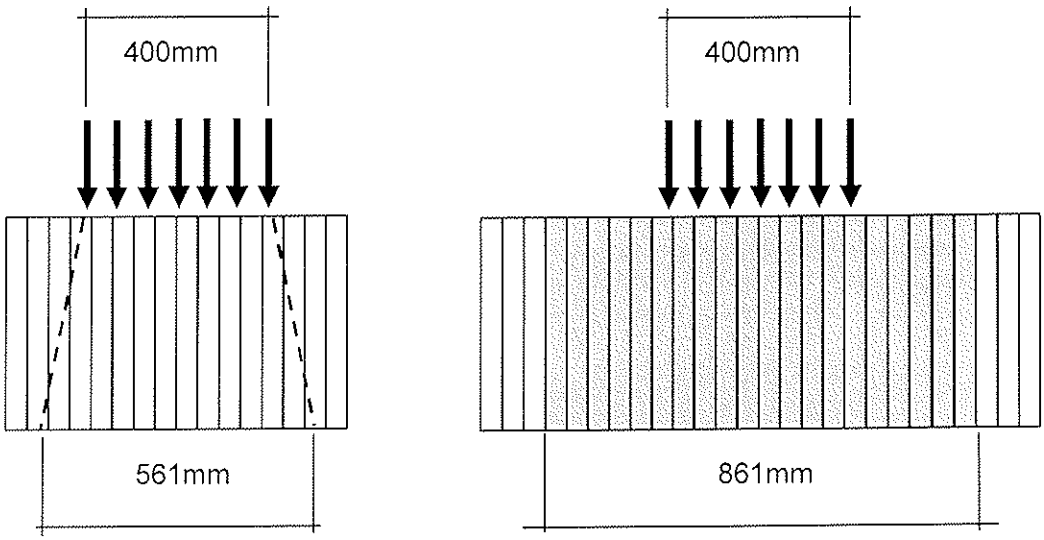

Figure 6 – (a) Dispersion of load, and (b) Distribution width – calculated using EN1995-2: 2004

4.2 DEFLECTION AREA METHOD

A relatively simple technique for predicting distribution widths from wheel path loads for plate decks is presented by Bakht [*1988*]. This involves using the deflections obtained from application of a wheel load and comparing the total area under the deflected shape of the orthotropic plate with the maximum or peak deflection, as indicated in equation 1:

$$D_t = \frac{A}{\Delta_{max}} \qquad \textit{equation: 1}$$

Where:
- D_t = the distribution width for a single wheel path load
- A = the total area under the deflected shape (at the critical transverse section)
- Δ_{max} = the peak value of deflection (at the critical transverse section)

Load testing of prototype bridges undertaken in Canada confirms that this method is acceptable, although perhaps slightly conservative. A similar technique has been used to derive the expressions for predicting distribution widths contained in the initial Australian limit states design procedures, using data obtained from extensive load testing on full scale bridge decks under both laboratory and field conditions. These expressions were based on a prestress of 1000 kPa (1.0 N/mm^2) (regardless of the timber species) which is the assumed serviceability prestress for Australian decks. For lower prestress levels the distribution widths calculated using equations 2 and 3 need to be reduced by 5% at 700 kPa (0.7 N/mm^2) and 10% at 550 kPa (0.55 N/mm^2) .

The expressions for predicting distribution widths [*Crews - 1995*] are reproduced below:

Single lane bridges (normal vehicle – 400mm wheel width):

$$D_{wi} = \left(\frac{E}{10000}\right)^{0.5} + \frac{L}{25} + 0.45 \qquad \textit{equation: 2}$$

Two lane bridges (normal vehicle – 400mm wheel width):

$$D_{wi} = \left(\frac{E}{18000}\right)^{0.4} + \frac{L}{30} + 0.45 \qquad \textit{equation: 3}$$

Where:

D_{wi} = the effective equivalent beam distribution width (m) - based on a 1 in 4 butt joint pattern for normal vehicle loading

E = the modulus of elasticity (MPa or N/mm^2)

L = the effective design span (m)

4.3 DEVELOPMENT OF SIMPLE PREDICTION FORMULAS

Equations 2 and 3 were originally developed to take account of the significantly higher values for flexural modulus of elasticity that occur for native Australian hardwoods. However, subsequent testing indicated that variations in MoE did not greatly change the distribution width, whereas the effect of prestress is more significant. As such, the equations have been simplified (as indicated below), based on a lower serviceability prestress of 700 kPa (0.7 N/mm^2), to take account of creep related losses which gradually occur over time.

Single and Two lane bridges (one design vehicle – 400mm wheel width):

$$D_{wi} = 1.5 + \frac{L}{20} \qquad \textit{equation: 4}$$

Two lane bridges (two design vehicles – 400mm wheel width):

$$D_{wi} = \left(1.5 + \frac{L}{20}\right) \times 0.85 \qquad \textit{equation: 5}$$

The effectiveness of these equations is illustrated in Tables 3 and 4. In Table 3 the "observed" distribution width for each of three load tests on a prototype bridge indicated in Figure 7, is estimated using Equation 1 (column 4). Equations 4 & 5 have been used to calculate the predicted value of distribution width shown in column 5. It is noted that the Equation 4 can be slightly conservative for a single truck on a two lane bridge, although for narrower two lane bridges the ratio is generally about 95%.

Table 3 – Analysis of deflection data to predict Distribution Width

LOAD TEST:	*Maximum deflection (mm)*	*Approx Area (mm^2)*	*Estimated Dw*	*Predicted Dw*	*Predicted / Estimated*
Run 1 – One vehicle u/s	21.5	94460	2196	1980	90%
Run 2 – Two Vehicles	26	176600	1698	1683	99%
Run 3 – One vehicle d/s	20	91170	2170	1980	91%

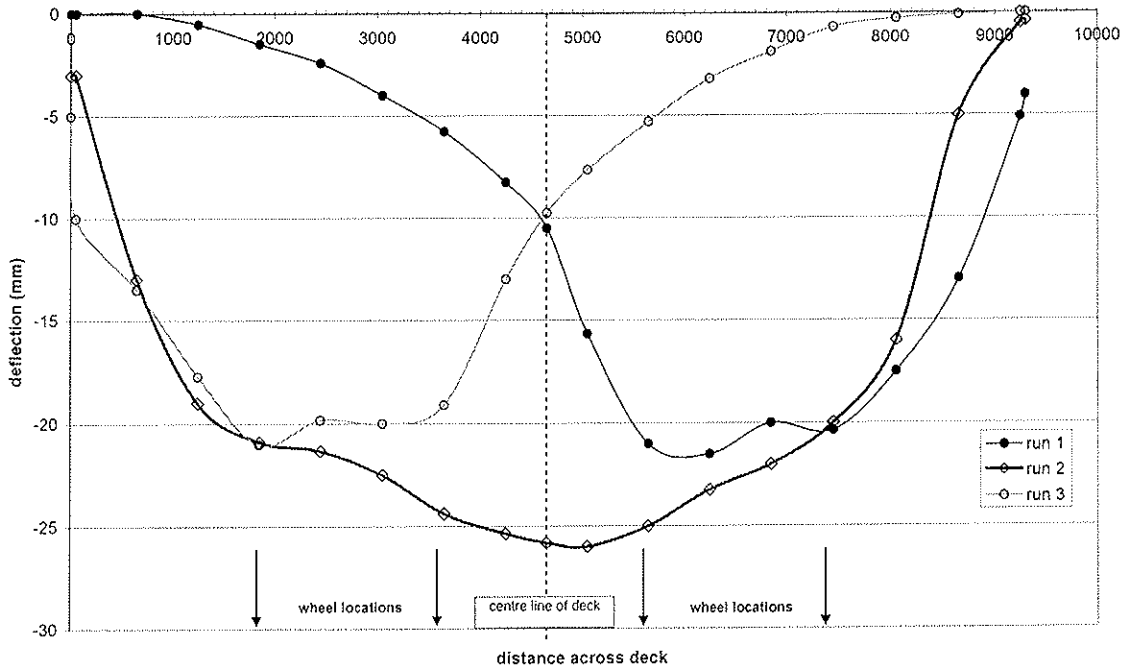

Figure 7 – Deflection data at midspan – Prototype bridge spanning 9.6m

Table 4 presents a summary of maximum deflection results obtained from testing 3 different plate bridges, where the distribution width has been estimated using equations 4 and 5.

Table 4 – Comparison actual and predicted maximum deflections, using predicted values of Distribution Width

Yarramundi Lagoon (800 kPa)	span (m)	depth (mm)	MOE (MPa)	Dw (m)	theoretical deflection	approx observed deflection	ratio (ob/th)
one lane loaded	9.3	290	18200	1.965	22.50	23	102%
two lanes loaded	9.3	290	18200	1.670	26.48	26	98%
McGraths Flat Lagoon (700 kPa)							
one lane loaded	9.6	340	12200	1.980	22.77	22	97%
two lanes loaded	9.6	340	12200	1.683	26.79	26	97%
McCarrs Creek (700 kPa)							
one lane loaded	6	290	12800	1.800	9.07	9	99%
two lanes loaded	6	290	12800	1.530	10.67	10.5	98%

4.4 COMPARISON OF INTERNATIONAL PRACTICES

A comparison of the various methods that have been used in North America, Australia and Europe for prediction of distribution width in SLT decks is presented in Figures 8 and 9. The Figures assume that the bridges have all been designed using softwood timber with an MoE of 10500 MPa (N/mm^2), with a live load deflection limitation of span / 400. The relevant equations from the OHBDC [*1991*] are reproduced below and it can be seen that the Canadian and Australian equations are quite similar.

Single lane bridges (one design vehicle – 400mm wheel width):

$$D_{wi} = 1.55 + \frac{L}{25}$$ *equation: 6*

Two lane bridges (two design vehicles – 400mm wheel width):

$$D_{wi} = 1.30 + \frac{L}{30}$$ *equation: 7*

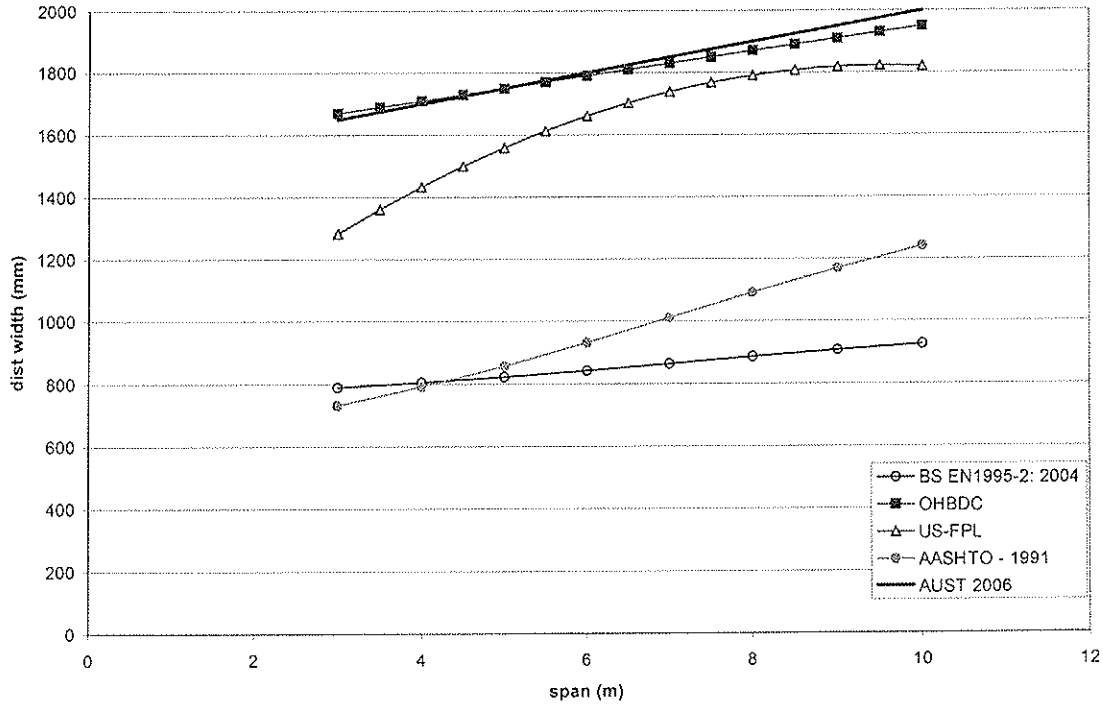

Figure 8 – Comparison of distribution width predictions – single lane bridges

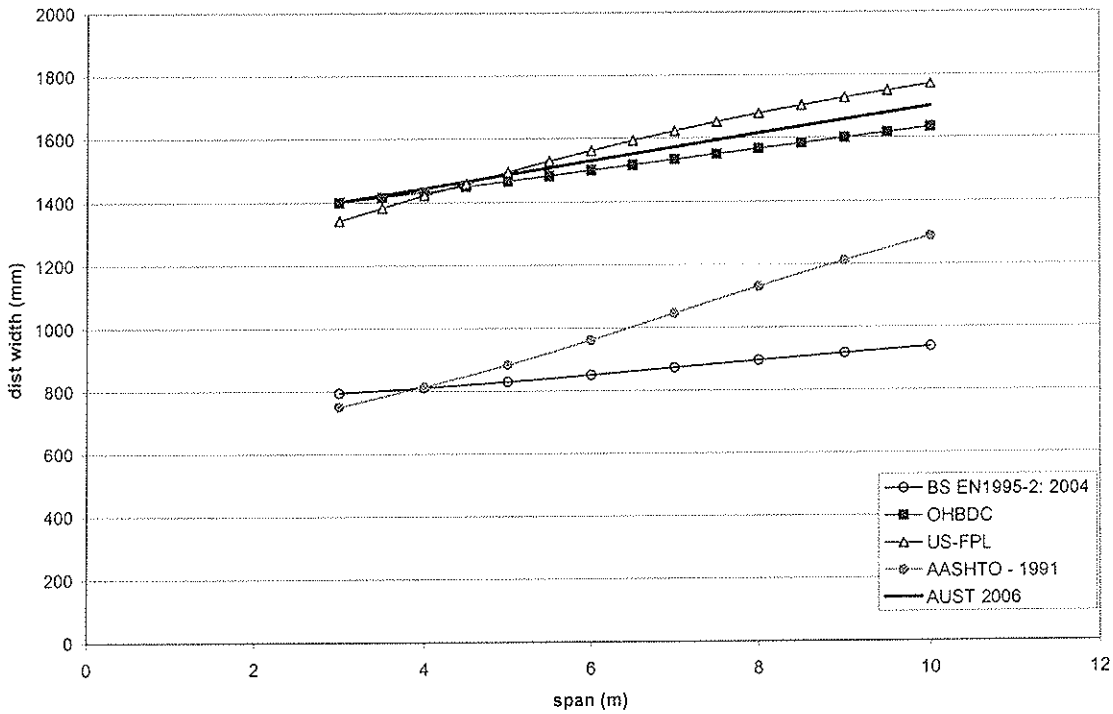

Figure 9 – Comparison of distribution width predictions – two lane bridges

The AASHTO [*1991*] method was first published in the interim design guidelines for use in the USA, but was later superseded by the "FPL" method, which was developed by Ritter [*1990, 1995*] following a widespread load testing program of prototype bridges. The OHBDC method was also developed from load testing and is now incorporated into the Canadian Bridge Design Code.

Distribution width predictions using equations 4 and 5 have also been compared with load test results from field monitoring programs undertaken in both Australia and North America and close correlations have been observed. The equations consistently predict maximum deflection for design load effects to within ± 5%; for example, maximum deflection of the bridge deck indicated in Figure 5, are 2% higher than those predicted using equation 5.

5 CONCLUSIONS AND RECOMMENDATIONS

Accurate prediction of the distribution width for design of an SLT plate deck has a major bearing on the economics of the structure, as well as being important for providing realistic assumptions for modelling the structural behaviour of the deck system. From Figures 8 and 9 it can be concluded that the current simplified method for determining distribution width specified in BS EN1995-2: 2004, is conservative when compared with other international methods, which have been derived from load testing of prototype stress laminated timber bridge decks.

Both the Canadian and Australian methods for predicting the distribution width are based on simple equations that have been found to have acceptable levels of accuracy and reliability when compared with the results of full scale load testing. It is therefore recommended that these same equations be assessed for applicability for modelling the load responses of European stress laminated timber plate bridge decks. This assessment should ideally be undertaken by analysis (using the equations presented in Section 4 of this paper) of data obtained from load testing of suitable bridges constructed from European timber species. The applicability of the equations would then be determined and if necessary adjustments made to produce a simplified set of equations that replace the current provisions of Clause 5.1.3 of BS EN1995-2: 2004 for longitudinal SLT decks.

6 REFERENCES

AASHTO [*1991*] - *"Guide Specifications for the Design of Stress-Laminated Wood Decks"* - American Association of State Highway and Transportation Officials, Washington DC

Bakht, B [*1988*] - *"Load Distribution in Laminated Timber Bridge Decks"* - ASCE Journal of Structural Engineering, Vol 114 - No 7 - July 1988

Crews, K [*1995*] - *"Recommended Guide for the Design of Stress Laminated Timber Plate Bridge Decks"* - Design Procedures & Commentary (pp 98) - Roads & Traffic Authority of NSW - Sydney, (edition 1.51) - May 1995 ISBN: 1 86365 146 2

OHBDC [*1991*] - *"Ontario Highway Bridge Design Code - Commentary "* - Ontario Ministry of Transportation, Downsview, Ontario - ISBN : 0-7729-9611-3

Oliva, M; Dimakis, A; Ritter, M; Tuomi, R [*1990*] - *"Stress-Laminated Wood Bridge Decks - Experimental and Analytical Evaluations"*, USDA- Forest Products Laboratory Research Paper FPL-RP-495, March 1990

Ritter, M [*1990*] - *"Timber Bridges - Design, Construction, Inspection and Maintenance"* - United States Department of Agriculture, Forest Service - Madison Wisc - June 1990

Ritter, M; Wacker, J; Duwadi, S [*1995*] - *"Field Performance of Stress Laminated Timber Bridges on Low-Volume Roads"* - 6th International Conference on low volume roads - Minneapolis MN - Proceedings Vol 2, pp 347 - 356, National Academy Press

Tsai, S [*1965*] - *"Experimental Determination of the Elastic Behaviour of Orthotropic Plates"* - Journal of Engineering for Industry. Transactions of American Society of Mechanical Engineers, August 1965 pp 315 -318

West, T [*1993*] - *"Investigation into Short span Stress Laminated Timber Bridges"* - University of Technology, Sydney, Undergraduate Project, June 1993

INTERNATIONAL COUNCIL FOR RESEARCH AND INNOVATION
IN BUILDING AND CONSTRUCTION

WORKING COMMISSION W18 - TIMBER STRUCTURES

IN-SITU STRENGTHENING OF TIMBER STRUCTURES WITH CFRP

K U Schober
S Franke
K Rautenstrauch

Department of Timber and Masonry Engineering
Bauhaus-University of Weimar

GERMANY

MEETING THIRTY-NINE
FLORENCE
ITALY
AUGUST 2006

Presented by S Franke
K Crews asked how many specimens were tested. S Franke responded that 4 very old beams were tested with debonding failure observed.
P Quenneville received confirmation that the FRP was not prestressed.
H Larsen discussed whether this type of work would be worth continuing on the basis of small gains. R Marsh suggested that the work dealt with existing structures up to 100 years old. Engineers would need guidelines to increase confidence on the performance of such structure to ascertain its engineering or economic life.
R Steiger stated that the R^2 value in figure 5 was meaningless.
L Uzielli wondered what would happen when one made a cut to insert the reinforcement when there was spiral grain. H Blass responded that it would depend on the size of t he cut and the severity of the spiral grain.
B Dujic commented on the issue of higher strength and stiffness but lower ductility would not be desirable.
T Williamson asked about glass versus carbon fibre. S Franke responded that glass fibre would be too soft and other projects have been underway.

In-situ strengthening of timber structures with CFRP

K. U. Schober, S. Franke and K. Rautenstrauch
Department of Timber and Masonry Engineering
Bauhaus-University of Weimar, Germany

1 Introduction

Particularly old timber structures in residential houses are designed for lower live loads as specified in performance and design standards and need new technologies to increase the load-carrying capacity of the members for state-of-the-art housing conditions. Therefore, a study of reinforcement techniques for restoration and strengthening of existing timber floors under bending loads has been carried out at the Bauhaus-University of Weimar, based on the use of carbon fibre reinforced plastics on the building site, whereby the removal of the overhanging part of the structure as well as the inserted ceiling is not necessary.

Reinforcement techniques for structural timber elements, based on the use of adhesives on site, have been applied for some decades as an extension of procedures that became very common for the repair or the upgrading of other structures. Some problems have prevented the wider use of adhesives, particularly in historical timber structures. One reason is that a life-long service life has not yet been fully proven for synthetic adhesives, since the oldest bonded joints are around sixty years and greater ages cannot be simulated by existing accelerated ageing tests. Although epoxy based adhesives have been used in most cases for on-site repair jobs, most formulations were developed for other materials. On-site application of adhesives is somewhat difficult and the consequent quality of adhesive bond is not easy to evaluate. Since properties of reinforced elements very much depend on the care put in the work, such difficulties have to be overcome and first procedures for applying and controlling were established (CEN TC 193/SC1/WG11 2003).

2 Experimental study

Two basic approaches are discussed here:

- the use of reinforcement materials embedded internal in the wood specimen,
- the use of external reinforcement resulting in a system of composite type.

The old solid wood beams were reinforced with a continuous carbon fibre lamella S&P 150/2000 with intermediate modulus fibres and 3.15 m length within the clear span for external reinforcement, otherwise over the full length of 3.50 m embedded in the wooden beams. The CFRP layer with a cross-section of 1.4 x 50 mm was embedded by means of the commercially available epoxy resin StoPox SK 41. The mean mechanical properties are shown in Table 1.

Table 1 Mean material properties of used epoxy resin and CFRP

Property	Unit	Epoxy Matrix	CFRP
Tensile Strength	MPa	75	2200
Tensile Modulus of Elasticity	GPa	2.8	164
Ultimate elongation	%	3.5	1.4
Density	g/cm³	--	--

Three different reinforcement schemes were evaluated in the testing program (Table 2). The gluing of the lamellas was done under practice-related conditions. The timber surface was primed using StoJet HIS, a two-part epoxy to saturate the wood prior gluing to avoid desiccation of the resin and to ensure a full compound between resin and wood surface.

Table 2 Dimensions of used timber beams and reinforcement schemes

Series	Height [cm]	Width [cm]	Type	Description
Vh	15.42...19.33	15.14...20.30	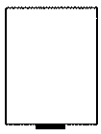	1 x 1.4 x 50 mm bonded centrally to the tension zone, horizontal on bottom
Vs	14.64...21.28	15.30...18.28		2 x 1.4 x 25 mm bonded laterally to tension zone 3 cm from bottom in slot
Vv	15.74...21.09	15.00...19.33	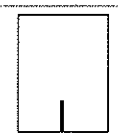	1 x 1.4 x 50 mm bonded centrally to the tension zone, vertical on bottom

For practice related investigations, preloaded spruce rafters and ceiling joists were used for the tests. The influencing factors like pre-ageing and weathering, moisture content when bonding, wood species, density, cross-section, existing cracks, knots and damages were analyzed. For determination of the strengthening effect after bonding and the Young's modulus of the specimen, the cross-sectional data including cracks and damages A, I and the averaged properties A_m, I_m where taken into account. A typical cross section and the outline for calculating the real cross section data are shown in Figures 1-2. Due to the usual existing cracks in historic timber beams, a reduction of the moment of inertia of about 8-23% (mean 17 %) could be observed. Based on the reviewed test specimen cross section, a section modulus modification factor, k_a of 0.8 may be justified generally for old timber beams that have similar properties and history as the beams used in this study.

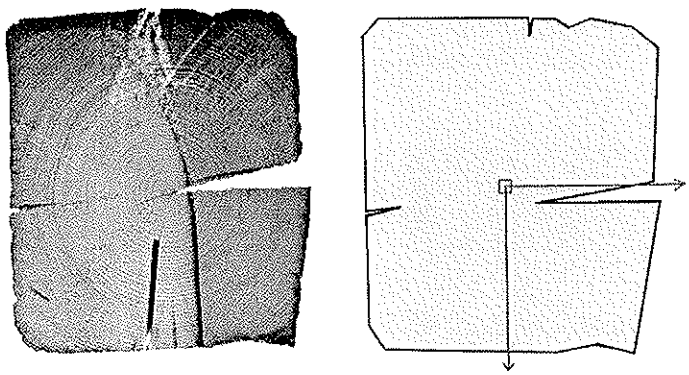

Figure 1-2 Typical cross-section of test specimen

For investigating the strengthening effect of the carbon fibre reinforcement in different, practice-related positions the flexural behaviour of all specimen were tested first within the elastic range with and without reinforcement (Schober and Rautenstrauch 2005a, 2005b). The tests of the un-reinforced beams were accomplished to determine the bending stiffness and the Modulus of Elasticity of the specimen within the elastic range. The tests were executed as a four-point bending test according to EN 408. The vertical and horizontal displacements of the beams were measured using inductive transducers in the span and on the support brackets (Figure 3), as well as 2D close range photogrammetry in the midspan of the specimen (Rautenstrauch et al. 2004). In test series 1 with external reinforcement strain gauges were placed on the external bonded CFRP lamella to obtain the elongation of the reinforcement itself (Figure 4).

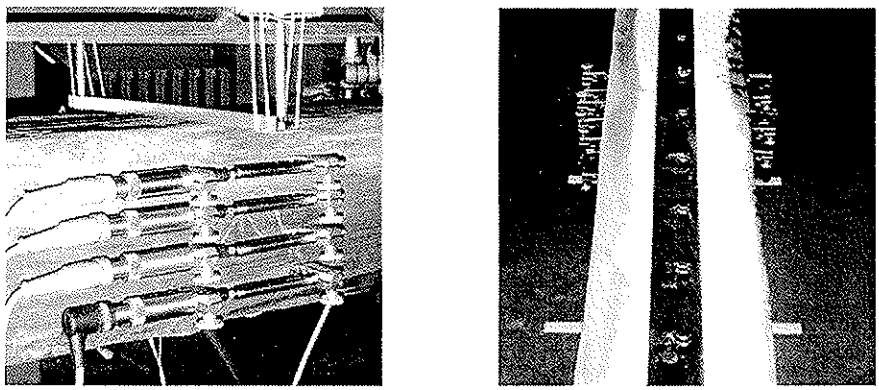

Figure 3-4 Deflection measurement on face and bottom of the specimen

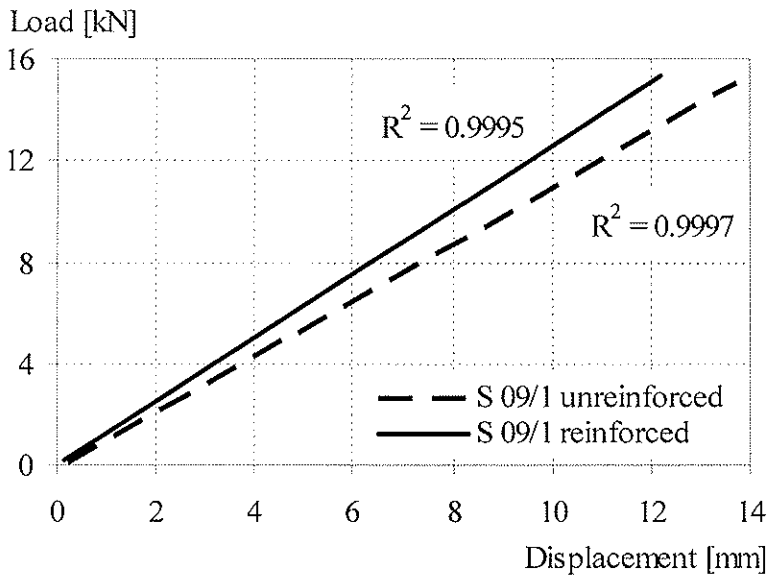

Figure 5 Load-deflection curve within the elastic range (regression line of 106 data points)

3 Structural response

Each piece of wood differs in the amount of stiffness-reducing defects such as knots, splits, and checks and therefore, it is hard to say at what stress level the other reinforced beams would have failed if they had not been reinforced. Such is the nature of wood. Several experimental tests (Triantafillou 1997; Borri et al. 2003) showed that the most frequent fracture mechanism is caused by the failure of the traction zone without the complete plasticization of the compression region, depending on the quality of the wood. First, the section shows a more ductile behaviour, while the stresses in the FRP material with reinforcement are highly increased and therefore, the composite material is more involved. Initially the load defection is shown to be linear elastic up to local failures induced by the presence of defects e.g. knots and cracks. Wood yielding produced a non-linear response terminated by a sudden drop of the load because of CFRP rupture. This was immediately followed by wood fracture in the tension zone, resulting in the collapse of the beams. The load-deflection behaviour of the different reinforcement schemes is shown in Figure 6.

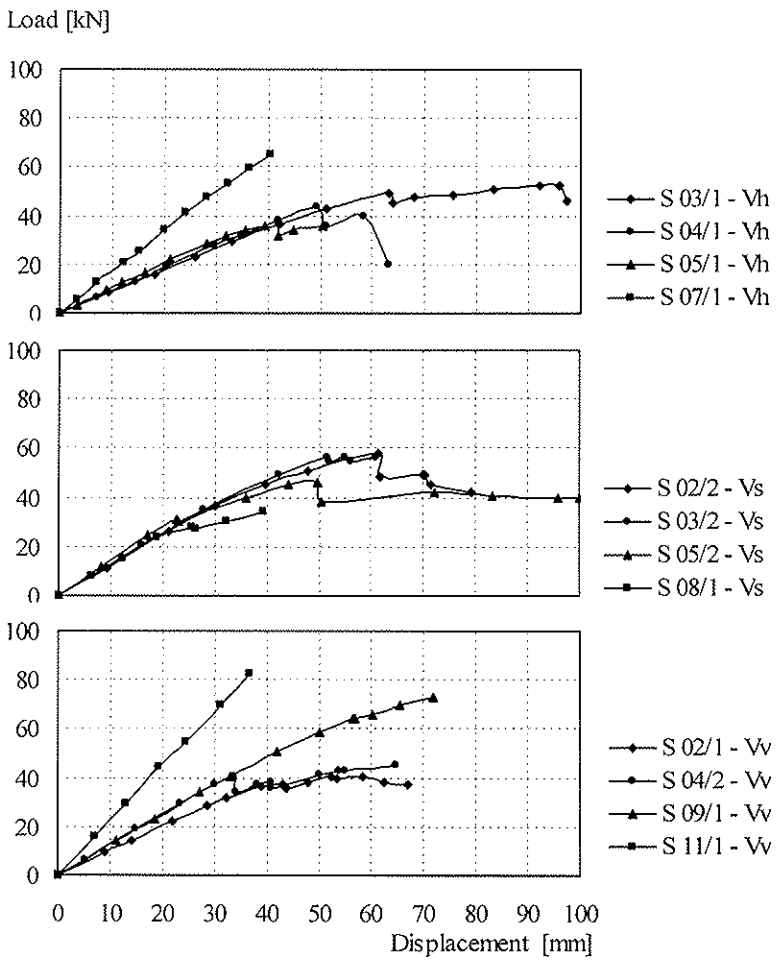

Figure 6 Load-deflection curves for different reinforcement types

The tests have shown that the most frequent failure mechanism is the one in which traction failure and shear failure occurs with or without partial plasticization of the compressed zone. The different failure modes for different strengthening methods are described in Schober and Rautenstrauch (2005a). A similar experimental and numerical approach for new glulam beams with pre-fabricated horizontal reinforcement over the full with was published by Blaß and Romani (2000, 2001). There, the bending stiffness is calculated in

the linear-elastic range and plastic deformations are not considered, since the stiffness is used for serviceability limit states and the stiffness increase for horizontal reinforced beams with a reinforcement over the full with.

It could be ascertained that on all tests in series 1 and 3 the Ultimate Load is reached within the linear range and on all tests of series 2 the specimen could not support further load increments after the first break. The increasing of the bending stiffness by applying CFRP reinforcement can been done by defining a fictitious Modulus of Elasticity, calculated from the cross-section data of the un-reinforced specimen:

$$E_{fict} = \frac{a \cdot \ell_1^2 \cdot (F_2 - F_1)}{16 \cdot I_m \cdot (w_2 - w_1)} \tag{1}$$

where F_2-F_1 denote the load increase in the elastic range, w_2-w_1 the equivalent deflection values difference, a the distance from the support to the loading point and ℓ_1 the span of the specimen. The reinforcing scheme increased the load bearing capacity by mean 5.86 % in comparison to the values measured for the un-reinforced wooden beams. The strength increase $k_{r,b}$ was defined as the bending stress of the reinforced specimen at the deflection in linear range before failure divided by the bending stress of the un-reinforced specimen at the same deflection value and shown for each series in Table 3.

$$k_{r,b} = \frac{max.\, w_{lin}}{max.\, w_{r,lin}} \cdot \frac{F_r(w_{r,lin})}{F(w_{lin})} \cdot \frac{(EI)_r}{EI} \tag{2}$$

Table 3 Comparison of the different load levels and the load-carrying capacity

Specimen	F_s [kN]	F_u [kN]	F_m [kN]	MOR [MPa]	MOE [MPa]	MOE_{fict} [MPa]	E_{fict} / E [%]	k_a ---	$k_{r,b}$ (series)
S03/1-Vh	22.00	50.46	53.46	53.52	12,622	14,390	113.99	0.78	
S04/1-Vh	18.00	44.46	44.46	48.14	14,900	15,546	104.34	0.79	
S05/1-Vh	21.00	38.06	38.06	35.68	13,229	14,875	112.45	0.83	
S07/1-Vh	39.00	66.23	66.23	39.01	10,744	12,163	113.20	0.80	1.12
S02/2-Vs	22.00	58.93	58.93	43.49	17,675	17,891	101.22	0.82	
S03/2-Vs	25.00	57.03	57.03	38.13	13,954	14,762	105.79	0.77	
S05/2-Vs	21.00	47.03	47.03	52.77	16,373	16,982	103.72	0.86	
S08/1-Vs	18.00	35.03	35.03	55.07	11,156	11,642	104.36	0.78	1.07
S02/1-Vv	22.00	38.96	41.06	58.17	15,837	16,742	105.71	0.91	
S04/2-Vv	27.00	41.76	46.16	44.75	18,747	17,823	095.07	0.88	
S09/1-Vv	32.00	73.86	73.86	37.57	10,837	11,427	105.45	0.92	
S11/1-Vv	49.00	86.13	86.13	25.07	17,770	18,604	104.96	0.79	1.09
						Mean	105.86	0.83	1.09
E_{fict} / E = $EI_{,reinf}$ / EI						COV	5.03	6.38	2.61

The wood beams reinforced with CFRP lamellas revealed more ductile behaviour with respect to un-reinforced beams. The presence of CFRP reinforcement arrest crack opening, confines local rupture and bridges local defects in the timber. Especially in reinforcement type Vh and Vs, with in wood embedded lamellas, an improvement of the load-carrying behaviour can be observed. The failure of the structure in this cases occurred by shear due to ripping of the section in longitudinal direction between cracks.

4 Numerical verification and design applications

Predicting the stiffness and strength increase that occurs when a timber beam is reinforced with carbon fibre is a complex problem and difficult to establish because of the natural defects that occur in wood and drastically reduce the stiffness. However, design of wood structures has been accomplished for decades by applying stress modification factors to the allowable design stress values according to national codes for a given size and grade of timber. Accordingly, allowable stress modification factors have been conceptually developed based on the experimental results from this study. With further research and more comprehensive testing, these modification factors could be used by engineers to determine the safe load carrying capacity of old timber beams reinforced with carbon fibre. A review of the load versus deflection curves shows the beams in this study behaved mostly in a linear manner up until failure. In addition to providing confinement, the carbon fabric adds tensile strength and allows the beams to yield more in compression before they fail in tension. Based on test results showing increases in bending stiffness of about 6% and flexural strength up to 25%, a bending stress modification factor, $k_{r,b}$ of 1.07 to 1.12, depending on the type of reinforcement, may be justified for beams reinforced with carbon fibres that have similar mechanical properties as the fibre used in this study. Further testing has to be done with a larger number of specimens to confirm these modification factors.

For investigation of the different reinforcement schemes and failure modes a non-linear finite element analysis was obtained using a delamination analysis and interface damage law described mathematically by Barenblatt (1962) and Needleman (1987). For a single-mode delamination, the non-smooth model results in an elastic relationship between the relative displacement and the traction in the interface between CFRP lamella, glue line and timber as long as the specific elastic energy stored Ψ is lower than the critical energy release rate G_c, and in a sudden loss of adhesion when $\Psi = G_c$. For mixed-mode delamination, an interaction criterion is adopted which is often used in practical applications (Allix and Corigliano 1996) and implemented in cohesive zone formulations for finite element codes. Full delamination occurs and the crack propagates as soon as the equation is satisfied which involves the ratio between the dissipated energy for each mode and the critical energy release rate characteristic of the mode itself.

Delamination of composite laminates, such as CFRP, have the peculiarity that the non-linear constitutive behaviour can be limited to a small region around the lamella where the crack propagates, while the remaining part of the structure can be assumed as linear elastic. The timber beam was modeled using symmetry conditions and the anisotropic properties obtained from the beam specimen, for the glue line cohesive interface elements were used. The geometry and load conditions are described above and illustrated with the cross-section mesh for lateral reinforcement in Figure 7-8.

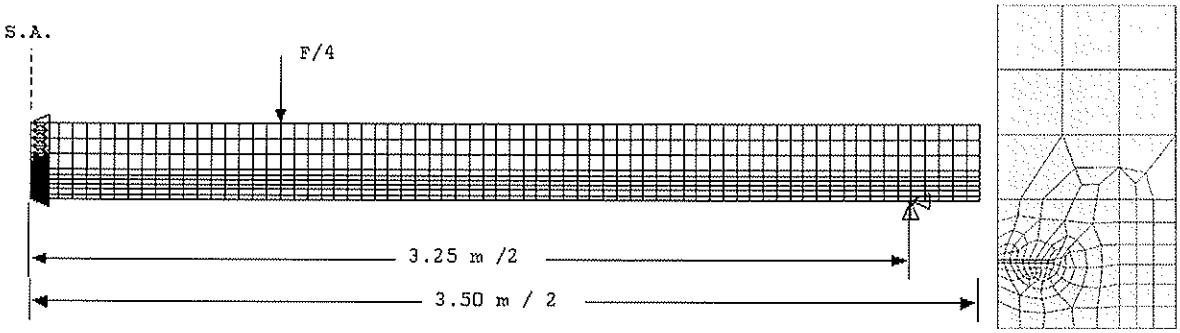

Figure 7-8 Test specimen for delamination simulation

The comparison of the obtained flexural behaviour and the numerical simulation are shown in Figure 9. Pre-existing cracks and fissures in the structure result in an overestimation of the bending stiffness in the delamination model. The investigation on this issue currently going on and will be reported after reviewing all results.

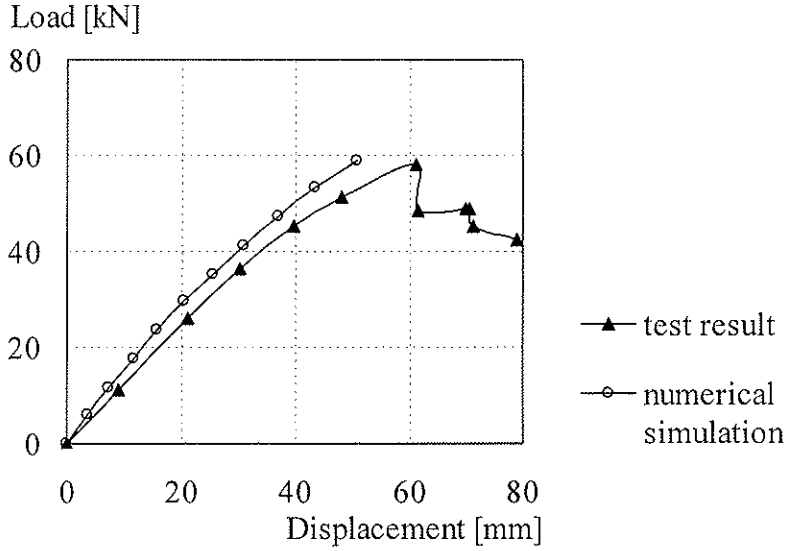

Figure 9 Load-deflection behaviour of specimen S02/2-vs with lateral reinforcement

5 Conclusions

The use of CFRP as a strengthening technique can be applied without necessitating the removal of the overhanging part of the structure. This is very promising in many cases of reinforcement of old, historical structural wood parts. Upgrading traditional timber structures of old solid wood with carbon fibre reinforcement on different locations are described and discussed here based on experimental investigations. For practice related investigations effective cross-sectional data including existing cracks, knots and damages were used with a reduction of the initial bending stiffness and the moment of inertia respectively of about 17 % compared to the cross-sections without defects. The results of the experiments have highlighted the limitations of the composite structure as well as the advantages of the various reinforcement positions and present numerous interesting aspects. The wood beams reinforced with CFRP lamellas revealed more ductile behaviour with compared to un-reinforced beams. The presence of CFRP reinforcement arrests crack opening, confines local rupture and bridges local defects in the timber especially for reinforcement types other than on the bottom face.

The various theories of bonding developed so far are not able to explain comprehensively the observed effects. Chemical bonding always has been seen as the optimal form of combining two surfaces with each other, but its contribution to the overall bonding mechanism is still unclear. The properties of the glue line can be described among other methods by the analysis of the microstructure of the bond surface. This includes the adhesive penetration into the wood surface, the effect of ageing of a glue bond as well as the description of the cohesive strength of the glue line in terms of an optimization of the brittle and elastic ratio of the glue line. These methods took into account by applying a numerical model for this reinforcement types using finite element cohesive zone modelling. These investigations are currently going on.

6 References

Allix, O. and Corigliano, A. (1996). "Modeling and simulation of crack propagation in mixed-modes interlaminar fracture specimens", *International Journal of Fracture*, 77, 111-140.

Barenblatt, G.I. (1962). "The mathematical theory of equilibrium cracks in brittle fracture", *Advances in Applied Mechanics*. 7, 55-129.

Blaß, H.J. and Romani, M. (2000). "Load-bearing capacity and deformation behaviour of FRP reinforced glulam composite beams", *Research report: Schlussbericht AiF-Vorhaben 11407/N*. Karlsruhe.

Blaß, H.J. and Romani, M. (2001). "Design model for FRP reinforced glulam beams", *International Council for Research and Innovation in Building and Construction, Working Commission W18-Timber Structures*, CIB-W18/34-12-3, Venice.

Borri, A *et al.* (2003). "FRP reinforcement of wood elements under bending loads", *Proceedings, Structural Faults and Repair*, London.

CEN TC 193/SC1/WG11 (2003). "Adhesives for on-site assembling or restoration of timber structures. On-site acceptance testing":

Part 1: Sampling and measurement of the adhesives cure schedule. Doc. N20.
Part 2: Verification of the shear strength of an adhesive joint. Doc. N21.
Part 3: Verification of the adhesive bond strength using tens. proof-loading. Doc. N22.

EN 408: (1995). "Timber structures - Structural timber and glued laminated timber. Determination of some physical and mechanical properties", CEN European Committee for Standardization.

Needleman, A. (1987). "A continuum model for void nucleation by inclusion debonding", *Journal of Applied Mechanics*, 54, 525-531.

Plevris, N. and Triantafillou, T.C. (1992). "FRP Reinforced wood as structural material", *Journal of Materials in Civil Engineering*, 4 (3), 300-315.

Rautenstrauch, K. *et al.* (2004). "Strain analysis of solid wood and glued laminated timber constructions by close range photogrammetry", *Third International Conference of the European Society for Wood Mechanics*, Villa Real, Portugal, 2004.

Schober, K.U. and Rautenstrauch, K. (2005a). "Strengthening of timber structures in-situ with an application of fiber-reinforced polymers", *FRP Composites in Civil Engineering – CICE 2004*, Seracino (ed). Taylor & Francis Group, London, ISBN 90 5809 638 6, 697-704.

Schober, K.U. and Rautenstrauch, K. (2005b). "Experimental investigations on flexural strengthening of timber structures with CFRP", *Proceedings of International Symposium on Bond Behaviour of FRP in Structures (BBFS 2005)*, Chen and Teng (eds). The International Institute for FRP in Construction, Hong Kong, 2005, ISBN 962-367-506-2, 465-472.

Triantafillou, T.C. (1997). "Shear reinforcement of wood using FRP materials", *Journal for Materials in Civil Engineering*, ASCE, 9(2), 65-69.

INTERNATIONAL COUNCIL FOR RESEARCH AND INNOVATION
IN BUILDING AND CONSTRUCTION

WORKING COMMISSION W18 - TIMBER STRUCTURES

EFFECT OF CHECKING AND NON-GLUED EDGE JOINTS ON THE SHEAR STRENGTH OF STRUCTURAL GLUED LAMINATED TIMBER BEAMS

B Yeh
T G. Williamson
Z A Martin

APA - The Engineered Wood Association

U.S.A.

MEETING THIRTY-NINE
FLORENCE
ITALY
AUGUST 2006

Presented by B Yeh
P Quenneville asked whether the effect of checks around the neutral axis would be evaluated. B Yeh stated that it was already done. If the length of crack was too long, one would need to consult engineer to investigate; therefore, only examined the most common cases.
A Ranta-Maunus stated in Finland work was performed in similar issue for the code.
I Smith stated that critical length and real length are very different and natural versus man-made cracks are also very different.
A Leijten commented that there must be natural reasons why these cracks occurred. B Yeh confirmed that the non-glue situation was artificial and not intended for production.
F Lam asked whether the artificially induced crack would close during loading and if so friction might develop. B Yeh stated that the gaps did closed but would not expect large shear transfer.
E Karacabeyli asked if there would be guidance when one had more than one check. B Yeh answered that the neutral axis case should be governing.
J Van de Kuilen suggested the case with cracks near the support, crack near the top of the beam rather than the bottom of the beam would be more serious because of compression perpendicular to grain. B Yeh answered that the bottom of the beam would see more shear stress.

Effect of Checking and Non-Glued Edge Joints on the Shear Strength of Structural Glued Laminated Timber Beams

Borjen Yeh, Ph.D., P.E.
Thomas G. Williamson, P.E.
Zeno A. Martin, P.E.
APA - The Engineered Wood Association, U.S.A.

Abstract

Shear strength of structural glued laminated timber (glulam) beams may be affected by the in-service conditions or manufacturing processes. While glulam is typically manufactured with kiln-dry lumber and therefore less susceptible to checking and splitting, glulam beams still check or split, usually at the first or second glueline and at the beam ends, as they gain or lose moisture in response to direct exposure to water, changing relative humidity and temperature in the surrounding environment.

Literature is available for determining the effect of checks or splits on the horizontal shear strength of glulam beams based on conservative assumptions. It is not uncommon for the architect, builder or homeowner to be alarmed when a significant check or split is found on a glulam beam. In many instances, however, the check or split may have limited influence on the horizontal shear strength of a glulam beam and the structural integrity of the glulam beam is not compromised. In order to define the boundaries of checks or splits, upon which the influence of such checks or splits can be safely ignored, APA - The Engineered Wood Association (APA) conducted a series of full-scale glulam beam tests based on the most common configurations and locations of checks or splits.

The glulam manufacturing processes may also affect the horizontal shear strength of a glulam beam. For example, the U.S. design code reduces the horizontal shear strength of a glulam beam when manufactured with non-glued edge joints using multiple pieces of side-by-side lumber and loaded in the direction parallel to the wide face of the laminations (y-y axis). The shear strength reduction is not required when such a glulam beam is loaded in the direction perpendicular to the wide face of the laminations (x-x axis). However, there is only limited data available to substantiate these cases. In support of a revision to the Japanese Agricultural Standard (JAS) for Structural Glued Laminated Timber, APA conducted a series of full-scale glulam beam tests to evaluate the effect of non-glued edge joints in multiple-piece layups on the horizontal shear strength of glulam beams. This paper describes the test results and findings from the checking and non-glued edge joint studies.

1. Introduction

Shear strength of structural glued laminated timber (glulam) beams may be affected by the in-service conditions or manufacturing processes. While glulam is typically manufactured with kiln-dry lumber and therefore less susceptible to checking and splitting, glulam beams still check or split, usually at the first or second glueline and at the beam ends, as it gains or loses moisture in response to direct exposure to water, changing relative humidity and temperature in the surrounding environment.

It is not uncommon for the architect, builder or homeowner to be alarmed when a significant check or split is found on a glulam beam. In fact, the effect of checking on the structural integrity of glulam beams is one of the most frequently asked questions received by the APA Helpdesk, which provides technical and educational support to timber engineers, specifiers, builders, distributors, building officials, and general public. In many instances, the check or split may be of limited influence on the horizontal shear strength of a glulam beam and the structural integrity of the glulam beam is not compromised.

While there are mathematical models, such as the fracture mechanics and finite element method, that are available for analyzing the effect of checks on glulam strength, most designers in the U.S. typically prefer to use a less sophisticated method, such as the prescriptive methods published by the glulam industry in North America [1]. In general, the glulam industry has recommended a simple methodology by proportioning the shear strength with the remaining unchecked cross section for side checks at the shear critical zone, defined as the areas at both ends of a simply supported beam within a distance from each end equal to 3 times the beam depth and within the middle 1/2 depth of the beam. For example, for a side check of 1/4 of the beam width, the shear strength of the glulam is assumed to be 3/4 of the published design value. Note that the length of the side check is not regarded as a factor. For end checks or splits, the effect is governed by the length of the end check, which is assumed to be 1/3 of a side check. For example, an end check of 30 mm (1.18 in.) in length is considered to be equivalent to a side check of 10 mm (0.39 in.) into the beam width.

While these simplistic guidelines have been successfully used in North America for years, there is very limited data available to support them. Furthermore, the existing methodology requires an engineering analysis to determine the extent of the strength reduction as long as there are any checks present. Throughout the years, many designers have expressed their desire to have an even simpler methodology by quantifying the limitation of checks upon which the effect of checks can be safely ignored. Accordingly, APA conducted a series of full-scale bending tests on glulam beams made with artificial checks, as described in the following sections.

On a related subject, the effect of non-glued edge joints in multiple-piece width layups on the glulam shear strength was recently questioned by glulam experts in Japan. In the U.S. design code, the horizontal shear strength of a glulam beam is reduced when the glulam beam is manufactured with non-glued edge joints in the laminations and loaded in the direction parallel to the wide face of the laminations (y-y axis). However, the shear strength reduction is not required when the glulam beam is loaded in the direction perpendicular to the wide face of the laminations (x-x axis). These code provisions have very limited data available to substantiate them. In support of a revision to the JAS glulam standard [2], APA conducted a series of full-scale glulam beam tests in November 2005 to evaluate the effect of non-glued edge joints on the horizontal shear strength of glulam beams.

2. Materials and Test Methods

2.1 Checking Study

Glulam beams with no glue on a portion of the wide face of certain laminations were manufactured to simulate the effect of seasoning checks. Two sets of artificially checked beams were manufactured and tested. One set of beams had "checks" (unglued faces) in the ends (Group E), while the other set had a check in the middle (Group M) of the beam

span at the first glueline. Note that the end checks were actually full-width splits that represent the worse case conditions for a check or split.

Douglas-fir glulam beams with a dimension of 130 mm x 457 mm x 4724 mm (5-1/8 in. x 18 in. x 186 in.) were manufactured in accordance with the *American National Standard for Wood Products - Structural Glued Laminated Timber*, ANSI A190.1 [3], using the 24F-V4/DF layup combination that is the most popular in the U.S. The beam size was selected in accordance with the full-scale test setup for evaluating the shear strength of glulam beams, as specified in Annex A7 of ASTM D3737 [4], with the exception that the span-to-depth ratio was set at 10:1 and the loading was applied at the third points of the span. The span-to-depth ratio of 10:1 was determined based on a structural analysis as the critical ratio for the shear strength to govern the ultimate beam performance for a simply supported beam subjected to uniform loads. When the span-to-depth ratio is greater than 10:1, the bending strength or deflection is expected to govern the beam design. The locations of the unglued faces used to simulate the seasoning checks are shown in Figures 1 and 2. The bearing plates were 152 mm (6 in.) in length.

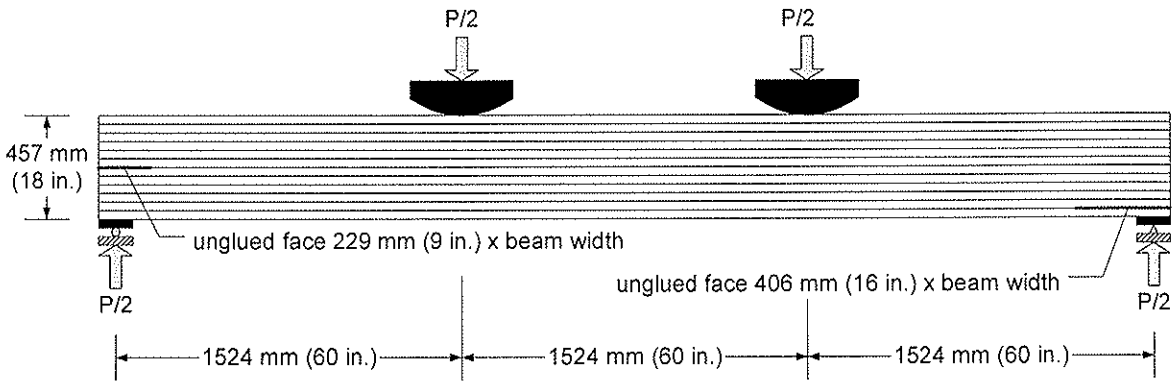

Figure 1. Group E beam test setup, and size and location of unglued faces

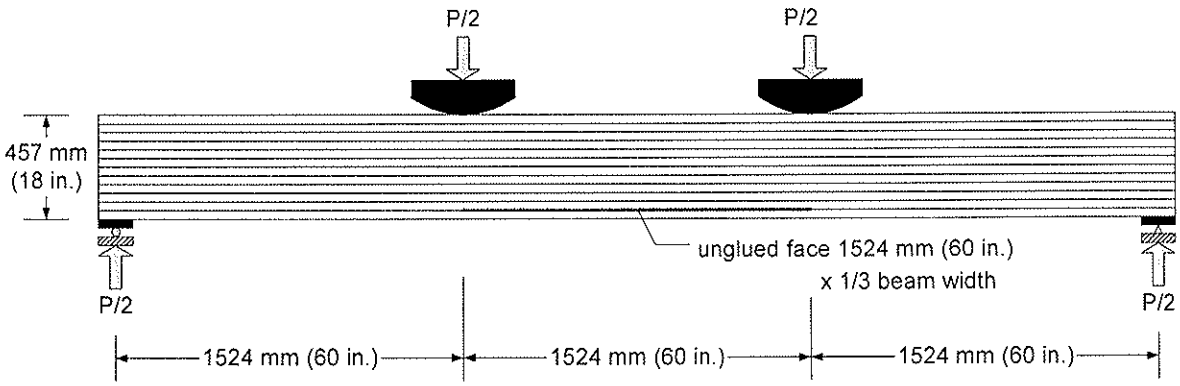

Figure 2. Group M beam test setup, and size and location of unglued faces

The locations of the unglued faces for Group E beams (Figure 1) were selected to evaluate the end checks in a "green zone", as shown in Figure 3. Based on a survey of major glulam distributors in North America, the end check within the green zone represents the vast majority of end checks observed in the field. It was anticipated that within the "green zone," the end checks, as simulated by the unglued faces, would not affect the beam performance. The location of the unglued faces for Group M beams (Figure 2) was intended for the evaluation of the side checks in the moment critical zone due to the

frequently occurred checks at the first glueline. The actual depth of the side check manufactured into Group M beams was 51 mm (2 in.), which is 1/3 of the nominal beam width of 152 mm (6 in.).

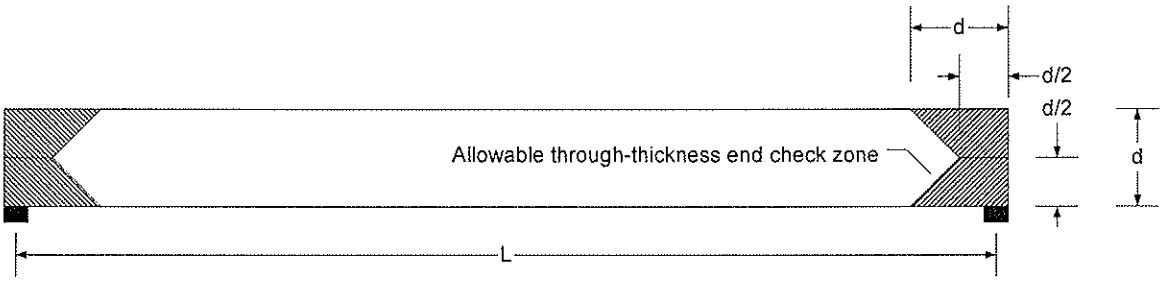

Figure 3. "Green zone" for end checks or splits

In order to create the unglued faces, wax paper and tape were used to cover a portion of a lamination as it went through a glue spreader, as shown in Figures 4 through 6. The tape and wax paper were then removed, leaving a clean non-glued face on the lamina, before the beam layup and clamping.

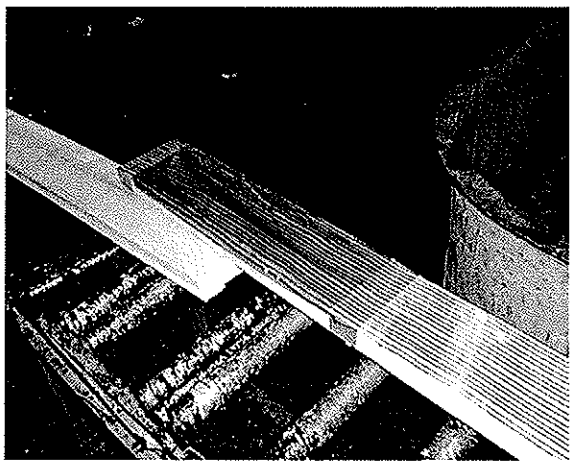

Figure 4. Taped wax paper was applied to a lamina as glue was spread (Group E)

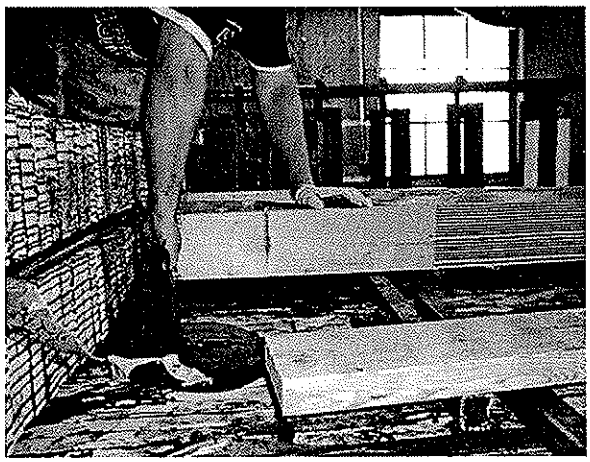

Figure 5. Taped wax paper was then removed from the lamina prior to clamping (Group E)

2.2 Non-Glued Edge Joint Study

The glulam beams used for the non-glued edge joint study were manufactured with Douglas-fir laminations using the JAS E120-F330 layup combination. Since the objective of this study was to evaluate the effect of non-glued edge joints on the glulam shear strength, the tested beams were manufactured without end joints to minimize bending failures. The beam sizes and non-glued edge joints are shown in Figures 7 and 8.

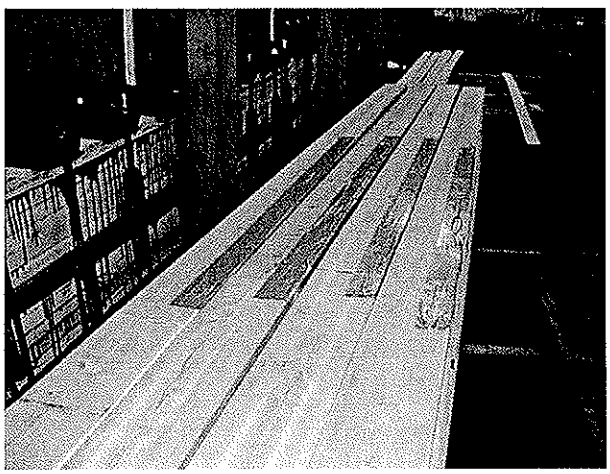

Figure 6. Tape used to create unglued surface (Group M)

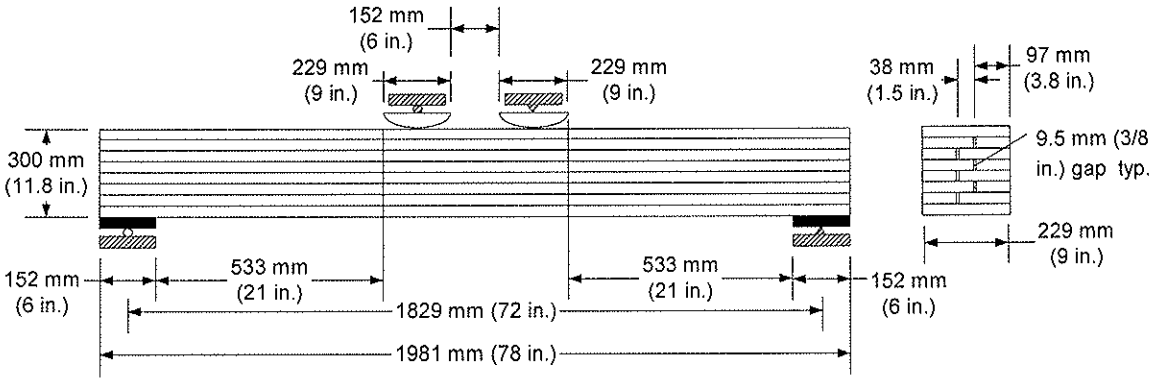

Figure 7. Group X beams

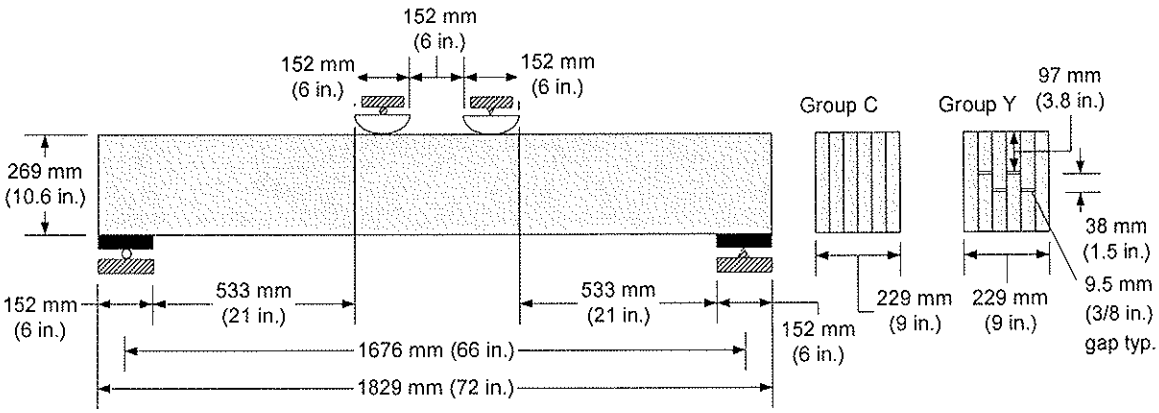

Figure 8. Groups C and Y beams

The face laminations for all beams tested in this study were full width. Middle and inner laminations for Group X in the x-x orientation and Group Y in the y-y orientation were not edge-glued. The gap of the non-glued edge joints between side-by-side lumber laminations was manufactured to 9.5 mm (3/8-in.), which is the maximum gap permitted in ANSI A190.1 [3]. The "control" beams (Group C in the y-y orientation) were manufactured from full-width laminations in accordance with the JAS E120-F330 layup combination.

3. Test Methods

Full-scale beam tests were conducted in accordance with ASTM D198 [5] and D3737 [4]. All beams were tested in the as-received conditions. The mean moisture content and specific gravity (based on oven-dry weight and as-received volume) of the glulam beams used in the checking study was approximately 14% and 0.46, respectively.

4. Results and Discussions

4.1 Checking Study

A summary of test results is given in Tables 1 and 2. All beams failed in bending for both beam groups with the exception of Beam E6, which failed in shear (at the end check location), and Beam M9, which failed as a result of bearing failure at one of the end reactions. Note that the mean MOR values from both beam groups are very similar and the minimum MOR values are still at the expected level, 2.1 x 16.5 or 34.7 MPa, (2.1 x 2,400 or 5,040 psi) for 24F glulam beams despite the simulated checks at the shear and moment

critical zones. Beam E6 that failed in shear at the end check location still had a shear strength, 2.96 MPa (430 psi), which meets the allowable shear stress of 2.92 MPa (265 x 1.6 or 424 psi) for Douglas-fir glulam beams after taking into account the short load duration at test. These results suggest that the glulam beam performance is not compromised by the end checks and side checks tested in this study.

Table 1. Summary of test results for Group E beams

Beam #	Width (mm)	Depth (mm)	Max Load (kN)	Bending Stress[(a)] (MPa)	Shear Stress[(a)] (MPa)	Failure Mode
E1	130.3	457.2	232.7	39.1	2.93	Bending
E2	129.9	457.2	207.9	35.0	2.62	Bending
E3	130.0	457.2	217.9	36.7	2.75	Bending
E4	130.0	457.2	216.0	36.3	2.73	Bending
E5	129.9	457.2	210.7	35.5	2.66	Bending
E6	130.1	457.2	235.0	39.5	2.96	Shear
E7	130.0	455.6	247.0	41.8	3.13	Bending
E8	129.7	456.4	270.3	45.7	3.42	Bending
E9	129.5	456.4	219.1	37.1	2.78	Bending
E10	130.2	454.8	243.7	41.4	3.09	Bending
E11	129.7	455.6	246.0	41.8	3.12	Bending
E12	129.8	454.8	238.0	40.5	3.02	Bending
N	12	12	12	12	12	
Minimum	129.5	454.8	207.9	35.0	2.62	
Maximum	130.3	457.2	270.3	45.7	3.42	
Mean	129.9	456.4	232.0	39.2	2.93	
COV	--	--	0.079	0.082	0.081	

[(a)] Stress at the time of beam failure

Table 2. Summary of test results for Group M beams

Beam #	Width (mm)	Depth (mm)	Max Load (kN)	Bending Stress[(a)] (MPa)	Shear Stress[(a)] (MPa)	Failure Mode
M1	129.6	457.2	268.8	45.4	3.40	Bending
M2	129.7	457.2	280.0	47.2	3.54	Bending
M3	129.9	457.2	215.9	36.3	2.73	Bending
M4	129.9	457.2	231.7	39.0	2.93	Bending
M5	129.8	457.2	226.6	38.2	2.86	Bending
M6	130.1	457.2	224.4	37.7	2.83	Bending
M7	130.1	457.2	251.3	42.2	3.17	Bending
M8	129.7	456.4	211.2	35.8	2.68	Bending
M9	130.0	456.4	239.2	40.4	3.02	End bearing
N	9	9	9	9	9	
Minimum	129.6	456.4	211.2	35.8	2.68	
Maximum	130.1	457.2	280.0	47.2	3.54	
Mean	129.9	457.0	238.8	40.2	3.02	
COV	--	--	0.099	0.099	0.099	

[(a)] Stress at the time of beam failure

4.2 Non-Glued Edge Joint Study

The Group X beam results (shear in the x-x orientation with non-glued edge joints) are given in Table 3. All 3 beams failed in shear.

Table 3. Summary of test results for Group X beams

Beam #	Width (mm)	Depth (mm)	Max Load (kN)	Bending Stress[(a)] (MPa)	Shear Stress[(a)] (MPa)	Failure Mode
X1	231.7	302.4	394.7	40.4	4.22	Shear
X2	231.8	302.2	392.7	40.3	4.20	Shear
X3	231.8	303.0	425.4	43.4	4.54	Shear
Mean	231.8	302.5	404.2	41.4	4.32	
COV	--	--	0.045	0.043	0.044	

[(a)] Stress at the time of beam failure

The mean shear strength of these beams, 4.32 MPa (627 psi), is comparable to the mean shear strength of 4.41 MPa (639 psi), as reported in CIB W18/34-12-2 [6] for 171-mm (6-3/4-inch) wide Douglas-fir glulam beams without any edge joints (full-width laminations). Therefore, the non-glued edge joints in this study did not have an effect on the shear strength of glulam beams in the x-x orientation.

The Group C (control without edge joints) and Group Y beam test results (shear in the y-y orientation with non-glued edge joints) are given in Tables 4 and 5. Noted that 4 out of 10 Group C beams failed in bending. This percentage of shear failure is parallel to the results given in CIB-W18/34-12-2 [6]. On the other hand, all Group Y beams failed in shear. With this difference in failure modes, the data can be compared as follows:

Table 4. Summary of test results for Group C (control) beams

Beam #	Width (mm)	Depth (mm)	Max Load (kN)	Bending Stress[(a)] (MPa)	Shear Stress[(a)] (MPa)	Failure Mode
C1	228.0	271.1	428.7	52.7	5.20	Bending
C2	228.8	271.1	450.8	55.1	5.45	Shear
C3	227.4	270.6	438.1	54.1	5.34	Bending
C4	227.9	271.2	407.7	50.0	4.95	Shear
C5	228.9	270.6	440.5	54.1	5.33	Bending
C6	229.8	270.8	420.8	51.4	5.07	Shear
C7	229.3	270.8	444.1	54.3	5.36	Shear
C8	229.0	270.7	308.5	37.8	3.73	Shear
C9	229.0	270.7	442.5	54.2	5.35	Bending
C10	229.0	270.9	398.0	48.7	4.81	Shear
N	10	10	10	10	10	
Minimum	227.4	270.6	308.5	37.8	3.73	
Maximum	229.8	271.2	450.8	55.1	5.45	
Mean	228.7	270.9	418.0	51.3	5.06	
COV	--	--	0.101	0.101	0.101	

[(a)] Stress at the time of beam failure

1) If the difference in the failure mode is ignored, the mean shear strength of 4.32 MPa (626 psi) for Group Y beams is about 85% of the mean shear strength of 5.06 MPa (734 psi) for Group C beams. Similarly, the minimum shear strength of 3.64 MPa (528

psi) for Group C is about 98% of the minimum shear strength of 3.73 MPa (541 psi) for Group C beams. Note that the minimum shear strength for Group C beams was caused by a shear failure.

Table 5. Summary of test results for Group Y beams

Beam #	Width (mm)	Depth (mm)	Max Load (kN)	Bending Stress[(a)] (MPa)	Shear Stress[(a)] (MPa)	Failure Mode
Y1	229.1	270.2	370.7	45.6	4.49	Shear
Y2	228.7	270.1	299.8	37.0	3.64	Shear
Y3	228.9	270.5	328.1	40.3	3.97	Shear
Y4	229.5	271.2	383.4	46.7	4.62	Shear
Y5	228.7	270.8	382.9	47.0	4.64	Shear
Y6	229.0	270.7	385.3	47.3	4.66	Shear
Y7	229.4	271.1	334.2	40.8	4.03	Shear
Y8	228.8	270.5	341.8	42.0	4.14	Shear
Y9	229.0	271.2	395.6	48.3	4.78	Shear
Y10	229.1	270.8	348.6	42.7	4.22	Shear
N	10	10	10	10	10	
Minimum	228.7	270.1	299.8	37.0	3.64	
Maximum	229.5	271.2	395.6	48.3	4.78	
Mean	229.0	270.7	357.1	43.8	4.32	
COV	--	--	0.087	0.086	0.086	

[(a)] Stress at the time of beam failure

2) If the data due to bending failure in Group C is ignored, the mean shear strength for Group C beams that failed in shear is 4.90 MPa (710 psi). Therefore, the mean shear strength of 4.32 MPa (626 psi) for Group Y is about 88% of the mean shear strength of 4.90 MPa (710 psi) for Group C beams. The comparison on the minimum shear strength, as given in 1) above, remains unchanged.

Based on the methodology currently adopted by the glulam industry in the U.S., the Group Y beams with non-glued edge joints would be designed with 2/3 of the shear strength of the Group C (control) beams because the non-glued edge joints result in a 1/3 less area at the critical shear plane. However, according to the analysis given above, the glulam beams with non-glued edge joints in the y-y orientation have 85 - 88% of the shear strength obtained from the control beams. Therefore, results from this study confirm that the methodology currently adopted by the glulam industry in the U.S. is quite conservative.

5. Conclusion

Based on the test results, the presence of unbonded areas between laminations, as could be caused by seasoning checks, does not affect the performance of glulam beams. A new publication on this subject, *Owner's Guide to Understanding Checks in Glued Laminated Timber* [7] was developed and released by APA in March 2006. Figure 9 shows a flow chart included in the Guide, which provides simple guidance for evaluating glulam checks. Note that an engineering analysis is still required when a check exceeds the limitations specified in the Guide. For simplistic reasons, the Guide does not prescribe the "green zone" shown in Figure 3, which is justifiable based on the test data given in this paper.

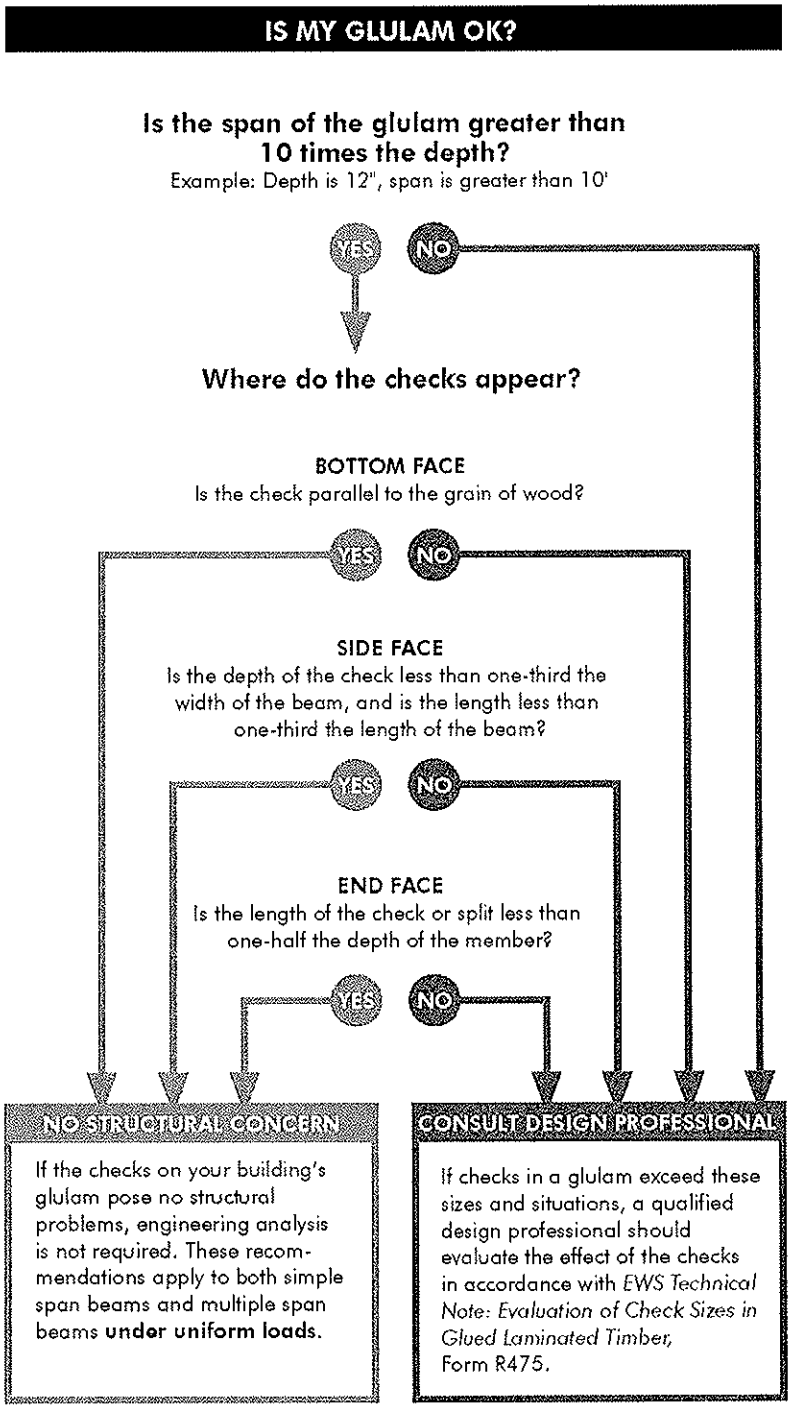

Figure 9. Guidelines for evaluating glulam checks

For the non-glued edge joints, the glulam shear strength is not affected by the non-glued edge joints in the x-x orientation based on the test results reported above. The effect of non-glued edge joints on the glulam shear strength in the y-y orientation can be conservatively estimated in accordance with the methodology currently adopted by the glulam industry in the U.S. These results have been used to support the revision of the JAS glulam standard to permit the use of non-edge glued joints in the core and inner laminations of JAS glulam beams. Further research on a more realistic strength reduction factor due to non-glued edge joints is recommended.

6. References

1. APA - The Engineered Wood Association. 1999. Evaluation of Check Size in Glued Laminated Timber Beams. Form R475. Tacoma, WA.

2. JAS. 2003. Japanese Agricultural Standard for Structural Glued Laminated Timber. Notification No. 235. The Ministry of Agriculture, Forestry and Fisheries. Tokyo, Japan.

3. American National Standards Institute. 2002. American National Standard for Wood Products - Structural Glued Laminated Timber. ANSI A190.1. New York, NY.

4. ASTM International. 2005. Standard Practice for Establishing Allowable Properties for Structural Glued Laminated Timber (Glulam). ASTM D3737. West Conshohocken, PA.

5. ASTM International. 2005. Standard Test Methods of Static Tests of Lumber in Structural Sizes. ASTM International. ASTM D198. West Conshohocken, PA.

6. Yeh, B. and T.G. Williamson. 2001. Evaluation of glulam shear strength using a full-size four-point test method. In proceedings of the 34th International Council for Research and Innovation in Building and Construction, Working Commission W18 - Timber Structures. Venice, Italy.

7. APA - The Engineered Wood Association. 2006. Owner's Guide to Understanding Checks in Glued Laminated Timber. Form F450. Tacoma, WA.

INTERNATIONAL COUNCIL FOR RESEARCH AND INNOVATION
IN BUILDING AND CONSTRUCTION

WORKING COMMISSION W18 - TIMBER STRUCTURES

A CONTRIBUTION TO THE DESIGN AND SYSTEM EFFECT OF CROSS LAMINATED TIMBER (CLT)

R A Jöbstl
Th Moosbrugger
Th Bogensperger
G Schickhofer

Institute for Timber Engineering and Wood Technology
Graz University of Technology

AUSTRIA

MEETING THIRTY-NINE
FLORENCE
ITALY
AUGUST 2006

Presented by R Jöbstl
A Leijten and R Jöbstl discussed the last formula dependency on COV and why system factors increased when COV increased and the issue of COV for tensile strength became a very important factor.
H Larsen questioned that when one set up the model, why not use the mean values rather than the characteristic values. G Schickhofer stated that this could be done.
B Dujic discussed the possible use of the CLT beam on its side and wondered if one would expect different failure mode. G Schickhofer stated that this was not known as this would be a different system and the current system behaved as a plate.
H Larsen asked how many companies would be making these members. H Blass responded that 7 or 8 German groups were making these systems and the number would increase.
H Larsen wondered would they require EU technical approval if so why these companies were not asked to develop a large database. H Blass stated one system has EU technical approval.
R Foschi asked when you tested these systems what was the failure (1st failure or sequential failures). G Schickhofer stated that it was not a brittle failure mode and sequential failures were observed. R Foschi stated this would explain why system factors would go up with larger COV same as lumber floor system.
A Buchanan asked about nailed system without glue. H Blass stated that nail system and beech dowel as connection system have been approved in Germany. Tests results were developed but not generally available for the public.
P Quenneville asked about the 4 laminae wide versus larger number of laminae. R Jöbstl answered that it was done.

L Uzielli announced planning a new COST action on wood science concerning conservation of cultural heritage structures. The idea would be to mix structural engineering and wood science as a subject. Interested parties should contact L Uzielli directly.

A Contribution to the Design and System Effect of Cross Laminated Timber (CLT)

R.A. Jöbstl, Th. Moosbrugger, Th. Bogensperger, G. Schickhofer
Institute for Timber Engineering and Wood Technology
Graz University of Technology, Austria

Abstract

The design code of Germany DIN 1052:2004 [1] is the first national code where the verification process for the engineered building product 'Cross Laminated Timber' (CLT) is defined. In this code the calculation of stresses for the layers of a bending stressed element has to be done for each single layer as a combination of the tensile stress in the center line and the bending stress, as a difference between the center line stress and the edge stress of the applied layer.

The present study has been done to evaluate an improved model of design for the homogenised product 'Cross Laminated Timber' (CLT). Starting from the base material 'boards', visual graded as S10 (according to the German standard DIN 4074-1) which should give a strength class of C24 (according to EN 338), tension tests have been made to get the characteristic properties (tensile strength and modulus). Four series of 5-layered CLT-elements of different widths have been produced and tested in bending. For comparison two small series with unidirectional build-up – quasi GLT – have been made.

The results indicate a clear affinity between CLT and GLT. On this findings a design concept for CLT based on the beam model' for GLT, has been suggested. It includes the difference of homogenisation in the vertical direction (laminating effect) between CLT, and GLT by defining the factor $k_{CLT/GLT}$. Furthermore the so called 'system strength factor k_{sys}' – given in EN 1995-1-1 (for *'equally spaced similar members'*) and EN 1995-2 (for timber deck systems working as parallel acting components) has been worked out for CLT to describe the load bearing behaviour in the horizontal direction.

1 Introduction

CLT is a plate-like product typically build-up in a cross layering of the single layers which are arranged orthogonally. Normally the parallel oriented boards in each layer are not connected together in their smaller side.

CLT is used in Europe for timber constructions like residential houses, multi-storey buildings, halls and bridges since more than ten years.

The verification process for CLT has to be done for each single layer as a combination of the tensile stress in the center line and the bending stress, as a difference between the center line stress and the edge stress of the applied layer.

This design method doesn't consider any homogenisation effects; only the characteristic properties of the base material are kept in mind.

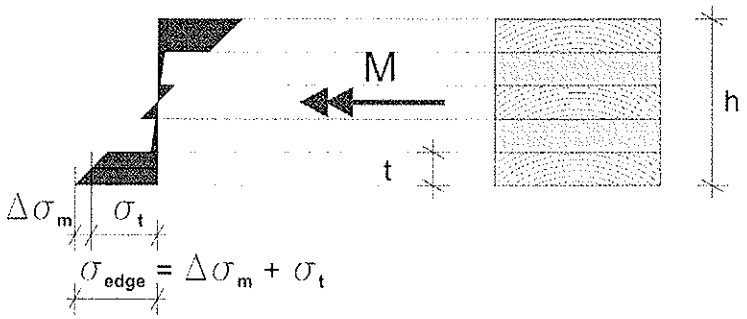

Verification process

(according to DIN 1052:2004 [1])

$$\frac{\sigma_{t,d}}{f_{t,0,d}} + \frac{\Delta\sigma_{m,d}}{f_{m,d}} \le 1$$

with: $f_{t,0,k} = 0{,}6^{*} \cdot f_{m,k}$

(according to EN 384 [2])

* Factor depending on timber quality (see paper CIB-W18/39-6-2 Steiger et. al. [5])

Figure 1 Assumed stress distribution over a CLT cross section due to bending for the verification prozess ($E_{90} \neq 0$)

Because of the different strengths for tension and bending ($f_{t,0} = 0{,}6 \cdot f_m$) this design rule leads to an uneconomic design. To demonstrate this uneconomic verification process for CLT a comparison with glued laminated timber (GLT) - also a laminated product – has been shown.

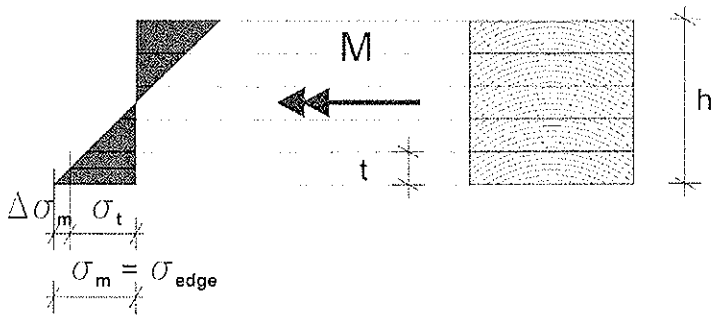

Verification process:

$$\frac{\sigma_{m,d}}{f_{m,d}} \le 1$$

Figure 2 Assumed stress distribution over a GLT cross section due to bending for the verification prozess

If all layers - respectively boards - have the same thickness, the two above-mentioned stresses, tensile σ_t and bending $\Delta\sigma_m$, can be expressed by the edge stress $\sigma_{edge} = \sigma_m$ and by the geometrical properties, the thickness of the single layer t and the height of the whole plate h.

$$\Delta\sigma_m = \sigma_m \cdot \frac{t}{h} \qquad \sigma_t = \sigma_m \cdot \frac{h-t}{h}$$

The equation for the verification process – given above for CLT – can be expressed by a simple function between the design edge stress $\sigma_{edge,d} = \sigma_{m,d}$ and the design bending strength for the single board $f_{m,d}$.

$$\frac{\sigma_{t,d}}{f_{t,0,d}} + \frac{\Delta\sigma_{m,d}}{f_{m,d}} = \frac{\sigma_{m,d} \cdot \frac{h-t}{h}}{\frac{3}{5} \cdot f_{m,d}} + \frac{\sigma_{m,d} \cdot \frac{t}{h}}{f_{m,d}} = \frac{\sigma_{m,d} \cdot \left(\frac{5}{3} - \frac{2}{3} \cdot \frac{t}{h}\right)}{f_{m,d}} \le 1$$

Considering the ratio t/h for a 5-layered plate (t/h = 1/5) the following equation, based on the well known design strength for bending $f_{m,d}$, is given:

$$\frac{\sigma_{m,d}}{0{,}65 \cdot f_{m,d}} \leq 1$$

2 Aim of this work

One aim of this work has been to get information about the homogenisation beginning from the base material 'single board' and finishing by the engineered building product CLT. The homogenisation for glued elements, e.g. products where (simple) boards are used, is composed of the so called 'laminating effect' (predominantly serial linking) – naturally in the vertical direction (e.g. GLT) – and the so called 'system effect' (predominantly parallel linking) – naturally in the horizontal direction (e.g. deck system for timber bridges). Both together gives the 'homogenisation effect', a parallel-serial linking effect, especially important for the verification process of CLT.

The first effect – the laminating effect – describes the characterisation of beam-like products normally in the vertical direction. In this context there exists the same effect between GLT and CLT, if CLT is build-up as a beam-like element with the width of one board (figure 3). For GLT the so called 'Beam Model' considers this 'laminating effect' which is given in EN 1194:1999. Therefore the GLT-model could be a basis for the description of a CLT-model (chapter 5).

CLT is generally applied as a plate-like and not as a small beam-like product. Hence it exist a benefit for CLT-elements in comparision to GLT regarding the second effect – the system effect in the horizontal direction –, because a CLT element is normally produced with greater widths or rather with a greater number of parallel arranged single boards in the outer layer (figure 3).

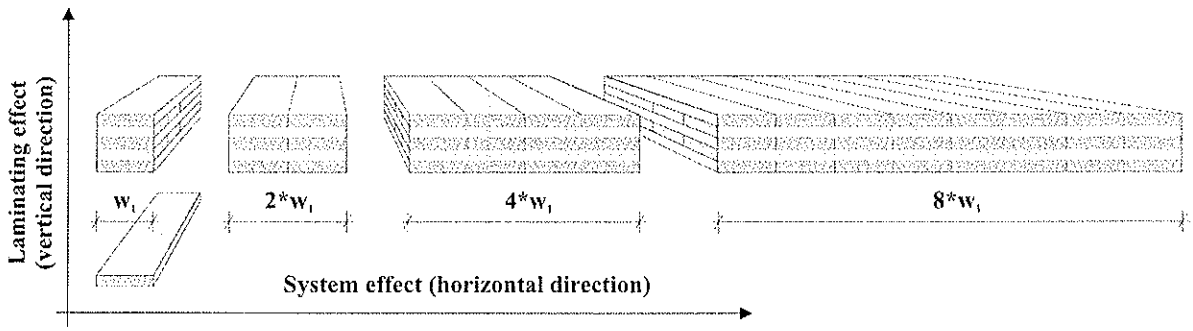

Figure 3 CLT elements with a width from $w = w_1$ to $w = 8 \cdot w_1$

3 Method

To achieve a verification of the bearing potential of CLT the following method has been used:

The base material 'boards' for all tested series and specimens has been visual graded (S10 according to the German standard DIN 4074-1) to strength class C24 according to EN 338. Boards have been taken as a sample from the source of production (figure 4) to get on one

hand the 124 tensile specimens and on the other hand material for production of the CLT and GLT bending specimens.

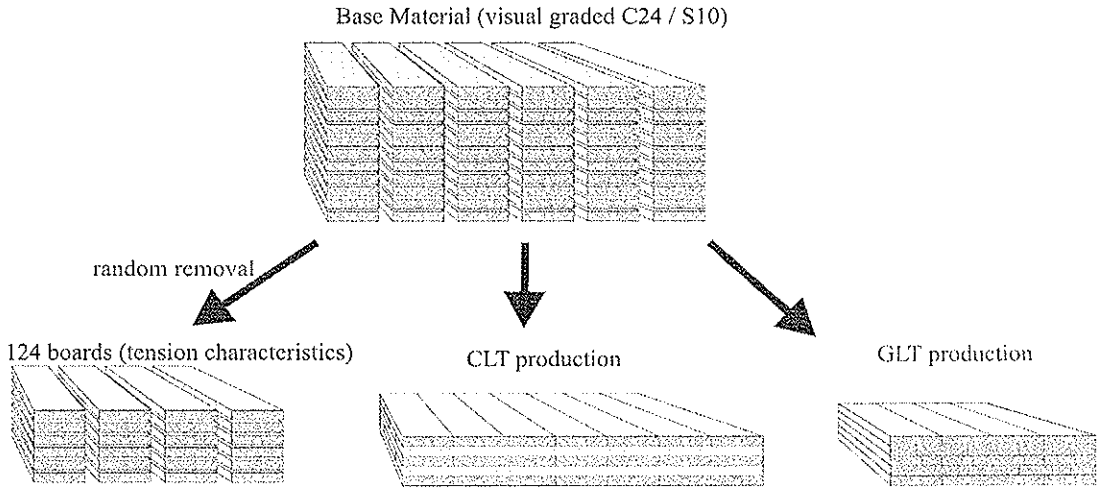

Figure 4 Material flow of the test program – tensile tests on boards – bending tests on CLT and GLT

3.1 Experimental program

Table 1 gives the experimental program of this project. To evaluate the tension characteristics of the base material 124 boards with the cross section of 22 mm/120 mm have been tested in tension according to EN 408 [3]. The cross laminated timber elements have been tested in four different widths starting with w_1 = 120 mm (width of one board; series '1c', 1 board in the outer layer, cross laminated) followed by the multiple of board width of w_1 of 2-times (series '2c'), 4-times (series '4c') and 8-times (series '8c'). For establishing a relationship between CLT and GLT regarding the homogenisation additional tests have been done on GLT elements with the same thickness of 110 mm and two widths (series '1u': w_1 = 120 mm, series '4u': w_4 = 480 mm; see table 1).

	Boards	CLT				GLT	
Notation of series		'1c'	'2c'	'4c'	'8c'	'1u'	'4u'
Width w	120	120	240	480	960	110	480
Number of specimens	124	40	20	15	10	16	5
Type of test	Tension	Bending					
c … cross laminated u … unidirectional							

Table 1 Experimental programm

3.2 Experimental setup

For the tensile tests the boards with cross section of 22 mm / 120 mm have been tested according to EN 408 (l ≥ 9b) with free testing length of 2095 mm (also in accordance to

EN 1194:1999 [4]). The tensile MOE has been determined deviant to the EN 408 above the whole length and not in the scope of 5·w in the middle section of the board (figure 5).

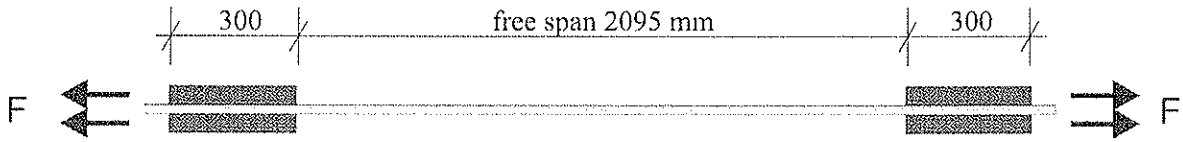

Figure 5 Test setup for tensile tests on the base material

The bending tests on CLT and GLT elements have been carried out in accordance to EN 408 (figure 6) by consideration of test arrangements for measuring the local and global MOE.

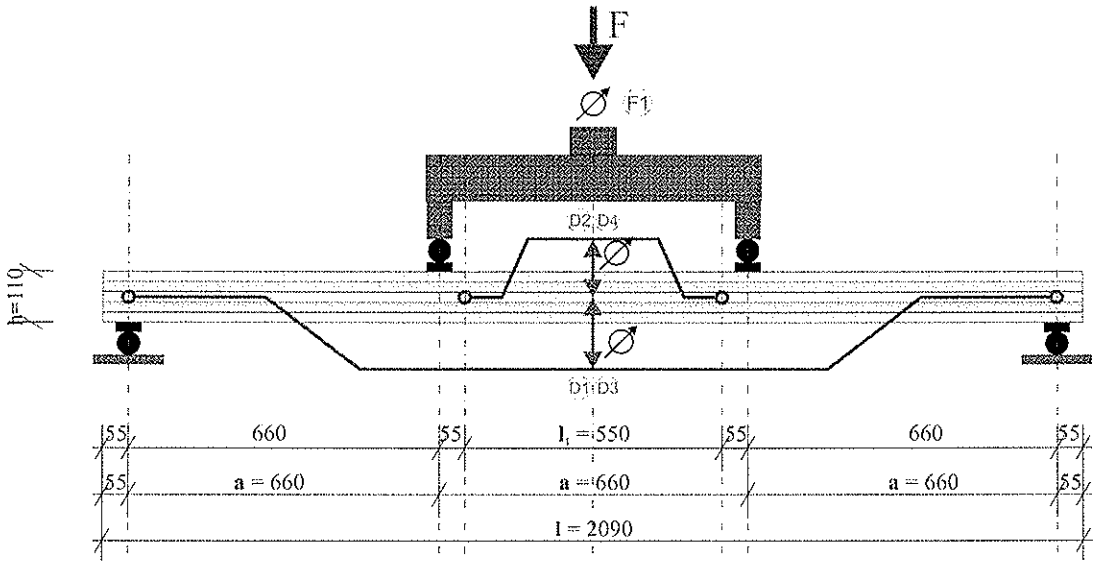

Figure 6 Test setup for bending tests on CLT and GLT elements

3.3 Evaluation of test results

Tensile tests on boards and bending tests on GLT elements have been analysed in accordance to EN 408.

The bending tests on CLT elements, which are highly statical undefined, have been calculated by three methods:

Name of the method	Description
'FEM'	FEM analysis with a plane stress modelling (abaqus)
'NUM'	exact differential equation with fourier discretication [6]
'Beam'	beam model with rigid composite cross section and modified and calculated shear correction factor ($\kappa = 4{,}9$ for a five layered element)

Table 2 Description of the three methods used for calculation

For all three methods three optimisation processes have been applied:

Name of the optimisation process	Description
'2 para'	The stiffness properties E_{90} and G_{090} have been fixed with the values 300 N/mm² and 700 N/mm². The stiffness properties E_0 and G_{9090} have been varied as long as the two measured deformations – local and global - were equal to the calculated ones.
'60'	In addition to the requirements above the stiffness property G_{9090} has been fixed with the value of 60 N/mm². Only the stiffness property E_0 has been varied till the measured deformation in the middle matched with the identical calculated point.
'100'	Equal to '60' but with a G_{9090} of 100 N/mm².

Table 3 Description of the three optimisation processes used for calculation

4 Results

4.1 Tensile tests of the base material

Table 4 shows the results of the tensile tests of the base material.

	Density [kg/m³]	MOE tensile [N/mm²]	MOR tensile [N/mm²]
Mean	447 (420)	10977 (11000)	26,1
COV_t [%]	9,7	20,3	**39,4**
5% fractile	376 [1] (350)	7303 [1] (7400)	**12,5** [2] (14,0)
[1] Normal distributed			
[2] Lognormal distributed (according to EN 384 without functional distribution - order statistic / nonparametric approach - 13,1 N/mm²)			
Values in braces shows the properties of C24 according to EN 338			

Table 4 Results of tensile tests of the base material

As shown in table 4 the density reach the requirements of C24. The MOE calculated from the tensile tests, scarcely do not reach the demanded MOE of C24 regarding EN 338. In this regard it should be noted that the bending MOE as required value for allocation to a strength class according to EN 338, is about 6% to 9% higher than the tensile MOE [7], [8], [9]. By that the MOE of C24 can be fulfilled (10977*1,06 = 11640: +5,8%). The tensile strength shows a low mean value ($f_{t,0,l,mean}$ is generally in the scope of 30 ± 5 N/mm² [10]) and a high COV_t (COV_t is generally in the scope of 35 ± 5 % for visual graded boards [11]). This results in a low 5%-fractile for the tensile strength, where the lognormal distribution gives the best fitting.

4.2 Bending tests – stiffness considerations

The four point bending tests according to EN 408 shows high sensibility due to the shear modulus G_{9090}. The results, based on a finite element analysis using the software 'Abaqus' (method 'FEM'), yields to comparable values with the analytical model (method 'NUM'). Considering the deformation, the difference is less than 0,1%, when the knots in the FEM analysis are fixed together over the thickness (rigid in the thickness direction). This should be fulfilled as a requirement of the analytical model to compare both methods. The more realistic model with orthotropic constraint considering the MOE perpendicular to grain E_{90} = 300 N/mm² in the thickness direction leads to differencies of about 10% in the calculated MOE. Using the method 'Beam', considering the modified and calculated shear correction factor, comparable results with the method 'FEM' are given (figure 7).

Above all series (table 1) and widths the mean values of the calculated bending MOEs are nearly constant in the area of about 12000 N/mm². The tensile MOE of the base material gives $E_{t,0,l,mean}$ = 11000 N/mm². Multiplying this tensile MOE with the factor of 1,06 and 1,09 respectively a bending MOE between 11660 N/mm² and 11990 N/mm² is reachable. As a result it can be shown, that the calculated bending MOE $E_{m,l,mean}$ for the base material is in the area of the calculated MOE for the CLT elements (figure 7).

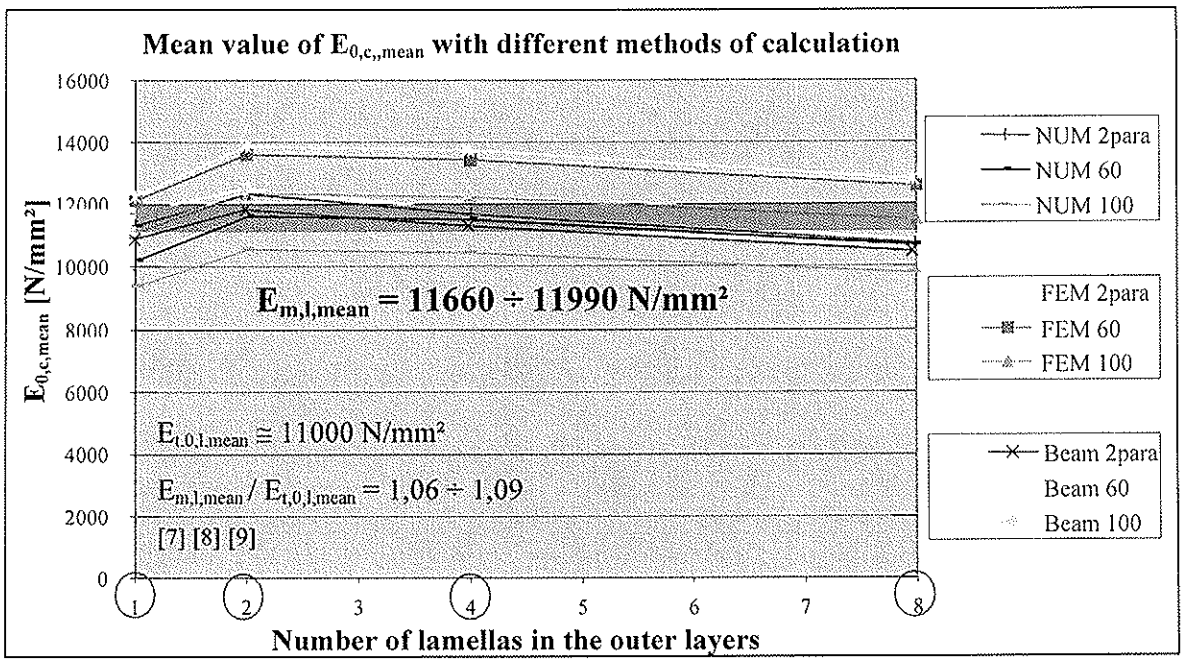

Figure 7 Mean value of bending MOE of CLT $E_{0,c,mean}$ calculated with different methods and for different widths of the elements

By consideration of all three methods (table 3) and optimisation processes (table 4) during the calculation process similar behaviour regarding the COV_E for bending MOE is given (figure 8).

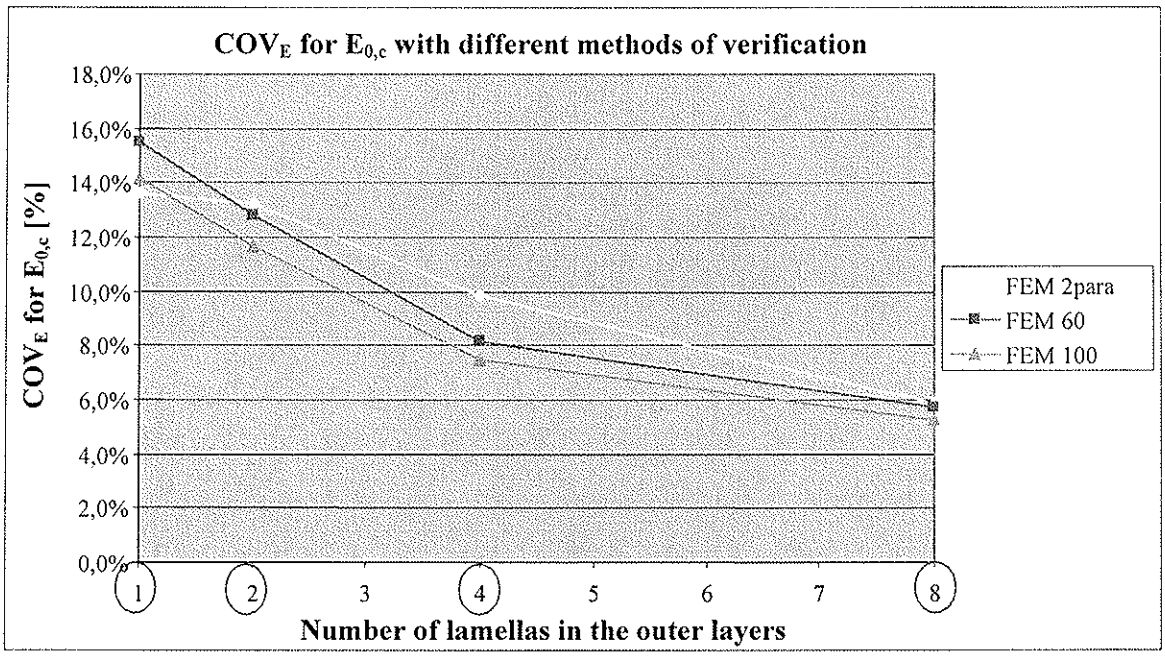

Figure 8 COV$_E$ for bending MOE of CLT calculated with different methods and for different widths of the elements

It states that series '1c' (beam-like elements) gives a coefficient of variation of about 14% to 16% which is similar to test results for GLT. With increasing of width the COV$_E$ decreases till about 6% for series '8c' (elements with 8 boards in the outer layers). By that a first step of homogenisation can be recogniced from the base material board to the beam-like element (width of one board) and a second step with increasing of width.

4.3 Bending tests – calculation of stresses

The variety of stresses, calculated with different methods and consideration of different optimisation processes (table 3 and 4), is not as high as the calculated bending MOEs for CLT. A simple example by application the beam theory for a 5-layered element gives further impact.

The edge normal stress has to be calculated by: $$\sigma_{edge} = \frac{M}{W_{eff}}$$

The bending moment M is given by the test results and therefore constant. The effective section modulus may be calculated by:

$$W_{eff} = \frac{b \cdot h^2}{6} \cdot \frac{1}{125}\left(99 + 26 \cdot \frac{E_{90}}{E_0}\right)$$

By fixing E_{90} with 300 N/mm² and varying the bending MOE (E_0 = 11000 N/mm² ± 10%) a variation of W_{eff} less than ± 0.1% can be examined and therefore compatible deviation is reachable for the edge normal stress.

Figure 9 reflects that clearly. All calculation methods lead to comparable results. Above all widths the mean value $f_{edge,c,mean}$ is nearly constant within the area of 37,2 N/mm² and 39,4 N/mm². Series '1u' (unidirectional plate GLT) reaches obvious higher mean value of 44,2 N/mm². The five unidirectional elements with the width of four boards (series '4u') reach a mean value of 42,4 N/mm².

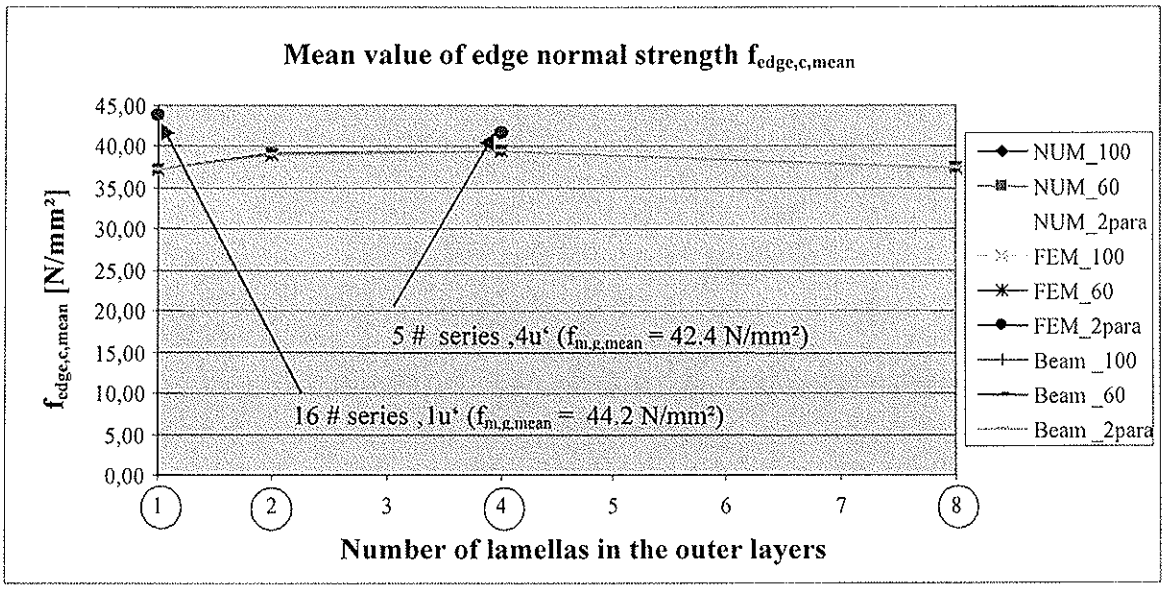

Figure 9 Mean value of edge normal strength $f_{edge,c,mean}$ calculated with different methods and for different widths of the elements

As stated in figure 10 the coefficient of variation (COV) decreases constantly from about 16 % for series '1c' - which is common for GLT - towards to about 8 % for series '8c'. The 16 quasi GLT elements (series '1u') show a higher variation with a COV_{edge} of 20,1 %. This can be explained by the small lot. For series '4u' (only 5 GLT specimens) the COV_m is mentioned but not relevant because of the low quantity of specimens.

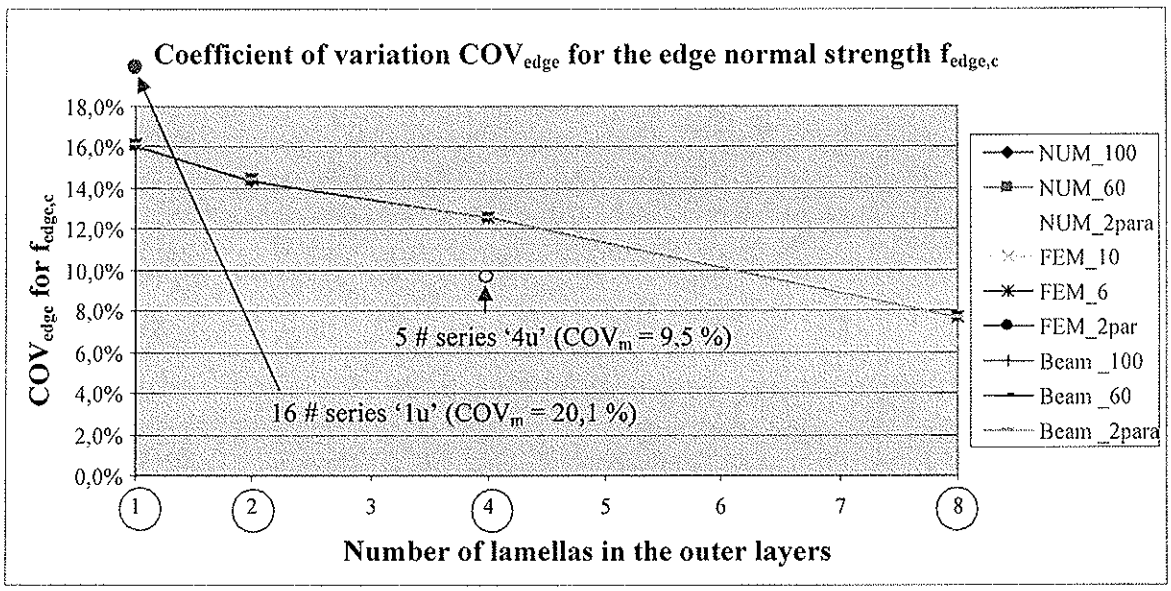

Figure 10 COV_{edge} of edge normal strength $f_{edge,c}$ calculated with different methods and for different widths of the elements

Figure 11 shows the 5 % fractile values of the edge normal stresses of the series '1c' to '8c' and also for series '1u'. The increasing of the 5 % fractile with increasing of width is apparent. Beginning with series '1c' (27.3 N/mm²) it increases to 29.8 N/mm² for series '2c', 31.3 N/mm² for series '4c' and to 32.6 N/mm² for series '8c'. Series '1u' for GLT elements reaches a value of 29.0 N/mm² which gives about 6% higher 5% fractile values than series '1c'.

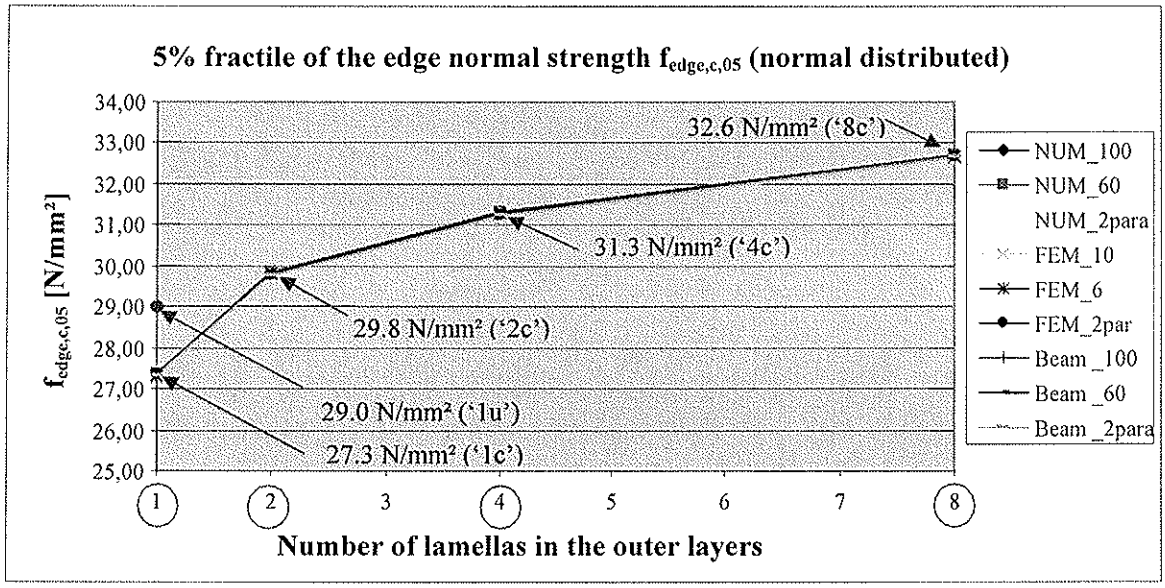

Figure 11 5% fractile of edge normal strength $f_{edge,c,05}$ calculated with different methods and for different widths of the elements

Based on the 5 % fractile of series '1c' a system strength factor k_{sys} for each series width may be calculated as shown in figure 12. In comparison to the system strength factor used in EN 1995-1-1 or DIN 1052:2004, where factors of 1.2 for glued elements and 1.1 for mechanical connected elements are defined, a system strength factor $k_{sys,CLT} = 1.1$ is proposed. Despite glued elements a lower value seems to be more adequate for CLT due to the small range of this test series on one hand and on the other hand because of the weaker connection from one board to the adjacent board in the outer layer of CLT elements.

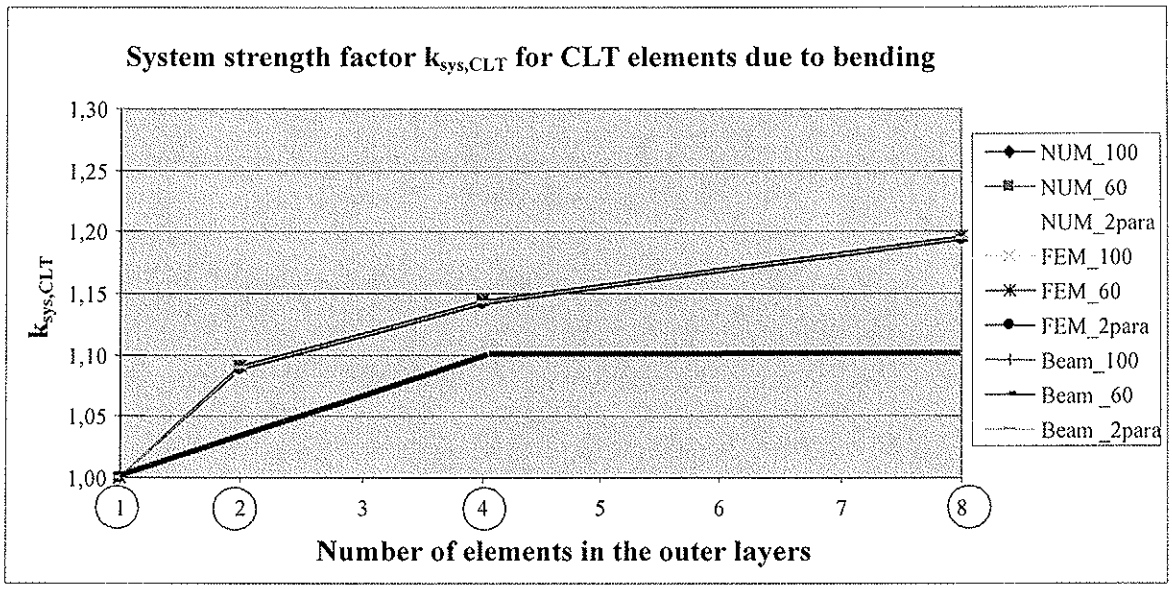

Figure 12 System strength factor $k_{sys,CLT}$ of edge normal strength $f_{edge,c,05}$ calculated with different methods of verification and for different widths

5 Design of cross laminated timber CLT

As an outcome of the test results a design rule for cross laminated timber CLT is proposed.

5.1 Design concept according to DIN 1052:2004

Based on the design concept according to DIN 1052:2004 as shown in chapter 1 the design value for the edge normal stress for a CLT element build-up by boards of the strength class C24 and five layers has to be calculated as follows:

$$\frac{\sigma_{t,d}}{\frac{3}{5}\cdot f_{m,d}} + \frac{\Delta\sigma_{m,d}}{f_{m,d}} = \frac{\left(\frac{5}{3} - \frac{2}{3}\frac{t}{h}\right)\cdot \sigma_{edge,d}}{f_{m,d}} \leq 1$$

$$\sigma_{edge,d} \leq \frac{f_{m,k}}{\left(\frac{5}{3} - \frac{2}{3}\frac{t}{h}\right)} \cdot \frac{k_{mod}}{\gamma_M} = 0{,}65 \cdot 24{,}0 \cdot \frac{k_{mod}}{\gamma_M} = 15{,}7 \cdot \frac{k_{mod}}{\gamma_M}$$

The strength value 15,7 N/mm² should be kept in rememberance for a comparison with the new model (chapter 6).

5.2 Beam model for GLT

The results in chapter 4 suggest an affinity between the homogenised products CLT and GLT which are both produced using the base material board. That is the reason why the beam model of GLT is used as basis for the following considerations.

According to EN 1194:1999 the bending strength of GLT has to be calculated using the tensile characteristics of the base material board:

$$f_{m,g,k} = 7{,}0 + 1{,}15 \cdot f_{t,0,l,k}$$

Various research projects on GLT since 1999 particularly show that there exist an overestimation of the higher strength classes or in other words the tensile stength of the base material has to be raised to reach the highest strength classes for GLT [11].

Furthermore the given function in EN 1194:1999 does not consider the distribution of the tensile strength of the base material. A new research work at the Institute for Timber Engineering and Wood Technology considers the COV_t for tensile strength and the COV_m for the bending strength of GLT to formulate a new beam model ('Grazer Holzbau-Workshop'06' [11]).

$$f_{m,g,k} = a_{GLT} \cdot f_{t,0,l,k}^{\,0,82} \qquad \text{with:} \qquad a = \begin{cases} 2{,}422 & COV_t = 0{,}25 \\ 2{,}811 & COV_t = 0{,}35 \end{cases}$$

A simple modification leads to following function (best fitting by a linear regression; differenz in common area within 2 %)

$$f_{m,g,k} = 1{,}06 \cdot (1{,}4 + 4{,}0 \cdot COV_t) \cdot f_{t,0,l,k}^{\,0,8}$$

This new beam model applied to the test results of the base material (from table 4: $f_{t,0,l,05}$ = 12,5 N/mm², COV_t = 39,4%) and the GLT beams (from figure 11: series '1u': $f_{m,g,05}$ = 29,0 N/mm²) shows the application for these values:

$$f_{m,g,05} = 1{,}06 \cdot (1{,}4 + 4{,}0 \cdot COV_t) \cdot f_{t,0,l,05}{}^{0,8} = 1{,}06 \cdot (1{,}4 + 4{,}0 \cdot 0{,}39) \cdot 12{,}5^{0,8} = 23{,}8$$

Corresponding to the reference dimensions for GLT in accordance to EN 1194:1999 (h = 600 mm, w = 150 mm) the factor k_{size} has to be considered for the calculation of the bending strength based on the test results for the series '1u' (GLT) and '1c' (CLT) respectively (h = 110 mm, w = 120 mm).

$$k_{size} = \left(\frac{600}{h}\right)^{0,1} \cdot \left(\frac{150}{w}\right)^{0,05} = \left(\frac{600}{110}\right)^{0,1} \cdot \left(\frac{150}{110}\right)^{0,05} = 1{,}20 \qquad \text{N/mm}^2$$

The calculated bending strength for GLT based on the new beam model is only insignificant lower than the edge normal strength gained from test results.

$$f_{m,g,05,h} = k_{size} \cdot f_{m,g,05} = 1{,}20 \cdot 23{,}8 = 28{,}6 \leq 29{,}0$$

5.3 Beam model for CLT

Because of the weaker cross layers a reduced effect of homogenisation for the product CLT can be assumed (figure 11). It is suggested that this effect can be considered by the factor $k_{CLT/GLT}$ gained from presented test results.

$$k_{CLT/GLT} = \frac{f_{edge,c,05,h}}{f_{m,g,05,h}} = \frac{27{,}3}{29{,}0} \cong 0{,}94$$

The **calculated** edge normal (bending) strength for a CLT element with a width of one board in the form of a product of the factor $k_{CLT/GLT}$ and the bending strength for a GLT element with also the width of one board gives a value of 26,9 N/mm². As demanded this is marginally less than the edge normal (bending) strength $f_{edge,c,1c,05}$ = 27,3 N/mm² (series '1c') from the presented test results.

$$f_{edge,c,beam,05} = k_{CLT/GLT} \cdot f_{m,g,05,h} = 0{,}94 \cdot 28{,}6 = 26{,}9 \leq 27{,}3 \qquad \text{N/mm}^2$$

As mentioned above CLT is a plate-like element. Therefore the proposed system strength factor $k_{sys,CLT}$ = 1,1 (figure 12) may be considered for CLT elements which are build-up by **four or more** parallel arranged boards in the outer layers.

$$f_{edge,c,plate,05} = k_{sys,CLT} \cdot f_{edge,c,beam,05} = 1{,}1 \cdot 26{,}9 = 29{,}6 \leq 31{,}3 \qquad \text{N/mm}^2$$

Comparing the calculation above with the test results from series '4c' (31,3 N/mm²) it can be seen that the calculation process is on a conservative basis.

5.4 Design proposal for CLT

The design of CLT should be economic concerning the 'correct' use of the material potential and the calculation process. To reach this a design concept is proposed for CLT elements with a width of more or equal than four parallel arranged boards in the outer layers with a reference depth of 150 mm. Because of missing knowledge regarding the volume and build-up effect of CLT – further research work is needed – the factor k_h (without consideration of the width) as given for GLT is used for the following explanation.

$$k_h = \left(\frac{600}{150}\right)^{0,1} = 1,15$$

If all the above mentioned factors ($k_{sys,CLT}$, $k_{CLT/GTL}$, k_h) are considered the new simplified beam model for GLT may be written for CLT in the following form:

$$f_{m,c,05} = f_{edge,c,plate,05} = k_{sys,CLT} \cdot k_{CLT/GLT} \cdot k_h \cdot 1,06 \cdot (1,4 + 4,0 \cdot COV_t) \cdot f_{t,0,l,05}^{0,8}$$

$$k_h = \left(\frac{600}{h}\right)^{0,1} = \left(\frac{600}{150}\right)^{0,1} = 1,15$$

$$k_{CLT/GLT} = 0,94$$

$$k_{sys;CLT,\geq 4} = 1,1$$

$$f_{m,c,05} = 1,26 \cdot (1,4 + 4,0 \cdot COV_t) \cdot f_{t,0,l,05}^{0,8} = (1,76 + 5,0 \cdot COV_t) \cdot f_{t,0,l,05}^{0,8}$$

5.5 Comparison between CLT and GLT model

The comparison has been done for two different COV_t's (25% - normally given for machine graded material and 35% - normally given for visual graded material [10]) whereas a tensile strength for the base material has been assumed with $f_{t,0,l,05}$ = 14,0 N/mm².

For GLT (reference height **h = 600 mm** and reference width **w = 150 mm**) the following can be determined regarding the above findings:

$$f_{m,g,05} = a_{GLT} \cdot f_{t,0,l,05}^{0,82}$$

Using

$$a_{GLT} = 2,422 \qquad \text{for } COV_t = 0,25$$

$$a_{GLT} = 2,811 \qquad \text{for } COV_t = 0,35$$

the bending strength for GLT is given with

$$f_{m,g,05} = 2,422 \cdot 14,0^{0,82} = 21,1 \quad \text{N/mm}^2$$

$$f_{m,g,05} = 2,811 \cdot 14,0^{0,82} = 24,5 \quad \text{N/mm}^2$$

For CLT (reference height **h = 150 mm** build-up as a **5-layered element** by more than **four parallel arranged boards** in the outer layers) the following can be stated regarding the above findings:

$$f_{m,c,05} = a_{CLT} \cdot f_{t,0,l,05}^{0,8}$$

Where

$$a_{CLT} = 1,76 + 5,0 \cdot COV_t$$

Using

$$a_{CLT} = 3{,}0 \qquad \text{for } COV_t = 0{,}25$$

$$a_{CLT} = 3{,}5 \qquad \text{for } COV_t = 0{,}35$$

the bending strength for CLT is given with

$$f_{m,c,05} = 3{,}0 \cdot 14{,}0^{0{,}8} = 24{,}8 \qquad N/mm^2$$

$$f_{m,c,05} = 3{,}5 \cdot 14{,}0^{0{,}8} = 28{,}9 \qquad N/mm^2$$

1	2	3	4	5	6
COV_t	**GLT** $f_{m,g,05}$ **[N/mm²]** **h = 600 mm, w = 150 mm**	GLT $f_{m,g,05}$ [N/mm²] h = 150 mm, w = 150 mm	**CLT** $f_{m,c,05}$ **[N/mm²]** **h = 150 mm 5-l., ≥4 boards**	CLT $f_{m,c,05}$ [N/mm²] h = 150 mm, 5-l., w = 150 mm (1 b.)	$\Delta_{2:4}$ [%]
0,25	**21,1**	24,2	**24,8**	22,6	17,5
0,35	**24,5**	28,1	**28,9**	26,4	18,0

Table 5 Comparison of the bending strength values for GLT and CLT

For CLT elements with a width less than four boards the calculated bending strength values have to be reduced (column 5 – w = 150 mm/1 board – of table 5). The function for CLT is only valid for a maximum thickness of h = 150 mm in combination with a 5-layered build-up of the element). In the future further research has to be done regarding the build-up of the CLT elements to extend the application of the CLT model (build-up factor).

6 Summary

In the presented project the base material 'boards' **visual graded** in the grading class **S10** (strength class C24 respectively) has been tested to get the tensile properties.

The tensile MOE achieves the required value of about **11000 N/mm²**. The tensile strength shows a low mean value ($\mathbf{f_{t,0,l,mean}}$ **= 26,1 N/mm²**) but a high COV_t (**39,4%**) and therefore a low 5% fractile ($\mathbf{f_{t,0,l,05}}$ **= 12,5 N/mm²**, lognormal distributed).

Based on the above mentioned starting material CLT elements have been produced in four series (**'1c', '2c', '4c' and '8c'**, where the number in the notation stands for the number of the parallel arranged boards in the outer layers) as well as into two series of GLT elements (**'1u' and '4u'**, where 'u' stands for unidirectional). All specimens have been built-up as 5-layered elements and have been tested in bending in accordance to EN 408.

Three methods of calculation have been used – exact differential equation with fourier discretization, finite element analysis with plane stress discretisation, conventional beam model with rigid cross section and modified shear correction factor (κ = 4,9 for a five layer element). All these methods have been calculated by use of three optimisation models, whereas the stiffnesses E_{90} and G_{090} have been fixed – a two parametric model to optimise E_0 and G_{9090} (rolling shear), and two one parametric models with additional fixed G_{9090} (60,100) to optimice E_0. All calculation models leads to comparable results. For calculation the beam model with modified shear correction factor is proposed.

The bending test results suggest an affinity between the homogenised product CLT and GLT. Due to this situation it is comprehensible to use the same basis (beam model) for both products. The tests represent an increasing of the 5% fractile with increasing of width of the elements. Hence a so called **system strength factor $k_{sys,\,CLT}$ = 1,1** could be defined, if four or more parallel arranged boards are given. Furthermore a factor **k_h = 1,15** to consider the depth effect and the **factor $k_{CLT/GLT}$ = 0,94** considering the difference in the homogenisation between GLT and CLT could be defined.

If all the three factors are multiplied a factor **k_{CLT} ~ 1,2** ($k_{sys,\,CLT} \cdot k_h \cdot k_{CLT/GLT}$) is given for a **5-layered CLT** element with a **thickness of 150 mm** and a width, where **four or more** parallel arranged boards in the outer layers are used.

New research works at the Institute of Timber Engineering and Wood Technology [11] clearly showed that it is of importance to consider the **COV_t** (tensile strength) for the boards and the **COV_m** (bending strength) of GLT when defining a new beam model.

In [11] the following model for GLT is expected (reference height **h = 600 mm** and reference width **w = 150 mm**) where **a_{GLT} = 2,811** for COV_t = 0,35 (normally given for visual graded material) and COV_m ~ 0,15:

$$f_{m,g,05} = a_{GLT} \cdot f_{t,0,l,05}^{\,0,82}$$

Based on this new beam model the following model for CLT can be expected (reference depth **h = 150 mm**, 5-layered element, four or more boards in the outer layers) with a_{CLT} = 1,76 + 5,0.COV_t (**a_{CLT} = 3,5** for COV_t = 0,35 (normally given for visual graded material) and COV_m ~ 0,15):

$$f_{m,c,05} = a_{CLT} \cdot f_{t,0,l,05}^{\,0,8}$$

Based on the respected results and on the verification concept for GLT it is proposed to use a comparable concept for CLT. Instead of splitting the edge normal stress and strength resprectively the following simple verification function can be used, when CLT is treated like a beam-like element (e.g. single-span beam).

$$\frac{\sigma_{m,c,d}}{f_{m,c,d}} \leq 1$$

The difference between the design concept according to DIN 1052:2004 and the presented concept in this paper is in the range of about 50% and more (depending on the used strength classes and given COVs), where the DIN-concept is on the conservative side.

7 Acknowledgment

The research work within the project 'shell_structures' has been financed by the competence centre holz.bau forschungs gmbh and performed in collaboration with the Institute of Timber Engineering and Wood Technology of the Graz University of Technology and partners from industry (StoraEnso Timber Oy).

The project is aided by the funds of the Federal Ministry of Economics and Labour, the Styrian Business Promotion Agency GmbH, the province of Styria and the city of Graz.

8 Symbols

E_0	Modulus of elasticity parallel to the grain
E_{90}	Modulus of elasticity perpedicualar to the grain
G_{090}	Shear modulus acting in the plane of grain-direction and perpendicular to the grain
G_{9090}	Shear modulus acting in the plane perpendicular to the grain; known as 'rolling shear modulus'
σ_t	Normal (axial) stress due to tension
σ_m	Normal (axial) stress due to bending
$\Delta\sigma_m$	Part of normal (axial) stress with stress distribution due to bending
σ_{edge}	Normal (axial) stress on the edge of cross section
f_t	Strength due to tension
f_m	Strength due to bending
a	Prefactor for beam model
c	CLT, short description
d	Design value
g	Glulam
h	Depth
k	Characteristic value
l	Lamella
t	Tensile
mean	Mean value
05	5 % fractile value
k_h	Depth factor
k_{size}	Size factor
$k_{CLT/GLT}$	Factor to consider lower effect of homogenisation for CLT compared to GLT
$k_{sys,CLT}$	System factor for the product CLT

References

[1] DIN 1052:2004: ‚Entwurf, Berechung und Bemessung von Holzbauwerken – Allgemeine Bemessungsregeln und Bemessungsregeln für den Hochbau', DIN Deutsches Institut für Normung e.V., 2004

[2] ON EN 384: ‚Structural timber - Determination of characteristic values of mechanical properties and density', Austrian Standards Institute, Austria, 2004

[3] ON EN 408: ‚Timber structures - Structural timber and glued laminated timber - Determination of some physical and mechanical properties', Austrian Standards Institute, Austria, 2005

[4] ON EN 1194: , Timber structures - Glued laminated timber - Strength classes and determination of characteristic values', Austrian Standards Institute, Austria, 1999

[5] Steiger, R.; Arnold, M.; Fontana, M.: ‚Revisting EN 338 and EN 384 Basics and Procedures', Proceedings of CIB-W18/39-6-2, Florence, Italy, 2006

[6] Schickhofer, G.: ‚Starrer und nachgiebiger Verbund bei geschichteten flächenhaften Holzstrukturen', Doctoral thesis, Graz University of Technology, 1994

[7] Burger, N.; Glos, P.: ‚Verhältnis von Zug- und Biege-Elastizitätsmoduln von Vollholz', Holz als Roh- und Werkstoff, 53, pp 73-74, 1995

[8] Unterwieser, H.: ‚"Long-Span"-E-Modulmessung sowie Vierpunkt-Biegeprüfungen von BSH-Lamellen im Rahmen des Zulassungsprocederes für den amerikanischen Markt', holz.bau.forschungs.gmbh, internal test report, 2006

[9] Klann, A.: ‚Ermittlung des Potentials von steifigkeitssortiertem keilgezinktem Konstruktionsvollholz', Master thesis, Wismar University of Technology, Business and Design, Wismar, 2006

[10] Glos, P.: ‚Zur Modellierung des Festigkeitsverhaltens von Bauholz bei Druck-, Zug- und Biegebeanspruchung', Berichte zur Zuverlässigkeitstheorie der Bauwerke, Heft 61, Laboratorium für konstruktiven Ingenieurbau, Technische Universität München, München, 1981

[11] Brandner, R.: ‚Darstellung der Festigkeits- und Steifigkeitspotentials von BSH-Lamellen in Hinblick auf das ‚Trägermodell'', Vortragssammlung zum 2. Grazer Holzbau-Workshop '06, Graz, Austria, 2006

INTERNATIONAL COUNCIL FOR RESEARCH AND INNOVATION
IN BUILDING AND CONSTRUCTION

WORKING COMMISSION W18 - TIMBER STRUCTURES

BEHAVIOR OF GLULAM IN COMPRESSION PERPENDICULAR TO GRAIN IN DIFFERENT STRENGTH GRADES AND LOAD CONFIGURATIONS

M Augustin
G Schickhofer

Institute for Timber Engineering and Wood Technology
Graz University of Technology

A Ruli
R Brandner

holz.bau forschungs gmbh, Graz

AUSTRIA

MEETING THIRTY-NINE
FLORENCE
ITALY
AUGUST 2006

Presented by M Augustin
A Leijten commented that the listed references were not cited in text. He stated that when comparing Cases ABC to prismatic case, model was lacking. A model presented in past CIB W18 meeting can be used in here.
H Riberholt discussed the issue of boundary conditions of glulam used in the test. The issue of compression on both top and bottom of beam versus compression on side of beam would influence test results.
H Larsen stated the paper lacked practical implications. The paper missed mean values and COV. One would need this statistical information to assess results. It would not be appropriate if one defined compression perpendicular failure as "collapse" rather than serviceability. M Augustin received confirmation from the Chair that it would be possible to revise the paper.
G Schickhofer stated that one would need to be careful with rounded values in code.

Behavior of Glulam in Compression Perpendicular to grain in Different Strength Grades and Load Configurations

M. Augustin[1], A. Ruli[2], R. Brandner[2], G. Schickhofer[1]
[1] Institute for Timber Engineering and Wood Technology,
Graz University of Technology / Austria, Europe
[2] holz.bau forschungs gmbh, Graz / Austria, Europe

Abstract

In the European standard for glulam EN 1194:1999 the strength values perpendicular to the grain are specified in dependence on the tensile strength and grading class of the used boards respectively. By consideration of the test results given in this paper this correlation could not be confirmed. For all glulam strength classes the specification of a constant characteristic strength value perpendicular to the grain $f_{c,90,g,k}$ of about 2,1 N/mm² to 2,3 N/mm² can be recommended and has to be discussed. This is also the fact for the characteristic modulus of elasticity perpendicular to the grain where a constant mean value of 300 N/mm² valid for all glulam strength classes should be considered. For the design of structural members with different loading situations adjustments of these values are necessary.

1 Introduction

In many practical applications timber and glulam respectively (resp.) is loaded perpendicular to the grain. For design purposes realistic strength and stiffness values have to be determined. It has to be mentioned that a definite point of failure due to stresses perpendicular to the grain can not be obtained and – apart from special configurations where a collapse as stability problem can occur – restrictions of deformations are needed. As a result for the determination of strength values for this type of loading serviceability limit states are rather crucial than ultimate limit states ([7], [8], [9]).

In the relevant testing standard EN 408:2005 [16] the needed force $F_{c,90}$ and stress $f_{c,90}$ resp. for reaching a defined deformation (in EN 408:2005: 1% of the specimens height h_0) are specified as strength values for compression perpendicular to grain. For the determination of the stiffness parameters a secant (in EN 408:2005: between 0,1 $F_{c,90,max}$ and 0,4 $F_{c,90,max}$) has to be approximated into the load-deformation-curve whereby the slope enables the calculation of the modulus of elasticity perpendicular to the grain $E_{c,90}$.

The mechanical properties for this type of loading are depending on wood technological characteristics like the annual ring width and - curvature, in particular the position of the board to the pith and in local areas by the knottiness ([3], [5], [6]). Apart from this in particular the geometrical situation of the loaded area (at the end, at a distance from the end, "in the center"), the type of loading (full area loading, partial area loading) and the loading and bearing length resp. have a strong influence on the mechanical parameters in compression perpendicular to the grain ([1], [2], [4], [5], [11]). Because of the large variability of loading situations in practical cases basic values for the strength and stiffness

perpendicular to the grain in the european codes are determined on cubic specimens loaded on the whole surface. For the design of structural members the so specified values have to be adjusted by coefficients for the loading configuration (in Eurocode: $k_{c,90}$) and the loading length to represent the realistic situation.

For the determination of strength values such in most codes for glulam also in the European standard EN 1194:1999 [14] the so called "beam model" is given. According to this model with increasing tensile strength and grading class of the boards resp. the bending strength of hence build-up glulam increases. Based on this relation also other characteristic values for glulam are defined.

Because of the appearance of juvenile wood and the higher knottiness near to the pith resp. in general boards with higher tensile characteristics are from the outer zones of the log. Such a board can be characterized by flat curved annual rings where boards near to the pith have upstanding ones. Obviously these boards have lower stiffness perpendicular to grain and – because of the definition of the strength – also lower strength values ("spring-model"). That is in fact a contradiction to the given "beam model" based on the fact that boards of flat curved annual rings are characterized by lower compression strength perpendicular to grain but higher MOE and tensile strength. Therefore the above mentioned assumption is verified with tests on cubic specimens of different heights. In addition for the evaluation of a practical case tests on members with a continuous support on the opposite side of the loadings (sills) with different heights and various loading situations have been conducted.

2 Codes and Standards

2.1 EN 1194:1999 [14]

The "beam model" in the European standard EN 1194:1999 applied on the compression strength perpendicular to the grain specifies the correlation between the tensile strength and grading class of the boards resp. and the strength of the glulam perpendicular to the grain by the following function:

$$f_{c,90,g,k} = 0{,}7 \cdot f_{t,0,l,k}^{\,0,5}$$

$f_{c,90,g,k}$ .....characteristic glulam compression strength perpendicular to the grain [N/mm²]
$f_{t,0,l,k}$ .....characteristic tensile strength of the used boards [N/mm²]

For the glulam strength classes defined in this standard and the characteristic tensile strength of the boards needed for their lay-up the following stiffness and characteristic strength values for compression perpendicular to the grain can be calculated as listed in the following Tab. 1.

Strength class of the glulam			GL24h	GL28h	GL32h	GL36h
Tensile strength of the board acc. to EN 1194:1999	$f_{t,0,l,k}$	[N/mm²]	14,5	18,0	22,0	26,0
homogeneous build-up glulam	$f_{m,g,k}$	[N/mm²]	24,0	28,0	32,0	36,0
	$E_{0,g,mean}$	[N/mm²]	11600	12600	13700	14700
	$E_{90,g,mean}$	[N/mm²]	**390**	**420**	**460**	**490**
	$f_{c,90,g,k}$	[N/mm²]	**2,70**	**3,00**	**3,30**	**3,60**

Tab. 1: Glulam strength classes defined in EN 1194:1999 and appropriate mechanical properties

2.2 EN 408:2005 [16]

In the European standard EN 408:2005 regulations and an instruction for the testing procedure to determine the mechanical properties perpendicular to the grain are given. For glulam specimens specifications for the geometry (cubic specimens) and size ($b \cdot l = 25000$ mm²; $b_{min} = 100$ mm; $h = 200$ mm) as well as a method for the calculation of strength and stiffness values is included.

For the determination of the maximum compression load $F_{c,90,max}$ in a first step an estimated load $F_{c,90,max,est}$ is needed, then the values 0,1 $F_{c,90,max,est}$ and 0,4 $F_{c,90,max,est}$ can be calculated and drawn into the load-deformation-curve. Through the intersection points of these values with the recorded testing curve of the specimens a line 1 can be drawn. This line has to be shifted parallel on the x- coordinate by a distance of 0,01 h_0 to get line 2. Where this line intersects the load-deformation-curve of the tested specimens a value $F_{c,90,max}$ can be obtained. If this value is within a range of 5% of the estimated value $F_{c,90,max,est}$ the procedure ends otherwise it has to be repeated until the value is within this tolerance limit.

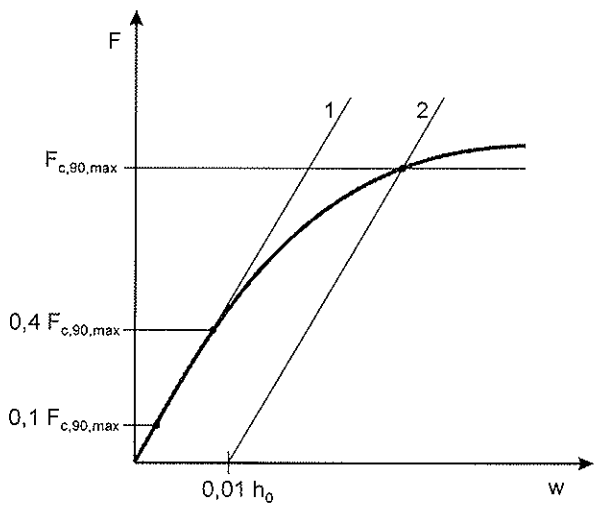

Fig. 1: Definition of the maximum compression load perpendicular to the grain in accordance with EN 408:2005

By knowledge of the load $F_{c,90,max}$ the strength perpendicular to the grain $f_{c,90}$ can be calculated by

$$f_{c,90} = \frac{F_{c,90,max}}{b \cdot l}$$

$f_{c,90}$ ..... compression strength perpendicular to the grain [N/mm²]
$F_{c,90,max}$ ..... maximum compression load perpendicular to the grain [N]
b, l ..... width, length of the specimens [mm]

The modulus of elasticity perpendicular to the grain can be computed by

$$E_{c,90} = \frac{(F_{40} - F_{10})\, h_0}{(w_{40} - w_{10})\, b\, l}$$

$E_{c,90}$ ..... modulus of elasticity in compression perpendicular to the grain [N/mm²]
F_{10}, F_{40} ..... load at 0,1 and 0,4 of $F_{c,90,max}$ [N]
w_{10}, w_{40} ..... corresponding deformations at the above mentioned loads [mm]
h_0 ..... gauge length [mm]
b, l ..... width, length of the specimens [mm]

2.3 Execution and analysis of the tests

In the below mentioned tests no gauges have been used as mentioned in EN 408:2005. Instead deformations in relation to piston ways of the testing machine have been measured. As a consequence the specimen height is equivalent to the gauge length and further the load-stiffness-behaviour of the testing apparatus has been determined and considered in the calculation of the test results.

The characteristic MOE $E_{c,90,g,k}$ and density ρ_k in accordance to EN 384:2004 [15] have been determined as mean and 5%-quantile value resp. For the determination of the characteristic compression strength perpendicular to the grain $f_{c,90,g,k}$ the required minimum number of 40 specimens could not be reached for all series. Therefore the calculation of the strength values in general has been carried out in accordance to prEN 14358:2006 [17].

The characteristic values of the sill-like specimens have been determined in the same way as it has been mentioned for the normative regulated cubic specimens. Thus the effect of the load spreading on the stiffness and strength has not been considered.

3 Objective of the tests

Because of the reasons mentioned above a verification of the specifications given in the European standard EN 1194:1999 has been conducted. Especially the correlation between the tensile strength of the boards and their grading class resp. and the compression strength perpendicular to the grain of glulam has been investigated.

To clear-up the influence of the deformation limit (0,01 h_0) on the strength perpendicular to the grain given in EN 408:2004 tests have been analysed also with the deformation limits 0,02 h_0 (2%) and 0,05 h_0 (5%).

As mentioned the strength and stiffness values tested on cubic specimens are of less practical interest. In the field of timber engineering compression forces perpendicular to the grain often appear as local loadings in joints. Examples for such loading configurations are bearing areas of girders, loadings where the member rests on a firm foundation (sill) or are transmitted trough a member and below washers. For the calculation in the design process it is of importance how the members are loaded and on which length the load is applied.

In the Eurocode this fact is considered by the $k_{c,90}$-factor for the loading situation and a factor for the bearing length. The increased stiffness and strength perpendicular to the grain of practical loading configurations can be explained with the supporting effect of wood fibers beside the direct loaded areas (see Fig. 2).

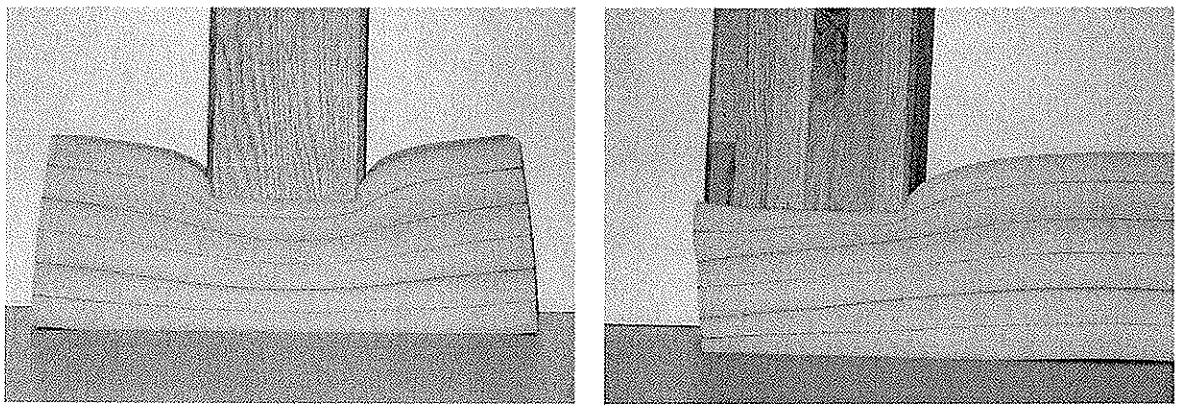

Fig. 2: Illustration of the supporting effect of wood fibers beside the direct loaded area by means of a loaded cellular material

To find out the stiffness and strength values for a case of practical interest tests on sill-like specimens with loadings at the end, at a distance of 100 mm from the end and in an "adequate" distance form the end ("in the center") have been conducted. The bearing length of all sill-like specimens has been 150 mm so that this influence can not be answered with the below mentioned tests.

For the evaluation of a possible influence of specimens height on the strength perpendicular to the grain also tests with two different heights for the cubic and the sill-like specimens (h = 200 mm and h = 480 mm) have been performed.

4 Testing programme

4.1 Material

The investigated species has been spruce (Picea Abies) from a middle European provenience. All specimens have been conditioned before the tests to an equilibrium moisture content of u = 12 ± 2 % at 20°C temperature and 65 % relative humidity.

The glulam specimens have been produced with a polyurethane adhesive (Purbond HB 110) in the lab.

4.2 Tests

For the verification of the above mentioned questions two series (I and II) have been tested:

4.2.1 Series I

For test series I 160 boards of dimensions l/b/h = 4000/175/40 mm have been obtained and graded into three stiffness classes (K1, K2, K3) by means of dynamical modulus of elasticity (MOE_{dyn}) measurement determined with an ultrasonic apparatus (Sylvatest). Subsequently the boards have been cut as shown in Fig. 3 to obtain on one hand 90 specimens (= 30 specimens per stiffness class) for tensile tests according to EN 408:2005 (free testing length of 1600 mm; distance of the displacement sensors for the determination of the tensile MOE = 5 · b = 870 mm). On the other hand the remaining pieces have been used to produce 62 cubic glulam specimens (l/b/h = 160/160/200 mm) for the determination of the compression properties perpendicular to the grain in accordance to EN 408:2005. Threshold values of the MOE_{dyn} for the three stiffness classes and the number of specimens for the tests of series I are given in Tab. 2.

Stiffness class of the boards	K1	K2	K3
MOE_{dyn} of the boards [N/mm²]	MOE_{dyn} > 17200	15500 < MOE_{dyn} < 17200	MOE_{dyn} < 15500
Number of tensile tests [-]	30	30	30
Series I - Specimens for tests perpendicular to the grain – cubic specimens (160/160/200 mm)	19	22	21

Tab. 2: Threshold values for MOE_{dyn} and specimens number of series I

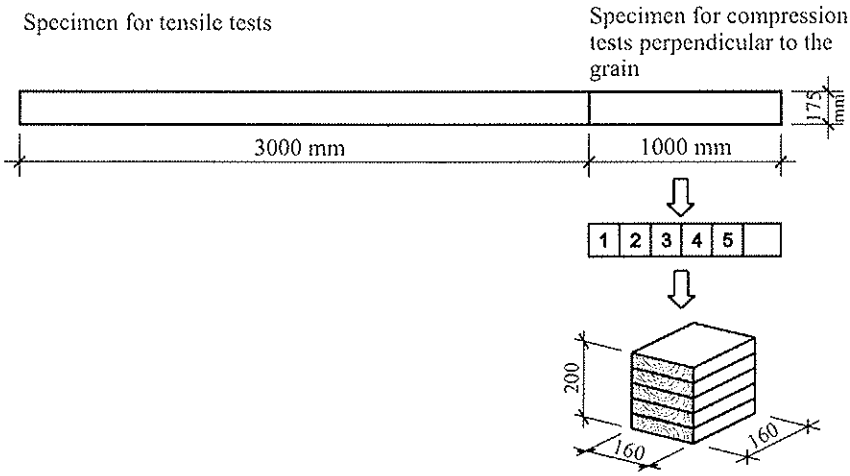

Fig. 3: Geometry and lay-up for the specimens of series I

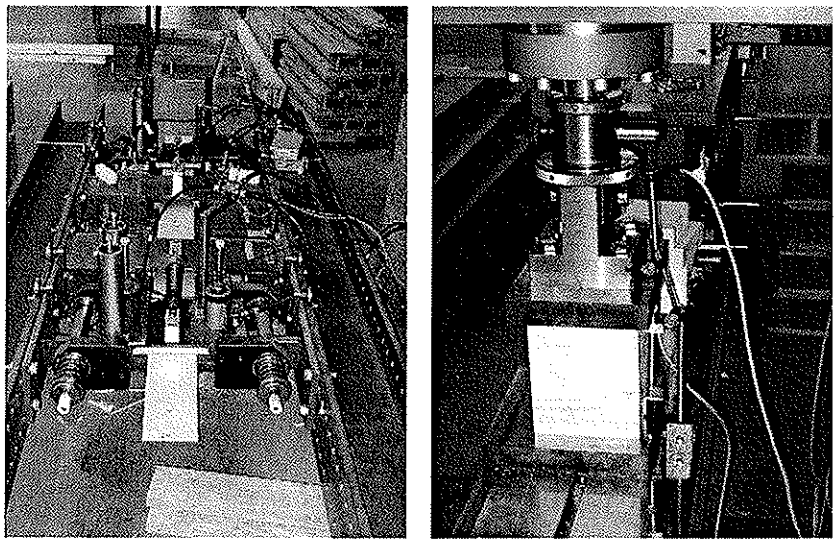

Fig. 4: Test configuration for the tensile tests (left) and the tests for the determination of compression properties perpendicular to the grain (right)

4.2.2 Series II

Series II has been split-up into four sub-series with two heights (cubic specimens l/b = 160/160 mm; h_0 = 200 mm and h_0 = 480 mm) to investigate the influence of specimens height and various loading conditions resp. and geometrical influences (sill-like specimens l/b = 980/160 mm; h_0 = 200 mm and h_0 = 480 mm). The material consisted of machine graded boards (graded with the approved grading device Dimter Grademaster 403) of the strength grades MS10 (C24M), MS13 (C35M) and MS17 (C40M) in accordance to ON DIN 4074-1:2004 and EN 338:2003 resp. The cubic specimens have been cut, build-up as shown in Fig. 3 and tested as described for series I (tensile tests; compression tests perpendicular to the grain). Boards for the production of the sills have been cut as shown in the upper part of Fig. 3. With the longer parts (l = 3000 mm) tensile tests have been conducted and with the shorter parts (l = 1000 mm) sill-like specimens have been produced and tested in compression at the end, 100 mm from the end and "in the center" as shown in Fig. 5. A summary with the denotations of the sub-series, the dimensions and the number of specimen build-up with boards of the different grading classes is given in Tab. 3.

Grading class of the boards according to ON DIN 4074-1:2004 and EN 338:2003 resp.	**MS10 (C24M)**	**MS13 (C35M)**	**MS17 (C40M)**
Tensile tests - Number of specimens	131	134	127
Series II/1 Number of cubic specimens (160/160/200 mm)	41	40	41
Series II/2 Number of cubic specimens (160/160/480 mm)	6	6	6
Series II/3 Number of sill-like specimens (980/160/200 mm)	18	18	18
Series II/4 Number of sill-like specimens (980/160/480 mm)	5	5	5

Tab. 3: Denotation of the sub-series, dimensions, grading classes and number of specimens of series II

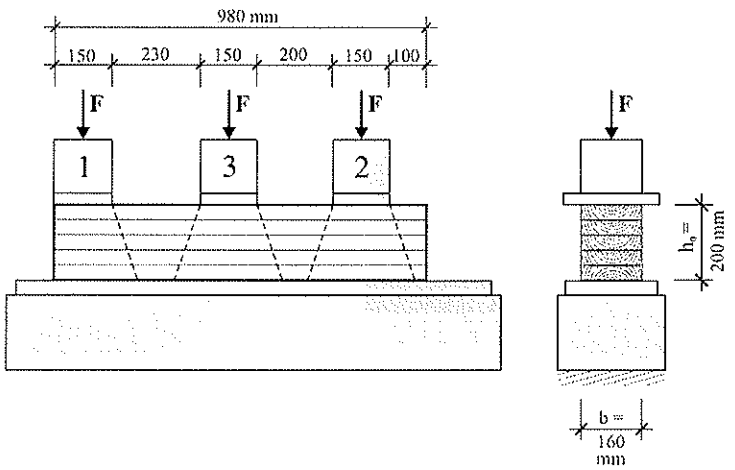

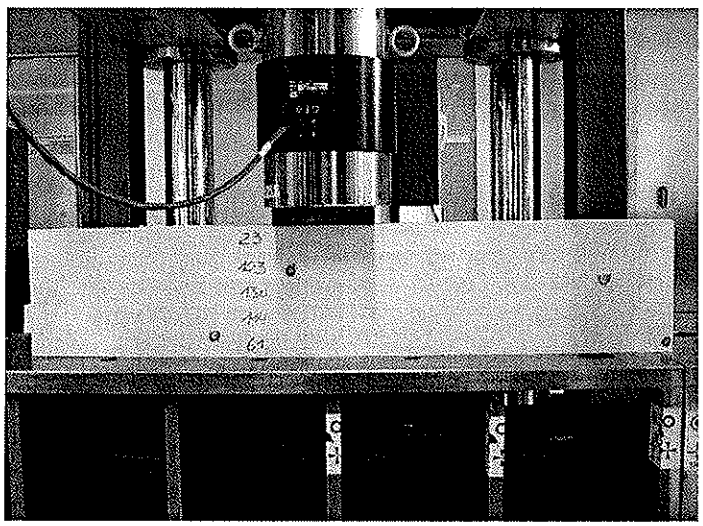

Fig. 5: Loading situations, dimensions (above) and test configuration (below) of the sill-like specimens of series II (sub-series II/3 and II/4)

6 Results

The results given below in general have been calculated in accordance with the specifications given in EN 384:2004. Where this has not been possible because the number of specimens was lower than 40 the regulations of prEN 14358:2006 has been applied.

6.1 Series I

Stiffness class of the boards			K1	K2	K3
Boards					
Specimens number		[-]	30	30	30
Density ρ_l	Mean	[kg/m³]	481	450	408
	COV	[%]	4,36	4,61	5,43
	$\rho_{l,k}$	[kg/m³]	**446**	**416**	**372**
(Tensile-) MOE $E_{t,0,l}$	Mean	[N/mm²]	**14730**	**12290**	**10340**
	COV	[%]	10,16	6,88	12,79
	$E_{t,0,l,05}$	[N/mm²]	12270	10890	8160
Tensile strength $f_{t,0,l}$	Mean	[N/mm²]	49,54	33,73	27,64
	COV	[%]	23,87	26,07	33,87
	$f_{t,0,l,k;\ EN\ 14358}$	[N/mm²]	**30,50**	**19,72**	**15,71**
Glulam specimens					
Specimens number		[-]	19	22	21
Density ρ_g	Mean	[kg/m³]	490	439	418
	COV	[%]	5,02	4,99	11,98
	$\rho_{g,k}$	[kg/m³]	**449**	**403**	**335**
MOE $E_{c,90,g}$	Mean	[N/mm²]	**299**	**301**	**320**
	COV	[%]	19,86	12,02	22,91
	$E_{c,90,g,05}$	[N/mm²]	201	241	200
Compression strength perpendicular to the grain $f_{c,90,g}$	Mean	[N/mm²]	3,10	3,01	3,12
	COV	[%]	22,10	17,58	18,01
	$f_{c,90,g,k;\ EN\ 14358}$	[N/mm²]	**1,99**	**2,13**	**2,18**

Tab. 4: Test results of series I

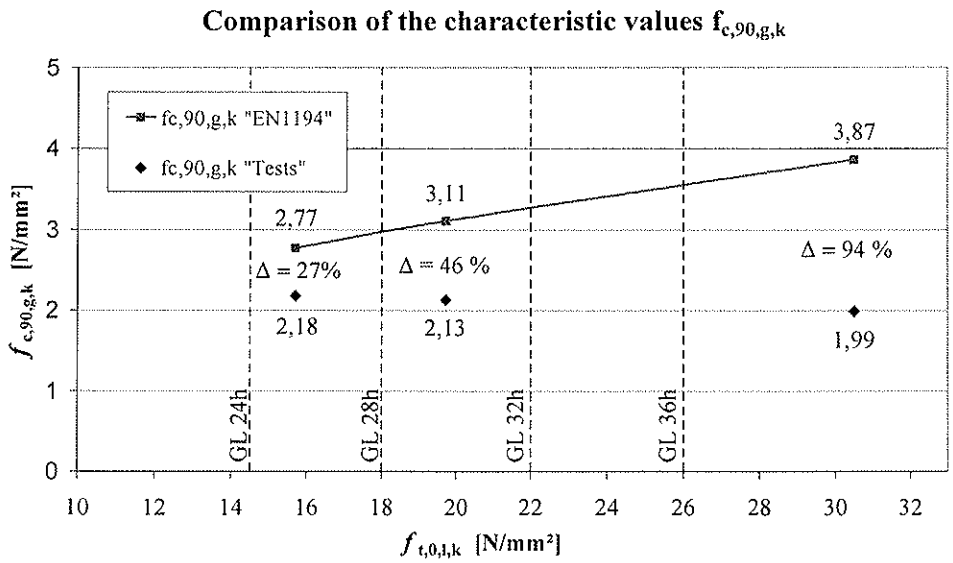

Fig. 6: Comparison of the characteristic values $f_{c,90,g,k}$ calculated with the functions in EN 1194:1999 and the test results of series I

6.2 Series II

In table 5 results from the tests of subseries II/1 and II/2 (tests on cubic specimens with heights h_0 = 200 mm and h_0 = 480 mm) are listed.

Grading class of the boards			**MS 10 (C24M)**	**MS 13 (C35M)**	**MS 17 (C40M)**
Boards					
Specimens number		[-]	131	134	127
Density ρ_l	Mean	[kg/m³]	419	452	489
	COV	[%]	6,33	6,47	6,95
	$\rho_{l,k}$	[kg/m³]	**375**	**404**	**433**
(Tensile-) MOE $E_{t,0,l}$	Mean	[N/mm²]	**9690**	**11830**	**14400**
	COV	[%]	12,17	7,82	12,98
	$E_{t,0,l,05}$	[N/mm²]	7750	10310	11330
Tensile strength $f_{t,0,l}$	Mean	[N/mm²]	22,05	30,32	43,21
	COV	[%]	30,76	24,01	33,19
	$f_{t,0,l,05;\ EN\ 384}$	[N/mm²]	**11,40***	**19,23***	**24,03***
	$f_{t,0,l,k;\ EN\ 14358}$	[N/mm²]	**11,98**	**19,21**	**23,38**
Glulam Specimens					
Subseries II/1					
Specimens number		[-]	41	40	41
Density ρ_g	Mean	[kg/m³]	417	447	493
	COV	[%]	7,71	6,04	6,04
	$\rho_{g,k}$	[kg/m³]	**364**	**402**	**444**
MOE $E_{c,90,g}$ (h_0 = 200 mm)	Mean	[N/mm²]	**265**	**292**	**318**
	COV	[%]	21,24	15,64	16,81
	$E_{c,90,g,05}$	[N/mm²]	172	217	230
Strength perpendicular to the grain $f_{c,90,g}$ (h_0 = 200 mm) (EN 384 / EN 14358)	Mean	[N/mm²]	3,35	3,43	3,16
	COV	[%]	19,62	21,05	17,58
	$f_{c,90,g,05;\ EN\ 384}$	[N/mm²]	**2,46***	**2,45***	**2,45***
	$f_{c,90,g,k;\ EN\ 14358}$	[N/mm²]	**2,33**	**2,33**	**2,30**
Subseries II/2					
Specimens number		[-]	6	6	6
MOE $E_{c,90,g}$ (h_0 = 480 mm)	Mean	[N/mm²]	**272**	**255**	**312**
	COV	[%]	10,87	9,63	19,48
	$E_{c,90,g,05}$	[N/mm²]	223	214	212
Strength perpendicular to the grain $f_{c,90,g}$ (h_0 = 480 mm)	Mean	[N/mm²]	2,89	2,87	2,84
	COV	[%]	14,50	13,59	11,73
	$f_{c,90,g,k;\ EN\ 14358}$	[N/mm²]	**2,10**	**2,11**	**2,17**
* The given values have been determined as 5%-quantile values by means of order statistics.					

Tab. 5: Results of series II – subseries II/1 and II/2

In table 6 results of scenarios characterized by consideration of deriving deformation limits of 0,02 h (2%) and 0,05 h (5%) are listed. Further a comparison with values calculated in accordance to EN 408:2005 (deformation limit 0,01 h and 1% resp.) is included.

Analysed deformation limit	**In acc. to EN 408:2005 (1%)**	**Deformation limit 0,02 h (2%)**	**In comparison to EN 408:2005 [%]**	**Deformation limit 0,05 h (5%)**	**In comparison to EN 408:2005 [%]**
Mean value					
MS 10 (C24M)	3,35	3,69	**110**	3,93	**117**
MS 13 (C35M)	3,43	3,74	**109**	3,97	**116**
MS 17 (C40M)	3,16	3,54	**112**	3,81	**121**
Characteristic value					
MS 10 (C24M)	2,33	2,65	**114**	2,89	**124**
MS 13 (C35M)	2,33	2,67	**115**	3,02	**130**
MS 17 (C40M)	2,30	2,64	**115**	2,96	**129**

Tab. 6: Compression strength perpendicular to the grain of subseries II/1 by consideration of different deformation limits (0,02 h_0 and 0,05 h_0)

Strength values determined from tests with the sill-like specimens depending on different loading situations (loading at the end, at a distance of 100 mm from the end and "in the center") and the different grading classes of the used boards are given in Tab. 7.

Grading class of the boards			**MS 10 (C24M)**			**MS 13 (C35M)**			**MS 17 (C40M)**		
Type of loading (see also Fig. 5)			**1**	**2**	**3**	**1**	**2**	**3**	**1**	**2**	**3**
Subseries II/3											
Specimens number			18	18	18	18	18	18	18	18	18
Density ρ_g	Mean	[kg/m³]	422			461			475		
	COV	[%]	6,17			6,27			5,19		
	$\rho_{g,k}$	[kg/m³]	**379**			**413**			**434**		
MOE $E_{c,90,g}$ (h_0 = 200 mm)	Mean	[N/mm²]	**374**	**574**	**629**	**387**	**580**	**650**	**416**	**609**	**675**
	COV	[%]	8,25	13,11	13,95	7,88	9,08	9,08	8,57	7,40	8,51
	$E_{c,90,g,05}$	[N/mm²]	323	450	485	337	493	553	357	535	580
Strength perp. to the grain $f_{c,90,g}$ (h_0 = 200 mm)	Mean	[N/mm²]	4,40	5,82	6,14	4,49	5,86	6,27	4,38	5,41	5,67
	COV	[%]	7,44	12,76	15,20	11,54	11,01	15,64	10,24	11,80	14,53
	$f_{c,90,g,k;\ EN\ 14358}$	[N/mm²]	**3,79**	**4,51**	**4,51**	**3,59**	**4,71**	**4,63**	**3,59**	**4,29**	**4,32**
Subseries II/4											
Specimens number			5	5	5	5	5	5	5	5	5
MOE $E_{c,90,g}$ (h_0 = 480 mm)	Mean	[N/mm²]	**399**	**585**	**851**	**400**	**635**	**876**	**398**	**614**	**849**
	COV	[%]	17,84	17,37	15,40	9,11	9,71	16,44	9,44	13,11	8,99
	$E_{c,90,g,05}$	[N/mm²]	282	418	635	340	533	639	336	482	724
Strength perp. to the grain $f_{c,90,g}$ (h_0 = 480 mm)	Mean	[N/mm²]	4,59	5,69	6,11	4,79	5,90	6,66	4,59	5,70	6,29
	COV	[%]	10,17	14,22	5,93	5,47	8,98	12,53	6,98	6,63	6,33
	$f_{c,90,g,k;\ EN\ 14358}$	[N/mm²]	**3,53**	**3,93**	**5,32**	**4,20**	**4,78**	**4,95**	**3,86**	**4,84**	**5,43**

Tab. 7: Results of series II – subseries II/3 and II/4 (1... loading at the end, 2 ... loading in a distance 100 mm from the end, 3 ... loading "in the center")

In table 8 the results of the sill-like specimens with different loadings (subseries II/3 and II/4) are listed expressed as increasing factors in relation to the results obtained from the cubic specimens with the same height.

Grading class of the boards	MS 10 (C24M)			MS 13 (C35M)			MS 17 (C40M)		
Type of loading (see also Fig. 5)	1	2	3	1	2	3	1	2	3
Subseries II/3									
Mean value									
MOE $E_{c,90,g,mean}$ (h_0 = 200 mm) [-]	1,41	2,17	2,37	1,33	1,99	2,23	1,31	1,92	2,12
Strength perp. to the grain $f_{c,90,g,k;\ EN\ 14358}$ (h_0 = 200 mm) [-]	1,31	1,74	1,83	1,31	1,71	1,83	1,39	1,71	1,79
5%-quantile and characteristic value resp.									
MOE $E_{c,90,g,05}$ (h_0 = 200 mm) [-]	1,88	2,62	2,82	1,55	2,27	2,55	1,55	2,33	2,52
Strength perp. to the grain $f_{c,90,g,k;\ EN\ 14358}$ (h_0 = 200 mm) [-]	1,63	1,94	1,94	1,54	2,02	1,99	1,56	1,87	1,88
Subseries II/4									
Mean value									
MOE $E_{c,90,g,mean}$ (h_0 = 480 mm) [-]	1,47	2,15	3,13	1,57	2,49	3,44	1,28	1,97	2,72
Strength perp. to the grain $f_{c,90,g,k;\ EN\ 14358}$ (h_0 = 480 mm) [-]	1,59	1,97	2,11	1,67	2,06	2,32	1,62	2,01	2,21
5%-quantile and characteristic value resp.									
MOE $E_{c,90,g,05}$ (h_0 = 480 mm) [-]	1,26	1,87	2,85	1,59	2,49	2,99	1,58	2,25	3,42
Strength perp. to the grain $f_{c,90,g,k;\ EN\ 14358}$ (h_0 = 480 mm) [-]	1,68	1,87	2,53	1,99	2,27	2,35	1,78	2,23	2,50

Tab. 8: Increasing factors for mechanical properties of the sill-like specimens concerning different loading situations in relation to the cubic specimens of the same height

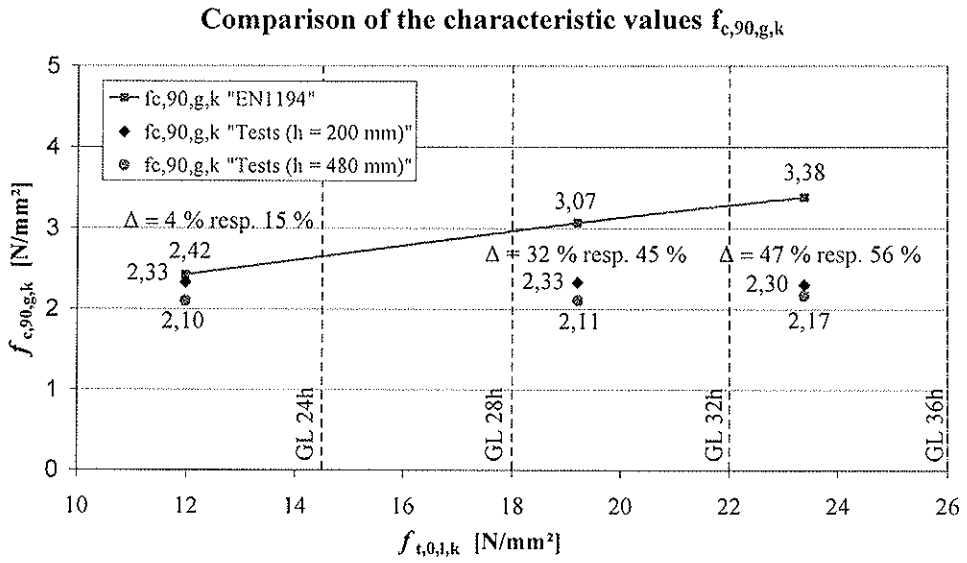

Fig. 7: Comparison of the characteristic values $f_{c,90,g,k}$ calculated with the function in EN 1194:1999 and the test results of series II/1 and II/2

The following diagram (Fig. 8) shows the correlation between the density and the compression strength perpendicular to the grain of the cubic specimen from series I and II/1. Additionally to the regression line also their 95%-confidence interval and the 95%-interval for the regression model is drawn.

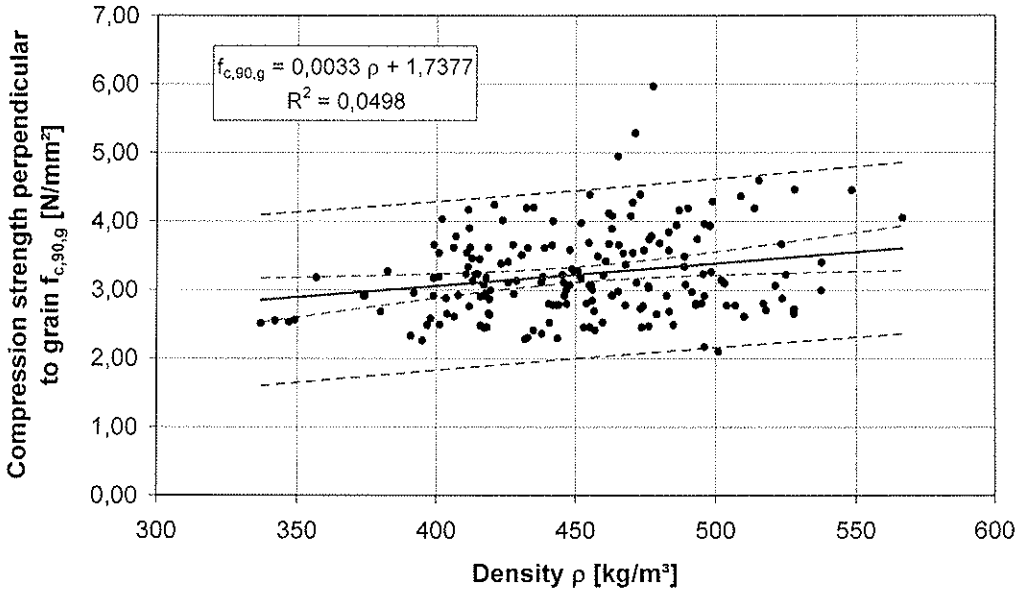

Fig. 8: Correlation between the density and the compression strength perpendicular to grain of the cubic specimen of series I and II/1 with 95%- confidence interval for the regression line and 95%-interval for the regression model

In Fig. 9 the results of series II for the different loadings (cubic specimens – full area loading; sill-like specimens: loading at the end, 100 mm from the end and "in the center"), the different strength classes of the boards and specimens heights h_0 = 200 mm and h_0 = 480 mm are shown.

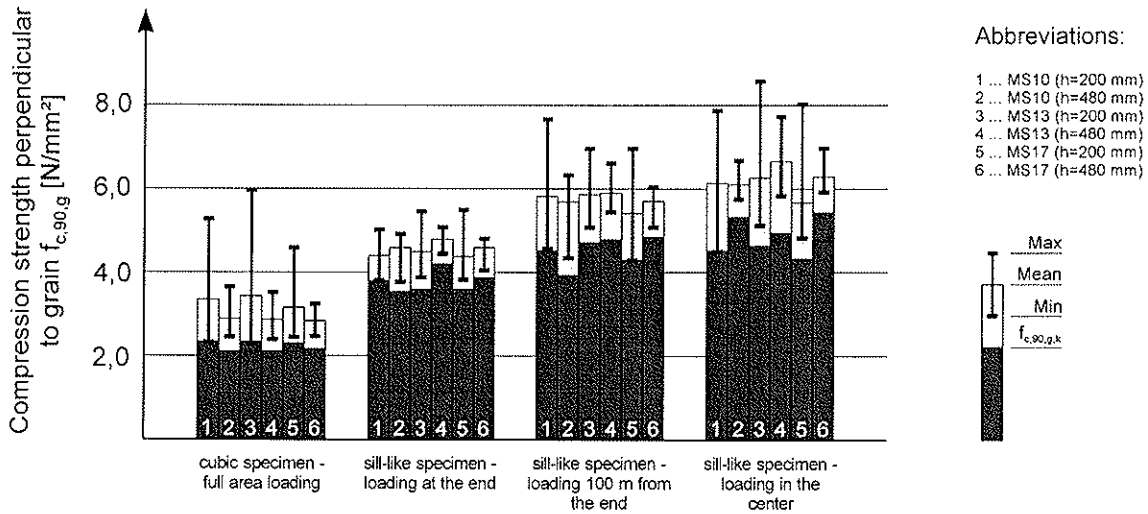

Fig. 9: Comparison of the results for the compression strength perpendicular to the grain depending on the different loading situations, strength classes of the boards and specimens heights

7 Summary and Discussion

As can be seen from the results in Fig. 6 and Fig. 7 the proposed correlation in EN 1994:1999 between the tensile strength and grading class of the boards resp. and the compression strength perpendicular to the grain for glulam could not be confirmed. For a specification in standards a value between 2,1 N/mm² and 2,3 N/mm² for cubic specimens (loaded on the whole surface) independent from the glulam strength class is recommended and has to be discussed. For the mean MOE $E_{c,90}$ a constant value of about 300 N/mm² (for the cubic specimens) valid for all glulam strength classes (see Tab. 4 and Tab. 5) should be introduced. These values confirm exactly the results published by [10].

From the wood technological point of view no definitely characteristic influencing the mechanical properties of this type of loading has been found. Between the density and the strength perpendicular to grain a slightly correlation with pronounced fuzziness of the test data could has been observed. The analysis of the board's annual ring pattern used for the lay-up of the cubic specimens has been shown a slightly dependence on the mechanical properties perpendicular to grain. Specimens with upstanding annual ring pattern resulted in slightly higher stiffness and strength than those with flat-lying annual rings.

If the analysis is done with a deformation limit of 0,02 h_0 and 0,05 h_0 resp. the characteristic compression strength values are increasing by about 15% and 30% resp. compared with those calculated in accordance with the procedure given in EN 408:2005 (0,01 h_0 deformation limit).

The results from the cubic specimens with two different heights (h_0 = 200 mm and h_0 = 480 mm) showed no significant difference. Thus a dependence on the height of the characteristic stiffness and strength values for the cubic specimens could not be observed.

The tests on sill-like specimens revealed a strong dependence on the loading situation. This can be explained with the supporting effect of wood fibers beside the loaded area. For specimens with a height of h_0 = 200 mm the mean stiffness values increased by a factor of 1,35 for the specimens loaded at the end, 2,03 for those with a distance of 100 mm from the end and 2,24 for those loaded "in the center". For the characteristic compression strength perpendicular to the grain values increased by a factor of 1,58 (at the end), 1,94 (at a distance 100 mm from the end) and 1,94 (load "in the center").

The corresponding factors for the specimens with height h_0 = 480 mm are: 1,44 (at the end), 2,20 (at a distance of 100 mm from the end) and 3,10 (load "in the center") for the mean MOE values and 1,82 (at the end), 2,12 (at a distance of 100 mm from the end) and 2,46 ("in the center") for the characteristic compression strength perpendicular to the grain. It has to be mentioned that these values are linked to a bearing length of 150 mm.

Unlike to the results of the cubic specimens those of the stiffness and strength values perpendicular to the grain for the sill-like specimens showed an increasing tendency with increasing height. This fact is a consequence of the definition of the mechanical parameters and due to the spreading of the load under the loading area resp. Furthermore if the distance of the loaded area is more or equal than 100 mm from the end no significant difference of the mechanical properties could be found.

For design purposes of loaded sills the application of the strength perpendicular to the grain of $f_{c,90,g,k}$ = 2,30 N/mm² and a factor $k_{c,90}$ = 1,50 for the loading situation at the end and a factor $k_{c,90}$ = 1,80 for loadings at a distance of ≥100 mm from the end can be suggested. As a conservative approach the mentioned $k_{c,90}$-factors can also used for the calculation of the stiffness.

It has to be mentioned that the given data for the sills can be explained in an excellent way with the theoretical model given in [12].

8 Acknowledgement

The presented research work of series I was in the main part carried out within the diploma thesis of A. Ruli [13] at the Institute of Timber Engineering and Wood Technology at Graz University of Technology / Austria. Additionally A. Ruli and R. Brandner were employed during the time they were working on Series II at the competence centre holz.bau forschungs gmbh which is supported with funds from the Federal Ministry of Economics and Labour (BMVA), of the Province of Styria and the City of Graz as a part of the programme Centres and Networks of Excellence for Technology Development of the BMWA in Austria.

We would like to thank our colleagues G. Meinhardt for the co-supervision on A. Ruli's thesis and B. Heissenberger, Y. Halili and H. Krenn (all holz.bau forschungs gmbh) for their support during the tests in the lab and the analysis of the data. Special thanks goes also to E. Gehri for his valuable discussions and his helpful suggestions during the tests and the analysis of the data.

9 Literature

[1] Graf, O.
„Beobachtungen über den Einfluss der Größe der Belastungsfläche auf die Widerstandsfähigkeit von Bauholz gegen Druckbelastung quer zur Faser“,
Der Bauingenieur, 18 (1921), p. 498-501

[2] Suenson, E.
"Zulässiger Druck auf Querholz",
Holz als Roh- und Werkstoff, 1 (1938), No. 6, p. 213-216

[3] Kennedy, R.W.
„Wood in Transverse Compression“,
Forest Products Journal, Vol. 18, No.3, p. 36-40, 1968

[4] Korin, U.
"Timber in Compression Perpendicular to Grain"
Proceedings of the CIB-W-18, Paper 23-6-1, Lisbon, Portugal, 1990

[5] Pellicane, P.J.; Bodig, J.; Mrema, A.L.
"Behavior of Wood in Transverse Compression",
Journal of Testing and Evaluation, Vol. 22, No. 4, p. 383-387, 1994

[6] Ethington, R.L.; Eskelsen, V.; Gupta, R.
"Relationship between compression strength perpendicular to grain and ring orientation", Forest Products Journal, 46 (1), p. 84-86, 1996

[7] Gehri, E.
"Timber in compression perpendicular to the grain"
International Conference of IUFRO S 5.02 Timber Engineering, Copenhagen, Denmark, 1997

[8] Leicester, R.H.; Fordham, H.; Breitinger, H.
"Bearing Strength of Timber Beams"
Proceedings of the CIB-W-18, Paper 31-6-5, Savonlinna, Finland, 1998

[9] Madsen, B.
"Behaviour of Timber Connections"
Timber Engineering Ltd., Vancouver, Canada, 2000

[10] Damkilde, L.; Hoffmeyer, P.; Pedersen, T.N.
"Compression Strength Perpendicular to Grain of Structural Timber and Glulam"
Holz als Roh- und Werkstoff, 58 (2000), p. 73-80

[11] Blass, H.-J.; Görlacher, R.
"Compression perpendicular to the grain",
Proceedings of the 8th World Conference on Timber Engineering, Vol. II,
Lahti, Finland, 2004

[12] van der Put, T.A.C.M.; Leijten, A.J.M.
"Evaluation of Perpendicular to Grain Failure of Beams caused by Concentrated Loads of Joints", Appendix II
Proceedings of the CIB-W-18, Paper 33-7-7, Delft, The Netherlands, 2000

[13] Ruli, A.
"Längs und quer zur Faserrichtung auf Druck beanspruchtes Brettschichtholz",
Diploma thesis, Institute for Timber Engineering and Wood Technology, Graz University of Technology, Graz, 2004

[14] EN 1194:1999
"Timber structures – Glued laminated timber; Strength classes and determination of characteristic values"

[15] EN 384:2004
"Structural timber – Determination of characteristic values of mechanical properties and density"

[16] EN 408:2005
"Timber structures – Structural timber and glued laminated timber; Determination of some physical and mechanical properties"

[17] prEN 14358:2006
"Timber structures – Calculation of 5-percentile values and acceptance criteria for a sample"

INTERNATIONAL COUNCIL FOR RESEARCH AND INNOVATION
IN BUILDING AND CONSTRUCTION

WORKING COMMISSION W18 - TIMBER STRUCTURES

EFFECT OF TRANSVERSE WALLS ON CAPACITY OF WOOD-FRAMED WALL DIAPHRAGMS

U A Girhammar
Civil Engineering, Department of Applied Physics, Umeå University

B Källsner
School of Technology and Design, Växjö University
SP Swedish National Testing and Research Institute, Stockholm

SWEDEN

MEETING THIRTY-NINE
FLORENCE
ITALY
AUGUST 2006

Presented by B Källsner
H Blass asked how the capacity of the nailed connection was calculated. B Källsner answered that some old test results of similar connections were used for this paper. The work was still a preliminary evaluation and would be doing more.
B Dujic and B Källsner agreed that the influence of length of transfer wall have a limit as maximum value should be the case of fully anchored wall. Also linear beam elements would also influence the load path.
I Smith suggested the completion of the box would be of interest. B Källsner agreed that consideration of the rest of the structure would be important.
E Karacabeyli commented that two story tests without hold-down showed that they behaved well. This analytical approach offered theoretical explanation and support of the experimental results.
B Dujic commented that based on this work every wall with transverse wall can make use of the added capacity.

Effect of Transverse Walls on Capacity of Wood-Framed Wall Diaphragms

Ulf Arne Girhammar
Civil Engineering, Department of Applied Physics, Umeå University, Sweden

Bo Källsner
School of Technology and Design, Växjö University, Sweden
SP Swedish National Testing and Research Institute, Stockholm, Sweden

Abstract

It is well known that the structural behaviour of a wood-framed wall diaphragm is to a large extent dependent on the 3-dimensional behaviour of the whole building. In this connection the influence of transverse walls is an issue of special interest.

A plastic design method capable of analyzing the behaviour and capacity of partially anchored wood-framed wall diaphragms has been presented in previous papers. In this paper the plastic model is applied to the case where a wall diaphragm is connected to a transverse wall. The tying-down effect of the transverse wall on the vertical uplift is studied and the effect on the horizontal load-bearing capacity of the wall diaphragm is analyzed. In an ongoing study, tests are being conducted to evaluate the strength and stiffness of these transverse walls.

The paper describes the theoretical analyses and the experimental results for sheathed wood-framed transverse walls of different geometrical configurations and with different boundary conditions. Transverse walls are studied by varying the number of sheet segments and the horizontal fixing of the top rail. The extreme cases of horizontally fixed and free top rail are investigated. The effect of the tying-down action of transverse walls on the load-carrying capacity of wall diaphragms and the agreement between theoretical and experimental results are presented.

1 Introduction

1.1 Background

The structural behaviour and capacity of wall diaphragm are primarily dependent on the sheathing-to-timber joints, the anchorage of studs, the vertical loads, and on the transverse walls and the inter-component connections between the wall diaphragms and the surrounding structures. Due to the conditions for stud anchoring and the action of vertical loads on the studs, the wall diaphragm will behave as fully or partially anchored. A new plastic method capable of analyzing the behaviour and capacity of both, with respect to vertical uplift, fully and partially anchored wood-framed wall diaphragms frequently used in practice has been presented in previous papers, see e.g. Källsner and Girhammar (2005). The method covers static loads and can be applied when mechanical fasteners with plastic or partially plastic characteristics are used.

It is well known that the structural behaviour of a wood-framed wall diaphragm is to a large extent dependent on the 3-dimensional behaviour of the whole building. In this connection the influence of transverse walls is an issue of special interest. These transverse

walls, connected to the wall diaphragms, may have the corresponding restraining effect on the vertical uplift of the wall diaphragms as do tying-down devices or vertical loads. This tying-down effect will depend on the strength and stiffness of the transverse wall itself as well as the inter-component connection between the two walls. In this paper, attention is given to the capacity of the transverse wall itself.

1.2 Objective and scope

The overall purpose of the research project is to develop an analytical method for the design of wood-framed wall diaphragms in the ultimate limit state with different anchoring, loading and geometrical conditions and with different sheet and framing materials, and fasteners used.

The objective of this paper is to describe the theoretical analyses and the experimental results for sheathed wood-framed transverse walls of different geometrical configurations and with different boundary conditions. Transverse walls are studied by varying the number of sheet segments and the horizontal fixing of the top rail. The extreme cases of horizontally fixed and free top rail will be investigated. The effect of the tying-down action of transverse walls on the load-carrying capacity of wall diaphragms and the agreement between theoretical and experimental results will be presented.

The purpose of this paper is also to investigate the effect of transverse walls on the load-carrying capacity of partially anchored wood-framed wall diaphragms and to give some design recommendations.

In this paper, the plastic model is applied to the transverse wall and its tying-down effect on the vertical uplift and the effect on the horizontal load-bearing capacity of the wall diaphragm is analyzed. In an ongoing study, tests are being conducted to evaluate the strength and stiffness of these transverse walls and to enable a verification of the analytical results. Here it will be assumed that the build-up of the transverse walls and the wall diaphragms is similar. Only the tests on transverse walls with free top rail will be included here.

2 Testing program

2.1 Specification of transverse walls tested

Tests on sheathed wood-framed transverse walls of different geometrical configurations and with different boundary conditions subjected to a vertical uplifting force have been conducted. The testing arrangements are shown in Figure 1.

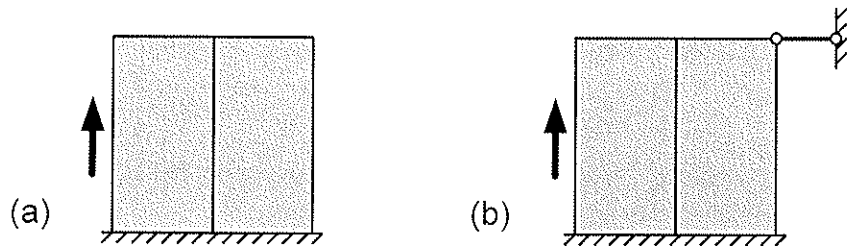

Figure 1. Testing of transverse walls subjected to vertical uplift and (a) top rail free to displace horizontally and (b) top rail fixed against horizontal displacement.

One series refers to transverse walls with different numbers of sheet segments and the top rail free to displace horizontally, series 1. The other series refers to transverse walls with different numbers of sheet segments and the top rail fixed against horizontal displacement, series 2. The free and fixed top rail, respectively, constitute the extreme cases for the behaviour of transverse walls in practice. The different types of tests are summarized in Table 1.

Table 1. Specifications of transverse walls tested. Bottom rail was fully anchored to the substrate in both series.

Series	Configuration	Boundary conditions	Number of tests
1	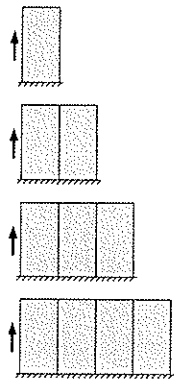	Top rail free to displace horizontally	4 3 4 4
2	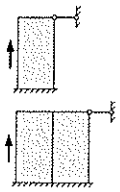	Top rail fixed against horizontal displacement	

Here the tests with top rail fixed against horizontal displacement will not be reported.

2.2 Test specimens and testing procedure

All walls tested were made of sheathing fastened to a timber frame. Only one side of the frame was sheathed. The test specimens were designed as follows:

- Frame members: Pine (Pinus Silvestris), C24, 45×120 mm, stud spacing 600 mm.
- Sheathing: Hardboard, 1200 × 2400 × 8 mm (wet process fibre board, HB.HLA2, Masonite AB).
- Sheathing-to-timber joints: Annular ringed shank nails, 50×2.1 mm (Duofast, Nordisk Kartro AB). The joints were hand-nailed and the holes were pre-drilled, 1.7 mm. Nail spacing was 100 mm along the perimeter and 200 mm along the vertical centre line of the sheets. Edge distance was 11.25 mm along the vertical studs and 22.5 mm along the bottom and top rails.
- Framing joints: Two annular ringed shank nails of dimension 90×3.1 mm were applied in the grain direction of the vertical studs.

All tests were performed under displacement control with a constant rate of 8 mm/min. The vertical load was applied as a tension force along the side of the leading stud. The

horizontal displacement and the reaction force were measured at the centre of the top rail for the two tests series, respectively. The bottom rail was anchored against vertical uplift to the substrate along the entire length of the wall.

For each test, the density and moisture content were determined and a choice of fasteners was tested with respect to the bending yield stress. However, these results are not yet available.

3 Test results for transverse walls with free top rail

The test results for transverse walls with one, two, three, and four sheet segments and top rail free to displace horizontally are summarized in Table 2. A ductile type of joint failure by yielding and withdrawal of nails from the bottom rail took place, where the main direction of the nail forces was essentially perpendicular to the bottom rail. The final failure mode of the wall was ductile.

Table 2. Test results for transverse walls with different number of sheet segments and top rail free to displace horizontally.

Series 1	Maximum load in different tests [kN]	Mean value of maximum load [kN]	Coefficient of variation [%]
One segment	6.0, 6.5, 7.9, 7.4	6.95	12.4
Two segments	9.6, 12.0, 11.7	11.1	11.8
Three segments	16.4, 17.2, 18.8, 18.0	17.6	5.87
Four segments	20.0, 20.5, 21.0, 22.2	20.9	4.51

4 Analytical model

4.1 Basic assumptions

For the analytical evaluation of the capacity of the partially anchored transverse walls subjected to vertical uplift a plastic lower bound method is proposed. This means that a force distribution is chosen that fulfils the conditions of force and moment equilibrium for each timber member and sheet. The basic assumptions are given in Källsner & Girhammar (2005). However, in this paper we apply the methods somewhat differently. The full vertical shear model is used together with a strict use of the lower bound method, but neglecting the influence of the framing joints, in two ways: First, we consider the different sheets as one entire sheet, i.e. the internal equilibrium between sheets is not taken into account; and second, we consider the different sheets as separate sheets and fulfil the internal equilibrium.

In order to obtain simple expressions for the capacity of the transverse walls, the fastener forces are assumed continuously distributed along the timber members. The load-carrying capacity of the sheathing-to-timber joints is consequently given in force per unit length. In

all the examples presented below, it is assumed that the fastener spacing around the perimeter of the sheets is constant.

4.2 Vertical load-bearing capacity

4.2.1 General

According to the static theorem, a wall free to displace horizontally and subjected to a vertical uplifting load equals the sum of the two sub-cases according to Figure 2.

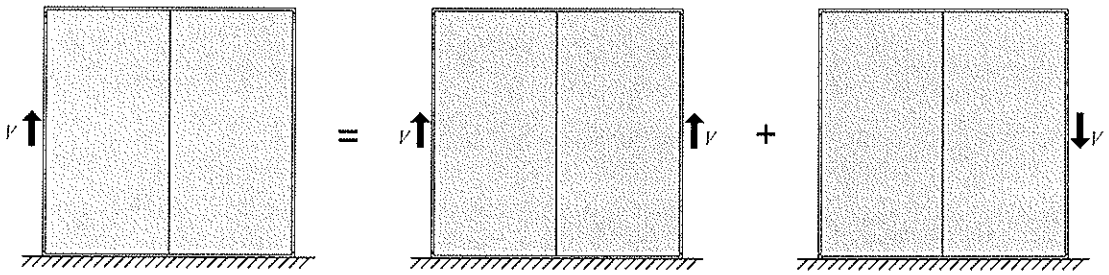

Figure 2. Original transverse wall subjected to vertical uplift is divided into two sub-cases.

4.2.2 One segment transverse walls

Top rail free to displace horizontally: Consider Figure 3a. f_p represents the plastic shear capacity per unit length of the sheathing-to-timber joints.

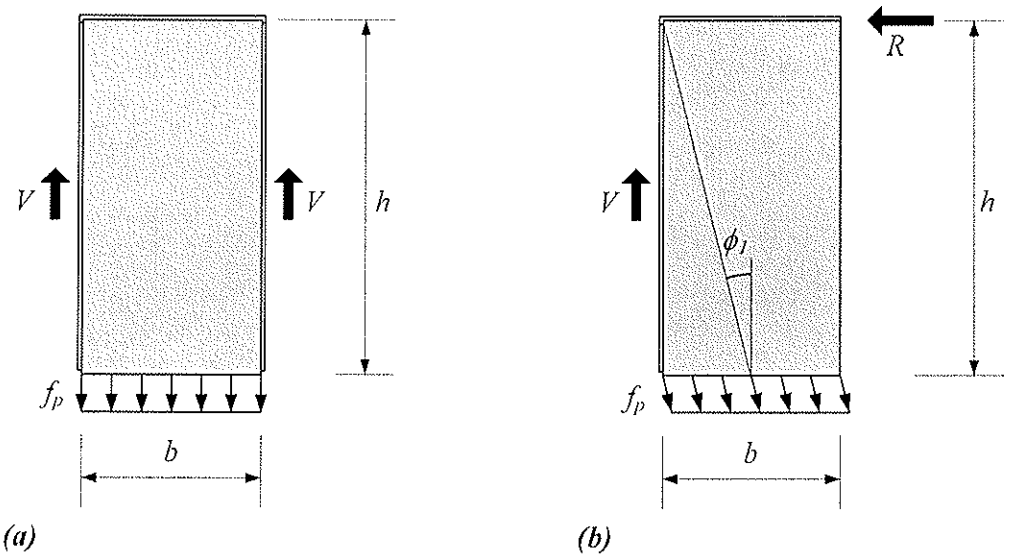

Figure 3. Plastic capacity of a one segment wall diaphragm in case of (a) top rail free to displace horizontally and (b) top rail fixed against horizontal displacement.

Equilibrium for vertical forces gives the capacity of the free transverse wall as

$$V = \frac{1}{2} f_p b \qquad (1)$$

Top rail fixed against horizontal displacement: Consider Figure 3b. R represents the reaction force at the horizontally fixed support. Assuming $h = 2b$, force equilibrium gives that the resultant of the fastener forces along the bottom rail must pass through the upper left corner of the wall i.e.

$$\phi_1 = \arctan\frac{b}{2h} = \arctan\frac{1}{4} = 14.0^\circ \tag{2}$$

Considering vertical equilibrium gives the capacity of the horizontally fixed transverse wall as

$$V = f_p b \cos\phi_1 = 0.970 f_p b \tag{3}$$

4.2.3 Two segment transverse walls

Top rail free to displace — Not considering internal equilibrium between sheets: Consider Figure 4.

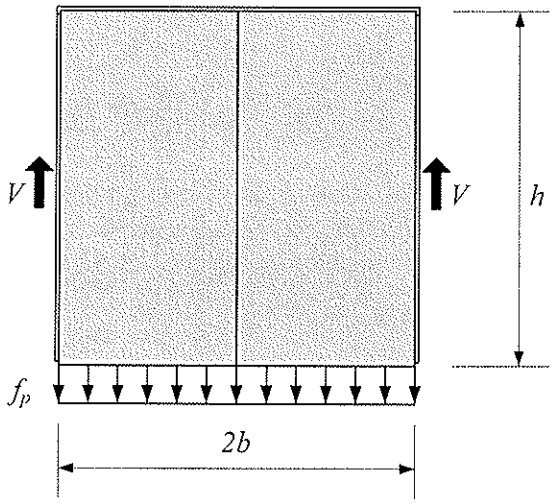

Figure 4. Plastic capacity of a two segment wall diaphragm in case of top rail free to displace horizontally and no regard taken to the internal equilibrium between the sheets.

Vertical force equilibrium gives the capacity of the free transverse wall considered as one sheet unit (no regard to equilibrium between the sheets) as

$$V = f_p b \tag{4}$$

Top rail free to displace — Considering internal equilibrium between sheets: Consider Figure 5.

Each sub-case corresponds to that for the fixed one segment case, i.e. the capacity of the free transverse wall with internal equilibrium between the sheets is given by

$$V = f_p b \cos\phi_1 = 0.970 f_p b \tag{5}$$

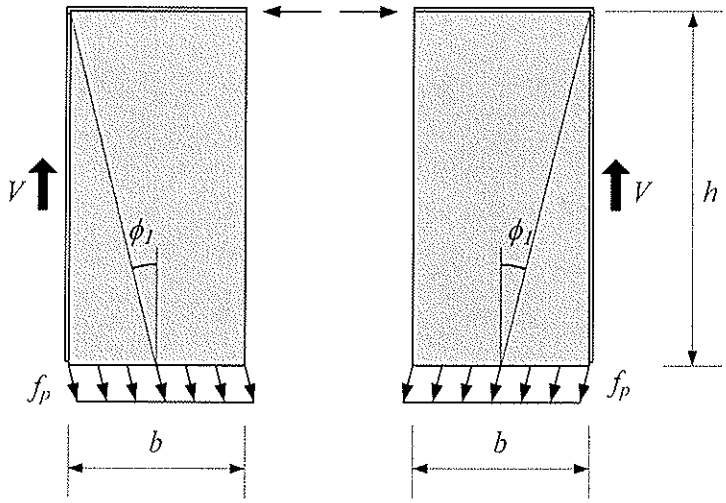

Figure 5. Plastic capacity of a two segment wall diaphragm in case of top rail free to displace horizontally and the internal equilibrium between the sheets taken into account.

Top rail fixed against displacement — Not considering internal equilibrium between sheets: Consider Figure 6.

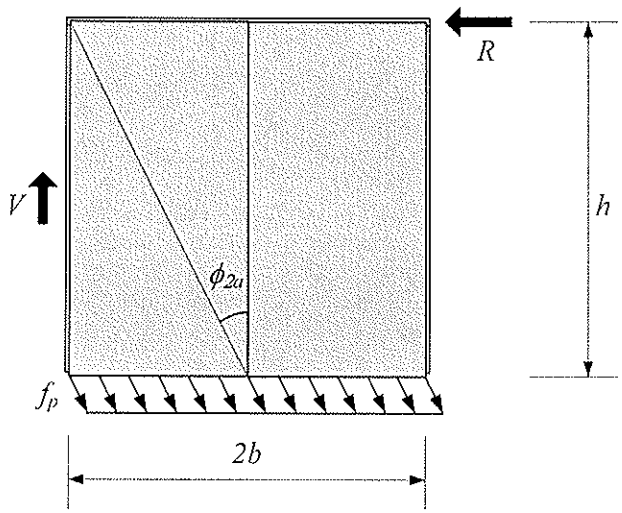

Figure 6. Plastic capacity of a two segment wall diaphragm in case of top rail fixed against horizontal displacement and no regard taken to the internal equilibrium between the sheets.

Force equilibrium gives

$$\phi_{2a} = \arctan\frac{b}{h} = \arctan\frac{1}{2} = 26.6^\circ \qquad (6)$$

and the capacity of the horizontally fixed transverse wall with no regard to internal equilibrium as

$$V = 2f_p b\cos\phi_{2a} = 1.79 f_p b \qquad (7)$$

Top rail fixed against horizontal displacement — Considering internal equilibrium between sheets: Consider Figure 7.

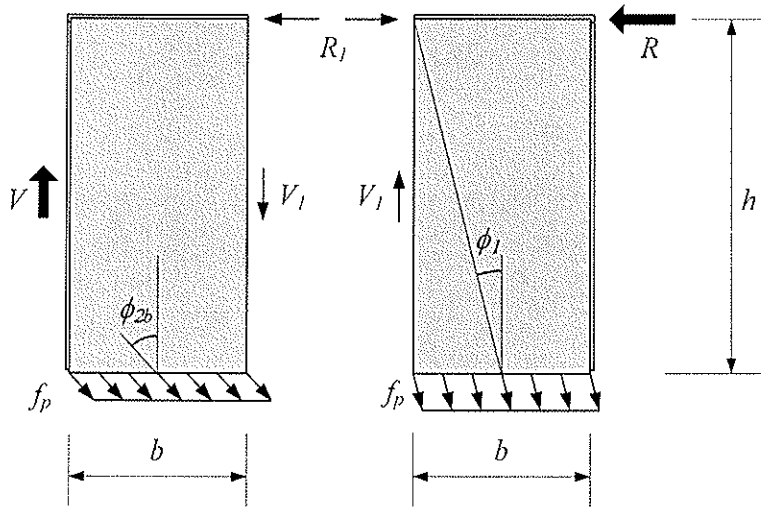

Figure 7. Plastic capacity of a two segment wall diaphragm in case of top rail fixed against horizontal displacement and the internal equilibrium between the sheets taken into account.

The right sub-case in Figure 7 corresponds to the fixed one segment case, i.e. the vertical capacity equals equation (5), i.e. $V_1 = f_p b \cos\phi_1 = 0.970 f_p b$. Considering that $R_1 = f_p\, b \sin\alpha_{2b}$ and $V\text{-}V_1 = f_p\, b \cos\alpha_{2b}$, moment equilibrium for the left segment around the centre of the bottom rail gives

$$4\sin\alpha_{2b} - \cos\alpha_{2b} = 2V_1/f_p b = 1.94, \quad \text{i.e.} \quad \alpha_{2b} = 42.1^\circ \tag{8}$$

Vertical equilibrium gives the capacity of the fixed transverse wall with internal equilibrium between the sheets as

$$V = f_p b \cos\phi_{2b} + V_1 = (\cos\phi_{2b} + \cos\phi_1) f_p b = 1.71 f_p b \tag{9}$$

4.2.4 Three and four segment transverse walls

The detailed derivations are not shown here. The resulting expressions are given in Table 3.

5 Comparison between analytical and measured results

The plastic capacity of the sheathing-to-timber joints, f_p, used to compare the experimental and theoretical values are those obtained for single sheathing-to-timber joint tests according to Girhammar et al. (2004), i.e. f_p = 10.5 kN/m.

The results obtained by analytical methods and those measured by testing are compared in Table 3.

Table 3. Comparison of theoretical and experimental results for vertical load-bearing capacity of transverse walls with different number of segments. The top rail is free with respect to horizontal displacements.

Test wall	Load-carrying capacity V			$\frac{V_{measured}}{V_{calculated}}$	
	Mea-sured	Analytical values		Internal equilibrium not regarded	Internal equilibrium regarded
		Internal equilibrium not regarded	Internal equilibrium regarded		
One	6.95	$0.5 f_p b = 6.30$		1.10	
Two	11.1	$1.0 f_p b = 12.6$	$0.970 f_p b = 12.2$	0.88	0.91
Three	17.6	$1.5 f_p b = 18.9$	$1.38 f_p b = 17.4$	0.93	1.01
Four	20.9	$2.0 f_p b = 25.2$	$1.71 f_p b = 21.5$	0.83	0.97

The results according to Table 3 are preliminary. It is obvious that there is fairly good agreement between theoretical and experimental values.

6 Effect of transverse walls on the capacity of wall diaphragms

The horizontal load-carrying capacity of partially anchored wall diaphragms can be written as (Källsner & Girhammar, 2005)

$$H = f_p l_{eff} \tag{10}$$

where the effective wall length is given by

$$l_{eff} = \begin{cases} l - \frac{h}{2}\left(1 - \frac{V_0}{f_p h}\right)^2 & ; \quad l \geq h(1 - \frac{V_0}{f_p h}) \\ l\left(\frac{l}{2h} + \frac{V_0}{f_p h}\right) & ; \quad l \leq h(1 - \frac{V_0}{f_p h}) \\ l & ; \quad \frac{V_0}{f_p h} \geq 1 \end{cases} \tag{11}$$

where V_0 is the vertical downward load on the leading stud and corresponds to the vertical capacity of the transverse walls.

If it is assumed that the vertical capacity of the transverse walls can be utilized in tying down the leading stud of wall diaphragms made of the same number of segments as in the transverse walls, the horizontal load-carrying capacity of these wall diaphragms will increase as shown in Table 4. $V_0 = f_p h$ corresponds to the case fully anchored leading stud.

Table 4. Effect of transverse wall on the horizontal load-carrying capacity of wall diaphragms with different number of segments. The number of segments is the same in both wall diaphragms and transverse walls.

Wall diaphragm	Horizontal load-carrying capacity of wall diaphragm, H			Increase of horizontal load-carrying capacity
	$V_0 = 0$	$V_0 = f_p h$	$V_0 = V_{test}$	
	$0.250 f_p b$	$1 f_p b$	$0.526 f_p b$	$0.276 f_p b$
	$1 f_p b$	$2 f_p b$	$1.69 f_p b$	$0.69 f_p b$
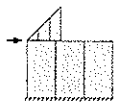	$2 f_p b$	$3 f_p b$	$2.91 f_p b$	$0.91 f_p b$
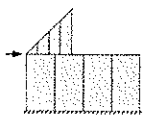	$3 f_p b$	$4 f_p b$	$3.97 f_p b$	$0..97 f_p b$

Table 4 clearly shows the big effect of the tying down action of the transverse walls on the load-carrying capacity of wall diaphragms with different number of segments. The geometrical configuration is assumed to be the same in both the transverse walls and the wall diaphragms. For a one segment wall diaphragm, for example, the load-bearing capacity is more than twice that of a wall diaphragm without tie-downs.

7 Conclusions

A plastic lower bound method is used to study the effect of transverse walls on the load-carrying capacity of partially anchored wood-framed wall diaphragms. The load-bearing capacity for transverse walls with various number of sheet segments subjected to a vertical uplifting force is derived.

The analytical values are compared to preliminary test results and are found to agree fairly well. A more comprehensive experimental study and evaluation need to be conducted to verify the analytical models.

The tying down effect of transverse walls with the same geometrical configurations as for the wall diaphragms is demonstrated for walls with one to four sheet segments. The effect is found to be very significant.

References

Girhammar U.A., Bovim N.I., and Källsner B., "Characteristics of sheathing-to-timber joints in wood shear walls", *8th World Conference on Timber Engineering*, Lahti, Finland, 2004.

Källsner B., and Girhammar U.A., "Plastic design of partially anchored wood-framed wall diaphragms with and without openings", *Proceedings CIB-W18 Meeting*, Karlsruhe, Germany, 2005.

INTERNATIONAL COUNCIL FOR RESEARCH AND INNOVATION
IN BUILDING AND CONSTRUCTION

WORKING COMMISSION W18 - TIMBER STRUCTURES

WHICH SEISMIC BEHAVIOUR FACTOR FOR MULTI-STOREY BUILDINGS MADE OF CROSS-LAMINATED WOODEN PANELS?

A Ceccotti, M Follesa, M P Lauriola

C Sandhaas

CNR-IVALSA

ITALY

Chikahiro Minowa

NIED

Naohito Kawai

BRI

Motoi Yasumura

Shizuoka University

JAPAN

MEETING THIRTY-NINE

FLORENCE

ITALY

AUGUST 2006

Presented by A Ceccotti

H Blass commented that the real time behaviour was better than the static behaviour.

B Dujic commented that the testing of the wall was better than the testing of the anchors. How the anchor behave is important. Two of his walls were recently tested and would present the work next week in a different meeting. He asked about the one story test where q was less than 3.

A Ceccotti stated that the nails were not randomly put. 12 nails were used in an anchor to ensure the nail and not steel failures. Also Additional story improved the behaviour.

A Buchanan stated that the strength of the wall was not chosen for seismic reason. If there were a wood failure would one worry about collapse.

A Ceccotti stated that it would be impossible in this case. The matter is not to make the wall thinner. In Italy and Central Europe people want the feel of solid wall.

I Smith stated that light frame system also behaved better than single wall but this would not be the same in the case of masonry.

F Lam asked about the rigidity of the diaphragm. A Ceccotti stated that the rigid diaphragm was assumed in the model but non rigid diaphragm was observed in test. F Lam also asked whether torsional response was observed in the tests. A Ceccotti stated that it was observed in pseudo dynamic tests but less in the shake table test.

G Schickhofer stated that in Graz a 7x7 system was tested in racking but could not destroy the wall; therefore, the wood failure would be unlikely.

R Steiger stated that in shake table test accurate reproduction of the ground acceleration would obviously be important but what about the displacement. C Minowa stated that the maximum displacement was 10 cm from the supplied record because high pass filter was originally used. In this test low pass filter was used and ~40 cm of peak ground motion was obtained on the table.

R Marsh asked about some shake table test results done in 2001 in Japan. M Yasumura has agreed to check on this.

Which Seismic Behaviour Factor for Multi-Storey Buildings made of Cross-Laminated Wooden Panels?

Ario Ceccotti, Maurizio Follesa, Marco Pio Lauriola, Carmen Sandhaas
CNR-IVALSA, Italy

Chikahiro Minowa
NIED, Japan

Naohito Kawai
BRI, Japan

Motoi Yasumura
Shizuoka University, Japan

1 Abstract

Day by day, multi-storey buildings made of cross-laminated wooden panels (XLam) are becoming a stronger and economically valid alternative to their counteracts built with concrete and masonry. Throughout Europe and even in seismic prone zones, this construction type is gaining a broader acceptance.

However, until now, in Eurocode 8 this constructive system is not yet included and no recommendations are given regarding constructive details. Especially regarding the value of the seismic behaviour factor to be used in seismic design of this new typology of wooden buildings, no comprehensive investigations have yet been undertaken.

In this paper, results from shaking table tests on a three-storey cross-laminated wooden building are presented and the value of the seismic behaviour factor is found on the base of the actual response of the building to one quake.

2 Introduction

The SOFIE Project is a cooperative research project supported by the Trento Province, Italy and coordinated and conducted by the CNR-IVALSA (Italian National Research Council – Trees and Timber Institute).

The main purpose of this project is to analyse multi-storey buildings built with solid wooden panels with cross interlayers considering every aspect of the building behaviour such as static, fire, acoustic, thermal and, particularly, seismic performance.

Especially regarding the seismic performance, a comprehensive testing programme has been undertaken jointly by CNR-IVALSA and NIED (National Institute for Earth Science and Disaster Prevention, Japan), consisting in the following stages:

- tests on connections,

- in-plane cyclic tests on wall panels with different connections and opening layouts and with different dimensions and amounts of vertical load,
- pseudo-dynamic tests on a one-storey specimen in 3 different opening layouts in the external walls parallel to the shaking direction and without vertical load,
- shaking table tests on a three-storey building of about 7m x 7m in plan and 10m of total height with a pitched roof in 3 different configurations (3 different opening layouts, A, B and C) and with 3 different earthquakes (Kobe, El Centro and Nocera Umbra) at 2 growing levels of PGA (0.15g and 0.5g),

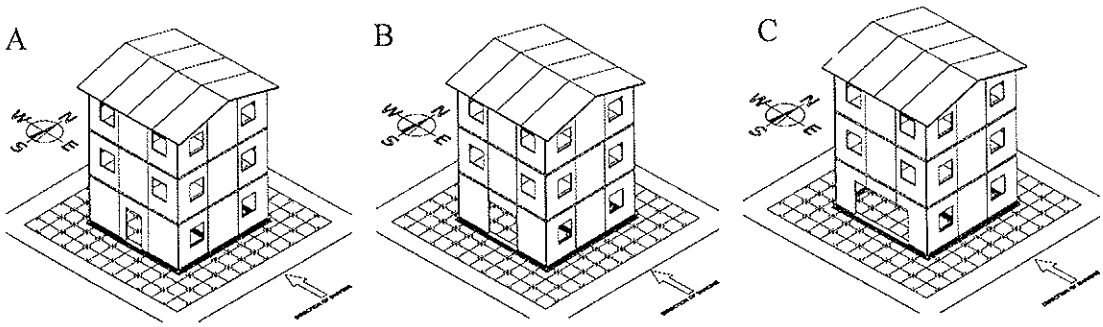

Figure 1: Three different configurations in which the building has been tested. While Configuration A and B are symmetric, Configuration C is asymmetric as the opening of the other external wall parallel to the shaking direction is equal to the one in Configuration B.

- Finally, configuration C of the building has been tested applying Kobe and Nocera Umbra at growing levels of excitation until the "near collapse" status was reached.

Here, for the sake of this paper, reference will be made to this last phase, while the rest of collected data and discussion will be matter of further papers to be published soon.

2.1 How to determine the q value

Most seismic design codes contain action reduction factors (ARF) to evaluate the forces to be accounted for when designing the structure using a simple elastic global analysis. ARF then reflects the capability of a structure to dissipate energy through inelastic behaviour such that it survives even exceptional earthquakes without complete collapse, i.e. the so-called "near-collapse" limit state.

This philosophy is the same of Eurocode 8 in which the ARF is called "seismic behaviour factor *q*" which according to the definition is *the factor used for design purposes to reduce the forces obtained from a linear analysis, in order to account for the non-linear response of a structure, associated with the material, the structural system and the design procedures.*

The main way to follow in order to assess the correct q value for a given structural system is based on mathematical calculations using an appropriate computer model. This model is capable of giving the non-linear response of the structure under a certain number of real earthquake excitations. The following procedure must be applied:

- Design the structure for an anticipated q value according to the relevant codes ("static" and seismic codes, e.g. Eurocode 5 and 8 [1]) and the design PGA_u prescribed by the code ($PGA_{u,code}$). At the end of this step, the resistant system will be completely decided.
- Model the building's mechanical behaviour on the base of its mechanical characteristics (obtained by tests, eventually calibrated on results of full-scale testing on

a shaking table) using a suitable computer analysis programme capable of calculating the non-linear response of the structure under a quake in the time domain.

- Use this programme for a chosen quake anticipated for the construction site increasing the intensity, the quake's peak ground acceleration (PGA), until the building will reach a previously determined "near-collapse" state (for example a maximum inter-storey drift, or a failure in joints or in timber elements). The intensity at this "near-collapse" state determines the $PGA_{u,eff}$.
- Compare this $PGA_{u,eff}$ against $PGA_{u,code}$ prescribed by the code: if $PGA_{u,eff} > PGA_{u,code}$, the previously chosen design ARF value is adequate (for that quake).
- This procedure must be repeated for a series of earthquakes suitable for the design site, in order to have a global picture according to different possible inputs.

The above procedure can be used both with a probabilistic [2] or a semi-probabilistic approach [3]. For example, in the semi-probabilistic approach, appropriate safety coefficients are considered in the codes both for the design action and the design resistance to take into account the relevant uncertainties.

This is a long procedure which is still undergoing and whose outcomes will be published shortly after this paper.

However – under the above assumptions and based on the test results, i.e. without mathematical modelling, it is possible to determine the q value - even though only for a particular building and ground motion record.

- Design the structure using q=1 according to the seismic code for the prescribed design $PGA_{u,code}$ and the resistant system according to the relevant codes (seismic and "static" codes) with the design values for seismic actions,
- Define an appropriate "near-collapse" criterion,
- Perform shaking table tests until the actual "near-collapse" state, i.e. $PGA_{u,eff}$, is reached,
- Calculate q as the ratio between the $PGA_{u,eff}$ value that caused the "actual" near-collapse of the building and the design value $PGA_{u,code}$.

2.2 Chosen strategy

The strategy used in this paper to evaluate the q value at least for the ground motion records used for the shaking table tests is therefore the following:

- Design the structure using q=1 according to the seismic code for a given design $PGA_{u,code}$ (0.35g - which is the design ground acceleration corresponding to the more hazardous seismic zone of Italy),
- Define as "near-collapse" criterion the failure in holdown anchors (one or more),
- Analyse the test results and calculate q as the ratio between the $PGA_{u,eff}$ value that caused the near-collapse of the building and the design value of the $PGA_{u,code}$.

3 Design of the test building according to Eurocode 8

The reference building considered is the one shown in Fig. 1 which has been tested in June and July 2006 at the NIED shaking table facility in Tsukuba, Japan. As above explained,

the procedure to follow in order to assess the q value starting from test results needs by definition the reaching of a near collapse status. Therefore, as this condition has been fulfilled only for Configuration C, plans and elevations of the building are referred only to this configuration and are shown in Fig. 2.

Figure 2: Plans and elevation of the test building.

The distribution of dead and additional loads at each floor in the test house is the following:

Floor	Dead [kN]	Additional [kN]	Total [kN]
1st	60	150	210
2nd	60	150	210
Roof	45	0	45
Total	165	300	465

Table 1 Load distribution at each floor

According to Eurocode 8, the base shear force is calculated according to the following equation:

$$F_b(T_1) = S_d(T_1) \times W$$

where $S_d(T_1)$ is the ordinate of the design spectrum at period T_1 and W is the total mass of the building.

From the outcomes of the tests, the period T_1 of the building is 0.20 s, therefore the ordinate of the design spectrum is

$$S_d(T_1) = a_g \times S \times \frac{2,5}{q}$$

where:

a_g is the design ground acceleration corresponding to the seismic zone. According to the Italian Seismic Building Code, a_g is taken equal to 0.35g, corresponding to the most hazardous value of the Italian territory

S is the soil factor (taken equal to 1,25 accounting for type B soil, e.g. deposits of very dense sand, gravel, or very stiff clay)

q is the behaviour factor taken equal to 1.

Therefore, the calculation of the seismic forces and the shear at each floor is the following:

Total Weight

roof		45 kN
2° floor		210 kN
1° floor		210 kN
	TOT	**465 kN**

seismic action

base shear			
zone 1; a_g =		0.35	
T1		0.20	
soil B S=		1.25	
q		1	
$F_b = 2,5*(W*S*a_g)/q$		**509**	**kN**
distribution on storeys			
height			
	Hr (roof) =	9.40	m
	H2 (2nd floor) =	6.18	m
	H1 (1st floor) =	3.09	m
horizontal forces at each floor			
	Fr =	91	kN
	F2 =	279	kN
	F1 =	139	kN
shear at each floor			
	Tr =	91	kN
	T2 =	370	kN
	T1 =	509	kN

3.1 Design of holdown anchors at ground level

To resist the shear forces, steel angles have been used. To resist the uplifting forces, holdown anchors have been used.

The holdown anchors used to connect the building at ground floor are SIMPSON STRONG-TIE holdown anchors HTT22, connected to the basement by means of 8.8 Class M16 anchor bolts and to the cross-laminated walls with ϕ 4 annular ringed nails.

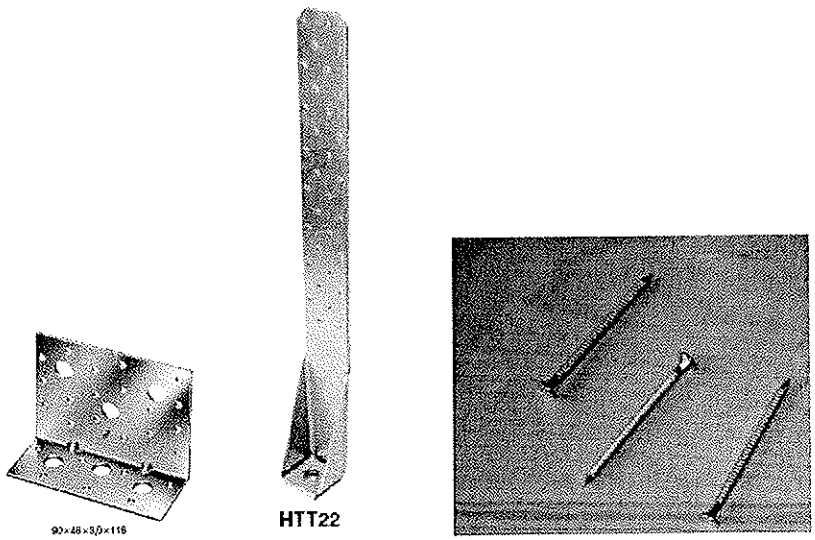

Figure 3: Steel angles BMF 90x48x3,0x116, holdown anchors HTT22 and ϕ 4 annular ringed nails used to fasten both connectors to the cross-laminated walls

The distribution of holdown anchors at the ground floor and of the seismic forces at each floor is shown in Fig. 4

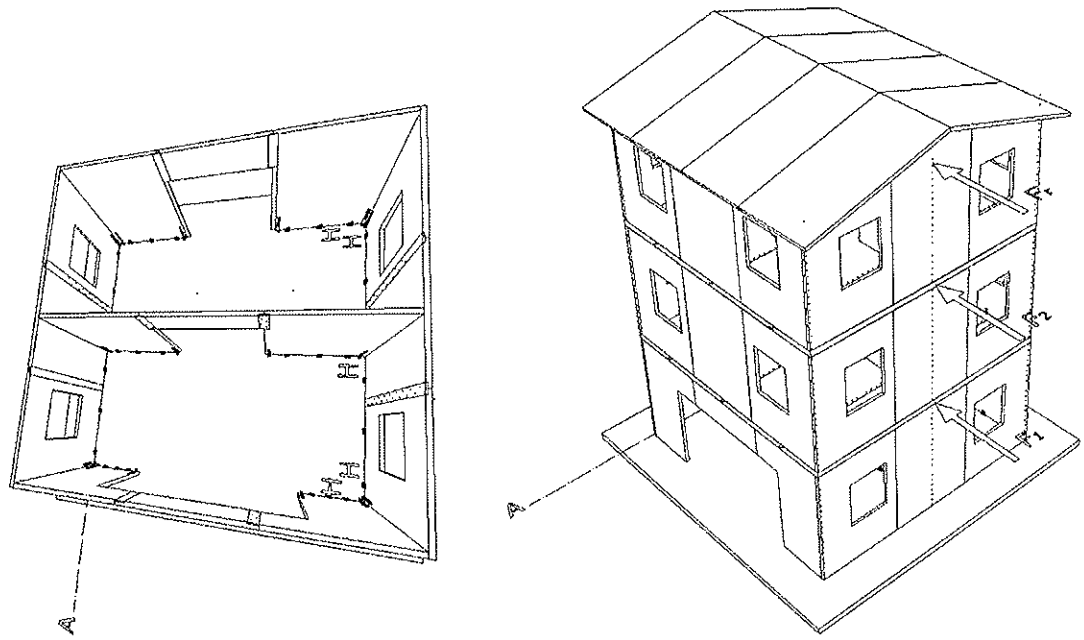

Figure 4: Distribution of holdown anchors and steel angles at ground floor and distribution of seismic forces at each floor. In the left side picture, the holdown anchors marked with H are those taken into account in the design.

Considering only the design of the holdown anchors at the ground floor and considering also the contribution of the holdowns in the walls perpendicular to the shaking direction, the calculation gives the following result (moment equilibrium around the A line and neglecting the contribution of the holdowns at openings):

$$F_r \times h_r + F_2 \times h_2 + F_1 \times h_1 - W \times \frac{6{,}93}{2} - 5 \times H \times 6{,}93 = 0$$

$$91 \times 9{,}40 + 279 \times 6{,}18 + 139 \times 3{,}09 - 465 \times \frac{6{,}93}{2} - 5 \times H \times 6{,}93 = 0 \quad \Rightarrow \quad \text{H} = 40{,}34 \text{ kN}$$

From the results of the experimental tests on the steel-to-timber connections using annular ringed nails, each nail has an ultimate shear resistance of 4 kN, which is taken as the 5-percentile value of strength. Therefore, according to Eurocode 5 and 8, the strength design value of each nail is:

$$R_d = \frac{R_k \times k_{\text{mod}}}{\gamma_M} = \frac{4 \times 1{,}1}{1{,}3} = 3{,}38\ kN$$

Hence to resist the uplift force, each holdown anchor is connected using 12 nails.

$H_r = 12x3{,}38 = 40{,}56\ kN > H = 40{,}34\ kN$

Note that the design tensile strength of the Class 8.8 ϕ16 anchoring bolt, considering the effective cross section is:

$$N_r = \frac{A_{res} \times f_y}{\gamma_M} = \frac{157 \times 640}{1000 \times 1{,}1} = 91{,}35\ kN$$ which is greater than H_r

4 Test outcomes

The test outcomes are summarised in Table 2. Under Nocera Umbra 1.20g, the "near-collapse" state was reached.

Record	**PGA [g]**	**Restoring intervention (before the test)**	**Observed damage (after the test)**
Nocera Umbra	0.50	Tightening of holdown anchor bolts	None
El Centro	0.50	Tightening of holdown anchor bolts. Replacing of screws in vertical joints between panel	None
Kobe	0.50	Idem	None
Kobe	0.80	Idem	Slight deformation of screws in vertical joints between panels
Kobe	0.50	Idem	None
Kobe	0.50	Tightening of holdown anchor bolts	None
Kobe	0.80	Replacing of holdown anchors and tightening of bolts. Replacing of screws in vertical joints between panel	Slight deformation of screws in vertical joints between panels
Nocera Umbra	1.20	Tightening of holdown anchor bolts. Replacing of screws in vertical joints between panel	**Holdown failure** and deformation of screws in vertical joints between panels

Table 2 Results of shaking table tests for Configuration C in terms of observed damage.

5 Discussion

Being the design ground acceleration $PGA_{u,code}$ equal to 0.35g, by applying the procedure given in 2.2, the q value is:

$$q = \frac{1.20}{0.35} = 3.4$$

Of course the above value is valid only referring to the used Nocera Umbra ground motion record. A series of different quakes should be used with the same procedure. This is obviously impossible, therefore the importance of a good mathematical model that can simulate different quakes and cases is obvious.

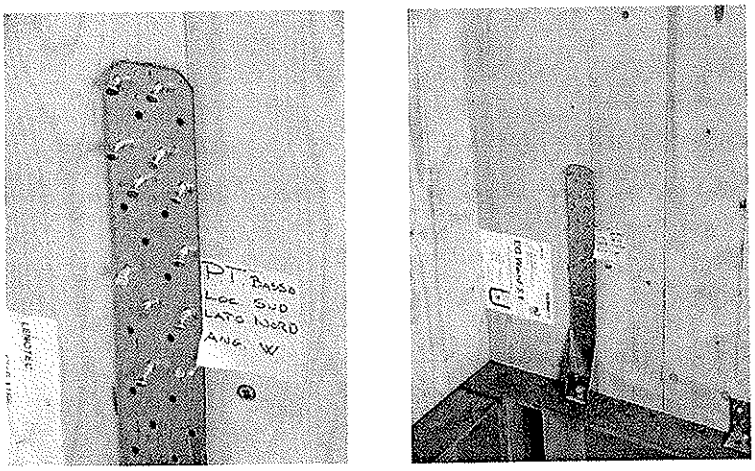

Figure 5: Holdown failure after Nocera Umbra 1.2g test.

In any case, the above value has its own significance as an indicator. Moreover, it must be considered that the building has passed without any important reparation at least 14 "destructive" quakes in a row. It has kept its shape even with the last quake that has produced the near-collapse state. That means that this typology seems very promising when the design philosophy in seismic areas would convert to the NDD - no damage design – approach [4].

6 Acknowledgements

This paper is published in the frame-work of the SOFIE project on XLam buildings funded by the Autonomous Province of Trento, Italy.

A special thank for their contribution to this work to Gabriele Bonamini, Mario Moschi and Mario Pinna of CNR-IVALSA and Minoru Okabe and Masateru Sudou of Center for Better Living, Tsukuba.

7 References

[1] EN 1998-1:2004: "Eurocode 8: Design of structures for earthquake resistance - Part 1: General rules, seismic actions and rules for buildings"

[2] A.Ceccotti- R.O.Foschi: "Reliability assessment of wood shear walls under earthquake excitation", Proceedings of Santorini Conference on Stochastic Mechanics, 1998, Greece.

[3] A. Ceccotti, M. Follesa, E. Karacabeyli "3D Seismic Analysis of Multi-Storey Wood Frame Construction" 6th World Conference on Timber Engineering, Whistler Resort, British Columbia, Canada, 2000

[4] A. Buchanan, *Personal communication*, 2005

INTERNATIONAL COUNCIL FOR RESEARCH AND INNOVATION
IN BUILDING AND CONSTRUCTION

WORKING COMMISSION W18 - TIMBER STRUCTURES

LAMINATED TIMBER FRAMES UNDER DYNAMIC LOADINGS

A Heiduschke
P Haller
University of Technology Dresden
Department of Civil Engineering

GERMANY

B. Kasal
Pennsylvania State University
Department of Civil and Environmental Engineering, PA

USA

MEETING THIRTY-NINE

FLORENCE

ITALY

AUGUST 2006

Presented by A Heiduschke
R Steiger commented on peak ground displacement of the records (11 and 18 cm). He stated that the equation used in the calculation of period depended on damping; therefore, they were only approximate.
B Dujic commented that free displacement without resistance was shown in the hysteretic loop.
A Ceccotti asked which computer software was used. A Heiduschke answered ANSYS; therefore, simple hysteretic laws were needed.
E Karacabeyli asked would one recommend this type of frame or would one wait for bracing system wall. A Heiduschke answered as pointed out in the conclusion bracing system work would be needed.
A Leijten and A Heiduschke discussed the issue of improving structural performance by the introduction of stronger and stiffer connections.

Laminated Timber Frames under Dynamic Loadings

A. Heiduschke, P. Haller

University of Technology Dresden, Department of Civil Engineering, Dresden, Germany

B. Kasal

Pennsylvania State University, Department of Civil and Environmental Engineering, PA, USA

Summary

This paper discusses the results of time-history analyses of four-story moment-resisting timber frames subjected to various seismic loadings. The purpose of the case study was to document the difficulties, which arise due to large story drifts of the frames caused by the soft character of moment transmitting connections using dowel-type fasteners. Two frames were designed: one according strength and the second according stiffness requirements stipulated by the seismic code - EC8. From the design procedure it follows that, in general, the serviceability limit state design is the limiting criteria. Unacceptable lateral drifts made it necessary to increase the joint stiffness. Since connection stiffness increases significant with the depth of the member, the member size inclusive the number of the fasteners was enlarged. This, in combination with densified and textile reinforced wood resulted in a frame design with an adequate lateral stiffness keeping the inter-story drift within the limit stipulated by the seismic code. The numerical model used to simulate the structural response of the frames utilized the hysteretic formulation of nonlinear connection behavior. The results of the dynamic pushover analysis were used to evaluate and verify the behavior factor q. In the seismic code, the elastic spectrum is modified with this factor to obtain an inelastic design response spectrum that is used to determine equivalent static forces.

1 Introduction

Shake table tests of the two-story frames have demonstrated, that laminated timber frames perform well under dynamic loads due to their low mass density, high specific strength and high capacity to dissipation energy [1, 2]. The critical issue is the semi-rigid beam-to-column connection, which suffers from relatively low rotational stiffness.

In order to demonstrate the seismic performance of laminated timber frames a case study was performed on a multistory structure designed according the EC5 and EC8 - prEN1998-1:2003 [3]. To analyze the dynamic behavior of the nonlinear system, a numerical simulation, including the nonlinear connection models presented in [4], was performed. The model was capable of simulating the full time-history response of the structure

subjected to seismic excitations. Such a transient analysis requires an accurate and sophisticated modeling of the structural details. The properties of the nonlinear connections were shown to be the primary influence on the response of the entire structure [1, 2].

Such time-history analyses can be time consuming for nonlinear systems, so a simplified method is proposed in the EC8. In the seismic code the earthquake design base shear F_b [kN] is evaluated as:

$$F_b = S_d(T_1) \cdot m \qquad \textbf{(equ. 1)}$$

where: m = total weight of the building [kN]
$S_d(T_1)$ = ordinate of the design spectrum, depending on the fundamental period T_1 of the building and assuming 5% viscous damping

Equation 1 calculates the maximum base shear force that the structure would sustain without collapse. The inelastic design response spectrum $S_d(T_1)$ is evaluated by a set of equations (see EC8 - 3.22), but in general, equation 2 will be used to determine the maximum ordinate of the inelastic design spectrum.

$$S_d(T_1) = \frac{S_e(T_1)}{q}; \quad \text{with } S_e(T_1) = a_g \cdot S \cdot 2.5 \qquad \textbf{(equ. 2)}$$

where: $S_d(T_1)$ = ordinate of the design spectrum
$S_e(T_1)$ = ordinate of the elastic response spectrum
a_g = design ground acceleration [g]
S = soil parameter factor
q = behavior factor

In the seismic code, the elastic response spectrum $S_e(T_1)$ is modified with a behavior factor, namely the q-factor, to obtain an design spectrum that is used to determine equivalent static forces. This factor reflects the ability to sustain a design earthquake without collapse by exceeding the elastic limit and accounts for 5% viscous damping of the building.

The evaluation of the q-factor is an important issue to achieve reliable results. The primary problem faced is the definition of the collapse and/or admissible structural damage. Therefore, aspects such as inter-story drift limitations and early brittle failures of structural members have to be considered. The general definition of the actual q-factor, proposed by Ballio [5], is given by the ratio between the peak ground acceleration (PGA_u) producing the ultimate rotation (global plastic mechanism) and the PGA_y that produces the first yielding of the joints (first plastic hinge) - equation 3.

$$q = \frac{PGA_u}{PGA_y} \qquad \textbf{(equ. 3)}$$

This method was applied by Ceccotti and Karacabeyli [6], to determine the q-factor for a laminated timber frame with semi-rigid connections. Such a procedure requires a suitable nonlinear analysis program capable of following the displacement-history of the structure in time domain. Several dynamic analyses must be performed for a large set of ground motions. For simple one-story frames, a q-factor of 2 was determined by Ceccotti and Karacabeyli [6]. They concluded that q-factor of 3 to 4 might be possible for multistory frame buildings, provided the structures have sufficient energy dissipation capacity. This is in accordance with the EC8, where a factor of 4 is recommended for hyperstatic portal frames with a high capacity to dissipate energy. The cyclic connection tests presented in [7] have shown that the textile reinforced joints are ductile and capable to dissipate large

amounts of energy. Hence these frames can be classified as structures having high capacity to dissipate energy.

The design procedure presented above is the check at the ultimate limit state (USL) to prevent the collapse of the structure under the most severe design earthquakes. In order to avoid excessive damage of structural and nonstructural elements, the EC8 gives rules for allowable inter-story drifts. The inter-story drift at the serviceability limit state (SLS) is limited to:

$\Delta/h * \nu = 0.005$ (buildings having brittle nonstructural elements attached to the structure) **(equ. 4)**
$= 0.0075$ (buildings having ductile nonstructural elements attached)
$= 0.01$ (buildings having nonstructural elements fixed in a way so as not to interfere with structural deformations)

where: Δ = story drift [m]
h = story height [m]
ν = reduction factor = 0.4 or 0.5 - accounts for lower return period of a seismic action

One can expect that the drift limits of the seismic code will lead to over-designed structural elements due to the large connection areas necessary for the required connection stiffness. De Matteis et al. [8] pointed out that even the design of moment-resisting steel frames according to the EC8 leads to strongly over-resistant structures with excessive member strengths, due to the insufficient lateral stiffness of these frames. The fulfillment of the SLS requirements usually limits their efficiency in seismic areas.

2 Case Study on Four-Story Frames

To monitor the difficulties in the design process with regard to a balanced structural design, a case study was performed where a four-story timber frame was subjected to several ground motions.
First a frame-C (C – Capacity Design, ULS) was designed according to the EC5 and EC8 strength and ductility criteria, but without the SLS restrictions. The critical frame locations were checked against their plastic moment capacity. Since the frame was not designed according to the stiffness requirements, it is characterized by low lateral strength as compared to the design forces thus resulting in higher sways.

Then a second frame-S (S – Stiffness Design, SLS) was designed according to the stiffness requirements. Over-sized members, having a lateral strength larger than the design story shear as determined by the strength requirements, characterize this frame.
In order to evaluate the improvement in structural behavior due to the treatment of the material, two connection designs: 1) undensified and textile reinforced - UD-R and 2) partially densified and textile reinforced - PD-R per frame-type were studied (see [7]).

The nonlinear spring elements that were used to simulate the hysteretic behavior of the joints were presented elsewhere [4]. Figure 1 shows a comparison between experimental versus numerical results for different joint design.

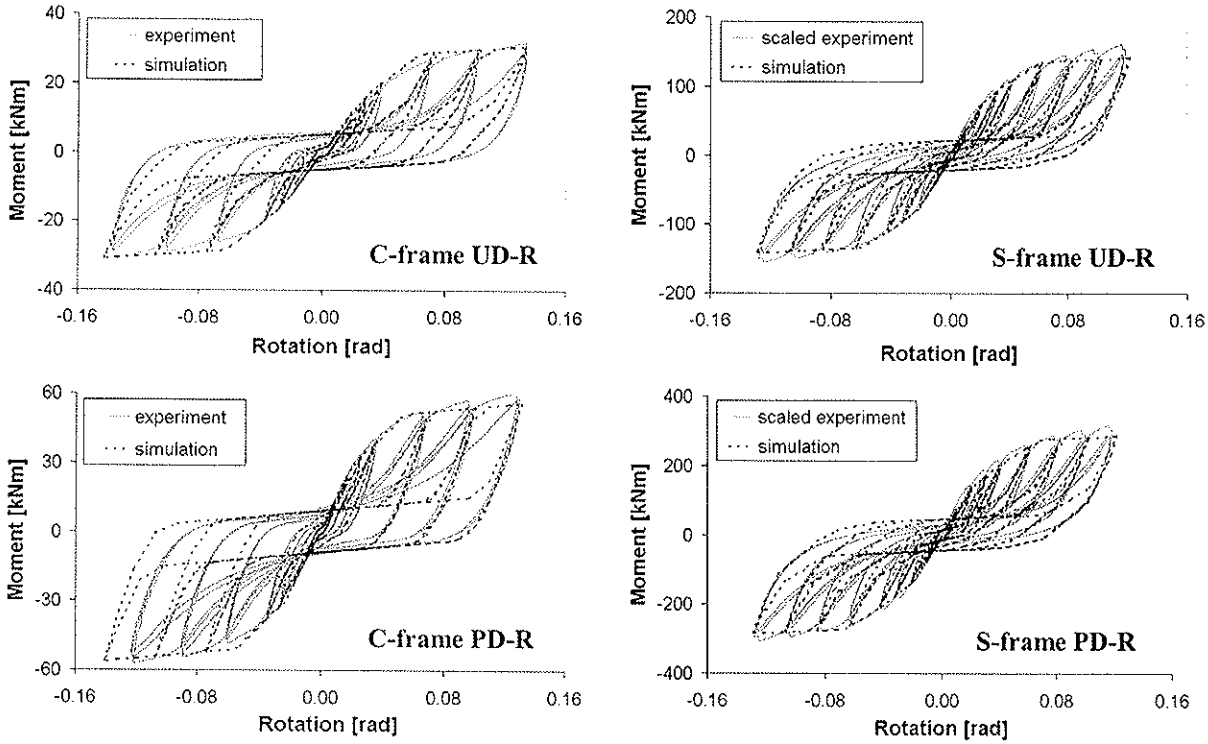

Figure 1. Moment-rotation relationship of the simulation versus experiment

In the seismic design procedure, a design ground acceleration a_g equal to 0.25 g, the sub-soil class B (medium density sand - $S = 1.2$) and a design q-factor equal to 2.5 have been assumed. Figure 2 shows the dimensions of the four-story frame model.

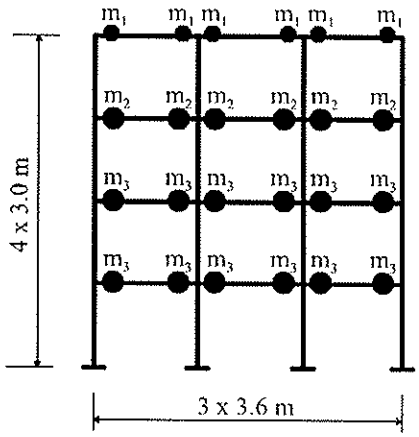

Frame-C:
Column: 160x290 mm
Beams: 2x 80x290 mm

Frame-S:
Column: 200x500 mm
Beams: 2x 100x500 mm

Seismic design:
$m_1 = 1.0$ kNs^2/m
$m_2 = 1.4$ kNs^2/m
$m_3 = 1.2$ kNs^2/m

Figure 2. Schematic of the 2D analytical model of the four-story frame

The three-bay frame had a total height H of 12 m, where the spacing between the plane frames was 3.6 m. Beams and columns were modeled via 2D, linearly elastic beam elements with 3 degrees of freedom at each node. A modulus of elasticity of 12500 MPa with a mass density of 380 kg/m^3 was used. The masses used to simulate the dead and live load were defined as lumped masses attached to the beams. A dead load of 1.5 kN/m^2 and a live load of 2 kN/m^2 have been chosen for this study. No live load was placed at the roof. The inter-story drift Δ/h_{SLS} has been limited to 0.005 (equation 4), where a reduction factor of $\nu = 0.5$ was assumed. The most restrictive drift limit has been chosen to illustrate the

difficulties in the design process with regard to the drift restrictions in the seismic code. The damping of the system was primarily due to the hysteretic behavior of the connections. An additional 2% equivalent viscous damping was added to account for other unknown sources of damping.

Frame C – Capacity Design

The beams and columns of the first frame had cross sections of 2x 80x290 mm and 160x290 mm, respectively. The dimensions of the members as well as the connection design were identical to those of the two-story frame (see [1]). This was done to use the known moment-rotation behavior as obtained in the experiments (Figure 1).

The results of the design procedure showed that only the frame with densified connections was capable to fulfill the ULS criteria although neither of the frames provided a sufficient lateral stiffness to fulfill the SLS criteria.

Frame S - Stiffness Design

The beams and columns of the second frame had cross sections of 100x500 mm and 200x500 mm, respectively. Due to the dimensions of the members, a connection with circular dowel arrangement was chosen. The circle was 380 mm in diameter and contained 12 dowels with a diameter of 20 mm. Since test data were not available for this connection, experimental results of small-scale tests were used to get an approximation for the moment-rotation behavior of the full-scale connections. Figure 1 shows the resulting moment-rotation hysteresis of the UD-R and PD-R connections with circular dowel arrangement.

The results of the design procedure showed that only the densified-reinforced frame was capable of fulfilling all requirements of the code.

3 Results and Discussion

3.1 Dynamic Pushover Analysis

First a modal analysis was performed to approximate the fundamental periods for the different frame designs. These values are useful indicators how the ground motion will affect the structural response of the frame. The fundamental periods of the frame-C with undensified and/or densified connections were $T_{1,C,UD\text{-}R} = 2.6$s and $T_{1,C,D\text{-}R} = 1.9$s, whereas the frame-S values were $T_{1,S,UD\text{-}R} = 1.05$s and $T_{1,S,D\text{-}R} = 0.78$s.

Since the results of a time-history analysis vary according to the input ground motions different four ground motion records have been selected for the numerical analyses. They all had a PGA similar to the design one of 0.25 g. An arbitrary signal (SYN) has been generated to simulate a large number of real earthquakes while representing their frequency and amplitude contents. The Montenegro earthquake (MON) has been chosen to represent a near fault recording. In order to get reasonable structural deformations, two special earthquake signals were selected, characteristic for regions with soft soil conditions. These are the Bagnoli-Irpinia (BAG) and the Vrancea earthquake (VRA). This selection was necessary due to the long fundamental periods, especially of the C-frames, that do not fall within the period range of typical earthquakes (0.1s – 0.8s see EC8 design spectrum).

For the evaluation of the seismic performance of the frames the relationship between the ground motion damage potential, here represented through the PGA in terms of g, and the structural damage, here represented through the maximum inter-story drift Δ/h, was used. The structural response was investigated up to a Δ/h of 0.1. Since the elastic deformations

of the structural elements were small, the inter-story drift was nearly coincident with the joint rotation. The performance curves are given in Figure 3.

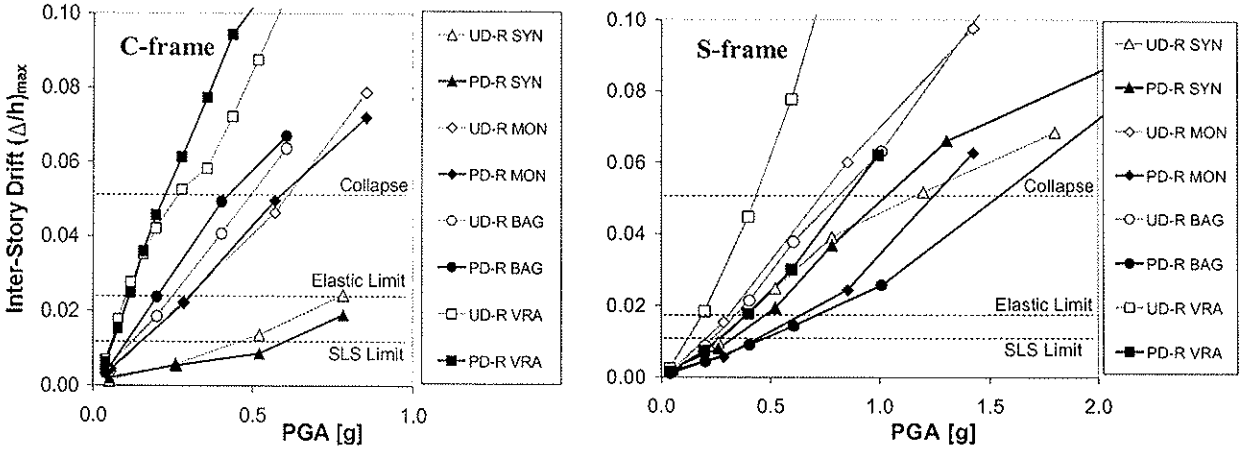

Figure 3. Performance curves for frame-C and frame-S

Figure 3 shows that the response of the C-frames was strongly dependent on the input earthquake signal. A significant damage was obtained for the ground motions of the Vrancea earthquake. The influence of this record on the response of the frames was significant because of the high amplitude in its response spectrum for long periods. Already the original record with a PGA of 0.199g led to an inter-story drift larger then 0.04. On the other hand the synthetic earthquake did not affect the frame response significantly, since this record was not representative for structures having long fundamental periods. For this reason the differences between undensified and densified frame designs were small.

The enhancement in frame performance due to densified connections of the S-frames was significant. Strengthening the connections led to story drift reduction in a range of 25% to 160%. In general, the PD-R frame-S had an adequate lateral stiffness to limit the inter-story drifts to be less then 0.03 even for strong ground motions up to 0.6g.

3.2 Evaluation of q-factor

To verify the q-factor of 2.5, proposed by the seismic code for hyperstatic frames, the evaluated database was used. In accordance to equation 3, q-factor is defined by the ratio of PGA_u over PGA_y. This method still requires the definition of yielding and collapse conditions. For this study the results of the cyclic connection tests [7] were used to define yielding and collapse conditions. The first yielding in the frame-C connections occurs at a joint rotation of 0.022 rad (Figure 1) while the joints of the frame-S exceeded the elastic rotation limit at 0.015 rad. To keep the deformations at a reasonable level, Δ/h has been limited to 0.05 as the definition of the collapse condition. Such deformation criterion was also applied by Cecotti and Karacabeyli [6] for multi-story timber frames.

Based on the performance curves in Figure 3 of the dynamic analysis, the minimum q-factor of the investigated frames was 2.2. As a consequence of the large elastic range (yield rotations > 0.015 rad), a q-factor larger then 3 was difficult to achieve. It appears that the point of first plastic yielding was the limiting factor, while the collapse conditions were of less importance.

4 Conclusions

From the design procedure it follows, that in general the SLS design will be the limiting criteria in the design process of moment-resisting frames. The inter-story drift of the frame-C, designed in accordance to the strength and ductility criteria, exceeded the seismic code limitation at the SLS. The unacceptable deformations made it necessary to increase the joint stiffness. Since the stiffness increases significantly with the depth of the member size inclusive the number of the fasteners was enlarged. This, in combination with densified and textile reinforced wood, resulted in a frame design with an adequate lateral stiffness keeping the inter-story drift within the limit stipulated by the code. Over-sized members and a lateral strength larger then the design story shear characterize this frame-S, designed according to the stiffness requirements.

From the modal analysis one can conclude that for the evaluation of the first fundamental period of the system, the connection behavior has to be taken into account. For the frame-C, long periods (T_1 > 2s), were evaluated due to the low rotational stiffness of the connections. The structures were not within the period range of typical earthquakes and this results in small inertia forces. In order to get reasonable structural deformations, specific earthquakes, characterized by soft soil conditions were selected for the nonlinear time-history analysis.

The frame-S had an adequate lateral stiffness to keep the inter-story drift at a reasonable level for strong ground motions up to 0.6g. In either simulation the frame performance improved with story drift reductions of 25% to 160% when using densified wood.

The cyclic test on connections have shown that textile reinforced joints have at least medium ductility, so that these frame types can be classified as structures having a medium capacity to dissipate energy. As a consequence, a q-factor of 2.5 can be assumed for the studied statically indetermined frames. The numerical time-history analysis showed that a q-factor of 2.5 is acceptable for the investigated frames.

References

1. Kasal, B., Pospíšil, S., Jirovsky, I., Heiduschke, A., Drdacky, M. and Haller, P. Seismic performance of laminated timber frames with fiber reinforced connections. *Earthquake Engineering and Structural Dynamics.* John Wiley & Sons, UK, Vol. 33. (5): 633-646, 2004.
2. Kasal, B., Heiduschke, A., Kadla, J. and Haller, P. Laminated timber frames with composite fiber reinforced connections. *Prog. in Structural Engr.,* John Wiley, UK, Vol. 6(2): 84-93, 2004.
3. EC 8. EUROCODE 8 - Design of structures for earthquake resistance. Part 1: General Rules prEN 1998-1 December 2003 final draft, CEN, Brussels, Belgium, 2003.
4. Heiduschke A, Kasal B & Haller P. Analysis of Wood-Composite Laminated Frames under Dynamic Loads – Analytical Models and Model Validation. Part I: Connection Model and Part II: Frame Model. *Progress in Structural Engineering and Materials* (in press).
5. Ballio, G. ECCS approach for the design of steel structures against earthquakes. *Proceedings of the ECCS IABSE Symposium*, Luxembourg, 1985.
6. Ceccotti, A. and Karacabeyli, E. Seismic performance of moment resisting timber frames. *Proc. of 5th World Conference on Timber Engineering,* Montreux, Switzerland, 540-547, 1998.
7. Heiduschke A. Seismic behavior of moment-resisting timber frames with densified and textile reinforced connections. Dissertation, TU-Dresden, Faculty of Civil Engineering, ISSN 1613-6934, KID Heft 7 (eds. Haller, Curbach etc.) 2006.
8. De Matteis, G., Landolfo, R. and Mazzolani, F.M. Seismic response of moment-resisting steel frames with low-yield shear panels. *Engineering Structures* 25, 155-168, 2003.

INTERNATIONAL COUNCIL FOR RESEARCH AND INNOVATION
IN BUILDING AND CONSTRUCTION

WORKING COMMISSION W18 - TIMBER STRUCTURES

CODE PROVISIONS FOR SEISMIC DESIGN OF MULTI-STOREY POST-TENSIONED TIMBER BUILDINGS

A Palermo
Dipartimento di Ingegneria Strutturale, Politecnico di Milano

ITALY

S Pampanin
A Buchanan
M Fragiacomo
B Deam
Department of Civil Engineering, University of Canterbury, Christchurch

NEW ZEALAND

MEETING THIRTY-NINE
FLORENCE
ITALY
AUGUST 2006

Presented by A Palermo
I Smith asked about the need for shear along with moment transfer. A Palermo stated that a shear key could be used.
A Leijten received confirmation that code design recommendations would be intended for next CIB.
A Jorissen and A Palermo discussed the observed failure mode; no fatigue as the number of cycles was low.
V Rajcic and A Palermo discussed shrinkage issue for long span and how to account for loss of tension. There was agreement that more work would be needed.

Code Provisions for Seismic Design of Multi-Storey Post-Tensioned Timber Buildings

S. Pampanin[(1)], A. Palermo [(2)], A. Buchanan[(1)], M. Fragiacomo[(1)], B. Deam[(1)]

[(1)] Department of Civil Engineering, University of Canterbury, Christchurch, New Zealand

[(2)] Dipartimento di Ingegneria Strutturale, Politecnico di Milano, Italy

1 Introduction

Recent developments and successful preliminary experimental validations of innovative types of ductile connections for multi-storey seismic-resisting laminated veneer lumber (LVL) timber buildings have opened major opportunities for extensive use of structural timber in seismic regions. These particular solutions, named *jointed ductile connections* or *hybrid systems* are based on post-tensioning techniques to assemble structural LVL members for both frame and shear wall systems which are designed to exhibit controlled rocking deformations during seismic loading. These systems have been proposed and successfully tested using concepts developed for high-performance seismic-resisting precast concrete buildings, currently being approved in major seismic codes and design guidelines worldwide. The extremely satisfactory results of quasi-static cyclic and pseudo-dynamic experimental tests on exterior beam-column joint subassemblies, column-to-foundation connections and shear wall systems have provided valuable confirmation of the high seismic performance of these LVL systems, as well as the reliability of the adopted design criteria and methodology. In this paper, after a brief introduction to the concept of post-tensioned seismic-resisting LVL structures and an overview of experimental results, particular focus will be given to seismic design aspects, within a performance-based design approach, as a sound basis for the preparation of seismic design code provisions.

2 Developments in High-Performance Seismic Systems

2.1 Refinements in performance based seismic design approaches

In the last decade, significant development and refinements of performance-based seismic engineering (PBSE) philosophies (SEAOC Vision 2000, 1995) and corresponding compliance criteria, have been driven by the recognized importance of designing ductile structural systems to undergo inelastic cycles during earthquakes while sustaining their integrity and minimizing structural and non-structural damage after the earthquake. Within a typical performance-based design framework, different levels of structural damage and, consequently, repair costs (associated with performance levels related to Operational Conditions, Damage Control, Life Safety and Collapse Prevention) may be expected, depending on the seismic intensity and the importance given to the structural facilities during the design process.

Structural damage is typically accepted as an unavoidable result of inelastic behaviour during an earthquake. Following the common goal of reducing severe socio-economical losses due to earthquake events to an "acceptable" level in seismic-prone countries, an increased focus has been given to the development of design approaches and adequate technology to respect the performance requirements typical of a damage control objective, after having prevented life safety and structural collapse.

Recent developments in performance-based design and assessment (MacRae and Kawashima, 1997, Pampanin et al., 2002 Christopoulos and Pampanin, 2004) have highlighted the limitations and inconsistencies related to current PBSE approaches, and have emphasised the critical role of permanent residual deformations, typically sustained by a structure after a seismic event even when "well designed" according to current codes. Residual damage is a major additional and complementary damage indicator to those typically adopted, i.e. inter storey drift, ductility and/or cumulative energy. Considering the impact of residual deformations on the cost of repairing and expected downtime (including the difficulty of straightening a building to its original position) after an earthquake event, seismic resisting systems or devices with re-centering properties naturally attract favourable attention.

2.2 Traditional solutions for seismic resisting ductile systems

Regardless of the structural material adopted (i.e. concrete, steel, timber), traditional solutions to achieve adequate global and local ductile structural behaviour rely on the inelastic behaviour of the material, allowing for plastic deformations to occur within selected discrete and sacrificial regions (typically referred to as "plastic hinge regions"), designed according to capacity design principles in order to protect the whole system from undesired inelastic mechanisms.

Alternatively, seismic protection can rely on the use of energy dissipation and supplemental damping devices (including base isolation), designed with passive, active or semi-active control to protect the main structural skeleton from inelastic mechanisms and damage.

In timber engineering, several alternative solutions have been studied and developed in literature to provide moment-resisting connections in timber construction, for both lateral load resisting wall or frame systems. Feasibility studies of multi-storey timber buildings have been described by Halliday & Buchanan (1993) and Thomas et al. (1993). Depending on the type of connection and structural details, many alternative arrangements are available ranging from mechanically fastened solutions with nailed, bolted or dowel connections to glued or epoxied steel rods. These solutions apply to solid sawn timber in large sizes, glue laminated timber (glulam), or LVL. Significantly different forms of inelastic behaviour can occur, leading to different levels of ductility capacity and hence different overall structural performance. Typical pinching phenomena can be observed in the hysteresis behaviour of nailed or steel rod connections (Fig. 1a) which leads to a reduction of stiffness (both loading and unloading) as well as a reduction of energy dissipation capacity, hence higher displacement demand (thus damage) than in well designed steel or concrete structures. These hysteresis loops are similar to those achieved in structural walls with nailed plywood sheathing (Deam 1997).

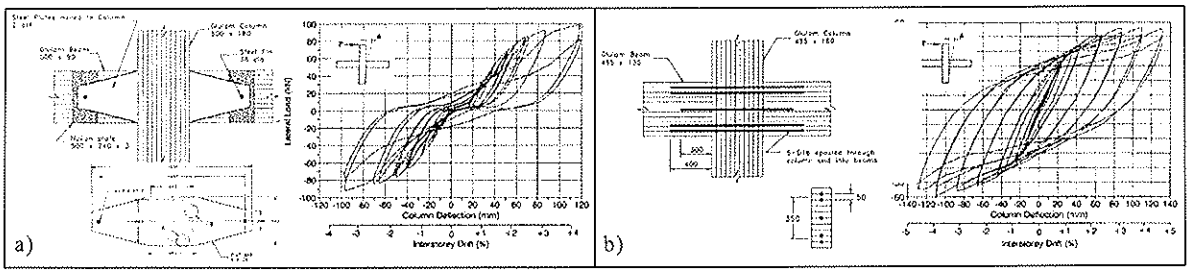

Figure 1. Layout and hysteresis loops for glulam frame systems: a) multiple-nailed connection; b) epoxied rods (Buchanan & Fairweather, 1993).

An overview of seismic resisting solutions for multi-storey glulam timber buildings (Buchanan & Fairweather, 1993) proposed alternative arrangements for steel epoxied connections with or without additional sacrificial steel brackets to accommodate the inelastic behaviour. In particular the simplest version of the connection (Fig. 1b) showed satisfactory behaviour under cyclic loading, similar to the behaviour of a properly designed plastic hinge in reinforced concrete members, with stable dissipating hysteresis loops and limited stiffness degradation. However, in line with the previous discussion on performance based design requirements, excessive permanent residual deformations would be expected after an earthquake event, as in typical monolithic concrete or steel structures.

2.3 Jointed ductile connections: damage-resistant, self-centering and dissipative systems

Recent developments in precast concrete moment-resisting frames or interconnected shear walls (Priestley 1996, Priestley et al., 1999) (Fig. 2a), under the U.S. PRESSS (PREcast Seismic Structural System) program as well as subsequently in steel moment-resisting frames (Christopoulos et al., 2002b), (Fig. 2b), have resulted in the revolutionary development of high-performance, cost-effective, seismic resisting systems which can undergo inelastic displacements similar to their traditional counterparts, while limiting the structural damage and assuring full re-centering capability. These innovative solutions, typically referred to as *jointed ductile connections*, differ from monolithic solutions (i.e. cast-in-place reinforced or precast concrete; welded or bolted connections in steel) in that prefabricated structural elements are connected by using unbonded post-tensioning, the inelastic demand is accommodated within the connection through opening and closing of an existing gap, while the structural elements are kept in the elastic range with a very limited level of damage. These connections can be located at the beam-column, column-foundation or wall-foundation interface. A particularly efficient solution is provided by the *hybrid* system (Fig. 2a) where an adequate combination of self-centering capacity (unbonded tendons plus axial load) and energy dissipation (mild steel or other dissipation devices) leads to a sort of controlled rocking motion defined by a peculiar "flag-shaped" hysteresis loop (Fig. 2c).

Extensive numerical and analytical studies have recently focused on further refinement of these systems, and development of simple and reliable modelling and design procedures. Several on-site applications adopting PRESSS-type technology have been implemented in seismic countries around the world including U.S., Europe, South America, Japan, and New Zealand. Major seismic codes or design guidelines (*fib* Bulletin *27* 2004, EC8, Architectural Institute of Japan (AIJ), ACI T1.2-03 2003, NZS3101:2006) have incorporated the possibility of using similar solutions, typically referred to as *jointed ductile connections* or *connections with concentrated ductility*. An overview of recent

developments of hybrid solutions in precast concrete construction including research outcomes, modelling and design aspects, code provisions and guidelines as well as practical applications can be found in Pampanin (2005).

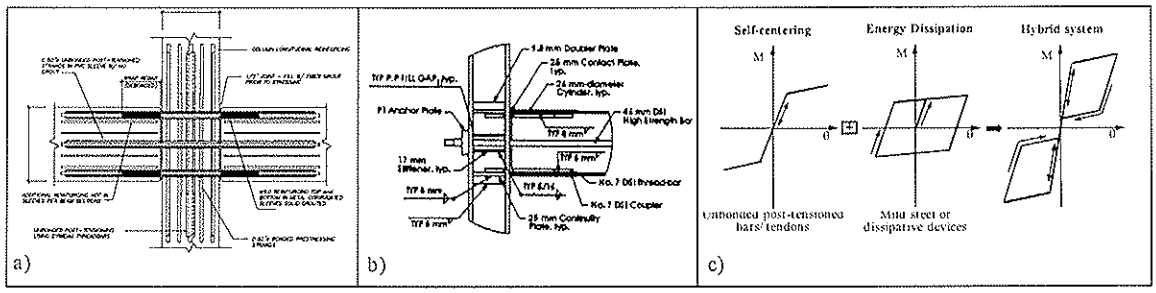

Figure 2. Hybrid solutions: a) for precast concrete frame systems (PRESSS program, Priestley et al., 1999); b) for steel moment resisting frames (Post-Tensioned Energy Dissipation, PTED, Christopoulos et al. 2002b); c) idealised flag shape hysteresis loop.

3. Extension of the Hybrid System Concept to LVL Seismic-Resisting Multi-Storey Buildings

In recent contributions from the authors (Palermo et al., 2005, 2006) the concept of hybrid or controlled rocking systems has been proposed for multi-storey timber seismic-resistant structures with particular emphasis on Laminated Veneer Lumber (LVL).

As a structural material, LVL is a superior alternative to sawn timber or glulam because the 3 mm thick veneers are specially selected, then staggered during processing so that the selected wood material is thoroughly mixed and the defects, such as knots, are randomised to a point where their influence on the material properties can be assumed negligible. Due to the higher homogeneity, the tension strength of LVL can reach values at least 3 times that of sawn timber from the same population of trees. However it is worth underlining that the hybrid connection (Fig. 3) is not significantly affected by the strength of the material, provided that proper confinement is given to the compression area to avoid crushing of the edge layers, hence this connection can be used with different wood-based materials (i.e., sawn timber, glulam etc).

Figure 3 shows a conceptual hybrid solution for LVL beam-column connections based on the combination of post-tensioning and internal dissipaters (e.g. epoxied mild steel bars). In the following paragraphs, an overview of the connection mechanism and design philosophy will be given, supported by the very satisfactory results of experimental validation on prototype connections for beam column joints, cantilever columns and wall systems.

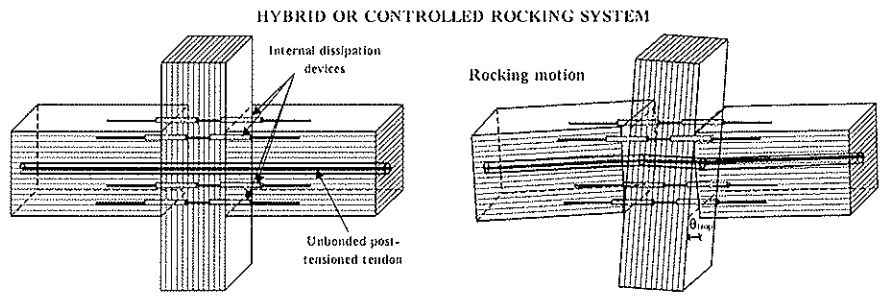

Figure 3. Basic concept of *hybrid* jointed ductile connections for LVL frame systems.

3.1 Controlled rocking mechanism at the connection interface

As shown in Fig. 4, in a post-tensioned jointed ductile connection a "controlled rocking" motion occurs with the opening and closing of an existing gap at the critical interface. When compared to pure rocking motion, the prestressing force (initial prestress plus additional contribution due to elongation of the tendons) provides a restoring force counteracting excessive opening (rotation demand), reversing the rocking motion, and closing the gap completely after an earthquake. The additional non-prestressed reinforcement can provide further limitations to the gap rotation demand, by increasing the strength of the connection as well as reducing the seismic demand (energy dissipation contribution).

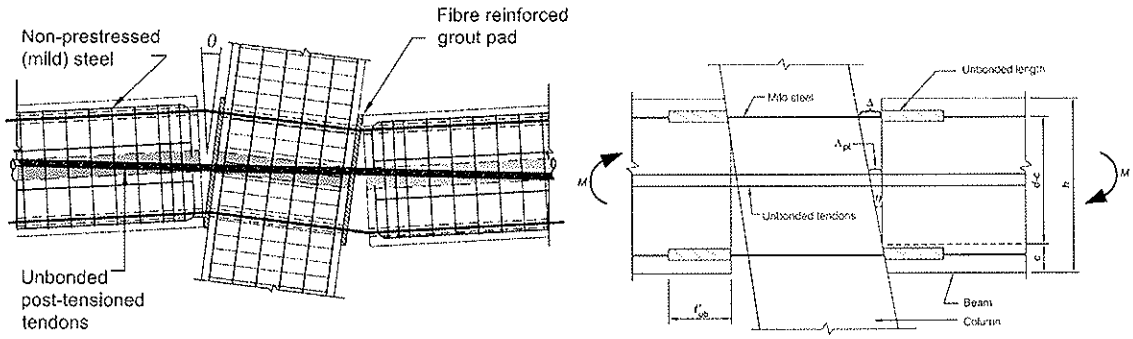

Figure 4. Controlled rocking mechanism at the critical connection in a hybrid beam-column connection (NZS3101:2006, Appendix B, after Pampanin et al., 2001).

Evaluation of flexural strength

Referring to the peculiar mechanism (gap opening and closing at the critical interface) of the hybrid beam-column connection shown in Figure 4, the strain levels in the unbonded post-tensioned tendons due to the gap rotation θ, $\varepsilon_{pt}(\theta)$, and in the non-prestressed steel reinforcement (with a short unbonded length at the critical section in the case of internal mild steel, to avoid premature fracture), $\varepsilon_s(\theta)$, can be evaluated by basic geometrical considerations as : $\varepsilon_{pt} = \frac{n\Delta_{pt}}{\ell_{ub}}$ and $\varepsilon_s = \frac{(\Delta_s - 2\Delta_{sp})}{\ell'_{ub}}$ respectively. where: n is the number of total joint openings along the beam (at beam-column interfaces); ℓ_{ub} and ℓ'_{ub} are the unbonded lengths in the tendons and in the non-prestressed steel reinforcement, respectively; Δ_{pt} and Δ_s, are the elongations at the level of the tendons and of the non-prestressed steel reinforcement respectively; Δ_{sp} is the elongation due to strain penetration of the non-prestressed steel reinforcement (assumed to occur at both ends of the unbonded region).

Once the position of the neutral axis and the value of the compression strain in the extreme LVL fiber is derived by translational equilibrium, the moment capacity can be simply derived by rotational equilibrium. However, due to the presence of unbonded post-tensioned tendons possibly in combination with partially epoxied longitudinal mild steel bars (or externally located dissipaters), or a combination of the above, the assumption of strain compatibility between the basic material (timber in this case) and the post-tensioned steel, typically required for a section analysis approach is violated at a section level. As a result, traditional cross section analysis methods typically adopted for the design or flexural strength evaluation of a section cannot be directly applied to these systems. The special provisions for precast concrete jointed ductile connections in NZS3101:2006 adopt a

simplified yet extensively validated procedure for the definition of the moment-rotation curve for connections with unbonded reinforcement where section strain compatibility assumption are violated. This is described by Pampanin et al. (2001) also adopted by the *fib* guidelines for the seismic design of precast concrete connections. Based on a member compatibility concept, the method, named "Monolithic-Beam-Analogy" (MBA) and further refined by Palermo (2004), relies on an analogy with equivalent monolithic solutions. Extensive experimental validations of the aforementioned general procedure for jointed ductile connections have been carried out for precast concrete beam-column joints, frames and shear walls (Pampanin et al., 2001; Palermo et al., 2005), as well as for concrete bridge piers (Hewes et al., 2002, Palermo et al., 2006) and for post-tensioned dissipating, PTED, steel frame solutions (Christopoulos et al. 2002a). Preliminary validation with the experimental results on LVL hybrid systems have provided satisfactory confirmation. Following the aforementioned moment-rotation procedure and on-going validation with the experimental tests, dimensionless design tables and charts related to different section shapes and reinforcement layouts are under preparation, as already done for precast concrete systems (Palermo, 2004).

4. General Design Philosophy and Criteria

4.1 Force-based or displacement-based design approach

Either a force-based or a displacement based design procedure can in principle be adopted for the design of jointed ductile systems, including those using timber members. The special provisions for jointed ductile systems and connections included in Appendix B of NZS3101:2006 are the first worldwide to suggest and allow the use of displacement design of jointed ductile connections.
Limits and drawbacks of traditional force-based design approaches have been well recognized and critically discussed in the literature (Priestley, 1998).A displacement-based design procedure would more naturally capture and control the peculiar rocking behaviour (the rotations at the critical interfaces) of these systems. According to a "flexible" design approach for hybrid systems proposed by Pampanin (2000), the self-centering and energy dissipation contributions of a hybrid system, recognized as key design parameters, can be adequately selected to control maximum displacement and limit residual displacement, while maintaining a given moment capacity. A framework for a Direct Displacement Based design procedure for generic hybrid systems, regardless of the material adopted, was proposed by Pampanin (2000). A more comprehensive displacement based design procedure for precast concrete jointed systems including design examples for frames and wall systems has been recently provided by Priestley (2002). Development of a displacement-based design procedure for timber LVL hybrid systems is continuing and will be presented in the future.

When using a force-based design approach, as typical of major seismic code provisions, appropriate values for the reduction factor R (or the behaviour factor q defined in Eurocode 8) should be defined. As mentioned, provided that an adequate amount of hysteretic damping is given to the flag-shape hysteretic rule, the performance of a hybrid system is expected to be at least as satisfactory as an equivalent monolithic ductile system. Numerical comparisons, again material-independent, between the seismic response of flag-shape and standard dissipating hysteresis loops (Pampanin, 2000, Christopoulos et al., 2002a, Palermo et al., 2006) have demonstrated that the maximum displacements, ductility

or inter storey drift values of a hybrid system will be similar, provided that adequate dissipation capacity is given (in the order of 15% of equivalent viscous damping). Similar values for the reduction factors can thus be suggested for hybrid systems and their monolithic counterparts (Pampanin 2000), as recently adopted in Eurocode 8 for concentrated ductility connections. When designing timber structures, equivalent reduction or behaviour factors (R or q) typical of standard high-ductile connection (i.e. epoxied rods or multi-nailed connections) can be thus be adopted. Extensive numerical investigations are on-going to compare the seismic response of multi-storey timber buildings using traditional connections (i.e. plywood shear walls with nailed connections, or glulam frames with multi-nailed steel plates or epoxied rod connections) with the performance of hybrid (rocking/ dissipating) connections. It is anticipated that, given the relatively limited energy dissipation capacity of a multi-nailed connection due to the extensive "pinching" in the hysteresis loops when compared to the more stable flag-shape hysteresis loops provided by the alternative hybrid connections tested under simulated seismic loading, elastic spectra reduction (or behaviour) factors for these new solutions may be even higher than for conventional construction.

4.2 Controlling the flag-shape hysteresis behaviour: damping vs. re-centering

As consistently confirmed by the results of experimental results, (quasi-static or pseudo-dynamic tests) a wide range of hybrid solutions can be obtained, depending on the moment contribution ratio between self-centering and dissipating contribution, typically defined as $\lambda = M_{pt} / M_s$ where M_{pt} is the flexural strength contribution of the post-tensioning tendons and M_s is the flexural strength contribution of the energy dissipating devices.

Upper and lower bounds of an hybrid system would thus be given by a) a pure rocking system relying on unbonded post-tensioning and/or axial load to provide re-centering (behaviour described by a Non Linear Elastic rule) and b) a dissipative only system with non-prestressed reinforcement and typical elasto-plastic or similar hysteresis rule.

By combining, for a given target strength, the percentage of prestressed and non-prestressed reinforcement within the connection, or, better, the moment contributions between rocking (or re-centering) and energy the properties of the flag-shape hysteresis would vary accordingly (Figure 5) and could be controlled. In particular, it can be noted that the static (maximum feasible) residual deformation and the equivalent viscous damping evaluated from the hysteretic rule can be adopted as main design parameters. By increasing the moment contribution due to the post-tensioning, lower dissipation capacity will be obtained, thus leading to higher displacement demand. On the other hand, a low contribution from the post-tensioning, could impair the re-centering capacity, thus leading to not-negligible residual deformations and a higher cost of repair. Ultimately, a balanced combination of prestressed and non-prestressed steel given by a adequately selected value of $\lambda = M_{pt} / M_s$ can control the maximum lateral displacement, expected under a design level of earthquake intensity, under target limits in accordance with performance based design considerations, while guaranteeing minimum values of residual deformations.

Simplified design charts such as those shown in Figure 5 can be used to define an adequate ratio $\lambda = M_{pt} / M_s$ in the preliminary design phase in order to satisfy the desired requirements.

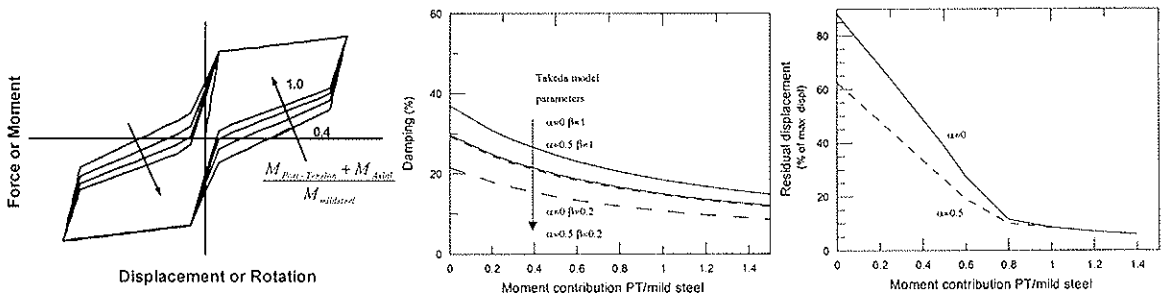

Figure 5 – Influence of the moment contribution ratio λ between post-tensioning steel (PT) and non-prestressed steel on the flag-shape hysteresis of a hybrid system. and on its key parameters (equivalent viscous damping and static residual (Pampanin, 2000; fib, 2003, NZS3101:2006)

4.3 Targeting fully re-centering behaviour

As anticipated, a full re-centering capacity can be achieved at a connection level when the tendons are able to overcome the resistance of the dissipaters and re-close the gap. When using ordinary yielding devices to dissipate the energy, the tendon's restoring moment must be sufficient to yield back in compression the non-prestressed steel which has previously yielded in tension.

In general, regardless of the material and the dissipation systems adopted, a fully re-centering condition can be obtained by selecting an appropriate moment contribution ratio $\lambda \geq 1$. Material overstrength due to steel hardening and Bauschinger effects should be accounted for. In this regard, the NZS3101:2006 guidelines suggest a value of $\lambda \geq \alpha_0$, where α_0 is the expected material overstrength for the non-prestressed steel reinforcement or the energy dissipation devices. In absence of clear information a value of $\alpha_0 \geq 1.15$ (thus $\lambda \geq 1.15$) should be adopted. As a result of a full-re-centering requirement or targeted behaviour, the value of the initial prestress in the tendon are bounded by lower and upper limits. A minimum amount of initial prestress should be used (lower bound) to guarantee the target strength as well as the desired re-centering contribution at a target drift level. Additionally, if coulomb friction due to the post-tensioning is relied upon for partial transfer of shear force (typically seismic shear component) at the critical interface (as in a beam-column connection) a minimum prestress level should be guaranteed at all times. On the other hand, a maximum level of initial prestress should be adopted (upper bound) in order to ensure that the tendons remain in the elastic range at the target inter storey drift levels.

5. Experimental Validation of LVL Hybrid Connections

An extensive research program has been planned and partly carried out at the University of Canterbury to investigate the seismic performance of innovative LVL jointed ductile connections for application in multi-storey timber buildings consisting of seismic resisting frames and/or walls and floors. The program, divided in three phases, involves both comprehensive numerical and experimental investigations at subassembly level (beam-column, column-to-foundation) and global level (whole frames or walls in the complete building). A brief overview is given here, confirming the high performance of the developed solutions and reliability of the design approach. More details can be found in recent publications (Palermo et al. 2005, 2006a, 2006b). The numerical and experimental investigations have provided excellent confirmation of the efficiency of hybrid solutions in multi-storey LVL buildings in seismic regions.

Either quasi-static or pseudo-dynamic tests have been carried out on exterior beam-column subassemblies, wall-to foundation as well as column-to foundation connections. Typical test-setups are shown in Fig. 6. Yielding-type dissipaters have been provided, consisting of deformed mild steel bars machined down to guarantee fuse action, either epoxied inside the main structural elements or located externally. Figure 7 shows details of the construction process and final appearance of typical internal and external dissipaters for the beam-column subassemblies.

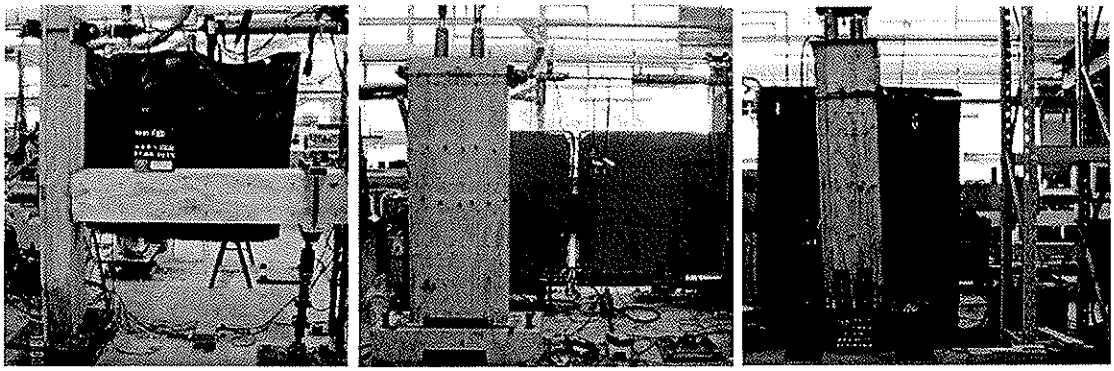

Figure 6. Test set-up of Exterior beam-column, wall-to-foundation, column-to-foundation specimens.

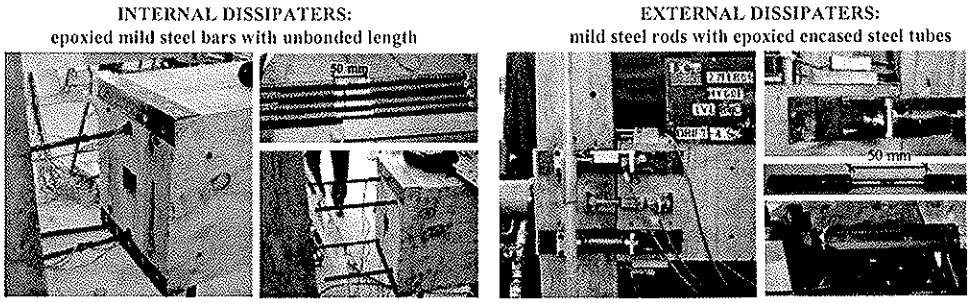

Figure7. Construction details of beam-column subassemblies with internal and external dissipaters.

Following the design principles outlined above, the size, location and other details of the dissipaters and the location and initial prestress of the post-tensioned tendons were carefully designed to guarantee different target levels of re-centering vs. dissipating contribution (moment ratio, λ) while maintaining a flag-shape response.

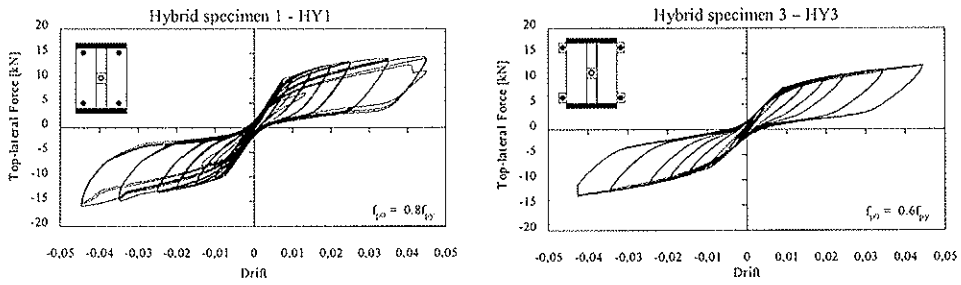

a) b)

Figure 8: Hysteresis force vs. drift response of hybrid solution beam-column joint: a) hybrid solution with internal dissipaters; b) hybrid solution with external dissipaters

The experimental results have confirmed the unique design flexibility of hybrid connections, where similar force-drift (or moment-rotation) capacity envelopes associated with different values of λ have been consistently found, as shown in Figure 8a (internal dissipaters) and Figure 8b (external dissipaters), where the force-displacement curves of four tests on exterior beam-column subassemblies are represented. It can be seen that the overall force-drift envelope curve of the specimen HY1 is very similar to HY3 despite the

adoption of a different combination of dissipaters (internal vs. external, with different unbonded lengths) and initial post-tensioning forces ($0.8f_{py}$ vs. $0.6f_{py}$, respectively). Several unbonded post-tensioned-only configurations have also been tested with different levels of the initial post-tensioning force. Similar design procedures and connections details have been implemented for wall-foundation (Fig. 9a) and column-foundation (Fig. 9b) specimens.

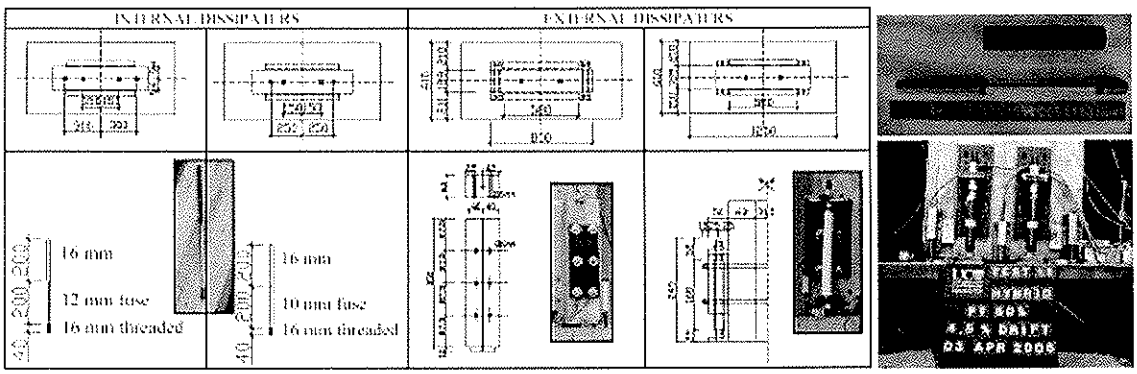

a) b)

Figure 9: a) Details of internal and external dissipaters used for the wall specimens; b) dissipaters detail for of the column-to-foundation specimens.

The results of a series of pseudo-dynamic tests on wall-foundation and column-foundation connections under different level of seismic intensity, confirmed the excellent performance of the post-tensioned/dissipating solutions. Depending on the seismic intensity of the region or on the targeted performance level, alternative arrangements can be obtained by using different combination of tendons and dissipaters. As confirmed by previous studies and applications on precast concrete connections (Pampanin et al., 2005), it is worth noting that in low-to-moderate seismic regions the use of post-tensioning alone, without additional dissipation devices, can be sufficient to control the deflection within targeted (desired or acceptable) levels.

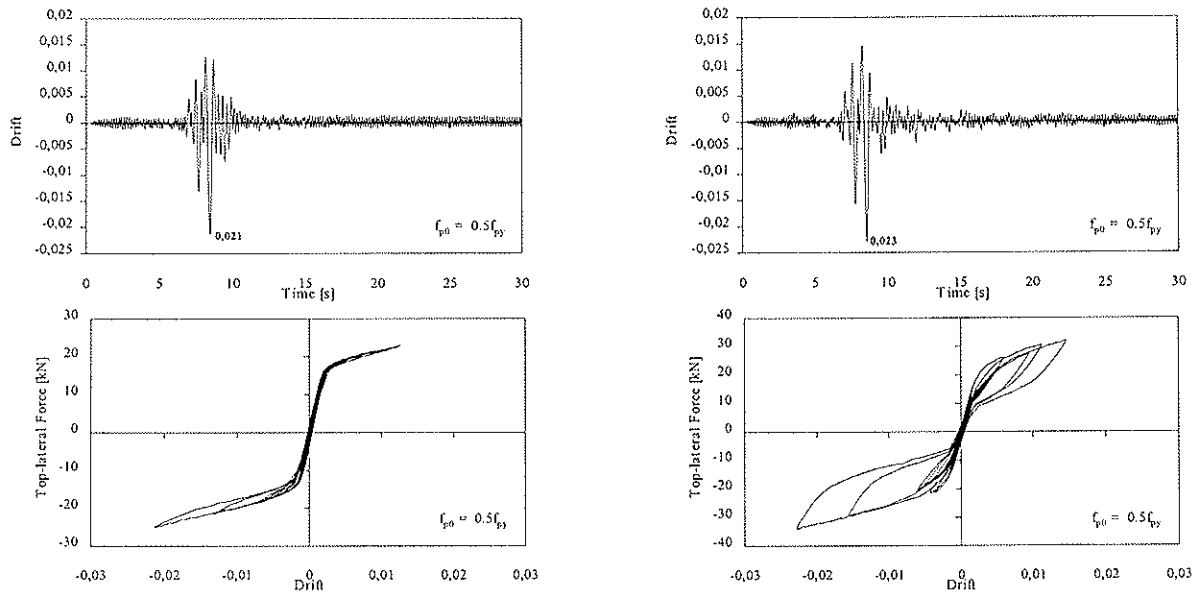

a) b)

Figure 10 Pseudo-dynamic experimental test response of cantilever column-to-foundation systems a) unbonded post-tensioned only (under 100% input motion) b) hybrid system (under 150% input motion)

Multi-storey timber post-tensioned buildings could thus represent a very efficient solution for most of "gravity load dominated" structures. The additional use of dissipaters, would not only enhance the overall strength but also the energy dissipation contribution, thus meeting similar code-based displacement or drift limits in higher seismic region. This concept is clearly illustrated in Figure 10: two alternative solutions, one post-tensioned-only and one hybrid, have been designed according to a displacement based design procedure to achieve similar target drift (around 2-2.5 %) when subjected to two different levels of seismic input intensity (100% and 150% of an earthquake record from the Loma Prieta event, 1989) corresponding to a different earthquake return period (e.g. 500 years and 2500 years respectively). As expected, a non-linear hysteresis response is emphasized by the unbonded post-tensioned-only solutions with a small amount of dissipation due to minor plastic deformation of the LVL material in the compression zone, while a typical flag-shape hysteresis with higher strength is obtained by the solutions with additional external dissipaters, which yielded at around 0.7% of drift. Confirming the reliability of the design procedure, both systems showed similar maximum drift response (2.1% and 2.3% drift respectively) while maintaining negligible residual deformations (full re-centering condition respected). Furthermore, in both cases and in spite of the drift level achieved, no appreciable damage was observed.

6. Conclusions

Innovative damage-resistant solutions have been developed for the seismic design of multi-storey LVL timber buildings, following current international trends towards performance based seismic design and technological solutions for high seismic performance, based on limited levels of damage. The results of an ongoing extensive experimental campaign have confirmed the enhanced performance of jointed ductile connections (also referred to as hybrid systems) with a combination of post-tensioned tendons and energy dissipaters. When compared to traditional solutions widely used in timber construction (e.g. nailed, bolted or steel dowel connections) limited levels of damage can be achieved thanks to controlled rocking mechanisms at the critical connection interfaces. Re-centering properties, leading to negligible residual deformations and limited cost of structural repairing, are provided by unbonded post-tensioned tendons. Simple and reliable design and modelling procedures, developed for precast concrete structures and implemented in major seismic codes, can be adopted with minor modifications for the design of innovative high performance LVL structures and can be proposed for adoption in the next generation of timber design codes and guidelines. It is clearly anticipated that the flexibility of design and the speed of construction of prefabricated LVL buildings, combined with the intrinsic enhanced seismic performance of hybrid systems, creates unique potential for future development and increased use of this type of construction in low-rise multi-storey buildings on a world scale.

References

ACI T1.2-03, (2003) Innovation Task group 1 and collaborators, Special Hybrid moment frames composed of discretely jointed precast and post-tensioned concrete members (ACI T1.2-03) and commentary (ACI T1.2R-03) American Concrete Institute Farmington Hills, MI

Buchanan, A.H. & Fairweather R.H. (1993). Seismic Design of Glulam Structures, Bulletin of the New Zealand National Society for Earthquake Engineering, Vol 26(4) 415-436.

Christopoulos, C., Filiatrault, A. and Folz, B. (2002a). Seismic response of self-centering hysteresis SD & F Systems," Earthquake Engineering and Structural Dynamics, Vol. 31, pp. 1131-1150

Christopoulos, C., Filiatrault, A., Uang, C.M. & Folz, B. (2002b). Post-tensioned Energy Dissipating Connections for Moment Resisting Steel Frames, ASCE Jo. of Structural Engg, Vol. 128(9) 1111-1120.

Christopoulos, C. and Pampanin, S. (2004). Towards performance-based design of MDOF structures with explicit consideration on residual deformations, ISET Journal of Struct. Eng., Special Issue on "Performance-Based Seismic Design", paper 440.

Deam, B. (1997). Seismic Design and Behaviour of Multi-storey Plywood sheathed timber framed shear walls, Research Report No 97/3, Department of Civil Engineering, University of Canterbury.

EC8 (2003). Eurocode 8: Design of structures for earthquake resistance. ECS, Brussels, 2003.

fib, International Federation for Structural Concrete, (2004). Seismic Design of Precast Concrete Building Structures, Bulletin 27, Lausanne, 254 pp.

Halliday, M.A. & Buchanan, A.H. (1993). Feasibility of Medium Rise Office Structures in Timber, IPENZ Transactions, Vol. 19, No.1/CE. 13-20.

Hewes, J.T. & Priestley, M.J.N. (2001). Experimental Testing of Unbonded Post-tensioned Precast Concrete Segmental Bridge Columns, Proc. of the 6th Caltrans Seismic Research Workshop, Sacramento, California.

MacRae, G. A. and Kawashima, K. (1997). Post-earthquake residual displacements of bilinear oscillators, Earth. Eng. and Struct. Dynamics, 26, 701-716.

NZS 3101:2006. Standards New Zealand, Design of Concrete Structures, Appendix B: Special Provisions for the Seismic Design of Ductile Jointed Precast Concrete Structural Systems.

Palermo, A. (2004). The use of controlled rocking in the seismic design of bridges, Ph.D. thesis, Structural Engineering Dept., Technical University of Milan, Italy.

Palermo A., Pampanin S., Buchanan A., Newcombe M. (2005). Seismic design of multi-storey buildings using Laminated Veneer Lumber (LVL), NZEES Conference, March 11- 13, 2005, New Zealand.

Palermo A., Pampanin, S., Calvi, G.M. (2005) Concept and development of Hybrid Systems for Seismic-Resistant Bridges, Journal of Earthquake Engineering, Imperial College PRESS, Vol. 9 (6), pp. 899-921

Palermo, A., Pampanin, S., Carr, A., (2005). Efficiency of Simplified Alternative Modelling Approaches to Predict the Seismic Response of Precast Concrete Hybrid Systems, fib Symposium, Budapest

Palermo A., Pampanin S., Fragiacomo M., Buchanan A., Deam B., (2006a). Innovative seismic solutions for multi-storey LVL timber framed buildings, World Conf on Timber Engg, August 2006, Portland, USA.

Palermo A., Pampanin S., Buchanan A., (2006b). Experimental Investigations on LVL seismic resistant wall and frame subassemblies, ECEES, First European Conference on Earthquake Engineering and Seismology, September 3- 8, 2006, Geneva, Switzerland, (paper accepted).

Palermo A., Pampanin S., Fragiacomo M., Buchanan A., Deam B., Pasticier L., (2006c). Quasi-static cyclic tests on seismic-resistant beam-to-column and column-to-foundation subassemblies using Laminated Veneer Lumber (LVL), 19th ACMSM, December, 2006, Christchurch, New Zealand, (paper accepted).

Pampanin S. (2000). Alternative Design Philosophies and Seismic Response of Precast Concrete Buildings, Ph.D Dissertation, Technical University of Milan, December.

Pampanin, S., Priestley, M. J. N., Sritharan, S. (2001). Analytical modelling of the seismic behaviour of precast concrete frames designed with ductile connections, Journal of Earth. Eng., 5(3), 329-367.

Pampanin, S., Christopoulos, C., Priestley, M. J. N. (2002). Residual deformations in the performance-based seismic assessment of frame structures, Report Rose-2002/02, IUSS PRESS, Pavia.

Pampanin S., (2005). Emerging Solutions for High Seismic Performance of Precast/Prestressed Concrete Buildings, Jo. of Adv. Concrete Technology, invited paper, "High performance systems" 3(2), 202-223.

Priestley, M. J. N. (1996). The PRESSS program – Current status and proposed plans for phase III", PCI Journal, 41(2), 22-40.

Priestley, M.J.N. (1998) Displacement-Based Approaches to Rational Limit States Design of New Structures, Keynote address of the 11th European Conference on Earthquake Engineering, Paris, France.

Priestley, M.J.N. (2002), Direct Displacement-Based Design of Precast/Prestressed Concrete Buildings" PCI Journal, Vol 47 No. 6, pp 66-78

Priestley, M.J.N., Sritharan, S., Conley, J. R. & Pampanin, S. (1999). Preliminary Results and Conclusions from the PRESSS Five-story Precast Concrete Test-building, PCI Journal, Vol 44(6) 42-67.

SEAOC Vision 2000 Committee, (1995). Performance-Based Seismic Engineering Structural Engineers Association of California, Sacramento, California.

Thomas, G.C., Buchanan, A.H. & Dean J.A. (1993). The Structural Design of a Multi-storey Light Timber Frame Residential Building, IPENZ Transactions, Vol. 19, No.1/CE. 35-41.

INTERNATIONAL COUNCIL FOR RESEARCH AND INNOVATION
IN BUILDING AND CONSTRUCTION

WORKING COMMISSION W18 - TIMBER STRUCTURES

FIRE PERFORMANCE OF FRP REINFORCED GLULAM

T G. Williamson
B Yeh

APA - The Engineered Wood Association

U.S.A.

MEETING THIRTY-NINE
FLORENCE
ITALY
AUGUST 2006

Presented by T Williamson
A Buchanan asked whether steel trusses shown in the slide would have a 1 hr fire rating. T Williamson answered in US steel would be considered as non-combustible and fire rating would not be an issue for them.
A Buchanan asked whether a full or reduced design load was used in the fire test. T Williamson answered in US fire tests would be performance at full design load.
A Asiz asked about the fire rating of LVL hybrid glulam. T Williamson stated that LVL member would be typically of smaller dimension and would not seek the same level of rating. But LVL would be expected to perform similar to glulam.
H Larsen asked what would be the economy of this system and could one develop a standard for a patented producer. T Williamson explained the recent history and issues of the patented FRP glulam and that alternative patented products have been introduced into the market. The cost of glass reinforced system would be approximately 20% cheaper than normal glulam and 10% cheaper than steel. Finally ASTM standard would be focused on mechanics based model not patent specific product.
I Smith received clarification that in US only a single passing fire rating test would be required to achieve a certain target fire rating.
J König commented that it is well known that bigger beams would be needed to achieve the target fire rating. He questioned what would the strength of deeper beam be without the FRP in comparison to using the FRP reinforced deeper beam. He commented that since one would need the deeper beam anyway to achieve the fire rating why one would need the FRP.

Fire Performance of FRP Reinforced Glulam

Thomas G. Williamson, P.E.
Borjen Yeh, Ph.D., P.E.
APA - The Engineered Wood Association, U.S.A.

Abstract

One of the emerging advanced engineered wood technologies in the United States and other countries is the use of high strength fiber-reinforced polymers (FRP) to reinforce the tension zone of structural glued laminated timber (glulam). Glulam is used in numerous long-span commercial building applications where the glulam is exposed for architectural reasons. For some occupancy use classifications, the U.S. building code mandates that these exposed glulam members be rated for one-hour fire construction. The most structurally efficient use of FRP reinforcement is to place the FRP on the outermost face of the glulam member. However, there is no published information on how a glulam beam reinforced in this manner will perform when directly exposed to fire.

In order to address this concern, representatives of APA - The Engineered Wood Association (APA), the Market Development Alliance (MDA) Engineered Wood Team, and the University of Maine Advanced Engineered Wood Composites Center (AEWCC) sponsored a fire test program of FRP reinforced glulam beams at Omega Point Laboratories in San Antonio, Texas. The purpose of the testing was to gain an understanding of the performance of FRP composites exposed to fire when used as a structural reinforcement for glulam beams.

This paper describes the results of two test programs conducted in accordance with ISO Standard 834. The first test program was a pilot study involving relatively small FRP reinforced glulam beams. Based on the results of this pilot study, a second test program was then undertaken to evaluate the fire performance of FRP reinforced glulam beams designed to achieve a one-hour fire rating. The results of these tests led to the development of a design methodology to permit establishing fire ratings for FRP reinforced glulam.

1. Introduction

Structural glued laminated timber (glulam) is used in numerous commercial building applications where the glulam is exposed for architectural reasons such as in the roof framing of a school gymnasium, the sanctuary of a religious facility or many other similar situations. In some instances the applicable building code, such as 2006 International Building Code (IBC) in the United States [1], requires that these exposed glulam members be rated for one-hour or greater fire resistive construction.

The determination of fire ratings for glulam is described in Chapter 16 of the National Design Specification (NDS) for Wood Construction [2] promulgated by the American Forest and Paper Association (AF&PA) and published as an American National Standard Institute (ANSI) standard, which is referenced by the 2006 IBC. The methodology is based on the approach of determining an effective char rate based on published nominal one-hour char rate data. Fire endurance times of 1 hour, 1-1/2 hours and 2-hours may be calculated using this methodology. Further details are provided in American Wood

Council (AWC) Technical Report 10, *Calculating the Fire Performance of Exposed Wood Members* [3].

To achieve these fire ratings, it is required that the glulam members be manufactured using an additional outer tension lamination per each one hour of fire rating to be achieved. It is assumed that this outermost tension lamination will serve as a sacrificial lamination to protect the next innermost tension lamination form exposure to the fire and thus maintain the structural integrity of the beam.

One accepted way in the U.S. to achieve a one-hour fire rating for an FRP reinforced glulam is to use a similar approach of positioning a so-called "bumper lamination" (sacrificial lamination) on the exposed face of the beam to protect the FRP layer from direct exposure to the fire. However, the use of a bumper lamination introduces other design considerations that must be addressed, such as defining ultimate failure of the beams. In addition, the most structurally efficient use of FRP reinforcement is to place the FRP on the outermost face of the glulam member. However, there is little published information on how a glulam beam reinforced with FRP in this manner will perform when directly exposed to fire.

In order to address this concern, representatives of APA - The Engineered Wood Association (APA), the Market Development Alliance (MDA) Engineered Wood Team, and the University of Maine Advanced Engineered Wood Composites Center (AEWCC) sponsored a fire test program of FRP reinforced glulam beams at Omega Point Laboratories in San Antonio, Texas. The purpose of the testing was to gain an understanding of the performance of FRP composites exposed to fire when used as a structural reinforcement for glulam beams.

The tests were conducted in accordance with ASTM E 119 [4], which is the prescribed U.S. standard for evaluating products exposed to a fire of controlled extent and severity. It is noted that the *International Standard for Fire Resistant Test – Elements of Building Components,* ISO 834 [5], is very similar to ASTM E 119. Both of these test methods are intended to evaluate the duration for which assemblies will contain a fire, retain their structural integrity, or exhibit both properties.

Since fire testing can be complicated and expensive and virtually no fire test data was available for this type of FRP reinforced member, the research team decided to start with a small-scale pilot study involving relatively small FRP reinforced glulam beams. Based on the results of this pilot study, a second test program was then undertaken to evaluate the fire performance of larger FRP reinforced glulam beams designed to achieve a one-hour fire rating.

2. Phase I Testing

Lacking published data, the research team initially evaluated a set of relatively small size FRP reinforced glulam beams to develop benchmark data. Several MDA companies expressed interest in supplying FRP reinforcement for this test phase. Based on their experience working with this type of reinforcement technology, the AEWCC staff required that any products offered for testing had to pass two screening tests: The FRP products bonded to wood had to pass ASTM D 2559 [6] for adhesive durability and ASTM D 905 [7] for shear compression loading. The first test was to determine the resistance to

delamination during accelerated exposure of FRP/wood laminations based on a modified ASTM D 2559. The second test was to determine the resistance to shear by compression loading. Two companies, Creative Pultrusions and Gordon Composites, submitted products and passed the screening tests established by the University of Maine.

Creative Pultrusions and Gordon Composites fabricated two samples each that were 2.5 mm x 127 mm x 3.94 m and 6.4 mm x 127 mm x 4.3 m. A manufacturer certified to produce glulam in accordance with the *American National Standard for Wood Products - Structural Glued Laminated Timber*, ANSI A190.1 [8], which is the U.S. manufacturing standard applicable to glulam, produced glulam beams made of Douglas Fir that were 127 mm x 229 mm x 4.3 m in length. The beams were manufactured in accordance with industry lay-up provisions for a beam having an allowable bending strength of 16.5 MPa and a modulus of elasticity of 12,410 MPa with no additional special tension lamination. These non-reinforced beams were then shipped to the AEWCC where the FRP layer was applied. A total of 9 beams (8 with FRP reinforcement and one control) were fabricated. Four FRP reinforced beams were destructively tested in the as-received conditions at the University of Maine prior to fire testing to determine the design loads to be applied during the fire test.

As noted, it was decided to test the glulam beams without the bumper lam to evaluate the effect of the FRP directly exposed to fire. These beams were tested in accordance with ISO 834/ASTM E 119 at the Omega Point Laboratories in San Antonio, Texas. Table 1 summarizes the results of these Phase I tests.

Table 1. Summary of Fire Test Measurements and Observations for Phase I Tests

	Test #1	Test # 2	Test # 3	Test # 4	Test # 5
Beam Reinforcement	2.50%	Control	2.50%	1.20%	1.20%
Laminate Construction	Roving/CSM	None	Roving	Roving	Roving/CSM
FRP Materials	E-glass/urethane	None	E-glass/epoxy	E-glass/epoxy	E-glass/urethane
Manufacturing Process	Pultrusion	None	Continuous lamination	Continuous lamination	Pultrusion
Center-point Load	29.3 kN	18.7 kN	29.3 kN	24.5 kN	24.5 kN
Time to break (min:sec)	27:47	36:37	21:42	24:26	20:44
Deflection (mm) @ min:sec	60.3 @ 27:30	77.8 @ 36:00	61.9 @ 21:00	52.4 @ 24:00	38.1 @ 20:00
Type of failure	Tension	Tension	Delamination	Tension	Delamination

Figure 1 shows one of the FRP beams positioned in the test element prior to placing it in the furnace. Figure 2 shows one of the FRP layers was delaminated and fell onto the bottom of the furnace after the completion of the test. Figure 3 shows the resulting cross-sections after the fire. Specimen A shown in Figure 3 was a reinforced beam and Specimen B was the control beam showing the greater charring of the control beam.

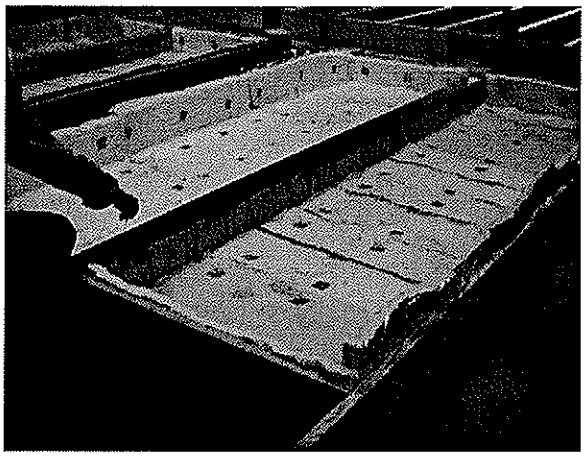

Figure 1. An FRP beam positioned in the test element

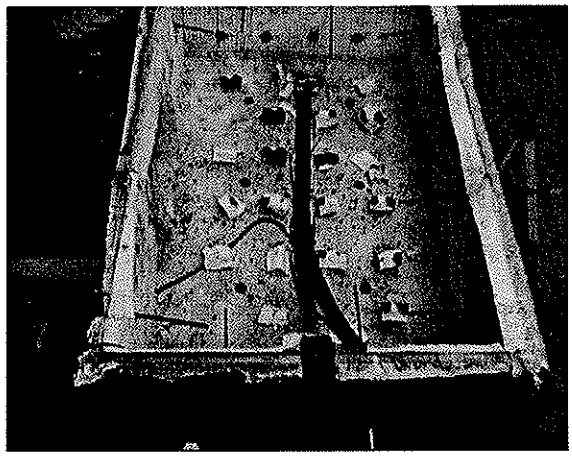

Figure 2. A delaminated FRP layer fell onto the bottom of the furnace

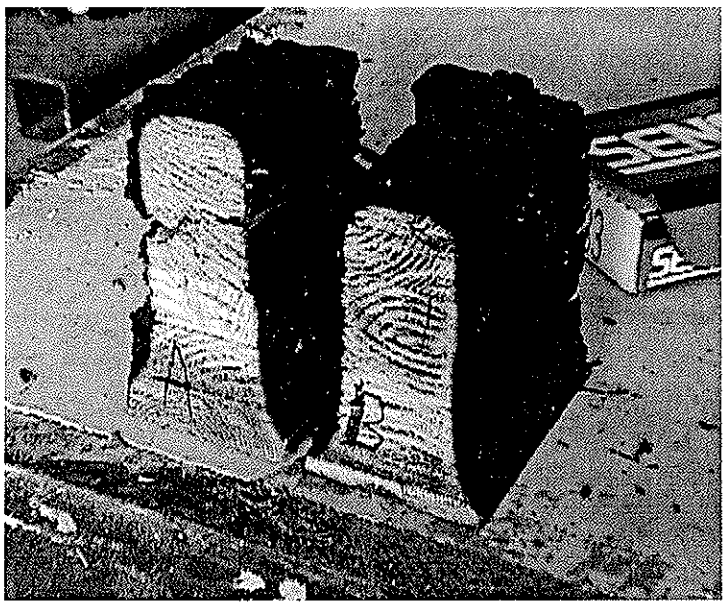

Figure 3. The resulting cross-sections after the fire

One observation to note from the test results is the load difference of the control beam (18.7 kN) compared to the FRP reinforced beams (24.5 kN or 29.7 kN). Based on an analysis by the AEWCC, the FRP reinforced beams had higher allowable bending stresses, 19.3 MPa for the 1.2% reinforced beams and 22.7 MPa for the 2.5% reinforced beams, as compared to 16.5 MPa for non-reinforced beams, resulting in the higher allowable design loads for beams of the same size. To test the control beam at the same load as the FRP reinforced glulam, it would have been necessary to use a larger cross-section for the control beam and it was decided this could significantly bias the results by testing the larger cross-section.

Visual observations by the research team of this testing indicated that the FRP materials began to burn at approximately 2 minutes after the ignition of the furnace and that the FRP layers began to delaminate from the beams at approximately 15 and 20 minutes.

The four FRP reinforced beams lasted from 21 to 28 minutes in comparison to the 36.5 minutes for the control beam. Neither the reinforcements nor the bond was designed to

specifically resist exposure to fire since the focus of these tests was primarily on meeting the requirements of ASTM D 2559 and D 905. Given the low Tg values (150°C to 200°C) for the matrix and adhesive used in the reinforcements, it was concluded that the beams performed well. As expected, while the fire endurance of the FRP reinforced glulam beams was less than that for the control beam, the results were encouraging and provided insights for the next testing phase involving larger beams.

An analysis of the char rates indicated an average rate of 37.3 minutes per 25mm of char. This equates to 40mm/hr. A nominal char rate of 38mm/hr is normally assumed for glulam manufactured using softwoods. For a one-hour rated beam this results in an effective char rate of 46mm/hr per the NDS.

3. Phase II Testing

In order to achieve a one-hour fire rating according to the NDS methodology, typically a 170 mm wide x 343 mm deep glulam is required. The goal was thus to design a similar size beam reinforced with FRP composites that would meet the one-hour test criteria to satisfy the building code requirements. APA staff conducted some preliminary analyses based on the results of the Phase I pilot study and the accepted methodology of rating glulam beams using the char rate as published in the NDS. The analysis hypothesized that an FRP reinforced beam with a depth of 10% greater than that required for full design load plus one additional tension lamination could achieve a one-hour rating.

For example, if the non-reinforced design depth is 343 mm, then the FRP reinforced beam would need to be 343 mm x 1.1 plus one additional tension lamination. Based on a lamination thickness of 38 mm, the required size for a one-hour rating would be 377 mm + 38 mm or 415 mm. Thus, it was determined that a beam having a cross-section of 165 mm x 420 mm should meet the one hour criteria. However, due to the uncertainty of the analysis and the fact that the width was only 165 mm vs. the standard minimum width of 170 mm for a non-reinforced beam, it was decided to also test beams having a cross sectional dimension of 165 mm x 455 mm. The reason for the slightly narrower width was to accommodate the manufacturing process for the FRP materials. Also the depths used represented standard multiples of the 38 mm lamination thickness.

It should be noted that the 10% depth increase plus one additional tension lamination for the FRP reinforced beam is intended to compensate for the reduction in the beam strength by the increase in the section modulus when the FRP layer fails during the one-hour fire exposure. Therefore the percentage of depth increase required for a one-hour fire rating is dependent on the bending strength ratio between the reinforced and non-reinforced beams. For the beams tested in Phase II, the strength ratio between the reinforced and non-reinforced beams was determined to be 1.25. Therefore, the depth ratio could be calculated as $\sqrt{1.25}$ or 1.12. From the example given above, the 420 mm deep beam provides a depth ratio of 1.22 over the 343 mm deep beam.

The FRP used was again supplied by the same manufacturers involved in Phase I and consisted of 0.6 mm x 165 mm x 4.3 m samples using a pultruded E-glass/urethane and a continuous E-glass/epoxy lamination.

The non-reinforced Douglas fir glulam beams were manufactured by an ANSI-certified manufacturer using a 24F-V4 lay-up (F_b = 16.5 MPa and MOE =12,410 MPa) combination

with a second tension lamination added per the requirements for a one-hour rated beam. An approved phenol-resorcinol adhesive typical of those used by the glued laminated timber manufacturing industry in the U.S. was used. APA staff witnessed the grading of the lumber, the lay-up of the test beams and the manufacturing of the beams. Two of the beams were 165 mm x 420 mm x 4.3 m and the other two beams were 165 mm x 455 mm x 4.3 m.

After manufacturing, the non-reinforced beams were shipped to the AEWCC at the University of Maine where the FRP was installed on the bottom face of the test beams. Based on an analysis by the AEWCC staff, it was determined that the allowable bending stress for these FRP reinforced glulam was equivalent to 20.7 MPa and this was used to establish the design loads applied during the fire test. The beams were then shipped to the Omega Point Laboratory in San Antonio, Texas and tested using the ISO 834 test protocol.

Figure 4 shows one of the test beams being installed in the furnace and Figure 5 shows the application of the design load. The design load for the 420 mm deep beams was 69.4 kN and the design load for the 455 mm deep beams was 85.4 kN.

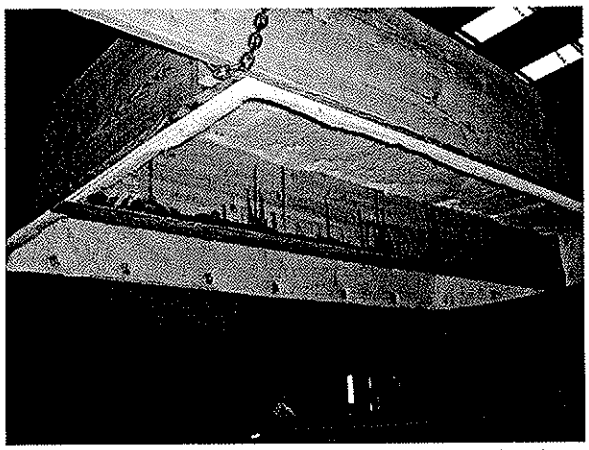

Figure 4. A test beam being installed in the furnace

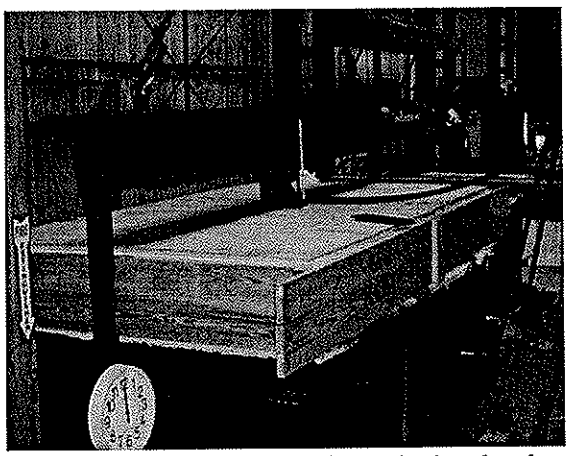

Figure 5. Application of the design load

Results of these tests supported the proposed design hypothesis of adding 10% plus one lamination to the beam depth to achieve a one-hour fire rating. Three of the test beams reached 60 minutes with the beams still maintaining full design loads. The fourth beam, one of the 420 mm deep beams, achieved 56 minutes, but it was felt that this result was within the variability associated with glulam beam fabrication and fire testing. Following the extinguishment of the fire, the three test beams that had achieved the one-hour rating were loaded to failure and all three had at least 15% additional reserve capacity after the one-hour fire exposure.

Figure 6 shows the residual cross sections of test beams after the one-hour test visually demonstrating the charring effect. The two beams on the left are the 420 mm deep beams and the two beams on the right are the 455 mm deep beams. There was no noticeable difference in the performance of the two sets of beams with the approximate percentage of wood remaining ranging between 47% and 49% indicating that both FRPs used performed similarly. In fact, the ultimate failure load for the two 455 mm deep beams was identical.

Figure 6. Residual cross sections of tested beams

4. Conclusions

Based on these tests, it was clearly demonstrated that a glulam beam with an FRP applied to the bottom face of the beam and directly exposed to a fire (no bumper lamination) can be designed to achieve a one-hour fire rating when evaluated in accordance with the ASTM E 119 or ISO 834 fire test protocol. It was also shown that for the two different FRP reinforcement layers used in this study there were no discernible differences in overall fire and structural performance. These results should open up new market opportunities for FRP reinforced glulam when a one-hour fire rating is required with the FRP applied to the outermost tension face.

Results of these tests suggested that the FRP reinforced glulam could be designed for fire rating in a similar manner as the conventional non-reinforced glulam. Test data from these studies supported the proposed mechanics-based methodology by increasing the depth of the FRP reinforced beam to achieve a one-hour fire rating. As manufacturers in the U.S. seek building code acceptance of proprietary FRP reinforcement systems, this testing will provide the basis for justifying one-hour rated assemblies using FRP reinforced glulam beams.

5. References

1. ICC. 2006. International Building Code. International Code Council. Country Club Hills, IL.

2. American Forest & Paper Association. 2005. National Design Specification for Wood Construction. Washington, DC.

3. American Forest & Paper Association. 2003. Calculating the Fire Performance of Exposed Wood Members. Technical Report 10. Washington, DC.

4. ASTM International. 2005. Standard Test Methods for Fire Tests of Building Construction and Materials. ASTM International. ASTM E 119. West Conshohocken, PA.

5. ISO. 1999. Fire-Resistance Tests -- Elements of Building Construction -- Part 1: General Requirements. ISO 834-1. International Organization for Standardization. Geneva, Switzerland.

6. ASTM International. 2004. Standard Specification for Adhesives for Structural Laminated Wood Products for Use Under Exterior (Wet Use) Exposure Conditions. ASTM International. ASTM D 2559. West Conshohocken, PA.

7. ASTM International. 2003. Standard Test Method for Strength Properties of Adhesive Bonds in Shear by Compression Loading. ASTM International. ASTM D 905. West Conshohocken, PA.

8. American National Standards Institute. 2002. American National Standard for Wood Products - Structural Glued Laminated Timber. ANSI A190.1. New York, NY.

INTERNATIONAL COUNCIL FOR RESEARCH AND INNOVATION
IN BUILDING AND CONSTRUCTION

WORKING COMMISSION W18 - TIMBER STRUCTURES

AN EASY-TO-USE MODEL FOR THE DESIGN OF WOODEN I-JOISTS IN FIRE

J König
SP Trätek/Wood Technology

B Källsner
SP Trätek/Wood Technology
Växjö University

SWEDEN

MEETING THIRTY-NINE
FLORENCE
ITALY
AUGUST 2006

Presented by J König
A Frangi asked about the issue of rock fibre versus glass fibre used in the model. J König stated that the model would be okay for cavity and glass fibre would be okay if cladding was intact. After cladding failed the glass fibre performance would be compromised as the melting point is ~ 500C. H Blass questioned that knowing rock fibre would be better why would one consider glass fibre. J König stated that glass fibre user would need the data.
B Yeh asked about the charring of web material as typical real failure mode. T Williamson stated in US insulation would typically not be provided in the cavity. J König stated that in Sweden no one would use non-insulated system because of sound transmission issue etc.
A Buchanan commented that the model required assumed knowledge of the cladding and glass performance etc which could be product manufacturer dependent. Also the model would be based on standard fire curve and questioned what about parametric fire.
J König stated that full size testing would be needed to calibrate the model. Different gypsum producers would need to provide fire test data to put in the model if they would want their product considered. Finally parametric fire would be tricky. Thermo properties of wood would only be valid for standard fire.

An easy-to-use model for the design of wooden I-joists in fire

Jürgen König
SP Trätek/Wood Technology, Sweden

Bo Källsner
SP Trätek/Wood Technology, Sweden
Växjö University, Sweden

Abstract

A numerical study was conducted with the objective to determine cross-sectional and strength properties of I-shaped joists subjected to charring under ISO 834 standard fire exposure. The outcome of this work should be design parameters in terms of Eurocode 5 (EN 1995-1-2) for I-joists in bending where the tension flange is on the fire exposed side of the joist; these are the time of start of charring, charring depths and modification factors for strength. The I-joists are assumed to be integrated in floor assemblies consisting of joists, linings made of gypsum plasterboard or wood-based panels, cavities completely filled with batt-type rock or glass fibre insulation, and a decking. Heat transfer analyses were performed using SAFIR. This software permits to study the effect of the lining falling off at specified times that are known from full-scale testing or using the criterion of insufficient penetration length of fasteners into unburnt wood. For the determination of the notional charring depth in the flange and the modification factors of the whole cross-section, a computer program CSTFire, written as a Visual Basic macro embedded in Excel, was developed, using the temperature output from the heat transfer calculations and relative strength and stiffness values given by EN 1995-1-2, i.e. compressive strength, tensile strength and moduli of elasticity in compression and tension. The notional charring depth is calculated such that the notional residual cross-section of the flange remains rectangular and the section modulus of the I-section is unchanged. The effect of various parameters on the notional charring rate is shown, such as charring phases (i.e. a distinction is made whether the I-section is initially unprotected, protected by a lining, or unprotected after failure of the lining), flange dimensions and depth of cross-section. Modification factors for bending and shear strength are shown as functions of the notional charring depth for different charring phases. In order to simplify these relationships, simple expressions are given for increased user-friendliness and code specification.

1 Introduction

Wooden I-shaped joists and studs, consisting of flanges made of solid timber or LVL and a web made of wood-based panels (such as particle board, fibreboard or OSB), are increasingly used in timber frame construction. While design models for fire exposed timber frame construction with solid timber joists and studs are available [1] [2] there is still a need to develop corresponding rules for timber frame assemblies with I-shaped joists and studs. For the time being, fire resistance classification is normally done by fire testing of floor and wall assemblies.

The constructions dealt with in this paper consist of wooden I-joists with a lining, a decking (generally called as fire protective claddings) and cavities that are completely filled with batt-type rock or glass fibre insulation. The lining may be fixed to the I-joists or to resilient channels or battens in perpendicular direction to the I-joists. This paper deals with I-joists in bending where the tension

flange is on the fire exposed side of the floor assembly.

The normal design procedure of timber members exposed to fire consists of several steps:
- Determination of action effects (internal forces and moments);
- Determination of the residual cross-section of the member taking into account the effect of fire protective claddings on the charring depth (thermal analysis);
- Determination of the degradation of strength and stiffness properties, e.g. by modification factors or the use of an effective residual cross-section where applicable;
- Calculation of the mechanical resistance of the member.

The goal of the study presented here was to derive simple, easy-to-use expressions from the results of thermal and mechanical analyses for the following parameters:
- Time of start of charring;
- Charring rates;
- Modification factors for the reduction bending and shear strength.

Since failure times of fire protective claddings are not known for all types of claddings used in practice, the design model should also be applicable where failure times of fire protective claddings must be determined by testing.

For application of the results from the thermal and mechanical analyses in a simplified design model, the following goals were set up:
- The design model should be easy to use and available to all designers; it was not the purpose to create a design tool that could be felt as a "black box";
- Charring and strength parameters should be given as linear expressions;
- The charring model should be consistent with testing and be modified where other species or engineered wood with different charring performance are used.

This paper highlights some of the issues of the background report [3].

2 The simplified model

2.1 General

The design model developed for I-joists follows the method and terminology and describes relevant parameters given in EN 1995-1-2 [1]. Charring rates and charring depths are expressed as notional values in order to simplify design work. Different charring phases are taken into account with respect to the effect of claddings and their failure. The degradation of strength due to elevated temperature is taken into account by multiplying the bending and shear strength values at ambient temperature by modification factors.

With respect to the degree of protection provided by the cladding, three different charring phases are defined [1]:
- Charring phase 1 for initially unprotected timber surfaces. For timber frame assemblies with I-joists this charring phase won't exist in practice.
- Charring phase 2 for the phase between start of charring of the timber member behind the cladding until failure of the cladding.
- Charring phase 3 for the phase after failure of the cladding.

For timber floors with I-joists and linings made of gypsum plasterboard or wood-based panels, charring phase 3 is the most likely to occur near failure of the floor.

2.2 Cross-section

The dimensions of an I-joist are shown in Figure 1a. At ambient temperature, the characteristic moment resistance is calculated as:

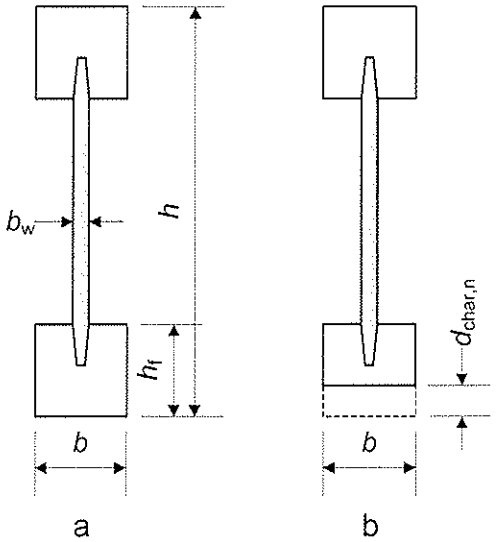

Figure 1: Cross-section of I-joist, a: at ambient conditions, b: in the fire situation

$$M_k = f_{m,k}\, W_{ef} \tag{1}$$

where $f_{m,k}$ is the characteristic bending strength of the flanges and the effective section modulus W_{ef} takes into account the different moduli of elasticity of the web and the flanges. Where the bending resistance of the I-joist was derived from testing, $f_{m,k}$ is the characteristic bending strength of the I-joist declared by the producer of the I-joist, implying that no further verification of axial stresses in the web is necessary.

In the fire situation, for I-beams in floor assemblies with cavities that are completely insulated, the cross-section shown in Figure 1b should be used to calculate the mechanical resistance for the required period of fire exposure t.

For failure during charring phase 3, that is the cladding has fallen off at the time t_f, the notional charring depth, $d_{char,n}$, should be taken as:

$$d_{char,n} = \beta_n\, (t - t_{f,ef}) \tag{2}$$

where:

$$\beta_n = \beta_0\, k_{b,ch}\, k_3\, k_n \tag{3}$$

$$k_{b,ch} = \frac{27,4}{b} + 1 \tag{4}$$

$$k_3 = 0,0157\, t_f + 1 \tag{5}$$

$$t_{f,ef} = 0,9\, t_f \tag{6}$$

$k_n = 1,4$

β_0 is the one-dimensional charring rate given in EN 1995-1-2 [1], that is β_0 = 0,65 mm/min for solid softwood and LVL;

t_f is the failure time of the cladding, in minutes; it may be given by EN 1995-1-2 [1] or by the producer or be determined with respect to withdrawal failure of cladding fasteners;

$t_{f,ef}$ is the effective failure time of the cladding;

b is the flange width in mm.

The penetration length into unburnt wood of fasteners for fixing claddings or resilient channels should be at least 10 mm. The charring depth may be taken as the notional charring depth $d_{char,n}$.

2.3 Strength parameters

For I-joists in bending where the fire-exposed flange is in tension, the modification factor for bending strength, $k_{mod,fm,fi}$, should be calculated as:

$$k_{mod,fm,fi} = 1 - 0,016\, d_{char,n}\, k_{b,fm}\, k_{hf,fm}\, k_{h,fm} \tag{7}$$

with

$$k_{b,fm} = 0,76 + \frac{11,5}{b} \tag{8}$$

$$k_{hf,fm} = \frac{68}{h_f} - 0,41 \tag{9}$$

$$k_{h,fm} = 1,4 - \frac{80}{h} \tag{10}$$

where the notional charring depth $d_{char,n}$, the flange width b, the flange depth h_f and cross-section depth h are in mm, while all k-factors are dimensionless.

For shear strength verification of the web, the maximum temperature of the web in degrees Celsius should be calculated as:

$$\Theta_{w,max} = \frac{160\, k_b\, d_{char,n}}{h_f} - 47 \tag{11}$$

For wood-based webs the modification factor for shear strength, $k_{mod,fv,fi}$, may be calculated, using the reduction factor for shear strength given in Figure B4 of EN 1995-1-2 [1], as:

$$k_{mod,fv,fi} = \begin{cases} 1 & \text{for} \quad \dfrac{48\, k_{b,ch}\, d_{char,n}}{h_f} \le 20 \\ 1,47 - \dfrac{1,13\, k_{b,ch}\, d_{char,n}}{h_f} & \text{for} \quad \dfrac{48\, k_{b,ch}\, d_{char,n}}{h_f} > 20 \end{cases} \tag{12}$$

For shear strength verification of the glue-line between the web and the flange, the temperature in degrees Celsius should be taken as:

$$\Theta_{joint} = \max \begin{cases} 666\, d_{char,n}\, \dfrac{k_b}{\sqrt{b}\, h_f} - 12 \\ 20 \end{cases} \tag{13}$$

In equations (7) to (13) all sizes are in mm.

3 Determination of model parameters

3.1 Methodology

The charring and mechanical properties of I-joists were determined in two steps. The charring properties were determined using the residual cross-section from the thermal analysis, assuming that all parts of the cross-section with temperatures greater than 300°C have undergone charring. Since the irregular shape of the residual cross-section of the fire-exposed flange is unfavourable to be used in design calculations, a notional charring depth, $d_{char,n}$, of the fire exposed flange was determined (see Figure 2), assuming that:

- the notional residual cross-section of the fire exposed flange is rectangular and the flange width is equal to the original flange width b;
- the section modulus of notional residual cross-section, W_r, is equal to the residual cross-section obtained by the thermal analysis.

Since the bending moment resistance of a fire-exposed beam is dependent on charring and bending strength reduction, the modification factor for the reduction of bending strength, $k_{mod,fm,fi}$, was determined from

$$k_{mod,fm,fi} = \frac{M_{fi}\, W}{M\, W_r} \tag{14}$$

where:

M is the bending moment resistance under ambient conditions;
M_{fi} is the bending moment resistance in the fire situation;
W_r is the section modulus of the residual cross-section of the I-joist;
W is the section modulus of the original cross-section of the I-joist.

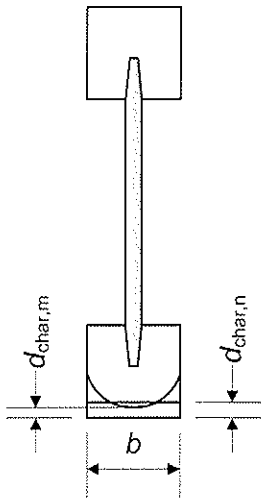

Figure 2 – Determination of the notional (equivalent) charring depth

A typical cross-section of an I-joist is shown in Figure 3a. Most calculations were conducted for an I-joist (H200) with h = 200 mm, b = 48 mm, h_{fl} = 48 mm and b_w = 8 mm. Thereafter the flange width was varied from 36 to 88 mm and the depth of the cross-section was increased to 300 mm. With respect to the web properties some simplifying assumptions were made. The flanges of I-joists and studs are produced using solid timber or engineered wood products such as LVL, while the web is normally made of wood-based panels (particleboard, OSB or wood fibreboard). Since the effect of the web is small on both temperature development in the web and the resistance of the cross-section, (the modulus of elasticity of the web is between 20 and 50 % of the modulus of elasticity of the flanges), the modulus of elasticity of the web was taken equal to zero in the bending resistance analysis and the determination of the notional charring depth, see Figure 3b, while thermal properties of wood were assumed for the web in the thermal analysis, see Figure 3c. Further, the bonded-in part of the web was given the same properties as the flange; this simplification compensates, to some extent, for the effects of disregarding the web.

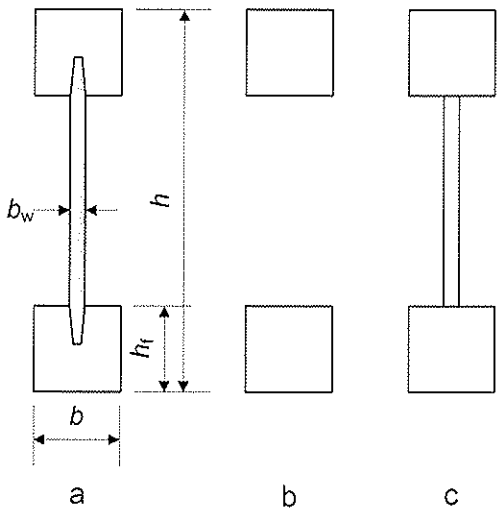

Figure 3 – a) Dimensions of I-shaped section, b) Cross-section for mechanical analysis (bending) and determination of notional charring depth, c) Cross-section for thermal analysis

Although floor and wall assemblies always include claddings on the fire exposed side, calculations were also conducted on assemblies consisting of an I-joist plus the cavity insulation (without cladding). The results of these calculations were used for studying the effect of parameters such as the flange width, flange depth and the total depth of the cross-section.

3.2 Thermal analysis

The thermal analysis, using the ISO 834 standard fire curve for the temperature development in the compartment, was executed using the software SAFIR 2004. This version of SAFIR permits modelling the failure of claddings at specific times, e.g. when a pre-defined failure criterion has been reached (a specific temperature on the unexposed side of gypsum plasterboard linings, or pull-out failure of fasteners, or a value known from full-scale fire tests), by using the temperature field from the first run as the start temperature field in the following calculation without the cladding that is assumed to have fallen off. An example of typical results of the thermal analysis is shown in Figure 4. The graph indicates a rounded shape of the residual cross-section of the fire exposed flange; the char-line of which is defined as the location of the 300°C isotherm. The propagation of the 300°C isotherm can be seen from Figure 5.

3.3 Structural analysis

For the structural analysis, a computer program CSTFire, written as a Visual Basic macro embedded in Excel, was developed, using the temperature output from the heat transfer calculations and the

relative strength and stiffness values given by EN 1995-1-2 [1], i.e. compressive and tensile strengths, f_c and f_t, and moduli of elasticity in compression and tension, E_c and E_t. These values are given as bi-linear functions of temperature from 20 to 300°C with breakpoints at 100°C, also taking into account the effects of transient moisture situations and creep, see Figure 6. The software takes into account the possibility of permitting ductile behaviour of wood under elevated temperature. Contrary to ambient conditions where failure on the tension side of a beam is brittle, in the fire situation tensile failure of the outermost fibres won't cause immediate collapse of the member since a redistribution of internal stresses will take place as long as equilibrium is maintained.

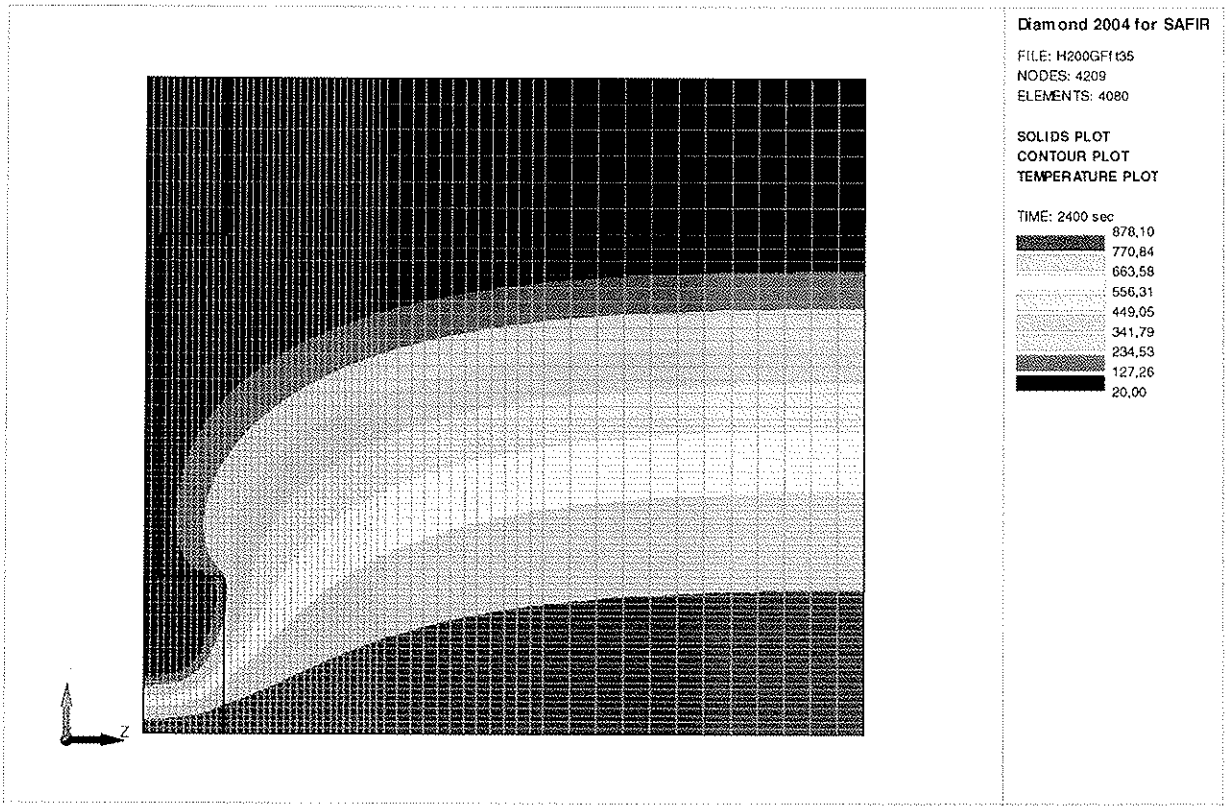

Figure 4 – Example of temperature field of assembly after 40 minutes, 5 minutes after failure of fire protective cladding

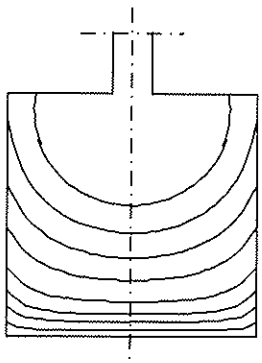

Figure 5 – Propagation of char front in fire-exposed flange

Since the reduction of strength and stiffness properties is different for tension and compression, CSTFire uses an iteration process, increasing the curvature of the member until the maximum moment resistance is reached. The element size used for the structural analysis was chosen as 1 mm × 1 mm. Since a coarser grid was used in the thermal analysis, intermediate temperature values were determined by linear interpolation.

The calculations were conducted assuming material properties that are representative for I-joists used in practice, using the stress-strain relationship shown in Figure 7. Since the values of tensile and compressive strength of solid timber given in design or product standards, e.g. EN 338 [4], are values of the whole cross-section and were determined on the assumption of a linear relationship between stress and strain until failure, the use of these values in a finite element analysis would not be correct [5]. Therefore, compressive strength values were determined using the data from Thunell [6] as shown in [5]. For the I-joists assumed here the compressive strength was f_c = 30 N/mm^2, while the tensile strength of the solid timber flanges was taken as f_t = 27 N/mm^2, that is the

same value as the bending strength of the I-joist. For I-joists with the tension flange on the fire exposed side, from the calculations below could be seen that there is no influence of compressive strength on the results as long as it is greater than the tensile strength.

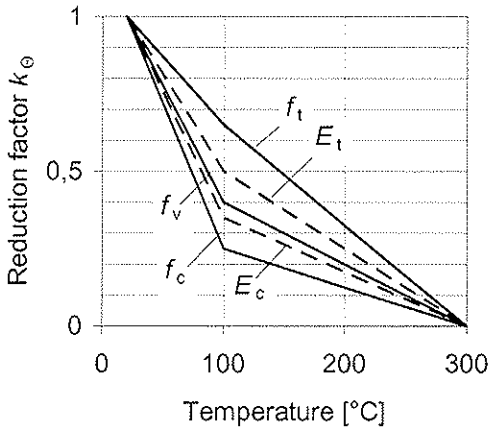

Figure 6 – Reduction factors for strength and stiffness properties according to EN 1995-1-2 [1]

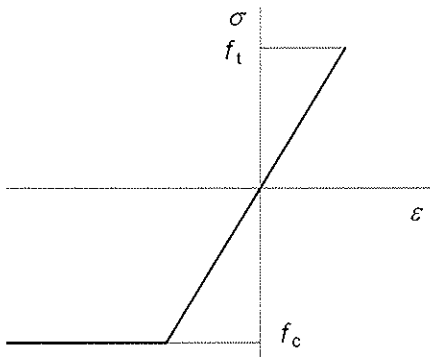

Figure 7 – Stress-strain relationships of wood

4 RESULTS AND MODELLING

4.1 Resistance

Calculations were made of an I-shaped section H200 with h = 200 mm, and $b_f = h_f$ = 48 mm, see Figure 3, with a fire exposed tension flange and various gypsum plasterboard claddings and failure times of the claddings. In all cases the cavities were completely filled with rock fibre insulation. In Figure 8 the results of the calculations are shown as relative resistances versus time for various charring scenarios.

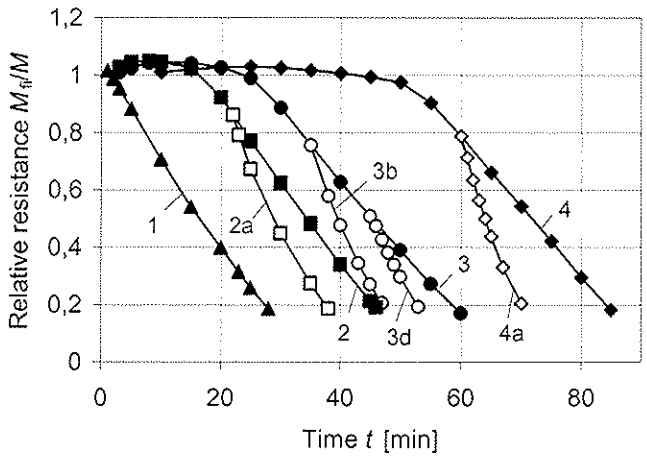

Figure 8 – Relative resistance of I-joist H200 with different gypsum plasterboard claddings and different failure scenarios assumed for claddings , see Table 1

Table 1 – Assemblies and failure scenarios of claddings

Case	**Cladding**	**Failure time of cladding** t_f min
1	none	
2	12,5 mm GA	none
2a	12,5 mm GA	21
3	15,4 mm GF	none
3a	15,4 mm GF	32
3b	15,4 mm GF	35
3c	15,4 mm GF	40
3d	15,4 mm GF	45
4	12,5 mm GA + 15,4 mm GF	none
4a	12,5 mm GA + 15,4 mm GF	60
4b	12,5 mm GA + 15,4 mm GF	70

Case 1 is shown as a reference scenario to demonstrate the effect of the claddings. For the effect of the flange width b and the depth of the joist h, see Figure 9 and Figure 10 (the effect of flange depth is not shown here). In all cases 1, 2, 3 and 4, the resistance increases initially above the values at ambient

temperature since the wood on the fire exposed tension side becomes ductile at elevated temperatures, permitting the redistribution of internal stresses utilizing that the compressive strength is larger than the tensile strength and/or the material is assumed as elastic-plastic in compression, see Figure 7.

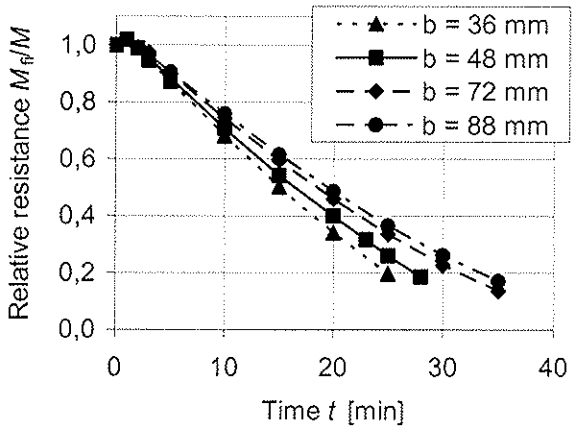

Figure 9 – Effect of flange width on relative resistance (h = 200 mm)

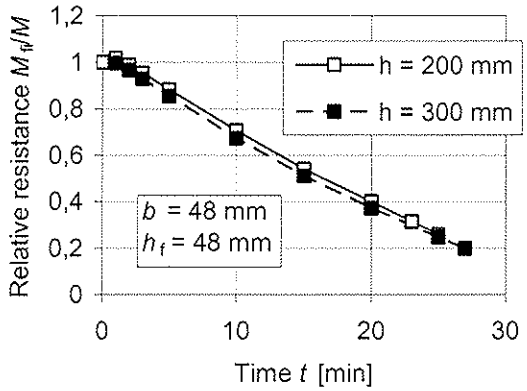

Figure 10 – Effect of depth on relative resistance (b = 48 mm)

4.2 Temperatures and charring

Relationships of charring depth in the middle of the flange versus time are shown in Figure 11. Most curves correspond to the cases shown in Figure 8. Again case 1 (initially unprotected by a cladding) serves as the reference scenario. In cases without failure of the cladding, after some time charring starts at time t_{ch}, initially at a lower rate than in case 1 (charring phase 1), but later on with an increasing rate, see also Figure 12. When the cladding fails at time t_f, an immediate increase of the charring takes place, however after a few minutes the charring rate has slowed down and stabilized (charring phase 3), but it is greater than the charring rate during charring phase 1. For simplification, for charring phases 1 and 2, the non-linear relationships were replaced by secant values for $d_{char,m}$ = 20 mm. When the charring depth has reached that value, the relative resistance is about 0,3. Thus, for charring phases 1 and 2, secant values give slightly conservative results at load levels that are common in practice and slightly non-conservative values for lower resistances.

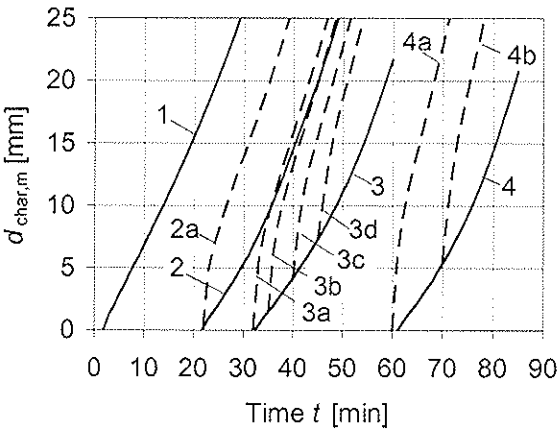

Figure 11 – Charring depth vs. time in the middle of the flange

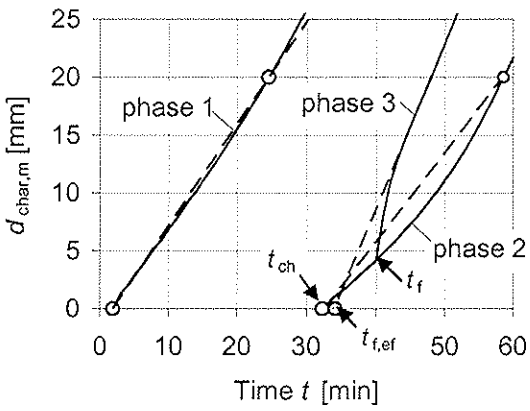

Figure 12 – Modelling of charring depth by linearization at different charring phases 1, 2 and 3

For charring phase 3 after failure of the cladding, the relationship of charring depth versus time was fitted to the final, almost linear parts of the curves; the intersection with the time axis gives the effective failure time $t_{f,ef}$ of the panel (see Figure 12), determined as 90 % of the actual failure time (see Figure 13). With $k_2 = \frac{\beta_{char,m,2}}{\beta_{char,m,1}}$ and $k_3 = \frac{\beta_{char,m,3}}{\beta_{char,m,1}}$, where the figures 1, 2 and 3 in the subscripts refer to the corresponding charring phases, k_2 was determined as approximately equal to 1 (not shown) and k_3 as shown in Figure 14.

The influence of the flange width on the charring depth in the middle of the flange, $\beta_{char,m}$, is shown in Figure 15 and 16 for charring phase 1. Again, the corresponding charring rates were determined as the secant values for $d_{char,m}$ = 20 mm. The ratio $k_{b,ch}$ shown in Figure 16, is defined as $k_{b,ch} = \frac{\beta_{char,m}}{\beta_{char,0}}$, where $\beta_{char,0}$ = 0,65 mm/min, that is the one-dimensional charring rate of a semi-infinite wood slab, given by EN 1995-1-2 [1].

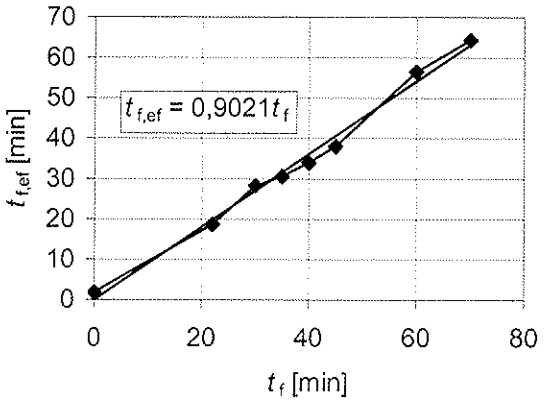

Figure 13 – Determination of effective failure time of cladding

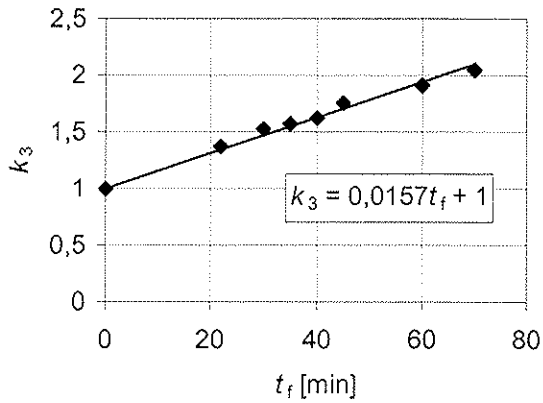

Figure 14 – Determination of k_3 for charring rate after failure of cladding (phase 3)

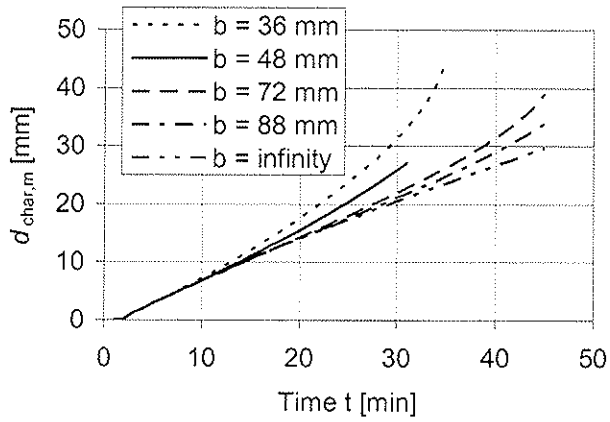

Figure 15 – Effect of flange width on charring depth in the middle of the flange (charring phase 1)

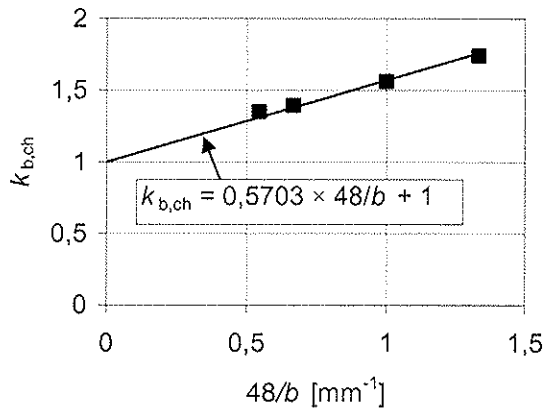

Figure 16 – Determination of flange width on flange width factor (and charring rate β_m)

4.3 Notional charring depth

Using the above mentioned software CSTFire, from the section modulus of the residual cross-section, for various time steps the notional charring depths $d_{char,n}$ were determined and compared with the

charring depth in the middle of the flange, $d_{char,m}$, denoting

$$k_n = \frac{d_{char,n}}{d_{char,m}} \tag{15}$$

Relationships of k_n versus $d_{char,m}$ are shown in Figure 17. For small charring depths $d_{char,m}$ the values of k_n are greater when the flange is protected by a cladding, since the residual cross-section of the flange is smaller, see Figure 18, however for resistances relevant in practice, the differences are small. As a reasonable approximation, $k_n = 1{,}4$ can be used in all cases. No influence of flange dimensions and the depth of the cross-section was found.

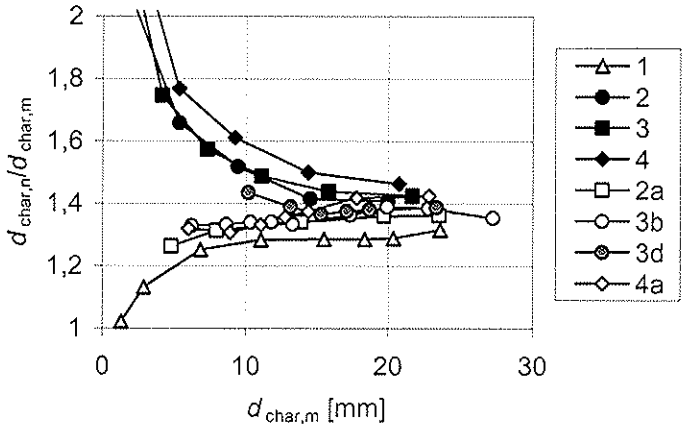

Figure 17 – Relationship of $k_n = d_{char,n}/d_{char,m}$ vs. $d_{char,m}$

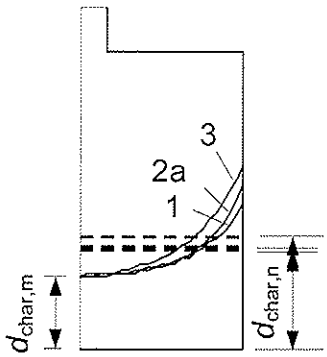

Figure 18 – Real and notional charring depths in flange for charring phases 1 (curve 1), 2 (curve 3) and 3 (curve 2a); for curve numbering see Table 1

4.4 Bending strength

Since the designer will always determine the notional charring depth, $d_{char,n}$, the modification factors for bending, $k_{mod,fm,fi}$, are presented as functions of $d_{char,n}$, see Figure 19, where the different curves refer to the cases of Table 1. Comparing curves 1, 2, 3 and 4, we can see that that there is a greater strength reduction during charring phase 2 than charring phase 1, the greatest strength reduction for claddings consisting of several layers (case 4). After failure of the cladding, a fast (within 3 minutes) recovery of strength takes place with modification factors even greater than for curve 1. An explanation of this effect is that the temperature gradient largely depends on the heating rate: at smaller heating rates as during charring phase 2 greater parts of the flange are affected by elevated temperature, and vice versa, at very large heating rates of the flange, the temperature affected zone is small, see Figure 20 showing temperature profiles below the char-line for $d_{char,m} = 12$ mm.

For I-joists used as floor joists, gypsum plasterboard claddings will normally fall off the floor due to thermal degradation of the cladding, or due to pull-out failure of fasteners. Therefore the most frequent scenario would be charring phase 3 (cases 2a, 3a, 3b or 4a, see Figure 8). For design, the following expression, obtained by fitting to curve 1, can be used:

$$k_{mod,fm,fi} = 1 - 0{,}016\, d_{char,n} \tag{16}$$

The effect of the flange width, see Figure 21, that, although being small, can be taken into account by extension of Equation (16) to

$$k_{mod,fm,fi} = 1 - 0{,}016\, d_{char,n}\, k_{b,fm} \tag{17}$$

with

$$k_{b,fm} = \frac{11{,}5}{b} + 0{,}76 \tag{18}$$

Correspondingly, the effect of the flange depth h_f and the cross-section depth h were taken into account by adding the coefficients $k_{hf,fm}$ and $k_{h,fm}$, see Equation (7).

An example of stresses and strength distributions along the symmetry axis of the cross-section is shown in Figure 22. It can be seen that tensile failure has occurred in a zone close to the char-line.

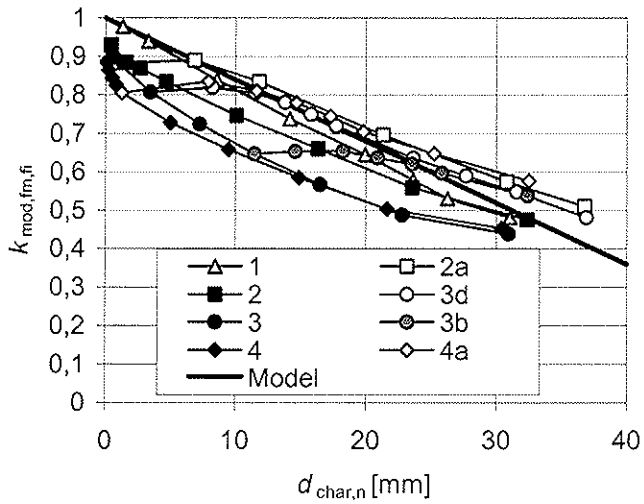

Figure 19 – Modification factors for bending strength vs. notional charring depth

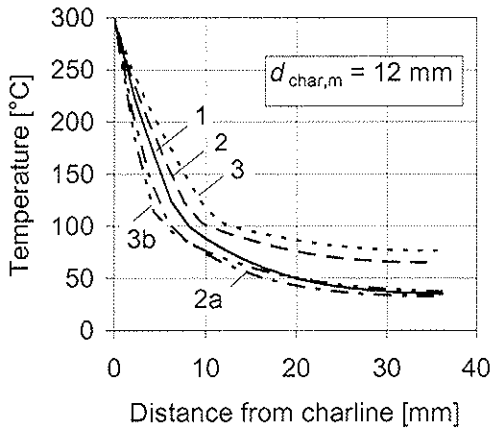

Figure 20 – Temperature profiles below char-line along axis of symmetry

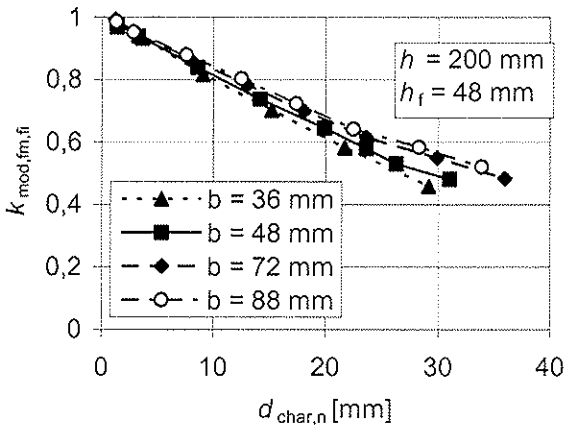

Figure 21 – Effect of flange width on modification factor for bending strength

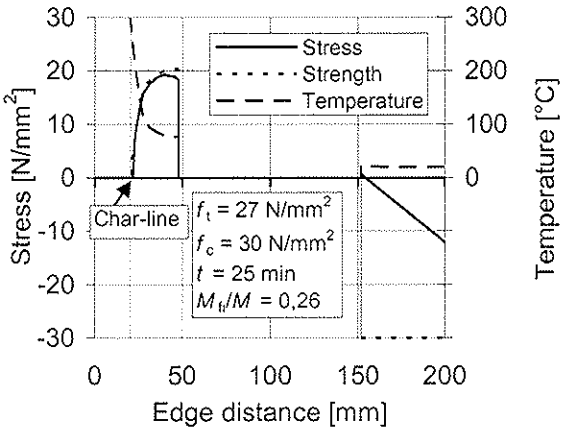

Figure 22 – Example of stress distribution along axis of symmetry of cross-section

4.5 Shear failure

A check of shear resistance close to supports should be done by determining shear strength at locations of the web with maximum temperature elevation. From Figure 4 can be seen that maximum web temperatures are reached at a distance of about 20 mm from the upper edge of the fire exposed flange (A in Figure 23). In Figure 24 temperature histories at A are shown. By normalizing the curves as functions of 48 k_b $d_{char,n}/h_f$, uniform curves were obtained for the same charring phase, see Figure 24. Assuming that the reduction of shear strength of wood-based panels is the same as for wood, a modification factor for shear strength was determined by multiplying these curves by the reduction factor for shear strength k_Θ given in Figure 6, see Figure 25. Considering phase 3 after failure of panels as the most relevant failure scenario, the curves can be fitted by a bi-linear expression shown in the chart. Similarly, temperature histories of B were determined for shear resistance verification of the joint between flange and web.

Web temperatures of 100°C (that is $k_{mod,fv,fi}$ = 0,4) are reached when the relative bending resistance is about 0,3 or smaller. Therefore, shear resistance is normally not decisive in the design of I-joists.

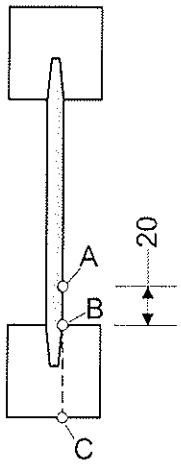

Figure 23 – Location of A and B for shear strength verification

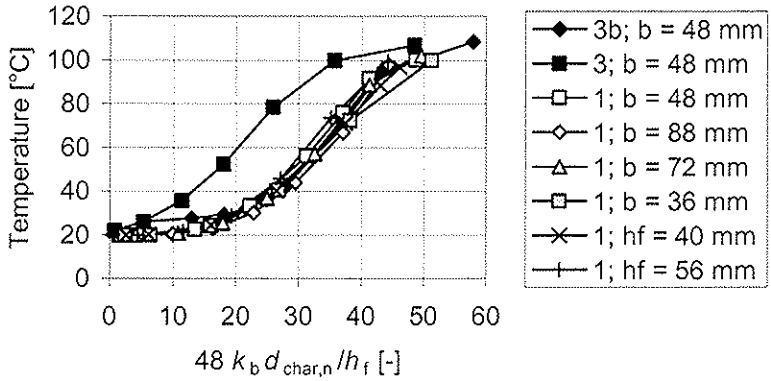

Figure 24 – Temperature histories at A 20 mm above lower flange

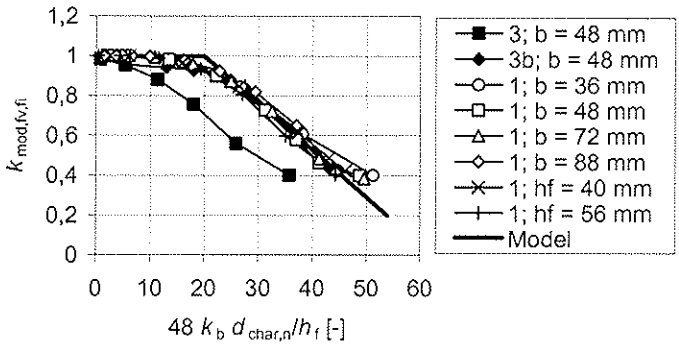

Figure 25 – Modification factor for shear strength vs. notional charring depth

5 Acknowledgement

The investigation described in this paper was funded by Nordic producers of wooden I-joists, the Nordic Innovation Centre (NICe) and the Swedish Agency for Innovation Systems (Vinnova).

6 References

[1] EN 1995-1-2:2004 Eurocode 5: Design of timber structures – Part 1-2: General – Structural fire design. European Standard. European Committee for Standardization, Brussels, 2004.

[2] Östman, B., König, J., Mikkola, E., Stenstad, V., Carlsson, J., and Karlsson, B., Brandsäkra trähus. Version 2. Trätek, Swedish Institute for Wood Technology Research, Publ. nr 0210034, Stockholm, 2002.

[3] König, J., Fire exposed simply supported wooden I-joists in floor assemblies. SP, Swedish National for Testing and Research Institute. In preparation.

[4] EN 338:2003, Structural timber – Strength classes. European Standard. European Committee for Standardization, Brussels, 2003.

[5] Källsner, B. and König, J., Thermal and mechanical properties of timber and some other materials used in light timber frame construction. Proceedings of CIB W18, Meeting 33, Delft, Lehrstuhl für Ingenieurbau, University Karlsruhe, Karlsruhe, Germany, 2000.

[6] Thunell, B., Hållfasthetsegenskaper hos svenskt furuvirke utan kvistar och defekter. Royal Swedish Institute for Engineering Research, Proceedings No. 161, Stockholm, 1941.

INTERNATIONAL COUNCIL FOR RESEARCH AND INNOVATION
IN BUILDING AND CONSTRUCTION

WORKING COMMISSION W18 - TIMBER STRUCTURES

A DESIGN MODEL FOR TIMBER SLABS MADE OF HOLLOW CORE ELEMENTS IN FIRE

A Frangi
M Fontana

Institute of Structural Engineering, ETH Zürich

SWITZERLAND

MEETING THIRTY-NINE
FLORENCE
ITALY
AUGUST 2006

Presented by A Frangi
I Smith and A Frangi discussed the issues of passive versus active resistance in major building.
R Marsh and A Frangi discussed the need of educating insurance company about the latest developments in fire engineering of timber buildings to recognize their performance so that novel timber construction would not be penalized.
A Jorissen questioned whether glass fibre should be banned based on the results. A Frangi replied that banning a particular material would not be the issue but understanding the performance of the material would be of interest.

A design model for timber slabs made of hollow core elements in fire

Andrea Frangi & Mario Fontana
Institute of Structural Engineering, ETH Zurich, 8093 Zurich, Switzerland

1 Introduction

Prefabricated timber assemblies made of hollow core elements are often used for slabs in residential and commercial buildings. Besides the advantage of element prefabrication and a high structural performance, the thermal and acoustic insulation of the timber assemblies can be significantly improved by insulating batts in the cavities and sound absorbers placed behind the perforated acoustic layer.

Timber is a combustible material and thus differs from most other common structural building materials. When sufficient heat is applied to wood, a process of thermal degradation (pyrolysis) takes place producing combustible gases, accompanied by a loss in mass. A charred layer is then formed on the fire-exposed surfaces and the char layer grows in thickness as the fire progresses, reducing the cross-sectional dimensions of the timber member. Because of its low thermal conductivity, the char layer protects the remaining unburned residual cross-section against heat. Because of the small size of the timber members of the hollow core elements, the fire action can lead to very irregular residual cross-sections with charring depths much greater than for heavy timber structures. For fire resistance calculations it is therefore of primary importance to know the development of the charring depth during the fire exposure.

A comprehensive research project on the fire behaviour of timber slabs made of hollow core elements has been recently performed at the ETH Zurich [6]. The objectives of the research project were to enlarge the experimental background of timber slabs in fire and to permit the development of a simplified design model for the fire resistance of timber slabs made of hollow core elements. In addition to a large number of small-scale fire tests, the fire behaviour of the timber slabs was experimental analysed with 2 large-scale fire tests. All fire tests were based on ISO-fire exposure and performed at the Swiss Federal Laboratories for Materials Testing and Research in Dubendorf. The test specimens were manufactured by the Swiss firm Lignatur, Waldstatt. Lignatur elements consist of hollow core elements made of spruce (picea abies) with a mean density of 450 kg/m^3. The strength properties of the timber elements correspond to the strength class C24 according to EN 338 [3]. Figure 1 shows a typical cross-section of Lignatur timber assemblies made of hollow core elements. The vertical members have a thickness of 33 mm.

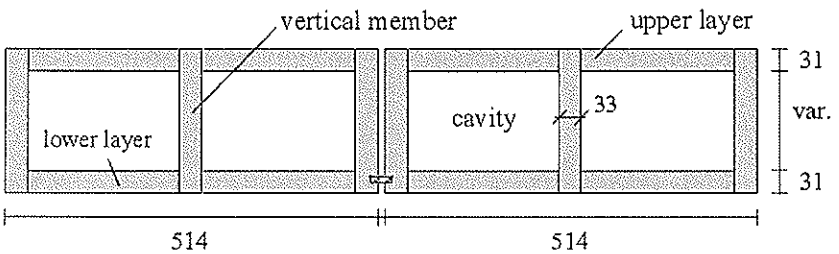

Figure 1 Typical timber slab made of hollow core elements

The paper describes the simplified design model for the calculation of the fire resistance of timber slabs made of hollow core elements. Particular attention is given to the analysis of different strategies used in order to improve the fire behaviour of the timber slabs in fire. The first part of the paper describes the simplified calculation model, in the second part the test results are compared to the simplified calculation model.

2 Timber slabs made of hollow core elements in fire

The fire behaviour of timber assemblies made of hollow core elements is characterised by two different charring phases, before and after the timber layer directly exposed to fire is completely charred. Before the fire-exposed timber layer is completely charred, the timber assembly is exposed to fire only on one side and a more or less homogenous regular one-dimensional charring similar to that of a heavy timber slab can be assumed, as confirmed by fire tests on timber assemblies performed within the framework of the research project (see figure 2).

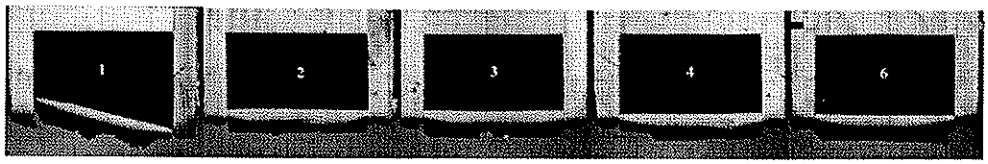

Figure 2 Residual cross-section of a timber slab after 70 minutes ISO-fire exposure; the fire-exposed timber layer was so designed that a fire penetration into the cavities was prevented

After the fire-exposed timber layer is completely charred and the char-layer begins falling off, the thin vertical timber members are exposed to fire on 3 sides, leading to very irregular residual cross-sections with charring depths much greater than for heavy timber structures where the char-layer performs as an effective protection of the remaining unburned residual cross-section (see figure 3).

Figure 3 Residual cross-section of a timber slab after 40 minutes ISO-fire exposure; the thin vertical timber members have been exposed to fire on 3 sides, leading to very irregular residual cross-sections

From a fire design point of view it is therefore desirable that the vertical timber members are not exposed to fire on 3 sides. This can be achieved in two different ways:

- the fire-exposed timber layer is so designed that a fire penetration into the cavities is prevented (the timber slab shown in figure 2 was designed according to this criteria).
- the cavities are filled with insulation material, so that after failure of the fire-exposed timber layer charring occurs mainly on the narrow side of the vertical members, while the wide sides are more or less protected by the insulation.

A series of small-scale fire tests looked at the behaviour of the hollow core elements filled different insulation materials. Figure 4 shows the residual cross-section of hollow core elements filled with rock fibre batts and glass fibre batts. It can be see that rock fibre batts were able to protect the wide sides of the vertical members from charring, so that one-dimensional charring can be assumed. On the other hand, cavity insulation made of glass fibre batts melted when exposed directly to fire temperatures, being incapable of protecting the wide sides of the vertical members.

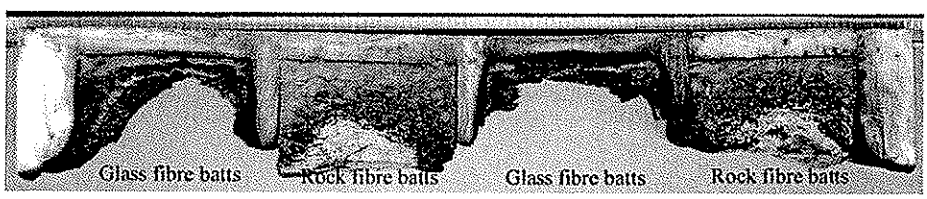

Figure 4 Residual cross-section of a timber slab after 60 minutes ISO-fire exposure with hollow core elements filled with different insulation materials

3 Simplified design model

In order to assess the fire performance of structural timber members exposed to fire the loss in cross-section due to charring as well as the reduction in strength and stiffness near the charred layer due to elevated temperature has to be considered. EN 1995-1-2 [2] gives two alternative simplified methods for the determination of cross-sectional properties for the calculation of load-bearing capacity of structural timber members for 3- and 4-sided fire exposure: the "Reduced cross-section method" and the "Reduced properties method". The "Reduced cross-section method" considers the strength and stiffness reduction near the charred layer by adding an additional depth to the charred layer. The "Reduced properties method" takes into account the influence of the temperature reducing the timber stiffness and strength properties of the residual cross-section by a factor $k_{mod,fi}$. The reduction of the timber strength and stiffness properties were derived using test results [8], which do not well reflect the physical behaviour of timber in fire [12]. Further this method was developed for structural members (beams, columns) exposed to fire on 3 or 4 sides [16] and should not be used for slabs exposed to fire only on one side [13]. For these reasons the "Reduced properties method" was not considered as appropriate to calculate the fire resistance of timber slabs made of hollow core elements.

The proposed simplified design model based on the reduced cross-section method according to EN 1995-1-2 and takes into account the two different charring phases as shown in figure 5 and generally discussed in the previous paragraph. For simplicity linear relationships between charring depth and time are assumed for each phase. Further it is assumed that the vertical timber members are not exposed to fire on 3 sides during the required fire resistance. Thus the fire-exposed timber layer is so designed that a fire penetration into the cavities is prevented or the cavities are filled with insulation material which remain intact up to 1000°C like rock fibre batts.

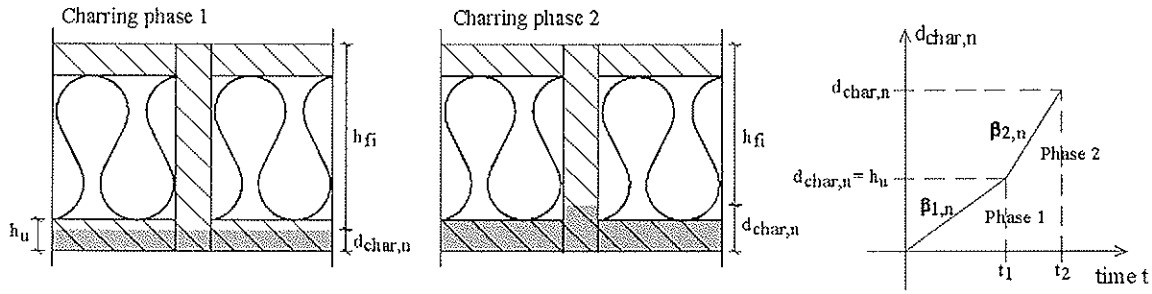

Figure 5 Charring model for the calculation of the residual cross-section of the hollow core elements

The first phase is defined as the time period, during which the charring depth has not yet reached the thickness of the fire-exposed timber layer ($d_{char,n} \leq h_u$). The notional charring rate $\beta_{1,n}$ describes the more or less one-dimensional charring of the timber slab during the first phase and takes into account the influence of joints and insulation material (see paragraph 4.1). The time t_1, when the charring depth has reached the thickness of the fire-exposed timber layer ($d_{char,n} = h_u$) can be calculated as following:

$$t_1 = \frac{h_u}{\beta_{1,n}} \tag{1}$$

The second phase is characterised by the charring of the vertical timber members after the charring depth has reached the thickness of the fire-exposed timber layer ($d_{char,n} \geq h_u$). The notional charring rate $\beta_{2,n}$ during this phase is mainly influenced by the thickness of the vertical members. Because of the small thickness of the vertical members of only 33 mm in the case of the Lignatur hollow core elements, a superposition of the heat flux from the sides and below occurs and increased charring has to be considered in comparison to one-dimensional charring (see paragraph 4.2).

For a required time t_{req} of fire resistance, the notional charring depth for the vertical members of the hollow core elements can be calculated as following:

$$d_{char,n} = \beta_{1,n} \cdot t_{req} \qquad \text{for } 0 \le t_{req} \le t_1 \qquad (2)$$

$$d_{char,n} = h_u + \beta_{2,n} \cdot (t_{req} - t_1) \qquad \text{for } t_{req} \ge t_1 \qquad (3)$$

The effective cross-section is calculated by reducing the initial cross-section by the effective charring depth d_{ef}, which is calculated as following:

$$d_{ef} = d_{char,n} + k_0 \cdot d_0 \qquad (4)$$

The additional depth $k_0 \cdot d_0$ takes into account the temperature-dependent reduction of strength and stiffness in the heat affected zones of the residual cross-section, permitting the designer to use for the effective cross-section the strength and stiffness properties at normal temperature. The modification factor is therefore taken as $k_{mod,fi} = 1.0$ for the effective cross section. The factor k_0 linearly increases from 0 to 1 with time during the first 20 minutes of fire exposure, as it takes normally about 20 minutes to get stabilized temperature profiles in the heat affected zones of the residual cross-section [13].

Table 1 Values of the notional charring rate $\beta_{1,n}$ and $\beta_{2,n}$ as well as the factor d_0 for the different charring phases

Charring phase	Notional charring rate	Factor d_0
First charring phase: $d_{char,n} \le h_u$	$\beta_{1,n} = 0.8$ mm/min	7 mm
Second charring phase: $d_{char,n} > h_u$	$\beta_{2,n} = 1.6$ mm/min	20 mm

Values of β_n and d_0 for the first and second charring phase are given in table 1 and discussed in detail in the following paragraph. The values $\beta_{2,n}$ and d_0 for the second charring phase have been determined for hollow core elements with 33 mm thick vertical members and a fire resistance up to 60 minutes. For thicker vertical members the values are conservative. Further the minimal thickness of the fire-exposed layer should be $h_u = 40$ mm for a fire resistance of 60 minutes. This restriction is necessary to respect the range for which the charring of the vertical members was validated with fire tests.

4 Discussion of the charring model

4.1 First charring phase

The fire tests showed that during the first phase the timber assembly is exposed to fire only on one side and a more or less homogenous regular one-dimensional charring similar to that of a heavy timber slab can be assumed. Table 2 shows measured average charring rates for the fire tests performed on timber slabs as well as the small-scale fire tests. Details of the fire tests can be found in [6].

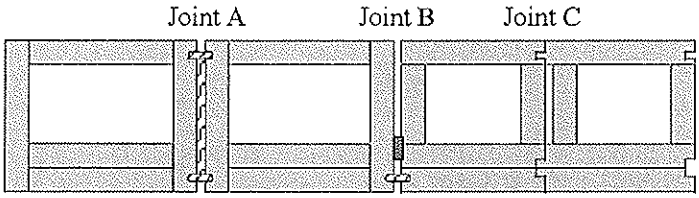

Figure 6 Different joints of the hollow core elements tested under ISO-fire exposure

For the hollow core elements without insulation the charring rate measured at the fire-exposed lower layer varied between 0.60 and 0.73 mm/min. At the vertical members, because of the influence of the joints, the measured charring rate was higher and varied between 0.70 and 0.80 mm/min. Details of the joints tested can be seen in figure 6. For the hollow core elements filled with insulation material the charring rate measured at the fire-

exposed lower layer as well as at the vertical members was higher than for the elements without insulation. The measured charring rate varied between 0.80 and 0.82 mm/min. A possible reason is that the insulating batts in the cavities significantly improve thermal performance, but they also cause the fire-exposed layer to heat more rapidly, possibly increasing the charring rate [1].

Table 2 Measured average charring rates in mm/min for the fire tests on timber slabs as well as the small-scale fire tests; details of the joints can be seen in figure 6

Position of measurement		Hollow core elements without insulation			With insulation	
		Small-scale test EI60	Test on slab REI60	Test on slab REI90	Small-scale test EI60-31	Small-scale test EI60-40
Fire-exposed lower layer		0.60	0.68	0.73	0.82	0.81
Vertical member	Joint type A	0.70	0.80	0.79	-	-
	Joint type B	0.77	0.76	0.70	-	-
	Joint type C	0.70	0.76	0.77	-	-
	No joint	-	-	-	0.81	0.80

The fire tests showed that for the calculation of the charring depth during the first phase a notional charring depth $\beta_{1,n} = 0.8$ mm/min can be assumed giving mostly safe results. The notional charring rate $\beta_{1,n}$ takes into account the influence of the insulation material in the cavities as well as the influence of the joints. For simplicity, a value $d_0 = 7$ mm is assumed for the calculation of the effective cross-section during the first charring phase. The values $\beta_{1,n} = 0.8$ mm/min and $d_0 = 7$ mm correspond to the values given in EN 1995-1-2 for solid timber and for the calculation of the effective cross-section based on the reduced cross-section for 3- and 4-sided fire exposure making the model easier for the designer.

4.2 Second charring phase

An extensive research [10, 11] has been recently conducted on the fire behaviour of light timber frame assemblies permitting the development of a design model which takes into account different charring stages due to the protection provided by the lining [12]. The design model has been included in EN 1995-1-2, Annex C [2]. The assemblies considered consisted of solid timber members (joist or studs), linings of gypsum plasterboards, and cavity insulation made of rock or glass fibre. In a series of fire tests without lining on the fire-exposed side, the fire behaviour of the timber members with rock fibre insulation was studied. The fire tests showed that rock fibre insulation was capable of protecting the wide sides of the timber members from fire, however due to two-dimensional heat flux in the insulation material close to the timber members, increased charring occurred in comparison to one-dimensional charring. This confirms the test results performed within the framework of this research project. In order to take into account this effect and convert the irregular residual cross-section caused by corner roundings into a notional rectangular cross-section, a cross-section factor k_s as well as a conversion factor k_n were derived from the fire tests. Values of k_s for different member thicknesses are given in Table 3.

Table 3 Cross-section factor k_s for different member thicknesses according to [12]

Member thickness in mm	33	38	45-48	60	90
Cross-section factor k_s	1.5	1.4	1.3	1.1	1.0

It can be seen that for wide members where the heat flux is mainly one-dimensional k_s is 1.0. The conversion factor k_n is a function of area, section modulus and moment of inertia. For simplicity these three values can be replaced conservatively by a single value of 1.5. Starting from one-dimensional charring β_0 the notional charring rate β_n can be finally calculated as following:

$$\beta_n = k_n \cdot k_s \cdot \beta_0 \qquad (5)$$

Thus for timber members with a thickness of 33 mm a charring rate of about 1.5 mm/min can be calculated according to equation 5 ($\beta_n = 1.5 \cdot 1.5 \cdot 0.65 \approx 1.5$ mm/min, where $\beta_0 = 0.65$ mm/min according to EN 1995-1-2 for softwood). It can be seen that this value is slightly smaller than the notional charring rate $\beta_{2,n}$ assumed for the calculation of the charring depth of the vertical members of the hollow core elements during the second phase.

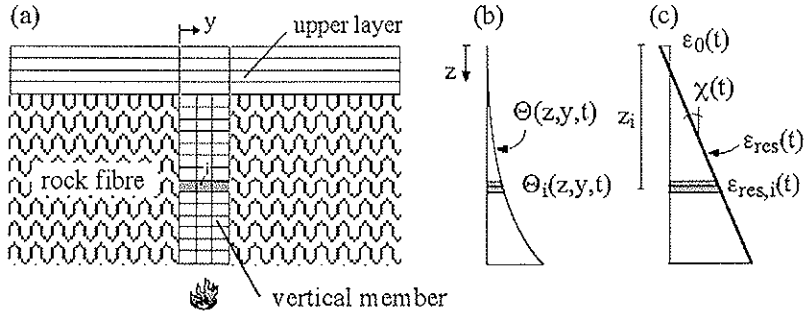

Figure 7 Calculation model: (a) cross-section composed of different layers, (b) temperature gradient of the cross-section, (c) resulting strains ε_{res}

Although the insulation material is able to protect the wide sides of the vertical members, the fire tests showed that because of the small size of the vertical members the temperatures measured in the vertical members are higher than in comparison to heavy timber cross-sections. For the calculation of the factor d_0, which takes into account the temperature-dependent reduction in strength and stiffness in the heat affected zones of the vertical members, an advanced calculation model as shown in figure 7 has been used. The cross-section of the timber assembly is divided into n finite elements with different stiffness and strength properties as a function of the measured temperature $\Theta_i(t)$. Unfortunately temperature-dependent properties of wood reported in the literature exhibit a large scatter and are partially in contradiction to each other [7, 8, 9, 14, 15, 17]. The main reason is that the test results are highly influenced by differences in the test methods used to collect those data [12].

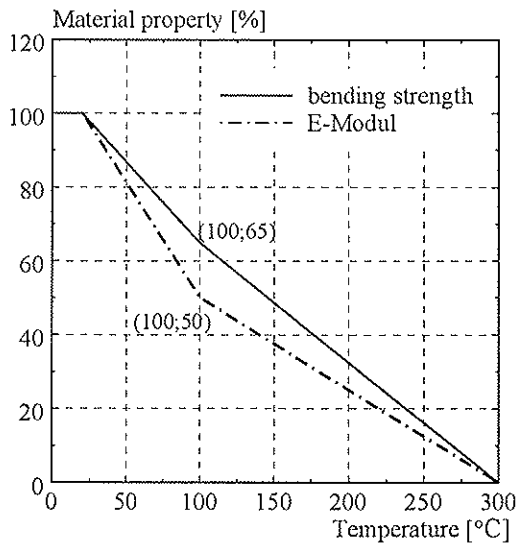

Temperature-dependent properties of wood given in EN 1995-1-2 were derived from many results of large-scale fire tests on loaded timber frame members in bending [11] and were considered as appropriate to model the structural behaviour of the timber assemblies made of hollow core elements in fire. However EN 1995-1-2 gives only the stiffness and strength reduction in tension and compression as a function of the temperature. As the fire-exposed side of the timber slabs are mostly subjected to tension, the stiffness and strength reduction in tension given in EN 1995-1-2 was assumed in the advanced calculation model for the E-modul and the bending strength (see figure 8).

Figure 8 Material properties of timber (modulus of elasticity and bending strength) as a function of the temperature used in the advanced calculation model

Temperatures, material properties, strains and stresses are assumed in the centre of gravity of each element and are constant with regard to thickness of the element. Further it is assumed that Bernoulli's hypothesis of plane sections is valid also in fire. The resulting time-dependent strains $\varepsilon_{res,i}(t)$ can be calculated taking into account the strain of the upper layer $\varepsilon_0(t)$ and the curvature $\chi(t)$ of the cross-section as following:

$$\varepsilon_{res,i}(t) = \varepsilon_0(t) + \chi(t) \cdot z_i \qquad (6)$$

The effect of thermal expansion of timber can lead to residual thermal stresses. However the residual thermal stresses are small in comparison to the stresses due to external mechanical loads and therefore can be neglected in the calculation of the fire resistance of structural timber members [4]. Under assumption of a linear elastic material behaviour and neglecting the influence of thermal expansion the resulting time-dependent stresses $\sigma_{res,i}(t)$ can be calculated as following:

$$\sigma_{res,i}(t) = E_i(\Theta_i) \cdot [\varepsilon_0(t) + \chi(t) \cdot z_i] \tag{7}$$

The strain of the upper layer $\varepsilon_0(t)$ and the curvature $\chi(t)$ of the cross-section can be found from static equilibrium requiring that the internal bending moment M_Θ and the internal axial force N_Θ are in equilibrium with the external mechanical loads. For a simply supported member which is subjected only to external bending moment M (external axial force N=0) the conditions of equilibrium can be written as following:

$$N_\Theta(t) = \sum_{i=1}^{n} \sigma_{res,i}(t) \cdot A_i = 0 \qquad M_\Theta(t) = \sum_{i=1}^{n} \sigma_{res,i}(t) \cdot A_i \cdot z_i = M \tag{8}$$

The solutions of the above equation system are:

$$\varepsilon_0(t) = \frac{-\left(\sum EA_i \cdot z_i\right) \cdot M}{\left(\sum EA_i\right) \cdot \left(\sum EA_i \cdot z_i^2\right) - \left(\sum EA_i \cdot z_i\right)^2} \tag{9}$$

$$\chi(t) = \frac{\left(\sum EA_i\right) \cdot M}{\left(\sum EA_i\right) \cdot \left(\sum EA_i \cdot z_i^2\right) - \left(\sum EA_i \cdot z_i\right)^2} \tag{10}$$

The bending resistance M_R of the cross-section can be finally calculated using following failure criteria:

$$\sigma_{res,i}(M_R) = f_{d,fi,i} \tag{11}$$

where $f_{d,fi,i}$ is the bending strength taking into account the strength reduction due to the influence of the temperature.

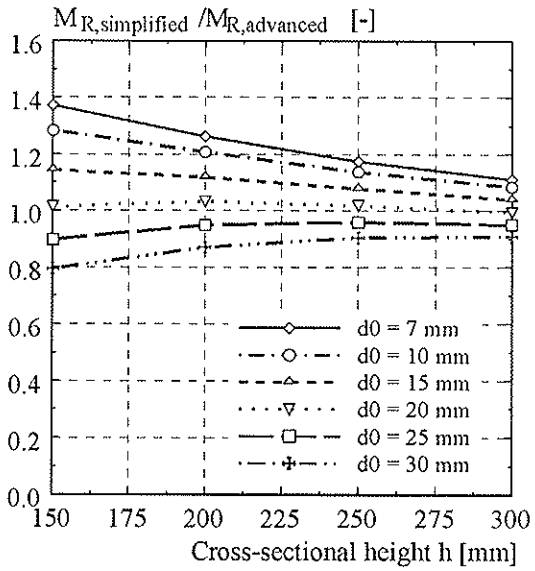

The advanced calculation model was used in order to calculate the bending resistance of timber slabs made of hollow core elements with different heights varying between 150 and 300 mm subjected to 60 minutes ISO-fire. For the calculation it was assumed that the fire-exposed timber layer has a thickness of 40 mm.
Figure 9 compares the results of the advanced calculation model to the simplified calculation model based on the reduced cross-section method. In the figure the ratio $M_{R,simplified}/M_{R,advanced}$ as a function of different assumptions for the factor d_0 is given.

Figure 9 Comparison of the fire resistance after 60 minutes fire exposure as a function of the height of the cross-section according to the advanced calculation model and the simplified design model assuming different values of d_0

It can be seen that under the assumption of a factor of d_0 = 7 mm the simplified calculation model leads to bending resistances which are 20 up to 40% higher than in comparison to the advanced model. Thus the simplified calculation model leads in this case to unsafe

results. The main reason is that the vertical members because of the small size are more affected by the heat in comparison to heavy timber sections. On the other hand under assumption of a factor of d_0 = 20 mm a good agreement between the advanced and the simplified calculation model is observed. Thus it is proposed to use d_0 = 20 mm for the simplified calculation model.

5 Comparison to fire tests

The small-scale fire tests were conducted with unloaded specimens and looked at the charring behaviour of the hollow core elements using different insulation materials and type of joints. Another series of small-scale fire tests studied the influence of acoustic perforations on the charring behaviour of the hollow core elements. The charring rate during the first phase was derived from the test results as a function of the size and position of the acoustic perforations [5]. Details of these fire tests can be found in [6]. Figure 10 left compares the measured charring depths with the charring depths calculated according to the simplified calculation model. For the calculation of the charring depth the values given in table 1 were used. A good agreement between simplified calculation model and fire tests can be observed. The average ratio between $d_{char,model}/d_{char,test}$ is 1.08, i.e. the simplified calculation model leads to safe results.

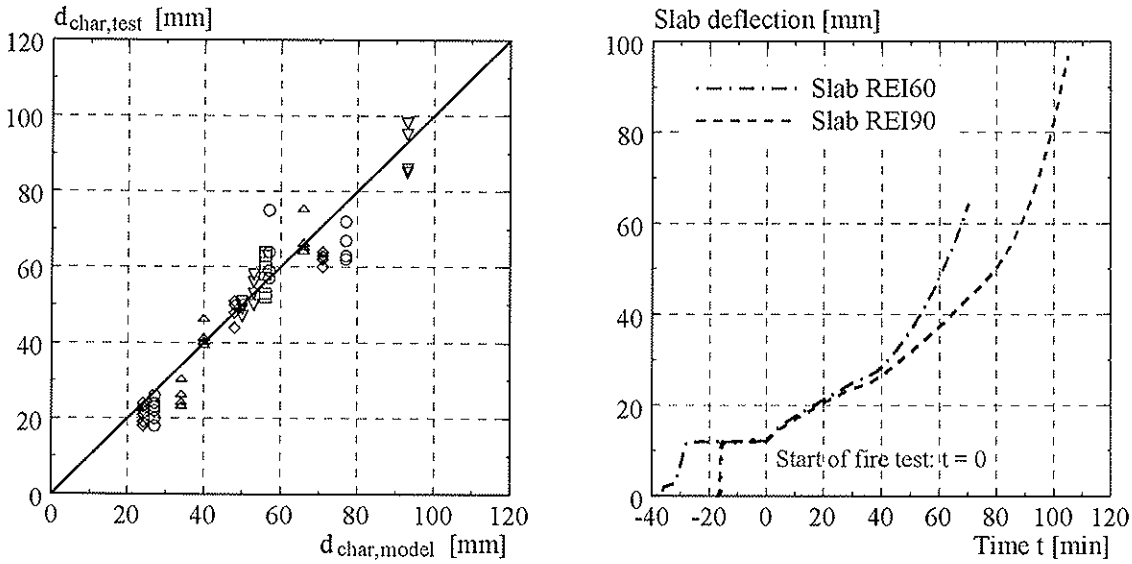

Figure 10 Comparison between measured and calculated charring depths according the simplified design method (left) and measured deflections during the large-scale fire tests on the slabs REI60 and REI 90 (right)

The global behaviour of the timber slabs made of hollow core elements was analysed with two fire tests on slabs performed in EMPA's horizontal furnace (3.0 x 4.85 m). The timber slabs were made of 0.2 m high hollow elements of spruce with a mean density of 450 kg/m^3 and moisture content of 10±2%. Two different slabs with three different joints between the timber elements were designed for a fire resistance of 60 and 90 minutes. The slabs called in the following REI60 and REI90 were designed so that a fire penetration into the cavities was prevented. The fire-exposed timber layer had a thickness of 64 mm for the slab REI60 and 97 mm for the slab REI90. The load level during the fire tests was set in such a way that the maximum bending moment corresponded to that in a slab of about 7.10 m span, with a permanent load of 1.5 kN/m^2 and a reduced accompanying live load of 1.5 kN/m^2. In the fire tests the temperatures in selected locations, the vertical deflections and the horizontal deformations were measured.

The fire tests showed a fire resistance of more than 60 minutes and 90 minutes respectively. No relevant smoke or flame penetration was observed through the three different joints between the timber elements during the fire tests. For security reasons the

tests were not conducted until failure of the slab. The fire test on the slab REI60 was stopped after 70 minutes. After the test, the slab was loaded until failure which occurred under 1.08 times the load applied during the fire test. For this slab a fire resistance of 77 minutes was estimated based on the increase of the deformations measured during the fire test (see figure 10 rigth). The fire test on the slab REI90 was stopped after 105 minutes. For this slab a fire resistance of 107 minutes was estimated based on the increase of the deformations measured during the fire test (see figure 10 rigth). The fire resistance of the slabs was calculated using the simplified calculation model based on the reduced cross-section method (see table 4). It can be seen that the simplified calculation model was able to predict the fire resistance quite well.

Table 4 Comparison between test results and simplified calculation model

Fire test	t_{test} [min]	$t_{R,test}$ [min]	$t_{R,modell}$ [min]	$t_{R,model} / t_{R,test}$ [-]
slab REI60	70	77	85	1.10
slab REI90	105	107	109	1.02

6 Summary and conclusions

The paper presents a simplified design method for the calculation of the fire resistance of timber slabs made of hollow core elements. The simplified design method is based on the reduced cross-section method according to EN 1995-1-2 and takes into account two different charring phases, before and after the fire-exposed layer is completely charred. For simplicity linear relationships between charring depth and time are assumed for each phase. Further it is assumed that the vertical timber members are not exposed to fire on 3 sides. This can be achieved in two different ways:

- the fire-exposed timber layer is so designed that a fire penetration into the cavities is prevented
- the cavities are filled with insulation material, so that after failure of the fire-exposed timber layer charring occurs mainly on the narrow side of the vertical members, while the wide sides are more or less protected by the insulation.

As cavity insulation, rock fibre batts which remain intact up to 1000°C and in place after failure of the fire-exposed timber layer can be used. On the other hand, cavity insulation made of glass fibre batts is not recommended because it melts when exposed directly to fire temperatures, being incapable of protecting the wide sides of the vertical member.

Before the fire-exposed timber layer is completely charred, the timber assembly is exposed to fire only on one side and a more or less homogenous regular one-dimensional charring similar to that of a heavy timber slab can be assumed, as confirmed by fire tests on timber assemblies performed within the framework of the research project. The charring rate measured during the fire tests at the fire-exposed lower layer as well at the vertical members varied between 0.60 and 0.82 mm/min. For the calculation of the charring depth during the first phase a notional charring depth $\beta_{1,n}$ = 0.8 mm/min can be assumed giving safe results. This value corresponds to the notional charring rate given in EN 1995-1-2 for solid timber.

Because of the small thickness of the vertical members of the hollow core elements, a superposition of the heat flux from the sides and below occurs during the second phase and increased charring has to be considered in comparison to one-dimensional charring. Thus the notional charring rate $\beta_{2,n}$ during this phase is mainly influenced by the thickness of the vertical members. For the hollow core elements tested with a thickness of the vertical members of 33 mm a notional charring rate $\beta_{2,n}$ = 1.6 mm/min. can be assumed. This is confirmed by fire tests conducted within the framework of this research project and other fire tests [11]. Although the insulation material is able to protect the wide sides of the vertical members, the fire tests showed that because of the small size of the vertical members the temperatures measured in the vertical members are higher than in comparison to heavy timber cross-sections. For the calculation of the factor d_0, which takes into

account the temperature-dependent reduction in strength and stiffness in the heat affected zones of the vertical members, an advanced calculation model has been used. The cross-section of the timber assembly has been divided into n finite elements with different stiffness and strength properties as a function of the measured temperature $\Theta_i(t)$. The reduction of the E-modul and bending strength has been assumed according to EN 1995-1-2. Under assumption of a factor d_0 = 20 mm a good agreement between the advanced and the simplified calculation model was observed.

The global behaviour of the timber slabs made of hollow core elements was analysed with two fire tests on slabs performed in EMPA's horizontal furnace (3.0 x 4.85 m). The fire tests showed a fire resistance of more than 60 minutes and 90 minutes respectively. When verifying the simplified design method, a good agreement between fire test results and the simplified design method was observed.

7 References

[1] Buchanan H., *Fire performance of timber construction*, Progress in Structural Engineering and Materials, Vol. 2, 2000.

[2] EN 1995-1-2 (Eurocode 5), *Design of timber structures, Part 1-2 General rules-Structural fire design*, CEN, Brussel, 2004.

[3] EN 338, *Structural timber – Strength classes*, CEN, Brussel, April 2003.

[4] Frangi A., Fontana M., *Thermal expansion of wood members under ISO-fire*, 7th International Symposium on Fire Safety Science (IAFSS), Worcester Polytechnic Institute, Massachusetts, USA, June 6-21, 2002.

[5] Frangi A., Fontana M., Schleifer V., *Fire behaviour of timber surfaces with perforations*, Fire and Materials, Vol. 29, 2005.

[6] Frangi A., Fontana M., *Brandverhalten von Hohlkastendecken aus Holz (Fire performance of hollow core slabs made of wood)*, Bauphysik, Vol. 27, 2005.

[7] Gerhards CC., *Effect of moisture content and temperature on the mechanical properties of wood: An analysis of immediate effects*, Wood and Fiber, Vol. 14, 1982.

[8] Glos P., Henrici D., *Festigkeit von Bauholz bei hohen Temperaturen*, Abschlussbericht 87505, Institut für Holzforschung der Universität München, 1990.

[9] Knudson RM., Schniewind AP., *Performance of structural wood members exposed to fire*, Forest Products Journal, Vol. 25, 1975.

[10] König J., *Fire resistance of timber joists and load bearing wall frames*, Swedish Institute for Wood Technology Research, Trätek Rapport I 9412071, Stockholm, 1995.

[11] König J., Norén J., Olesen FB., Hansen FT., *Timber frame assemblies exposed to standard and parametric fires, Part 1: fire tests*, Swedish Institute for Wood Technology Research, Trätek Rapport I 9702015, Stockholm, 1997.

[12] König J., Walleij L., *Timber frame assemblies exposed to standard and parametric fires, Part 2: a design model for standard fire exposure*, Swedish Institute for Wood Technology Research, Trätek Rapport I 0001001, Stockholm, 2000.

[13] König, J., *Structural fire design according to Eurocode 5 - Design rules and their background*, Fire and Materials, Vol. 29, 2005.

[14] Schaffer EL., *Elevated Temperature Effect on the Longitudinal Mechanical Properties of Wood*, Ph.D. Thesis, University of Wisconsin, Madison, WI, 1971.

[15] Van Zeeland I.M., Salinas J.J., Mehaffey J.R., *Compressive strength of lumber at high temperatures*, Fire and Materials, Vol. 29, 2005.

[16] Wesche J., Klingsch W., Tavakkol-Khah M., Kersten-Bradley M., *Temperaturentwicklung in brandbeanspruchten Holzquerschnitten*, Schlussbericht, Forschungsvorhaben F-90/1 der Deutschen Gesellschaft für Holzforschung, München, November 1993.

[17] Young SA., Clancy P., *Compression mechanical properties of wood at temperatures simulating fire conditions*, Fire and Materials, Vol. 25, 2001.

INTERNATIONAL COUNCIL FOR RESEARCH AND INNOVATION
IN BUILDING AND CONSTRUCTION

WORKING COMMISSION W18 - TIMBER STRUCTURES

POSSIBLE CANADIAN / ISO APPROACH TO DERIVING DESIGN VALUES FROM TEST DATA

I Smith

A Asiz

M Snow

Ying Hei Chui

Faculty of Forestry and Environmental Management

University of New Brunswick, Fredericton, NB

CANADA

MEETING THIRTY-NINE

FLORENCE

ITALY

AUGUST 2006

Presented by A Asiz

H Larsen stated when you compared test results to theory one should use mean values. However design should not be based on mean values as coefficient of variation would come into play. I Smith answered that as long as results would be similar, it would only depend on how the format was put together. H Larsen disagreed and cited the example of structural timber having high COV compared to glulam. With characteristic values and phi approach the differences would be considered appropriately. Also his supporting document for European design code allowed mean value based test results with large penalty. Alternative approach of polled data to combine various data sets could also be used. Further discussion on the subject took place.

JW van de Kuilen stated that ISO standard on general principle of reliability assessment already existed. What the difference would be between the proposed approach and ISO standard. A Asiz stated 4 ranges of failure modes have been considered in this work.

A Ceccotti suggested that different definition of ductility to be checked. J Köhler and A Asiz discussed the approach of using the approximate formula originated in the 1970 compared to more accurate method. A Asiz stated that this approach would make it easier for engineers to use.

F Lam commented that this simplified approach has limitations because the phi formula would be based on the assumption of lognormal distributions and we knew loads followed extreme value distribution.

Possible Canadian / ISO Approach to Deriving Design Values From Test Data

Ian Smith, Andi Asiz, Monica Snow and Ying Hei Chui

Faculty of Forestry and Environmental Management,
University of New Brunswick, Fredericton, NB, Canada

ABSTRACT

This paper proposes principles for a standard practice for deriving factored design resistances of structural components or subsystems directly from test data. This applies to, for example, members, connections, trusses and shear-walls. The approach is intended as a fully consistent alternative to practices embodied in existing design codes. It is assumed that parent design standards (national loading and timber design codes) are based on Load and Resistance Factor Design (LRFD) concepts. The likely level of consistency between design solutions based on testing evidence and those based on existing LRFD codes is evaluated based on examples applicable to Canadian wood products.

1. Introduction

The available range of proprietary products and subsystems, and special design situations involving structural use of wood products, has grown rapidly in recent years. Proprietary products are evaluated based on test data with the interpretations of evidence performed by product assessments organizations that are, in North America and elsewhere, independent of design code bodies. Assessment organizations produce documents containing suggested engineering design properties or equivalent information like limiting spans. The suggested properties only become validated within any regulatory jurisdiction if the appropriate building control authority accepts them. The purpose of this paper is to propose principles for a standardized approach that can be applied by product assessment organizations in Canada or elsewhere to derive engineering design values from test data. What is proposed is also thought suitable as guidance to engineers on how to make test based assessments of capacities of special components or subsystems. Here special means cases that do not lend themselves to 'traditional design' or are outside the scope of written design standards (e.g. use of components with non-standard dimensions).

Ideas presented were initially conceived as a parallel alternative way of designing connections that fall outside the scope of the design code Canadian Standard 086-01 "Engineering design in wood" [1]. However, it became apparent that the principles could be applied generally to other components and subsystems, and that they may be a suitable basis for creation of an international standard under the International Standards Organization (ISO) system. Hence the broadened scope herein. Starting with connections was fortuitous in the sense that practices for establishing their design capacities have historically been inconsistent and background reasoning often unknown. Thus there is no well framed or strongly conditioned thinking about what constitutes the best approach, as exists for example in the case of sawn lumber. This made it possible to start, so to speak, with an essentially blank piece of paper.

This paper builds on past discussion in CIB-W18 Paper *38-102-1* "New generation of timber

design practices and code provisions linking system and connection design" by Asiz and Smith [2]. It also dovetails with the parallel 2006 meeting papers: "Generalised Canadian approach for design of connections with dowel fasteners" by Quenneville et al [3], and "Overview of a new approach to handling system effects in timber structures" by Smith et al [4]. The hope is that simultaneous discussion of these topics within CIB-W18, ISO/TC 165 Committee "Timber Engineering" and the CSA/TC 086 "Engineering Design in Wood" will facilitate progress and harmonization of practices. Focus below is, as a first step, on principles without attempt to specify all details or to create language suitable for a written standard.

2. Scope and Premises

The scope is assessment of the behaviour of structural components and subsystems or special design situations through test evidence. Practices are intended to be adopted by product assessment agencies and be as far as is appropriate consistent with practices used to derive design properties specified in LRFD codes. It is recognized that test based product assessments will often be undertaken using quite limited amounts of test data, as compared to what underpins properties specified in design codes for some wood products (e.g. small dimension lumber).

Practices described here are based on the following premises:

- Test based assessment will not be used as a means of circumventing applicable design codes.
- Parent design standards (national loading and timber design codes) are based on LRFD concepts.
- Factored design resistances need to reflect target reliability indexes that relate to the nature of the expected failure mechanism(s).
- There is no ambiguity regarding the structural function of any component or subsystem being evaluated. Therefore all forces to be resisted can be defined.
- Interpolation is permissible in order to assign capacities to components or subsystems that are similar to and intermediate between those assessed based on test evidence. The term similar implies that the wood products employed, material conditioning, boundary conditions, load components, loading regimes and workmanship are directly comparable.

3. Sampling and Number of Replicates

3.1 Sampling

Specimens should be realistic and replicate expected field situations as closely as possible. Test materials and workmanship, and installation practices in the case of subsystems, must be representative of production situations.

3.2 Number of replicates

The number of test replicates should be sufficient for estimation of the average value and variance for each parameter used to characterize the structural response of any component or subsystem. The minimum acceptable number of replicates is six, and the Data Confidence Factor (C_f) defined in Section 7 accounts for the possibility of unrepresentative sampling. It is intended that product assessment organizations or engineer be allowed to balance tradeoffs concerning relationships between the number of test replications, the level of variability in parameters that characterize the studied structural response, and the level of precision desired.

4. Test Practices and Loading Regimes

Considerations to be taken into account will include, but may not be limited to:

- material conditioning prior to and after fabrication,

- long-term heating effects,
- boundary conditions,
- loading regime (e.g. time to failure, loading waveform and frequency), and
- workmanship.

An engineer should be responsible for design of the loading regimes best suited to procuring data from which to estimate properties defining the resistance of a component or subsystem to various applicable effects of loads. The necessary combination of loading regimes and other factors will vary depending on the type of component or subsystem and the intended field application. For components and subsystems manufactured using only traditional wood products (e.g. sawn lumber, plywood) assuming traditionally accepted methods for converting from the response under standardized static load tests of short duration to field situations can reasonably be considered reliable [e.g. 5]. Ditto if only well understood engineered wood products like Laminated-Veneer-Lumber (LVL) are used. In other circumstances it will be essential to establish data via a test matrix that properly addresses all of the issues itemised above, and possibly others. Professional judgement will apply.

As a minimum, tests should be carried out using a regime under which monotonic load is increased steadily at a rate that causes failure in about 0.1 hours, i.e. static load tests. If only this minimum requirement is met then it must be assumed that any static or cyclic fatigue effects on strength will depend on the wood product components. In such circumstances the Service Factor (k_S), as defined in Section 6.1, must take the most conservative possible values.

For situations where a component or subsystem is intended to resist the effects of seismic or extreme wind forces it is advisable to incorporate cyclic loading tests into the testing schedule, based on ISO or similar methods. This will permit determination of a degraded load-deformation envelope as the basis for determining strength properties. For situations where sustained loads are expected to be of long duration it is highly advisable to conduct sustained load tests. A sufficient range of durations is one that permits establishment of a Load Level (LL) versus Time to Failure (T_f) relationship that will not be extrapolated by more than one order of magnitude based on a plot of LL versus $\log(T_f)$. Collected data should extend to at least three decades in T_f.

5. Interpretation of Test Data

5.1 General philosophical principle

Because test data may be quite limited it is only realistic to expect to always accurately determine average design values for ultimate strength, or other properties that relate to assessment of a component or subsystem. The estimated variance associated with resistance properties may not be accurately characterized from available test data. Therefore it is proposed that average, rather than low exclusion level, characteristic test properties are the most appropriate base from which to derived design values. The determined Factored Design Resistance (ϕR) according to equation (3), Section 6.1, can be made technically equivalent irrespective of whether an average or low exclusion level characteristic value is used. As has been demonstrated previously by Smith [6], randomness in low exclusion level characteristic values leads to noisy and inconsistent estimates of Resistance Factors (ϕ values) and Modification Factors (k_i values). The result can be spuriously inconsistent design practices. The reason is easily demonstrated, in that, in reliability calibrations the process finds the value of ϕR that balances the equality in a prescribed design equation under certain conditions. Then the result is decomposed into ϕ, the Standardized Specified Resistance (R_S) and k_i values. Thus any uncertainty in variance of resistance introduces a first level of uncertainty into ϕR, and at a

second level inconsistency into separated components of that product. R_S is determined independently from analysis of test data, and that step causes second level noise in ϕ and k_i values during any decomposition process. The second level noise is minimized and estimates of ϕ and k_i are most robust if average characteristic resistance is used as the basis of establishing R_S. As can be further elucidated, for systems where effects of design variables are coupled it is also most consistent to base calibration practices on R_S that represents the average response. This is especially important when background data is from tests where the sample size is limited, which is itself the cause of noise in estimates of variance in resistance and therefore instability in low exclusion level estimates of resistance.

There may be concern that the proposal to characterize resistance at the average level differs from past practice [7] where 5th-percentile resistance has been the basis for decomposing ϕR into component parts. The authors believe that such concern is unfounded because, as already indicated, the results can be technically equivalent. The primary difference in calibrations done as proposed here and those in past reliability studies is that what is proposed here results in the relationship:

$$\frac{\phi_{R\_0.05}}{\phi_{R\_av.}} = \frac{R_{av.}}{R_{0.05}} \qquad \text{..... (1)}$$

where: $\phi_{R\_0.05}$ = resistance factor based on $R_{0.05}$, $\phi_{R\_av.}$ = resistance factor based on $R_{av.}$, $R_{0.05}$ = estimated 5th-percentile resistance under standard conditions, and R_{av} = estimated average resistance under standard conditions.

In Canada past approaches have introduced three additional manipulations into structural reliability calibration processes, as applied to design of isolated members [7]. First, the R_S values do not relate directly to strengths observed under standardized test conditions, but are taken as 0.8 x short-term static strength. This adjustment has the purpose of converting observed strengths to those applicable under Standard Term Loads on roofs (dead plus snow loads) and floors (dead plus occupancy loads). This allows for expected damage due to static fatigue, which in timber engineering circles is better known as 'the duration of loading effect on strength'. Second, there was smoothing across different sized products to allow for so-called size effects on apparent strengths of components, e.g. effect of member depth on apparent bending strength of sawn lumber. This was done for compact representation of data with design properties only being given for a reference member size, together with an adjustment rule for transforming properties so they apply to components of other sizes. This involved smoothing across reliability calculations in which component size was the variable of interest. Third, although nominally ϕ was consistently based on being used in conjunction with $R_{0.05}$, it was in fact given a constant value, with R_S rather than ϕ becoming the calibrated parameter. In North America this practice is termed Reliability Normalization of R_S values. The result is that the relationship in equation (1) is replaced by:

$$\frac{\phi_{Code}}{\phi_{R\_av.}} = \frac{R_{av.}}{R_S} = \frac{R_{av.}}{0.8 R_{0.05} \Psi} \qquad \text{..... (2)}$$

where: ϕ_{Code} = code specified resistance factor (typically 0.9), and Ψ = reliability normalization factor. The Ψ is a function of variance in the resistance and the target reliability index. Thus, neither ϕ nor R_S have been determined directly from basic concepts.

Despite what have been past practices, it is the view of the authors that for transparency it is important that R_S values be properties that are directly reproducible from test data. Preferably they should be free from adjustments from test (short-term static strength) values to resistances

applicable to standard term load conditions that are not reproducible in tests because the associated times to failure under sustained loads are not explicitly defined.

It is important when determining design properties not to confuse the precision of calculation methods with correctness of output. For this reason although it is accepted that structural reliability concepts are the appropriate basis for determining ϕ, this does not necessarily imply that the reliability analysis methods need be complex and numerically based. What is critical, as with standardized test methods, is that processes be repeatable and consistent. Calibration of the ratio of the Factored Effects of Loads to the Factored Resistance (ratio of right to left side of the design equation - equation (3)) is the main mechanism for controlling safety levels. Choice of a suitable Safety Index (β) is the most important decision, Section 7.

5.2 Classification of failure modes

It is proposed that failure modes be classified according to the observed level of apparent ductility under static load conditions, determined based on the Ductility Ratio (D) calculated according to Figure 1. Table 1 details the proposed categorization of D. Because failure mechanisms and the extent of ductility may be mixed between test replications, it is suggested that when more than 25 percent of D values imply more brittleness than $D_{av.}$ does, then the assigned classification should be 'reduced' by one category.

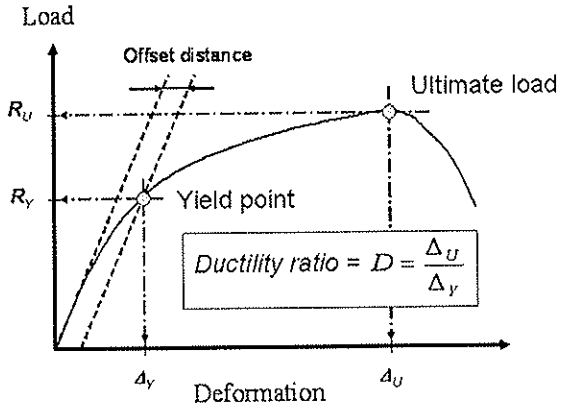

Figure 1 – Definition of characteristic deformations Δ_U and Δ_Y

Table 1 – Classification of failure mode

Classification	*Average ductility ratio, $D_{av.}$*
Brittle	$D \leq 2$
Low-ductility	$2 < D \leq 4$
Moderate-ductility	$4 < D \leq 6$
High-ductility	$D > 6$

NOTES: It is recognized that this system of classification may prove too challenging for practical implementation. An alternative is to adopt classifications such as 'No, Low, Moderate and High Reserve Capacity'. Various options are being investigated.

5.3 Determination of yield and ultimate loads

A range of options exist regarding the process for estimating the level of load at which damage and irreversible deformations start to accumulate. This level of load is commonly termed the Yield Load (R_Y) as for metals, even though wood products do not actually deform plastically. Subsystems may exhibit true plastic deformations if incorporated metal parts and fasteners are loaded beyond their yield point. Typically wood components and subsystems do not exhibit a clear transition from elastic to in-elastic response and unambiguous definition of R_Y can be impossible. In such cases the Offset Distance approach illustrated in Figure 1 is an acceptable

method for estimating R_Y. Acceptable values for the offset distance will depend on the type of component or subsystem, but as a rough guide they can be expected to be in the order of 0.1mm if the measured deformation is a translation, and 0.002 radians if the deformation is a rotation.

Many types of component and subsystem exhibit extensive post yield-point inelastic deformations, and in some cases apparent post-yielding hardening in the response. Under such circumstances the ultimate load is often not reached before termination of a test for reasons such as reaching the maximum deformation permitted by the test apparatus. In such circumstances an acceptable conservative method for estimating R_U, and the associated deformation Δ_U, is to substitute for those the maximum load applied and the associated deformation. Resulting classifications of failure mode according to Table 1 would result in conservative design. For some situations it may be desired to also estimate a so-called Failure Load (R_F) from the post-peak part of a load deformation envelope curve, and the associated deformation Δ_F.

6. Form of LRFD Design Equations

6.1 Strength Limit States

For strength controlled limit states the design equation is assumed to take the generic form:

$$\phi R \geq \text{effects of factored loads} \qquad \ldots\ldots\ldots (3)$$

where: ϕ= resistance factor, R= resistance adjusted for all design specific considerations. The adjusted resistance is calculated according to the generic form:

$$R = R_S k_S k_T k_N k_H \qquad \ldots\ldots\ldots (4)$$

where: R_S= standardized specified resistance, k_S= service factor, k_T= treatment factor, k_N= number of components or subsystems in series factor, k_H= system failure mechanism factor. The factor k_S accounts for the coupled cumulative effects of loading and service conditions. Specifics of equations (3) and (4) will vary depending on sensitivities of resistances to design variables, and exactly what parameters need appear will vary from situation to situation. It is of course necessary to have prior applicable evidence, or to collect such evidence by testing as already indicated in Section 4. The companion paper by Smith et al [4] also discusses the concepts underpinning k_N and k_H.

6.2 Deformation Limit States

Whether there is need to consider deformation limit states directly depends on the purpose for which any component or subsystem is intended, i.e. is end use dependent. The term deformation here is used in a very broad sense and includes the effects of all types of recoverable and non-recoverable movements. Although deformation limits are mostly applicable to systems and subsystems, there are situations where components have to be designed against the possibility of excessive deformability. The most likely applicable deformation limit states for components are associated with connections made by carpentry joints or using mechanical fasteners, or are deformations in linear elements that will be incorporated into plate or shell systems. As discussed in more detail by Smith et al in the context of systems [4], there are two reasons for such limits:

- Need to avoid basing design capacities on levels of resistances that are only attainable at deformations that the parent system will not permit until stages well past initiation of global failure. This need is linked to the system failure mechanism factor (k_H) in equation (4).
- Need to avoid none collapse related, commonly referred to as *Serviceability Limit States*.

For systems and subsystems deformation related limit states can fulfil a number of functions related to performance under normal use conditions. Examples include: avoidance of collision of adjacent buildings due to excessive inter-storey drift during strong wind or seismic events; avoidance of damage to the building envelope that leads to long term durability problems; and avoidance of annoying floor vibrations. Typically timber design codes will not be source documents for prescribing deformation limit state related criteria, even though some stray into that role [e.g. 1]. Therefore directives in any standard for test based assessment of design values should be restricted to guidance about collection of deformation data as ancillary information to the collection of strength information. The limit states and associated causal forces and excitations are best defined via building and loading codes, or if applicable from first principle.

7. Resistance Factors

As is widely documented, society's tolerance of building failures and associated risk to life is low, compared with risks for other life activities. The acceptable risk of death due to building failures has been estimated to be 0.14×10^{-6} per annum [8]. Consequently tolerated failure rates for components and subsystems of buildings are low. Assigned combinations of resistance and load factors within design equations are the tool used to control (in an informal sense) the likelihood of failures in components of systems. Even though structural reliability methods have been used as support to decisions concerning those factors, those methods primarily support relative scaling of ϕ values assigned for design of different types of component. Current knowledge of causal relationships is inadequate for true understanding of how choice of one value of ϕ versus another choice will map to failure rates for components, or to failure rates for subsystems and systems that incorporate the components. Nevertheless, reliability methods are valuable tools allied to and supporting code committee decisions. The Safety Index (β) that is incorporated into reliability based calibrations of design equations is the parameter that is most widely accepted as a compact indicator of relative security again failure that different selections of ϕ will yield. Failure here, and elsewhere, is taken to mean that the effects of applied loads have equaled the available resistance of any component, presuming that both loads and resistances can be sensibly assumed to be the result of random processes. Estimates of acceptable β have been made based on inverse reliability analysis that shows what β values typify design solutions judged to be acceptable under historical engineering approaches like Allowable Stress Design. Acceptable in this sense implies that there is a desirable balance between the security against failure and the amount of materials required. Values of β that have been judged appropriate fall within the range of 2.5 to 4.5 for components within timber and steel structures [e.g. 7, 9]. Here that is the range assumed appropriate for standardized practice for deriving design resistances directly from test data. For simplicity it is proposed that the standardized practices be restricted to determination of the average characteristic resistance against failure and the necessary companion value of ϕ, Section 6.

Taking the simplest possible formulation, the resistance factor can be calculated as [9, 10]:

$$\phi = \exp(-\alpha\beta V)C_f \qquad \ldots\ldots\ldots\ldots (5)$$

where: α = calibration coefficient = 0.75, β = safety index applicable to the type of component or subsystem, V = coefficient of variation in resistance, and C_f = data confidence factor. The calibration coefficient is given the value 0.75 based on Smith [6]. Suitable choices for β are suggested within Table 2. There it is proposed that the safety index be a function of both the type of failure mode observed in tests, and whether or not the component or subsystem is to be part of a parent system that permits development of alternative load paths were a component or subsystem to fail [4].

The coefficient of variation in resistance should be calculated as:

$$V = \sqrt{V_{data}^2 + 0.1^2} \quad \text{..... (6)}$$

where V_{data} = coefficient of variation calculated from the test data. The term 0.1^2 is included to allow for general uncertainties in estimation of V. Data confidence factor C_f is given by [10]:

If sample size $n \geq 10$: $$C_f = 1 - \frac{2.7V}{\sqrt{n}} \quad \text{..... (7)}$$

If sample size $n < 10$: $$C_f = \frac{R_{\min}}{R_{0.05,data}} \left(\frac{n}{27}\right)^V \quad \text{..... (8)}$$

where: $R_{\min}$ = minimum strength of n test values, and $R_{0.05,data}$ = raw data estimate of 5th percentile strength (which can be estimated by fitting a statistical distribution).

Table 2 – Proposed values for Safety index (β)

***Classification of failure* (Table 1)**		***Brittle***	***Low-ductility***	***Moderate-ductility***	***High-ductility***
		β value			
Type of parent system	***No alternative load paths possible***	4.5	4.0	3.5	3.0
	Alternative load paths possible	4.0	3.5	3.0	2.5

In the above the there is no adjustment included to change the basis of the reference condition for the Standardized Specified Resistance (R_s) from short-term loading, as is the common standardized test situation, to some other basis. Allowing the option for that adjustment and other possible deviation of test conditions from those for standardized resistance, the final proposed standardized approach for determining 'factored standardized resistances' directly from test data is:

$$\phi R_S = \frac{R_{av,data} \exp(-0.75\beta V) C_f}{\prod k_{test,i}} \frac{1}{k_{test,DoL}} \quad \text{..... (9)}$$

where: $R_{av,data}$ = average strength of n test values, $\prod k_{test,i}$ = product of modification factors adjusting from the Standard Conditions associated with R_S to test conditions, and $k_{test,DoL}$ = modification factors adjusting from the Standard Term Loading Duration associated with R_S to the test duration. Based on past practices, for Canada $k_{test,DoL} = 1.25$ [7]. As will be noted, there is no actual need to separate ϕ from R_S. If that step is included to yield information in a more familiar LRFD format, it can be achieved using equation (5) as the basis for decomposing equation (9).

8. Expected Level of Consistence with Current Practice

Examples are given here to illustrate the likely level of consistency between design solutions based on the proposed approach for determining design resistances directly from test data and existing properties in the current edition of the Canadian timber design code [1]. Table 3

summarizes Standardized Factored Resistance (ϕR_S values) for data representing different levels of variability in resistance (apparent bending strength of relatively small dimension sawn lumber loaded as joists in a dry condition). In calculations for the proposed method β is taken equal to 3.5. This corresponds to a situation where the response exhibits low ductility (alternatively thought of as a component with Low Reserve Capacity) and members are employed in a parent system that can develop an alternative load path(s). That is the most typical application of such materials. All tabulated values are applicable to Standard Term Loading as defined in Canada ($k_{test,DoL} = 1.25$). The observed member strength data is taken from the literature [7] and is the same 'in-grade' data on which the design properties in the Canadian code are based. Factor C_f in calculations to the proposed method are based on $n = 400$ [7].

Table 3 – Comparison of Standardized Factored Resistances (ϕR_S values) – Apparent bending strength

Product definition			***Test data – bending strength*** (MPa)			***Standardized Factored Resistance*** (MPa)	
Species	***Grade***	***Nominal size*** (mm)	***Average***	***CoV***	***5 %tile***	***Canadian timber design code*** [1]	***Proposed Approach***
Douglas Fir - Larch	Select Struct.	38 x 241	40.44	0.27	21.60	16.3	14.6
		38 x 191	47.91	0.28	25.47	17.8	16.9
		38 x 89	56.02	0.21	35.45	25.2	23.4
	No. 3	38 x 241	27.55	0.43	9.55	4.55	3.86
		38 x 191	20.99	0.32	9.96	4.97	6.65
		38 x 89	46.19	0.46	14.47	7.04	10.1
Hem-Fir	Select Struct.	38 x 241	37.07	0.24	21.72	15.8	14.5
		38 x 191	50.41	0.29	25.69	17.3	17.3
		38 x 89	67.88	0.28	35.83	24.5	23.9
	No. 3	38 x 241	27.11	0.36	11.49	6.93	7.80
		38 x 191	27.30	0.32	12.86	7.56	8.65
		38 x 89	43.15	0.35	18.64	10.7	12.6
Spruce-Pine-Fir	Select Struct.	38 x 241	35.34	0.23	21.08	16.3	14.1
		38 x 191	39.87	0.25	23.01	17.8	15.2
		38 x 89	52.46	0.21	33.44	25.2	22.1
	No. 3	38 x 241	16.50	0.26	9.11	6.93	6.11
		38 x 191	24.29	0.30	12.08	7.56	8.11
		38 x 89	32.13	0.31	15.64	10.7	10.5

Based on tabulated comparisons, there is in general quite good consistency between design properties determined by the proposed approach and properties in the design code. Some discrepancies exist, but that has to be the case because the proposed approach is not a copy of the other one. It is deduced that designs proven based on test evidence according to the present proposal would yield acceptable levels of safety. The essence of this deduction would not change were more complex approaches to the reliability analysis to be inserted. An argument against use of simple reliability based approaches, like equation (5), could be that they do not accurately account for interactions between load and resistance sides of the design relationship. However, the authors believe that it is important not to overcomplicate processes that involve engineering judgment, and that calculations be treated as an aid to informed judgment. Unlike numerical methods, simple approaches do not obscure the relationship between calculated standardized factored resistances and the raw data on which they are based. Employing a kernel

equation like equation (9), which is a single step process, maximizes the transparency of interrelationships.

9. Conclusions

The approach proposed here for determining design properties for structural components and subsystems directly from test data is very simple, yet it appears to provide good consistency with provisions of existing code rules. Although created within the context of design practices in Canada it is believed that what is suggested is also the suitable basis for creating an ISO standard for data evaluation. A key concept embedded within the proposed approach is that the reliability index used within any analysis of test data be related to classification of the failure mode and the end use situation. Classification of failure modes would be according to a brittle – ductile scale. Definition of the intended end use would distinguish between whether a parent structural system incorporating components or subsystems of the type investigated is of a type capable to developing an alternative load path were any component or subsystem to fail. This dovetails with suggestions in a companion CIB-W18 meeting paper on Systems Level Design.

Acknowledgement

The authors gratefully acknowledge financial support from Natural Resources Canada under the project 'UNB2 - Design Methods for Connections in Engineered Wood Structures' (2003-06).

References

1. Canadian Standards Association (CSA). 2005. "Engineering Design in Wood", CAN/CSA Standard 086-01, CSA, Toronto, ON, Canada.
2. Asiz, A. and Smith, I. 2005. "New generation of timber design practices and code provisions linking system and connection design". CIB-W18 Meeting in Karlsruhe, Paper 38-102-1.
3. Quenneville, P., Smith, I., Asiz, A., Snow, M. and Chui, YH. 2006. "Generalised Canadian approach for design of connections with dowel fasteners". CIB-W18 Meeting in Florence (*in press*).
4. Smith, I., Chui, Y.H., and Quenneville, P. 2006. "Overview of a new approach to handling system effects in timber structures". CIB-W18 Meeting in Florence (*in press*).
5. Forest Products Laboratory. 1999. "Wood handbook--Wood as an engineering material". General Technical Report FPL-GTR-113. U.S. Department of Agriculture, Forest Service, Forest Products Laboratory, Madison, WI, USA.
6. Smith, I. 1985. "Methods of calibrating design factors in partial coefficients limit states design codes for structural timberwork: with special reference to mechanical timber joints". Research Report 1/85, Timber Research and Development Association, High Wycombe, Bucks, UK.
7. Foschi, R.O., Folz, B.R. and Yao, F.Z. 1989. "Reliability-based design of wood structures". Structural Research Series Report No. 34, Department of Civil Engineering, University of British Columbia, Vancouver, BC, Canada.
8. Reid, S.G. 2000 "Acceptable risk criteria". Progress in Structural Engineering and Materials, 2(2): 254-262.
9. Ravinda M.K. and Galambos T.V. 1978. "Load and resistance factor design for steel", ASCE Journal of the Structural Division, 104(ST9): 1337-1353.
10. Leicester R.H. 1986. "Confidence in estimates of characteristic values", CIB-W18 Meeting in Florence, Paper 19-6-2.

INTERNATIONAL COUNCIL FOR RESEARCH AND INNOVATION
IN BUILDING AND CONSTRUCTION

WORKING COMMISSION W18 - TIMBER STRUCTURES

COMPARISON OF THE PULL–OUT STRENGTH OF STEEL BARS GLUED IN GLULAM ELEMENTS OBTAINED EXPERIMENTALLY AND NUMERICALLY

V Rajcic
A Bjelanovic
M Rak

CROATIA

MEETING THIRTY-NINE
FLORENCE
ITALY
AUGUST 2006

Presented by V Rajcic
H Larsen discussed the principle of using glued-in rods where glue in rods should not be used unless ductile failure. In this case test data showed brittle failure. He further commented that the neural network was not verified. V Rajcic stated that the neural network approach would consider both training sample and testing set.
I Smith questioned whether these techniques should be limited to certain moisture class. V Rajcic agreed.
A Jorissen and V Rajcic discussed test setup and boundary conditions in the FEM analysis in relation to the observed failure mode.

Comparison of the Pull–out Strength of Steel Bars Glued in GluLam Elements Obtained Experimentally and Numerically

Vlatka Rajcic, Adriana Bjelanovic, Mladenko Rak

Prof, PhD, str. eng., Assist. Prof, PhD, str. eng., Prof, PhD, str. eng., Croatia

1. Introduction

The paper presents the comparison of results obtained experimentally and numerically as well as the efficiency of trained Neural Network in prediction of the strength capacity of the bolted joints made with bars of cold-drawn smooth steel and threaded steel bars glued-in GluLam elements. Joint specimens were undergone to destructive one–side pull–out test. The experiment was the starting point of the whole process with purpose of determining the tensile strength of joint. The whole research work and comparison of the experimentally obtained results have been made of several different levels and goals. The first one focused on fracture behaviour of joints made of cold-drawn smooth and threaded bars using the same adshesive layer, EPOCON 88 KGK. The second comparison level was focused on fracture behaviour of joints made of threaded bars while different species of bond layer was used SIKADUR 31 RAPID and EPOCON 88. The third level of research based on comparison of experimental and numerical results for joints bolted with threaded bars only where the results of 3D parametrically prepared models undergone to linear FE analysis in COSMOS/M program. Satisfactory correlation between experimentally obtained results and those that numerically produced was an ultimate issue that been intended to achieve.

Results of FE linear analysis obtained on 3D numerical models used for generating of NN database. The decisive thesis we try to verify was: if we could find the validity of relationship between results obtained experimentally and numerically, then we can use only numerical model to continue researching and make it extensively. We can use then only numerical FE model to explore an influence on joint strength capacity caused by variation of diameters, load angle and anchorage depths of threaded bars, as well.

We also try to make a move over and use results of the FE analysis to generate Neural Network databases. Why Neural Network? The most important fact is that inputs and outputs of FE analysis were recognisable for generated Neural Networks that we trained on them. The whole set of data inputs and outputs have been selected to represent a brief geometrical description of the joint as well as its state of load bearing capacity. The successful completion of an attempt have been achieved when trained NN models produced results of their own, based on, until then, unseen inputs. The interesting thing is correlation of the axial strength obteined by experiments, Neural network prediction strength and design rules suggested for characteristic axial capacity in tension given by Eurocode 5-Part 2-Appendix A.

2. EXPERIMENTAL RESEARCHING

2.1. Specimens and material properties

The laboratory tests were performed by one–side destructive pull–out test [1]. Each of four classified groups of specimens was characterised by different anchorage angle of bars (related to grains): 0° and 90° (see Fig.1), as well as by different glue type. Specimens were undergone to laboratory testing of their material properties (see Tab. 1), as well as glues were (see Tab. 2). The diameter of tested steel bars was varied for all specimens (d = 12mm, 16mm and 20mm). A hollow steel plate laid on the specimens of different shapes to prevent all possible displacements as well as to transfer a compressive load onto specimen over itself. All displacements were prevented in the zone of the steel plate on the parametrically prepared 3D models. A compressive load is transferred over the plate onto the specimen, and the bar is pulled out on the opposite side.

We varied an anchorage depth of bars (80mm, 120mm and 160mm), but the thickness of both types (two – component) epoxy glues to fill provided holes was kept constant (1,5mm).

Each of the four groups consists of approximately ten specimens with different anchorage depth

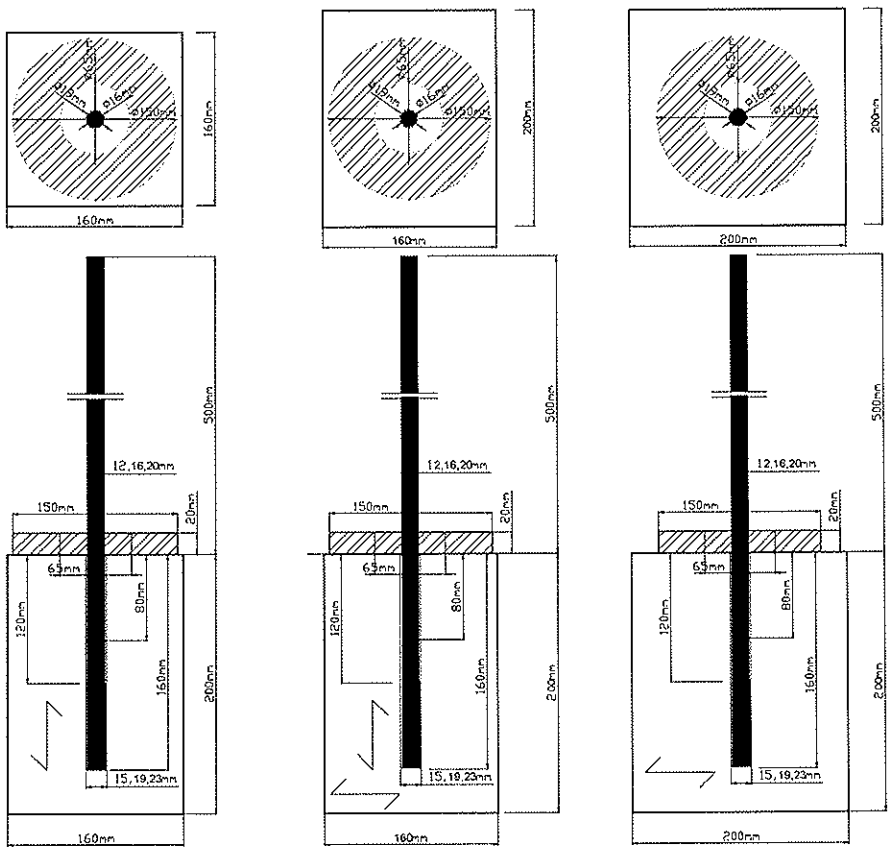

Fig 1: Shapes of tested groups of specimens with load angle of 0° and 90°

The threaded steel bars were manually embedded into the holes under constant pressure and rotation. The centring of the bars during embedding was visually performed.

Table 1: Measured material properties and moisture percentage of GluLam Fir specimens in [MPa]

$E_{0,mean} = 11700$	$\nu = 0{,}303$	$f_{v,0,FAILURE} = 8{,}33$	$u = 10\%$

Table 2: Material properties of steel bars and measured values in [MPa] for both epoxy two–component glues (SIKADUR 31 RAPID, EPOCON 88 KGK)

Steel material and epoxy glues	E–module	G–module	Poisson
Steel 235	210000	81000	0,27
SIKADUR 31 RAPID	4120	1420	0,45
EPOCON 88 KGK	7200	2170	0,336

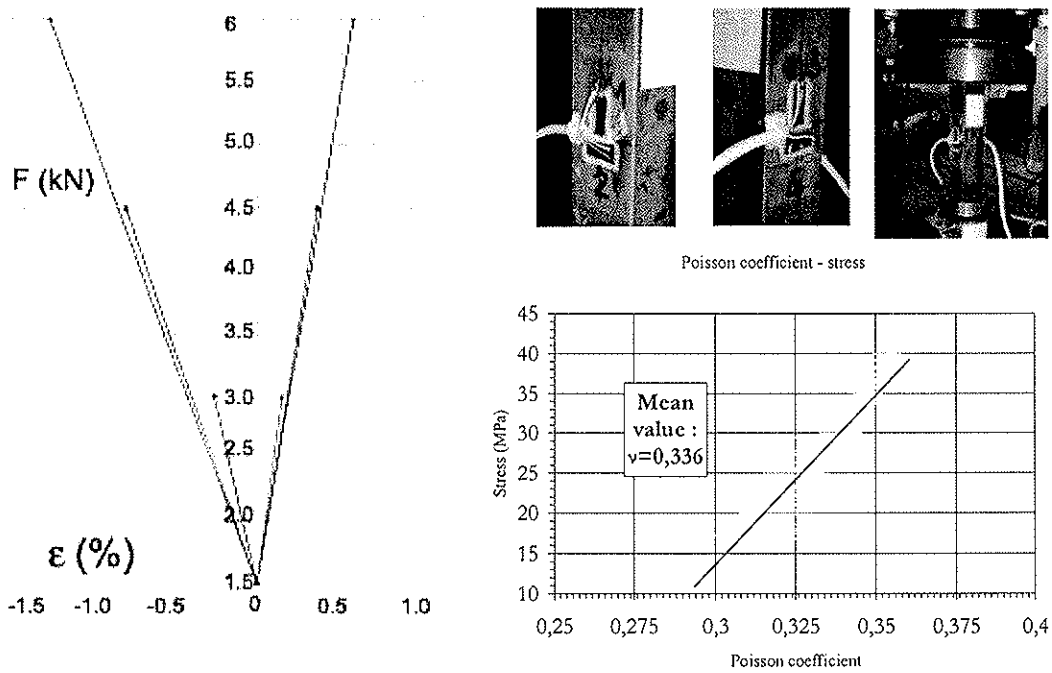

Fig 2: F –ε diagrams or SIKADUR 31 RAPID (left) and EPOCON 88 KGK (right) glues

The experiments to obteined axial tension strength of glued in smooth cold-drawn bars and rebars glued with EPOCON 88 were done by test machine system Zwick which can satisfy demands and performs superior test tasks. The tests were driven by the rule of the constant increase of the deformation. Software *testExpert* was used for data analysis and statistics. The digital technology drive system features a high control range. The lower exstensometers were placed on the top lavel of the wooden sample and the higher extensometers are placed on the steel bars. The measured displacement between wood sample and bar was difference between the results from two lavel extensometers. The result are given as the F-d diagrams.

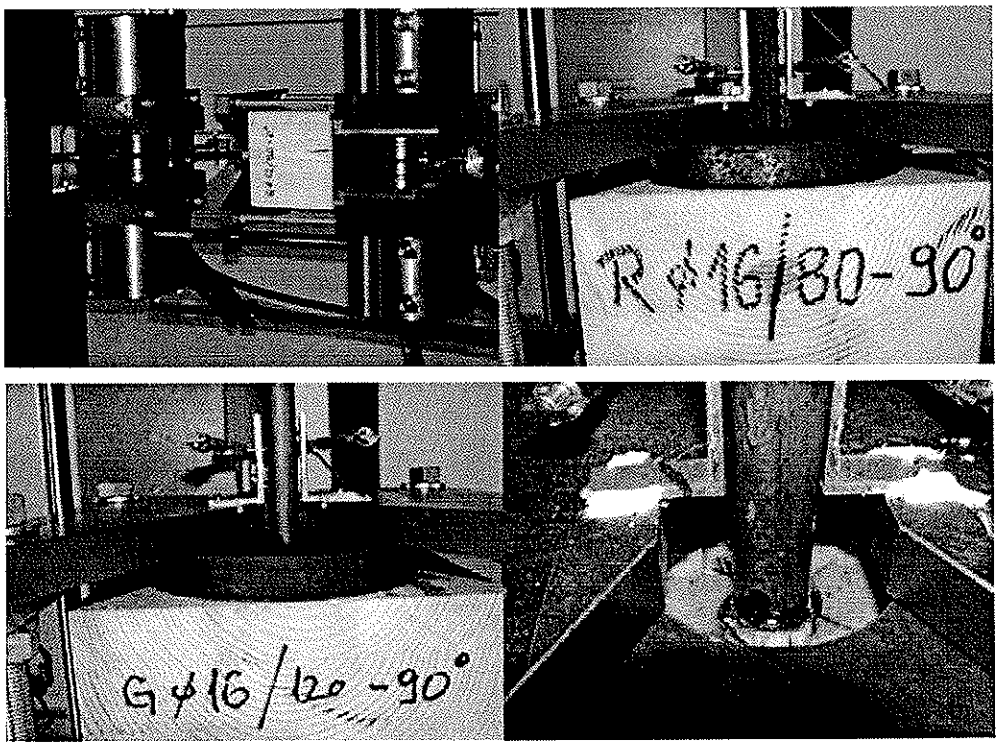

Fig 3: Setting up of experiments with EPOCON 88 glue

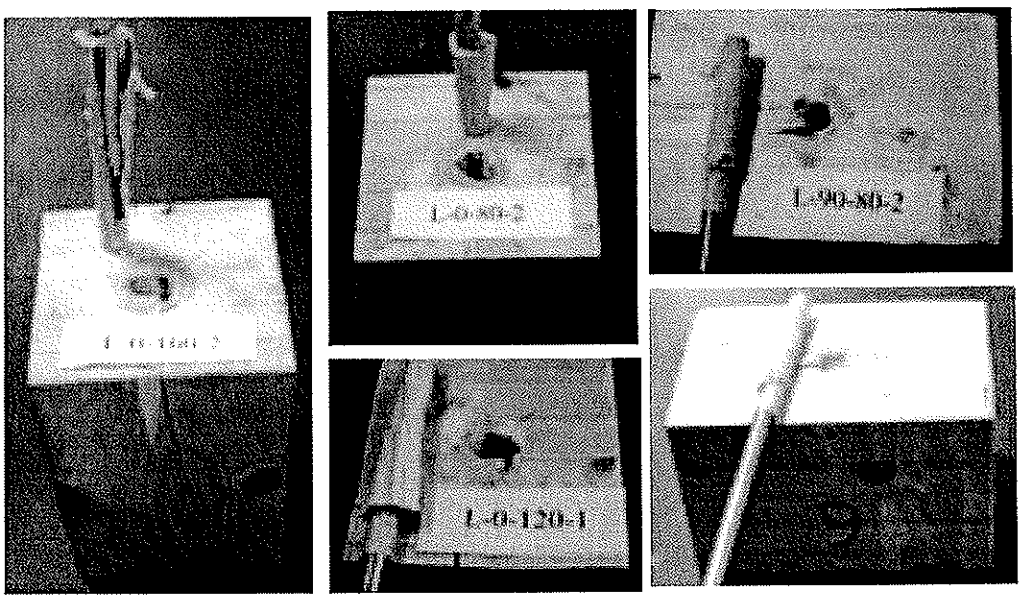

Fig. 4: The two basic types of fracture behaviour for joints with threaded bars due to load angle related to fibers

The first failure type is characteristic for 0° – tests (see Fig. 4 – 7) and threaded steel bars glued–in. The failure takes place in the wood along irregular surface, a few millimetres along the threaded bar, where there are the highest stress values. The second type of joint

strength capacity is characteristic by failure along the glue, which is typical for 90° – tests (see Fig. 4 – 7).

2.2. Experimentally Determined Joint Strength Failure

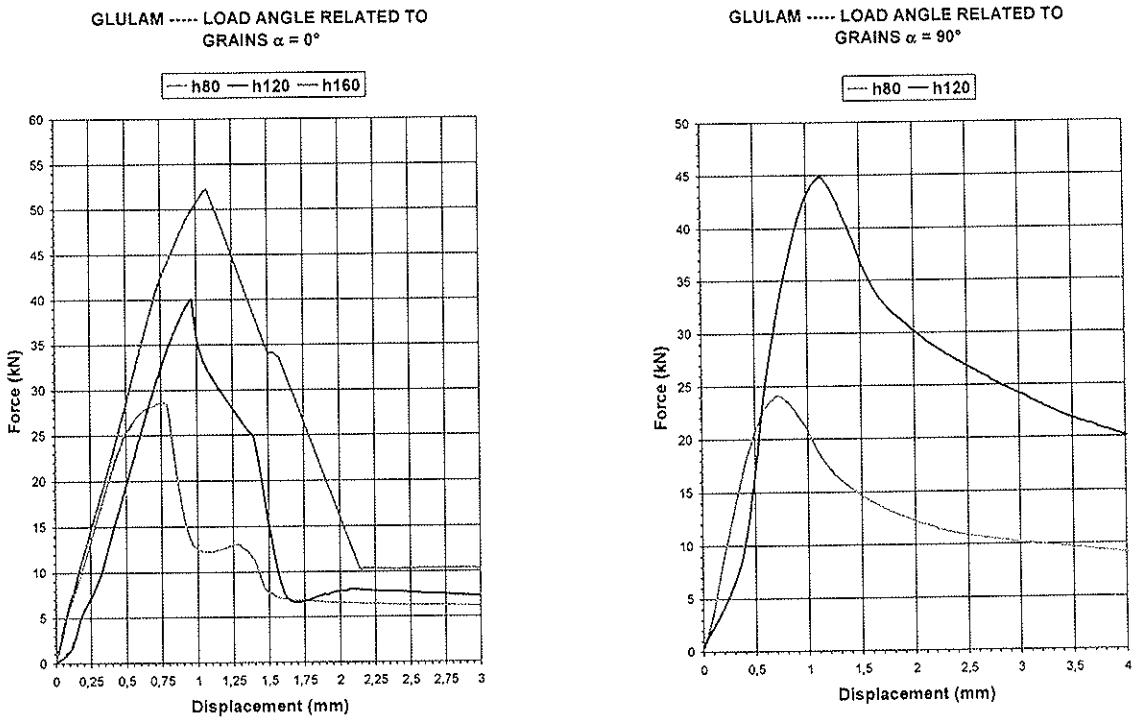

(a) Test Load Angle $\alpha = 0^o$

(b) Test Load Angle $\alpha = 90^o$

Fig. 5: Experimental results for threaded steel bars (d = 16mm) and SIKADUR glue: F–d diagram for various load angles (α) and anchorage depths (H)

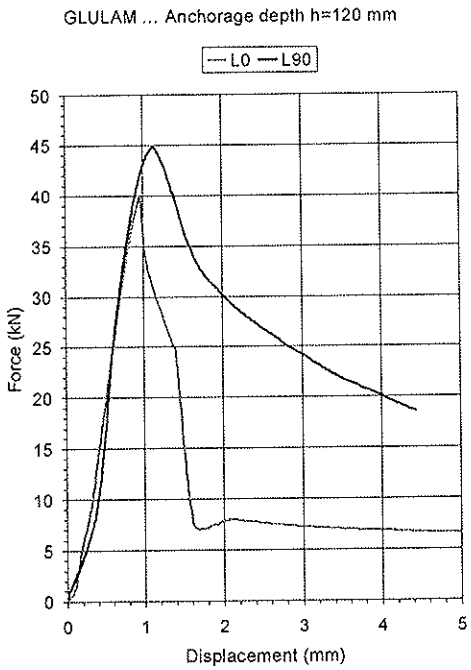

Fig. 6: Comparison of experimental results (F – d) for threaded steel bars (d = 16mm), SIKADUR glue and anchorage depth of h = 120mm due to load angle

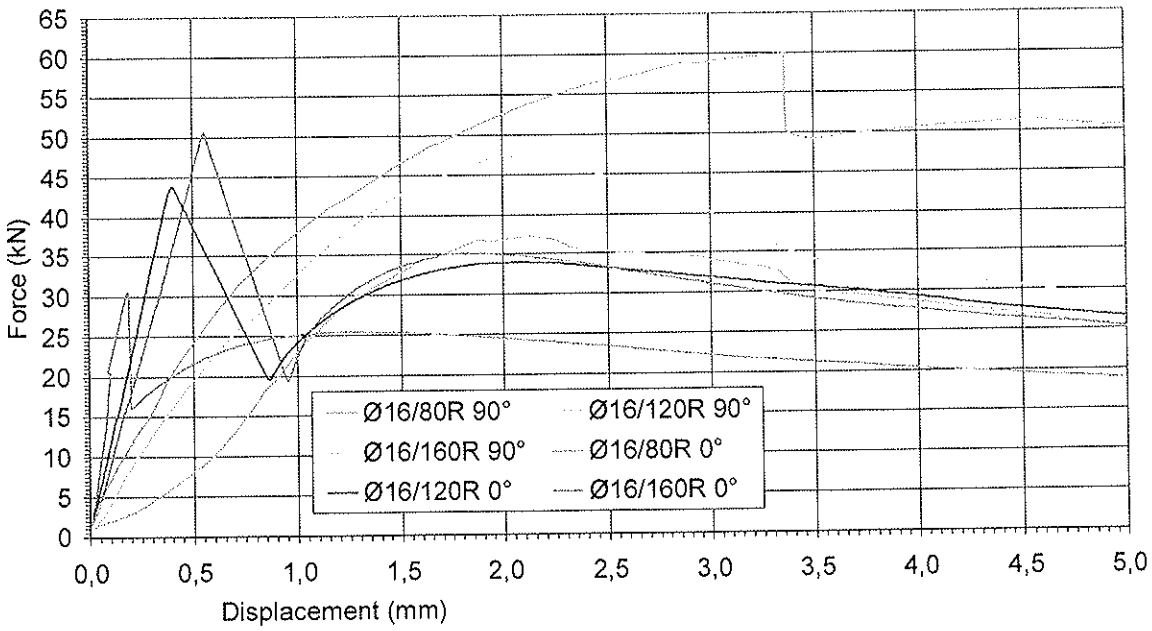

Fig. 7: Experimental results for steel rebars (d = 16mm) and EPOCON glue: F–D diagram for various load angles (α) and anchorage depths (H), R-rebar

Laboratory made one–side pull–out tests carried out the F–d diagram for an each specimen. A force increase was provoked by constant deformation increase. The connection involves possibility of plasticity, as it is apparent that after the elastic deformation and, upon reaching the failure strength of the cross section, there is a further strength possibility up to a certain level (see Fig. 5 – Fig. 6). Measuring results of all

medium values of the F–d relationship have been collected to represent the joint fracture behaviour during the tests.

It is clear that the anchorage depth (H), and loading conditions, the glue type as well as the bar type (threaded or cold-drawn smooth steel bars) are decisive for expression of the mean shear stress at the failure. We have found that the higher joint strength capacity for both glue types and for threaded bars was reached for the load angle of $\alpha = 90^{\circ}$ (see Fig. 5, Fig. 6 and Fig. 7). The failure force reached insignificantly higher values in tests where the EPOCON glue was used but this difference (related to SIKADUR bond) did not exceed approximately 10% of the measured failure value.

Significantly lower joint strength capacity was achieved for cold-drawn smooth steel bar (see Fig. 8 and Fig. 9) where the failure takes place in the glue, along the smooth surface of the cold-drawn smooth steel bar. We have also found that previously described failure type was characteristics for both load angles (of 0° and 90°, see Fig. 8 – 10) which means that the failure behaviour is very independent of load angle – fiber direction relation. Unfortunately, in spite of cold-drawn steel bars, we did not make test for both glue types (those were carried out only for EPOCON), so, we could not compare results and accomplish some conclusions in this field. However, it is obviously that a slipping along the smooth surface of a steel bar (placed between the bar and the glue) is predominance for the fracture behaviour. Slipping module is much higher for this type of steel bars (in comparison with threaded steel rods).

Also, there are no reliable proofs neither for the durability of adhesion of cold-drawn smooth steel bars nor for the influence of their corosion. Facts we have just mentioned, together with results which experiments carried out, do not speak in favor of smooth steel bars if we try to compare they with threaded rods (see Fig. 5 to Fig. 10).

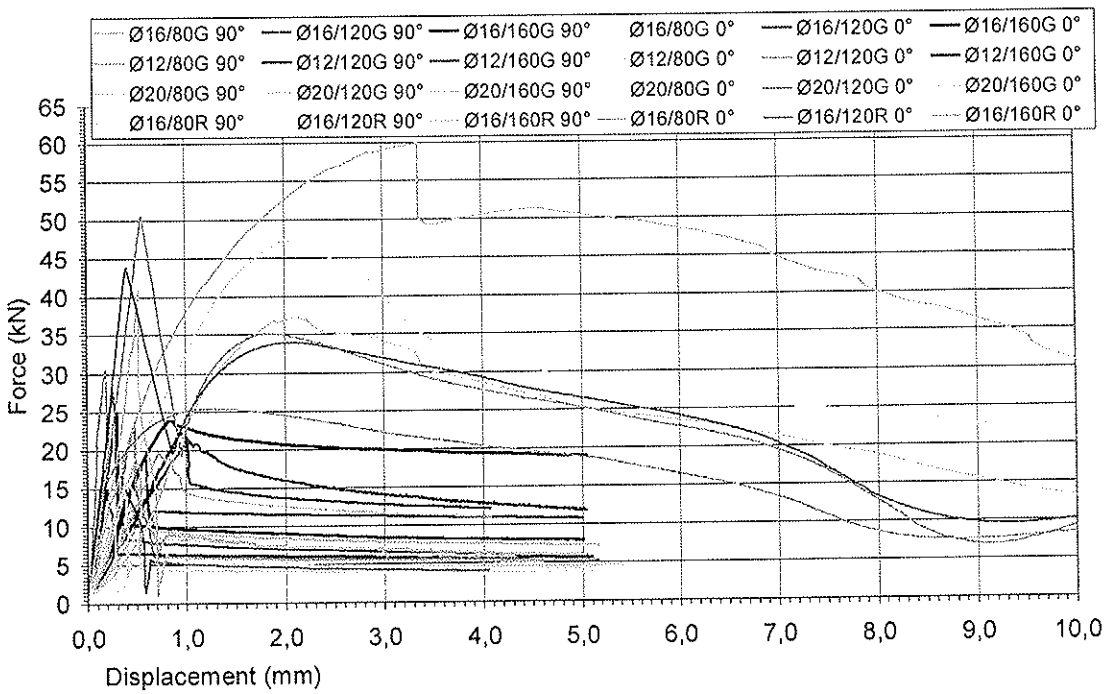

Fig. 8: Collected test results for both steel bars type and for the EPOCON glue: F–D diagrams for various load angles (α), diameters (d) and anchorage depths (H), (G)- smooth cold-drawn steel bars

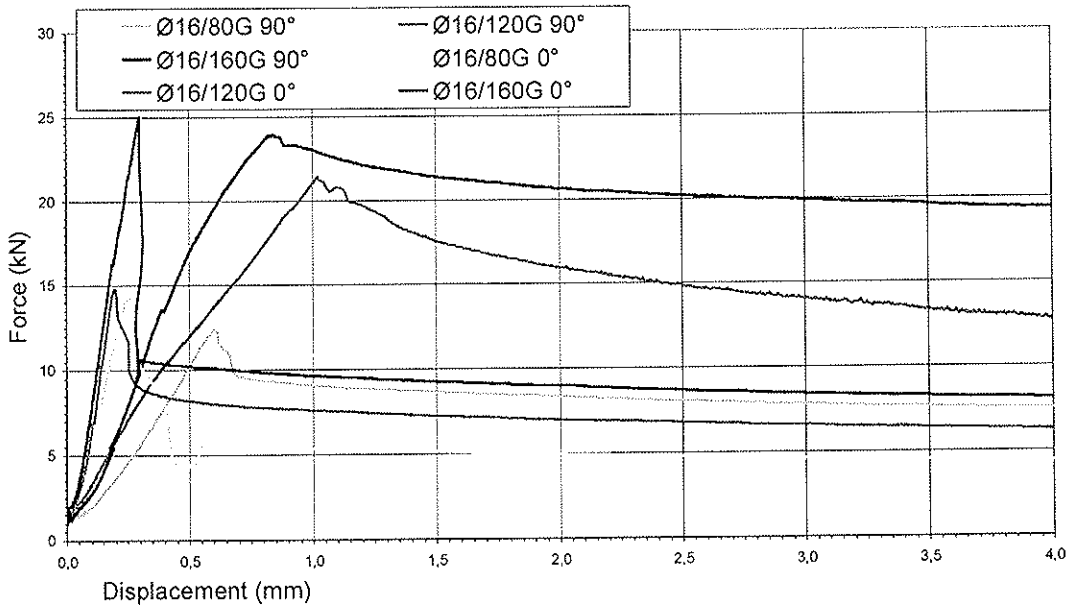

Fig. 9: Experimental results for cold-drawn steel bars of d = 16mm and EPOCON glue: F–d diagrams for various load angles and anchorage depths (H)

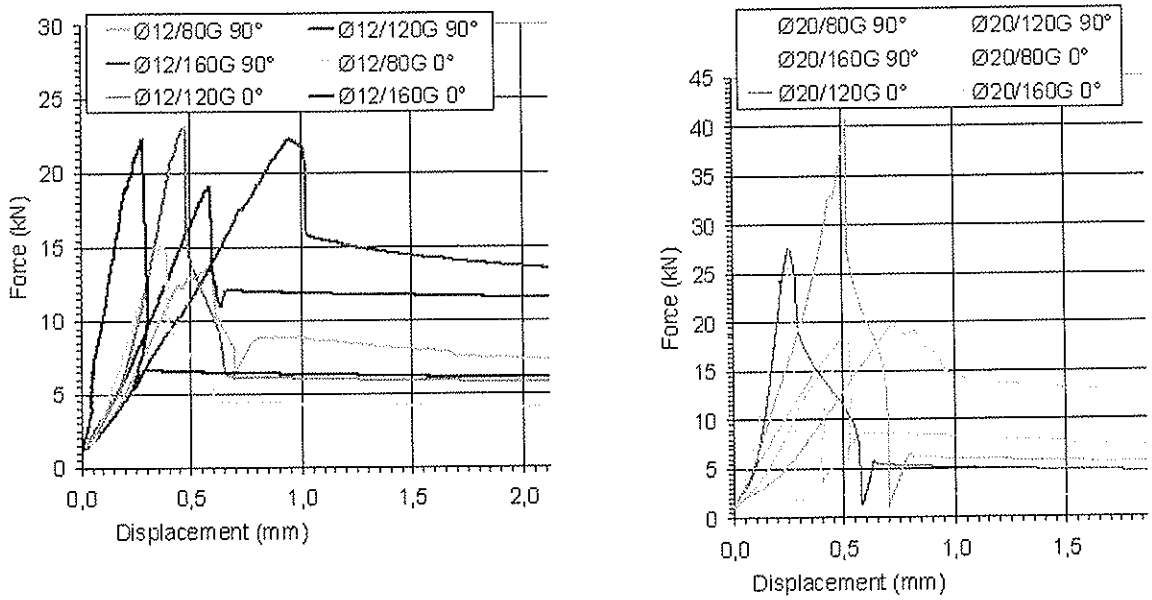

Fig. 10: Experimental results for cold-drawn bars of d = 12(20) mm and EPOCON glue: F–D diagrams for various load angles and anchorage depths (H)

3. NUMERICAL FE ANALYSIS

COSMOS /M programme was used for numerical analysis where only SOLID finite elements were constitutive part of an each 3D parametrically prepared model. SOLID is an 8–node three–dimensional where three translation degrees of freedom per node are considered for structural analysis. The direction of output stress components was defined

in the same way. Mechanical characteristics of an anysotropic GluLam Fir was defined in local coordinate system where a local x–axis always lies parallel with fibers direction (see Table 1 and Table 2). It is clear that the anchorage depth and the diameter of rods, glue fracture energy and loading conditions are decisive for expression of the mean shear stress at the failure. For small anchorage depths, like those we experimented with, the load is almost proportional with shear failure stress, so, we used only linear FE analysis to determine the failure stress values.

Comparison of results of experimental tests with results of analysis of 3D FE models was the next step of carried out researching. Numerical FE analysis is based on linear fracture mechanics analysis of the model of the adhesive layer's behaviour. Satisfactory correlation between experimentally and numerically obtained results was an ultimate issue we intended to achieve. During the linear analysis of FE models the following parameters had been varied (see Fig.11): the geometry of the model, the diameter of the bars, an anchorage depth of glued-in rods and the load angle in comparison with wooden fibers (0°and 90°). The thickness of the glue to fill provided holes was kept constant (1,5mm).

The decisive thesis that we tried to verify and to proof is: if we could find the validity of relationship between results obtained experimentally and numerically, then, we can dominantly use numerical model to continue researching and to explore an influence on joint strength capacity caused by variation of diameters and anchorage depths of steel bars (see Fig.12).

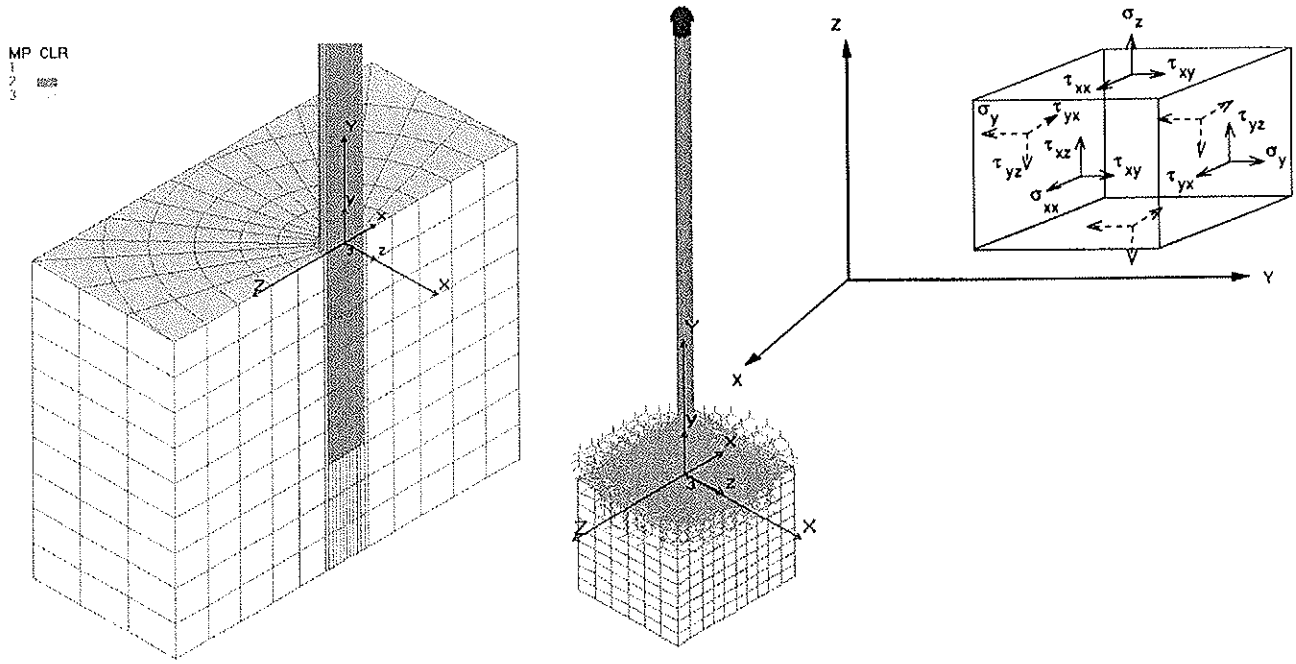

Fig. 11: Example of one FE 3D parametrically prepared model (geometrical parameters for 90°-load angle together with material property definition and the directions of stress components outputs for SOLID FE)

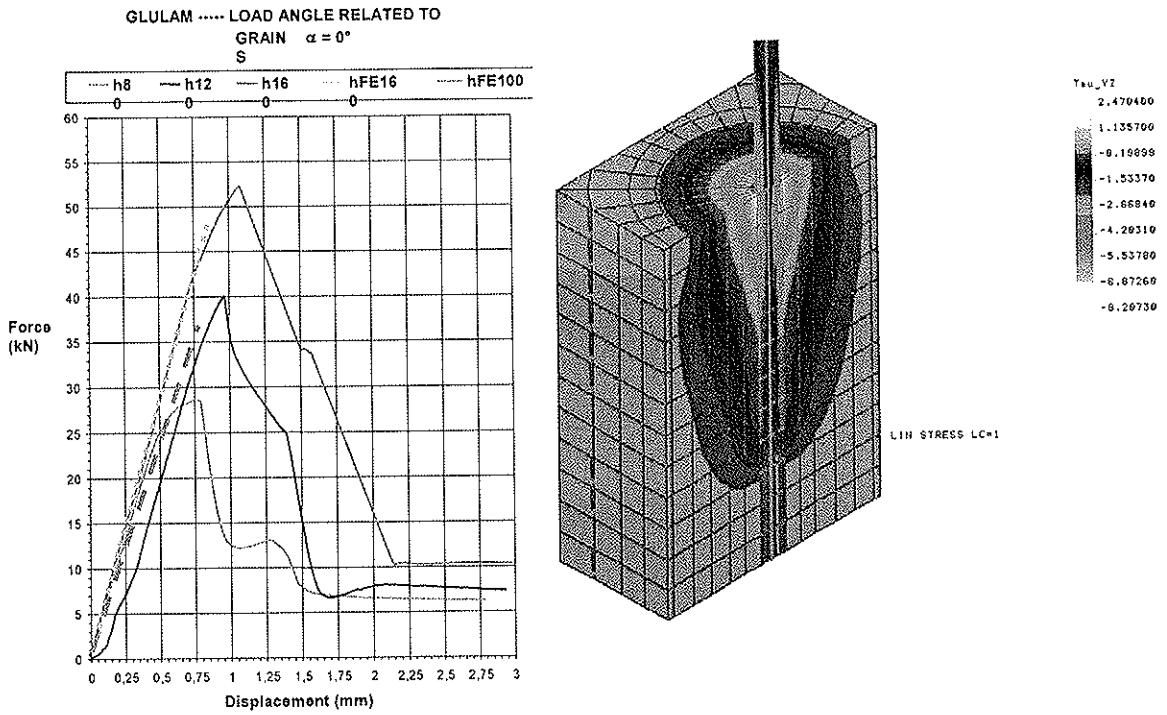

Fig. 12: Comparison of results obtain experimentally and numerically for load 0°-angle Strength failure type for load 0°-angle – shear stresses measured on fracture area

4. NEURAL NETWORK AS AN AUXILIARY TECHNIQUES FOR JOINT STRENGTH CAPACITY PREDICTION

The four Neural Network models (one for an each load angle related to wood fibers and one for an each type of glued-in steel bars) on the set pattern of an average number of fifty different cases per each NN model. Inputs had been separated as they follow: the width of the cross-section of specimens (A), the depth of the cross-section of specimens (B), the depth of specimens (HD), the diameter of threaded steel bars (D), the load angle (AL) and the depth of an anchorage of threaded steel bars (H), as well. The value of the tensional force of fracture (P) was the first output parameter. We have found that stress and deformation values, as well, significant for an each mode of strength failure, were the logical output values. They are as they follow: the shear stresses (TYZ) and normal stresses (SX, SY) as well) and the displacement measured on the contact line lay between the wood and the glue (for threaded bars) or between bar and glue (for cold-drawn smooth steel bars), as well as the displacement of the upper grain of the specimen.

We used the Back Propagation algorithm of Standard Connection and supervised learning for an each generated model of Neural Network. The learning was interrupted after approximately two hours, when the average error of test patterns reached value less than 0.25%. The successful completion of NN training was achieved when NN models had been claimed to produce results of their own based on, until, unseen inputs. When we have compared results produced by NN with expected values (by FE linear analysis of numerical models), it was clear that they correlate very well. Maximum deviation between them did not exceed 1.5–2.0%, and average values were less than the mentioned one.

Therefore, any potential user of trained NN, should be at least briefly informed (by NN) about joint strength capacity. Further researches into the scope of application of NN might be direct to provide the appropriate equation for describing the behaviour of this type of joint and predicting of their strength. Trained NN might be helpful in it because of its capability of "fitting" through dates.

Also, there is a big influence of the moisture contant and change of it and temperature condition that influence glue as well as wood. That influence was not predicted in design rules for axially loaded glued-in and laterally loaded bolts given in Eurocode 5-Part 2-Appendix A and could be nicely forseen using Neural Network results of learning.

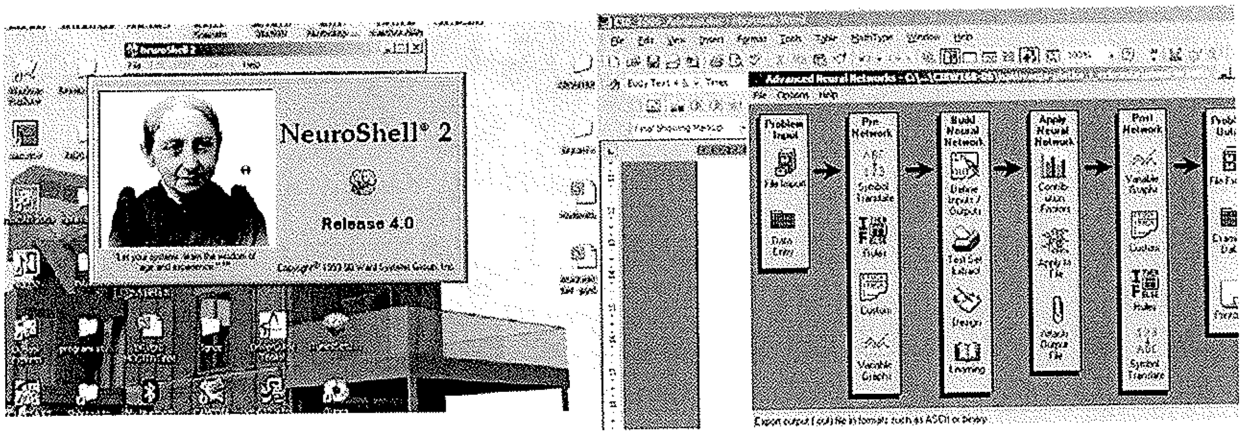

Fig. 13: Neural Network shell NeuroShell 2 was used for "training" the problem of the axial tension capacity of the glued-in bolts. Menu of the neural network shell is presented. Advanced learning with back propagation algorithm was used.

Datagrid: C:\...\clanci\CIBW168-06\ispitivanja-glatka_i_rebrasta\ulijepljenesopke.pat

File Edit Format Help

Number of row with variable names (blank if none): 1 — [X] left/right arrow keys and edit

First row containing actual training data: 2 — Size: 179 row 20 columns

Note: This is not a commercial spreadsheet and may not load fast enough for large files. The NeuroShell 2 Options menu allows you to change the datagrid call to your own spreadsheet. Search help file for "datagrid" for details.

	A	B	C	D	E	F	G
1	width of specimen	moisture	effective diameter	glued length of bolt	fract. tensile force (kN)	normal stress sx	perpendicular stress sy shear
2	20,000000000000	10,900000000000	16,000000000000	80,000000000000	14,080000000000	7,700000000000	0,570000000000
3	20,000000000000	12,300000000000	16,000000000000	80,000000000000	13,040000000000	6,800000000000	0,570000000000
4	20,100000000000	10,700000000000	16,000000000000	80,000000000000	14,050000000000	7,200000000000	0,560000000000
5	20,000000000000	11,300000000000	16,000000000000	80,000000000000	15,040000000000	7,200000000000	0,540000000000
6	20,000000000000	11,200000000000	16,000000000000	80,000000000000	14,950000000000	6,800000000000	0,430000000000
7	20,000000000000	10,900000000000	16,000000000000	80,000000000000	13,910000000000	7,100000000000	0,560000000000
8	20,200000000000	10,600000000000	16,000000000000	80,000000000000	14,550000000000	5,900000000000	0,450000000000
9	20,100000000000	10,400000000000	16,000000000000	80,000000000000	13,700000000000	6,100000000000	0,420000000000
10	20,000000000000	11,900000000000	16,000000000000	80,000000000000	14,750000000000	6,750000000000	0,440000000000
11	20,050000000000	10,500000000000	16,000000000000	80,000000000000	13,800000000000	6,900000000000	0,460000000000
12	20,000000000000	11,700000000000	16,000000000000	80,000000000000	14,130000000000	7,200000000000	0,570000000000
13	20,200000000000	11,400000000000	16,000000000000	80,000000000000	14,300000000000	5,860000000000	0,450000000000
14	20,100000000000	10,200000000000	12,000000000000	80,000000000000	14,030000000000	5,940000000000	0,550000000000
15	20,050000000000	9,900000000000	12,000000000000	80,000000000000	13,750000000000	6,120000000000	0,460000000000
16	20,030000000000	10,350000000000	12,000000000000	120,000000000000	18,510000000000	5,920000000000	0,450000000000
17	20,050000000000	11,200000000000	12,000000000000	120,000000000000	17,880000000000	7,000000000000	0,540000000000
18	20,000000000000	10,330000000000	12,000000000000	120,000000000000	19,630000000000	7,400000000000	0,440000000000
19	20,030000000000	12,100000000000	12,000000000000	120,000000000000	17,690000000000	7,500000000000	0,540000000000
20	20,000000000000	11,000000000000	12,000000000000	120,000000000000	18,360000000000	6,400000000000	0,490000000000
21	20,080000000000	10,400000000000	12,000000000000	120,000000000000	18,010000000000	7,200000000000	0,580000000000
22	20,000000000000	11,100000000000	12,000000000000	120,000000000000	17,650000000000	6,850000000000	0,580000000000
23	16,020000000000	12,100000000000	12,000000000000	120,000000000000	18,910000000000	7,120000000000	0,580000000000
24	16,000000000000	9,800000000000	12,000000000000	120,000000000000	17,670000000000	6,990000000000	0,440000000000
25	16,060000000000	11,200000000000	16,000000000000	120,000000000000	21,550000000000	5,880000000000	0,570000000000
26	20,060000000000	10,300000000000	16,000000000000	120,000000000000	22,460000000000	6,750000000000	0,410000000000
27	16,030000000000	11,150000000000	16,000000000000	120,000000000000	22,130000000000	7,005000000000	0,580000000000
28	16,050000000000	10,650000000000	16,000000000000	120,000000000000	21,780000000000	6,980000000000	0,580000000000
29	16,100000000000	11,350000000000	16,000000000000	120,000000000000	21,950000000000	7,200000000000	0,520000000000
30	16,000000000000	11,400000000000	16,000000000000	120,000000000000	23,010000000000	6,880000000000	0,540000000000
31	16,040000000000	10,200000000000	16,000000000000	120,000000000000	22,080000000000	5,880000000000	0,580000000000
32	16,030000000000	10,750000000000	16,000000000000	120,000000000000	21,860000000000	6,120000000000	0,400000000000
33	16,070000000000	11,250000000000	16,000000000000	120,000000000000	22,100000000000	5,210000000000	0,500000000000
34	16,300000000000	10,200000000000	16,000000000000	120,000000000000	22,400000000000	6,120000000000	0,570000000000
35	16,060000000000	11,670000000000	16,000000000000	120,000000000000	21,110000000000	6,000000000000	0,590000000000
36	16,070000000000	11,100000000000	16,000000000000	120,000000000000	21,960000000000	7,000000000000	0,510000000000

Start | CIB_2006_Adriana_novo... | NeuroShell 2 - C:\...\ulje... | Advanced Neural Networ... | Datagrid: C:\...\clanci... 14:43

Fig. 14: Part of the pattern file for learning Neural Network. All the datas come from experimental testings and some interpolations are made numerically by FEA on the presented model.

5. CONCLUSION REMARK

1. Although cold-drawn smooth bars are also declared for possible use in glued-in bolted connections, this paper with its results emphasize that we must be very careful with it. Adhesion between smooth steel bars and glue is questionable. There is also possibility of loosing strength due to corrosion of the steel bar. As it could be seen from the experiments, smooth steel bars just slips trough glue. Ultimate axial force (see Fig. 10) is significally smaller than characteristic axial capacity in tension suggested by Riberholt (1988) :

$R_{ax,k} = f_{ws} \cdot \rho_k \cdot d \cdot \sqrt{l_g}$, where $f_{w,s}$ is strength parametar. For brittle glues such as epoxy the value is 0.52

and about the same or smaller then characteristic axial capacity in tension suggested by Eurocode 5-Part2-Appendix A:

$F_{ax,\,Rk} = \pi \cdot d_{equ} \cdot l_a \cdot f_{v,\,k}$

It is of course logical to use rebars or threaded bars but somebody less informed must be warned that smooth steel bars are not allowed to be used in glued-in bolts joints. Or their axial tension strength capacity should be reduced.

2. From the diagrams (see Fig. 7-10.) it could be seen that the axial strength is somewhat higher for bolts glued-in perpendicular to grain direction.

3. The glued-in bolts joints should be used with lots of extra care, because during the experiments some of the results were significally failed regarding axial strength capacity witout mistakes in production.

4. Neural nerwork could be very good tool in prediction strength capacity of the glued-in bolts because it can contains much more datas which are valuable such as temperature in glue or in wood, moisture in both materials, production method, properties of various kind of glue.

5. REFERENCES

1.Bodig, J., Jayne, B.A. (1982): Mechanics of wood and wood composites. Van Nostrands Reinhold, New York, USA

2. Aicher, S., Herr, J. (1998.): Investigations on high strength glulam frame corners with glued-in steel connectors, Proceedings of 5th WCTE, Montreux, Switzerland, Vol 1.

3. Aicher, S (1992.): Testing of Adhesives for Bonded Wood-Steel Joints, Proceedings of the Meeting IUFRO S 5.02, Bordeaux, France.

4. COSMOSM 2.5 (2000.): Reference Guide, Vol1-Vol4, SRAC, USA

5. Rajčić,V, Bjelanović. A., Rak, M. (2004): Experimental Test of Glued in Bolt Joint using Threaded Steel Bars, Proceedings of 8th WCTE, Lahti, Finland, 317-320.

6. NeuroShell 2, Ward System, Reference Guide, USA.

INTERNATIONAL COUNCIL FOR RESEARCH AND INNOVATION
IN BUILDING AND CONSTRUCTION

WORKING COMMISSION W18 - TIMBER STRUCTURES

THE INFLUENCE OF THE GRADING METHOD ON THE FINGER JOINT BENDING STRENGTH OF BEECH

M Frese
H J Blaß

Universität Karlsruhe

GERMANY

MEETING THIRTY-NINE
FLORENCE
ITALY
AUGUST 2006

Presented by M Frese
I Smith asked about the finger joint profile and whether there had been any optimization work regarding softwood versus hardwood. M Frese answered the profile was based on softwood and more work would be needed to look into the optimization for hardwood.
G Schickhofer asked about bending versus tension testing of finger joint. M Frese answered that tension tests were also performed and the data could be made available.
G Schickhofer asked whether Formula 2 can be used if no finger joint in beam. The answer was yes. One could use higher value of finger joint strength so that tensile strength of the laminae governed. There was confirmation the Formula 2 was derived based on mean test data and beams were modelled to derive characteristic strengths.
H Larsen asked why tensile tests were performed if the model did not need it. H Blass responded that it was not known prior.

The influence of the grading method on the finger joint bending strength of beech

M. Frese, H.J. Blaß

Lehrstuhl für Ingenieurholzbau und Baukonstruktionen

Universität Karlsruhe, Germany

Abstract

During the last meeting in Karlsruhe the authors presented a paper [1] providing background information about the determination of the characteristic bending strength of beech glulam. A design proposal was derived to calculate the characteristic bending strength depending on the characteristic tensile strength of the lamellae and the characteristic finger joint bending strength. It was experimentally and numerically proved that visual strength grading of beech provide for strength class GL36 and mechanical grading for GL48.

The current paper gives now more detailed information about the influence of the strength grading method on the characteristic finger joint bending strength with regard to beech glulam requirements. Therefore 108 bending tests on finger joints manufactured from visually graded beech boards were performed. A further 319 tests on finger joints manufactured from mechanically graded beech boards were carried out. All the bending tests were conducted flatways according to EN 408 with a span of 15 times the height. The test results confirm a characteristic finger joint bending strength of 56 N/mm² in case of visual and 70 N/mm² in case of mechanical grading.

1 Introduction and background

The bending strength of glulam depends on the tensile strength of the lamellae and of the finger joints which may correlate. If the correlation is known, it is possible to determine the characteristic bending strength of glulam (= $f_{m,g,k}$) depending only on the characteristic tensile strength of the lamellae (= $f_{t,\ell,k}$). In the case of softwood this led to the calculation model in EN 1194, where a linear relation between the two values is given, see equation (1). Therein and in the following equation (2) the unit of the strength values is N/mm².

$$f_{m,g,k} = 7 + 1{,}15 \cdot f_{t,\ell,k} \tag{1}$$

The high tensile strength of beech (*fagus silvatica L.*) raises the question, whether the common relation (1) is also valid for a characteristic tensile strength exceeding 26 N/mm²

or if a different relation more accurately describes the laminating effect for beech glulam. It was the aim of the investigations [2], [3] and [4] to answer this question and to provide a design model for beech glulam. As a result equation (2) was derived. Therein the characteristic glulam bending strength is calculated from both the characteristic tensile strength of the boards and the characteristic finger joint bending strength (= $f_{m,j,k}$). For a better understanding equation (2) is evaluated in Fig. 1. The six curves represent different characteristic tensile strength values of beech boards, which correspond in part to the strength classes D35 – D70 in EN 338. Actually in DIN 1052 visual strength grading in class LS10 and LS13 as per DIN 4074-5 corresponds to strength class D35 and D40. In [4] it is numerically proved that visual strength grading of boards being free from knots enables even a characteristic tensile strength up to 32 N/mm² (D50) and mechanical strength grading up to 48 N/mm² (≥D60).

In the current paper the authors report on an extensive experimental investigation to determine the characteristic finger joint bending strength, which is necessary to establish beech glulam strength classes. They intend to give a basis for further standardisation of glulam made of hardwood e.g. birch or ash.

$$f_{m,g,k} = -2,87 + 0,844 \cdot f_{m,j,k} - 0,0103 \cdot f_{m,j,k}^2 \\ -0,192 \cdot f_{t,\ell,k} - 0,0119 \cdot f_{t,\ell,k}^2 + 0,0237 \cdot f_{m,j,k} \cdot f_{t,\ell,k} \qquad (2)$$

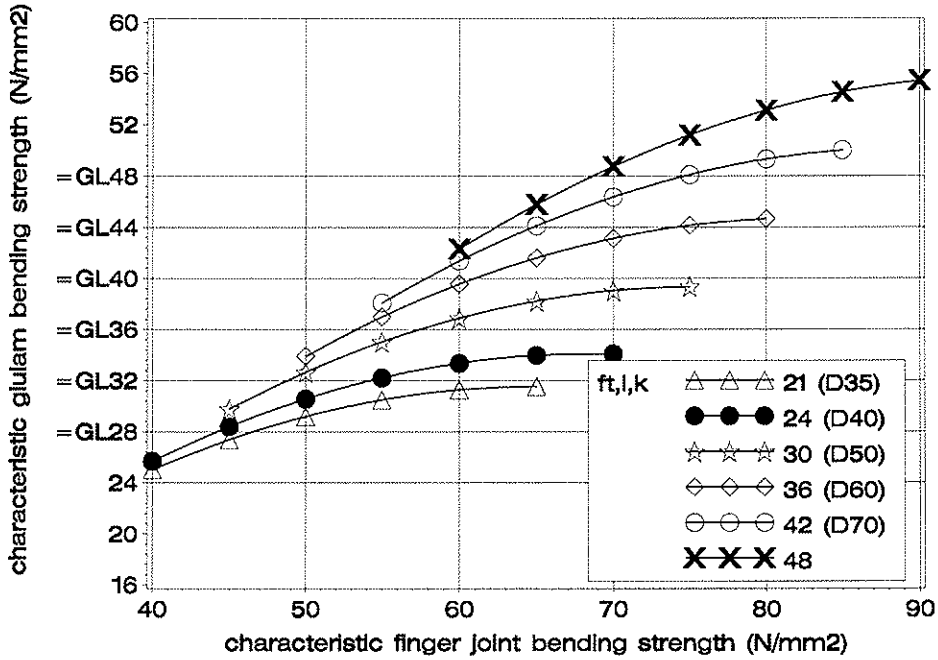

Fig. 1 Characteristic glulam bending strength depending on characteristic finger joint bending strength; evaluation of equation (2); comparison of characteristic tensile strength values corresponding to strength classes in EN 338

2 Finger joint bending strength

2.1 Material and methods

The boards to industrially manufacture the finger joint connection were delivered from three sawmills located in Germany (Nordhessen, Schönbuch and Spessart). The moisture content of the boards amounts to nearly 10%. The ends of the boards were prepared according to EN 385. The finger profile has a length of 15 mm and a division of 3,8 mm. A Melamine-Urea-Formaldehyde adhesive (Kauramin® adhesive 681 liquid and Kauramin® hardener 686 liquid) was used. 108 finger joint specimens differing in terms of source were manufactured from visually strength graded boards, see Table 1. The boards meet at least the criteria of LS10 as per DIN 4074-5 (compare Fig. 2). The MOE of the jointed boards was arbitrary, see Fig. 3 left. It is assumed that grading in LS10, LS13 or grading of boards being free from knots does not really affect the finger joint bending strength. This assumption is justified by the uniform requirements to the board ends in EN 385 and the missing grading criterion fibre deviation in case of beech in DIN 4074-5. A further 319 specimens were produced to study the influence of mechanical strength grading on the finger joint bending strength. Therefore the dynamic MOE (= E_{dyn}) as grading parameter of each board was calculated from (3).

$$E_{dyn} = (2 \cdot f \cdot \ell_{board})^2 \cdot \rho_{gross} \tag{3}$$

Therein f denotes the frequency of a longitudinal vibration, ℓ_{board} the board length and ρ_{gross} the gross density (= air dry mass/volume). The boards were graded according to the system in Table 2. Each specimen was manufactured from two boards belonging to a single grade, see Fig. 3. The 20 samples differing in terms of source and grade are assorted in Table 3. The flexural MOE of the finger joint specimens obtained by vibration methods is the bending strength reference parameter, see Fig. 4 and [6]. In Fig. 3 and Fig. 4 ℓ_j denotes the specimen length of about 20 times the height.

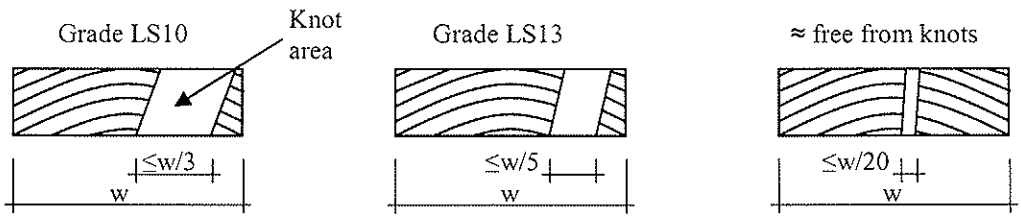

Fig. 2 Visual strength grading exemplified by the single knot: grades LS10 and LS13 according to DIN 4074-5 (left, middle) and recommended additional grade (right)

Table 1 Sample size and cross-sectional dimensions – visual grading

source	Nordhessen	Schönbuch	Spessart
N	56	21	31
width/height (mm)	100/30	105/36	110/34

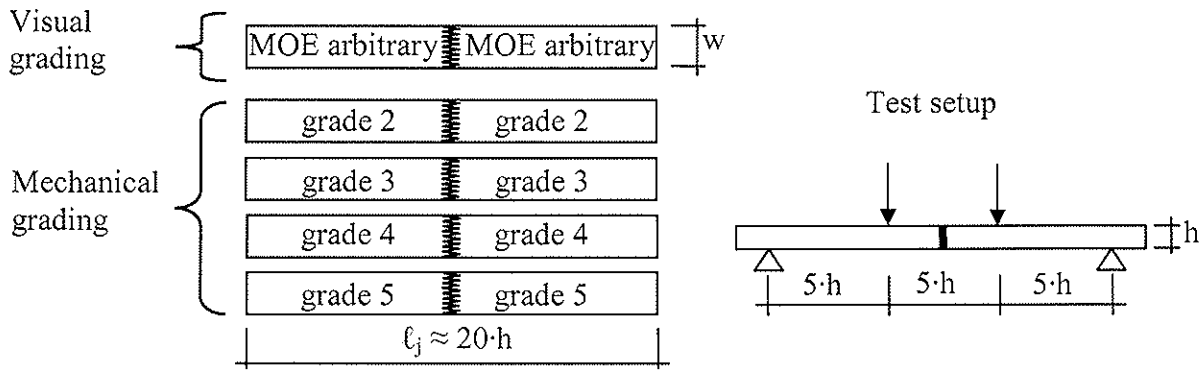

Fig. 3 Finger joint specimen manufacture (left) and test setup (right)

Table 2 Mechanical grading according to dynamic MOE; range in N/mm²

grade	2	3	4	5
range	$13000<E_{dyn}\leq14000$	$14000<E_{dyn}\leq15000$	$15000<E_{dyn}\leq16000$	$16000<E_{dyn}$

Table 3 Sample size N and cross-sectional dimensions – mechanical grading

source	Nordhessen I[1]	Schönbuch	Spessart	Nordhessen II[1]
grade 2	20	22	21	12
grade 3	22	22	25	22
grade 4	22	22	18	12
grade 5	19	22	24	14
width/height (mm)	100/29	105/34	110/33	100/28

[1] first sample coming from Nordhessen; [2] second sample coming from Nordhessen

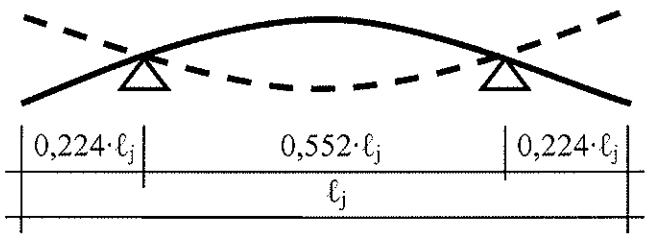

Fig. 4 Flatways flexural vibration; The connection is in the middle of the specimen.

2.2 Results

2.2.1 Visual grading of boards

The relation between bending strength and flexural MOE is shown in Fig. 5. The regression line confirms the influence of stiffness on the bending strength. Considering all specimens the 5th percentile is 56 N/mm². The range of the three 5th percentile values in terms of board source is from 50 up to 69 N/mm². This confirms in a single case a very high characteristic finger joint bending strength. The mean moisture content varies from 9,9% to 11% and the mean density from 684 kg/m³ to 695 kg/m³, see Table 4.

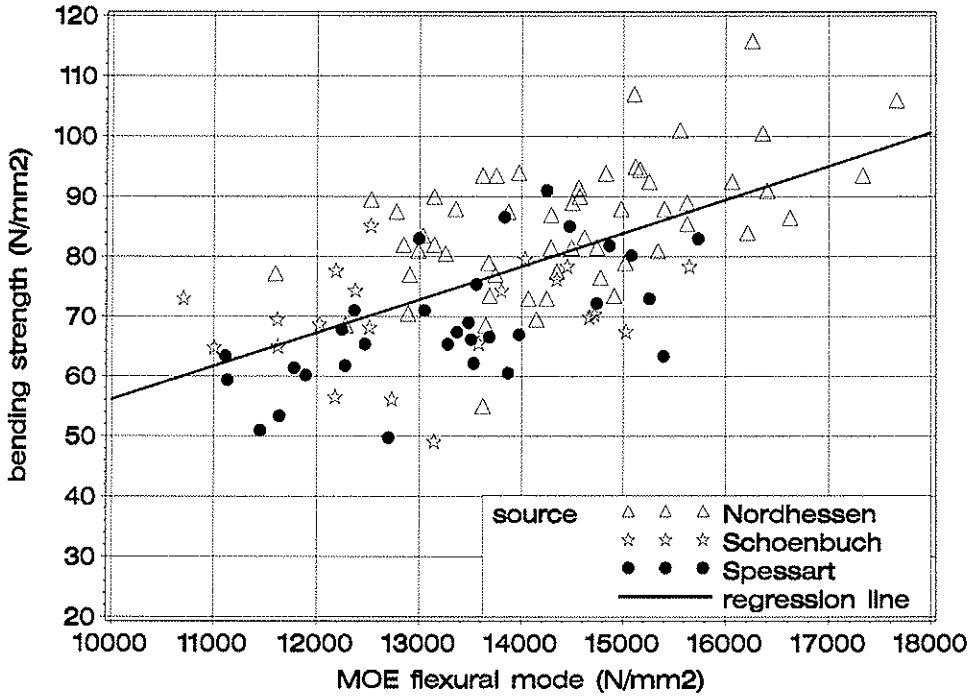

Fig. 5 Bending strength depending on reference parameter flexural MOE

2.2.2 Mechanical grading of boards

Fig. 6 shows the relation between bending strength and reference parameter flexural MOE. The symbols represent the grade of the connected boards. A correlation between the dynamic MOE of the boards determined by longitudinal vibrations and the dynamic flexural MOE of the specimens can be assumed. Hence specimens manufactured from boards of grade 2 and 3 lie on the left and those from boards of grade 4 and 5 on the right side of the diagram. The nonlinear regression curve and the 90% confidence limits indicate an upper limit for the mean and characteristic bending strength. For a better understanding of the influence of board grade and source on the mean and characteristic values Fig. 7 and Fig. 8 show the trend of these values (compare Table 6). It is remarkable that no increase of bending strength between grades 4 and 5 can be observed. Hence the specimens belonging to grade 4 and 5 were merged: The 5th percentile value amounts to 69,3 N/mm². In terms of technical feasibility mechanical grading of grades 4 and 5 can lead to a 5th

percentile value exceeding 70 N/mm². Concerning the 4 grades the mean bending strength values in the sample Nordhessen II is in part significantly higher than in the remaining samples. This may be caused by better steel of the finger joint cutter used only during the manufacture of this sample. This steel provides higher rigidity and longer tool life. The 5th percentile value (56 N/mm²) in case of visual grading is nearly equal to the 5th percentile value of specimens belonging to grade 3 (58,8 N/mm²). Hence the advantage of mechanical grading begins when grading boards which exceed a dynamic MOE of about 14000 or 15000 N/mm². The mean moisture content of the specimens in the four samples varies from 8,2% to 9,8% and the density from 672 kg/m³ to 681 kg/m³, see Table 5.

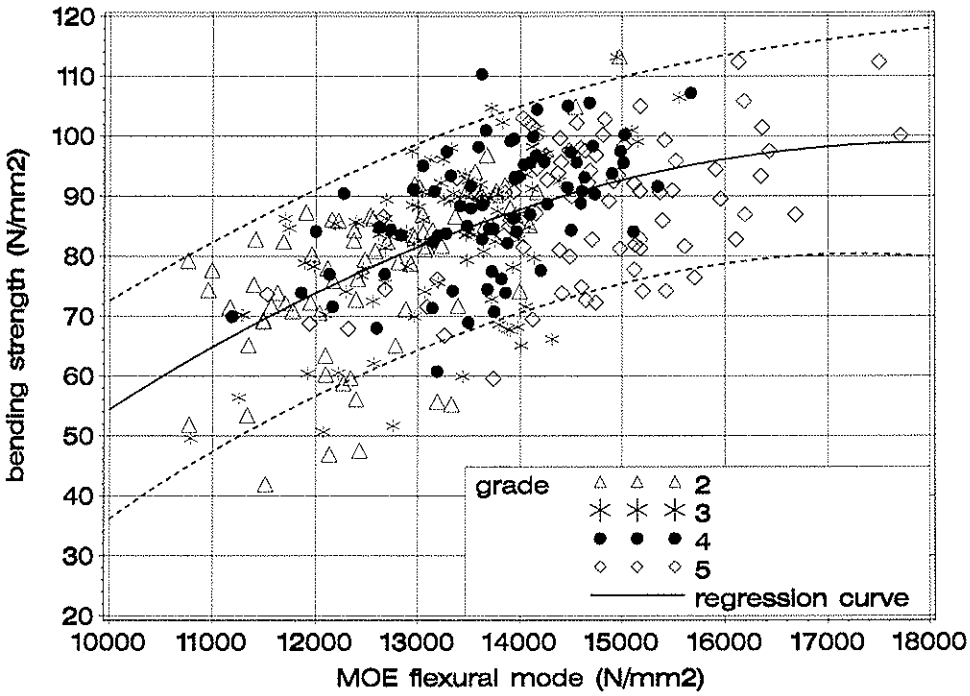

Fig. 6 Bending strength depending on reference parameter flexural MOE

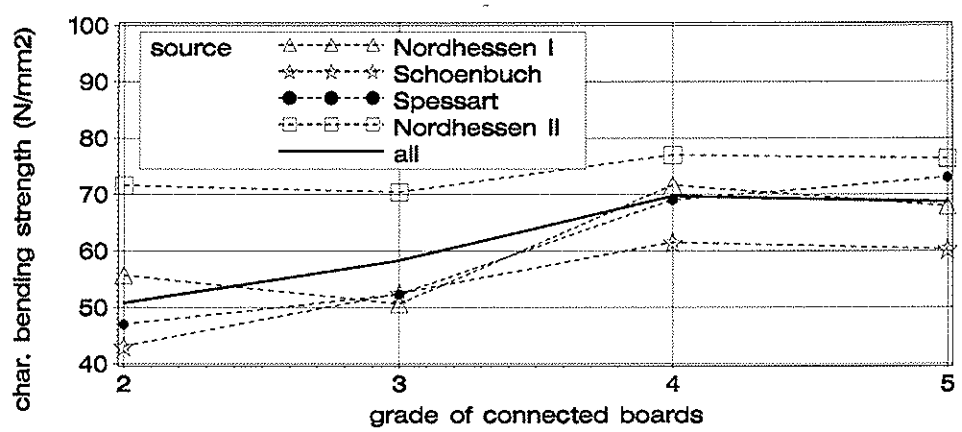

Fig. 7 5th percentile bending strength over grade of connected boards

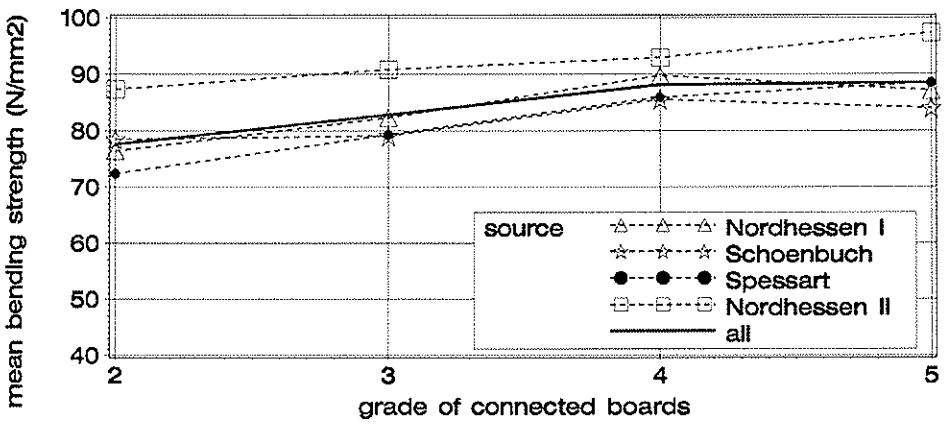

Fig. 8 Mean bending strength over grade of connected boards

3 Conclusions

On the basis of Fig. 1 and the experimental data the following conclusions can be drawn:

- In DIN 1052 visual strength grading of beech in class LS10 and LS13 corresponds to the strength classes D35 and D40, respectively. The characteristic finger joint bending strength of such visually graded boards amounts to nearly 56 N/mm². Hence it is possible to establish GL28 and GL32 with standard visual strength grading methods.

- Assuming that visual strength grading of beech boards being free from knots corresponds to D50 and that finger joint manufacture provides a characteristic bending strength of 58 N/mm² it is even possible to produce GL36.

- Mechanical strength grading of beech boards having a dynamic MOE determined from longitudinal vibrations of at least 15000 N/mm² and additional demands on knots are precondition for strength classes equal to or greater than D60. For those boards a characteristic finger joint bending strength amounts to nearly 70 N/mm². Under optimised production conditions in terms of finger joint manufacture higher values are even possible. Hence strength classes up to GL52 are imaginable.

4 References

[1] Frese M, Blaß HJ (2005). Beech Glulam Strength Classes. CIB-W18/38-6-2, Karlsruhe, Germany

[2] Blaß HJ, Denzler JK, Frese M, Glos P, Linsenmann P (2005). Biegefestigkeit von Brettschichtholz aus Buche – Bending strength of beech glulam (only available in German). Band 1. Karlsruher Berichte zum Ingenieurholzbau. Universitätsverlag Karlsruhe 2005

[3] Frese M, Blaß HJ (2006). Characteristic bending strength of beech glulam. Submitted for publication in Materials & Structures. Rilem France

[4] Frese M (2006). Die Biegefestigkeit von Brettschichtholz aus Buche - Experimentelle und numerische Untersuchungen zum Laminierungseffekt – The Bending strength of beech glulam – Experimental and numerical investigations (only available in German). Karlsruhe, Universität (TH). Dissertation

[5] Blaß HJ, Frese M (2006/2007). Die Biegefestigkeit von Keilzinkenverbindungen aus Brettern der Buche (*fagus silvatica L.*) – The finger joint bending strength of beech (only available in German). Manuskript zur Veröffentlichung bei Holz als Roh- und Werkstoff eingereicht.

[6] Görlacher R (1984). Ein neues Messverfahren zur Bestimmung des Elastizitätsmoduls von Holz – A new method for determining the modulus of elasticity of timber (only available in German). Holz als Roh- und Werkstoff. Vol. 42. P. 219-222

EN 338:2003. Bauholz für tragende Zwecke – Festigkeitsklassen – Structural timber – Strength classes

EN 385:2001. Keilzinkenverbindungen im Bauholz – Leistungsanforderungen und Mindest-anforderungen an die Herstellung – Finger jointed structural timber – Performance require-ments and minimum production requirement

EN 408:1995. Bauholz für tragende Zwecke und Brettschichtholz – Bestimmung einiger physikalischer und mechanischer Eigenschaften – Structural timber and glued laminated timber – Determination of some physical and mechanical properties

DIN 1052:2004-08. Entwurf, Berechnung und Bemessung von Holzbauwerken – Allgemeine Bemessungsregeln und Bemessungsregeln für den Hochbau – Design of timber structures – General rules and rules for buildings (only available in German)

EN 1194:1999. Brettschichtholz – Festigkeitsklassen und Bestimmung charakteristischer Werte – Glued laminated timber – Strength classes and determination of characteristic values

DIN 4074-5:2003-06. Sortierung von Holz nach der Tragfähigkeit, Teil 5: Laubschnittholz – Strength grading of wood - Part 5: Sawn hard wood (only available in German)

5 Appendix

Table 4 Bending strength, moisture content and density statistics in terms of source; specimens manufactured from visually graded boards

	Nordhessen	Schönbuch	Spessart	all
bending strength (N/mm²)				
n	56	21	31	108
$\bar{x}$	85,2	70,0	68,8	78
s	10,6	8,7	10,4	13
5%	68,5	49,5	50,4	56
CL_{95}[1]	62,6-71,5	47,9-60,4	44,5-56,4	52-60
moisture content[2] (%)				
$\bar{x}$	9,85	10,1	11	-
s	0,579	0,519	0,681	-
min-max	8,85-11,9	9,14-11,0	8,15-13,4	-
density[2] at given moisture content (kg/m³)				
$\bar{x}$	695	687	684	690
s	44,1	34,6	47,7	44
min-max	575-822	616-752	584-816	575-822
[1 and 2] see Table 6				

Table 5 Moisture content and density statistics in % in terms of source; specimens manufactured from mechanically graded boards

source	Nordhessen I	Schönbuch	Spessart	Nordhessen II
moisture content[2] (%)				
$\bar{x}$	8,88	9,84	9,64	8,24
s	0,345	0,432	0,822	0,228
min-max	7,98-9,70	8,95-10,6	8,80-12,1	7,69-8,85
density[2] at given moisture content (kg/m³)				
$\bar{x}$	672	681	681	672
s	39,2	32,3	33,8	38,9
min-max	583-817	606-786	595-781	588-786
[2] see Table 6				

Table 6 Bending strength and density statistics in terms of board grade; specimens manufactured from mechanically graded boards

source		grade				
		2	3	4	5	4+5
bending strength (N/mm²)						
Nordhessen I	n	20	22	22	19	41
	$\bar{x}$	76,4	82,3	89,7	87,1	88,5
	s	9,73	13,2	10,1	10,6	10,3
	5%	55,7	51,2	71,6	67,9	71,4
Schönbuch	n	22	22	22	22	44
	$\bar{x}$	78,5	79,1	85,5	84,0	84,7
	s	13,3	12,2	11	12,3	11,6
	5%	43,1	52,5	61,5	60,3	62
Spessart	n	21	25	18	24	42
	$\bar{x}$	72,4	79,3	85,9	88,5	87,4
	s	14,7	12,5	9,42	9,15	9,24
	5%	47	52,3	69,0	73,0	71,0
Nordhessen II	n	12	22	12	14	26
	$\bar{x}$	87,3	90,8	92,9	97,3	95,3
	s	12,5	10,6	10,2	9,47	9,87
	min/5%	71,6	70,4	77	76,4	76,6
all	n	75	91	74	79	153
	$\bar{x}$	77,6	82,8	88,1	88,5	88,3
	s	13,4	12,9	10,4	11,3	10,8
	5%	50,8	58,3	69,7	68,7	69,3
	CL_{95}[1]	50,2-59,7	57,0-65,3	66,8-74,2	65,6-73,4	67,6-72,9
density[2] (kg/m³)						
	$\bar{x}$	661	671	678	699	-
	s	37,6	28,7	36,4	31,5	-
	min-max	583-770	605-752	589-786	621-817	-

[1] 95% Confidence limits of the characteristic value assuming normal distributed data

[2] determined at both ends of the specimens as per EN 408

INTERNATIONAL COUNCIL FOR RESEARCH AND INNOVATION
IN BUILDING AND CONSTRUCTION

WORKING COMMISSION W18 - TIMBER STRUCTURES

FIRST EVALUATION STEPS OF DESIGN RULES IN THE EUROPEAN AND GERMAN CODES OF TRANSVERSE TENSION AREAS

S Franke

B Franke

K Rautenstrauch

Institute of Structural Engineering

Chair of Timber and Masonry Engineering

Bauhaus-University Weimar

GERMANY

MEETING THIRTY-NINE

FLORENCE

ITALY

AUGUST 2006

Presented by B Franke

H Blass stated that although the results showed values in the German design code to be conservative, volume effect was not considered; therefore, for larger beams this conservatism would disappear. Also S Aicher recently tested 900 mm deep beams with holes and results clearly showed a size effect.

I Smith stated that he planned to perform notch beam tests on large glulam members (7m long). I Smith commented that surface observation versus internal behaviour could be different. Even observation of behaviour on both sides show they are different.

B Franke agreed and thin cross section tended to give better results compared with thick cross sections.

First evaluation steps of design rules in the European and German codes of transverse tension areas

Steffen Franke
Bettina Franke
Karl Rautenstrauch

Institute of Structural Engineering
Chair of Timber and Masonry Engineering
Bauhaus-University Weimar, Germany

1 Introduction

Wood is an inhomogeneous, anisotropic and very porous material. This is reflected in the different failure mechanisms depending on the loading. In contrast to the ductile behaviour due to compression stress, the structural behaviour is characterized as brittle due to tension or shear stress. Characteristic parameters of strengths are used for the evaluation of the load-carrying capacity in the standards. As close-to-reality the capacity of transverse tension areas, e.g. notches and holes, can be estimated. The fracture mechanics methods allow the consideration of cracks and their behaviour. This approach is marginally included in parameters of the present standards.

In test series with small specimens of solid wood and practical specimens of glued laminated timber the strength behaviour of beams with notches and holes was determined. Additionally to the classical measuring methods, a new measuring procedure developed at the chair of timber and masonry engineering was used to determine the deformation behaviour. This new approach is based on the principle of photogrammetry. The principle of the photogrammetric measurement enables to determine the development of deformations and crack growth in several discrete ranges by determining coordinate vectors with extremely high accuracy. Strain distributions over the height of the specimen can be determined, deformations and stress concentrations on the specimen surface can be located by the evaluation of the deformations of the applied points.

Using this measuring method, fracture mechanics parameters could be directly determined due to the construction behaviour by the implementation of measured crack growth at the notches into numeric models. The comparison of the results with previously released assumptions leads to new conclusions.

2 Fracture Mechanic

2.1 Mode I

The conducted test series with only transverse tensioned stresses are the basis for fracture-mechanics evaluation of complex stress situations at notches and holes. The aim of the experimental investigations was to achieve a stable crack growth with a constant increasing of the load, in order to specify the softening behavior, for the calibration of numeric calculations. The photogrammetric measuring system developed at the department of wood and masonry engineering can detect the softening respectively the hardening behaviour of specimens during experimental investigations within the macroscopic range with a present frequency of up to 5 frames per second. The used test concept for investigations of mode I, tensile stress perpendicularly to the grain, referred to the Draft standard [3], developed for wood in context of CIB-W18A.

Using the experimentally gained complete load-displacement curves the median fracture energy can be determined according to [3]. Parallel to determining fracture energies the experimentally determined load-displacement curves implicitly the softening behavior for each specimen in numeric calculations, q.v. Fig. 1 can be reproduced. In further FE-simulations the crack resistance curves are determined on the basis of the path-independent line integral, which describes the energy release rate with linear elastic material behavior. The curve of the energy release rate related to the crack growth allows the determination of the critical energy release rate and the characterization of the crack growth in the post critical range. When the critical energy release rate is reached one speaks of the change of the stable to unstable crack growth. Fig. 2 presents exemplarily the developed crack resistance curve with the associated energy lines for a specimen tensile stressed in RL-plane. Additionally there, the level of the median fracture energy and the critical fracture energy is represented, too.

Schatz presented several publications in [20], in which is defined the ratio of the critical fracture energy and the median fracture energy. In most of them the ratio for the RL- such as TL-crack system is less than one. In contrast to this the ratio, as average value, for the RL-system was determined to $G_{IC}/G_F = 1{,}03$ and for the TL-system to $G_{IC}/G_F = 1{,}15$ in the context of this research project. This means that the released energy is approximately equal with the median fracture energy, determined throughout the failure process, when the instable crack behavior begins stressed by tension perpendicularly to the grain.

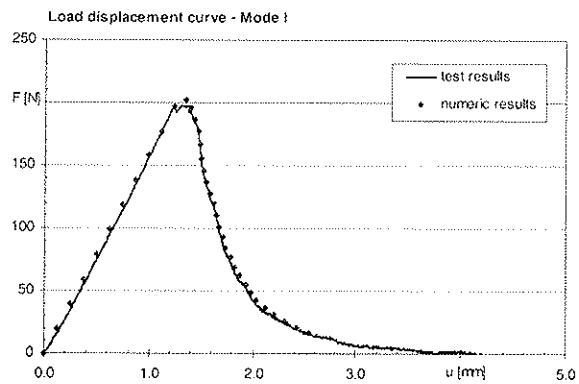

Fig. 1: Load displacement curve, RL-crack system

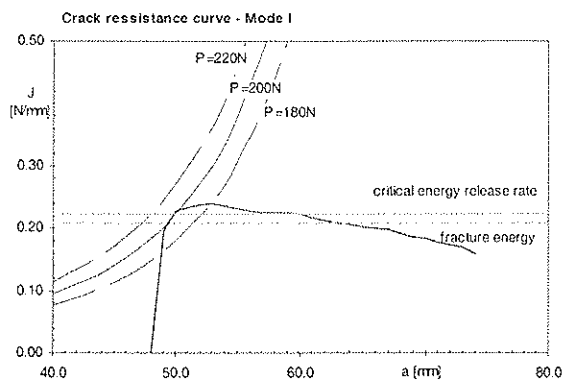

Fig. 2: Crack resistance curve for mode I with the specific energy levels, RL-crack system

2.2 Mixed Mode

At significant failure areas with stress concentrations, e.g. at notches or holes, no pure fracture modes are definable. In the process zones of the structural member an interaction of shear and transverse tension and/or transverse compression exists, called mixed mode. As basis for the estimation of the shear effect in interaction with transverse tension the specific fracture energies were determined by splitting the J-integral of the fracture mode I and II in plane stress on the basis of a parameter study with numeric simulations, q.v. Fig. 3. The fundamental algorithm for the determination of the fracture mechanics parameters including the interaction of transverse tension and shear stress could be verified with the numeric calculations. The diagram (Fig. 4) presents the determined relation between the released energy at constant load and constant crack length at different stress ratios separately for the RL- and TL-crack system. The trend of the released energy for the crack mode I, transverse tension, decreases continuously with the stress ratio. Whereas for the fracture mode II, shear stress, an energetically constant level within the range of this combined stress is presented.

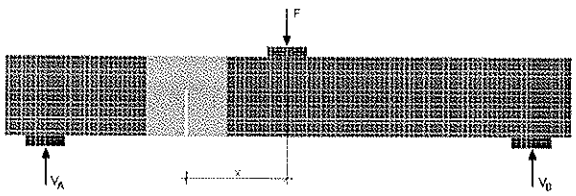

Fig. 3: Numeric model for the parameter studies

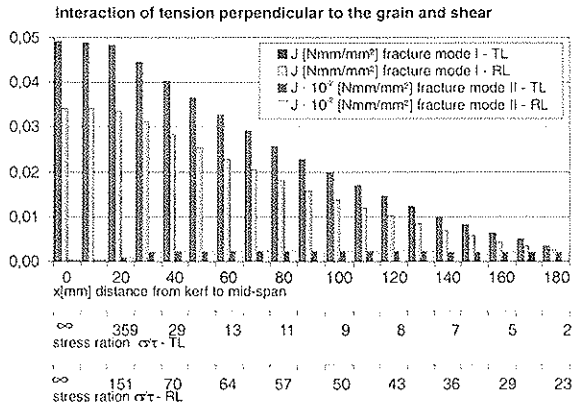

Fig. 4: Fracture energy of mode I and mode II with different stress ratios

3 Endnotched Beam

3.1 Failure Loads

Successively to the preliminary considerations, experimental investigations were executed with practically relevant endnotched beams of glued laminated timber. These investigations were aimed at the estimation of the load-carrying capacity of transverse tensioned areas and they were important for the consideration of the interaction of transverse tension with shear for the determination of fracture-mechanics parameters. The comparison of the experimentally determined failure loads and the calculated characteristic loads of the European and German codes indicates an enormous research necessity. Different cross sections and notch heights were tested way-controlled with a constant span of l_s = 160 cm as three point bending tests. In Fig. 5 and Fig. 6 it is visible, that a part of the reached fracture loads as well as their 5%-quantile are less than the characteristic values of DIN 1052:2004-08 and/or prEN 1995-1-1:2003 and the calculated loads of Gustafsson [7].

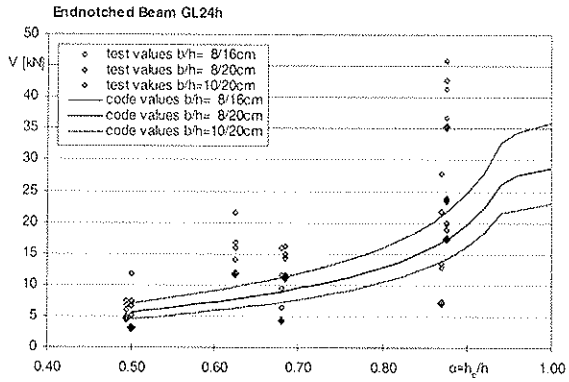

Fig. 5: Comparison of fracture loads with 5%-quantile and the values of DIN 1052:2004-08 with $f_{v,k}$=0,7·3,5 N/mm²

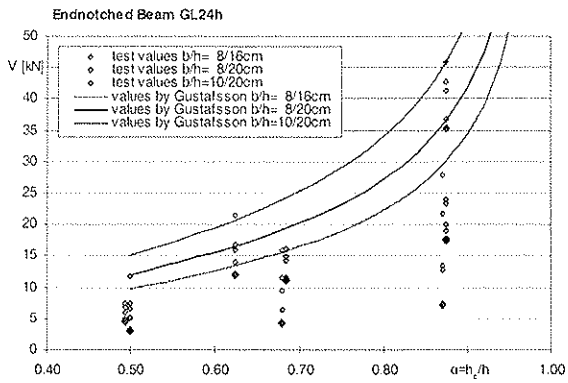

Fig. 6: Comparison of fracture loads with 5%-quantile and the method by Gustafsson with G_c = 0,3 N/mm

The approach developed by Gustafsson in [5] was the basis for the design method of the standards for the estimation of the load-carrying capacity of notched structures. In contrast to the conventional stress criterion Gustafsson obtained the energy balance consideration, which considers the change of the energy due to the crack propagation, in order to determine the limit value of the transverse force when the instable crack growth begins. Larsen [11] modified the approach of Gustafsson for the development of simple design equations for the standard. The ratio of the modulus of elasticity to the shear modulus E_0/G_v was set to 16 and it was assumed that $\sqrt{E_0 \cdot G_c}$ is proportional to the shear strength f_v of the material. Thus the necessary material parameter G_c was not again introduced but considered by an experimentally determined proportionality constant. The use of fracture mechanics for the evaluation of notched structures is principally appropriate, but the simple assumption of a constant critical energy release rate is to be regarded differentially. During the failure process an interaction of fracture mode I (transverse tension) and fracture mode II (shear stress) exists at the area of the notch.

3.2 Fracture Mechanics

The specific crack resistance curves for the fracture mode I and fracture mode II were determined by numeric simulation calculations with implemented continuous crack growth at selected specimens of the test series for notches. The applied crack length corresponds to the photogrammetric measured[1] crack length at the experimental investigations at notches. In Fig. 10 the crack resistance curves for fracture mode I and II with the corresponding energy lines are exemplary represented for an specimen with notch ratio $\alpha = 0.875$. The curves confirm the typical failure behavior of notches, observed in the test. With incipient crack a short crack growth exists by approximate constant load. In further crack growth with continuous increasing load the energy release rate increases constantly up to instable crack growth (collapse). Due to the natural defect distribution of wood the described crack growth can vary. Fig. 7 presents a defect free process zone with the associated crack resistance curve. In contrast to this, defects, e.g. knots parallel to the crack plane (Fig. 8) or knots normally to the crack plane (Fig. 9) can increase the crack resistance of wood. Likewise, these findings are mirrored in the crack resistance curve. One cannot compare the critical energy release rate determined from the mixed mode situation separately for the

[1] Testing of wood by photogrammetric measurement, see [4], [5]

part of transverse tension and the part of shear stress with the pure critical energy release rate, because they vary as a function of the existing interaction.

The critical energy release rates determined experimentally from the conducted test series for mode I and II are opposed in Fig. 11 separate to the notch ratio and the cross section. It shows clearly that the fracture mode II – mode I ratio of the critical energy release rate of notches at glued laminated timber beams converges to one with increasing of the effective height. The same was already determined at test series with solid timber beams [4].

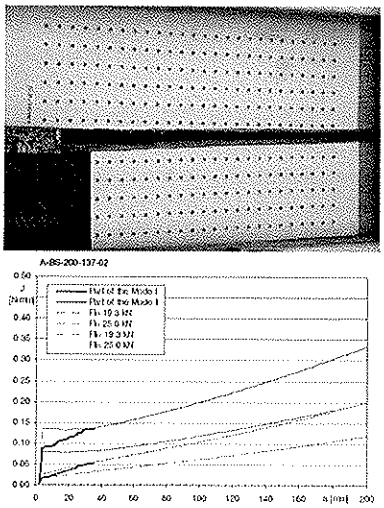

Fig. 7: Defect free process area; corresponding crack resistance curve

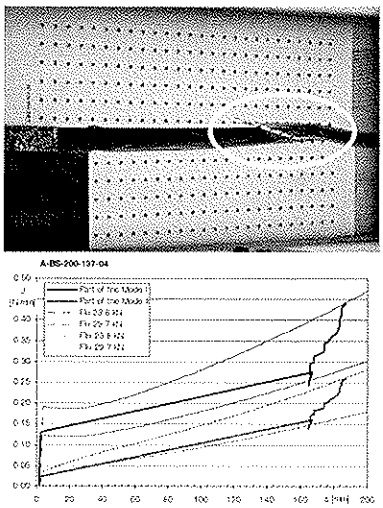

Fig. 8: One knot parallel to crack plane; corresponding crack resistance curve

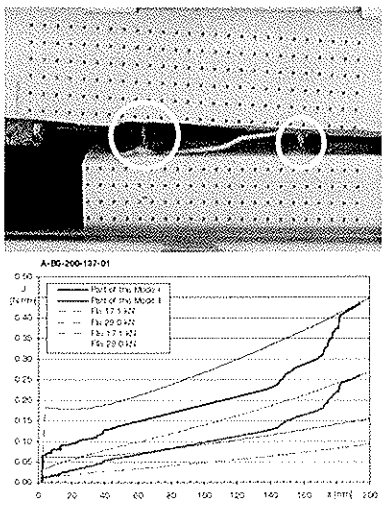

Fig. 9: Two knots normally to crack plane; corresponding crack resistance curve

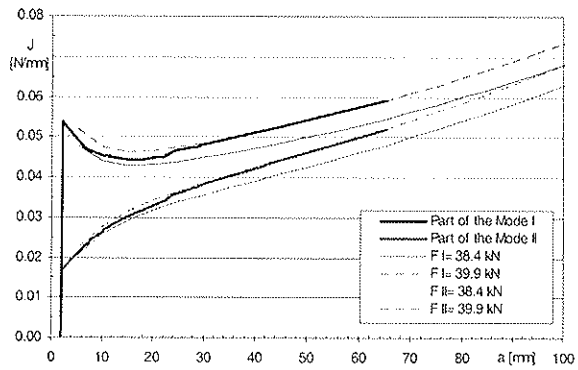

Fig. 10: Crack resistance curve of mode I and mode II for endnotched beam with $\alpha = 0.875$, b/h = 8/20cm

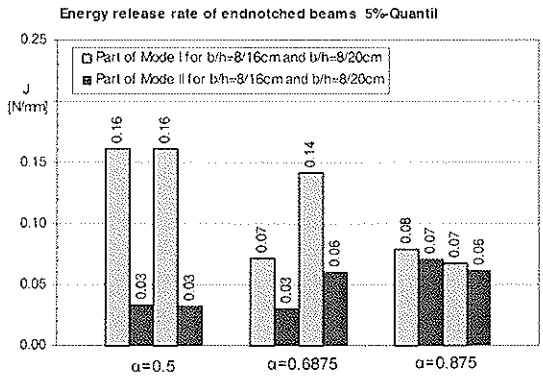

Fig. 11: Energy release rate of mode I and mode II for test specimen with b/h = 8/16cm and b/h = 8/20cm, GL 24h

4 Holes

4.1 General

In past years test series were made by different scientists, e.g. Aicher, Hoefflin [1] for the investigation of the influence of different internal force combinations or different geometry - sizes ratios. On this basis, four test series were carried out with different hole geometries for a fracture-mechanics evaluation of the influence of holes to the carrying and failure

behavior of glued laminated timber beams. The holes are placed in the range of combined transverse force and moment stress at ¼ of the span. The investigations were made at glued laminated timber beams with a quality GL24h and cross sections of b/h = 100/320mm, 100/400mm and 100/480mm with round and/or rectangular holes. The conditions l = 5·h and h_d = 0.4·h (centric) as well as the situation of the hole centrically with l/4 were constant for all beams. The specimens were way-controlled loaded as three point bending test.

For the investigation of the deformation and the failure behavior the strain distributions in the two transverse tension stressed areas of the holes and the crack growth were determined by means of photogrammetric measuring procedures. For this measuring, areas with a grid distance of approx. 8mm were applied at the transverse tension stressed areas analog to Fig. 12. Following crack resistance curves could be determined with the attained data using FE-simulations. These could be used for the estimation of the material resistance against cracking and thus for the estimation of the failure behavior.

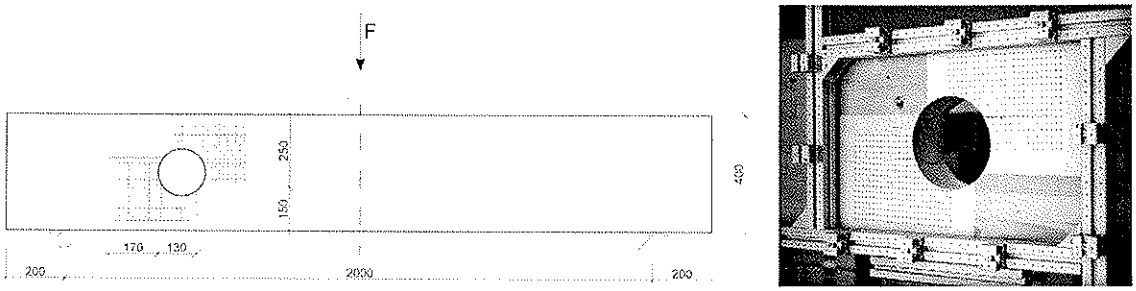

Fig. 12: Dimensions and arrangement of the measuring area as sketch as well as measuring photo of glued laminated timber 100/400 mm with round hole

4.2 Failure loads

Presently three different calculation concepts according to prEN 1995-1-1:2003 and DIN 1052:2004-08 as well as one of Gustafsson presented in [7] are available for the estimation of the load-carrying capacity of holes.

In prEN 1995-1-1:2003 based on a linear fracture-mechanics failure model the design led back to a design of endnotched bending beams with the half cross-sectional height and a halved transverse force. The fracture-mechanics failure model is integrated in the reduction factor for the shear strength $f_{v,k}$. In contrast to the DIN 1052:2004-08, the moment influence is completely ignored here. The design of round holes is provided by a notch with a notch inclination of 45°. The assumption is not used in the new Eurocode EN 1995-1-1:2004.

The design approach presented by Gustafsson in [7] is taken out of a Swedish design rule and is based on the concept of a classical shear stress proof like the procedure of the prEN 1995-1-1:2003. The reduction factor k_v is replaced here by the factor k_{hol}, in which only the relation between hole size and beam depth is considered. The moment influence is also ignored. In DIN 1052:2004-08 the proof is leaded back to a conventional stress verification of perpendicular tensile strength, $f_{t,90}$. The determination of the reference value of tension $F_{t,90}$ considers the parts of the action effects moment and transverse force, which are determined separately and added.

In Fig. 13 the calculated values of the presented dimensioning methods determined with characteristic strength values are confronted to the test results. The values of the dimensioning methods can reproduce the trend of the reached failure loads. However load

reserves to the 5%-Quantil values of the test results are visible in contrast to the determined notched results. A better utilization of the load-carrying capacity can result from adjusting the dimensioning methods.

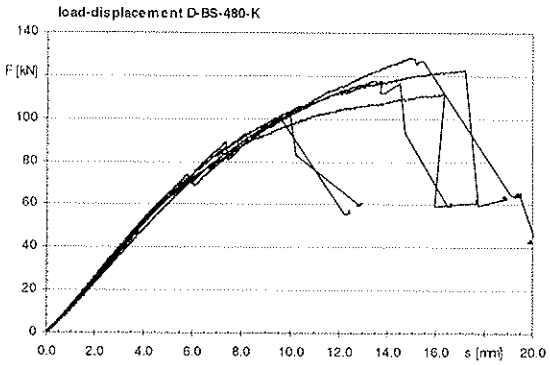

Fig. 13: Load-displacement-curves of test serie D-BS-480-K

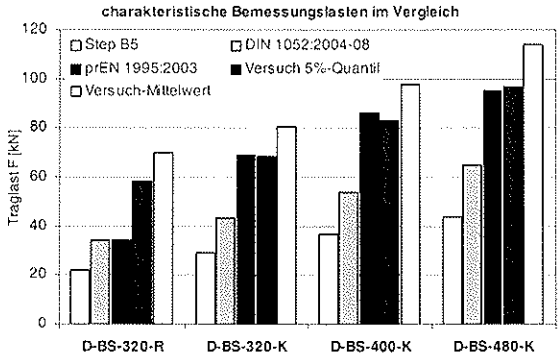

Fig. 14: Comparison of characteristic values of different methods with test values

4.3 Fracture Mechanics

Analog to the investigations of notches it was substantially more complex to determine the parameters for fracture behaviour at holes using numerical simulations with implemented crack growth. So far crack resistance curves could be determined only in the beginning in view of the changing multi-axial stresses and simultaneous consideration of the energies at two locally separated transverse tension areas with different crack growth. It must be noted that for an explicit correlation of the energy lines these are depended on their different crack growth and their position of the crack initiation.

In principle it could be observed that the crack initiation were at the right upper hole corner (area with higher moment, see Fig. 15) at first with approx. 70% of the tests. With approx. 13% a simultaneous crack growth begins. Aicher locates the area with superposed stress maximum between the extreme values of transverse force and moment ($\varphi_V = 40° \leq \varphi_{M/V} \leq \varphi_M = 60°$). The crack initiation places determined in the tests were at the lower range for DBS-320-K with $\alpha_o = \alpha_u \approx 42°$, $\alpha_o \approx 40°$ and for DBS-400-K with $\alpha_u \approx 42{,}5°$ and in the middle for DBS-480-K with $\alpha_o \approx 51°$ und $\alpha_u \approx 48°$.

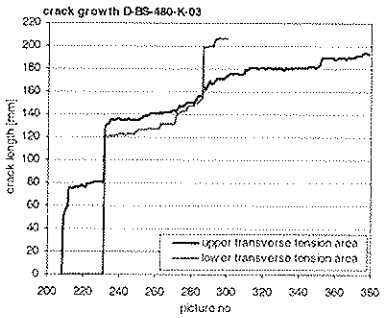

Fig. 15: Crack growth for D-BS-480-K-03

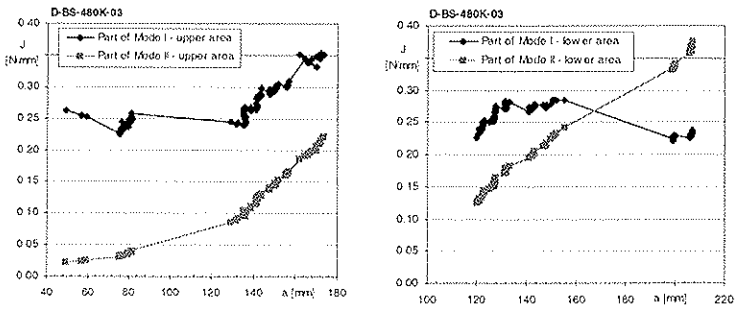

Fig. 16: Crack resistance curves for the mode I and II for the upper and lower tensioned area of D-BS-480-K-03

Areas with instable crack growth and following further stable crack growth can recognized in crack growth (Fig. 15) as well as the crack resistance curves (Fig. 16). This could be likewise observed well during the tests. In this phase the crack resistance curves for mode I decrease characteristically for all tests, however the crack resistance curves for mode II constantly increase. The failure usually happened at the lower support-sided hole edge with

shear failure. The tests and the determined results provide a basis for further investigations to improve the dimensioning methods.

5 Conclusion

The failure loads, reached in tests for endnotched glued laminated timber beams, show a clear deficit in the current dimensioning methods. In the presented fracture-mechanics studies about mixed mode situations at notches, the part of the fracture mode I and fracture mode II could be identified clearly. The determined critical energy release rates at practice-relevant test specimens show that the assumption of a constant critical energy release rate for all notch ratios is to be seen critically. The verified shear force at the notch or crack tip should not remain unconsidered contrary to the predominant transverse tension stress. The current dimensioning methods of the standards and the method from Gustafsson [5] could represent the developing of the reached failure loads. But the cause of the existing differences could be the simple assumption of a constant G_c. The presented results provide a basis for further investigations for the formulation of new or modified approaches for the estimation of the load-bearing capacity and to ensure the necessary parallel numeric parameter studies.

Holes have a stress situation consisting of transverse tension stress and shear stress like notches. The investigation of the failure behaviour is substantial more complex due to the failure that happens at two locally separated process areas and the different momentary stress. Crack resistance curves of the conducted tests could be already determined separately for mode I and mode II. During an instable crack growth these curves show a decrease for mode I and an increase for mode II. A clear load difference was detected in comparison with the presented failure loads and the calculated dimensioning loads of different dimensioning methods. The current results of the investigations can lead to an improvement of the dimensioning methods.

6 References

[1] Aicher, S.; Höfflin, L.; Reinhardt, H.-W. (2003): Verifizierung versagensrelevanter Dehnungsverteilungen im Bereich runder Durchbrüche in Brettschichtholzträgern. In: Bautechnik 80 (2003) 8, S. 523-533

[2] Blaß, H.J.; Bejtka, I. (2003): Querzugverstärkungen in gefährdeten Bereichen mit selbstbohrenden Holzschrauben. Forschungsbericht Universität Karlsruhe.

[3] Draft Standard (1989/1990): Determination of the fracture energy of wood for tension perpendicular to the grain. CIB-W18A

[4] Franke, S.; Franke, B.; Rautenstrauch, K. (2004): Determination of fracture mechanics parameters for wood with the help of close range photogrammetry. CIB-W18A/ 37-19-2, Edinburgh, United Kingdom

[5] Franke, S.; Franke, B.; Rautenstrauch, K. (2005): Beanspruchungsanalyse von Holzbauteilen durch 2D-Photogrammetrie. In: Bautechnik 82 (2005) 2, S. 61-68

[6] Gustafsson, P.J. (1988): A study of strength notched beams. CIB-W18A/ 21-10-1,.Parksville, Canada

[7] Gustafsson, P.J. (1995): Ausgeklinkte Träger und Durchbrüche in Brettschichtholz. In: Holzbauwerke Bemessung und Baustoffe nach Eurocode 5 Step1-B5/1. Fachverlag Holz, Düsseldorf

[8] Haase, K. (2003): Bruchmechanische Ansätze zur Bemessung von Durchbrüchen in Brettschichtholzträgern. In: Bautechnik 80 (2003) 8, S. 506-512

[9] Höfflin, L. (2004): Runde Durchbrüche in Brettschichtholzträgern – Experimentelle und theoretische Untersuchungen. Dissertation, Materialprüfanstalt Univ. Stuttgart

[10] Höfflin, L.; Aicher, S. (2003): Design of rectangular holes in glulam beams. In: Otto-Graf-Journal Vol. 14, S. 211-230

[11] Larsen, H.J. (1992): Latest development of Eurocode 5. CIB-W18A/ 25-102-1. Ahus, Sweden

[12] Larsen, H.J.; Gustafsson, P.J. (1991): The fracture energy of wood in tension perpendicular to the grain. CIB-W18A/ 24-19-1. Oxford, United Kingdom

[13] Larsen, H.J.; Gustafsson, P.J. (1989): Design of endnotched beams. CIB-W18A/ 22-10-1. Berlin, Germany

[14] Logemann, M. (1991): Abschätzung der Tragfähigkeit von Holzbauteilen mit Ausklinkungen und Durchbrüchen. Dissertation, VDI- Verlag Düsseldorf

[15] Logemann, M.; Schelling, W. (1992): Die Bruchzähigkeit von Fichte und ihre wesentlichen Einflussparameter – Untersuchungen im Mode-II. In: Holz als Roh- und Werkstoff 50 (1992) S.117-121

[16] Mall, S.; Murphy, J.F.; Asce, M.; Shottafer, J.E. (1983): Criterion for mixed mode fracture in wood. In: Journal of engineering mechanics 109 (1983) S. 680-690

[17] Mansfield-Williams, H.D. (2001): An end-notched beam test for specific fracture energy in mixed mode in timber. In: Materials and structures 34 (2001) S. 224-227

[18] Petersson, H. (1995): Fracture Design analysis of wooden beams with holes and notches, finite element analysis based on energy release rate approach. CIB-W18A. Copenhagen

[19] Petersson, H. (1992): On design criteria for tension perpendicular to the grain. CIB W18A/ 25-6-4. Ahus, Schweden

[20] Schatz, T. (1994): Zur bruchmechanischen Modellierung des Kurzzeit-Bruchverhaltens von Holz im Rissöffnungsmodus I. Universität Stuttgart, Institut für Werkstoffe im Bauwesen, Dissertation

[21] Tan, D.M.; Stanzl-Tschegg, S.E.; Tschegg, E.K. (1995): Models of wood fracture in Mode I and Mode II. In: Holz als Roh- und Werkstoff 53 (1995), S.159-164

[22] Valentin, G.; Caumes, P. (1989): Crack propagation in mixed mode in wood: a new specimen. In: Wood Science and Technology 23 (1989), S.43-53

INTERNATIONAL COUNCIL FOR RESEARCH AND INNOVATION
IN BUILDING AND CONSTRUCTION

WORKING COMMISSION W18 - TIMBER STRUCTURES

TIMBER DENSITY RESTRICTIONS FOR TIMBER CONNECTION TESTS ACCORDING TO ISO8970/EN28970

A Leijten
Delft University of Technology
THE NETHERLANDS

J Köhler
Swiss Federal Institute of Technology, Zürich
SWITZERLAND

A Jorissen
University of Technology, Eindhoven
THE NETHERLANDS

MEETING THIRTY-NINE
FLORENCE
ITALY
AUGUST 2006

Presented by A Leijten
H Blass stated that he agreed on the content of the paper; however, the reference section needed improvement. E.g. Eqn 9 was not from Ref 2 and correct paper could be downloaded from Karlsruhe homepage. He also stated that the reference list was incomplete e.g. some of the work done in Delft (Van de Kuilen's dissertation) was not referenced.
I Smith stated that work from TRADA did not show density influence within a species but between species. This was true and A Ceccotti has the report. There was discussion that within piece density variation could influence results and conclusions especially if a group of fasteners was considered rather than a single fastener.
J Köhler said that the aim of the paper was to show that although we might know the information of strength versus density, there might be inconsistency in using the results if a narrow range was considered.
H Larsen commented that code equations was based on assumption of density and strength relationship and suggested wider range should be considered.

Timber density restrictions for timber connection tests according to ISO8970/EN28970

Ad Leijten
Delft University of Technology, The Netherlands

Jochen Köhler
Swiss Federal Institute of Technology, Zürich, Switserland

André Jorissen
Eindhoven University of Technology, The Netherlands

Introduction

Eurocode 5 enables engineers to design timber connections with mechanical fasteners. If no design rules are given design by testing is optional and for this purpose EN28970 (equal to ISO8970 produced by ISO/TC165) is referenced. This standard specifies timber density requirements for the test pieces. The density range is narrow and several laboratories reported to have considerable difficulties to comply. Not only is the selection procedure time consuming the reason for such a selection is also questioned. This paper focuses on the effectiveness of the density selection requirements as well as certain interpretation problems in the evaluation of test results. Proposals for changes to the standard are made.

The test standard ISO8970/EN28970

ISO8970 - Testing of joints made with mechanical fasteners – Requirements for wood density, was first published in 1989. It was later adopted as EN28970. The most important part of the standard is being given below.

Scope

This standard specifies two methods for the selection of wood density for specimens, which are to be used in determining the **strength and stiffness** properties of joints made with mechanical fasteners.
The two methods are equally applicable.
It is assumed that the wood density is normally distributed with a coefficient of variation of about 0,15.
It is emphasized that the wood density is only one of the properties influencing the strength of a joint. Other relevant properties are, for example, growth ring size and slope of grain.

Method 1

A) The first method is based on all specimens having a density comparable with the characteristic density of the timber to which the test results should be applied; normally the test data can be used directly for calculating characteristic values, etc. of the joints.
NOTE The characteristic value of a material property corresponds in general to a fractile in the assumed statistical distribution of the particular property. The fractile - normally 0,05 or 0,5 is specified in the relevant standard.

B) The wood should be of uniform quality and without localized defects that could influence the test results. The mean density, ρ_m, of all specimens should satisfy the following condition:

$$\rho_m \leq 1{,}15\,\rho_k \qquad (1)$$

Where, ρ_m, is the required characteristic density for the timbers to which the test results should be applied determined in accordance with EN 3131 with mass and volume corresponding to equilibrium at a temperature of 20^0C ± 2^0C and relative humidity of (65 ± 5)%.
The density, ρ, of at least 20% of the specimen should satisfy the following condition:

$$\rho \leq \rho_k \tag{2}$$

where ρ_k is as in (1).

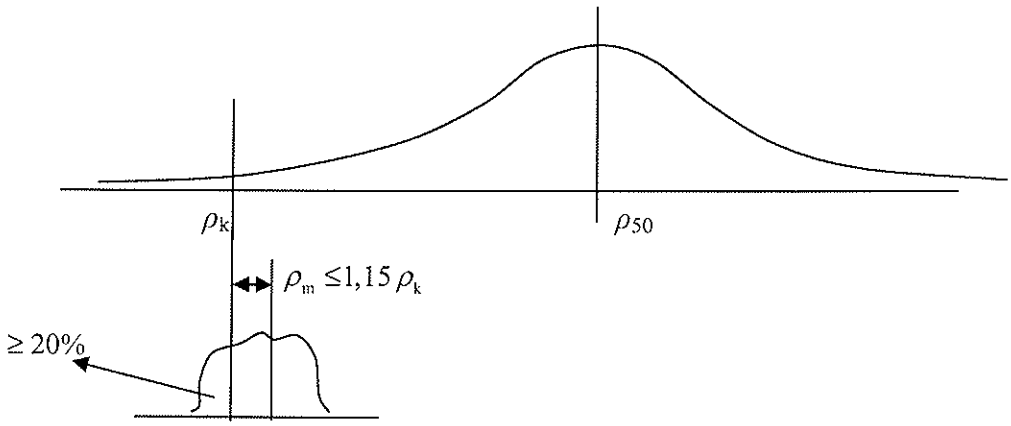

Figure 1: Graphical representation of the density requirements in method 1

Method 2
The wood should be of uniform quality and without localized defects that could influence the test results. The mean density, ρ_m, of all specimens should satisfy the following conditions:

$$1,05\,\rho_k \leq \rho_m \leq 1,1\rho_k \tag{3}$$

where, ρ_k, is the required characteristic density for the timbers to which the test results should be applied determined in accordance with EN3131 with mass and volume corresponding to equilibrium at a temperature of 20^0C ± 2^0C and relative humidity of (65 ± 5)%.
The density, ρ, of all single specimens should satisfy the following conditions:

$$0,9\,\rho_m \leq \rho \leq 1,1\rho_m \tag{4}$$

This method is aimed at getting specimens with a uniform density comparable with the mean density of the timber to which the test results should be applied: normally the characteristic values, etc, of the joints are calculated on the basis of corrected test values, F_{cor}, determined from the observed values, F_0, as:

$$F_{cor} = F_0\left(\frac{\rho_k}{\rho}\right)^c \tag{5}$$

where

ρ is the density of the wood in which failure took place.

ρ_k is the required characteristic density for the timbers to which the test results should be applied.

c is a power depending on the influence of the wood properties of the joint. It should be determined by tests or from theoretical considerations.

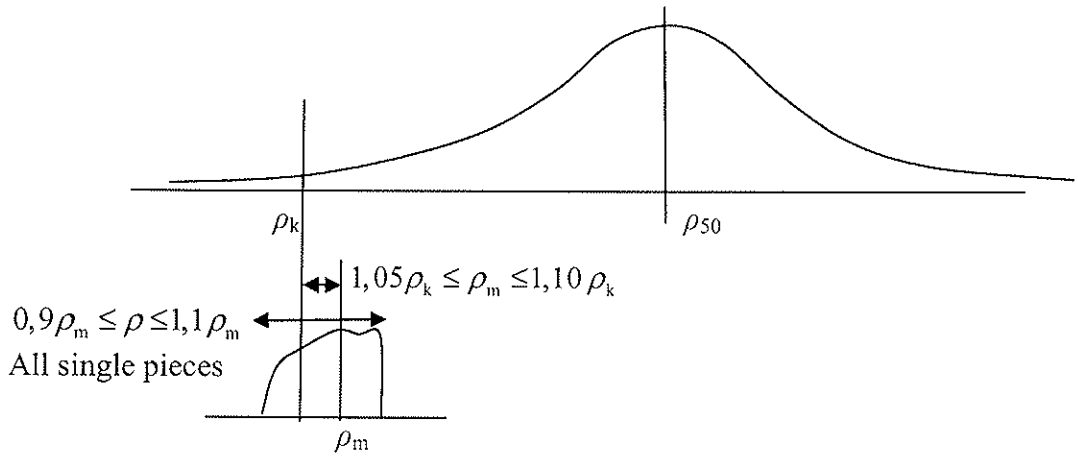

Figure 2: Graphical representation of the density requirements in method 2

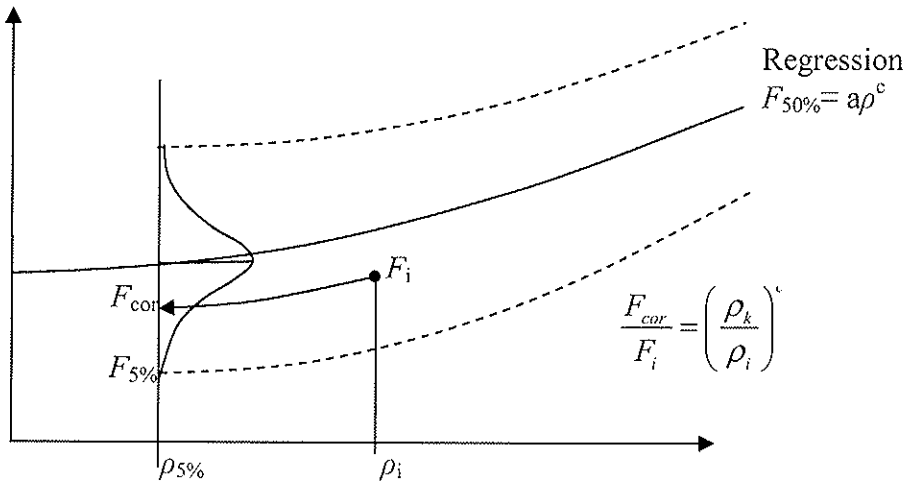

Figure 3: Data correction according to equation (5) for strength.

Both Figures 1 and 2 are not present in the standard but visualize both selection methods.

Figure 3 shows the effect of the correction factor to transform all data to the reference 5% density value. From the corrected data the 5% strength or stiffness value can be determined, $F_{5\%}$. However, the standard is not very specific in mentioning this. The reader might well believe that using specimens with a 5% density results in 5% test values.

Discussion of the density selection

One of the intentions of the drafters of ISO8970/EN28970 was to prevent manufacturers and/or researchers to cheat by using only specimens with high densities. Nevertheless, we can distinguish two cases:

- A) Strength and/or stiffness are **not** significantly correlated with density.
  Then, it does not make sense to have any density selection. The test specimens should reflect a representative part of the whole population. Applying

ISO8970/EN28970 is time consuming and the standard could better be ignored.

- B) Strength and/or stiffness are highly correlated with density.

  Even if the correlation between the density of the specimen and the observed connection strength or stiffness is assumed to be rather high the effect of the density selection is hard to justify. Statistics show that even for $R^2 = 0,7$:

  - the scatter of the test results is only decreased marginally by applying one of the selection methods for timber density and,
  - the mean value of the resulting set of test data is not representing the 5% fractile value.

  Method 2 might have a benefit of reducing the scatter using equation (5) compared to Method 1, the determination of the 5% fractile however is the same. The standard derivation procedure for the 5% fractile in EN 14358 does not reward any density selection of the specimens. Therefore, it is questionable to put effort into flowing ISO 8970 or EN28970.

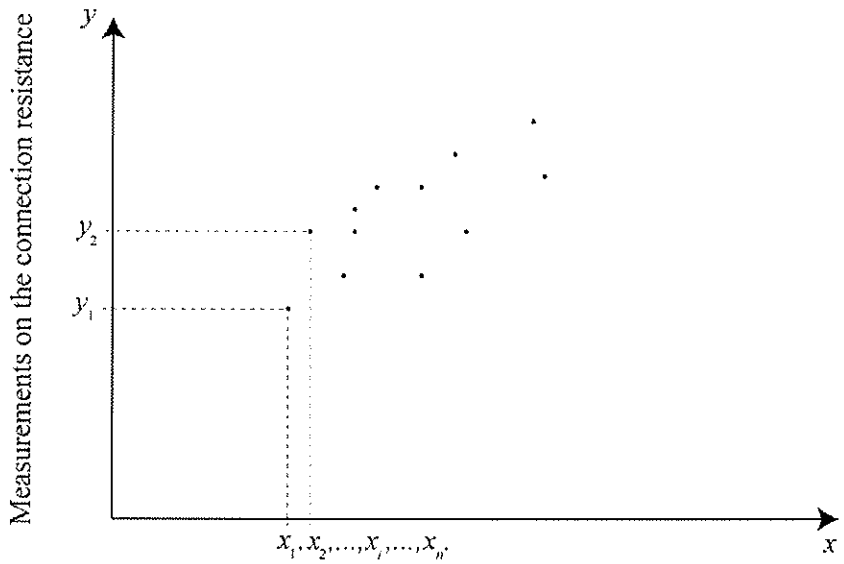

Figure 4: The effect of density selection

Consider the case of a set of two properties observed simultaneously like presented in Figure 4 e.g. the timber density **x** and the connection resistance **y**.
It may be assumed that both properties are normal distributed and the parameters may be estimated and represented by respective probability density functions (PDF). Their linear relationship may be assessed by regression analysis or correlation analysis, Figure 5.

Statistics provides a useful tool to analyse the effect of the density selection, which can be expressed by formulas (6) and (7).

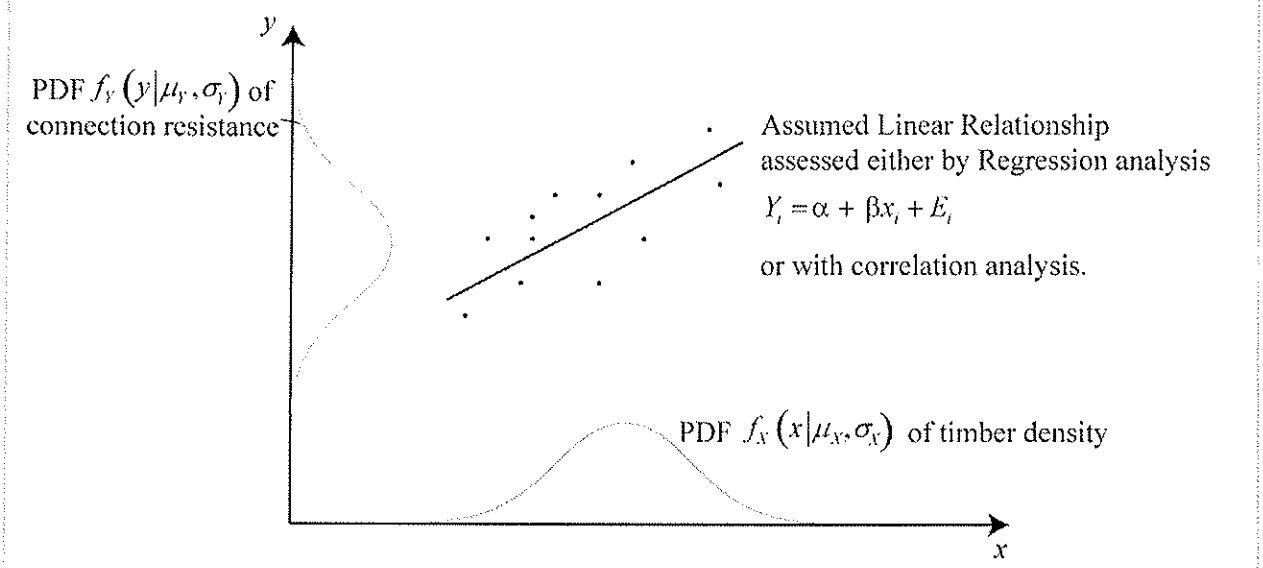

Figure 5: Relation between density and the connection resistance

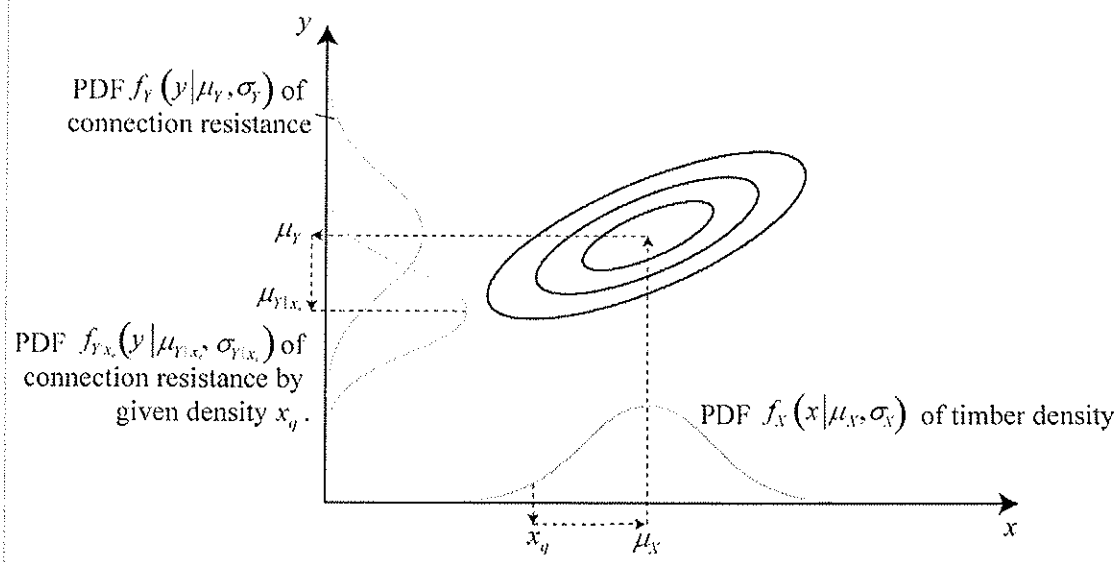

Figure 6: Influence of the density selection.

$$\mu_{Y|x_q} = \mu_Y + \rho\frac{\sigma_Y}{\sigma_X}\left(x_q - \mu_X\right) \tag{6}$$

$$\sigma_{Y|x_q} = \sqrt{\left(1-\rho^2\right)}\sigma_Y \tag{7}$$

Where:

$\mu_{Y|x_q}$ is the mean value of Y for given value of $X = x_q$.

$\sigma_{Y|x_q}$ is the standard deviation of Y for given value of $X = x_q$.

μ_Y, σ_Y is the mean value and the standard deviation of Y.

μ_X , σ_X is the mean value and the standard deviation of X.

ρ is the correlation coefficient of X and Y.

For example:
Assume a normal density distribution represented by the mean μ_x and standard deviation σ_x and the lower 5% fractile $x_q = 376$ kg/m^3. The test data is represented by μ_y and standard deviation σ_y and the lower 5% fractile $y_{0.05} = 75{,}4$ kN while the correlation with density is $\rho = 0{,}7$ which is rather high.

$$\mu_X = 450\,\text{kg/m}^3 \qquad \mu_Y = 100\,\text{kN}$$

$$\sigma_X = 45\,\text{kg/m}^3 \qquad \sigma_Y = 15\,\text{kN}$$

$$x_q = x_{0.05} = 376\,\text{kg/m}^3 \qquad y_{0.05} = 75{,}4\,\text{kN}$$

$$\rho = 0{,}7$$

Applying Equation (6) and (7) result in

$$\mu_{y|x_q} = 82{,}8\,\text{kN}$$

$$\sigma_{y|x_q} = 10{,}7\,\text{kN}$$

$$\left(y|x_q\right)_{0.05} = 65{,}2\,\text{kN}$$

The result confirms the low efficiency of the density selection scheme as prescribed by ISO8970/EN28970. Even if the range of the density values is restricted to exactly the 5% value x_q and the correlation of the density and the connection strength is assumed to be rather high, it can be observed that the mean value of the subsequent probability density function of the connection strength data is not close to the 5% fractile value of the entire connection strength data population.

Random variables should always be related to a meaningful and consistent set of populations. The description and modelling of these random variables should correspond to this set. A population with a unique set of specifications is referred to as elementary population; a population in which specification parameters vary is referred to as a composite population. The set of measurements associated with a certain population is referred to as an elementary or composite sample respectively. A sampling procedure may be representative or artificial. Representative samples or representative realisations of random variables are obtained through random sampling. Artificial means that no direct relation exist between the statistical properties of the sample and the statistical properties of the population. An artificial sample is e.g. when only weak specimen are selected for testing by engineering judgment or proof loading. Artificial samples are also termed censored samples.
When performing test according to the test standards ISO8970/EN28970 a so called artificial or censored data set of connection strength data is obtained. The statistical characteristics of these censored samples are not equivalent to the characteristics of the entire population of connection strength data (which is of general interest in timber engineering practice and research).
Since it is not possible to derive the characteristics of the connection strength population based on the characteristics of the obtained censored sample, the authors of this article recommend deleting Method 1 and 2 from the standard.

The only possibility to obtain a representative set of connection strength data is random sampling; i.e. no restrictions on the timber density of the test specimen.

Wood species

When the standard was drafted the European strength class system now in use was non-existing. The density profile of Spruce, the most used species in Europe, which the drafters must have had in mind, ranges from a mean of 451 kg./m^3 and a 5% fractile value of 379 and 95% fractile of 516 kg/m^3, respectively [3].
The density requirements according to both methods results in:
Method 1

Mean of the test specimens $\rho_m \leq 1{,}15\,\rho_k \rightarrow \rho_m \leq 436$ kg/m^3 (1a)

>20 % of specimens $\rho \leq \rho_k \rightarrow \rho \leq 379\,\text{kg/m}^3$ (2a)

Method 2

Mean of the test specimens $1{,}05\,\rho_k \leq \rho_m \leq 1{,}1\rho_k \rightarrow 398$ kg/m$^3 \leq \rho_m \leq 416\,\text{kg/m}^3$ (3a)

All specimens $0{,}9\,\rho_m \leq \rho \leq 1{,}1\rho_m$

for $\rho_m = 398$ kg/m$^3 \rightarrow 358\,\text{kg/m}^3 \leq \rho \leq 438\,\text{kg/m}^3$ (4a)

for $\rho_m = 416\,\text{kg/m}^3 \rightarrow 317\text{kg/m}^3 \leq \rho \leq 387\,\text{kg/m}^3$ (4b)

The density range of (4a) is shown in the left corner of Figure 4 and is satisfied by no more than 12% of the Spruce population the range of (4b) by about 5%.

Since the coniferous strength classes, C14 to C50, are introduced in Europe given in EN 338 and timber is classified accordingly, the 5% characteristic and mean density are specified for each class and irrespective of the wood species. The density ranges using method 2 for the respective strength classes are given in Figure 4. It seems rather difficult and therefore expensive to select the test pieces to meet these requirements. This is particularly true for class C18 and C24, which forms the majority of structural timber in practice that make up no more than 5% of the Spruce population.
For Method 1 the 20% requirement is hard to satisfy.

Interpretation of the c-factor

It has been observed that some researchers follow the method 2 procedure and apply the c-factor as prescribed in (5). This factor should be based on experiments or a theoretical consideration as the standard reads, without providing precise guidance. If based on tests it presumes appropriate data covering a wide density range as to determine the density effect. It also assumes timber failure is governing by definition. However, this type of information is generally not available. Especially, when a innovative connection is being tested. Modification of the data according to (5) is therefore not easy unless c = 0 is taken.
It is noted that in some cases researchers happen to be very creative in adopting certain c-factors that come from Eurocode 5 designs equations instead of initial tests over a wide density range. However, the density range prescribed by method 1 and 2 is usually so small that different c-factors only marginally affect the 5% strength or stiffness value.

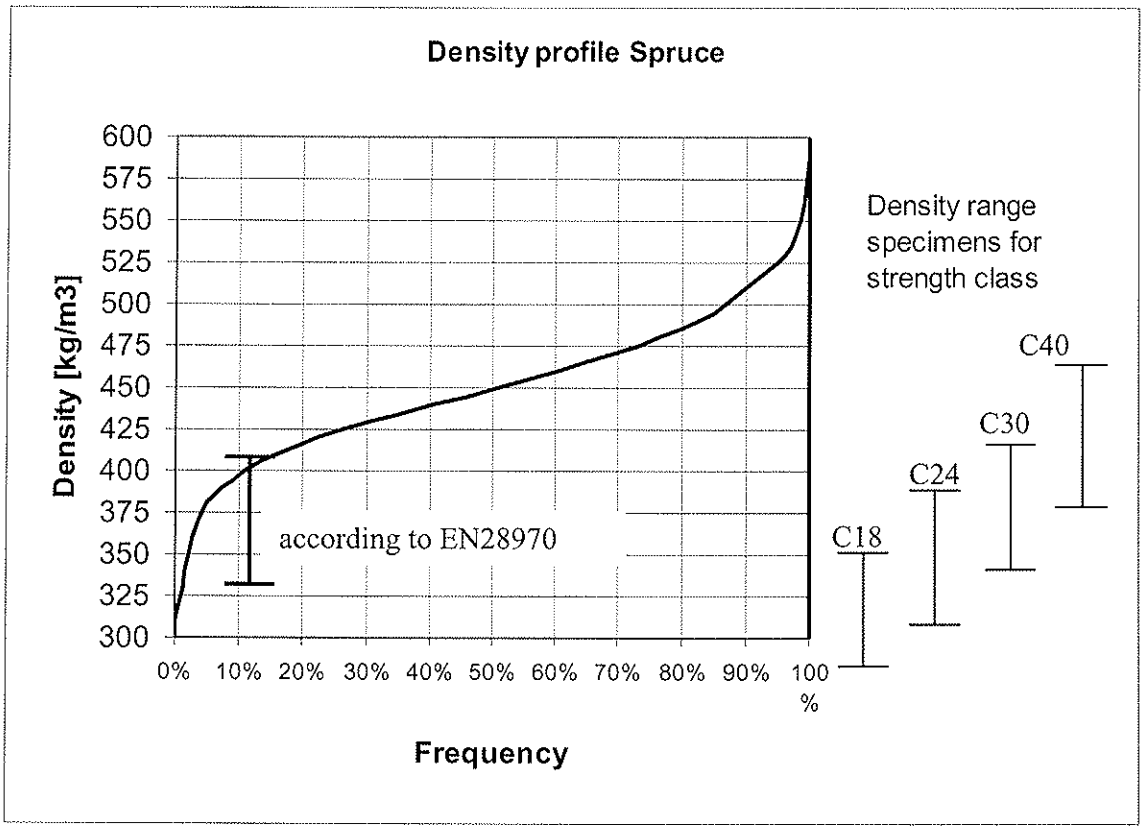

Figure 4: Density profile of Spruce and method 2 density ranges for several strength classes (EN 338).

Concluding

Regarding the application of ISO8970/EN28970 it can be concluded:

- the density restrictions for test specimens result in conservative 5% fractile values. An example where a correlation with density is 0,7 shows a 15% difference with the method where no density restrictions are set.
- the prescribed range of the density in the standard is not practical; it is small and hard to satisfy.
- The standard does not state clearly that the mean of the test results using Method 1 or 2 is not the 5% fractile of strength or stiffness.
- The standard does not mention that if timber failure does not govern the connection strength or stiffness the standard provisions do not apply.
- The derivation of the c-factor in (5) is open for free interpretation although its influence is considered small.
- A new method should be added as an alternative for Methods 1 and 2 disregarding any density restriction.

Code proposal changes and addition:

- The standard only applies when timber failure governs the strength or stiffness capacity.
- The new Method, replacing Method 1 and 2, should state that the density distribution of the test specimens should reflect the density distribution of the species to which results apply. This can be achieved by specifying a maximum deviation of the mean and standard deviation of the test pieces compared to the mean and standard deviation of the wood species.

INTERNATIONAL COUNCIL FOR RESEARCH AND INNOVATION
IN BUILDING AND CONSTRUCTION

WORKING COMMISSION W18 - TIMBER STRUCTURES

THE MECHANICAL INCONSISTENCE IN THE EVALUATION OF THE MODULUS OF ELASTICITY ACCORDING TO EN384

Th Bogensperger
G Schickhofer

Institute for Timber Engineering and Wood Technology, Graz
University of Technology

H Unterwieser
holz.bau forschungs gmbh, Graz

AUSTRIA

MEETING THIRTY-NINE
FLORENCE
ITALY
AUGUST 2006

Presented by T Bogensperger
A Ranta-Maunus wondered why one would need local MOE. If this was not needed, may be one could just work with global MOE with a 5% increase to make adjustment.
G Schickhofer stated that one need to repair the standard.
A Leijten asked about the background of the formula and B Källsner stated the formula originally based on low E material.
I Smith provided caution that some measurements could be subjected to 50% difference.

The Mechanical Inconsistence in the Evaluation of the Modulus of Elasticity According to EN384

Th. Bogensperger [1], H. Unterwieser [2], G. Schickhofer [1]

[1] Institute for Timber Engineering and Wood Technology, Graz University of Technology, Austria
[2] holz.bau forschungs gmbh, Graz, Austria

1 Introduction

The basic challenge is the determination of the bending modulus of elasticity (**MOE**) of timber beams (for example structural timber or glulam). EN 408 arranges a four-point bending test setup for the determination of the **MOE**. The test configuration shows a span length of 18·h and a symmetric loading in one and two thirds of the span.

In the middle third, where shear deformations do not appear, the local deflection over a local length of 5·h is frequently quantified for calculating the local bending modulus of elasticity $\mathbf{MOE}_{loc}$. Alternatively by using the global beam deflection a global bending modulus of elasticity $\mathbf{MOE}_{glob}$, refered to the total span length of 18·h, can be established. The advantage of the latter one is the consideration of a larger test volume. The global deflection constists of a bending and a shear part. The participation of both to the global deflection remains unknown, which can be seen as a drawback.

EN 384 introduces an equation for *'structural timber'*, which allows a conversion from the $\mathbf{MOE}_{glob}$ (on the basis of 18·h) to the $\mathbf{MOE}_{loc}$, which is more meaningful for mechanical calculations. The structure of the equation leads to the conclusion, that this equation was built of a linear statistical regression analysis between both items $\mathbf{MOE}_{glob}$ and $\mathbf{MOE}_{loc}$. Not any limitation (upper and lower limits of the $\mathbf{MOE}_{glob}$, wood species) is specified for this functional correlation in EN 384. In particular the mechanical consistence of the introduced equation is missing.

2 Standardisation

2.1 EN 408:2003

Inter alia, EN 408 arranges methods for test configurations and experiments for the determination of mechanical characteristics. In particular chapter 9 and 10 of this code are of basic interest to the topic of this paper. In both chapters four-point bending tests on simple supported beams with a length of 18·h between the bearings and the loading in one and two thirds of the length are specified. The test configuration for determination of $\mathbf{MOE}_{loc}$ is managed in chapter 9, whereas the determination of $\mathbf{MOE}_{glob}$ is specified in chapter 10. The $\mathbf{MOE}_{loc}$ is obtained directly with the measured local deformation value, but only about 28 % of the test volume is considered in this evaluation. By evaluation

the $\mathbf{MOE}_{glob}$, a larger test volume is consulted. If the mechanical energy is established with its alterable bending moment in both side parts and the constant one in the middle part, 56 % of the test volume, loaded with a constant bending moment, will deliver equal elastic internal energy.

The shear deformation free $\mathbf{MOE}_{loc}$ is adopted for a civil engineering like treatment. Thereby a mechanical correct, functional relationship between the $\mathbf{MOE}_{glob}$ and the $\mathbf{MOE}_{loc}$ is demanded.

2.2 EN 384:2004

A functional relationship between the $\mathbf{MOE}_{glob}$ and the $\mathbf{MOE}_{loc}$, as mentioned in chapter 2.1, is governed in EN 384 in section 5.3.2 in the following way:

$$\mathbf{MOE}_{loc} = 1,30 \cdot \mathbf{MOE}_{glob} - 2690\ [\frac{N}{mm^2}] \tag{1}$$

The method behind the derivation of this functional relationship is a linear regression analysis. For a $\mathbf{MOE}_{glob} \leq 8967\ \frac{N}{mm^2}$ the introduced function (eq. 1) allows the calculation of a $\mathbf{MOE}_{loc}$ value, which is lower than the $\mathbf{MOE}_{glob}$. This is mechanically inconsistent!

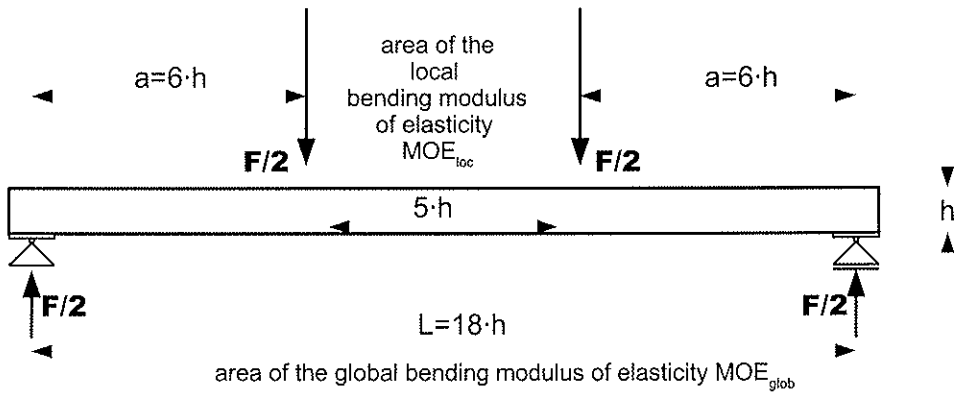

Figure 1: Test configuration according to EN 408

3 State of the art

The following relationship (eq. 2) was developed and published by **N. Burger** and **P. Glos** [3] at the Munich University of Technology (1995).

$$\begin{aligned} E_{B,EN} &= 1,107 \cdot E_{E,DIN} - 208\ [\frac{N}{mm^2}] \\ \text{also: } \mathbf{MOE}_{loc} &= 1,107 \cdot \mathbf{MOE}_{glob} - 208\ [\frac{N}{mm^2}] \end{aligned} \tag{2}$$

$E_{B,EN}$ conforms to the $\mathbf{MOE}_{loc}$, which is determined according to prEN 408 on the basis of 5·h length. $E_{E,DIN}$ accords to $\mathbf{MOE}_{glob}$, but in contradiction to EN 408 the span is governed with $\geq$ 15·h in DIN 52186 instead of 18·h.

The included shear deformations in the $\mathbf{MOE}_{glob}$ constitute the motivation for the introduction of a functional relationship [3]. But despite this clear mechanical cognition, a linear regression analysis

instead of a mechanical based solution was introduced in [3]. This fact leads analogous to eq. (1) to a limit point, below which the function is mechanically inconsistent. This limit point is given with $E_{E,DIN} \leq 1944\,[\frac{N}{mm^2}]$. Without doubts the value is very low, so that a restriction of the range of validity can be neglected.

4 Formal, mechanical correct relationship between $\mathbf{MOE}_{glob}$ and $\mathbf{MOE}_{loc}$

4.1 General

In order to govern a mechanically based relationship between $\mathbf{MOE}_{glob}$ and $\mathbf{MOE}_{loc}$, the deflection in the middle of the beam, calculated by the classical beam theory without any shear deformations is demanded to be equal to the deflection, calculated by a shear weak beam theory.

4.2 Deflection of a simply supported beam, according to the beam theory

The calculation of the deflection in the middle of a beam, seperated in the bending (eq. 3) and the shear part (eq. 4), is required, as stated in section 4.1.

- bending deflections:

$$w_B = \frac{23}{216} \cdot \frac{\frac{F \cdot L}{6}}{E \cdot I} \cdot L^2 = \frac{23}{216} \cdot \frac{M_{max}}{E \cdot I} \cdot L^2 \tag{3}$$

- deflections, caused by shear deformations:

$$w_S = \frac{F}{6} \cdot \frac{L}{\frac{G \cdot A}{\kappa}} = \frac{1}{3} \cdot \frac{Q_{max}}{\frac{G \cdot A}{\kappa}} \cdot L \tag{4}$$

κ is the shear deformation factor and is given with $\frac{6}{5}$ for a homogenious rectangular cross section.

4.3 Mechanical consistant relationship

With the approach of section 4.1, the following equation (eq. 5) can be established:

$$\frac{23}{216} \cdot \frac{\frac{F \cdot L}{6}}{\mathbf{MOE}_{loc} \cdot I} \cdot L^2 + \frac{F}{6} \cdot \frac{L}{G \cdot A_{shear}} \equiv \frac{23}{216} \cdot \frac{\frac{F \cdot L}{6}}{\mathbf{MOE}_{glob} \cdot I} \cdot L^2. \tag{5}$$

With eq.(6)

$$\mathbf{MOE}_{loc} = \frac{\mathbf{MOE}_{glob}}{1 - \frac{216}{23} \cdot \frac{\mathbf{MOE}_{glob} \cdot I}{G \cdot A_{shear} \cdot L^2}} \tag{6}$$

an improved relationship between $\mathbf{MOE}_{glob}$ and $\mathbf{MOE}_{loc}$ is attained in comparision to eq. (1).

4.4 Simplifications in the case of reference dimensions

If the length, the moment of inertia and the effective shear area are considered with $L = 18 \cdot h$, $I = \frac{b \cdot h^3}{12}$ and $A_{shear} = \frac{5}{6} \cdot b \cdot h$, the equation above (eq. 6) can be further simplified:

$$\mathbf{MOE}_{loc} = \frac{\mathbf{MOE}_{glob}}{1 - \frac{216}{23} \cdot \frac{\mathbf{MOE}_{glob} \cdot b \cdot h^3 \cdot 6}{12 \cdot G \cdot b \cdot h \cdot 5 \cdot L^2}} = \frac{\mathbf{MOE}_{glob}}{1 - \frac{108}{115} \cdot \frac{\mathbf{MOE}_{glob}}{G} \cdot \left(\frac{h}{L}\right)^2} = \frac{\mathbf{MOE}_{glob}}{1 - \frac{1}{345} \cdot \frac{\mathbf{MOE}_{glob}}{G}} \tag{7}$$

4.5 Mechanical consistant relationship with tolerances for the length L and a

If the tolerances according to EN 408 for the span length ($L = 18 \cdot h \pm 3 \cdot h$) and the location of the loading ($a = 6 \cdot h \pm 1,5 \cdot h$) are included, the governing equation can be written in the following form:

$$\mathbf{MOE}_{loc} = \frac{\mathbf{MOE}_{glob} \cdot \left(1 - \frac{4 \cdot a^2}{3 \cdot L^2}\right)}{1 - \frac{4 \cdot a^2}{3 \cdot L^2} - 8 \cdot \frac{\mathbf{MOE}_{glob} \cdot I}{G \cdot A_{shear} \cdot L^2}} = \frac{\mathbf{MOE}_{glob} \cdot \left(1 - \frac{4 \cdot a^2}{3 \cdot L^2}\right)}{1 - \frac{4 \cdot a^2}{3 \cdot L^2} - 4 \cdot \frac{\mathbf{MOE}_{glob} \cdot h^2}{G \cdot L^2}} \tag{8}$$

Eq. (8) can be converted to eq. (6) and eq. (7) respectively in the case of $a = \frac{L}{3}$.

4.6 Comparison to the function in EN 384

Both functional relationships (eq. (1), (6) and (7) respectively) are illustrated in figure 2. The new function (eq. (6) and (7) respectively) is a hyperbolic function, whereas the function in EN 384 (eq. 1) is linear.

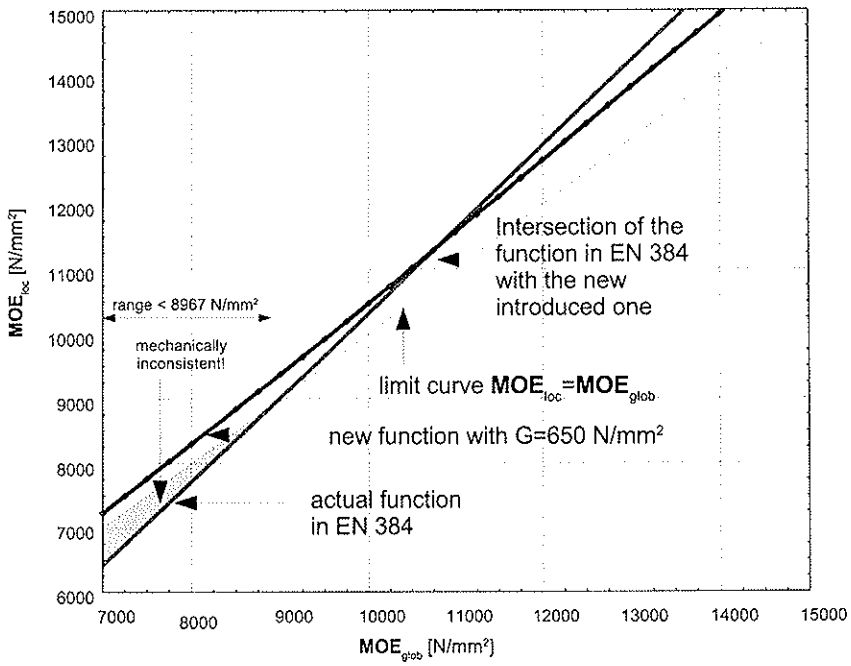

Figure 2: Comparison of the function acc. to EN 384 and the new function (eq. (6) and (7) respectively)

4.7 Additional effect due to local indentations

Eq.(1) delivers higher $\mathbf{MOE}_{loc}$ values for $\mathbf{MOE}_{glob} \geq 10782 \frac{N}{mm^2}$ (limit depends on the shear modulus and is valid for $G_{\parallel} = 650 \frac{N}{mm^2}$, see figure 2) than eq. (6) and (7) respectively. Local indentations are regarded as one major reason and are investigated in the following.

A numerical simulation is performed with the FEA-software ABAQUS, where the middle part is discretisized with beam elements, the area near the support is discretisized with planar 2D solid elements. Due to the symmetry only one half of the beam has to be modelled (see figure 3). Frictionless

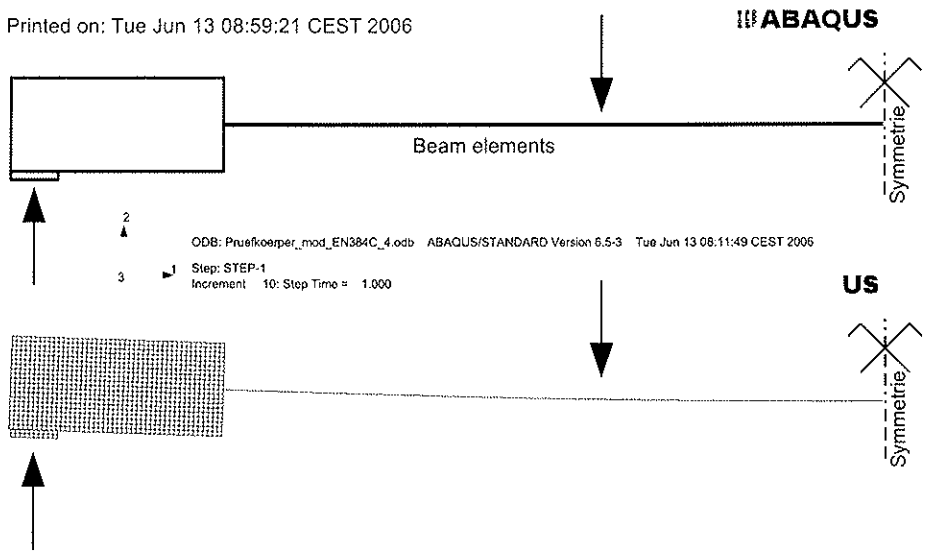

Figure 3: FE model for investigation of the influence of additional indentations

contact formulation is used between the supporting plates and the 2D solid elements of the beam. The deformated system near the supporting plates is shown in figure 4.

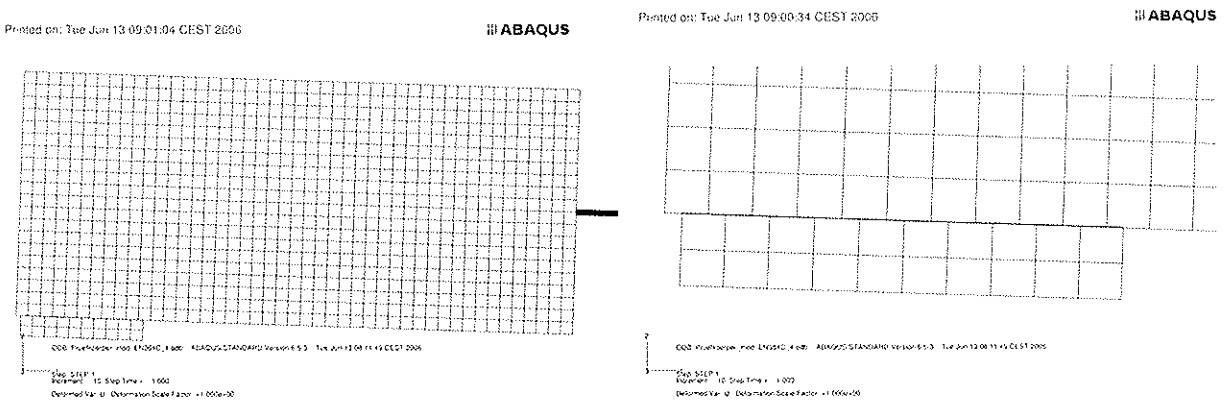

(a) Detail of the area near the supporting plates

(b) Detail of the area near the supporting plates - deformed model

Figure 4: Detail near the supporting plates

By including the effects due to the additional indentations, the function according to eq. (6) and (7) respectively is shifted towards function equation 1 (see figure 6). A compliance of both functions can not be found, merely a reduced difference between both ones.

The simulation is performed with a lateral modulus of elasticity of $E_{\perp} = 300\,\frac{N}{mm^2}$ and a shear modulus of $G_{\parallel} = 650\,\frac{N}{mm^2}$. The width of the supporting plates without any lateral overlap, which is an unfavourable case, was chosen with 0,25·h (= 150 mm width). A further simulation with a width of 0,167·h (= 100 mm width) of the support plate and an overlap of 100 mm, shows similar results to the previous case.

4.8 Influence of the mistake of the used shear modulus

If the shear modulus in eq. (6) and (7) respectively is not chosen accurately, the calculation of the $\mathbf{MOE}_{loc}$ value will remain improper, because the influence of the shear deformations is not regarded exactly. However the arising failure of $\mathbf{MOE}_{loc}$ remains small, because the importance of the shear deformations in comparision to the bending deformations is less then 5 % in the case of L = 18·h.

The arising failure is illustrated in figure 5 for two test configurations with span lengths of L = 18·h and L = 25·h, in which the failure of $\mathbf{MOE}_{loc}$ is a function of the mistake f of the shear modulus $G_{\parallel}$, which is used in eq. (6) and (7) respectively, from the real, effective but unknown shear modulus $G_{\parallel}^{*}$ of the beam. The mistake f is mathematically defined in the following equation and the failure of the $\mathbf{MOE}_{loc}$ value is shown in figure 5 for a mistake in a range $[-30\,\% \leq f \leq 30\,\%]$.

$$f = \frac{G_{\parallel} - G_{\parallel}^{*}}{G_{\parallel}^{*}} \cdot 100\,\% \tag{9}$$

In [4] the average of the shear modulus of timber boards is specified with $\sim 666\ \frac{N}{mm^2}$, the standard deviation is specified with $\sim 92\ \frac{N}{mm^2}$. Based on a normal distribution, the 95 %- and 5 %-quantile values can be calculated with 817 and 515 $\frac{N}{mm^2}$ respectively. If the real, effecitive shear modulus $G_{\parallel}^{*}$ captures one of these both quantile values and a nominal value $G_{\parallel}$ of 650 $\frac{N}{mm^2}$ (value corresponds to the actual value of shear modulus for glulam, but is still in discussion), the yielding deviations of the nominal shear value from the real, effective one achieves -20,4 % and 26,2 % respectively.

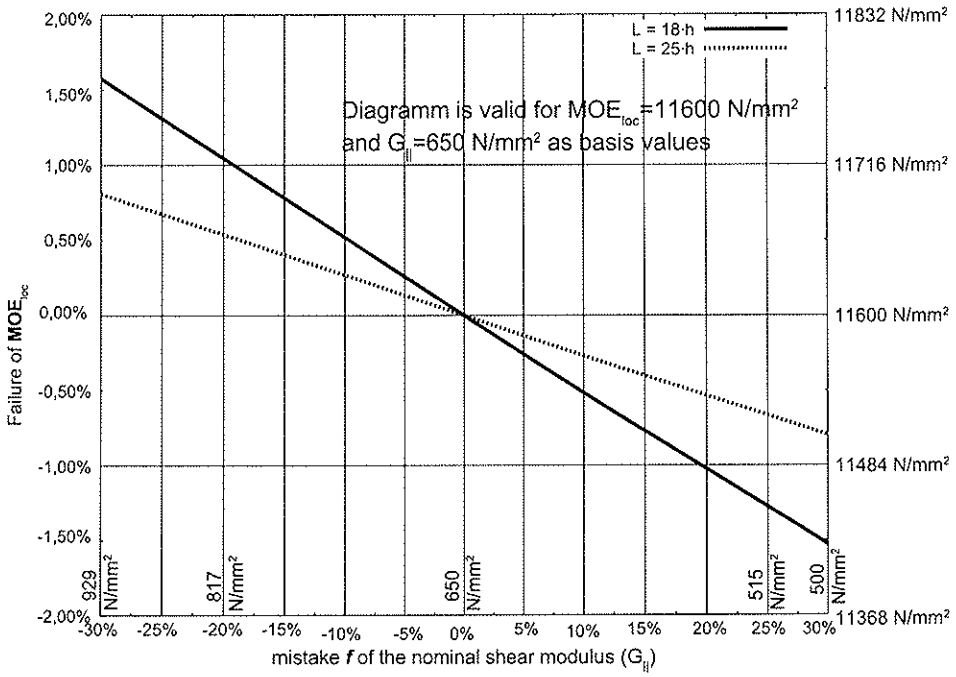

Figure 5: Influence of the mistake of the used shear modulus on $\mathbf{MOE}_{loc}$

In order to minimize the influence of the shear deformations, the length of the test configuration could be increased. In figure 5 the arising failures in the case of the standard length with L = 18·h and with an increased span length of L = 25·h is illustrated. With the increased length a deviation of the

shear modulus of almost 30 % (!) from the real, effective one results in a failure of only about 0,8 % for $\mathbf{MOE}_{loc}$, whereas in case of a span length with L = 18·h the deviation results in more than 1,6 %.

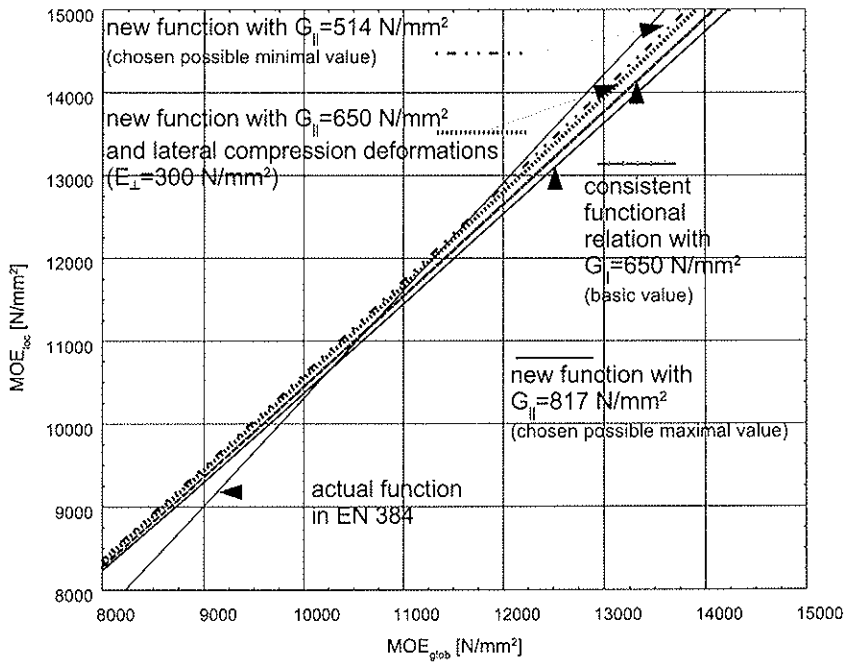

Figure 6: Effect of the local indentation as well as the deviation of the nominal shear modulus from the real, effective one (in eq. (6) and (7) respectively)

5 Application to research project test results

In the context of the research project **P05 grading** at the centre of competence for timber engineering and wood technology in Graz/Austria two series of glulam beams with depths of 300 mm and different widths were tested with a four-point bending test configuration.

5.1 Series A and B

From december 2005 to march 2006 a total of 95 glulam beams with depths of 300 mm and widths of 45 mm, 90 mm and 95 mm respectively, were tested with a four-point bending test configuration and followed by a statistical analysis. The beams with the width $b = 45\ [mm]$ were produced by resawing beams with widths of $b = 95\ [mm]$. The A series covers the cross-sections $b/h = 90/300\ [mm]$ (19 beams) and $b/h = 45/300\ [mm]$ (26 beams) respectively with a combined-symmetrically beam lay-up. The used grading classes MS10 (C24M), MS13 (C35M) and MS17 (C40M) were machine graded with the *Dimter GradeMaster 403*, which works with the principle of natural frequency measurement. The B series covers the cross-sections $b/h = 95/300\ [mm]$ (20 beams) and $b/h = 45/300\ [mm]$ (30 beams), whereas the combined-symmetrically beam lay-up consist of two grading classes MS10 (C24M) and MS13 (C35M) (machine graded with *Euro-GreComat, Type 702*).
The test program consisted of four point bending tests according to EN 408 for determination of the

global and local bending modulus of elasticity. Deformations for determining the global modulus of elasticity with a reference length of 18·h have been measured at the centre of the span. For determination of the local bending modulus of elasticity the deformation has been taken as the average of measurements on both faces at the neutral axis, and measured at the centre of a central gauge length of five times the depth of the section. Results see tables 1 and 2.

	Series A		Series B	
Cross-section	Series 45/300	Series 90/300	Series 45/300	Series 95/300
Beam lay-up	MS17/MS13/4#MS10/MS13/MS17		2#MS13/4#MS10/2#MS13	
MEAN	**13661**	**13905**	**11916**	**11871**
STA.DEV.	712	535	343	692
COV	5,21 %	3,84 %	2,88 %	5,83 %
MAX	14956	14651	12627	12921
MIN	12172	12577	11205	10576

Table 1: Test results of the global modulus of elasticity $\mathbf{MOE}_{glob}$

	Series A		Series B	
Cross-section	Series 45/300	Series 90/300	Series 45/300	Series 95/300
Beam lay-up	MS17/MS13/4#MS10/MS13/MS17		2#MS13/4#MS10/2#MS13	
MEAN	**14837**	**15048**	**12862**	**12875**
STA.DEV.	1015	794	419	893
COV	6,84 %	5,27 %	3,26 %	6,94 %
MAX	16852	16068	13653	14318
MIN	12680	12824	11957	11252

Table 2: Test results of the local modulus of elasticity $\mathbf{MOE}_{loc,5\cdot h}$

Notes to the tables 1 and 2:

1. The mean values of the global and local MOE are corrected up to a moisture content of 12 %.
2. The coefficient of variance of the resawn beams is generally higher than for broad beams. For the beam series B with widths of $b = 45\ [mm]$ and $b = 95\ [mm]$ a higher COV of the resawn beams was determined.

Apart from the evaluation of the local modulus of elasticity from the bending tests, the local MOE has been calculated with the new function ($\mathbf{MOE}_{loc}$) which includes the global modulus of elasticity (eq. (6) and eq. (7)). The shear modulus has been assumed to be constant (650 $\frac{N}{mm^2}$) over all beams, (see section 4.8 and table 3).

Note:
For the 90/300 mm series an additional correction considering local indentations was made. The local indentations were appraised with ABAQUS. This correction attenuates the global deformation which causes an increase of the global and local modulus of elasticity.

1. The mean value of $\mathbf{MOE}_{glob}$ increases from 13905 to 14037 $\frac{N}{mm^2}$, the mean value of the calculated local modulus of elasticity $\mathbf{MOE}_{loc}$ increases from 14766 to 14825 $\frac{N}{mm^2}$. The mean value of the local MOE determined from the bending tests, which refers to a length of 5·h, remains unchanged.

	Series A		Series B	
Cross-section	Series 45/300	Series 90/300	Series 45/300	Series 95/300
Beam lay-up	MS17/MS13/4#MS10/MS13/MS17		2#MS13/4#MS10/2#MS13	
MW	**14538**	**14766**	**12586**	**12536**
STABW	769	643	382	770
COV	5,29 %	4,35 %	3,04 %	6,14 %
MAX	15901	15698	13380	13711
MIN	12745	13153	11794	11100

Table 3: Results of the local bending modulus of elasticity $\mathbf{MOE}_{loc}$, determined with the new function

2. The additional correction considerung local indentations caused a change of the statistical dispersion. The COV of $\mathbf{MOE}_{glob}$ is increasing to 3,88 %, the COV of $\mathbf{MOE}_{loc}$ is decreasing to 4,09 %.

5.2 Regression analysis of the test results

If a linear regression is carried out with the experimental beam testing results, the following regression equation describes the linear relationship (with a square of coefficient of correlation $R^2 = 0{,}948$):

$$\mathbf{MOE}_{loc} = 1,146 \cdot \mathbf{MOE}_{glob} - 812 \tag{10}$$

Additionally, the confidence interval can be defined which covers the range of the regression line. The confidence level was fixed with 75 %, the confidence interval is plotted in figure. 7.

Because of the fact that the determined linear regression function, starting from a value of $\mathbf{MOE}_{glob} \leq 5562 \frac{N}{mm^2}$, computed a lower local modulus of elasticity $\mathbf{MOE}_{loc}$ than a global $\mathbf{MOE}_{glob}$, a new function is suggested, which conforms with the mechanically correct relationship of the MOE. The derived hyperbolic function, which is illustrated in figure. 7, can be described by

$$\mathbf{MOE}_{loc} = 1,018 \cdot \left(\frac{\mathbf{MOE}_{glob}}{1 - \frac{1}{345} \cdot \frac{\mathbf{MOE}_{glob}}{G}}\right) + 26 \tag{11}$$

with $G = 650 \frac{N}{mm^2}$. The square of coefficient of correlation R^2 is 0,949.

Figure. 7 shows that the linear regression produced a steeper function which causes mechanically inconsistent local modulus of elasticity in the lower range of values ($\mathbf{MOE}_{glob} \leq 5562 \frac{N}{mm^2}$). To draw a comparison, the function out of EN 384 already produces incorrect local modulus of elasticity $\mathbf{MOE}_{loc}$ starting from $\mathbf{MOE}_{glob} \leq 8967 \frac{N}{mm^2}$. The hyperbolic function and the mechanically consistent function show nearly the same derivation in the middle and higher range of values, whereas the hyperbolic function computed 2 % higher local modulus of elasticity. In the lower range of values (up to $\mathbf{MOE}_{glob} \leq 5000 \frac{N}{mm^2}$), the hyperbolic function becomes a lower derivation.

6 Summary

6.1 Suggested modifications in EN 384

Two general possibilities can be used for the determination of the effective or mechanical correct local modulus of elasticity $\mathbf{MOE}_{loc}$ for beams, built up as structural timber or glulam. One possibility

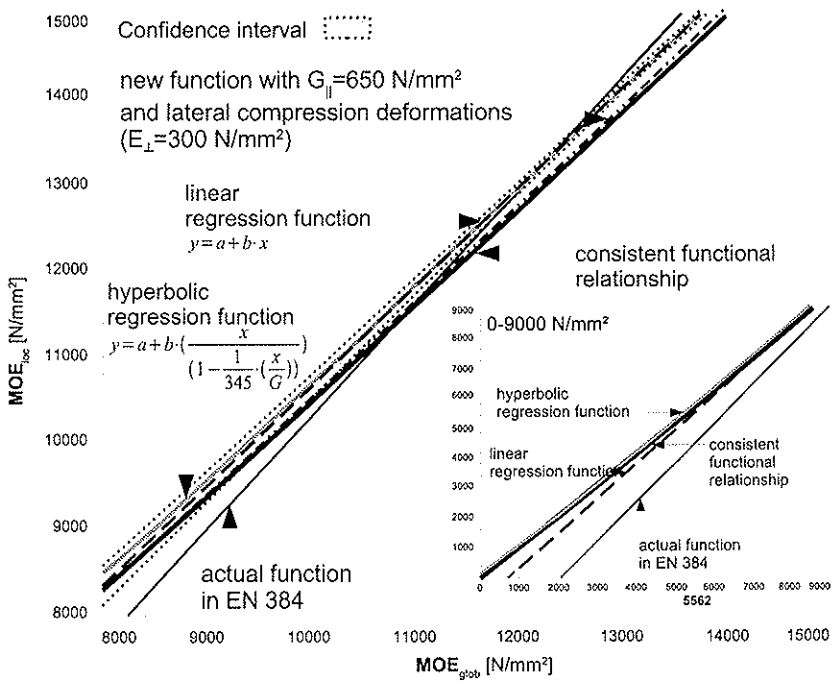

Figure 7: Relationship between the global and local modulus of elasticity with plotted confidence interval (75 % confidence level)

is the procedure according to chapter 9 of EN 408 with the direct determination of $\mathbf{MOE}_{loc}$. Only 28 % of the test volume is regarded in the evaluation of the test results, which can be stated as a drawback. The $\mathbf{MOE}_{loc}$ values features higher statistical dispersion in the range of 20 % up to 30 % than the associated $\mathbf{MOE}_{glob}$ values according to chapter 10 of EN 408. But this $\mathbf{MOE}_{glob}$ is only an apparent **MOE** value, because effects of the shear deformations are still included (see [3]). A function is introduced in EN 384, which allows the calulation of the interesting, mechanical correct $\mathbf{MOE}_{loc}$ with the determined $\mathbf{MOE}_{glob}$. It was shown, that this function provides mechanically inconsistent values for $\mathbf{MOE}_{glob}$ values $< 8967 \frac{N}{mm^2}$. For $\mathbf{MOE}_{glob}$ values $> 10782 \frac{N}{mm^2}$ higher values than the new introduced function (eq. (6) and (7) respectively), based on the beam theory, which is only partially explainable with local indentations. The function delivers higher values in comparison to our own linear regression analysis (eq. 10), based on 95 tests, too. Thus our suggestion yields in a replacement of the actual function in EN 384 by a mechanical consistent one (eq. (6), (7) and (11) respectively).

6.2 Suggested modifications in EN 408

Note 3 of chapter 10.2 in EN 408 should be modified in the following way, that local indentations should not be included in the measured values of the tests in principle (see figure 8), because this inclusion is a permanent source for dispensable errors. It can be shown by the introduced examples, that the $\mathbf{MOE}_{loc}$ values, calculated by eq. (6) and (7) respectively obtain less statistical dispersion than the $\mathbf{MOE}_{loc}$ values, based on the local deflection within a length of 5·h. This is not astonishing, because twice amount of test volume is included in the evaluation of $\mathbf{MOE}_{glob}$. The evaluation of eq. (6), (7) and (11) respectively should be conducted with values for the shear modulus $G_{\parallel}$ from

the literature or appropriate codes. It is shown, that the influence of mistake of the shear modulus $G_{\parallel}$ remains small in the calculation of $\mathbf{MOE}_{loc}$. Nevertheless an amendment of the test configuration in EN 408 chapter 10 is suggested, which allows optionally the determination of the shear deformations in both lateral parts of the test beams and out of that the determination of the shear modulus. This additional measurement is an option in particular (see figure 8). A measurement configuration is shown in figure 8, which neglects effects due to local indentations. Alternatively these local indentations can be acquired seperately or the measured global deflections can be adjusted by a mean local indentation, calculated e.g. by means of a FE-analysis.

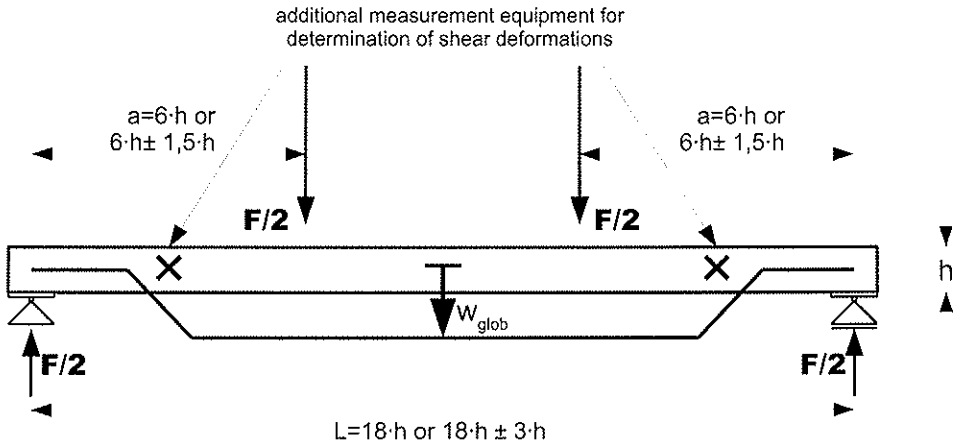

Figure 8: New test configuration an amendment for figure 3 of EN 408 with optional measurements of the shear deformations in both lateral parts of the test beam

Furthermore it should be clarified in chapter 10 of EN 408, whether length tolerances are allowed similar to chapter 9. In this case, the tolerances should be added to figure 3 similar as in figure 2. If length tolerances are not allowed in chapter 10 as indicated in figure 3 because of the missing illustrated tolerance values, the second sentence of the first clause should be cancelled, because length tolerances are explicitely allowed. Here a confict is given to figure 3, see also figure 9, which is copied from EN 408.

10.2 Procedure

The test piece shall be symmetrically loaded in bending at two points over a span of 18 times the depth as shown in Figure 3. If the test piece and equipment do not permit these conditions to be achieved exactly, the distance between the load points and the supports may be changed by an amount not greater than 1,5 times the piece depth, and the span and test piece length may be changed by an amount not greater than three times the piece depth, while maintaining the symmetry of the test.

(a) First clause in chapter 10.2 in EN 408

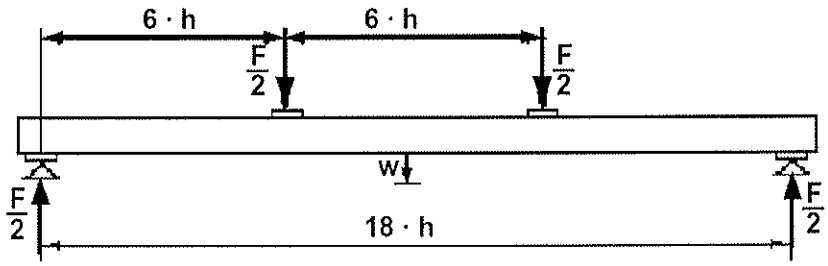

(b) Figure 3 in chapter 10.2 in EN 408

Figure 9: First clause and figure 3 of EN 408 (chapter 10.2)

Special thanks

The authors thank Mrs. Katja Frühwald for the support at the beginning of this work.

References

[1] EN 384:2004: *Structural timber - Determination of characteristic values of mechanical properties and density*, ratified 2003-02-20.

[2] EN 408:2003: *Timber structures - Structural timber and glued laminated timber - Determination of some physical and mechanical properties*, ratified 2003-06-20.

[3] Burger, N.; Glos, P.: *Verhältnis zwischen Zug- und Biege-Elastizitätsmoduln von Vollholz*, Holz als Roh- und Werkstoff 53 (1995), 73-74.

[4] Blaß, H.J.: *Ermittlung des 5 %-Quantils des Produkts aus Elastizitätsmodul und Torsionsschubmodul für Brettschichtholz*, available for members of WG3 (*Glulam*) (2005).

INTERNATIONAL COUNCIL FOR RESEARCH AND INNOVATION
IN BUILDING AND CONSTRUCTION

WORKING COMMISSION W18 - TIMBER STRUCTURES

CALIBRATION OF PARTIAL FACTORS IN THE DANISH TIMBER CODE

H Riberholt

Department of Structural Engineering
Technical University of Denmark

DENMARK

MEETING THIRTY-NINE
FLORENCE
ITALY
AUGUST 2006

Presented by H Riberholt
I smith asked how would one know that the extreme conditions had been experienced. H Riberholt explained that the wind load several years ago was very high yet no failures were experience; therefore, one would be comfortable with the proposed reduction.
R Marsh stated that one seemed to eliminate the problem during erection. Miss erection would be more of problem. H Riberholt stated that it was assumed for timber structures that the erections were done under normal conditions. A Ranta-Maunus stated that it would be difficult to quantify effect of erection errors. H Larsen stated that control during erection should be considered separately. Larsen did not like the statement that his research demonstrated Euler column formula did not apply to timber column.

Calibration of partial factors in the Danish Timber Code

Hilmer Riberholt
Adjunct Professor
Department of Structural Engineering
Technical University of Denmark

Abstract

The experience from recent strong gales in Denmark and also that experience shows no failures in structures designed in accordance with the codes have been the background for a reduction in the safety level of the structural codes, also the timber code.

Further, the introduction in Eurocode 0 – EN 1990 of reliability differentiation by a separation of the uncertainty of material and static model have by the Danish Standards association been used to set up a more clear specification of the factors resulting in new formal material partial factors.

The paper focuses on the effects of separating the uncertainty from partly the material parameters, partly the strength / static model.

As a consequence of the safety calibration work all Danish structural codes should now have the same safety level in accordance with Eurocode 0 – EN 1990.

1 Introduction and background

The safety format of the Danish structural codes have for many years been based on partial factors. In 1998 new values of the partial factors were published after a calibration of the safety had been performed to achieve the same safety index in the codes for the different structural materials.

During recent very strong gales with wind gusts similar to the characteristic wind velocity no structural failures were experienced. Further, in no cases there have been seen failures in structures designed according to the relevant structural code. Both facts indicate a too high safety level.

In 2005 it was decided to conduct another calibration of the safety in all structural codes to achieve the following:

- A lower general safety level than in the code from before 2005.
- The same safety level for all structural materials / codes
- A more clear specification of the factors resulting in the formal material partial factors, including the failure type, the uncertainty of the static model, the accuracy in the determination of the material parameters and the supervision during erection.

The new calibration was performed during a rather short period of 2005 and with limited information and resources. The background for the calibration is described in /Sørensen et al, 2005/.

2 Objective

The objective of this paper is to describe how the material partial factors have been determined according to the method developed by the Load- and safety committee at DS, Danish Standards.

3 Methods applied

According to EN 1990, clause 6.3.3 shall the design material or product property be determined from

$$X_d = \eta \frac{X_k}{\gamma_m} \tag{3.1}$$

where X_k the characteristic value of the material property
γ_m partial factor
η conversion factor taking into account effects of moisture, temperature and duration of load

EN 1990, clause 6.3.5 allows that the design resistance R of a member or component can be determined from a simplified formula

$$R_d = R\left\{\eta_i \frac{X_{k,i}}{\gamma_{M,i}}; a_d\right\} \quad i \geq 1 \tag{3,2}$$

where for material number i
$X_{k,i}$ the characteristic value of the material property
$\gamma_{M,i}$ partial factor
η_i conversion factor
a_d design value of a geometric size

The partial factor $\gamma_{M,i}$ covers the uncertainties from the model and the material since

$$\gamma_{M,i} = \gamma_{Rd}\gamma_{m,i} \tag{3.3}$$

where for material number i
γ_{Rd} partial factor associated with the uncertainty of the resistance model
$\gamma_{m,i}$ partial factor for a material property

EN 1990, Annex C, subclauses C7 – C10 describe that a practical way of ensuring that the reliability index is equal to or larger than the target value is to perform the calculations considering the design values of the material property X_d and the geometric property a_d plus the model uncertainty θ.

In EN 1990 it has been chosen to have a target reliability class RC2 $\beta = 4{,}7$ for a 1 year period for the consequence class CC2 (normal residential or office).

In the Danish safety format it has been chosen to lower the target reliability to $\beta = 4{,}3$ for a 1 year reference period, which corresponds to the lower RC3 class in EN 1990. Further it has been chosen to employ γ_M defined by the following equation

$$\gamma_{M,i} = \gamma_M = \gamma_0\gamma_1\gamma_2\gamma_3\gamma_4 \tag{3.4}$$

where the factors take into account

- γ_0 consequence of failure, see table 3.1
- γ_1 failure type, see table 3.2
- γ_2 uncertainty related to the resistance model, see table 3.3
- γ_3 extent of inspection during construction, see table 3.4
- γ_4 uncertainty related to the material property, see table 3.5

The different factors have been given values to achieve the above mentioned target reliability $\beta = 3{,}3$ for a structure in the so called Normal Safety Class corresponding to CC2.

The tables 3.1, 3.2 and 3.4 contain factors, which have been given the value 1,00 for normal situations and a larger 1,1 or a lower 0,90 / 0,95 for other situations.

As in EN 1990 it has been accepted to have different reliabilities for the different safety or consequence classes. Table 3.1 states that the partial factor can be decreased or increased 10 %.

Table 3.1. The factor taking into account the consequences of any failure

Safety class	Low (CC1)	Normal (CC2)	High (CC3)
γ_0	0,90	1,00	1,10

The failure type governs the factor γ_1 depending on whether the failure is without warning, or with warning without load-carrying reserves or with such reserves. Typical this is related to a brittle failure and a relatively ductile failure without or with reserves.

Table 3.2. The factor taking into account the amount of warning before complete failure.

Failure type	Warning with reserves	Warning without reserves	No warning
γ_1	0,90	1,00	1,10

The uncertainty related to the resistance model reflects how well the model predicts the measured load-carrying capacity of the member or component, e.g. how well does the column-equations predict the actual capacity of a column to carry the normal compressive force. Depending on the coefficient of variation, COV, determined from a reliability based calibration, the model factors γ_2 in table 3.3 have been determined by a reliability based calibration.

Table 3.3. The factor taking into account the uncertainty related to the resistance model.

COV for the calculation model	5%	10%	15%	20%	25%
γ_2	1,05	1,10	1,15	1,20	1,25

The extent of inspection during construction has been considered with the factor γ_3 stated in table 3.4.

Table 3.4. The factor taking into account the extent of inspection during construction

Inspection class	Intensified	Normal	Relaxed
γ_3	0,95	1,00	1,10

The uncertainty related to the material property was given the following relation to the COV of the material property. It is a noticeable fact that this relation is more relaxed than the previous.

Table 3.5. The factor taking into account the uncertainty related to the material property.

COV for the material property	≤5%	10%	15%	20%	25%	30%
γ_4	1,15	1,20	1,25	1,30	1,35	1,40

4 Partial factors, generally

It was recognized that it could be necessary with different partial factors for the different members in a timber structure, e.g. one for bending and one for the fasteners. It could even be necessary with different partial factors for bending and tension because of the different COV for bending and tension.

4.1 Timber members

However, for the determination of the partial factors for timber structures focus was set on the bending strength since this property frequently is the decisive one. In /Sørensen & Hoffmeyer, Paper No 206/ it has been concluded that for bending, compression and tension of graded, structural timber should the COV be assumed to have the values stated in table 4.1. The results in / Carl-Johan Johansson et all, 1998/ have been one of the important data bases.

Table 4.1 Coefficients of Variation for bending, compression and tension according to /Sørensen & Hoffmeyer, Paper No 206/

	Assuming 2 parameter Weibull tail fit	Assuming LogNormal distribution
Bending	20%	25%
Compression	15%	15%
Tension	25%	30%

In / Ranta-Maunus, VTT/ it has been concluded that the coefficient of variation for machine graded timber should be 30%, and that of plywood should be 20%, for glulam 15% and for LVL 10%. All values are applicable to the LogNormal distribution.

From the Load- and Safety committee it was argued that since the structural codes are based on the assumption that the LogNormal distribution should be used the large values of the COV should be employed.

It was discussed whether the model factor γ_2 could be put equal to 1,00 since the bending test is rather similar to the conditions in real structures. This argument was partially accepted, but it was added that the factor should also cover more complicated situations than a simple span beam and also uncertainty related to effects of duration of load and moisture. Therefore, it was agreed that the COV for the model should be assumed to 5% resulting in that γ_2 should be put equal to 1,05.

It has been taken into account that system effects can occur in timber structures, especially those with members close to each other. The effect can be attributed to

- Redistribution of loads to other components in the structure when the weakest fails, e.g. a continuous chord of a w-truss
- Redistribution of loads to neighbour members when one member fails, e.g. parallel beams with sheathing or battens which can carry the load to the neighbouring beams.

In /Sørensen, Damkilde and Munch-Andersen/ it is concluded that based on typical test data the COV for a W-truss can be assumed to be 10-15 % if a tail fitted Weibull distribution is used. Further, the characteristic load-carrying capacity is 10% larger.

The system effects in parallel timber beams with a relatively close spacing have been studied in /Hansson, 2005/. Based on the results in this report there has in /Stang & Munch-Andersen, 2004/ been concluded that COV of the load-carrying capacity of systems with such beams can be taken as 10 – 13 % and that the characteristic capacity is larger for the system than for the single beam. The increase in the characteristic load-carrying capacity has been considered in the Danish Timber Code by system factors.

Considering the fact that the load-carrying members in timber structures typically are spaced relatively close it was decided to assume a COV of 20%.

Since the tensile strength typically is decisive at the connections where the fasteners reduce the cross section the tensile stresses along the whole length of the member are

relatively small. To this can be added that the timber members frequently are loaded with a lateral load resulting in bending stresses. Therefore, the members in tension shall typically have their strength checked in a point or over a small length where the combination of tension and bending is maximum, so any length effect on the tensile strength may be disregarded in practice. The conclusion of the considerations has been that the partial factor for tension could be put equal to that of bending.

The same simplification has been applied to compression without stability phenomena, because it is on the safe side. Where stability effects occur special attention has been given to the model, see clause 5 of this paper.

For structural timber members it has been concluded that:

1. COV = 20% for the material property
2. COV = 5% for the uncertainty of the model, (this is a minimum value)
3. Warning is given before failure but without strength reserves

For glued laminated timber the COV has been set to 15% based on the tests reported in /H. J. Larsen, 1982/, which states that COV vary between 9% and 18%. Similar properties have been agreed for wood based panels and structural members produced under a third party control.

For glued laminated timber members, wood based panels and structural members produced under a third party control it has been concluded that:

1. COV = 15% for the material property
2. COV = 5% for the uncertainty of the model, (this is a minimum value)
3. Warning is given before failure but without strength reserves

The results and the partial factors are summarized in table 6.1.

4.2 Connections

For connections with metal dowel type fasteners the following has been the basis.

- For nails a lot of tests have shown COV values in the range of 10% - 15%.
- The COV for the embedment strength of bolts has been set to 10% according to test results in /Yasumura & Sawata, 2000/.
- The COV for the load-carrying capacity of a single bolt and multiple bolts have been found to min-**mean**-max: 4 – **6** - 10% respectively 4 -**10** – 17% according to /Jorissen, 1998/.
- The model uncertainty has been reported in /Köhler, 2005/. The COV for the model is around 10%.

For dowel type metal fasteners it has been concluded that:

1. COV = 13% for the material property
2. COV = 10% for the uncertainty of the model
3. Warning is given before failure but without strength reserves

For glued connections such as glued in rods it has been assumed that COV of the material is 20% and that no warning will be given before failure.

Table 6.1 states the compiled results.

5 Partial factors in cases where stability of the member is involved

The intention was to check whether the assumed characteristic properties and the formulas of DS 413 (EN 1995) documented the resistances.

Timber members subjected to compression, where the deflected state should be considered, were subjected to a more intensified analysis. Since several material properties are involved, it was necessary to carry out a more detailed analysis of the uncertainty of both the material and the model. The model described in /Sørensen et al, 2005/ is based on fitting with Maximum Likelihood. Here a model described in Annex D of EN 1990 will be used

5.1 Description of the method

Annex D gives guidance for how to separate the uncertainty from the material properties from that of the model.

The model analyzed is the column formulas given in EN 1995, part 1, which are the same as those in the Danish Timber Code DS 413. To achieve the best predicted load-carrying capacity from the column formulas and in accordance with Annex D of EN 1990 the mean values of the material properties were used. The mean values were calculated from the characteristic. They are the bending and the compression strengths plus the E-modulus.

The standard procedure described in Annex D has been used in a slightly different way. The basic assumption of Annex D is that the COV of the test results V_r shall be related to the COV of the uncertainty of the model V_δ and the COV of the material properties V_{rt}. For small values of COV as in this case:

$$V_r^2 = V_\delta^2 + V_{rt}^2 \qquad (5.1)$$

The analysis has been conducted on the ratio between the measured capacity and the one predicted by the model. Therefore, the uncertainty due to the material properties have been weighted by the capacity by using the coefficient of elastic sensitivity elasticity e for the bending strength, compression strength and E-modulus.

Bending $$e_m = \frac{dF}{df_m} \cdot \frac{f_m}{F} \qquad (5.2.a)$$

Compression $$e_c = \frac{dF}{df_c} \cdot \frac{f_c}{F} \qquad (5.2.b)$$

E-modulus $$e_E = \frac{dF}{df_E} \cdot \frac{E}{F} \qquad (5.2.c)$$

where :

e	coefficient of elastic sensitivity
F	capacity according to the model
f	strength or stiffness property

The COV from the material properties is calculated from

$$V_m^2 = \sum (e_i \cdot V_i)^2 \qquad (5.3)$$

and the COV of the model is then calculated from (5.1).

5.2 Analysis of test results

The available test results are those conducted and reported by H. J. Larsen in /Tests with centrally loaded timber columns, 1974/ and /Larsen & Theilgaard, 1977/. The last mentioned is also reported in /Laterally loaded timber columns, 1979/. All tests have been conducted with specially oil smeared bearings securing a perfect pinned joint.

The predicted load-carrying capacities have been calculated from the measured E-moduli and where no measurements have been performed by assuming that the mechanical properties approximately follow the Normal Distribution and that they have the previously mentioned COV values:

Bending strength	COV = 25%
Compression strength	COV = 15%
E-modulus	COV = 15%

The assumed characteristic values are those allocated to the grade T1, T2 and T3, which are similar to those of the strength classes C18, C24 and C30 except that the compressive strengths deviate a little.

Centrally loaded columns

Figure 5.1 shows the measured and the predicted capacities of the centrally loaded columns and the ratio of these versus geometric slenderness ratio λ for deflection around the strong and the weak axes. The mean values of the material parameters have been estimated from the Normal Distribution as described above.

By direct using the formulas given in DS 413 (EN 1995) it was found that the predicted capacities were too low. It was considered to change the material parameters, but this was rejected because it would interfere with EN standards. Instead, by increasing the relative slenderness factor by 5% the mean values of column capacities for deflection partly in the strong direction, partly in the weak direction became 0,98 and 0,99 respectively.

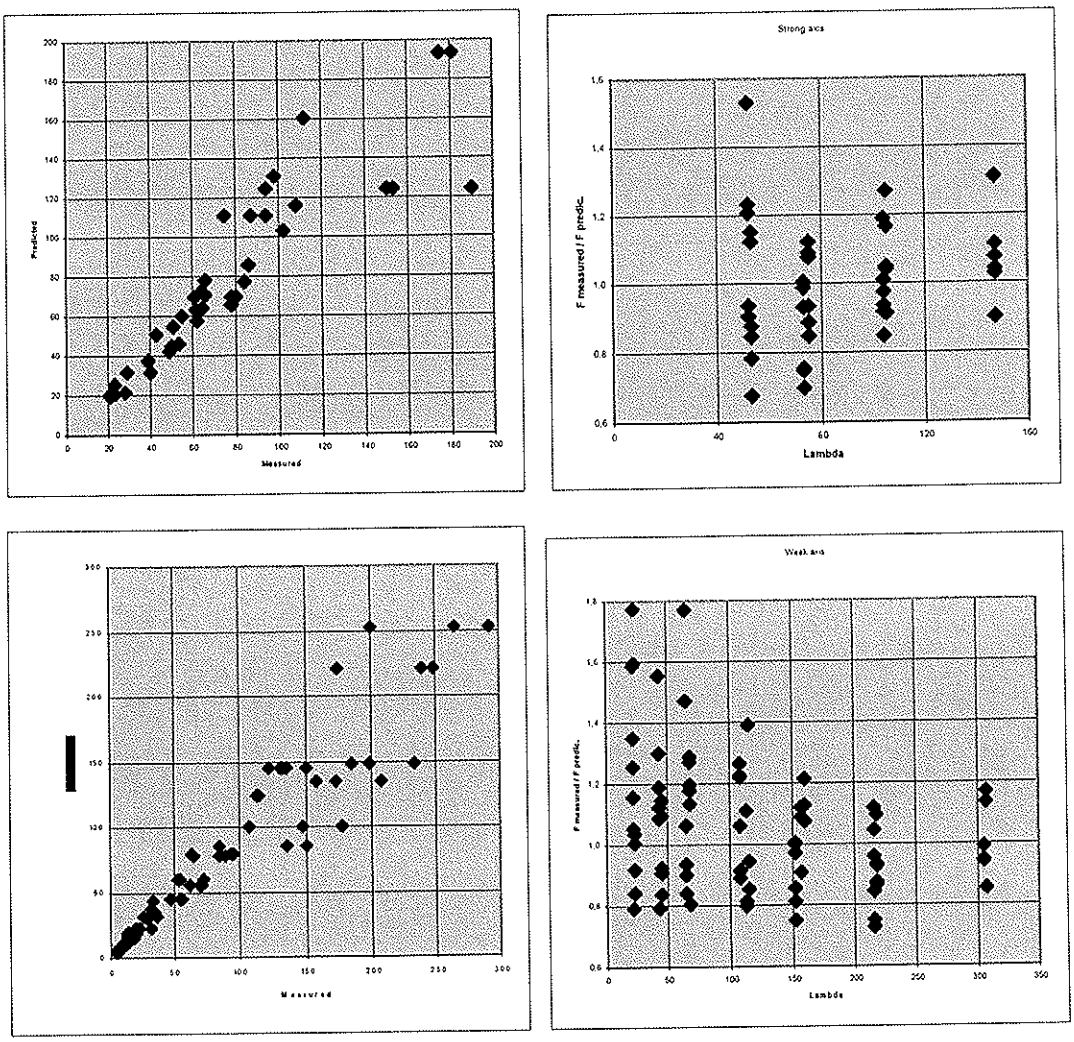

Figure 5.1 Measured versus predicted mean load-carrying capacity, and the ratio between these $F_{measure}/F_{predic.mean}$ versus the geometric slenderness ratio for a column deflecting partly in the strong direction, partly in the weak direction. Mean values are calculated from the characteristic ones.

It appears from figure 5.1 that there is a good agreement between measured and predicted capacities. The scatter is larger for small slenderness ratios, where the capacity of the column is controlled by the compressive strength, while for large slenderness ratios the scatter is smaller because the capacity is controlled by the E-modulus.

The coefficients of elastic sensitivity e have been determined numerically for small and large slenderness ratios. Table 5.1 states the results. The eccentricities from a straight line have been taken out of the column formula and it is estimated that their COV is small and negligible.

Table 5.1. Coefficients of elastic sensitivity e for deflection in the strong direction.

Material property	Small slenderness		Large slenderness	
	T300	ukl	T300	Ukl
Compression strength	0,48	0,8	0,035	0,054
E-modulus	0,48	0,18	0,96	0,94

The coefficients of elastic sensitivity have expected values. Using these values the weights in table 5.2 have been estimated and the uncertainties of the model have been calculated from formula (5.1).

Table 5.2. Weights for the material COV and the calculated COV of the model uncertainties.

				COV of model uncert.	
	f_m	f_c	E	Strong axis	Weak axis
Small slenderness ratio	0,5	1,0	0,5	0,29	0,18
Large slenderness ratio	0,2	0,2	1,0	0,17	0,06
All lengths	0,3	0,7	0,8	0,14	0,05

At DS it has been agreed to assume a COV of the model uncertainty of 10%.

Laterally loaded columns

The tests with the laterally loaded columns have been analyzed similarly using the models given in EN 1995 section 6.3.2 and 6.3.3. The combined Stress Index CSI for column bending in the formulas (6.23) and (6.24)

$$\frac{\sigma_{c,0,d}}{k_{c,y} f_{c,0,d}} + \frac{\sigma_{m,y,d}}{f_{m,y,d}} + k_m \frac{\sigma_{m,z,d}}{f_{m,z,d}} \qquad \text{(6.23) and (6.24) similar}$$

and that for combined bending and torsion in the formula (6.35)

$$\frac{\sigma_{c,0,d}}{k_{c,z} f_{c,0,d}} + \left(\frac{\sigma_{m,d}}{k_{crit} f_{m,d}} \right)^2 \qquad (6.35)$$

have been calculated using the calculated mean values of the strength properties and the stresses are those measured during the tests. The stresses have been calculated from the applied load at failure and the strengths in the denominator are predicted values. Since the largest value of CSI of the possible 3 failure modes corresponds to the lowest predicted capacity, the largest CSI value has been taken as a measure of the capacity of the column.

By considering only the combined Stress Index for column bending in the formulas (6.23) and (6.24) a mean value of CSI was found to 1,02 with a COV of 33%. By considering also the formula (6.35) for combined lateral and torsional buckling a mean value of 1,21 was found with a COV of 32%. So, considering combined lateral and

torsional buckling the formulas of DS 413 (Eurocode 5) are generally much on the safe side. The figures 5.2 and 5.3 show the relation between the geometric slenderness ratio and the Combined Stress Index CSI.

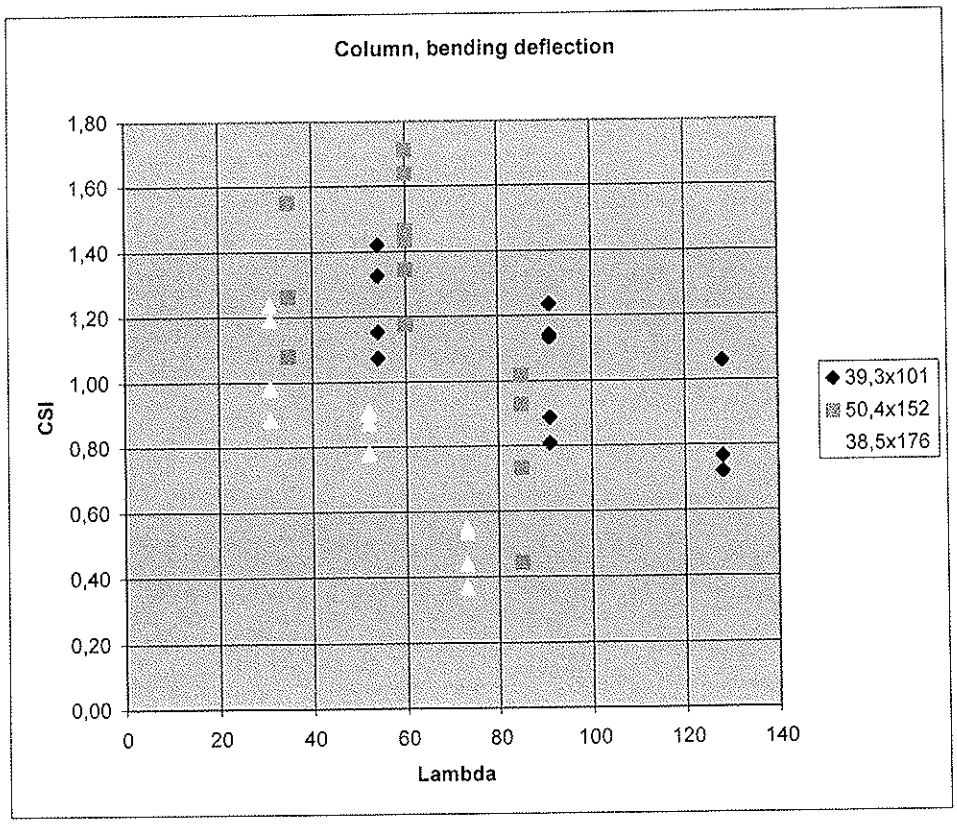

Figure 5.2. Combined Stress Index CSI for lateral buckling of laterally loaded columns in dependence on the slenderness ratio. Tested cross sections 39,3x101 mm, 50,4x152 mm and 38,5x176 mm.

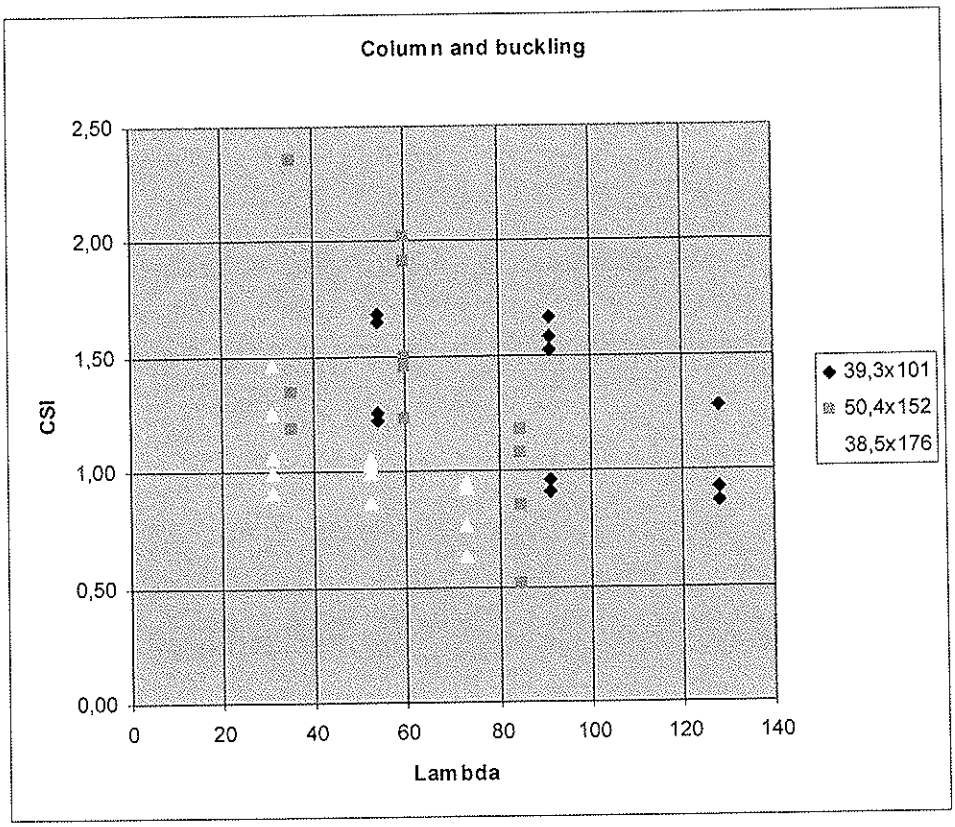

Figure 5.3. Combined Stress Index CSI for lateral and torsional buckling of laterally loaded columns in dependence on the slenderness ratio. Tested cross sections 39,3x101 mm, 50,4x152 mm and 38,5x176 mm.

It appears from figure 5.2 and 5.3 that the CSI-values decrease with increasing slenderness ration. If the model was perfect the CSI-values should remain constant around 1,0. Considering only flexural deflection, figure 5.2, the mean values of the CSI-value is 1,02, so in average these formulas are correct, but they are not safe for large slenderness ratios.

However, with the newly introduced strength requirement for combined lateral and torsional deflection of columns, formula (6.35) of EN 1995, the formulas in the DS 413 (Eurocode 5) are safe.

The coefficients of variation for CSI are larger for laterally loaded columns, around 35%, than for centrally loaded columns. Analyses similar to those performed for centrally loaded columns indicate that the COV of the model uncertainty is around 25%. Apparently, the column formulas of Eurocode 5 need more refinement.

6 Conclusions

The analysis has shown how the partial factors of the Danish Timber code have been derived. Table 6.1 states the values.

Table 6.1. Overview over coefficients of variation and γ-factors.

				γ-factors			
	Failure type	Model	Material	Failure type	Model	Material	
		COV_2	COV_4	γ_1	γ_2	γ_4	$\gamma_1\ \gamma_2\ \gamma_4$
Struc. timber Bending, tension, compression and others	Warning, no reserve	5%	20%	1,00	1,05	1,30	1,37
Glulam Bending, tension, compression and others	Warning, no reserve	5%	15%	1,00	1,05	1,20	1,31
Struc. Timber, glulam Columns and buckling	Warning, no reserve	10%	15%	1,00	1,10	1,25	1,37
Wood panels, and structural members produced under a third party control	Warning, no reserve	5%	15%	1,00	1,05	1,25	1,31
Dowel type metal fasteners	Warning, no reserve	10%	13%	1,00	1,10	1,23	1,35
Glued connections	No warning	10%	20%	1,10	1,10	1,30	1,57

The resulting partial factors $\gamma_1\ \gamma_2\ \gamma_4$ to be introduced into the Danish Timber Code DS 413 are:

Glulam, LVL and wood panels	1,30
Structural timber, trusses, elements	1,35
Dowel type connections	1,35
Glued connections	1,50

For laterally load columns it has been documented, that the models and formulas are safe, but the uncertainty of the model is relatively large. Further improvements are welcome.

References

Alpo Ranta-Maunus, VTT. Summary report on existing strength data submitted to Nordic Wood: Reliability of timber structures. 2004?

Martin Hansson. Probabilistic system effects in timber structures. Report TVBK-1030. Div. of Struc. Eng. Lund University.

Carl-Johan Johansson, Lars Broström, Lise Bräuner, Preben Hoffmeyer, Charlotta Holmqvist, Kjell Helge Solli. Laminations for glued laminated timber – Establishment of strength classes for visual strength grads and machine settings for glulam laminations of Nordic origin. SP Report 1998:38, Swedish National Testing and Research Institute.

André Jorissen. Double shear timber connections with dowel type fasteners. Delft University of Technology, doctor dissertation, 1998.

Jochen Köhler. A probabilistic framework for the reliability assessment of connections with dowel type fasteners. CIB W18/38-7-2, 2005

Jochen Köhler. PhD thesis, ETHZ, 2005.

H. J. Larsen & Svend S. Pedersen. Tests with centrally loaded timber columns. Aalborg Universitetscenter, Report R7405, 1974.

H. J. Larsen & Esko Theilgaard. Bæreevnen af tværbelastede træsøjler, Forsøg og teori. Aalborg Universitetscenter, Report R7707,1977.

H. J. Larsen & Esko Theilgaard. Laterally loaded timber columns. Jour. of Str. Div. July 1979.

H. J. Larsen. Strength of glued laminated beams – Part 5. Report No. 8201, 1982. Institute of Building Technology and Structural Engineering, Aalborg University.

Birgitte Dela Stang & Jørgen Munch-Andersen. Reliability of Timber Structures – Results of a study of the Danish codes, COST E24, Florence 27-28 May 2004.

John Dalsgaard Sørensen, Preben Hoffmeyer. Statistical analysis of Data for Timber Strengths. Paper No 206, 2001, Aalborg University.

John Dalsgaard Sørensen, Lars Damkilde and Jørgen Munch-Andersen. Load Bearing Capacity of Roof Trusses. 9th. ASCE Specialty Conference om Probabilistic Mechanics and Structural Reliability.

John Dalsgaard Sørensen et al. Background documents to revision of DS 409:2005 – Safety format etc. Draft November 2005. Danish Standard. Partly in Danish.

M. Yasumura & K. Sawata. Determination of yield strength and ultimate strength of dowel-type timber joints. CIB W18/33-7-1, 2000, Delft.